Zoosystematics and Evolution

99 (2) 2023

PENSOFT

für Natur
MUSEUM FÜR NATURKUNDE
BERLIN

Zoosystematics and Evolution
A Bulletin of Zoology since 1898

Zoosystematics and Evolution

2023. Volume 99. 2 Issue

ISSN: 1435-1935 (print), 1860-0743 (online)
Abbreviated keys title: Zoosyst. Evol.

In Focus

The cover picture shows shell and operculum of *Dalipaludina oxytropoides*

See paper of **Zhang L-J, Du L-N, von Rintelen T:** A new genus of river snails, *Dalipaludina* (Gastropoda, Viviparidae), endemic to the Yunnan Plateau of SW China

Cover design
Pensoft

Zoosystematics and Evolution
A Bulletin of Zoology since 1898

Content of volume **99** (**2**) 2023

Abstract & Indexing Information

Biological Abstracts® (Thompson ISI)
BIOSIS Previews® (Thompson ISI)
Cambridge Scientific Abstracts (CSA/CIG)
Web of Science® (Thompson ISI)
Zoological Record™ (Thompson ISI)

Zoosystematics and Evolution
A Bulletin of Zoology since 1898

Content of volume **99** (**2**) 2023

Zoosyst. Evol. 99 (2) 2023, 285–297 | DOI 10.3897/zse.99.102586

PENSOFT

für Natur MUSEUM FÜR NATURKUNDE BERLIN

A new genus of river snails, *Dalipaludina* (Gastropoda, Viviparidae), endemic to the Yunnan Plateau of SW China

Le-Jia Zhang[1], Li-Na Du[2,3], Thomas von Rintelen[1]

1 *Museum für Naturkunde, Leibniz, Institut für Evolutions und Biodiversitätsforschung, Berlin 10115, Germany*

2 *Key Laboratory of Ecology of Rare and Endangered Species and Environmental Protection, Guangxi Normal University, Ministry of Education, Guilin, Guangxi 541004, China*

3 *Guangxi Key Laboratory of Rare and Endangered Animal Ecology, College of Life Science, Guangxi Normal University, Guilin, Guangxi 541004, China*

https://zoobank.org/6856760F-3F9E-4B27-8AC2-B59D25845F67

Corresponding author: Le-Jia Zhang (lejia.zhang@mfn.berlin)

Academic editor: Frank Köhler ♦ **Received** 23 February 2023 ♦ **Accepted** 29 March 2023 ♦ **Published** 11 May 2023

Abstract

A new genus of viviparid snail, *Dalipaludina* **gen. nov.**, from the Yunnan Plateau of China is described within an integrative taxonomic framework based on data from the mitochondrial COI marker and morphology. *Dalipaludina* can be distinguished from all other viviparid genera by a unique combination shell, operculum and radula characters. Four species are assigned here to the new genus, *Dalipaludina delavayana* **comb. nov.**, *Dalipaludina oxytropoides* **comb. nov.**, *Dalipaludina occidentalis* **comb. nov.**, and *Dalipaludina pyramidella* **comb. nov.**, and one species is newly assigned to *Margarya*, *Margarya dianchiensis* **comb. nov.** The four species of *Dalipaludina* are allopatrically distributed in shallow water lentic habitats at high altitude regions of the Yunnan Plateau.

Key Words

High altitude, lentic habitat, phylogeny, taxonomy

Introduction

River snails (Viviparidae) are widely distributed freshwater gastropods that are found on all continents except for Antarctica and South America. The oldest fossil record of Viviparidae can be traced back to the mid Jurassic. About 28 extant genera and 125 to 150 extant species of this family worldwide are currently recognised (Van Bocxlaer and Strong 2019). China is the country with the highest biodiversity of Viviparidae, harbouring two subfamilies (Bellamyinae Rohrbach, 1937; Viviparinae J. E. Gray, 1847), 13 genera (*Amuropaludina* Moskvicheva, 1979; *Angulyagra* Rao, 1931; *Anularya* Zhang & Chen, 2015; *Cipangopaludina* Hannibal, 1912; *Filopaludina* Habe, 1964; *Idiopoma* Pilsbry, 1901; *Margarya* G. Nevill, 1877; *Mekongia* Crosse & P. Fischer, 1876 *Rivularia* Heude, 1890; *Sinotaia* F. Haas, 1939; *Tchangmargarya* He, 2013; *Ussuripaludina* Zatravkin & Bogatov, 1987; *Viviparus* Montfort, 1810), and at least 40 species (Liu et al 1995; Zhang et al. 2015; Van Bocxlaer et al. 2017).

The Yunnan Province of China, which covers an area of only 394,000 km^2, harbours nine genera (*Angulyagra*; *Anularya*; *Cipangopaludina*; *Filopaludina*; *Idiopoma*; *Margarya*; *Mekongia*; *Sinotaia*; *Tchangmargarya*) including three endemic ones (*Anularya*; *Margarya*; *Tchangmargarya*) and at least 24 species including 14 endemic ones of Viviparidae (Liu et al 1995; Zhang et al. 1997; Zhang et al. 2015). While it is the region with the highest diversity of Viviparidae at both the genus and species level not only in China but also worldwide, recent studies (Du et al. 2011; Zhang et al. 2015; Zhang 2017) have revealed that the diversity of Viviparidae in Yunnan is still underestimated. Based on an integrative study combining molecular and morphological data, we here revise the taxonomy of several viviparid species from the Yunnan Plateau, and describe a new genus. The phylogeny and ecology of the new genus, as well as conservation aspects, are discussed.

Materials and methods

Material

Type specimens of three Viviparidae species from Yunann kept in the Institute of Zoology, Chinese Academy of Sciences, Beijing (**IZCAS**), the Kunming Natural History Museum of Zoology, Kunming (**KIZ**), and the Museum of Comparative Zoology at Harvard University, Cambridge (**MCZ**), as well as other specimens in Museum für Naturkunde, Berlin (**ZMB**), have been examined. From 2011 to 2022, altogether 19 lakes of Yunnan and the surrounding aquatic habitats, including rivers, creeks, springs and wetlands, have been surveyed (Fig. 1A). Newly collected fresh samples of the species belonging to the new genus were collected by Le-Jia Zhang and Jiao-Wei Ning from 2018 to 2022 in northwest Yunnan (Fig. 1B–D). The newly sampled material is stored in ZMB and the private collection of Le-Jia Zhang (**ZLJ**) Jiao-Wei Ning (**NJW**).

Examination of morphology

Shell height (H) and width (W) of only mature and complete specimens were measured with a caliper to a precision of 0.1 mm (Table 1). The morphometric data of

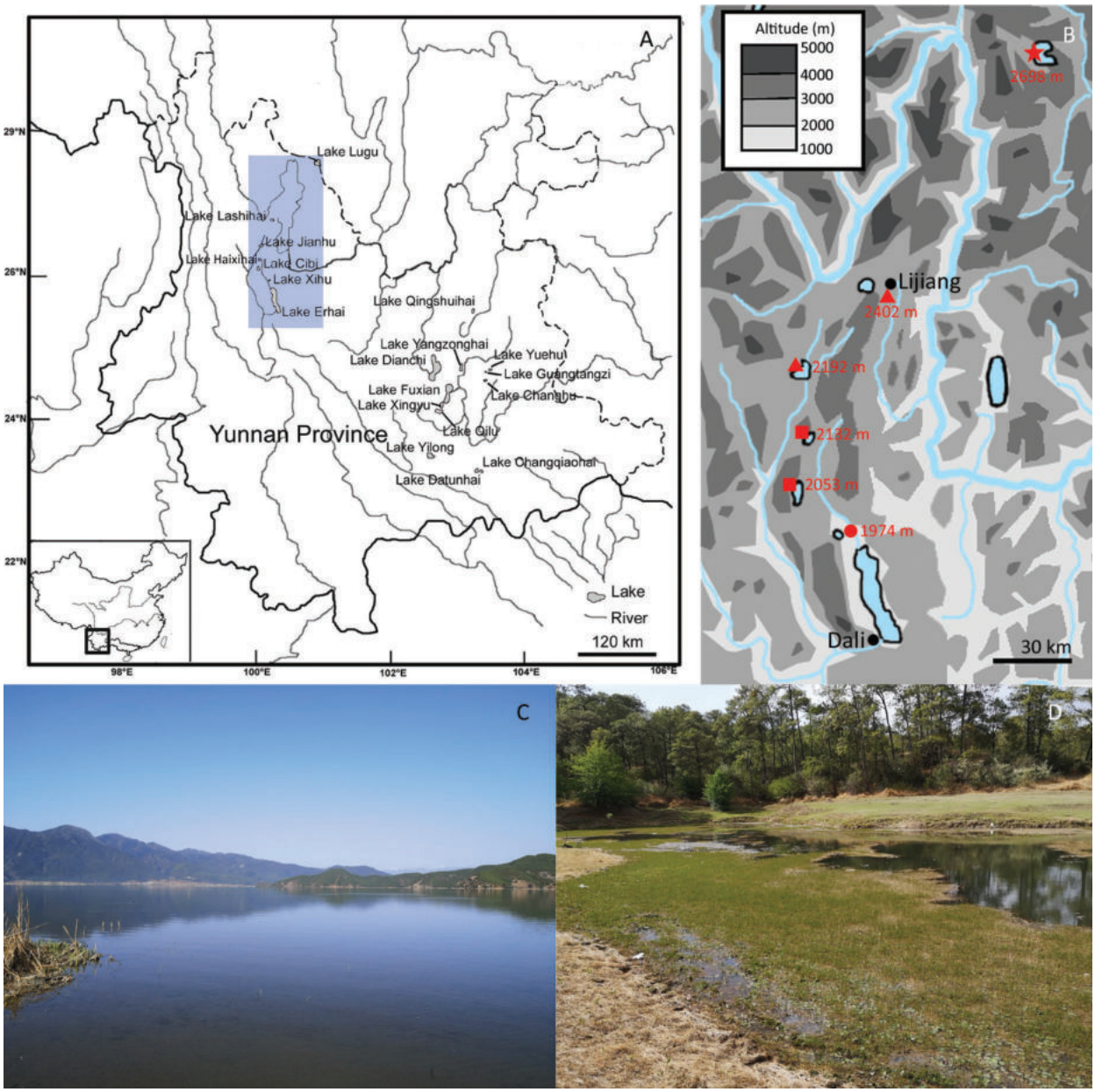

Figure 1. Collecting sites and habitats of *Dalipaludina* gen. nov. in Yunnan, China. **A.** Map of Yunnan Province showing 19 surveyed lakes (adapted from Zhang et al. 2015), study area in northwest Yunnan highlighted in blue, where *Dalipaludina* species were found during surveys; **B.** Map of study area in northwest Yunnan, star–*Dalipaludina oxytropoides*, triangle–*Dalipaludina occidentalis*, square–*Dalipaludina delavayana*, circle–*Dalipaludina pyramidella*; altitude of each collecting site is given; **C.** Environment of one collecting site of *Dalipaludina oxytropoides* in Lake Lugu; **D.** Environment of one collecting site of *Dalipaludina occidentalis* in an unnamed pond in Lijiang.

Dalipaludina oxytropoides kept in ZMB are from Wiese et al. (2022). The specimens were photographed in a consistent orientation using a Sony alpha 7R 4 camera. Radulae and embryonic shells were extracted through dissection; radulae were cleaned by boiling in 1% NaOH solution for half an hour and rinsed with distilled water. Radulae and embryonic shells were coated with gold before scanning electron microscopy with a Zeiss *EVO LS10* scanning electronic microscope. The terms used for describing the operculum are according to Zhang and von Rintelen (2021).

Table 1. Shell measurements of *Dalipaludina* species. Values are arithmetic means (mm).

Species	H	W	W/H
Dalipaludina delavayana (n=25)	58.30 ± 8.30	38.30 ± 5.27	0.70 ± 0.04
Dalipaludina oxytropoides (n=91)	44.60 ± 5.78	32.30 ± 3.82	0.70 ±0.04
Dalipaludina occidentalis (n=27)	50.17 ± 4.17	41.00 ± 2.38	0.82 ±0.05
Dalipaludina pyramidella (n=30)	47.86 ± 7.06	41.34 ± 5.48	0.87 ± 0.05

DNA extraction and amplification

DNA was extracted from the foot tissue of eight individuals (10–20 mg of each individual), using a mollusc-specific CTAB/chloroform extraction protocol (Winnepenninckx et al. 1993). A fragment of the mitochondrial cytochrome c oxidase subunit I (COI) gene was amplified through polymerase chain reaction (PCR) with the following primer pair: LCO1490, 5′-GGTCAACAAATCATAAAGATATTGG-3′ and COXB7R, 5′-ACCACCAGCTGGATCAAAAA-3′. (Schultheiß et al. 2011) PCR amplifications were conducted in 25 µl volumes under the following cycling conditions: initial denaturing step at 94 °C for 10 min, followed by 30 cycles of 94 °C for 1 min, 50 °C for 1 min, and 72 °C for 1 min, with a final extension step of 10 min at 72 °C. The purification and sequencing were conducted by Macrogen Europe, Amsterdam, Netherlands.

Phylogenetic analysis

Eight new DNA sequences (from eight individuals of two *Dalipaludina* species) have been uploaded to GenBank (accession numbers and museum voucher numbers, see Suppl. material 1). Additionally, three sequences of *Dalipaludina oxytropoides* published by Wiese et al. (2022) and sequences of 17 different genera of the subfamily Bellamyinae (Suppl. material 1) published by Stelbrink et al. (2020) and Hirano et al. (2019a) were downloaded from GenBank; *Viviparus viviparus* of the subfamily Viviparinae was selected as outgroup based on Stelbrink et al. (2020).

Sequences were aligned using MUSCLE as implemented in Geneious Prime 2020 (https://www.geneious.com). Genetic distances were calculated using MEGA X (Kumar et al. 2018). The dataset was tested in MEGA X for the best-fit model of sequence evolution by means of the Akaike and Bayesian information criteria; GTR+G+I was suggested as the best-fitting nucleotide substitution model. This model was employed in a maximum likelihood (ML) analysis conducted by RAxML as implemented in Geneious Prime 2020, with support estimated by 1,000 bootstrap replicates, and a Bayesian inference (BI) analysis performed with MrBayes 3.2.6 (Ronquist et al. 2012) as implemented in Geneious Prime 2020 with four independent chains for 5,000,000 generations, samplefreq = 1,000, burnin = 25%, and confirmed that convergence was reached based on the trace plots generated in Geneious Prime 2020.

Results

Genetic differentiation and phylogeny

COI p-distances between species of *Dalipaludina* are 1.81% to 3.98%; the p-distances between *Dalipaludina* and its closest relative, viz. the *Cipangopaludina*/*Margarya* complex, are 9.22%–14.98%, while p-distances within the *Cipangopaludina*/*Margarya* complex are 0–9.31%.

The phylogenetic trees reconstructed by BI and ML based on COI are highly congruent, therefore only the BI tree is shown (Fig. 2). The new genus *Dalipaludina* is monophyletic and distinct from all other included genera of Viviparidae. The three sequenced species of *Dalipaludina* are each recovered as monophyletic as well. *Dalipaludina occidentalis* is the sister species of *Dalipaludina delavayana*, and *Dalipaludina oxytropoides* is sister to both. *Dalipaludina* is the sister clade of a clade formed by the *Cipangopaludina*/*Margarya* complex, *Celetaia*, *Ussuripaludina*, *Hetergen*, *Torotaia*, *Anularya* and *Sinotaia*.

Systematics

Family Viviparidae J.E. Gray, 1847
Subfamily Bellamyinae Rohrbach, 1937

***Dalipaludina* Zhang, gen. nov.**
https://zoobank.org/6817CC4A-D98A-4D33-B890-49C91F64A1E5

Type species. *Paludina delavayana* Heude, 1889.

Etymology. "Dali" refers to the ancient Dali Kingdom (大理国) mostly situated in modern Yunnan, China; "paludina" refers the assignment to Viviparidae. The recommended Chinese name is "理田螺".

Diagnosis. Shell large, thin but solid; apex acute; teleoconch whorls with strong keel at suture, above suture relatively smooth or with several weak spiral threads or strong spiral cords, many thin and weak spiral threads on base; umbilicus narrow, sometimes bordered by a keel; exterior surface of operculum rather smooth, inner opercular region relatively small, nuclear region of operculum smooth, sometimes with small grains; outer marginal tooth with 9 to 11 small sharp cusps.

Comparative remarks. *Dalipaludina* gen. nov. resembles *Cipangopaludina* (widely distributed in East Asia), *Ussuripaludina* Zatravkin & Bogatov, 1987 (endemic to Far East), *Heterogen* Annandale, 1921 (endemic to Japan

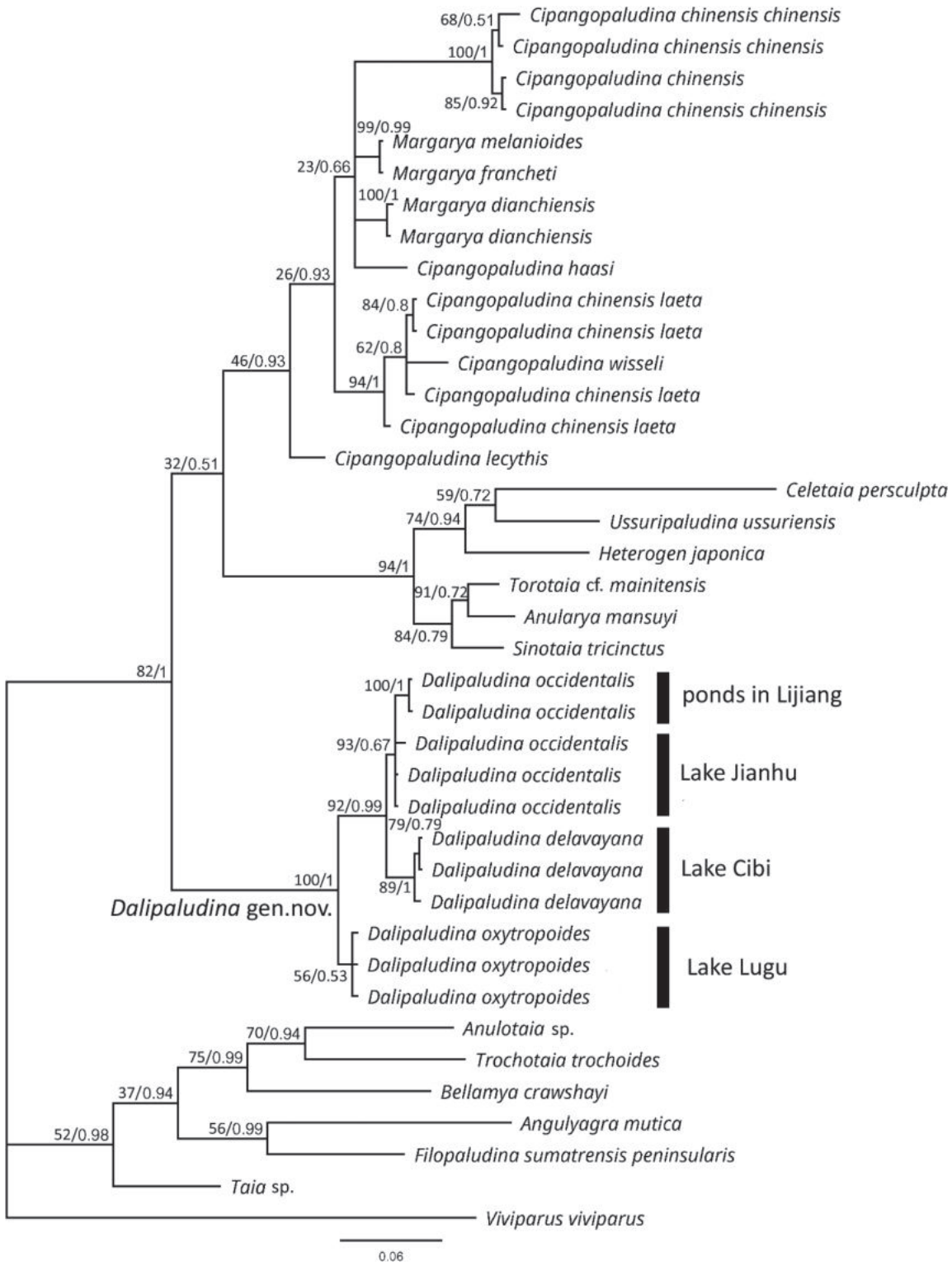

Figure 2. The BI tree based on cytochrome c oxidase subunit I (COI) showing the phylogenetic position of *Dalipaludina* gen. nov. within Viviparidae. Numbers above branches are ML bootstrap values/BI posterior probabilities.

and Korea), and *Torotaia* Haas, 1939 (endemic to Philippines, Sulawesi and New Guinea). It differs from *Cipangopaludina*, *Ussuripaludina*, *Heterogen* and *Torotaia* by having one strong keel at the suture, a shell base with many thin and weak spiral threads, a narrow umbilicus sometimes bordered by a keel, and operculum characters. The molecular phylogeny supports that *Dalipaludina* is distinct from *Cipangopaludina*, *Ussuripaludina*, *Heterogen* and *Torotaia*. The location of the testis in male *Dalipaludina* specimens in the mantle cavity supports the classification of this genus in the subfamily Bellamyinae. There are four known species of *Dalipaludina*.

Distribution. This genus is endemic to the lakes or ponds in northwest to northeast Yunnan, China.

Dalipaludina delavayana (Heude, 1889), comb. nov.

Paludina delavayana Heude, 1889: 47 ("lacu Ta-li fou", Lake Erhai).
Sinotaia delavayana – Qian et al. 2014.

Material examined. 2 ***syntypes***, IZCAS-FG-492553, IZCAS-FG-492554; 1 ***paratype***, MCZ-Mala-167342; 8 specimens in ZMB, collected by Le-Jia Zhang from around 0.5 to 1 metres depth in the north shore of Lake Cibi in Augest 2018, 2 specimens in ZMB, collected by Jiao-Wei Ning from around 1 to 2 metres depth in Lake Haixihai; 17 specimens in NJW, collected by Jiao-Wei Ning from around 1 to 2 metres depth in Lake Cibi.

Description. Shell (Fig. 3A–H) large, conical, thin, greenish yellow to dark olive in colour; up to six whorls at adulthood, including one relatively smooth protoconch whorl, apex acute, spire high; each teleoconch whorls with one strong keel at suture, above suture smooth or with many weak spiral threads, sometimes with additional two to three stronger cords, base of shell with many thin weak spiral threads, weak spiral cords and threads with short periostracal hairs; aperture ovate, less than half of shell in height, lip thin and simple, umbilicus narrow, sometimes bordered by a keel.

Operculum (Fig. 3I) corneous, ovate, rather thin, yellow, with reddish brown nuclear region, exterior surface of operculum rather smooth, inner opercular region relatively small, nuclear region smooth.

Radular (Fig. 7A, B) central tooth with one broad central denticle and with four small sharp cusps on either side; lateral tooth with one broad central denticle and four small sharp cusps on either side; inner marginal tooth with one broad central denticle and three small sharp cusps on either side; outer marginal tooth with 10 to 11 small sharp cusps.

Remarks. This species differs from the other *Dalipaludina* species by having a larger shell with a higher spiral. It may be difficult to distinguish from the smooth form of *Dalipaludina oxytropoides* from Lake Lugu based on morphology. However, this species is not recorded from Lake Lugu, and can be distinguished from *D. oxytropoides* based on differences in COI gene sequences. The recommended Chinese name of this species is "德拉维理田螺".

Habitat and distribution. shallow water area with sandy and muddy bottoms in Erhai, Cibi and Haixihai, Yunnan, China.

Dalipaludina oxytropoides (Heude, 1889), comb. nov.

Paludina oxytropoides Heude, 1889: 176 ('lacu prope Tchao-tong' = lake near Zhaotong City,Yunnan Province, China).
Vivipara oxytropoides – Kobelt 1909: 128.
Margarya sp. – Du et al. 2012: 45.
Margarya oxytropoides – Zhang et al. 2015: 777; Wiese et al. 2022.

Material examined. 2 ***syntypes***, IZCAS-FG-492586, IZCAS-FG-492587; 1 ***paratype***, MCZ-Mala-167343; 91 specimens in ZMB, collected by Frank Riedel from around 1 to 6 metres depth in all over the Lake Lugu in September and October 2014; 5 specimens in ZMB, collected by Le-Jia Zhang from 1 metre depth in the east shore of Lake Lugu in April 2022.

Description. Shell (Fig. 4A–H) large, conical, thin, greenish yellow to dark brown in colour; up to six whorls at adulthood, including one relatively smooth protoconch whorl, apex acute; each teleoconch whorls with one strong keel at suture, above suture with many rather weak spiral threads, sometimes with additional two to three strong cords, base of shell with many thin weak spiral threads, weak spiral cords and threads with short periostracum setae; aperture ovate, less than half of shell in height, lip thin and simple, umbilicus narrow, sometimes bordered by a keel.

Operculum (Fig. 4I) corneous, ovate, thin to relatively thick, yellow to reddish brown, with darker coloured nuclear region, exterior surface of operculum rather smooth, inner opercular region relatively small, nuclear region smooth or with small grains.

Radular (Fig. 7C, D) central tooth with one broad central denticle and three to four small sharp cusps on either side; lateral tooth with one broad central denticle and three to four small sharp cusps on either side; inner marginal tooth with one broad central denticle and four small sharp cusps on either side; each outer marginal tooth with 10 to 11 small sharp cusps.

Remarks. This species has the most variable shell within *Dalipaludina*. The form with strong cords of this species can be easily distinguished from the other *Dalipaludina* species. It used to be considered as a species of *Margarya* with a distribution in Lake Dianchi as well (Zhang et al. 2015). However, the COI-based phylogeny showed that "*Margarya oxytropides*" from Dianchi is not a species of *Dalipaludina*, but indeed a member of the *Cipangopaludina*/*Margarya* complex. The syntypes of *Paludina oxytropoides* Heude, 1889 from Zhaotong in Northeast Yunnan show a strong keel at the suture, two strong keels above the suture, a relatively smooth shell base with many weak spiral keels, and a narrow umbilicus with a keel around it. It is distinct from the "*Margarya oxytropides*" from Lake Dianchi but quite similar to the strongly keeled form of *D. oxytropoides* from Lake Lugu. Meanwhile, the shell morphology of "*Margarya oxytropides*" from Lake Dianchi matches the description and figure of *Cipangopaludina dianchiensis* Zhang, 1990 endemic to Lake Dianchi (Zhang 1990). Therefore, instead of *D. oxytropoides*, "*Margarya oxytropides*" from Lake Dianchi is here recognised as *Margarya dianchiensis* (Zhang, 1990) comb. nov. *Paludina oxytropoides* Heude, 1889 is reclassified as a member of *Dalipaludina*. The recommended Chinese name of this species is "尖龙骨理田螺".

Habitat and distribution. shallow to medium-depth water area with sandy bottoms in Lake Lugu, Yunnan/Sichuan, China; lakes in Zhaotong, Yunnan, China.

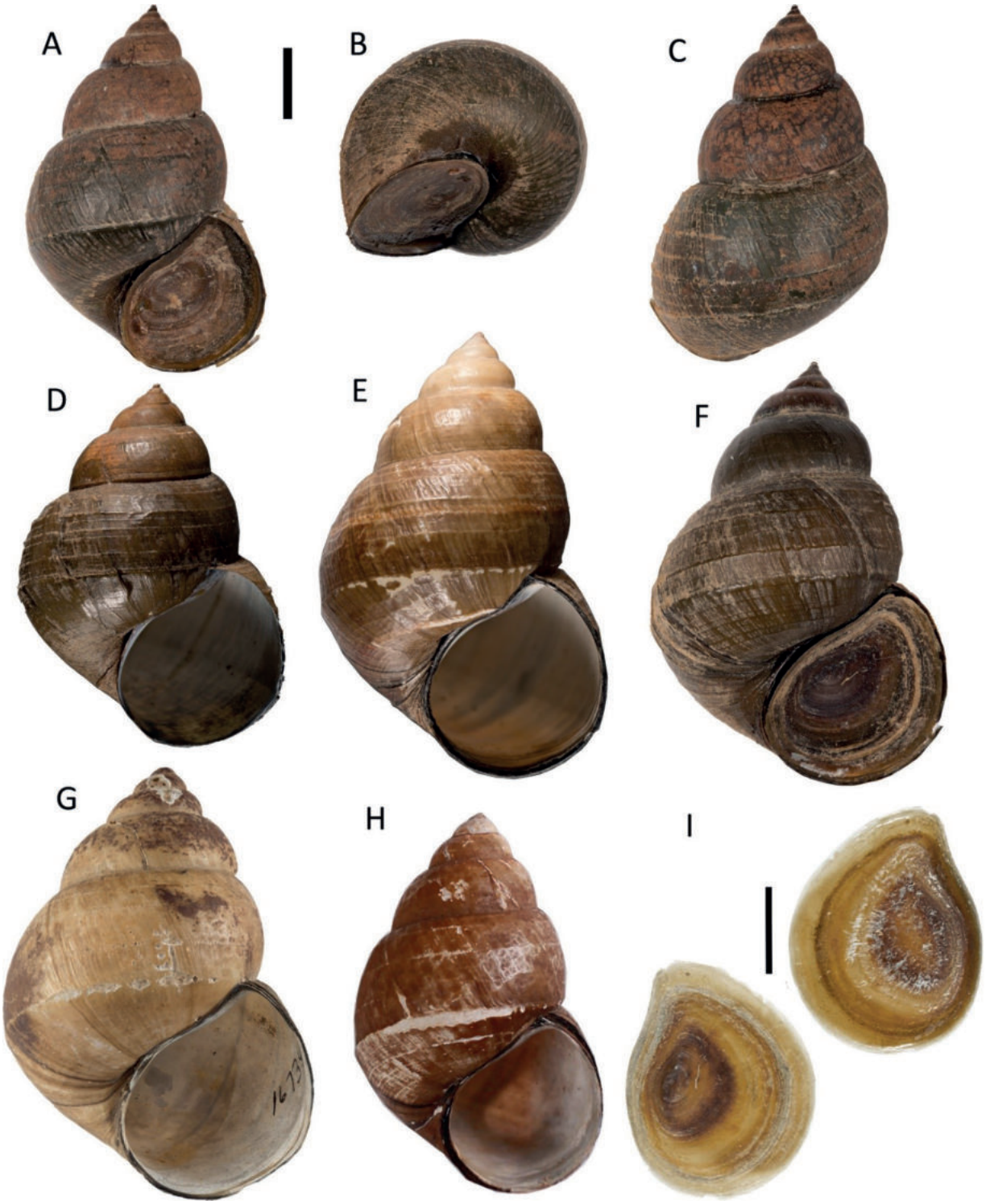

Figure 3. Shell and operculum of *Dalipaludina delavayana*. **A–C.** Specimen collected from Lake Cibi, ZMB Moll. 122707; **D, E.** Varieties collected from Lake Cibi, ZMB Moll. 122707; **F.** specimen collected from Lake Haixihai,LJZ; **G.** Paratype MCZ-Mala-167342, photo taken by Alana Rivera, Museum of Comparative Zoology, Harvard University, President and Fellows of Harvard College; **H.** Syntype IZCAS-FG-492554, photo taken by Kaibaryer Meng, Institute of Zoology, Chinese Academy of Sciences; **I.** Exterior (left) and interior (right) surface of operculum. Scale bar: 1 cm, **B–H** with the same scale bar of **A**.

Dalipaludina occidentalis (Annandale, 1924), comb. nov.

Lecythoconcha malleata f. *occidentalis* Annandale, 1924: 415 ("Ho-ching and Shihku", Heqing County and Shigu town, Lijiang City, Yunnan, China).

Viviparus occidentalis – Yen 1942.

Material examined. 8 specimens in ZMB, collected by local fishermen from 3 to 5 metres depth in the south shore of Lake Jianhu. February 2020; 4 specimens in

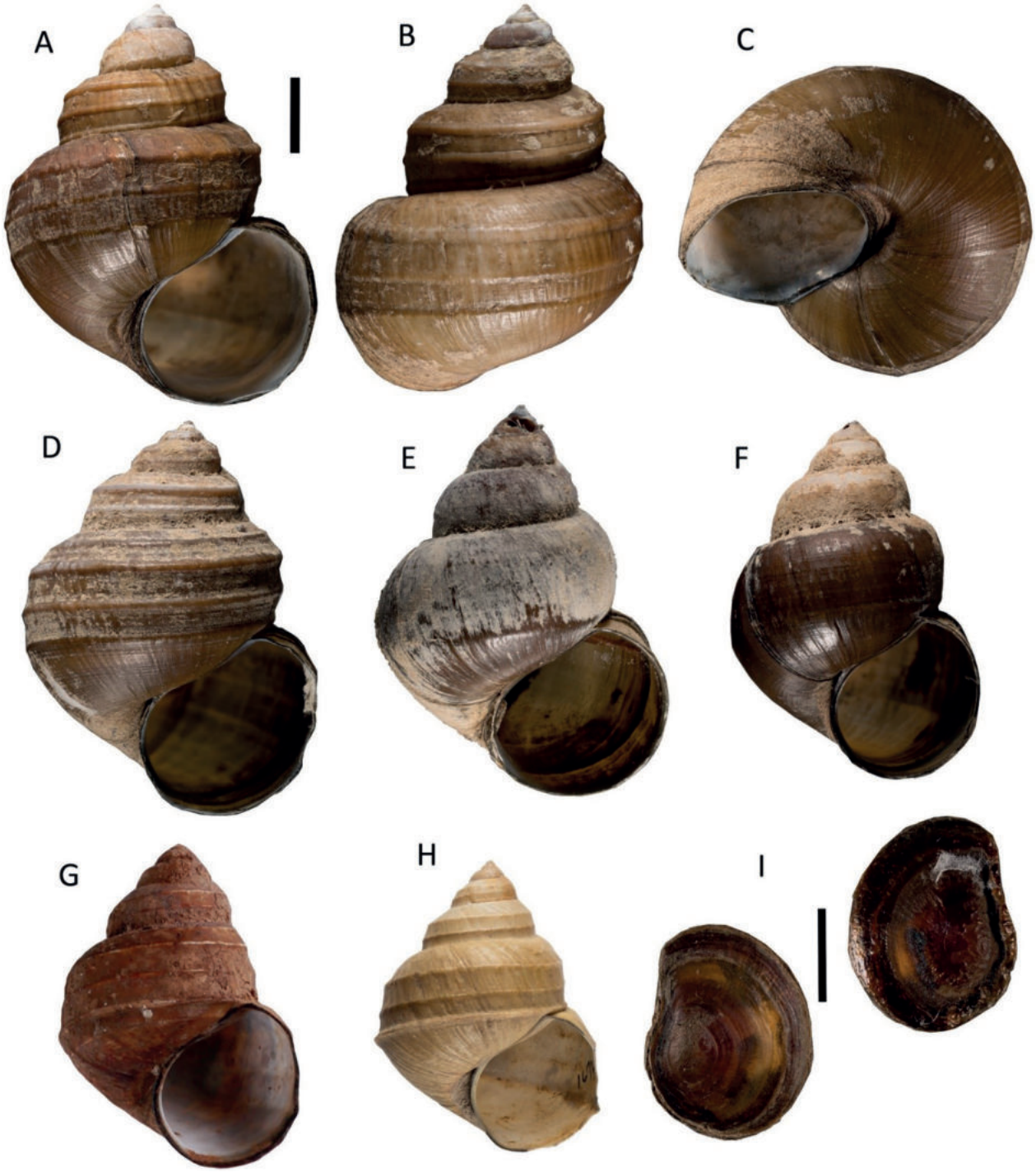

Figure 4. Shell and operculum of *Dalipaludina oxytropoides*. **A–C.** Specimen collected from Lake Lugu, ZMB.Moll. 250844; **D–F.** Varieties collected from Lake Lugu,ZLJ; **G.** Syntype IZCAS-FG-492587 from a lake in Zhaotong, Yunann, photo taken by Kaibaryer Meng, Institute of Zoology, Chinese Academy of Sciences; **H.** Paratype MCZ-Mala-167343 from a lake in Zhaotong, Yunann, photo taken by Alana Rivera, Museum of Comparative Zoology, Harvard University, President and Fellows of Harvard College; **I.** Exterior (left) and interior (right) surface of operculum. Scale bar: 1 cm, **B–F, H–I** with the same scale bar of **A**.

ZMB, collected by Le-Jia Zhang from 0.5 metres depth in an unnamed pond on the Sheshan hill in Lijiang City in April 2022; 19 specimens in NJW, collected by Jiao-Wei Ning from Lake Jianhu.

Description. Shell (Fig. 5A–G) large, broadly conical or sub globose, thin, olive to dark brown in colour; up to six whorls at adulthood, including one relatively smooth protoconch whorl, apex acute; teleoconch whorls inflated, occasionally shouldered, with one strong keel at suture, above suture with many weak spiral threads, sometimes with additional two to three stronger cords, base of shell with many thin weak spiral threads, weak spiral threads and cords with short periostracum setae; aperture ovate, slightly less than half of shell in height,

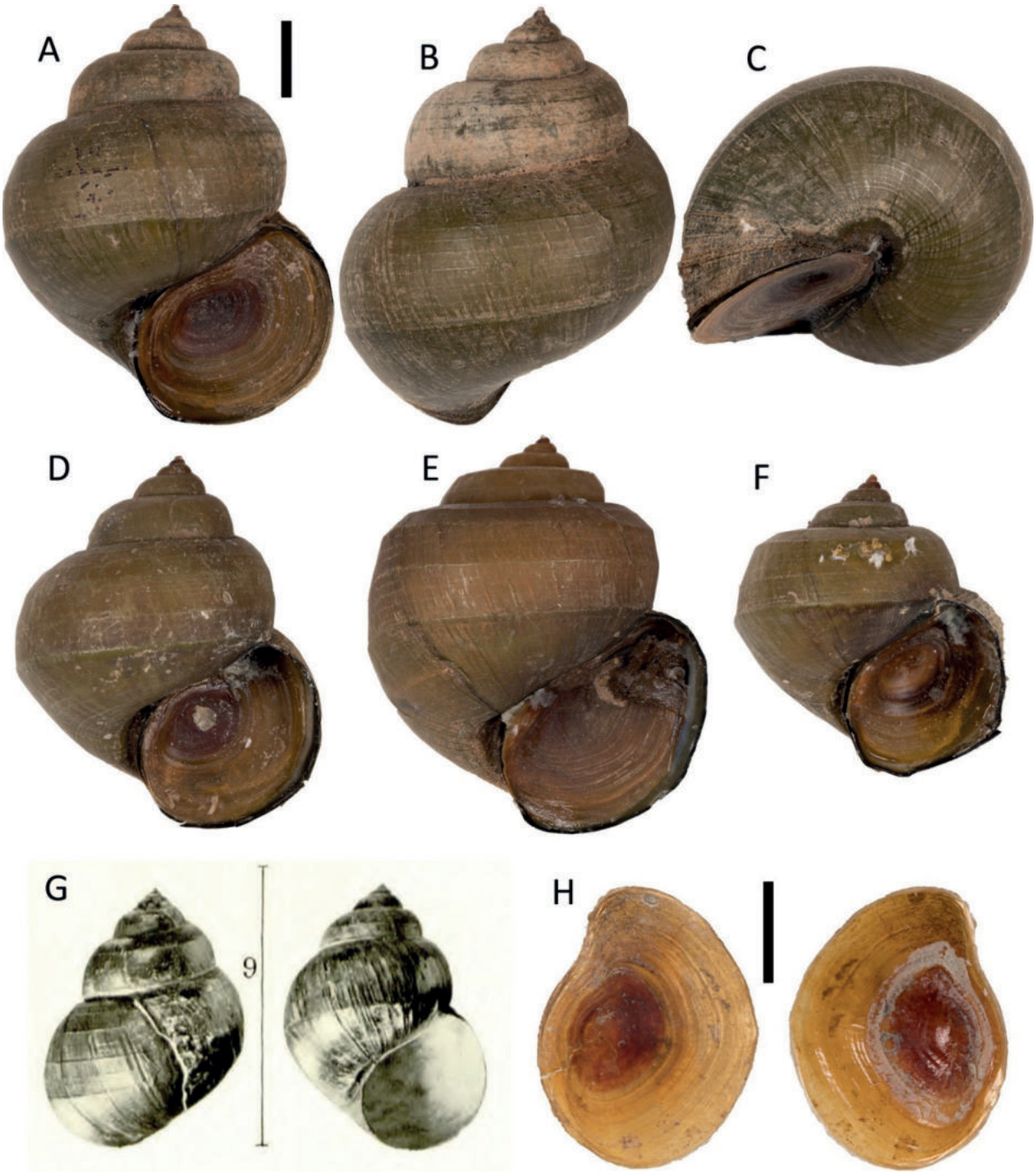

Figure 5. Shell and operculum of *Dalipaludina occidentalis*. **A–C.** Specimen collected from Lake Jianhu, ZMB.Moll. 122712; **D, E.** Varieties collected from Lake Jianhu, ZMB.Moll. 122713; **F.** Sub-adult collected from Lake Jianhu, ZMB.Moll. 122713; **G.** Original figure of the type specimen in Annandale, 1922; **H.** Exterior (left) and interior (right) surface of operculum. Scale bar: 1 cm, **B–F** with the same scale bar of **A**.

lip thin and simple, umbilicus narrow, sometimes bordered by akeel.

Operculum (Fig. 5H) corneous, ovate, rather thin, yellow, with red nuclear region, exterior surface of operculum rather smooth, inner opercular region relatively small, nuclear region smooth.

Radular (Fig. 7E, F) central tooth with one broad central denticle and four small sharp cusps on either side; lateral tooth with one broad central denticle and four small sharp cusps on either side; inner marginal tooth with one broad central denticle and four small sharp cusps on either side; outer marginal tooth with 9 to 10 small sharp cusps.

Remarks. This species differs from the other species of *Dalipaludina* by having rather inflated, shouldered whorls. Annandale (1924) presented a photo of the type specimen. The shell morphology and COI phylogeny of the speci-

mens collected from an unnamed pond in Lijiang City, which is very close to the type locality, confirm that this species should be assigned to *Dalipaludina*. The recommended Chinese name of this species is "滇西理田螺".

Habitat and distribution. Shallow ponds with muddy bottoms and abundant aquatic plants in Lijiang City, Yunnan, China; Shallow to medium-depth water area with muddy bottoms in Lake Jianhu, Jianchuan County, Yunnan, China.

Dalipaludina pyramidella (Du, Yang & Chen, 2011), comb. nov.

Trochotaia pyramidella Du, Yang & Chen, 2011: 85–89 (Yousuo village of Er-Yuan County, Yunnan, China).

Material examined. ***Holotype***, KIZ-DLN20100035; 19 ***paratypes***, KIZ-DLN20100036 to KIZ-DLN20100054; 3 specimens in ZMB, 7 specimens in NJW, collected by Jiao-Wei Ning from 1 metre depth in the ponds of Yousuo Village, Eryuan County.

Description. Shell (Fig. 6A–D) large, conical, thin, greenish brown to brown in colour; up to six whorls at adulthood, including one relatively smooth protoconch whorl, apex acute, spire low; each teleoconch whorls with one strong keel at suture, above suture smooth, with two rings of short periostracum setae, base of shell smooth, with many rather thin weak spiral threads; aperture ovate, almost half of shell in height, lip thin and simple, umbilicus narrow, sometimes bordered by a keel.

Operculum (Fig. 6E) corneous, ovate, rather thin, yellow or orange, with red nuclear region, exterior surface of operculum rather smooth, inner opercular region relatively small, nuclear region smooth.

Radular (according to Du et al. 2011) central tooth with one broad central denticle and three to four small sharp cusps on either side; lateral tooth with one broad central denticle and four small sharp cusps on either; inner marginal tooth with one broad central denticle and two small sharp cusps on either side; outer marginal tooth with 9 small sharp cusps.

Remarks. This species differs from the other species of *Dalipaludina* by having a relatively smooth shell with lower spire. Du et al. (2011) assigned this species to *Trochotaia* mainly based on the strongly keeled shell with lower spire. However, characters of the operculum, embryonic shells, the reduced number of cusps on the outer marginal teeth (9 in *D. pyramidella* vs 14–16 in *Trochotaia trochoides*) and the distribution in Yunnan strongly support its assignment to *Dalipaludina*. Species of *Trochotaia* have a very different operculum according to Zhang and von Rintelen (2021). This species is also quite similar to *Cipangopaludina miyagii* Kuroda, 1941 endemic to Kaohsiung, S Taiwan, China. It can be distinguished from *C. miyagii* by having a thinner shell, a shell base with many rather thin weak spiral threads, and a narrowly open umbilicus with a keel around it. The recommended Chinese name of this species is "塔形理田螺".

Habitat and distribution. shallow ponds with muddy bottoms and aquatic plant *Ottelia acuminata* (Gagnep.) in Yousuo Village, Eryuan County, Yunnan, China.

Discussion

The molecular and morphological data strongly support that four endemic viviparid species from Yunnan, formerly classified as species of *Cipangopaludina*, *Sinotaia*, *Margarya* or *Trochotaia*, should be assigned to a new genus described here: *Dalipaludina*. The former genus-level classification of these species was primarily based on shell morphology (Du et al. 2011; Qian et al. 2014). However, the shell morphology of freshwater snails can be quite similar due to convergence even between different genera. One remarkable example is the case of three highly sculptured but phylogenetically distinct viviparid genera (*Margarya*, *Tchangmargarya* and *Anularya*) endemic to the plateau lakes of Yunnan (Zhang et al. 2015). Our study has confirmed once again the importance of using an integrative approach in generic classification. In additional to shell characters, the operculum and radula, especially the cusps on the outer marginal teeth, provide important data for genus-level taxonomy of Viviparidae as well. The species-level phylogeny solely based on COI has been considered problematic in Viviparidae (Hirano et al. 2019b). However, at the genus level, it does not seem to be a big problem here (Fig. 2). Our BI tree based on partial COI sequences is broadly consistent with the genus-level topology for the Bellamyinae derived from an analysis of multiple genes in Stelbrink et al. (2020), suggesting that *Dalipaludina* likely falls into clade A of Bellamyinae proposed by Stelbrink et al. (2020).

Four species of *Dalipaludina* can be differentiated based on shell morphology. The scatter plot (Fig. 8) shows that *D. delavayana* has a larger and taller shell; *D. pyramidella* and *D. occidentalis* both have a lower spire, and *D. pyramidella* can be distinguished from *D. occidentalis* based on its less inflated whorls and comparatively smooth shell surface. The COI phylogeny has supported the reciprocal monophyly of the three sequenced species. The populations of *D. occidentalis* from two localities roughly 50 km apart cluster togther in the tree, without obvious geographic structuring (Fig. 2). The keeled, shouldered form of *D. occidentalis* (Fig. 5E) cannot be differentiated from the smooth form based on p-distance or phylogeny of COI as well. Moreover, the four species of *Dalipaludina* have allopatric distributions (Fig. 1B), and we have yet to find any lake or pond with more than one *Dalipaludina* species. Based on these results derived from morphological, molecular, and distribution data, we believe that there are four valid species of *Dalipaludina*.

Intraspecific diversity of shell morphology varies among the four species. *Dalipaludina delavayana* and *D. pyramidella* both display a relatively low intraspecific diversity; morphological diversity within *D. occidentalis* is higher; and that of *D. oxytropoides* is by far the

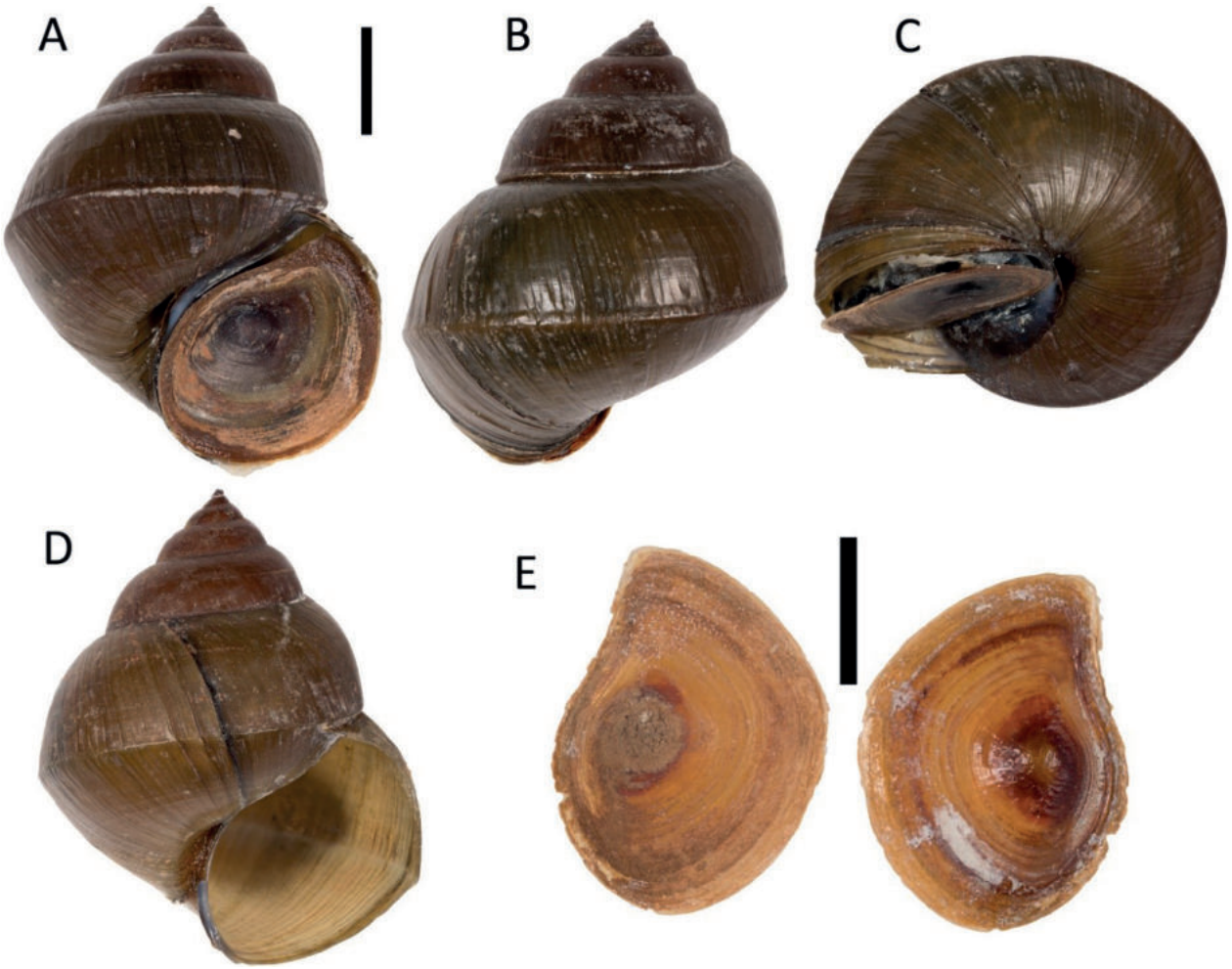

Figure 6. Shell and operculum of *Dalipaludina pyramidella.* **A–C.** Specimen collected from Eryuan County, ZMB.Moll. 122714; **D.** Varieties collected from Eryuan County, ZMB Moll. 122714; **E.** Exterior (left) and interior (right) surface of operculum. Scale bar: 1 cm, **B–D** with the same scale bar of **A**.

highest within the genus. An integrative study combining morphometrics and a COI phylogeny of *D. oxytropoides* from Lake Lugu ("*Margarya oxytropoides*" in Wiese et al. 2022) showed that it should be considered a single, but highly variable species. We have also observed many intermediate forms in this species.

In contrast to the other three endemic genera of Viviparidae from Yunnan (*Margarya*, *Tchangmargarya* and *Anularya*) mostly found in medium-depth to deep water (Zhang et al. 2015), *Dalipaludina* displays a preference for shallow water. In addition to large lakes like Lake Lugu or Jianhu, *Dalipaludina* also can be found in small shallow ponds, such as the artificial ponds for farming the aquatic vegetable *Ottelia acuminata* in Eryuan County (*D. pyramidella*) and an unnamed small pond on the top of Sheshan Hill in Lijiang (*D. occidentalis*). *D. oxytropoides* and *D. delavayana* are also more common in shallow water areas than in deeper water. However, *Dalipaludina* is only found in lentic environments. It has never been found in rivers or any other lotic environment.

The lowest altitude where we have found *Dalipaludina* species is in Eryuan County, around 1974 m a.s.l., and one historical record of *D. oxytropoides* in Zhaotong County from ~1920 m a.s.l. (Heude 1886); Lake Lugu harbouring *D. oxytropoides* is ~2698 m a.s.l., which is the highest altitude record of Viviparidae (Fig. 1B). Among the other three viviparid genera endemic to Yunnan Plateau, only *Margarya* is found within a similar but smaller altitudinal range (1886–2192 m a.s.l), while *Tchangmargarya* (1770–1907 m a.s.l.) and *Anularya* (1284–1721 m a.s.l.) inhabit a relatively lower altitude with no overlap with that of *Dalipaludina*. Viviparids from elsewhere in the world occur at much lower altitudes. In conclusion, *Dalipaludina* displays an adaptation to the shallow lentic environment in high altitude regions, and occurs at the highest altitude of any viviparid.

With the discovery of the new genus *Dalipaludina*, the Yunnan Plateau now harbours four endemic genera of Viviparidae, confirming again that it is the most important diversity hotspot of Viviparidae in the world. However, almost all of these species are threatened by human activities such as overharvesting, pollution, and habitat destruction (Yang et al. 2004; Zhang et al. 2015). *D. pyramidella* nearly disappeared from its only known site, the ponds in Eryuan County, during our recent surveys in 2021; the present population of *D. oxytropoides*

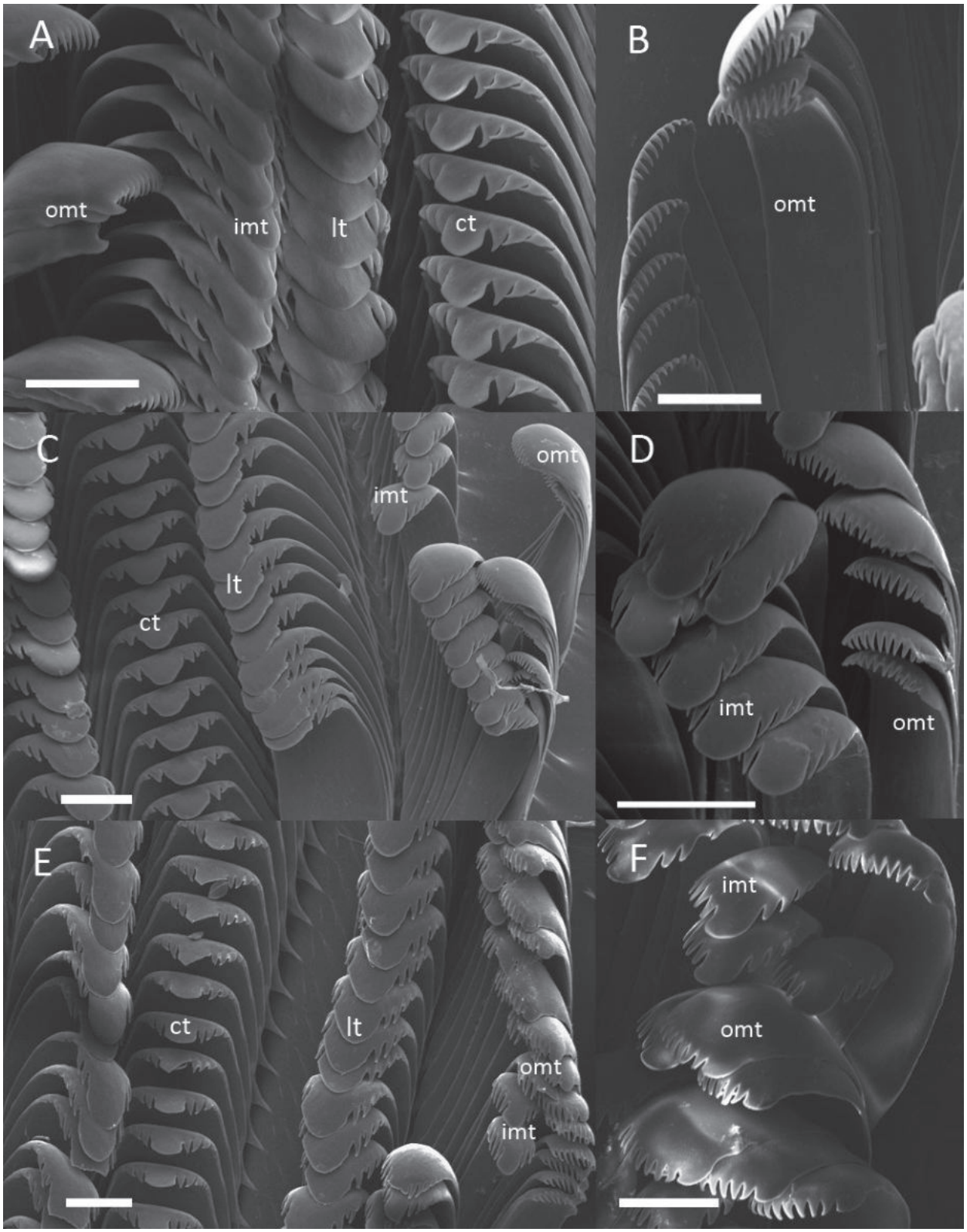

Figure 7. SEM photo of the radula and the protoconch of *Dalipaludina* species. **A, B.** Radula of *Dalipaludina delavayana*, A-ZMB. Moll. 181719, B-ZMB.Moll. 122707; **C, D.** Radula of *Dalipaludina oxytropoides*, ZMB.Moll. 250844; **E, F.** Radula of *Dalipaludina occidentalis*, ZMB.Moll. 122713. Abbreviations: ct–central teeth; lt–lateral teeth; imt–inner marginal teeth; omt–outer marginal teeth. Scale bars: 100 μm.

in Lake Lugu has declined dramatically compared to that in the 1990s according to local fishermen. Most endemic viviparid species of *Margarya*, *Tchangmargarya* and *Anulary*a are on the national Red List of China (Wang and Xie 2005), and one species *Margarya melanioides* Nevill, 1877 is a Class 2 species under state protection in the

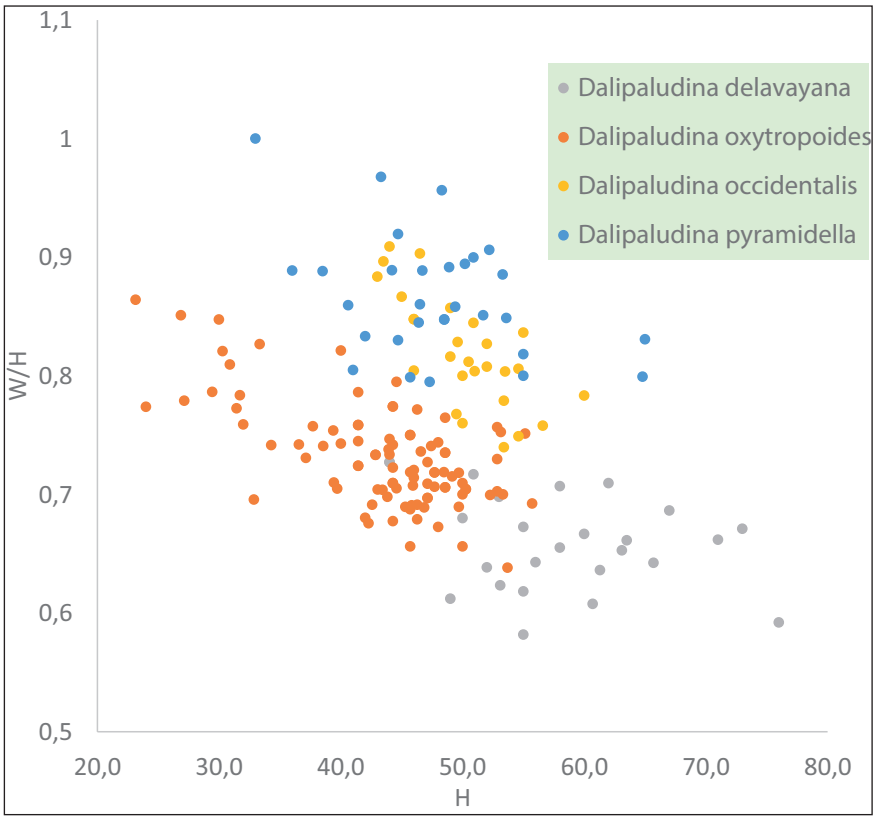

Figure 8. Comparison of *Dalipaludina* species with respect to parameters H (in mm) and W/H.

latest List of State Key Protected Wild Animals of China in 2021. Since all four *Dalipaludina* species are restricted to just one or two lakes or several small ponds, specific conservation measures should be applied urgently for each species based on more detailed population biology and ecology studies. The phylogeny based on genomic data, such as data from exon capture method, can also improve our understanding of the evolution of these rare species endemic to the plateau lentic environment.

Acknowledgments

The authors thank Jiao-Wei Ning from Yuxi, Yunnan and Hong-Quan Xiang (Yuxi Agriculture Agricultural Technology College) for collecting specimens, Bernhard Schurian (Museum für Naturkunde, Berlin) for help with photography, Kaibaryer Meng (Institute of Zoology, Chinese Academy of Sciences, Beijing), Adam Baldinger and Alana Rivera (Museum of Comparative Zoology at Harvard University, Cambridge) for providing the important type specimens for study.

References

Annandale TN (1924) Zoological results of the Percy Sladen Trust Expedition to Yunnan under the leadership of Professor J.W. Gregory, F.R.S., 1922. Aquatic gastropod molluscs. Journal and Proceedings of the Asiatic Society of Bengal, New Series 19(9): 399–422.

Du LN, Yang JX, Chen X (2011) A new species of *Trochotaia* (Caenogastropoda: Viviparidae) from Yunnan, China. Molluscan Research 31(2): 85. https://doi.org/10.1002/zoos.201000012

Du LN, Chen XY, Yang JX, Aldridge DC (2012) A survey of Molluscan compositions in four plateau lakes, Northwest Yunnan [In Chinese]. China. Journal of Hydroecology 33: 44–49.

Heude PM (1886) Notes sur les mollusques terrestres de la vallée du fleuve Bleu. Mémoires Concernant l'Histoire Naturelle de l'Empire Chinois 1: 1–188.

Hirano T, Saito T, Tsunamoto Y, Koseki J, Prozorova L, Do VT, Matsuoka K, Nakai K, Suyama Y, Chiba S (2019a) Role of ancient lakes in genetic and phenotypic diversification of freshwater snails. Molecular Ecology 28(23): 5032–5051. https://doi.org/10.1111/mec.15272

Hirano T, Saito T, Tsunamoto Y, Koseki J, Ye B, Do VT, Miura O, Suyama Y, Chiba S (2019b) Enigmatic incongruence between mtDNA and nDNA revealed by multi-locus phylogenomic analyses in freshwater snails. Scientific Reports 9(1): e6223. https://doi.org/10.1038/s41598-019-42682-0

Kobelt W (1909) Systematisches Conchylien-Cabinet von Martini und Chemnitz. Die Raublungenschnecken (Agnatha). Zweite Abtheilung: Streptaxidae und Daudebardiidae. Bauer & Raspe, Nuremberg, 128 pp.

Kumar S, Stecher G, Li M, Knyaz C, Tamura K (2018) MEGA X: molecular evolutionary genetics analysis across computing platforms. Molecular Biology and Evolution 35(6): 1547–1549. https://doi.org/10.1093/molbev/msy096

Liu YY, Zhang WZ, Wang YX (1995) Distribution of the Viviparidae from China (Mollusk: Gastropoda) [In Chinese].Transactions of the Chinese Society of Malacology 5–6: 8–16.

Qian ZX, Fang YF, He J (2014) A conchological review of Bellamyinae (Gastropoda: Viviparidae) of China. Shell Discoveries 1(3): 3–12.

Ronquist F, Teslenko M, van der Mark P, Ayres DL, Darling A, Höhna S, Larget B, Liu L, Suchard MA, Huelsenbeck JP (2012) MrBayes 3.2: Efficient Bayesian phylogenetic inference and model choice across a large model space. Systematic Biology 61(3): 539–542. https://doi.org/10.1093/sysbio/sys029

Schultheiß R, Wilke T, Jørgensen A, Albrecht C (2011) The birth of an endemic species flock: Demographic history of the Bellamya group (Gastropoda, Viviparidae) in Lake Malawi. Biological Journal of the Linnean Society 102(1): 130–143. https://doi.org/10.1111/j.1095-8312.2010.01574.x

Stelbrink B, Richter R, Köhler F, Strong EE, van Bocxlaer B, Albrecht C, Hauffe T, Page TJ, Aldridge DC, Bogan AE, Du LN, Manuel-Santos MR, Marwoto RM, Shirokaya AA, von Rintelen T (2020) Global diversification dynamics since the Jurassic: Low dispersal and habitat-dependent evolution explain hotspots of diversity and shell disparity in river snails (Viviparidae). Systematic Biology 69(5): 944–961. https://doi.org/10.1093/sysbio/syaa011

Van Bocxlaer B, Strong EE (2019) Viviparidae Gray, 1847. In: Lydeard C, Cummings KS (Eds) Freshwater Mollusks of the World: A Distribution Atlas. Johns Hopkins University Press, Baltimore, 43–50.

Van Bocxlaer B, Strong EE, Richter R, Stelbrink B, Von Rintelen T (2017) Anatomical and genetic data reveal that Rivularia Heude, 1890 belongs to Viviparinae (Gastropoda: Viviparidae). Zoological Journal of the Linnean Society 182(1): 1–23. https://doi.org/10.1093/zoolinnean/zlx014

Wang S, Xie Y (2005) China Species Red List (Vol. III). Invertebrates. Higher Education Press, Beijing, 299–306.

Wiese R, Harrington K, Hartmann K, Hethke M, von Rintelen T, Zhang HC, Zhang LJ, Riedel F (2022) Can fractal dimensions objectivize gastropod shell morphometrics? A case study from Lake Lugu (SW China). Ecology and Evolution 12(3): e8622. https://doi.org/10.1002/ece3.8622

Winnepenninckx B, Backeljau T, De Wachter R (1993) Extraction of high molecular weight DNA from molluscs. Trends in Genetics 9(12): e407. https://doi.org/10.1016/0168-9525(93)90102-N

Yang Y, Tian K, Hao J, Pei S, Yang Y (2004) Biodiversity and biodiversity conservation in Yunnan, China. Biodiversity and Conservation 13(4): 813–826. https://doi.org/10.1023/B:BIOC.0000011728.46362.3c

Yen TC (1942) A review of Chinese gastropods in the British Museum. The Journal of Molluscan Studies 24(5–6): 170–289.

Zhang L (1990) A new species of genus Cipangopaludina from Dianchi Lake in Yunnan Province, China. Acta Zootaxonomica Sinica 15(1): 25–27. [In Chinese]

Zhang LJ (2017) A new species of freshwater snail *Tchangmargarya* (Gastropoda: Viviparidae) endemic to a vanished small lake in Yunnan, China. Molluscan Research 37(4): 252–257. https://doi.org/10.1080/13235818.2017.1323369

Zhang LJ, von Rintelen T (2021) The neglected operculum: a revision of the opercular characters in river snails (Caenogastropoda: Viviparidae). Journal of Molluscan Studies 87(2): eyab008. https://doi.org/10.1093/mollus/eyab008

Zhang NG, Hao TX, Wu CY, Chen YX, Zhang W, Li JK, Zhang Y (1997) Primary investigation of freshwater Gastropoda in Yunnan Province. Studia Marina Sinica 39(2): 15–26. [In Chinese]

Zhang LJ, Chen SC, Yang LT, Jin L, Köhler F (2015) Systematic revision of the freshwater snail *Margarya* Nevill, 1877 (Mollusca: Viviparidae) endemic to the ancient lakes of Yunnan, China, with description of new taxa. Zoological Journal of the Linnean Society 174(4): 760–800. https://doi.org/10.1111/zoj.12260

Supplementary material 1

Accession numbers and museum voucher numbers

Authors: Le-Jia Zhang, Li-Na Du, Thomas von Rintelen

Data type: table (excel document)

Link: https://doi.org/10.3897/zse.99.102586.suppl1

Zoosyst. Evol. 99 (2) 2023, 299–305 | DOI 10.3897/zse.99.103893

PENSOFT

für Natur MUSEUM FÜR NATURKUNDE BERLIN

A new species of *Anatextrix* Kaya, Zamani, Yağmur & Marusik, 2023 (Araneae, Agelenidae, Textricini) from southern Türkiye, with a remarkable morphology of the male palpal femur

Rahşen S. Kaya[1], Alireza Zamani[2], Ersen Aydın Yağmur[3], Yuri M. Marusik[4,5]

1 *Department of Biology, Faculty of Arts and Science, Bursa Uludağ University, TR-16059, Bursa, Turkiye*
2 *Zoological Museum, Biodiversity Unit, FI-20014 University of Turku, Turku, Finland*
3 *Alaşehir Vocational School, Manisa Celal Bayar University, Manisa, Turkiye*
4 *Department of Zoology & Entomology, University of the Free State, Bloemfontein 9300, South Africa*
5 *Altai State University, Lenina Pr., 61, Barnaul, RF-656049, Russia*

https://zoobank.org/07CC7326-D124-47B8-9341-2BB7501AE86B

Corresponding author: Rahşen S. Kaya (rkaya@uludag.edu.tr; rahsens@gmail.com)

Academic editor: Danilo Harms ♦ **Received** 22 March 2023 ♦ **Accepted** 16 May 2023 ♦ **Published** 25 May 2023

Abstract

Anatextrix monstrabilis **sp. nov.** (Araneae: Agelenidae) is described and illustrated, based on male and female specimens collected from Adana Province, Türkiye. The new species has an L-shaped male palpal femur bearing multiple apophyses, which is a rare trait in spiders. *Anatextrix monstrabilis* **sp. nov.** is the second species of the recently described genus *Anatextrix* Kaya, Zamani, Yağmur & Marusik, 2023, currently known only from southern Türkiye.

Key Words

Adana, Ageleninae, Anatolia, Aranei, Mediterranean Region

Introduction

The funnel-weaver spider family Agelenidae C.L. Koch, 1837 is one of the most diverse families of spiders, currently comprising 93 genera and 1375 extant species in the subfamilies Ageleninae C.L. Koch, 1837 and Coelotinae F.O. Pickard-Cambridge, 1893 (Lehtinen 1967; WSC 2023). According to Lehtinen (1967), Ageleninae is subdivided into four tribes, including Textricini Lehtinen, 1967 which comprises four genera and more than 30 species primarily distributed in the Mediterranean Region. *Anatextrix* Kaya, Zamani, Yağmur & Marusik, 2023 — the most recently described genus of Textricini — is currently known only from southern Türkiye, a region with a high degree of endemism and a particularly high diversity of agelenids (Kaya et al. 2023).

Anatextrix was described by Kaya et al. (2023), with *A. spectabilis* Kaya, Zamani, Yağmur & Marusik, 2023 (from Mersin and Adana provinces of Türkiye) as its type species. The genus is characterised by a strongly modified male palpal femur bearing several processes/outgrowths, palpal patellar apophysis and a cymbial prolateral fold in males, and a thin septum and a lack of fovea or scape in females.

We recently found specimens of another species of this genus amongst the material collected in southern Türkiye. The new species displays a remarkable morphology of the male palpal femur and represents the second species of *Anatextrix*.

Materials and methods

Specimens were collected using a hand aspirator and preserved in 70% ethanol. Photographs were taken by a Canon EOS 7D camera attached to an Olympus SZX16 stereomicroscope at the Zoological Museum of the University of Turku. Digital images were montaged using Combine ZP and edited using CorelDraw graphic design software programme. Illustrations of internal genitalia were made after clearing and cleaning the epigyne in a 10% potassium hydroxide (KOH) aqueous solution, followed by a few minutes of treatment in Chlorazol Black. Lengths of leg segments were measured on the dorsal side and are listed as: total length (femur, patella, tibia, metatarsus, tarsus). All measurements are in millimetres (mm). Spination formula follows Bolzern et al. (2008, 2009).

The following abbreviations are used in the text and figures:

Eyes: **ALE** – anterior lateral eye, **AME** – anterior median eye, **PLE** – posterior lateral eye, **PME** – posterior median eye. Spination**: d** – dorsal, **Fe** – femur, **Mt** – metatarsus, **Pa** – patella, **pl** – prolateral, **rl** – retrolateral, **Ti** – tibia, **v** – ventral.

Male palp: ***Ca*** – anterior arm of conductor, ***Cf*** – cymbial fold, ***Cp*** – posterior arm of conductor, ***Ct*** – ventral tip of conductor, ***Db*** – distal bulge, ***Dc*** – dorsal extension of conductor, ***Eb*** – base of embolus, ***Kt*** – ventral keel, ***Pb*** – proximal bulge, ***Pt*** – prolateral apophysis, ***Rt*** – retrolateral apophysis, ***So*** – stump-like outgrowth, ***Sp*** – spine-like outgrowth, ***Va*** – ventral apophysis.

Epigyne: ***Cd*** – copulatory duct, ***Fd*** – fertilisation duct, ***Oc*** – copulatory opening, ***Re*** – receptacle, ***Se*** – septum.

The specimens are deposited in the following collections:

AZMM Alaşehir Zoological Museum of Manisa Celal Bayar University, Türkiye (E.A. Yağmur);
ZMUT Zoological Museum of the University of Turku, Finland (V. Vahtera);
ZMUU Zoological Museum of the Bursa Uludağ University, Türkiye (R.S. Kaya).

Results

Taxonomy

Family Agelenidae C.L. Koch, 1837
Subfamily Ageleninae C.L. Koch, 1837
Tribe Textricini Lehtinen, 1967

Genus *Anatextrix* Kaya, Zamani, Yağmur & Marusik, 2023

Type species. *Anatextrix spectabilis* Kaya, Zamani, Yağmur & Marusik, 2023 from southern Anatolia, by monotypy.

Emended diagnosis. The genus differs from all other genera of Textricini by having a strongly modified male palpal femur bent at the proximal or middle part with two digitiform outgrowths (*So* and *Sp*) and at least one proximal bulge (vs. not bent, with none or subdistal bulge), presence of the palpal prolateral tibial apophysis (*Pt*) and the cymbial baso-prolateral fold (*Cf*) (vs. lacking), straight mesal part of the embolic base *(Eb)* (vs. round) and a thin septum in the epigyne (vs. absent). Furthermore, the females of *Anatextrix* differ from those of *Textrix* Sundevall, 1833 by having no epigynal fovea and scape (vs. present). From the females of the two other genera of Textricini – *Maimuna* Lehtinen, 1967 and *Lycosoides* Lucas, 1846 – the females of *Anatextrix* differ by the anterior position of the receptacles (vs. mesal or posterior).

Composition. Two species: *A. spectabilis* and *A. monstrabilis* sp. nov.

Distribution. Southern Türkiye (Fig. 7).

***Anatextrix monstrabilis* sp. nov.**

https://zoobank.org/4EB359F3-3CFE-4016-BE35-97A91C6E8D85
Figs 1A, B, 2A–E, 3A–E, 4A–F, 5A–E

Type material. ***Holotype*** ♂ (ZMUU), Türkiye: Adana Province: Pozantı District, Akçatekir Village, 37°19'29"N, 34°46'33"E, 1336 m elev., 27.09.2018, hand collection (R.S. Kaya and E.A. Yağmur); Paratypes: 1♂2♀ (ZMUT), same data as for the holotype; 2♂2♀ (AZMM), same data as for the holotype; 10♂12♀ (ZMUU), same data as for the holotype.

Etymology. The specific epithet is derived from the Latin "*monstrabilis*", meaning "remarkable, excellent".

Diagnosis. The new species differs from the generotype, *A. spectabilis*, by having the male palpal femur bent at a right angle at the mesal part (vs. slightly bent at distal part), having no distal bulge (vs. present), a less protruding tip of the conductor (*Ct*) and a smaller dorsal extension of the conductor (*Dc*) (cf. Fig. 2A, F). The female of the new species differs from that of *A. spectabilis* by having diverging copulatory ducts (*Cd*) (vs. parallel; cf. Fig. 5A, F).

Description. Male (holotype). Habitus as in Fig. 1B. Total length 6.28. Carapace 3.17 long, 1.03 wide at pars cephalica, 2.18 wide at pars thoracica. Eye sizes: AME: 0.10, ALE: 0.14, PME: 0.20, PLE: 0.14. Carapace, sternum, labium and maxillae light brown; carapace with darker submedian bands. Chelicerae light reddish brown, with 3 pro- and 2 retromarginal teeth. Legs yellowish brown, with annulations. Abdomen dorsally dark greyish with lighter foliate pattern, light greyish ventrally. Spinnerets light greyish, darker basally. Measurements of legs: I: 7.04 (1.87, 0.88, 1.43, 1.74, 1.12), II: 7.06 (1.92, 0.89, 1.39, 1.78, 1.08), III: 7.09 (1.90, 0.85, 1.34, 1.90, 1.10), IV: 8.85 (2.25, 0.89, 1.78, 2.67, 1.26). Spination as shown in Table 1.

Palp as in Figs 2A–E, 3A–E, 4A–F; femur strongly modified, bent at right angle in mid-part, with proximal

Figure 1. Female (**A**) and male (**B**) of *Anatextrix monstrabilis* sp. nov., dorsal view of the habitus.

bulge (*Pb*) and two digitiform outgrowths (*So* and *Sp*); patella with ventral apophysis (*Va*); tibial about as long as wide, with small retrolateral apophysis extended retrolaterally *(Rt)* and ventral keel (*Kt*); tip of conductor with three processes in lateral view (Fig. 2A, C).

Female (paratype, ZMUT). Habitus as in Fig. 1A. Total length 6.33. Carapace 3.02 long, 1.01 wide at pars cephalica, 1.80 wide at pars thoracica. Eye sizes: AME: 0.10, ALE: 0.13, PME: 0.21, PLE: 0.15. Colouration as in male. Measurements of legs: I: 6.00 (1.59, 0.76, 1.23, 1.49, 0.93), II: 5.89 (1.62, 0.80, 1.14, 1.44, 0.89), III: 6.15 (1.69, 0.79, 1.19, 1.52, 0.96), IV: 7.95 (2.07, 0.85, 1.68, 2.26, 1.09). Spination as shown in Table 1.

Epigyne as in Fig. 5A–E; septum (*Se*) well distinct in posterior part; copulatory ducts (*Cd*) subparallel posteriorly and diverging anteriorly; receptacles (*Re*) elongated, ca. 3 times longer than wide, located anteriorly.

Table 1. Leg spination of *Anatextrix monstrabilis* sp. nov. The letter "p" indicates paired spines.

		Fe	Pa	Ti	Mt
		d-pl-rl	d-pl-rl	d-pl-rl-v	pl-rl-v
I	♂	3-1-1	2-1-1	1-2-1-1+1p	2-1-3p
	♀	3-1-1	2-1-1	1-2-1-1+1p	2-1-3p
II	♂	3-1-1	2-1-1	1-2-0-2	2-1-3p
	♀	3-1-1	2-1-1	1-2-1-2+1p	2-1-3p
III	♂	3-1-1	2-1-1	1-2-1-2	3-3-3p
	♀	3-1-1	2-1-1	2-2-2-2+1p	3-3-3p
IV	♂	3-1-1	2-1-1	1-2-1-2+1p	3-2-3p
	♀	3-1-1	2-1-1	2-2-2-2+1p	3-3-3p

Natural history. The type locality of the new species is located in the Eastern Taurus Mountain range. This species inhabits montane forests dominated by Taurus fir (*Abies cilicica* Carr.). All examined specimens were collected from their funnel-webs constructed under the rocks, crevices in the soil and trunks of fallen trees, in rocky areas along the forest (Fig. 6B).

Distribution. Known only from the type locality in Adana Province, southern Türkiye (Fig. 7).

Discussion

This paper describes and illustrates a new species of *Anatextrix*, representing the second species of this recently-established genus, which is currently known only from southern Türkiye. It seems that the species of *Anatextrix* primarily occur in montane forests (Fig. 6A, B).

Both currently-known species of this genus have been collected in closely-situated localities in the Taurus Mountains, a biodiversity hotspot that separates the Mediterranean coastal region from the central Anatolian Plateau (Noroozi et al. 2019). A higher diversity of *Anatextrix* is expected in this region, as mountain complexes, such as the Taurus, form barriers that contribute to the separation of populations and speciation (Çıplak 2003). Anatolian Agelenids demonstrate a very high degree of endemism: most species have restricted, local distributions and occur at high altitudes in mountainous areas (Kaya et al. 2010). This pattern of distribution is an indication of the important role of topography in the faunal evolution in this region (Çıplak 2003).

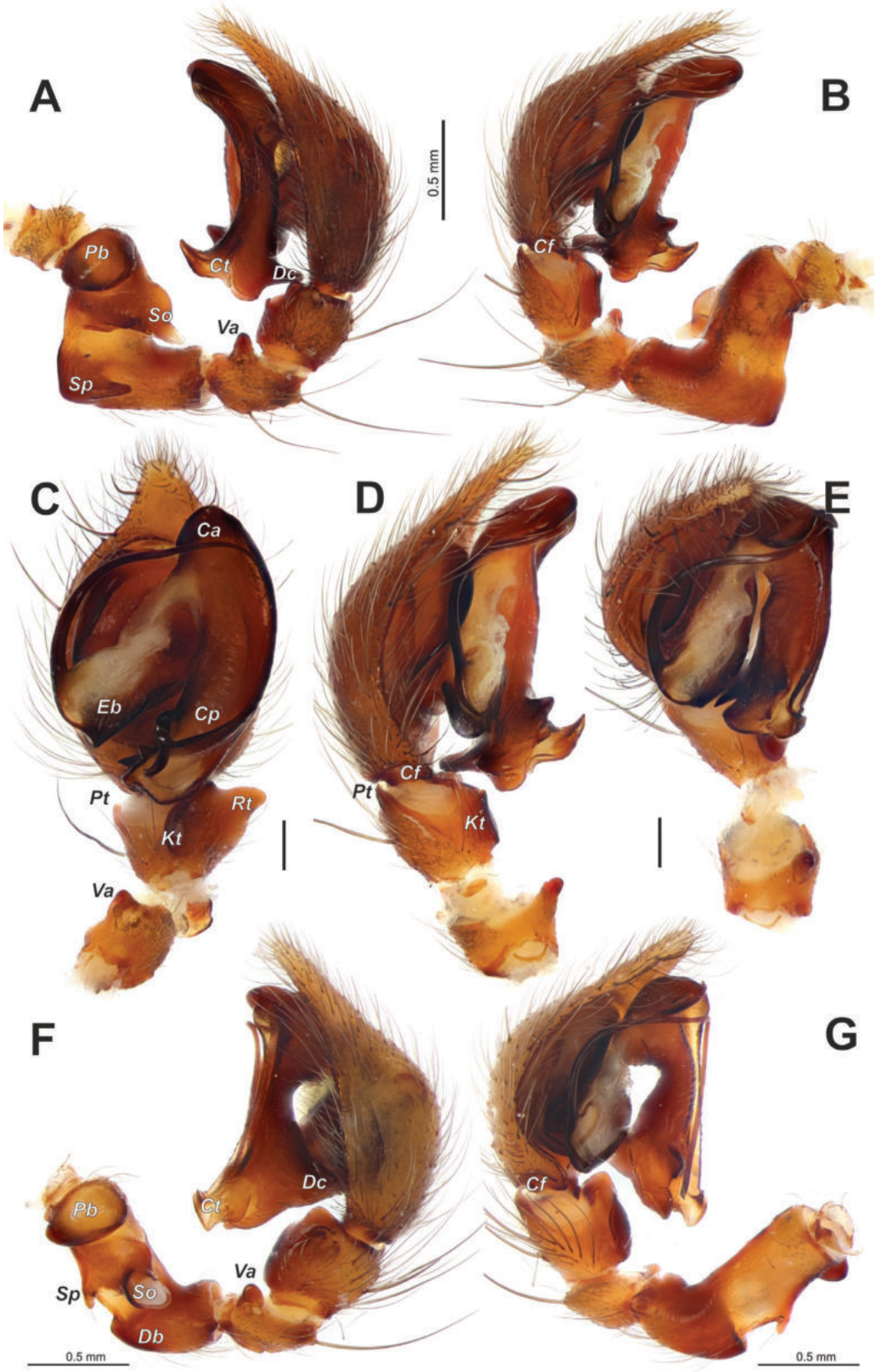

Figure 2. Male palps of *Anatextrix monstrabilis* sp. nov. (**A–E**) and *A. spectabilis* (**F, G**). **A, F.** Full palp, retrolateral view; **B, G.** Same, prolateral view; **C–E.** Palp with femur detached, ventral, prolateral and anterior views. Scale bars: 0.2 mm, unless stated otherwise. Abbreviations: *Ca* – anterior arm of conductor, *Cf* – cymbial fold, *Cp* – posterior arm of conductor, *Ct* – ventral tip of conductor, *Db* – distal bulge, *Dc* – dorsal extension of conductor, *Eb* – base of embolus, *Kt* – ventral keel, *Pb* – proximal bulge, *Pt* – prolateral apophysis, *Rt* – retrolateral apophysis, *So* – stump-like outgrowth, *Sp* – spine-like outgrowth, *Va* – ventral apophysis. **F** and **G** are reproduced from Kaya et al. (2023).

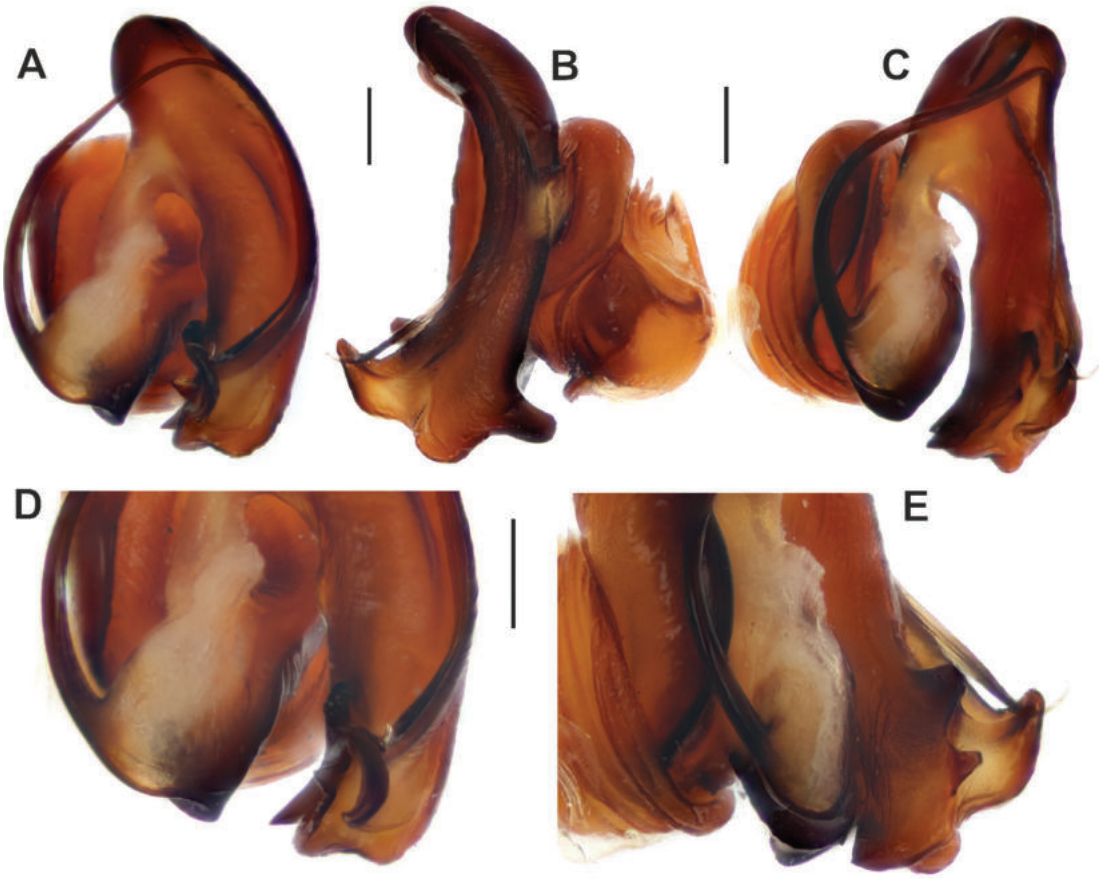

Figure 3. Bulb of *Anatextrix monstrabilis* sp. nov. **A, D.** Ventral view; **B.** Retrolateral view; **C.** Proventral view; **E.** Prolateral view. Scale bars: 0.2 mm.

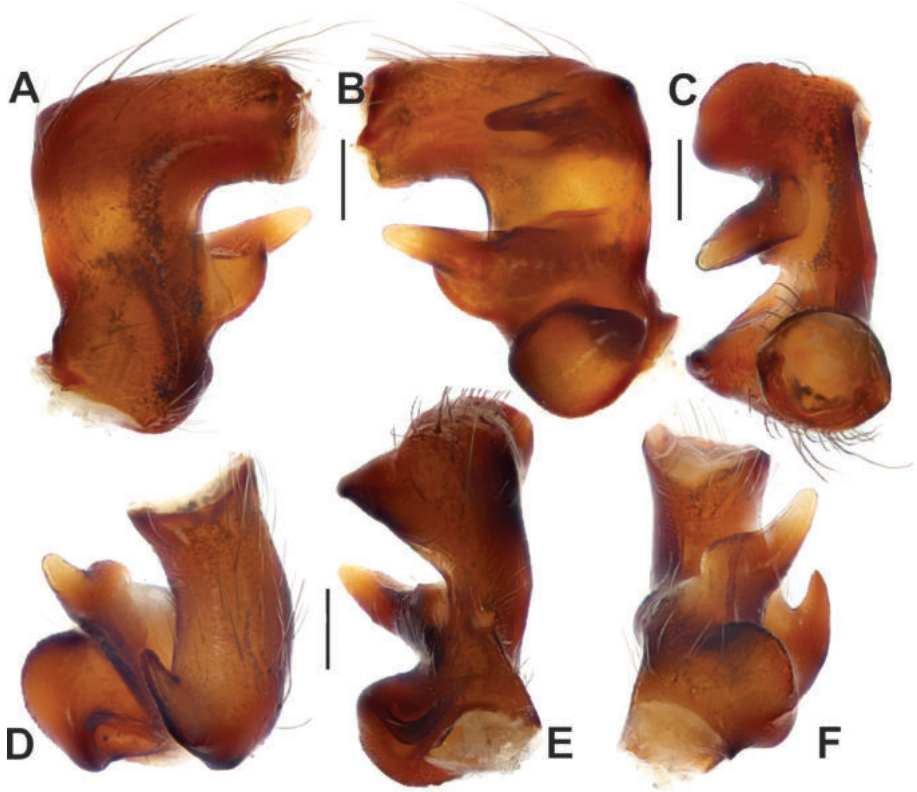

Figure 4. Male palpal femur of *Anatextrix monstrabilis* sp. nov. **A.** Prolateral view; **B.** Retrolateral view; **C.** Ventral view; **D.** Anterior view; **E.** Dorsal view; **F.** Posterior view. Scale bars: 0.2 mm.

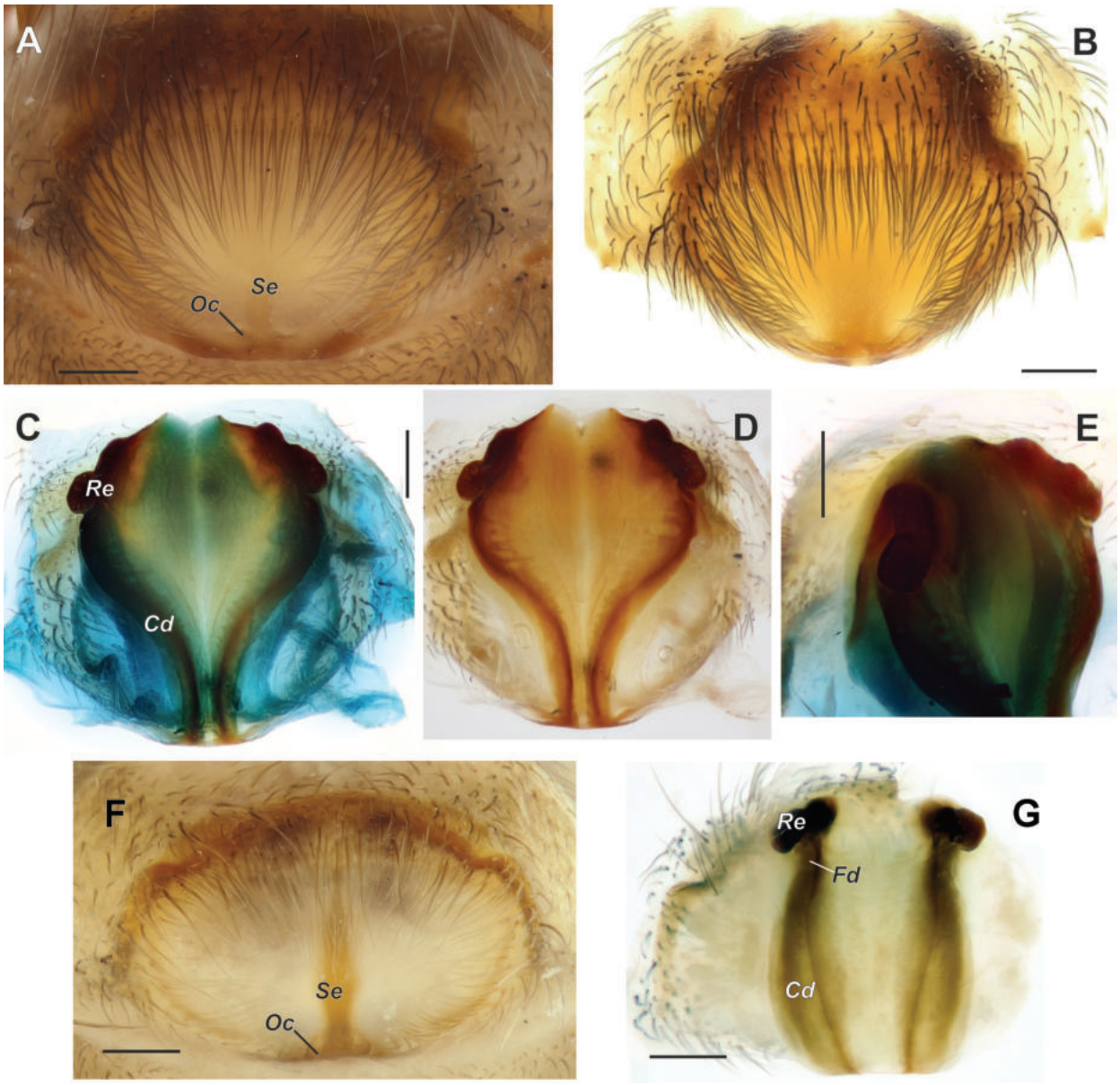

Figure 5. Epigynes of *Anatextrix monstrabilis* sp. nov. (**A–E**) and *A. spectabilis* (**F, G**). **A, F.** Intact epigyne, ventral view; **B.** Macerated epigyne, ventral view; **C, D, G.** Vulva, dorsal view; **E.** Same, dorsolateral view. Scale bars: 0.2 mm. Abbreviations: *Cd* – copulatory duct, *Fd* – fertilisation duct, *Oc* – copulatory opening, *Re* – receptacle, *Se* – septum. **F** and **G** are reproduced from Kaya et al. (2023).

Figure 6. Habitats of species of *Anatextrix* in Pozantı district of Adana Province, Türkiye. **A.** Habitat of *A. spectabilis* in Armutoğlu; **B.** Habitat of *A. monstrabilis* sp. nov. in Akçatekir.

Figure 7. Distribution records of *Anatextrix spectabilis* (circles) and *A. monstrabilis* sp. nov. (square).

The most interesting and remarkable characteristic of the new species described in this paper is the highly-modified male palpal femur, which is a relatively rare trait in spiders. Although the generotype of *Anatextrix* also displays a modified male palpal femur, the morphology of this segment is more remarkable in the new species (i.e., more distinctly L-shaped and bearing larger outgrowths). To the best of our knowledge, the combination of these two characters is unknown in any other species of spiders.

Generally speaking, male spiders use the apophyses on their palps or first pair of legs during copulation. Palpal apophyses (particularly the retrolateral tibial apophysis) are used to stabilise the palp on the epigyne (Huber 1995) or, in some cases, they are 'locked' into parts of the bulb, while apophyses of the legs are hooked to the chelicerae or appendages of the female to prevent her from attacking the male (Pérez-Miles and Perafán 2017). The morphology of these structures is often species-specific and widely believed to be shaped by sexual selection (Huber 1995). We believe that the mating behaviour of the species of *Anatextrix* should be an interesting case to study, as the large and numerous apophyses of the male palpal femur are likely to play a role in the copulation.

References

Bolzern A, Hänggi A, Burckhardt D (2008) Funnel web spiders from Sardinia: Taxonomical notes on some *Tegenaria* and *Malthonica* spp. (Araneae: Agelenidae). Revue Suisse de Zoologie 115: 759–778. https://doi.org/10.5962/bhl.part.80454

Bolzern A, Crespo L, Cardoso P (2009) Two new *Tegenaria* species (Araneae: Agelenidae) from Portugal. Zootaxa 2068(1): 47–58. https://doi.org/10.11646/zootaxa.2068.1.3

Çıplak B (2003) Distribution of Tettigoniinae (Orthoptera, Tettigoniidae) bush-crickets in Turkey: The importance of the Anatolian Taurus Mountains in biodiversity and implications for conservation. Biodiversity and Conservation 12(1): 47–64. https://doi.org/10.1023/A:1021206732679

Huber BA (1995) The retrolateral tibial apophysis in spiders-shaped by sexual selection? Zoological Journal of the Linnean Society 113(2): 151–163. https://doi.org/10.1111/j.1096-3642.1995.tb00931.x

Kaya RS, Kunt KB, Marusik YM, Uğurtaş İH (2010) A new species of *Tegenaria* Latreille, 1804 (Araneae, Agelenidae) from Turkey. ZooKeys 51: 1–16. https://doi.org/10.3897/zookeys.51.467

Kaya RS, Zamani A, Yağmur EA, Marusik YM (2023) A new genus of Textricini Lehtinen, 1967 (Araneae, Agelenidae) from Anatolia. ZooKeys 1151: 31–45. https://doi.org/10.3897/zookeys.1151.100430

Lehtinen PT (1967) Classification of the cribellate spiders and some allied families, with notes on the evolution of the suborder Araneomorpha. Annales Zoologici Fennici 4: 199–468.

Noroozi J, Zare G, Sherafati M, Mahmoodi M, Moser D, Asgarpour Z, Schneeweiss GM (2019) Patterns of endemism in Turkey, the meeting point of three global biodiversity hotspots, based on three diverse families of vascular plants. Frontiers in Ecology and Evolution 7: 159. https://doi.org/10.3389/fevo.2019.00159

Pérez-Miles F, Perafán C (2017) Behavior and biology of Mygalomorphae. In: Viera C, Gonzaga MO (Eds) Behaviour and ecology of spiders, contributions from the Neotropical region. Springer, Cham, 29–54. https://doi.org/10.1007/978-3-319-65717-2_2

WSC (2023) World Spider Catalog. Version 24. Natural History Museum Bern. [Online at:] http://wsc.nmbe.ch [accessed on 11.02.2023]

Zoosyst. Evol. 99 (2) 2023, 307–323 | DOI 10.3897/zse.99.101417

PENSOFT

für Natur MUSEUM FÜR NATURKUNDE BERLIN

Kangaraneus, a new genus of orb-weaving spider from Australia (Araneae, Araneidae)

Pedro de S. Castanheira[1], Volker W. Framenau[1,2,3]

1 *Harry Butler Institute, Murdoch University, 90 South St, Murdoch, Western Australia 6150, Australia*

2 *Department of Terrestrial Zoology, Western Australian Museum, Locked Bag 49, Welshpool DC, Western Australia, 6986, Australia*

3 *Department of Invertebrates, Museum of Nature Hamburg - Zoology, Leibnitz Institute for the Analysis of Biodiversity Change (LIB), Martin-Luther-King-Platz 3, 20146 Hamburg, Germany*

https://zoobank.org/F1A740F4-6BC2-44B4-9F9F-3222C428B23C

Corresponding author: Pedro de S. Castanheira (pedro.castanheira@murdoch.edu.au)

Academic editor: Danilo Harms ♦ **Received** 3 February 2023 ♦ **Accepted** 12 April 2023 ♦ **Published** 31 May 2023

Abstract

A new Australian genus in the orb-weaving spider family Araneidae Clerck, 1757 is described, *Kangaraneus* **gen. nov.**, with *K. arenaceus* (Keyserling, 1886) **comb. nov.** (New South Wales, Queensland, South Australia, Victoria and Western Australia) as the type species and also including two other species: *Kangaraneus amblycyphus* (Simon, 1908) **comb. nov.** (Australian Capital Territory, New South Wales, Queensland, South Australia, Victoria and Western Australia) and *K. farhani* **sp. nov.** (Australian Capital Territory, New South Wales, South Australia, Victoria and Tasmania). The new genus is included in the informally termed Australasian 'backobourkiine' clade due to the presence of its putative synapomorphies, specifically a single patellar macroseta on the male pedipalp and its median apophysis forming an arch over the radix. It includes medium-sized orb-weaving spiders (total length 3–12 mm) with distinct humeral humps on the almost triangular abdomen. Therefore, within the backobourkiines, it is somatically most similar to *Novakiella* Court & Forster, 1993 but differs considerably in male genitalic characters, including a C-shaped median apophysis with an acute tip. Genitalia are most similar to those in *Quokkaraneus* Castanheira & Framenau, 2023 from which the new genus differs by the lack of the white colouration and the shape of the abdomen.

Key Words

Araneus, backobourkiines, systematics, taxonomy

Introduction

A recent multi-gene molecular study on world-wide orb-weaving spiders in the family Araneidae Clerck, 1757 placed many Australian species in an informally termed clade, the 'backobourkiines' (Scharff et al. 2020). The study did not analyse morphological characters in detail but proposed two synapomorphies of the male pedipalp for this clade: a single macroseta on the pedipalp patella – most 'traditional' Araneinae Clerck, 1757 have two (Scharff and Coddington 1997) – and the base of the median apophysis forming an arch over the radix. The study by Scharff et al. (2020) spawned several genus-level revisions for the backobourkiines, a dominant Oriental and Pacific clade, that currently includes eleven genera in Australia (Table 1). Two of these genera, *Leviana* Framenau & Kuntner, 2022 and *Quokkaraneus* Castanheira & Framenau, 2022, were placed outside the backobourkiines in Scharff et al.'s (2020) preliminary phylogenetic hypothesis, but as their male pedipalps display the proposed synapomorphies, they are tentatively included in the backobourkiines pending further molecular and morphological studies (see discussions in Framenau and Kuntner (2022) and Castanheira and Framenau (2022)).

Table 1. Putative genera of the informally termed backobourkiine clade (sensu Scharff et al. 2020) occurring in Australia.

Genus	Total no. of species (World Spider Catalog 2023)	No. of species in Australia	Remarks
Acroaspis Karsch, 1878	5	5	included in Scharff et al. (2020); paraphyletic with respect to *Socca*; taxonomy unresolved
Backobourkia Framenau, Dupérré, Blackledge & Vink, 2010	4	4	revised in Framenau et al. (2010); *B. thyridota* likely senior synonym of either *B. heroine* (L. Koch, 1871) or *B. brounii* (Urquhart, 1885) pending an examination of type material (whereabouts currently unknown)
Carepalxis L. Koch, 1872	12	5	Taxonomy unresolved; Nearctic species reviewed in Levi (1992) and Ferreira-Sousa and Motta (2022)
Hortophora Framenau & Castanheira, 2021	13	10	revised in Framenau et al. (2021a)
Kangaraneus gen. nov.	3	3	this study
Lariniophora Framenau, 2011	1	1	monotypic (Framenau 2011)
Leviana Framenau & Kuntner, 2022	5	5	revised in Framenau and Kuntner (2022); not within backobourkiines in Scharff et al. (2020), but has putative synapomorphies of backobourkiines
Novakiella Court & Forster, 1993	2	2	revised in Framenau et al. (2021b)
Plebs Joseph & Framenau, 2012	22	7	revised in Joseph and Framenau (2012)
Quokkaraneus Castanheira & Framenau, 2022	1	1	monotypic (Castanheira and Framenau 2022); not within backobourkiines in Scharff et al. (2020), but has putative synapomorphies of backobourkiines
Salsa Framenau & Castanheira, 2022	5	5	revised in Framenau and Castanheira (2022)
Socca Framenau, Castanheira & Vink, 2022	12	12	revised in Framenau et al. (2022)
dehaani-group (sensu Yin et al. 1997)	3	1	*Parawixia dehaani* (Doleschall, 1859) was part of the backobourkiines in Scharff et al. (2020) and not monophyletic with true *Parawixia* F.O. Pickard-Cambridge, 1904 from the New World

The Australian *Araneus arenaceus* (Keyserling, 1886), originally described from New South Wales and Queensland, and *Araneus amblycyphus* Simon, 1908 from Western Australia, are morphologically very similar species and both display the proposed male genitalic synapomorphies of the backobourkiines as mentioned above. However, they do not display any of the genus-level synapomorphies that characterise the backobourkiine genera treated so far (Table 1). They were not included in Scharff et al.'s (2020) or any other recent molecular analysis including Australian araneids (e.g., Kallal and Hormiga 2018) that could facilitate their phylogenetic placement.

Due to their unique morphology, we consider *Araneus arenaceus* and *A. amblycyphus* to represent a new genus within the backobourkiines, pending a comprehensive molecular and systematic study of this clade. The aim of this study is to revise this new genus as a testable hypothesis for future systematic work, specifically to elucidate phylogenetic relationships to or within the backobourkiines.

Methods

This study is based on the examination of virtually all orb-weaving spider specimens in the major Australian museum collections and overseas collections where historical type material is lodged, totalling almost 12,000 records (vials) up to this date.

Descriptions and terminology follow recent publications on Australian backobourkiine orb-weaving spiders (e.g., Castanheira and Framenau 2022; Framenau et al. 2022; Framenau and Castanheira 2022; Framenau and Kuntner 2022). The generic and species descriptions of *Araneus arenaceus* and *A. amblycyphus* are based on recently collected, well preserved specimens in lieu of original type material. Colour patterns were described based on specimens preserved in ca. 75% ethanol.

Microscopic photographs were taken with two different stereo-imaging systems. A setup at the Natural History Museum, Copenhagen (Denmark) allowed taking images with a Nikon D300 digital SLR camera attached via a C-mount adapter to a Leica M16A stereomicroscope. Images of different focal plains were stacked with Automontage (vers. 5.02) software from Syncroscopy to increase depth of field. A second set-up at the Harry Butler Institute, Murdoch University (Australia) supported taking microscopic images in different focal planes with a Leica DMC4500 digital camera mounted to a Leica M205C stereomicroscope and combined using the Leica Application Suite X, v. 3.6.0.20104. All photos and plates were edited with Photoshop CC 2020.

All measurements are given in millimetres. They were taken with an accuracy of one tenth of a millimetre, except for the eye and labium measurements, taken with an accuracy of one hundredth of a millimetre.

Maps were compiled in the software package QGis v. 3.2.6 Buenos Aires (https://qgis.org/en/site/; accessed 1 September 2022). Geographic coordinates were extracted directly from original labels or the registration data as provided by the museums. When no detailed geographic information was available, localities were estimated based on Google Earth v. 9.1.39.3 (https://earth.google.com/web/ accessed 1 September 2022) to the closest minute of Latitude and Longitude.

Abbreviations

Morphology

ALE anterior lateral eyes
AME anterior median eyes
PLE posterior lateral eyes
PME posterior median eyes
TL Total length

Collections

AM	Australian Museum, Sydney (Australia);
CVIC	La Trobe University, Bendigo (Australia);
MNHN	Muséum National d'Histoire Naturelle, Paris (France);
MV	Museums Victoria, Melbourne (Australia);
NHMUK	Natural History Museum, London (United Kingdom);
QM	Queensland Museum, Brisbane (Australia);
QVMAG	Queen Victoria Museum & Art Gallery, Launceston (Australia)
SAM	South Australian Museum, Adelaide (Australia);
WAM	Western Australian Museum, Perth (Australia);
ZMB	Museum für Naturkunde, Zentralinstitut der Humboldt-Universität, Berlin (Germany);
ZMH	Zoologisches Institut und Zoologisches Museum, Universität Hamburg, Hamburg (Germany).

Taxonomy

Order Araneae Clerck, 1757
Family Araneidae Clerck, 1757

***Kangaraneus* gen. nov.**
https://zoobank.org/1AED6CD8-0E08-4945-83FB-9C1EB407717B

Type species. *Epeira arenacea* Keyserling, 1886 (designated here).

Etymology. The genus-group name is a compound noun composed of '*Kang*-' in reference to the Kangaroo, genus *Macropus* Shaw, 1790, the renowned Australian marsupial, and '-*araneus*', a genus-group name for orb-weaving spiders. The gender of the genus-group name *Kangaraneus* is masculine.

Diagnosis. Within the backobourkiines as circumscribed by Scharff et al. (2020; see also Table 1), the male genitalia of *Kangaraneus* gen. nov. are most similar to those of *Quokkaraneus*, due to a similar C-shaped median apophysis with a drawn-out, acute tip and the conductor having a basal protrusion (e.g., Castanheira and Framenau 2022; fig. 1C, D). However, *Kangaraneus* gen. nov. males differ distinctly by the presence of prominent humeral humps on the abdomen (lacking in *Quokkaraneus*) and the lack of white colouration on the carapace and legs (e.g., Castanheira and Framenau 2022; fig. 1A). Females of *Kangaraneus* gen. nov. differ from those of *Quokkaraneus* in somatic characters as described for males above, but also in the general shape of the epigyne scape, which is much wider basally in *Quokkaraneus* (Castanheira and Framenau 2022; fig. 3C), but not in *Kangaraneus* gen. nov. Due to the prominent humeral humps on the abdomen, *Kangaraneus* gen. nov. species are somatically similar to species of *Novakiella* but have a vastly different genital morphology; specifically, the male pedipalp lacks the greatly enlarged conductor lobe of *Novakiella* (e.g., Framenau et al. 2021b; figs 1C, 2A).

Description. Medium-sized orb-weaving spiders, with males (ca. TL 3.2–6.7) on average smaller than females (ca. TL 6.3–10.4). Carapace longer than wide with cephalic region slightly narrower in males than in females, light or dark brown (e.g., Figs 1A, 3A, 5A, 6A). Fovea longitudinal in males and transverse in females (e.g., Figs 1A, 3A). AME largest in males, row of posterior eyes recurved, lateral eyes almost touching; posterior lateral eyes largest in females and separated from PME by less than their diameter; AME slightly protruding from the carapace in both sexes (e.g., Figs 1A, 3A). Sternum slightly longer than wide, brown to beige and sometimes with dusky borders (e.g., Figs 1B, 3B). Labium wider than long, with anterior glabrous pale edge (e.g., Figs 6B, 8B). Maxillae with glabrous lighter antero-mesal section (e.g., Figs 6B, 8B). Chelicerae with four promarginal teeth and three retromarginal teeth (reduced to three and two respectively in *K. farhani* sp. nov.). Leg formula I > II > IV > III; tibiae II in males stronger than tibiae I and with strong prolateral spines (e.g., Figs 1A, 5A). Abdomen sub-triangular, generally wider than long, with two conspicuous humeral humps, but without specialized setae, condyles or other structures; colour dorsally varying from beige to olive-grey and black, sometimes with distinct folium pattern and large pale spot (e.g., Figs 1A, 3A, 5A). Venter brown or grey with irregular black setae, sometimes with two pale spots (e.g., Figs 1B, 3B, 5B, 9B).

Male pedipalp patella with a single macroseta (e.g., Figs 1C, 6C–E, 7A–D); paracymbium hook-shaped (e.g., Figs 1D, 6D, 7A–C, 9D); median apophysis C-shaped, basally strongest and tapering to an acute tip, at ca. half to ¾ length with a prominent bulge ('central protrusion'), base forming an arch over radix (e.g., Figs 1C–E, 7A–D); radix prominent (e.g., Figs 1C, 2A, 10A); terminal apophysis elongate, membranous, bubble-shaped or lanceolate, with a basal lobe and a pointed tip (e.g., Figs 1C, 2A–D, 10A–D); basal conductor lobe inconspicuous, terminally spatulate (e.g., Figs 1C, 2A, 6C, 10A); conductor prominent, laterally broad, apically with a protuberance and basally with an elongate protrusion tapering to a bifid tip (e.g., Figs 1C–E, 7A–D, 9C–E); embolus strong, basally elongate, rectangular, heavily sclerotised, with a curved, uncapped tip (e.g., Figs 1C, 2A–D, 9C). Epigyne wider than long, with very wide lateral borders encircling a wide and convex atrium (Figs 3E, 8C, 11C); central division narrow (Figs 3E, 8E, 11F); scape basally broadest, either tapering (Figs 3C, 8C) or truncated (Fig. 11D); spermathecae around half or more than half atrium length, ovoid, copulatory ducts curved, somewhat in a lyre-formation and heavily sclerotised (Fig. 4A–F).

Distribution. All Australian mainland states and Tasmania, excluding Northern Territory. (Fig. 12).

Included species. *Kangaraneus arenaceus* (Keyserling, 1886) comb. nov. (type-species), *K. amblycyphus* (Simon, 1908) comb. nov., and *K. farhani* sp. nov.

***Kangaraneus arenaceus* (Keyserling, 1886), comb. nov.**
Figs 1A–E, 2A–D, 3A–E, 4A, B, 5A–C, 12

Epeira arenacea Keyserling 1886: 145–148, plate 12, figs 2, 2a, 3, 3a, 3b.
Araneus arenaceus (Keyserling, 1886).- Rainbow 1911: 182; Bonnet 1955: 438.

Type specimens. ***Lectotype*** of *Epeira arenacea* Keyserling, 1886 (designated here): female, Sydney (33°53'S, 151°13'E, New South Wales, AUSTRALIA) (NHM 1890.7.1.4138), **examined**. ***Paralectotypes*:** 5 males, 3 females, same locality as lectotype (ZMH Rack (1961)-catalogue 224), **examined**; 1 male, same locality as lectotype (NHM 1890.7.1.4137), **examined;** 1 female, same locality as lectotype, misidentified (this is *K. amblycyphus* comb. nov.) (NHM 1890.7.1.4139), **examined**.

Other material examined. AUSTRALIA – **New South Wales** • 2 females, 3 juveniles, 'Allambi' Telegraph Point, 31°19'S, 149°15'E (AM KS.56967); • 1 male, Pittwater, 33°38'S, 151°18'E, (AM KS.31675). **Queensland** • 1 male, Blackdown Tableland, SW Rockhampton, 23°50'S, 149°03'E (QM); • 1 female, same locality (QM); • 1 female, Braemar State Forest, 27°13'S, 150°50'E (QM); • 1 male, 2 females, 4 juveniles, Peak Downs, 22°56'S, 148°05'E (ZMH); • 2 females, same locality (ZMH). **South Australia** • 1 female, Bridgewater, 35°S, 138°46'E (SAM); • 1 female, Cape du Couedic, on road to Flinder Chase Ranger Station, Kangaroo Island, 36°03'S, 136°42'E (SAM); • 1 female, Dudley

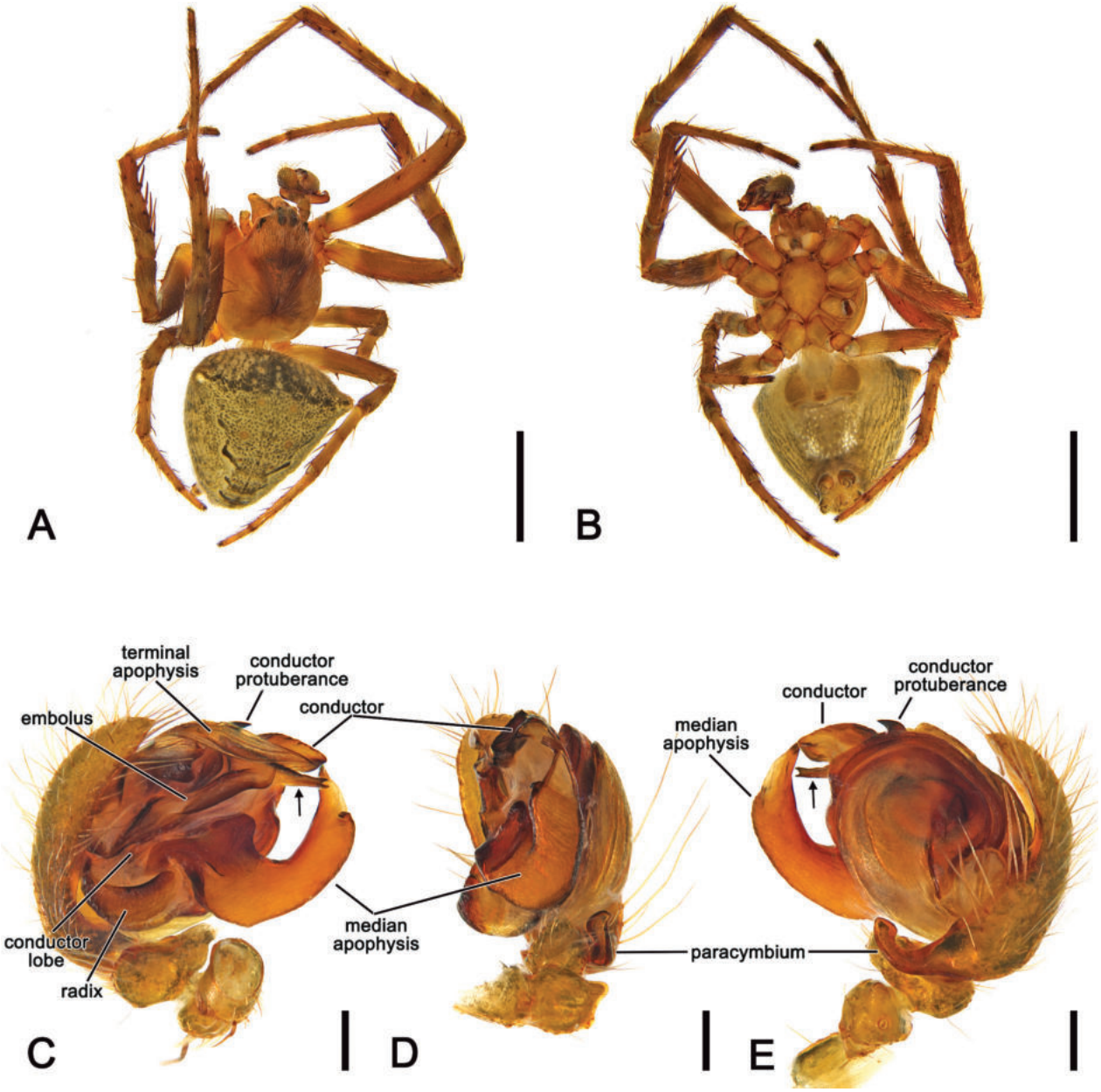

Figure 1. *Kangaraneus arenaceus* (Keyserling, 1886) comb. nov., male (WAM T64400). **A.** Dorsal habitus; **B.** Ventral habitus; **D.** Left pedipalp, ventral view; **E.** Left pedipalp, retrolateral view; **F.** Left pedipalp, dorsal view. Scale bars: 2 mm (**A, B**); 0.2 mm (**C–E**). Arrow points to the conductor basal protrusion.

Conservation Park, Kangaroo Island, 35°48'S, 137°51'E (SAM); • 1 female, Kuitpo Forest Reserve, 35°12'S, 138°40'E (SAM); **Victoria** • 2 females, unknown locality (MV K-10342); • 1 female, Berwick, Quarry Hill, 38°02'S, 145°20'E (QM); • 1 female, 1 juvenile, Spring Gully, 36°48'S, 144°17'E (CVIC 1174). **Western Australia** • 2 females, south-west Western Australia (no exact locality) (SAM); • 1 female, Boddington Bauxite Mine, 32°55'S, 116°26'E (WAM T77221); • 1 female, Busselton, 33°39'S, 115°20'E (AM KS.131227); • 1 female, Fitzgerald National Park, Twertup, 34°01'S, 119°20'E (WAM T75902); • 1 male, Fitzgerald River National Park, on track to Rose Rock, 34°04'S, 119°25'E (WAM T70101); • 1 male, Huntly Mine, 5 km E Banksiadale Dam, 32°39'S, 116°05'E (WAM T64598); • 1 male, same locality (WAM T64400); • 1 male, Jarrahdale (Alcoa) Mine area, 32°20'S, 116°03'E (WAM T48219); • 1 female, Pemberton, 34°26'S, 116°02'E (AM KS.32901); • 1 male, 1 female, 1 juvenile, Shannon National Park, 34°40'S, 116°22'E (WAM T70165).

Diagnosis. Males of *Kangaraneus arenaceus* comb. nov. are most similar to those of *K. amblycyphus* comb. nov. as both have pedipalp with a similar median apophysis with a blunt central protrusion and a conductor with an elongated basal protrusion (Figs 1C–E, 2A–D, 6C–E, 7A–D). However, *K. arenaceus* comb. nov. is identified by a lanceolate terminal apophysis with a more prominent and sclerotised basal lobe, and lacking a distal spine-like tip (present in *K. amblycyphus* comb. nov.). *Kangaraneus arenaceus* comb. nov. is the only species in the genus in which females have baso-lateral flaps on the epigyne base (Figs 3E, 4A, B), and in addition can be differentiated

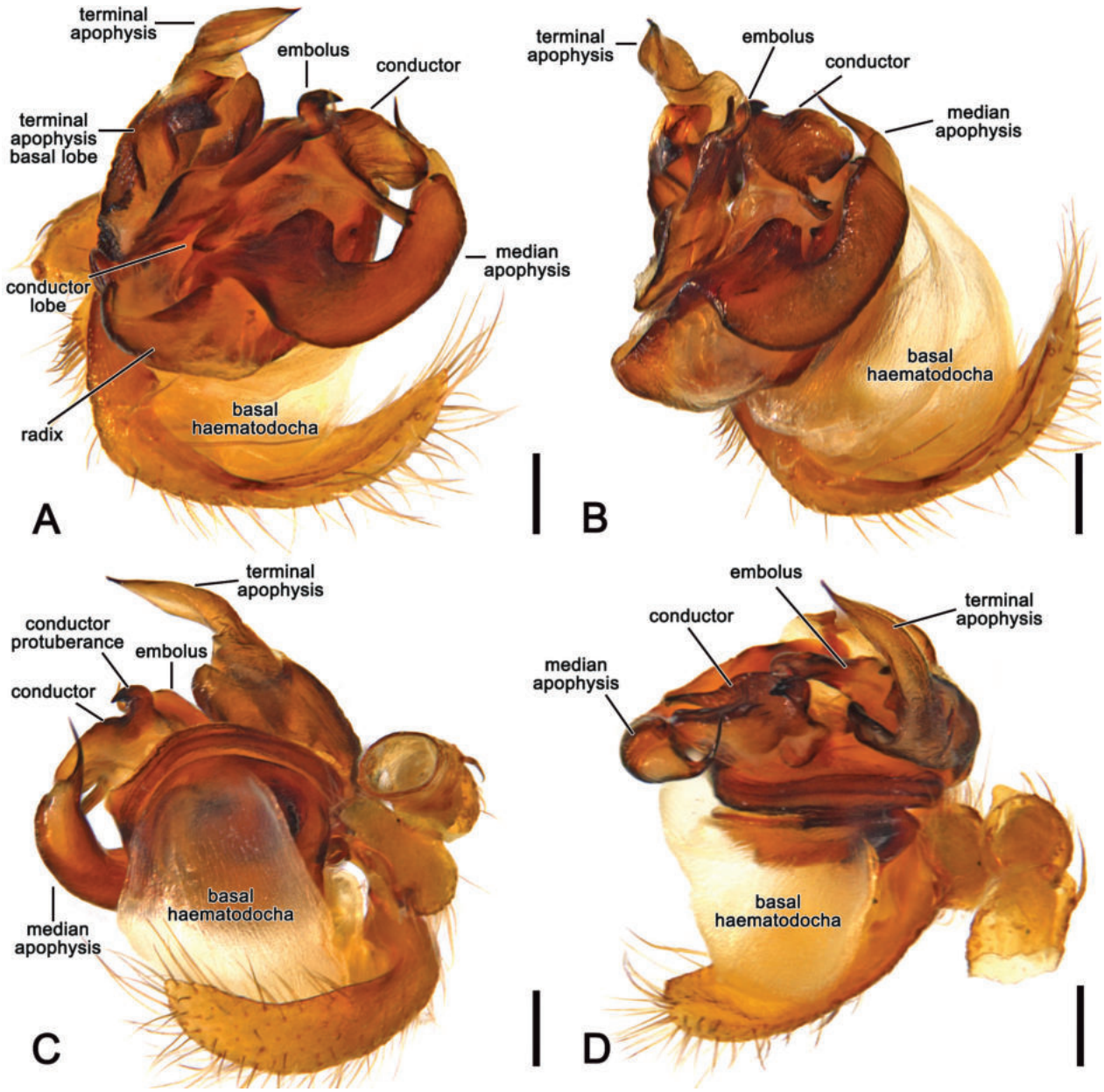

Figure 2. *Kangaraneus arenaceus* (Keyserling, 1886) comb. nov., male expanded left pedipalp (WAM T64598). **A.** Ventral view; **B.** Retrolateral view; **C.** Dorsal view; **D.** Apical view. Scale bars: 0.2 mm.

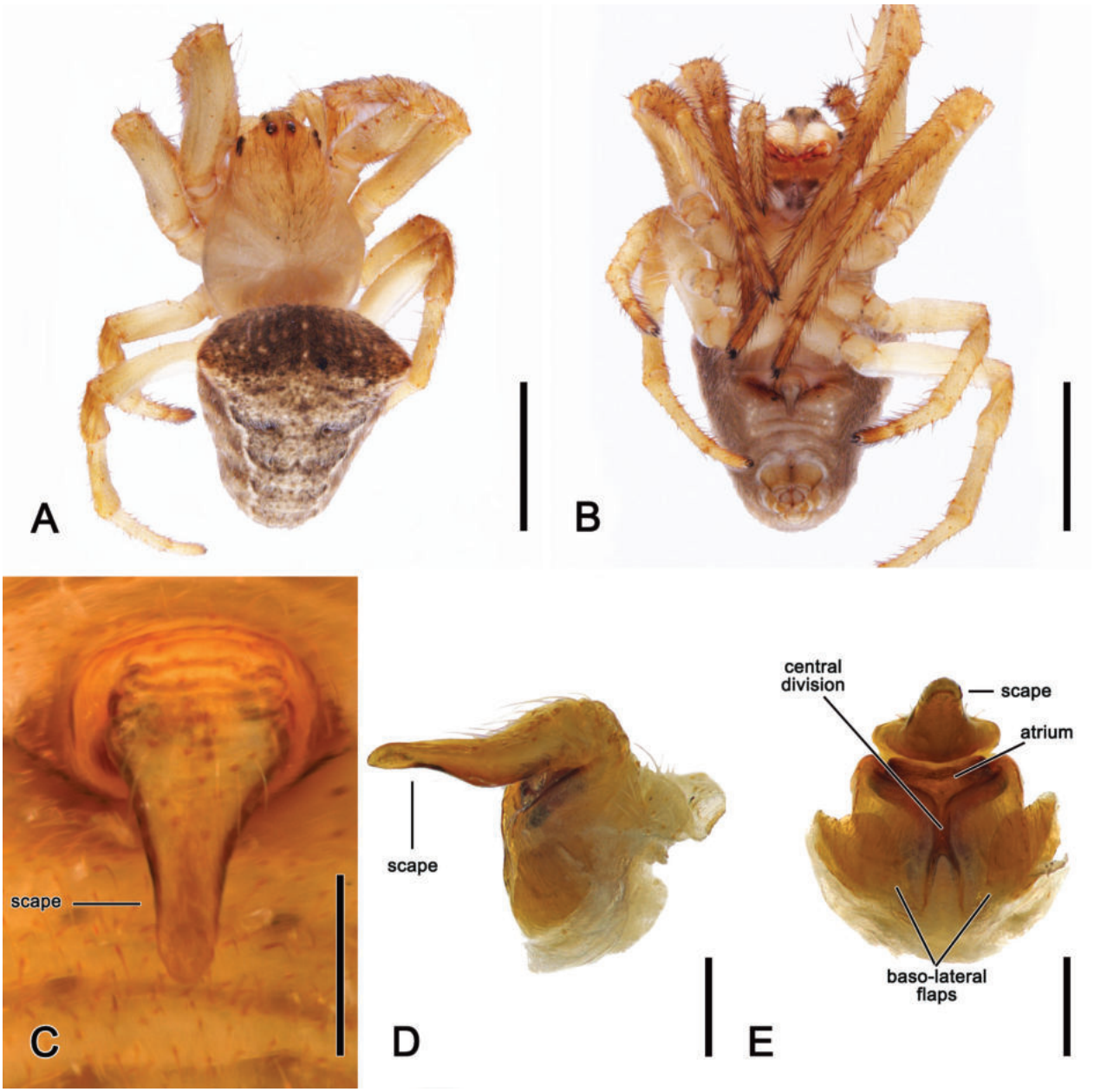

Figure 3. *Kangaraneus arenaceus* (Keyserling, 1886) comb. nov., female, (WAM T77221). **A.** Dorsal habitus; **B.** Ventral habitus; **C.** Epigyne, ventral view; **D.** Epigyne, lateral view; **E.** Epigyne, posterior view. Scale bars: 2 mm (**A, B**); 0.2 mm (**C–E**).

from *K. amblycyphus* comb. nov. by the epigyne scape completely covering the atrium (Figs 3C vs 8C).

Redescription. Male (based on WAM T64400). Total length 6.7. Carapace 3.0 long, 2.4 wide, light brown, centrally darker around fovea (Fig. 1A). Eye diameter AME 0.11, ALE 0.11, PME 0.12, PLE 0.07; row of eyes: AME 0.51, PME 0.42, PLE 1.12. Chelicerae light brown with four promarginal teeth (third largest) and three retromarginal teeth of similar size. Legs light brown mottled dark brown, base of femora lighter (Fig. 1A, B). Leg length of segments (femur + patella + tibia + metatarsus + tarsus = total length): I – 3.9+ 1.6 + 3.2 + 2.8 + 1.2 = 12.7, II – 3.1 + 1.5 + 2.4 + 2.3 + 1.0 = 10.3, III – 1.1 + 0.9 + 1.4 + 1.0 + 0.6 = 5.0, IV – 1.8 + 0.9 + 1.5 + 1.8 + 0.8 = 6.8. Labium 0.47 long, 0.35 wide, light brown; maxillae light brown, both beige anteriorly (Fig. 1B). Sternum 1.3 long, 1.0 wide, light brown with smooth darker radial shading (Fig. 1B). Abdomen 3.5 long, 3.6 wide, triangular with two conspicuous and pointed shoulder humps; dorsum with pale beige background, large olive-grey patch in cardiac area and irregular folium with olive-grey spots, laterally pale beige with dark streaks (Fig. 1A); venter same background colour as dorsum and with sparse guanine spots (Fig. 1B). Pedipalp (Figs 1C–E, 2A–D) length of segments (femur + patella + tibia + cymbium = total length): 0.6 + 0.4 + 0.2 + 1.0 = 2.2; paracymbium strong, hook-like and curved apically; median apophysis C-shaped, terminating in an acute tip, central protrusion small; radix strong; terminal apophysis elongated, membranous and lanceolate, bearing a large, sclerotised,

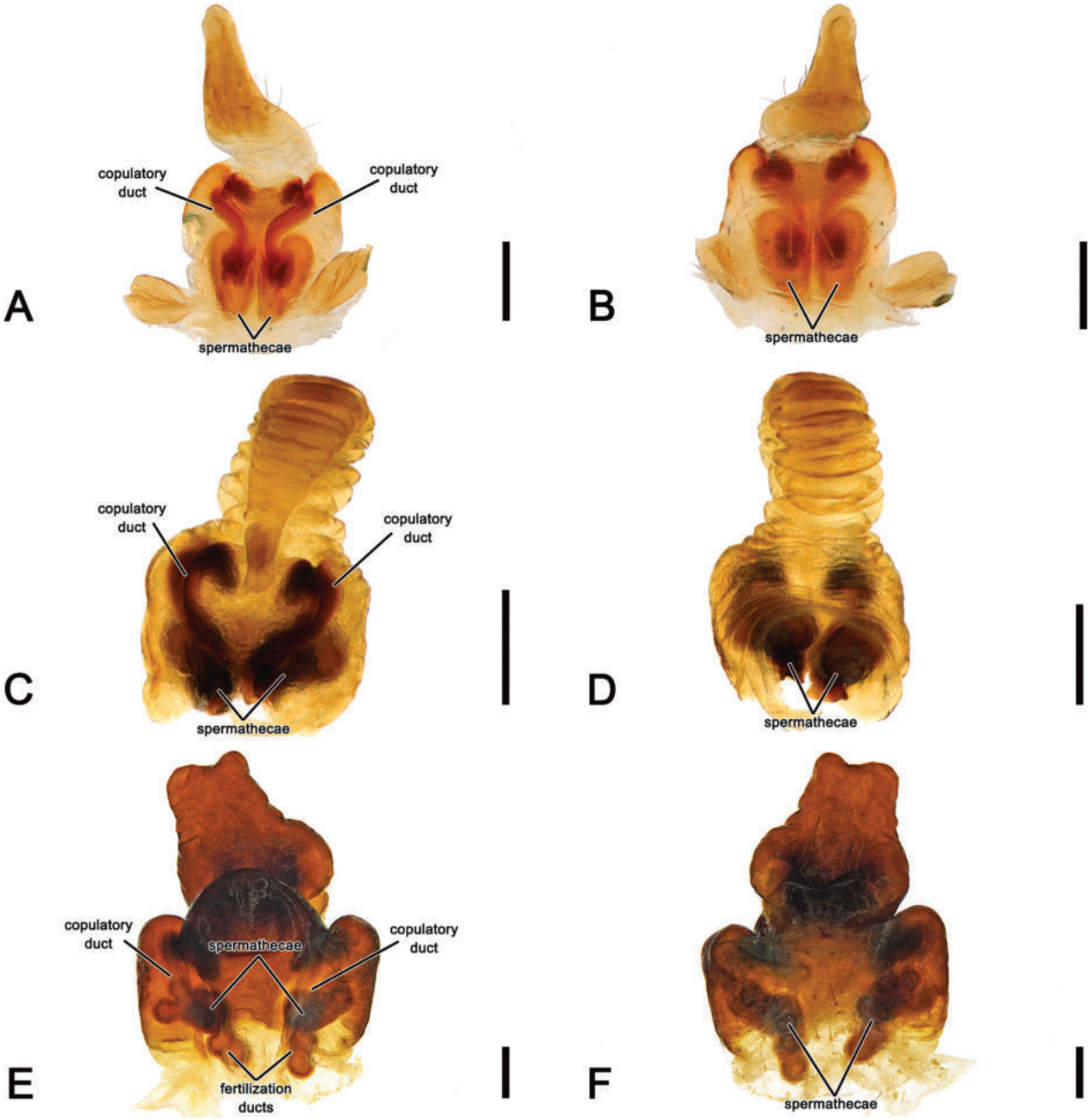

Figure 4. *Kangaraneus* gen. nov. female epigynes, cleared. **A.** *K. arenaceus* (Keyserling, 1886) comb. nov., ventral view (WAM T77221); **B.** *K. arenaceus* (Keyserling, 1886) comb. nov., dorsal view (WAM T77221); **C.** *K. amblycyphus* (Simon, 1908) comb. nov., ventral view (AM KS.131276); **D.** *K. amblycyphus* (Simon, 1908) comb. nov., dorsal view (AM KS. 131276); **E.** *K. farhani* sp. nov. ventral view (AM KS.131278); **F.** *K. farhani* sp. nov., dorsal view (AM KS. 131278). Scale bars: 0.2 mm.

round projection, ending in an acute tip; conductor large, round and laterally projected, bearing a hook-like apical protuberance and an elongated basal protrusion tapering to a bifid tip; basal conductor lobe inconspicuous; embolus prominent, elongate, heavily sclerotised with a curved tip.

Female (based on WAM T77221): Total length 5.6. Carapace 2.5 long, 2.4 wide; beige, cephalic area light brown (Fig. 3A). Eye diameter AME 0.11, ALE 0.10, PME 0.09, PLE 0.09; row of eyes: AME 0.46, PME 0.38, PLE 1.23. Chelicerae beige, with four promarginal teeth (apical and third largest) and three retromarginal teeth of similar size. Legs beige, patellae and tibiae apically slightly darker (Fig. 3A, B). Pedipalp length of segments (femur + patella + tibia + tarsus = total length): 0.6 + 0.4 + 0.4 + 1.2 = 2.6. Leg length of segments (femur + patella + tibia + metatarsus + tarsus = total length): I – 2.9 + 1.4 + 2.4 + 2.3 + 1.1 = 10.1, II – 2.4 +1.1 + 2.1 + 2.1 + 0.9 = 8.6, III – 1.4 + 0.9 + 1.0 + 1.0 + 0.8 = 5.1, IV – 1.8 + 1.0 + 1.5 + 1.7 + 1.0 = 7.0. Labium 0.25 long, 0.60 wide, beige; maxillae beige (Fig. 3B). Sternum 1.5 long, 1.2 wide, beige (Fig. 3B). Abdomen 3.5 long, 3.2 wide; dorsum of same colour background as male but almost completely covered greyish, laterally grey (Fig. 3A); venter grey with a few guanine

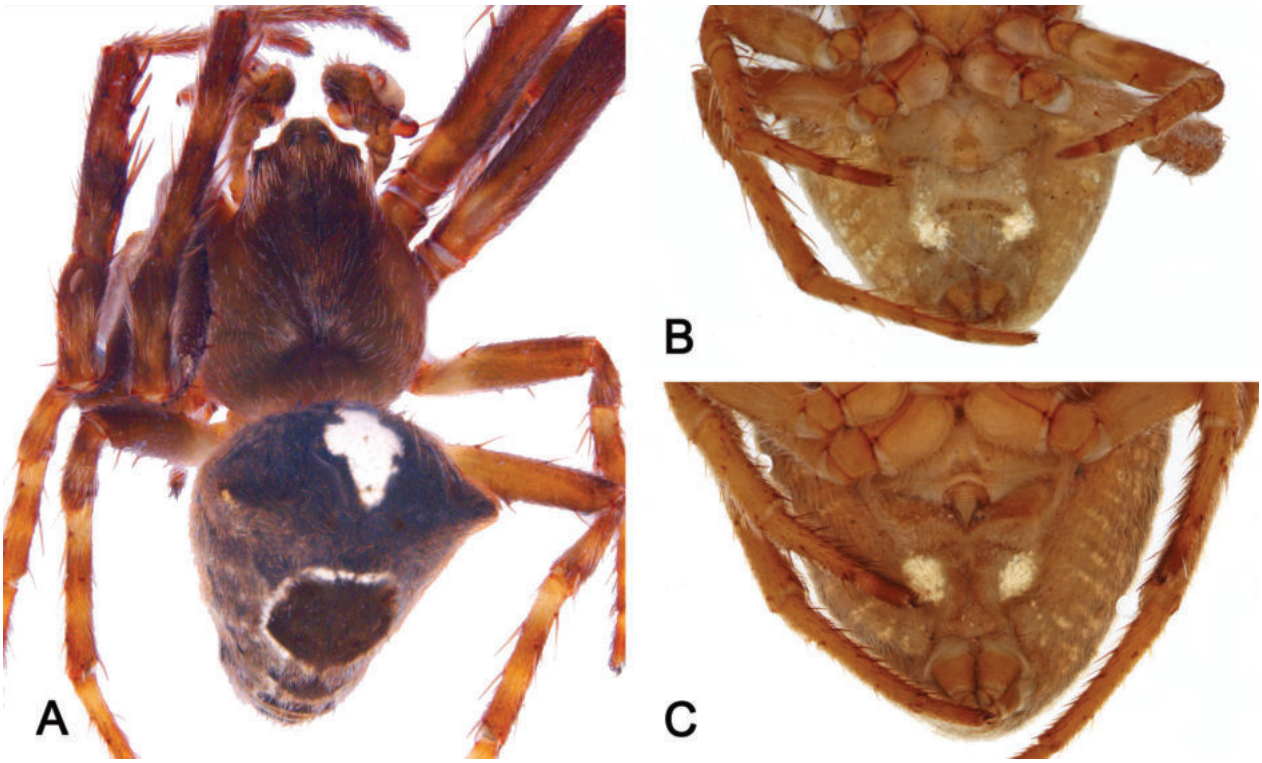

Figure 5. *Kangaraneus arenaceus* (Keyserling, 1886) comb. nov., variations. **A.** Male dorsal habitus (WAM T64598); **B.** Paralectotype male ventral abdomen (NHM 1890.7.1.4137); **C.** Lectotype female ventral abdomen (NHM 1890.7.1.4138).

spots (Fig. 3B). Epigyne base oval, wider than long, with wide lateral borders, atrium convex, barely visible in ventral view (Fig. 3C); central division narrow, baso-lateral flaps present (Figs 3E, 4A); scape elongate-triangular extending over the posterior epigyne border, basally broadly rounded and slightly wrinkled, almost straight in lateral view, tip flattened without terminal pocket (Fig. 3C, D); spermathecae elongate-ovoid, copulatory ducts sinuous and terminating at base of scape (Fig. 4A, B).

Variation. Males total length 4.5–6.7 (n = 6); females total length 5.6–8.7 (n = 6). The colouration of *K. arenaceus* comb. nov. males can vary considerably, with some specimens having a dark brown carapace and a black abdomen with a large white patch in the cardiac area (Fig. 5A). Examined females are less variable in colouration. Both males and females may have a pair of white spots ventrally on the abdomen, a character mentioned in the original description (see Keyserling 1886) (Fig. 5B, C).

Remarks. The syntypes of *Epeira arenacea* Keyserling, 1886 are deposited at the ZMH and NHM. A female paralectotype (NHM 1890.7.1.4139) was misidentified by Keysersing (1886); this is *K. amblycyphus* comb. nov. To unequivocally fix the species-group name of *K. arenaceus* comb. nov., we here designate a female collected in Sydney (NHM 1890.7.1.4138) as the lectotype of the species. We do not consider the specimens from Peak Downs (Queensland) at the ZMH syntypes of *K. arenaceus* comb. nov. as Keyserling's type locality is "Sydney. Museum Godeffroy".

Life history and habitat preferences. Specimens of *K. arenaceus* comb. nov. have mainly been found from October to January, with only a few specimens collected in the colder months like June and August. Therefore, the species seems to be largely spring to early summer mature.

Habitat descriptions on the collection labels include "cypress and brigalow" and "in low bush". Two labels indicated that the species falls prey to wasps ("in wasp nest" and "mud dauber wasp nest").

Distribution. *Kangaraneus arenaceus* comb. nov. has been found in eastern New South Wales and Queensland, the Fleurieu Peninsula and Kangaroo Island in South Australia, Victoria and south-western Western Australia (Fig. 12).

Kangaraneus amblycyphus (Simon, 1908), comb. nov.

Figs 6A–E, 7A–D, 8A–E, 12

Araneus amblycyphus Simon 1908: 427.

Araneus amblycyphus Simon, 1908.- Rainbow 1911: 182; Bonnet 1955: 432.

Type specimens. ***Lectotype*** of *Araneus amblycyphus* Simon, 1908 (designated here): 1 female Busselton (33°38'S, 115°20'E, Western Australia, AUSTRALIA) (MNHN 13309), **examined**. ***Paralectotype*****:** 1 juvenile, same locality (ZMB 13485), **examined**.

Other material examined. AUSTRALIA – **Australian Capital Territory** • 1 female, Corin Dam, 57 km W of Canberra, 35°34'S, 148°50'E (AM KS.32942); **New South Wales** • 1 female, Brooklana, W of Dorrigo, 30°16'S, 152°51'E (AM KS.34050); • 1 male, Hornsby, Waitara

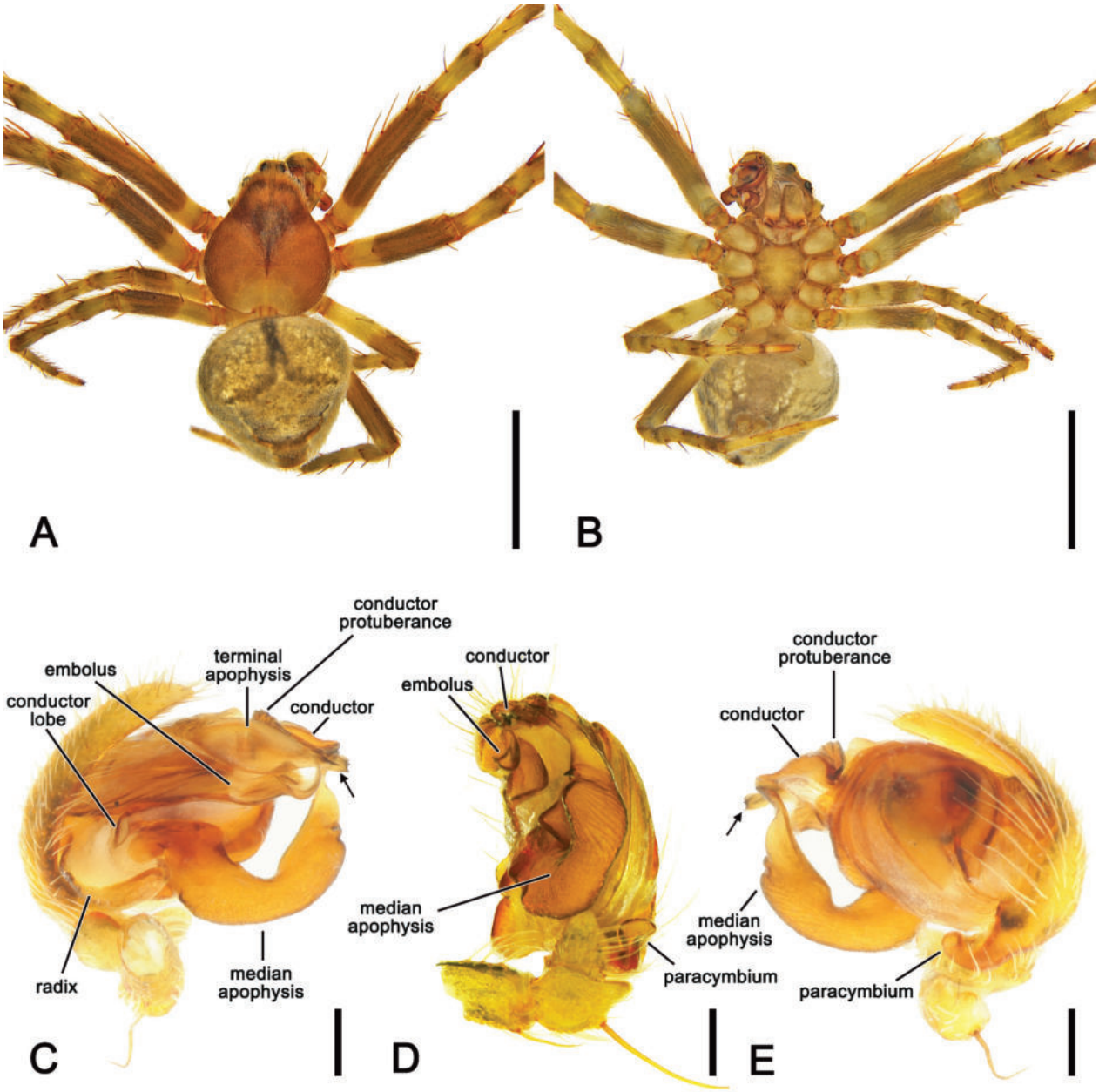

Figure 6. *Kangaraneus amblycyphus* (Simon, 1908) comb. nov., male (AM KS.131277). **A.** Dorsal habitus; **B.** Ventral habitus; **C.** Left pedipalp, ventral view; **D.** Left pedipalp, retrolateral view; **E.** Left pedipalp, dorsal view. Scale bars: 2 mm (**A, B**); 0.2 mm (**C–E**). Arrow points to the conductor basal protrusion.

Creek, 33°42'S, 151°05'E (AM KS.91125); • 1 female, same data (AM KS.91105); • 1 female, Howes Valley, 32°51'S, 150°51'E (AM KS.34043); • 1 male, Jamberoo Mountain, 34°40'S, 150°43'E (AM KS.54098); • 2 females, Scheyville, 33°36'S, 150°53'E (AM KS.98752); • 1 female, same data (AM KS.131276); • 1 female, Sydney, 33°53'S, 151°13'E (NHM 1890.7.1.4139; paralectotype of *K. arenaceus* comb. nov.); • 1 female, 3 juveniles, Wilson River Flora Reserve, Bellangry State Forest, 31°18'S, 152°29'E (AM KS.9666); **Queensland** • 1 female, Braemar State Forest, 27°13'S, 150°50'E (QM); • 1 male, same locality (QM); • 1 male, 6 juveniles, same locality (QM); • 1 female, 1 juvenile, Camira, 27°38'S, 152°55'E (QM S2462); • 5 females, same locality (QM); • 2 males, Malanda, SW, Lot 2, Meragallan Road, 17°25'S, 145°32'E (AM KS.86086); • 1 male, same data (AM KS.131277); • 1 male, Mt Lewis, 16°35'S, 145°17'E (QM); • 1 male, Mulgowie, 27°43'S, 152°22'E (QM); • 1 female, Tweed River, 28°18'S, 153°27'E (AM KS.32649); **South Australia** • 2 females, Dudley Conservation Park, Kangaroo Island, 35°48'S, 137°51'E, (SAM); **Victoria** • 1 female, German Creek, near Bright, 36°43'S, 147°02'E (QM); • 2 females, Snobs Creek, 37°15'S, 145°52'E (MV K-9440). **Western Australia:** • 2 males, 5 females, Stirling Range National Park, Moingup Spring, 34°24'S, 118°06'E (WAM T74424).

Diagnosis. Male *K. amblycyphus* comb. nov. can be distinguished from those of the very similar *K. arenaceus*

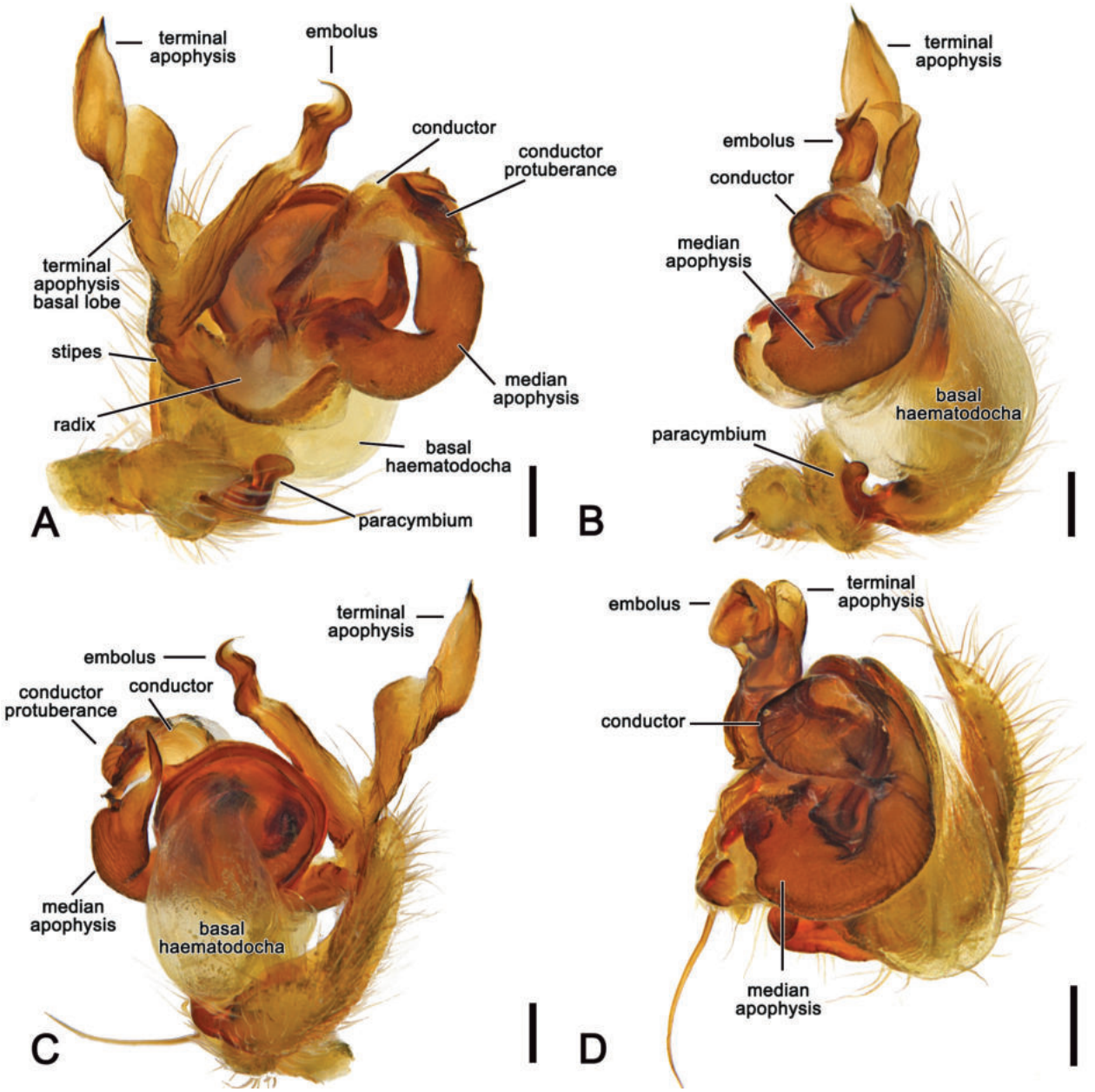

Figure 7. *Kangaraneus amblycyphus* (Simon, 1908) comb. nov., male expanded left pedipalp (AM KS.131277). **A.** Ventral view; **B.** Retrolateral view; **C.** Dorsal view; **D.** Apical view. Scale bars: 0.2 mm.

comb. nov. by the double central protrusion on the median apophysis, the bubble-shaped terminal apophysis, and the shorter and thicker basal protrusion of the conductor with a lamellar apical protuberance (Figs 6A–E, 7A–D). Females of *K. amblycyphus* comb. nov. can be differentiated from those of other *Kangaraneus* gen. nov. species by the epigyne scape not entirely covering the atrium (Fig. 8A, C).

Redescription. Male (based on AM KS.131277). Total length 5.8. Carapace 2.6 long, 2.4 wide, light brown, anteriorly darker (Fig. 6A). Eye diameter AME 0.12, ALE 0.11, PME 0.15, PLE 0.13; row of eyes: AME 0.54, PME 0.46, PLE 1.0. Chelicerae light brown, basally mottled dark brown; with four promarginal teeth (second from base largest) and three retromarginal teeth of similar size. Legs light brown, mottled in dark brown mainly on femora (Fig. 6A, B). Leg length of segments (femur + patella + tibia + metatarsus + tarsus = total length): I – 2.9 + 1.4 + 2.9 + 2.2 + 1.2 = 10.6, II – 1.9 + 1.2 + 2.3 + 1.8 + 1.1 = 8.3, III – 1.0 + 0.9 + 1.2 + 1.0 + 0.8 = 4.9, IV – 1.6 + 1.1 + 1.5 + 1.4 + 0.8 = 6.4. Labium 0.30 long, 0.43 wide, yellowish brown; maxillae yellowish brown (Fig. 6B). Sternum 1.0 long, 0.9 wide, light brown with black radial shading (Fig. 6B). Abdomen 2.8 long, 2.8 wide, oval with inconspicuous shoulder humps; dorsum with beige background and large olive-grey, irregular folium bordered anteriorly and posteriorly by brown bands, laterally beige with dark streaks (Fig. 6A); venter olive-grey, laterally with two pale bands (Fig. 6B). Pedipalp (Figs 6C–E, 7A–D) length of segments (femur + patella + tibia + cymbium

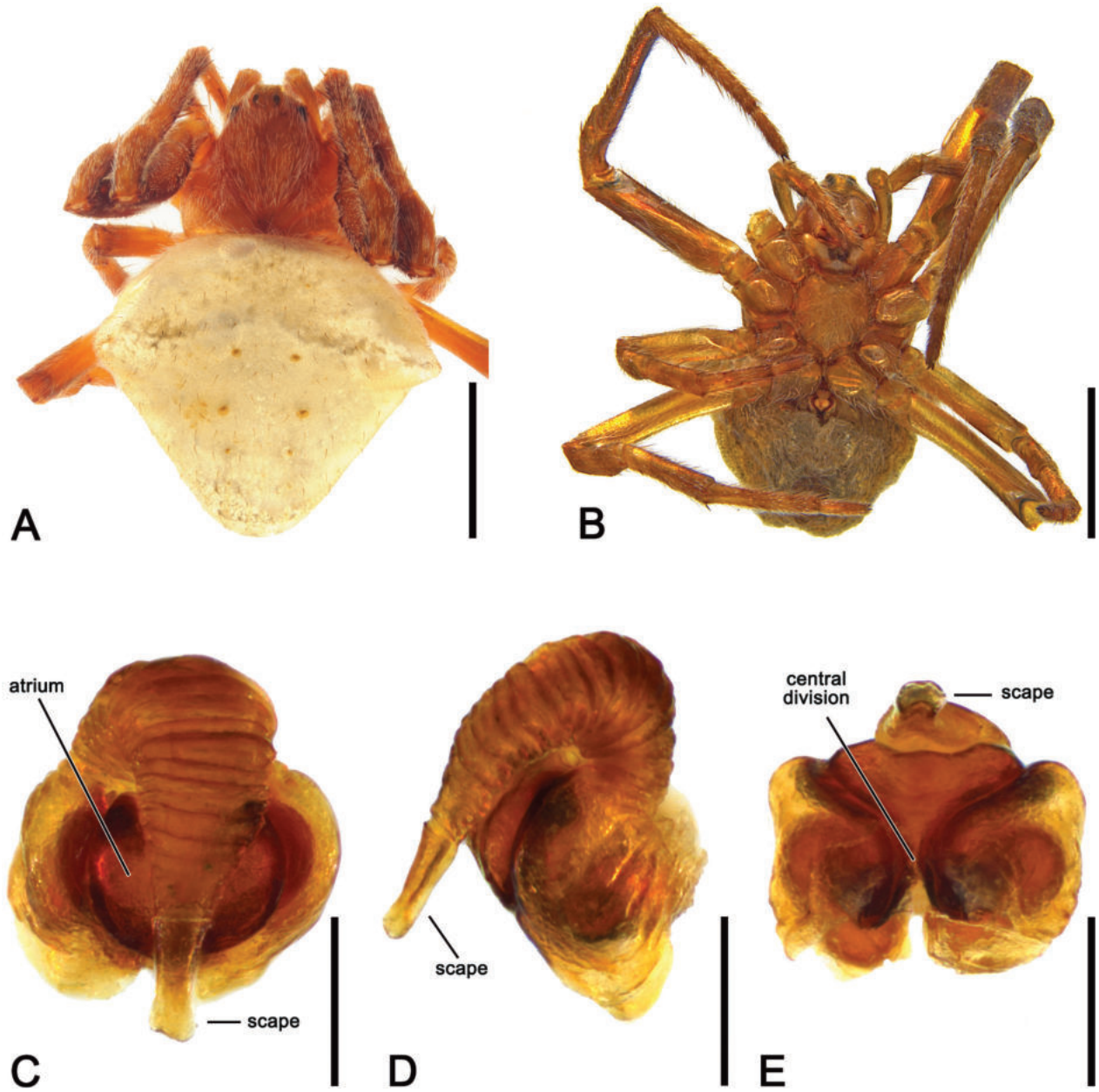

Figure 8. *Kangaraneus amblycyphus* (Simon, 1908) comb. nov., female, (AM KS.131276). **A.** Dorsal habitus; **B.** Ventral habitus; **C.** Epigyne, ventral view; **D.** Epigyne, lateral view; **E.** Epigyne, posterior view. Scale bars: 2 mm (**A, B**); 0.2 mm (**C–E**).

= total length): 0.7+ 0.2 + 0.3 + 1.1 = 2.3; paracymbium short, hook-like and slightly curved apically; median apophysis C-shaped, terminating in an acute tip, central protrusion accompanied by smaller bulge apically; radix comparatively slim; terminal apophysis elongate, slightly inflated and bubble-shaped, terminating in an acute spine-like tip; basal conductor lobe large; conductor prominent, bearing a strong protrusion tapering to a bifid tip; embolus short and elongate, heavily sclerotised with its tip curved apically.

Female (based on AM KS.131276): Total length 5.8. Carapace 2.7 long, 2.6 wide; dark brown, (Fig. 8A). Eye diameter AME 0.09, ALE 0.08, PME 0.10, PLE 0.07; row of eyes: AME 0.46, PME 0.41, PLE 1.15. Chelicerae dark brown, four promarginal teeth (second basal largest) and three retromarginal teeth of similar size. Legs brown with yellowish setae (Fig. 8A, B). Pedipalp length of segments (femur + patella + tibia + tarsus = total length): 0.9 + 0.5 + 0.7 + 0.8 = 2.9. Leg length of segments (femur + patella + tibia + metatarsus + tarsus = total length): I – 3.4 + 1.5 + 2.8 + 2.2 + 1.0 = 10.9, II – 3.4 + 1.4 + 2.7 + 2.2 + 1.1 = 10.8, III – 1.7 + 0.9 + 1.4 + 1.0 + 0.7 = 5.7, IV – 2.4 + 1.1 + 1.5 + 1.4 + 0.8 = 7.2. Labium 0.22 long, 0.49 wide, beige; maxillae beige (Fig. 8B). Sternum 1.3 long, 1.2 wide, dark brown, with yellow streaks (Fig. 8B). Abdomen 3.9 long, 5.4 wide; dorsum with two conspicuous shoulder humps, uniformly beige with indistinct darker line between humeral humps (Fig. 8A); venter dark olive grey (Fig. 8B). Epigyne base almost circular, slightly wider than long, with large and elevated borders (Fig. 8C); central division

narrow (Fig. 8E); scape elongate, longer than the epigyne base, with broad wrinkled base (Fig. 8C, D); spermathecae oval, almost as long as half of the epigyne length, copulatory ducts C-shaped and heavily sclerotised, copulatory openings near the base of scape (Fig. 4C, D).

Variation. Males total length 3.2–5.8 (n = 4); females total length 3.5–6.0 (n = 7). There was little colour variation in male *K. amblycyphus* comb. nov. Some female specimens had a large white patch completely covering the ventral part of abdomen and/or a rounded white patch in the cardiac area, similar to males of *K. arenaceus* comb. nov. and *K. farhani* sp. nov.

Remarks. There are only two syntypes for this species, one female deposited in Paris (MNHN 13309) and a juvenile deposited in Berlin (ZMB 13485), both from the type-locality of Busselton (Western Australia). We here designate the female as the lectotype of this species as the juvenile cannot be unequivocally identified and may be *K. arenaceus* comb. nov., which also occurs in Western Australia.

Life history and habitat preferences. Mature specimens of *K. amblycyphus* comb. nov. were mainly collected between September and December with few specimens collected in February and April; the species therefore appears to be spring to early summer mature.

Habitat descriptions on the labels include "cypress and brigalow" and "*Callitrus*"; the species was also found in a "wasp nest".

Distribution. The distribution of *K. amblycyphus* comb. nov. is very similar to that of *K. arenaceus* comb. nov. although it has been found much further north in Queensland. It occurs in all Australian states except Northern Territory and Tasmania (Fig. 12).

Kangaraneus farhani sp. nov.

https://zoobank.org/CD0DBA93-E176-468F-B6C0-238ED30A6FF0

Figs 9A–E, 10A–D, 11A–F, 12

Type-material. ***Holotype*** male, Frankston (38°09'S, 145°08'E, Victoria, AUSTRALIA), 25 September 1947 (MV K-9854).

Other material examined. AUSTRALIA – **Australian Capital Territory** • 2 females, Corin Dam, 35 km W Canberra, 35°34'S, 148°50'E (AM KS.33511). **New South Wales** • 1 female, Barrington Tops, 32°01'S, 151°29'E (MV K-9814); • 2 males, Jamberoo Mountain, 34°40'S, 150°43'E (AM KS.54090, KS.56902); • 2 females, same locality (AM KS.54096, KS.56898); • 1 female, Jenolan Caves, 33°49'S, 150°01'E (AM KS.32648); • 2 females, New England National Park, 30°29'S, 152°30'E (QM); • 1 female, Newnes State Forest, Sunnyside Road, 1.6 km from Blackfellows Hand Road, 33°22'S, 150°11'E (AM KS.93211). **South Australia** • 1 female, Mylor, 35°03'S, 138°46'E (SAM); • 1 female, Ravine des Casoars, Kangaroo Island, 35°48'S, 136°45'E (SAM). **Tasmania** • 1 female, King Island, 39°53'S, 143°54'E (MV K-9468); • 3 females, Launceston, 41°27'S, 147°10'E (AM KS.28590); • 1 female, same locality (AM KS.28697); • 1 male, 2 females, same locality (AM KS.28545); • 1 female, same locality (AM KS.131278); • 1 female, Lees Paddocks, 41°50'S, 146°06'E (QVMAG 13:0529); • 2 females, Lilydale, 41°15'S, 147°13'E (AM KS.8524); • 1 female, Maggs Mountain, 41°44'S, 146°10'E (QVMAG 13:0634); • 1 female, Picton area, 43°09'S, 146°38'E (MV K-10379); • 1 male, Ringarooma River, Gladstone, 40°57'S 148°01'E (QM S90595); • 1 female, Risdon, 42°49'S, 147°19'E (AM KS.28839); • 1 female, 2 juveniles, Southport, 43°25'S, 146°58'E (AM KS.28870); • 1 female, Stanley, 1 Ford St, 40°46'S, 145°17'E (QVMAG 13:0582); • 1 female, same locality (QVMAG 13:0584); • 1 female, Strahan, 42°09'S, 145°19'E (AM KS.34086). **Victoria** • 1 female, no exact locality (MV K-10377); • 1 female, Camberwell, 37°50'S, 145°4'E (MV K-10375); • 2 females, Frankston, 38°09'S, 145°08'E (MV K-10378); • 1 female, Macclesfield, 37°53'S, 145°29'E (MV K-10376); • 3 females, Narracan, 38°15'S, 146°13'E (MV K-10374).

Etymology. The specific name is a patronymic in honour of Farhan Bokhari, a colleague at the Harry Butler Institute (Murdoch University).

Diagnosis. Male *K. farhani* sp. nov. can be distinguished from the other two species of the genus by the central protrusion of the median apophysis being much longer, somewhat blade-like and heavily sclerotised (Figs 9C, D, 10A, B). Females can be differentiated from the other two *Kangaraneus* gen. nov. species by the truncated tip of the epigyne scape (tapering in the other two species) (Fig. 11D–F). *Kangaraneus farhani* sp. nov. is the only species in which females were found with a broken off scape exposing a distinct, shallowly V-shaped posterior edge of the atrium (Fig. 10C).

Description. Male (based on holotype MV K-9854). Total length 5.8. Carapace 3.6 long, 3.1 wide, light brown, slightly lighter in cephalic area (Fig. 9A). Eye diameter AME 0.23, ALE 0.18, PME 0.18, PLE 0.16; row of eyes: AME 0.64, PME 0.43, PLE 1.17. Chelicerae light brown, basally mottled dark; with three promarginal teeth (median largest) and two retromarginal teeth of similar size. Legs light brown, patched in beige on the base of femur (Fig. 9A, B). Leg length of segments (femur + patella + tibia + metatarsus + tarsus = total length): I – 3.9 + 1.3 + 2.6 + 2.9 + 1.2 = 11.9, II – 3.7 + 1.3 + 3.2 + 2.2 + 1.0 = 11.4, III – 2.2 + 0.8 + 1.6 + 1.0 + 0.5 = 6.1, IV – 3.2 + 0.7 + 1.8 + 2.0 + 1.0 = 8.7. Labium 0.39 long, 0.52 wide, light brown; maxillae light brown (Fig. 9B). Sternum 1.6 long, 1.2 wide, light brown with black contour (Fig. 9B). Abdomen 3.1 long, 3.1 wide, with conspicuous humeral humps; dorsum olive-grey, with short, pale longitudinal patch anteriorly and a dark, heart-shaped patch posteriorly, demarcated by a pale line (Fig. 9A); venter olive-brown with irregular light streaks (Fig. 9B). Pedipalp (Figs 9C–E, 10A–D) length of segments (femur + patella + tibia + cymbium = total length): 0.7+ 0.4 + 0.6 + 1.3 = 3.0; paracymbium strong and hook-like, curved apically; median apophysis C-shaped, tapering to an acute

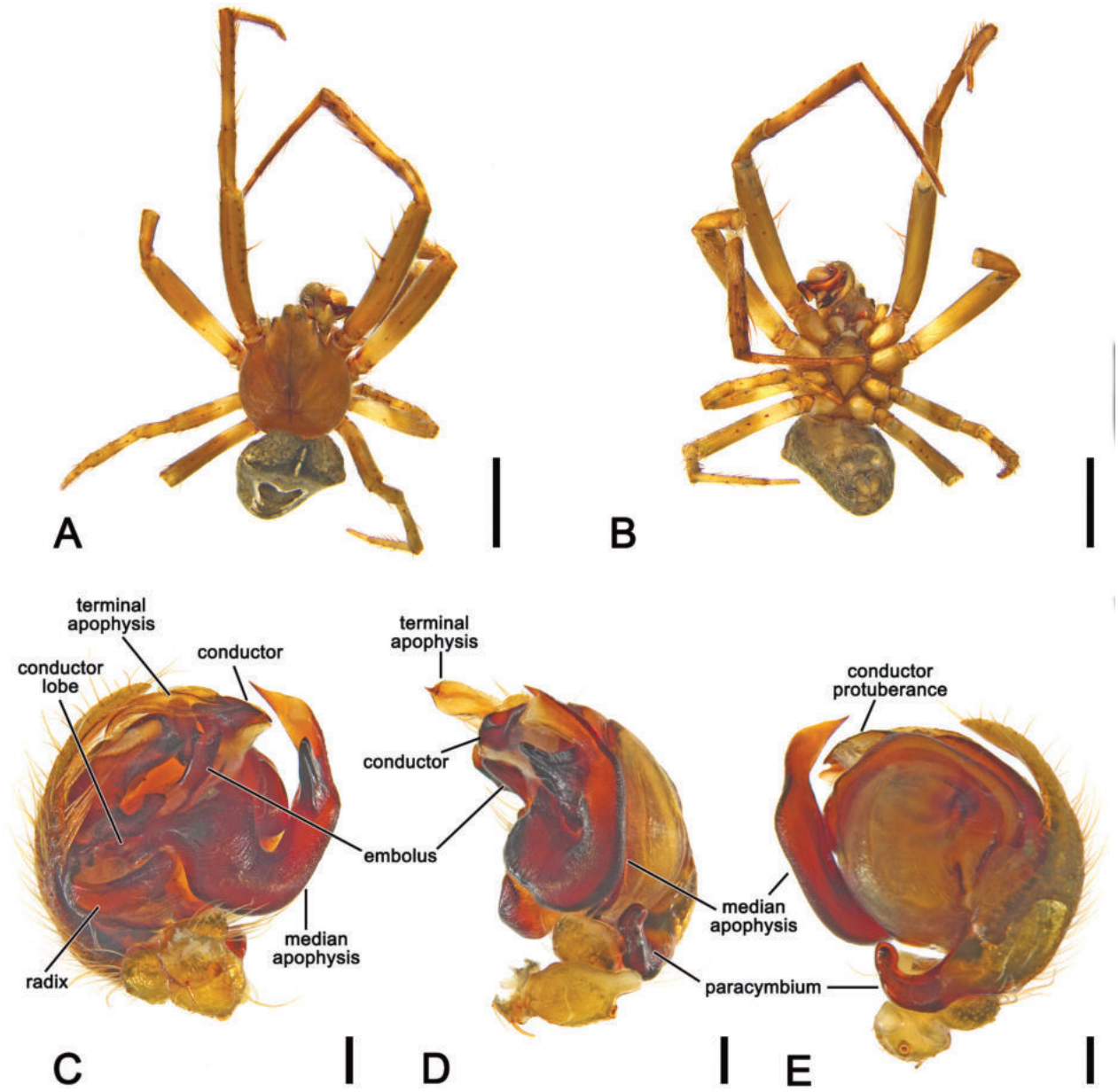

Figure 9. *Kangaraneus farhani* sp. nov., male holotype (MV K-9854). **A.** Dorsal habitus; **B.** Ventral habitus; **C.** Left pedipalp, ventral view; **D.** Left pedipalp, retrolateral view; **E.** Left pedipalp, dorsal view. Scale bars: 2 mm (**A, B**); 0.2 mm (**C–E**).

tip, central protrusion elongate, heavily sclerotised; radix canoe-shaped; terminal apophysis elongate, lanceolate, tapering to an acute tip; basal conductor lobe conspicuous, heavily sclerotised; conductor triangular, bearing a membranous apical protuberance and a short basal protrusion with a bifid tip; embolus heavily sclerotised with its tip curved apically.

Female (based on AM KS.54096): Total length 10.4. Carapace 3.7 long, 3.6 wide; colouration as in male (Fig. 11A). Eye diameter AME 0.13, ALE 0.11, PME 0.12, PLE 0.10; row of eyes: AME 0.51, PME 0.43, PLE 1.28. Chelicerae brown, four promarginal teeth (apical and third largest) and three retromarginal teeth of similar size. Legs light brown with covered in setae (Fig. 11A, B). Pedipalp length of segments (femur + patella + tibia + tarsus = total length): 1.3 + 0.5 + 0.8 + 1.7 = 4.3. Leg length of segments (femur + patella + tibia + metatarsus + tarsus = total length): I – 4.4 + 2.0 + 3.8 + 3.0 + 1.7 = 14.9, II – 3.9 + 1.8 + 3.3 + 2.6 + 1.4 = 13.0, III – 2.5 + 1.1 + 1.6 + 1.5 + 1.0 = 7.7, IV – 3.8 + 1.3 + 2.2 + 2.3 + 1.2 = 10.8. Labium 0.56 long, 0.89 wide, light brown; maxillae light brown (Fig. 11B). Sternum 2.0 long, 1.8 wide, colouration as in male (Fig. 11B). Abdomen 7.9 long, 6.7 wide; dorsum with two conspicuous humeral humps, golden brown with brown band between humeral humps (Fig. 11A); venter olive-grey with indistinct pale lateral bands (Fig. 11B). Epigyne base rounded, wider than long, with large and elevated borders including a V-shaped posterior rim (Fig. 11C, D); atrium convex (Fig. 11C, E, F); central division wide (Fig. 11F); scape slightly longer than wide, longer than the epigyne base, with rounded bulged base,

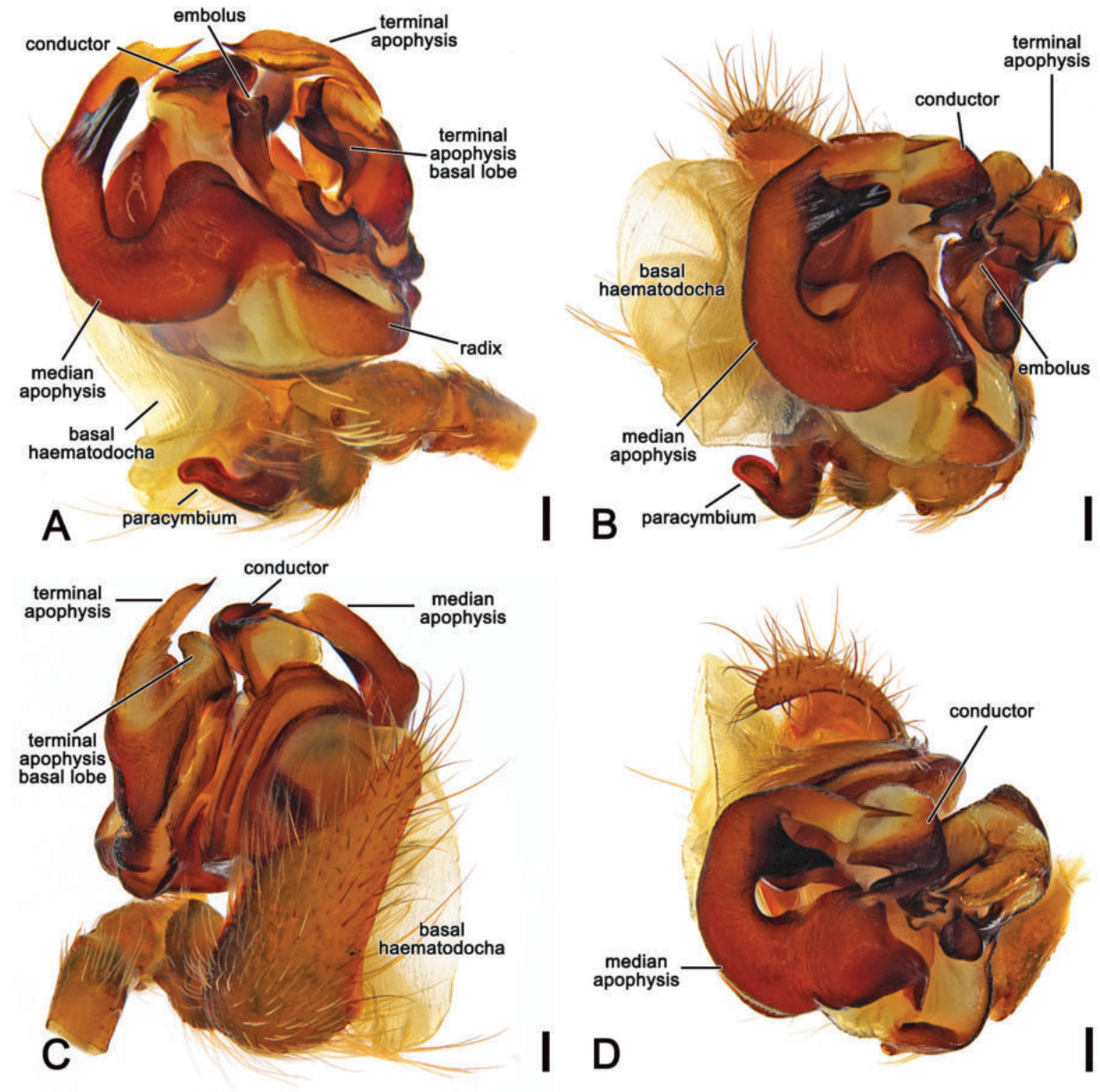

Figure 10. *Kangaraneus farhani* sp. nov., male expanded right pedipalp (AM KS.56902). **A.** Ventral view; **B.** Retrolateral view; **C.** Dorsal view; **D.** Apical view. Scale bars: 0.2 mm.

apically truncated (Fig. 11D, E); spermathecae oval, located basally on the genital plate, copulatory ducts short (Fig. 4E, F).

Variation. Males total length 5.6–5.8 (n = 2); females total length 6.3–10.4 (n = 8). Males display similar colour variations to *K. arenaceus* comb. nov. with one specimen having a large white patch in the cardiac area. Females do not display much colour variation, but half had the epigyne scape broken off.

Life history and habitat preferences. Mature specimens of *K. farhani* sp. nov. were collected between July and early December, except for one female collected in February. The species therefore seems to be largely winter- to spring mature.

Kangaraneus farhani sp. nov. generally appears to build its web low in grass, with original labels reading "among grass in garden", "garden", "orb-web near ground", "in grass at side of creek".

Distribution. *Kangaraneus farhani* sp. nov. occurs in south-eastern mainland Australia (Australian Capital Territory, New South Wales, South Australia, Victoria) and Tasmania (Fig. 12).

Discussion

We here consider *Kangaraneus* gen. nov. to be the twelfth genus within the backobourkiines sensu Scharff et al. (2020) due to the presence of a single patellar macroseta and the median apophysis forming an arch of the radix (Table 1). However, this placement remains ambiguous. Genital morphology, in particular that of the male pedi-

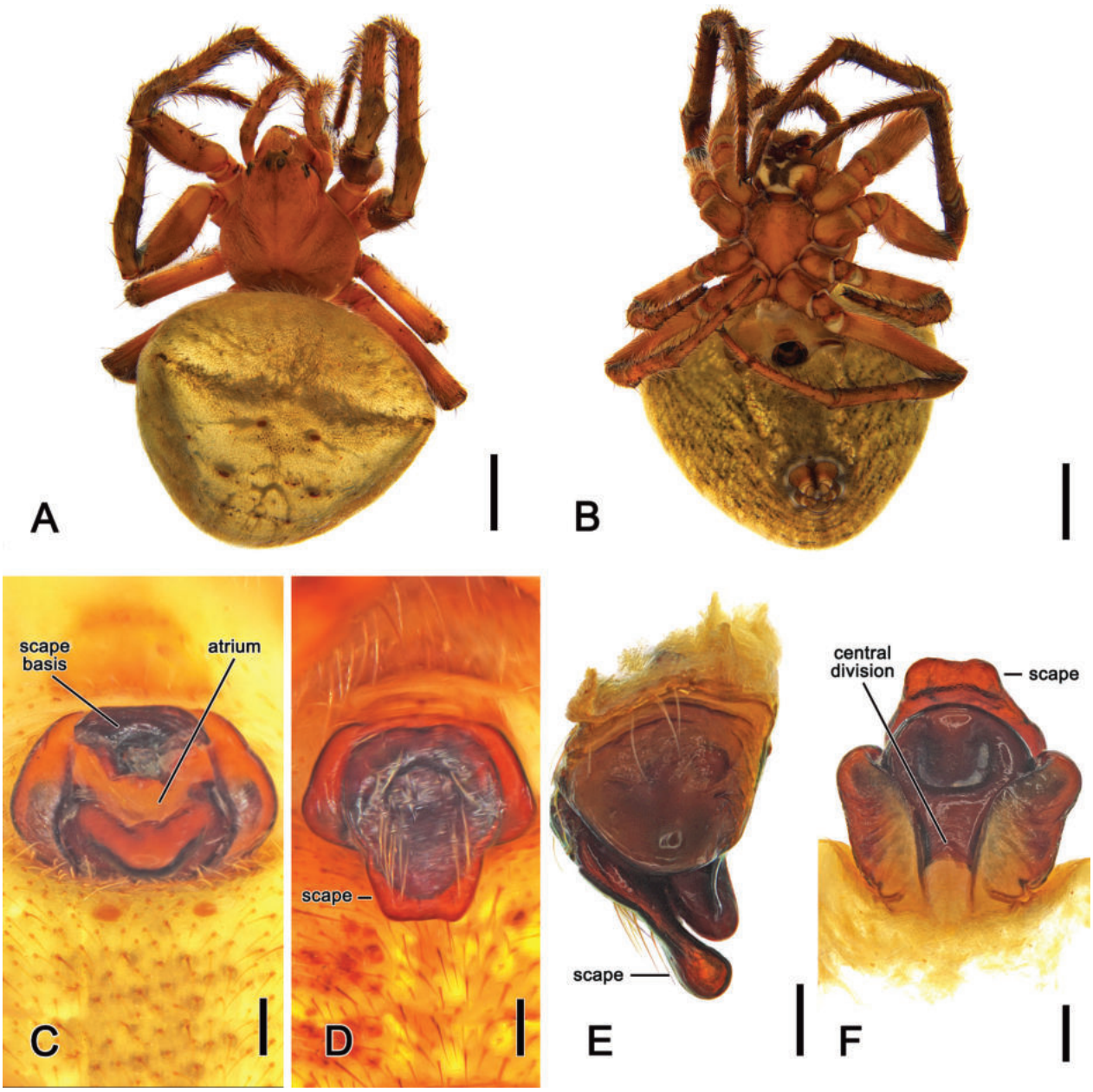

Figure 11. *Kangaraneus farhani* sp. nov., female. **A.** Dorsal habitus (AM KS.54096); **B.** Ventral habitus (AM KS.54096); **C.** Broken epigyne, ventral view (AM KS.54096); **D.** Epigyne, with scape, ventral view (AM KS. 131278); **E.** Epigyne, lateral view (AM KS.131278); **F.** Epigyne posterior view (AM KS. 131278). Scale bars: 2 mm (**A, B**); 0.2 mm (**C–F**).

palp, is most similar to that of *Quokkaraneus necopinus* (Keyserling, 1887), but that species was not recovered in the backobourkiines in Scharff et al. (2020); it was basal in their ARA-clade with the exception of 'caerostrines', phylogenetically far removed from the backobourkiines. However, Scharff et al. (2020; p. 16) stressed the preliminary aspect of their phylogenetic hypothesis: "*Little can be concluded other than araneid phylogeny remains a work in progress to be pursued with more data and more taxa.*" The same is true for the backobourkiines and their putative members (Table 1). More comprehensive phylogenetic analyses are required to elucidate their relationships and interpret the evolution of morphological characters, including genitalia.

The distribution patterns of *K. arenaceus* comb. nov. and *K. amblycyphus* comb. nov. are very similar, and there are several localities where both species were found together, even simultaneously (Busselton, Western Australia; Braemar State Forest, Queensland; Dudley Conservation Park, South Australia; Sydney, New South Wales). This made initial matching of sexes difficult. However, as multiple males and females of each species as diagnosed here were found together in several localities (Shannon and Sterling Range National Parks, Western Australia; Hornsby, Waitara Creek, New South Wales; Braemar State Forest, Queensland), we consider the results of our taxonomic revision the most likely match for males and females of *K. arenaceus* comb. nov. and *K. amblycyphus*

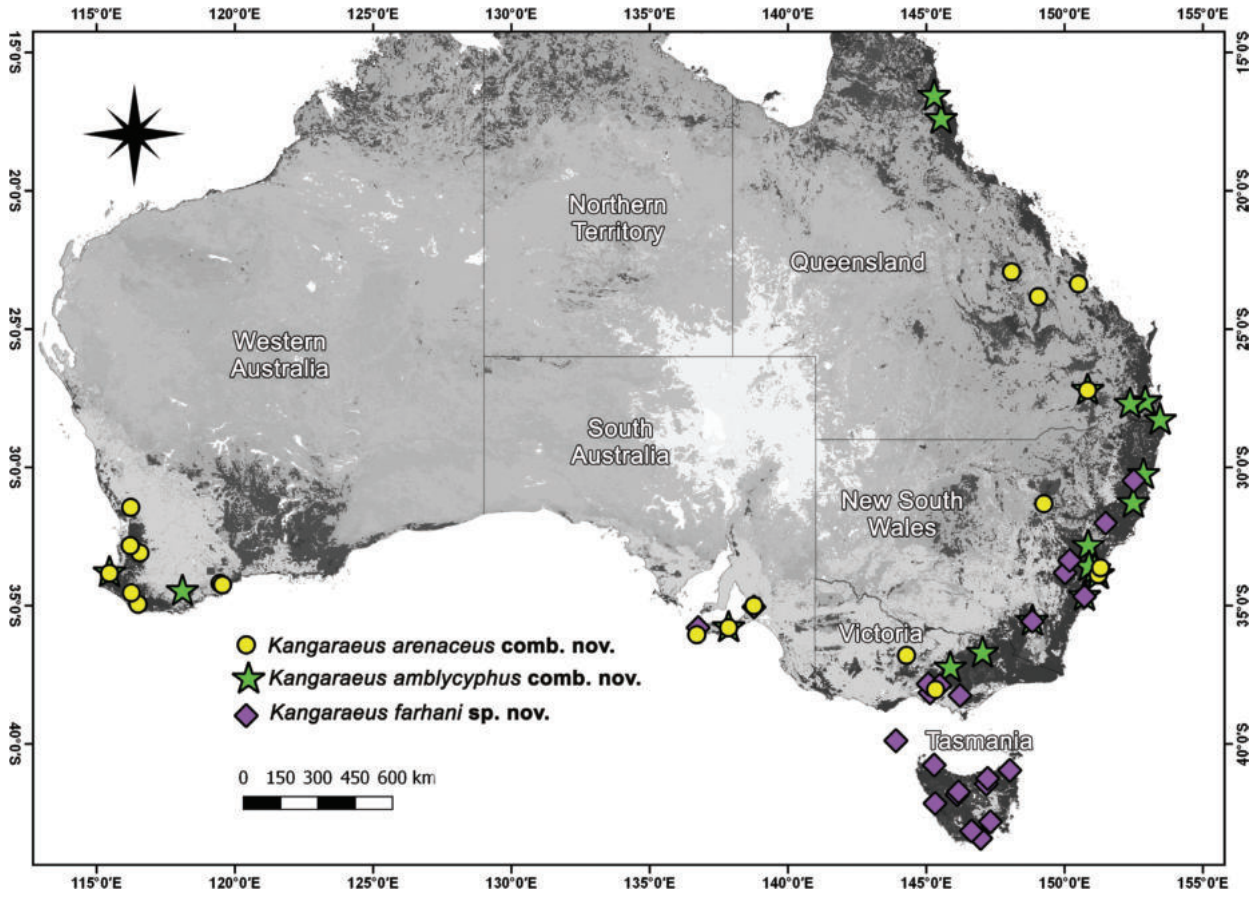

Figure 12. Distribution records of *Kangaraneus* comb. nov. species.

comb. nov. Our species diagnoses have been compiled based on best evidence and by arachnologists highly experienced in araneoid taxonomy. However, there remains the remote possibility that either males and females are matched incorrectly or, alternatively and even less likely, that male and female genitalia in these species are highly variable and both represent the same species. Future molecular analyses could confirm the matching and therefore the distribution patterns of these species.

Acknowledgements

We thank (in no particular order) Peter Lillywhite, Joseph Schubert, Catriona McPhee, Ken Walker, Richard Marchant, Simon Hinkley (NMV), Robert Raven (retired), Owen Seeman, Jeremy Wilson, Michael Rix (QM), John Douglas (retired) (QVMAG), David Hirst (retired), Matthew Shaw (SAM), Graham Milledge (retired), Helen Smith (AM), and Mark Harvey and Julianne Waldock (WAM), for the loan of specimens in their care and/or assistance when visiting their respective institutions. We also thank Christine Rollard and Yvan Montardi for sharing images of the *K. amblycyphus* comb. nov. lectotype. Janet Beccaloni and Nikolaj Scharff hosted both authors at a number of occasions in London and Copenhagen, respectively. Nikolaj also provided in-depth insights into araneid phylogeny and systematics.

Funding for revisions of the Australian Araneidae was provided by the Australian Biological Resources Study (ABRS) (grant no. 205-24 [2005–2008] to VWF and N. Scharff and grant number 4-EHPVRMK [2021–2023] to VWF, PSC, N. Scharff, D. Dimitrov, A. Chopra and R. Baptista). Additional funding was provided by a Synthesis project grant (GB-TAF-TA3-008) to PdSC to visit the NHMUK in London.

References

Bonnet P (1955) Bibliographia araneorum. Analyse méthodique de toute la littérature aranéologique jusqu'en 1939. Tome II. Systématique des araignées (Étude par ordre alphabétique) [1re partie: A–B]. Douladoure, Toulouse, 1–918.

Castanheira P de S, Framenau VW (2022) *Quokkaraneus*, a new monotypic genus of Australian orb-weaving spider (Araneae, Araneidae). Australian Journal of Taxonomy 10: 1–9. https://doi.org/10.54102/ajt.a7oq2

Castanheira P de S, Framenau VW (2023) *Abba*, a new monotypic genus of orb-weaving spiders (Araneae, Araneidae) from Australia. Evolutionary Systematics 7(1): 73–81. https://doi.org/10.3897/evolsyst.7.98015

Ferreira-Sousa L, Motta PC (2022) Diagnostic notes on the spider orb-weaving genera *Carepalxis* and *Ocrepeira* (Araneae: Araneidae), with description of three new species from Central Brazil. Zootaxa 5087(2): 389–399. https://doi.org/10.11646/zootaxa.5087.2.9

Framenau VW (2011) *Lariniophora*, a new monotypic orb-weaving spider genus from Australia (Araneae: Araneidae: Araneinae). Records of the Western Australian Museum 26(2): 191–201. https://doi.org/10.18195/issn.0312-3162.26(2).2011.191-201

Framenau VW, Castanheira P de S (2022) Revision of the new Australasian orb-weaving spider genus *Salsa* (Araneae, Araneidae). ZooKeys 1102: 107–148. https://doi.org/10.3897/zookeys.1102.82388

Framenau VW, Kuntner M (2022) The new Australian leaf-curling orb-weaving spider genus *Leviana* (Araneae, Araneidae). Evolutionary Systematics 6(2): 103–133. https://doi.org/10.3897/evolsyst.6.83573

Framenau VW, Dupérré N, Blackledge TA, Vink CJ (2010) Systematics of the new Australasian orb-weaving spider genus *Backobourkia* (Araneae: Araneidae: Araneinae). Arthropod Systematics & Phylogeny 68: 79–111.

Framenau VW, Baptista RLC, Oliveira FSM, Castanheira P de S (2021a) Taxonomic revision of the new spider genus *Hortophora*, the Australasian Garden Orb-weavers (Araneae, Araneidae). Evolutionary Systematics 5(2): 275–334. https://doi.org/10.3897/evolsyst.5.72474

Framenau VW, Vink CJ, Scharff N, Baptista RLC, Castanheira P de S (2021b) Review of the Australian and New Zealand orb-weaving spider genus *Novakiella* (Araneae, Araneidae). Zoosystematics and Evolution 97(2): 393–405. https://doi.org/10.3897/zse.97.67788

Framenau VW, Castanheira P de S, Vink CJ (2022) Taxonomy and systematics of the new Australo-Pacific orb-weaving spider genus *Socca* (Araneae: Araneidae). New Zealand Journal of Zoology 49: 263–334. https://doi.org/10.1080/03014223.2021.2014899

Joseph MM, Framenau VW (2012) Systematic review of a new orb-weaving spider genus (Araneae: Araneidae), with special reference to the Australasian-Pacific and South-East Asian fauna. Zoological Journal of the Linnean Society 166(2): 279–341. https://doi.org/10.1111/j.1096-3642.2012.00845.x

Kallal RJ, Hormiga G (2018) Systematics, phylogeny and biogeography of the Australasian leaf-curling orb-weaving spiders (Araneae: Araneidae: Zygiellinae), with a comparative analysis of retreat evolution. Zoological Journal of the Linnean Society 184(4): 1055–1141. https://doi.org/10.1093/zoolinnean/zly014

Keyserling E (1886) Die Arachniden Australiens nach der Natur beschrieben und abgebildet. Bauer & Raspe, Nürnberg.

Levi HW (1992) The American species of the orb-weaver genus *Carepalxis* and the new genus *Rubrepeira* (Araneae: Araneidae). Psyche, Cambridge 98(2–3): 251–264. https://doi.org/10.1155/1991/26493

Rack G (1961) Die Entomologischen Sammlungen des Zoologischen Staatsinstituts und Zoologischen Museums Hamburg. 2. Teil, Chelicerata 11: Araneae. Mitteilungen aus dem Hamburgischen Zoologischen Museum und Institut 59: 1–60.

Rainbow WJ (1911) A census of Australian Araneidae. Records of the Australian Museum 9(2): 107–319. https://doi.org/10.3853/j.0067-1975.9.1911.928

Scharff N, Coddington JA (1997) A phylogenetic analysis of the orb-weaving spider family Araneidae (Arachnida, Araneae). Zoological Journal of the Linnean Society 120(4): 355–434. https://doi.org/10.1111/j.1096-3642.1997.tb01281.x

Scharff N, Coddington JA, Blackledge TA, Agnarsson I, Framenau VW, Szűts T, Hayashi CY, Dimitrov D (2020) Phylogeny of the orb-weaving spider family Araneidae (Araneae: Araneoidea). Cladistics 36(1): 1–21. https://doi.org/10.1111/cla.12382

Simon E (1908) Araneae, 1re partie. In: Die Fauna Südwest-Australiens. Ergebnisse der Hamburger südwest-australischen Forschungsreise 1905 (ed. W. Michaelsen, R. Hartmeyer). Verlag von Gustav Fischer, Jena, 359–446.

World Spider Catalog (2023) World Spider Catalog Version 23.5. [Available from:] http://wsc.nmbe.ch [21 April 2023]

Yin CM, Wang JF, Zhu MS, Xie LP, Peng XJ, Bao YH (1997) Fauna Sinica: Arachnida: Araneae: Araneidae. Science Press, Beijing, 460 pp.

Zoosyst. Evol. 99 (2) 2023, 325–335 | DOI 10.3897/zse.99.103061

PENSOFT

MUSEUM FÜR NATURKUNDE BERLIN

A review of the genus *Sernokorba* Kamura, 1992 (Araneae, Gnaphosidae)

Nikolett Gallé-Szpisjak[1], Róbert Gallé[1,2], Tamás Szűts[3]

1 *ELKH Centre for Ecological Research, Lendület Landscape and Conservation Ecology Research Group, Alkotmány út 2-4. Vácrátót, 2163, Hungary*

2 *MTA-SZTE 'Momentum' Applied Ecology Research Group, Közép fasor 52, Szeged, 6726 Hungary*

3 *Department of Ecology, University of Veterinarian Medicine Budapest, Rottenbiller u. 50, Budapest, 1077, Hungary*

https://zoobank.org/8ABCBDD1-84C8-4761-8A6E-85EBF34D1507

Corresponding author: Nikolett Gallé-Szpisjak (szpisjak.nikolett@ecolres.hu)

Academic editor: Danilo Harms ♦ **Received** 6 March 2023 ♦ **Accepted** 16 May 2023 ♦ **Published** 2 June 2023

Abstract

The gnaphosid spider genus *Sernokorba* Kamura, 1992 is reviewed. While *Sernokorba pallidipatellis* (Bösenberg and Strand 1906) and *Sernokorba fanjing* Song, Zhu & Zhang, 2004, occur in the Far East and the Japanese archipelago, *Sernokorba tescorum* (Simon, 1914) is known from Europe. We here describe a fourth species, *Sernokorba betyar* **sp. nov.** (male and female) from the forest steppe vegetation in southern Hungary in Central Europe. Digital images, comparative drawings (except for *S. fanjing*) and a distribution map are provided for all the species, and an identification key is compiled. The cheliceral dentation as diagnostic character and its interpretation are discussed.

Key Words

Central Europe, forest steppe, identification key, new species, spider

Introduction

Kamura (1992) described the monotypic ground spider genus *Sernokorba* to accommodate *Prosthesima pallidipatellis* Bösenberg & Strand, 1906 from Japan, which was at that time placed in *Zelotes* Gistel, 1848, since it lacks the preening comb on metatarsi III–IV characteristic of the genus. The species occurs also in China (Song et al. 1999), Korea (Namkung 2002) and Russian Far East (Marusik 2009). According to Kwon et al. (2014), this ground-dwelling species occurs in a wide variety of habitats, in forests, vineyards and grasslands. Currently, three species of the genus are known. The second species, *Sernokorba fanjing* Song, Zhu & Zhang, 2004 was described from Mt. Fanjing, Guizhou, China.

The third species occurs in Europe. It was originally described as *Poechilochroa tescorum* Simon, 1914 on the basis of a female specimen. In their recent study, Cornic and Ledoux (2013) revised the species, described the male and proposed a new combination, *Sernokorba tescorum* (Simon, 1914). The species has been collected in nine locations in southern France, in grasslands and pine forests on calcareous soil. Later, Hernandez-Corral et al. (2017) and Breitling (2018) provided new occurrence data from the Iberian Peninsula, from a *Quercus rotundifolia*, Lamarck forest and a dry grassland, respectively. Naumova et al. (2021) reported the species from Bulgaria, from the leaf litter of a mixed forest of *Fagus sylvatica*, Linnaeus and *Pinus heldreichii,* Christ. In this paper we report, describe and illustrate *Sernokorba* specimens from Hungary for the first time, belonging to a hitherto unknown species, which we hereby describe as new to science. We provide an identification key, and illustrate occurrences of the genus, except for *S. fanjing*.

Materials and methods

The specimens of the new species were collected in the calcareous sand-dune area of the Kiskunság, central Hungary. The region belongs to the forest steppe zone, the transitional biome between the temperate deciduous forest and the steppe zones in Eurasia (Gallé et al. 2022a). The region has a semiarid continental climate, as the mean annual precipitation is between 500–550 mm and the annual temperature is between 10 °C and 12 °C (Gallé et al. 2022a). The calcareous soil is poor in organic matter (Tölgyesi et al. 2018). The forest steppe vegetation appears as a mosaic of (1) open dry grasslands: brome sward (*Brometum tectorum*), caliciphilous festuca steppe (*Festucetum vaginateae*) and Pannonian sand grassland (*Potentillo-Festucetum pseudovinae*), (2) wind-grooves between the sand dunes: more humid, with dune-slack purple moorgrass meadow (*Molinio-Salicetum rosmarinifoliae*) as main vegetation type, and (3) small forest patches of native arboreal plants such as *Populus alba*, *Crataegus monogyna* and *Juniperus communis*. Spiders were sampled with funnel traps (Császár et al. 2018), near Fülöpháza in an intact forest steppe fragment, approximately 3.3 km^2 (46°52'N, 19°24'E, Figs 1–4). A total of 10 sites were established, and in each site, three habitat types (grassland, forest and forest edge) were sampled with four traps in each habitat. Samplings were done between 18 May and 12 June 2014. We collected 21 out of the 28 specimens in the forest edges.

Type material of the new species will be deposited in the Hungarian Museum of Natural History, Budapest (HMNH, curator: E. Deákné Lazányi-Bacsó). A male of *S. tescorum* has been kindly loaned to us by Antonio Melic (Sociedad Entomológica Aragonesa: PCAM). Specimens of *S. pallidipatellis* have been kindly donated to HNHM (Hungarian Natural History Museum, Budapest,) by Prof. Takahide Kamura (Otemon Gakuin University). We did not have access to specimens of *S. fanjing*.

Specimens were photographed using a Nikon D300S camera and a Tucsen TrueChrome Metrics camera attached to a Nikon S800 stereomicroscope and a Nikon Eclipse E200 compound microscope at the Department of Ecology, University of Veterinarian Medicine Budapest. Digital multifocal images were assembled using HeliconFocus image stacking software. Epigynes were removed and illustrations of them were made after a day-long maceration in commercial pancreatic enzyme solution. Palps were examined immersed in methyl-salicylate and mounted in a slightly modified Coddington mount (Coddington 1983). We modified the mount as the coverslip is not horizontal, but touching the slide itself, thus creating a triangle allowing more precise manipulation and more stable fixation of the object. Illustrations of the new species, *S. tescorum* and *S. pallidipatellis* were redrawn from digital images, while for *S. fanjing* they were produced from the figures of the original description (Song et al. 2004). We used Adobe Illustrator CS6 vector graphics software. We illustrated the distribution of the Sernokorba species with Google Earth satellite images, and Adobe Photoshop CS6 software.

Measurements are given in mm. Lengths of leg segments and total length were measured on the dorsal view. Leg formula developed by Ono (1988) is used; lengths of leg segments are given as: total length (femur, patella, tibia, metatarsus, tarsus).

Abbreviations

AME	anterior median eyes;
d	dorsal;
p	prolateral;
r	retrolateral;
RTA	retrolateral tibial apophysis;
v	ventral.

Results

Key to the species

1 Females 2
– Males 5
2 Copulatory openings well visible (Figs 46, 47) ..... *Sernokorba fanjing*
– Copulatory openings not clearly visible (Figs 40–45) 3
3 Spermathecae relatively small (i.e., ~50% of the height of the vulva); sperm ducts straight (Figs 44, 45) ..... *Sernokorba pallidipatellis*
– Spermathecae relatively large (i.e., over 70% of the height of the vulva); sperm ducts with a proximal characteristic switchback (Figs 40–43) 4
4 Lateral edge of spermatheca with an angular posterior edge (Figs 28, 40, 41) ..... *Sernokorba betyar* sp. nov.
– Lateral edge of spermatheca round (Figs 42, 43) ..... *Sernokorba tescorum*
5 Embolar tip slightly bent (Figs 23, 33, 34) ..... *Sernokorba pallidipatellis*
– Embolar tip straight (Figs 20–22, 29–32) 6
6 Conductor blunt (Figs 29, 30, 35, 36), spermophore strongly bent as seen in retrolateral view, ventral bump on the RTA absent (Figs 13, 30) ..... *Sernokorba tescorum*
– Conductor with fin-like branches (Figs 17–19, 31, 32, 37, 38), spermophore almost straight as seen in retrolateral view, ventral bump on the RTA present (Figs 14, 15, 32) ..... *Sernokorba betyar* sp. nov.

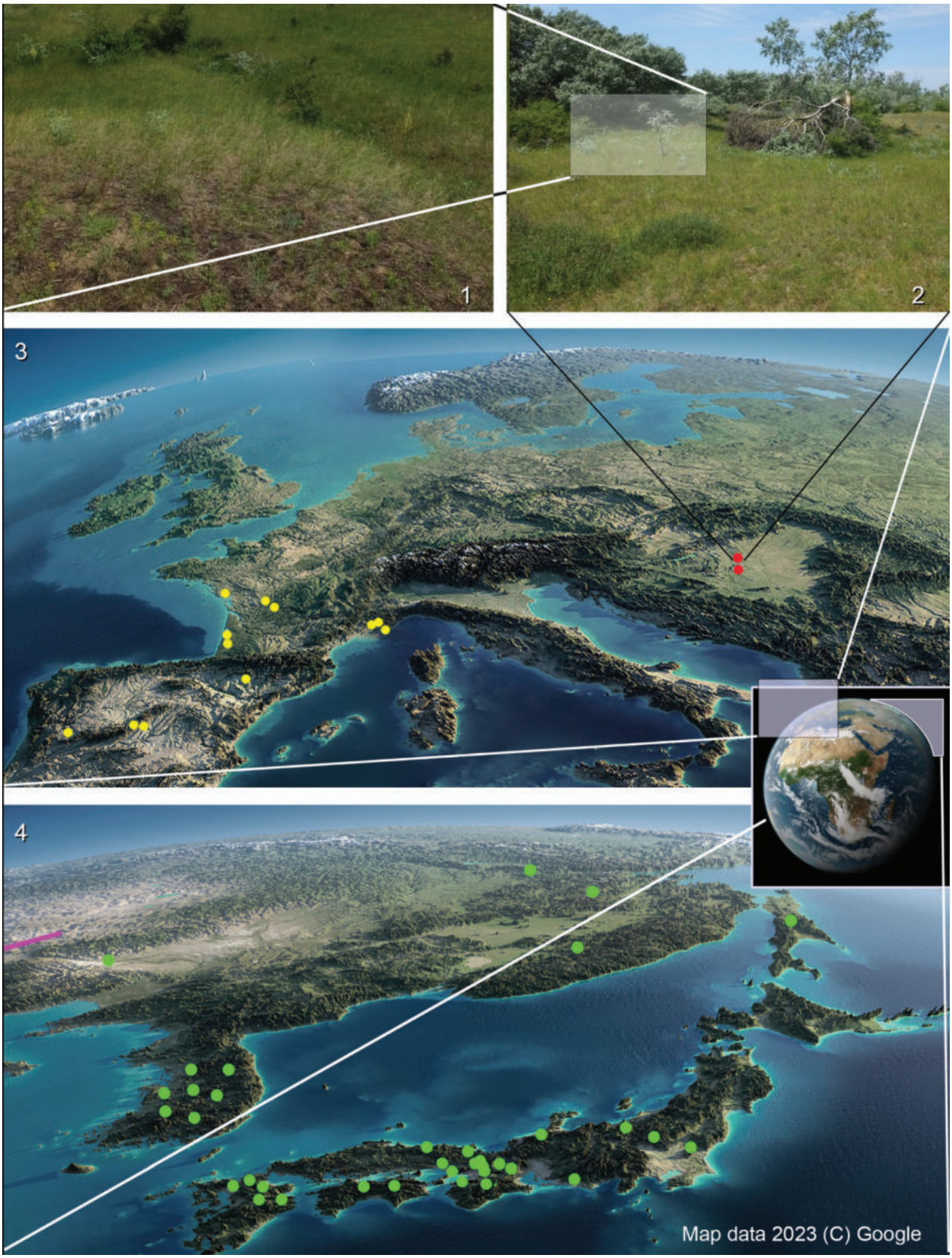

Figures 1–4. The habitat and distribution of *Sernokorba* species; **1, 2.** Habitat of *S. betyar* in Fülöpháza (Hungary); **3.** Occurrences in Europe, red dots: *S. betyar*, yellow dots: *S. tescorum*; **4.** Occurrences in Asia, green dots: *S. pallidipatellis*.

Taxonomy

Subfamily: Herpyllinae Platnick, 1990 (type genus *Herpyllus* Hentz, 1832)

Genus *Sernokorba* Kamura, 1992

Diagnosis. The genus is a members of the Herpylline group (Azevedo et al. 2018), with a conspicuous black and white abdominal pattern (Figs 5–7). Males can be recognized by the following combination of characters: a single RTA that is about as long as the cymbium, thin, slightly bent, evenly narrowing terminally, and with a hook–shaped end (Figs 13–16). The conductor is about as long or longer than the tegulum, not twisted around the embolus (Figs 9–11, 13–15, 29, 31, 33). Females can be recognized by the kidney–shaped spermathecae (Figs 40, 42) and the sperm ducts being as long as the height of the spermathecae (Figs 40, 42, 44, 46).

Description. See Kamura (1992). Furthermore, males in all the three examined species have a characteristic apical depression on the retrolateral side of gnathocoxae (Fig. 8), which females do not have (Kamura 1992: fig. 4, Murphy 2007: 296, 310). This sexually dimorphic character, was not mentioned in the original descriptions of *S. pallidipatellis* and *S. tescorum*, or in the description of the genus itself.

Distribution. The genus has been reported from East Asia (Korea, China, Russia and Japan) and from Western, Central and Southern Europe.

Type species. *Prosthesima pallidipatellis* Bösenberg & Strand, 1906 – by original designation by Kamura (1992); female holotype from Japan: Saga Pref., in Senckenberg Museum, Frankfurt am Main – not examined.

Sernokorba pallidipatellis (Bösenberg & Strand, 1906)

Figs 12, 16, 23, 33, 34, 39, 44, 45, 48–50

Remark. As mentioned by Kamura (1992), *Herpyllus coreanus* Paik, 1992 is most likely conspecific with *S. pallidipatellis*; however, we do not propose a formal synonymy as we did not examine the type specimen of *H. coreanus*.

Material examined. Japan: **Kyoto** 1 male, Kyoto-shi, Sakyo-ku, Matsugasaki, 28. April –5. May 1982 pitfall trap T. Kamura leg. (HNHM Araneae-9237); Japan: **Osaka** 1 male, Ibaraki-shi, Nishi-Ai, 26. May 1995 T. Kamura leg. (HNHM Araneae-9233); Japan: **Osaka** 1 female, Ibaraki-shi, Ai, 30. May 1997 T. Kamura leg. (HNHM Araneae-9219); Japan: **Osaka** 1 female, Ibaraki-shi, Nishi-Ai, 9. May 2003 T. Kamura leg. (HNHM Araneae-9007).

Diagnosis. Males can be recognized by the slightly bent embolar tip (Figs 23, 33) and by the large conductor reaching the tip of the embolus (Figs 33–34). Distal tip of the conductor is blunt and triangular. RTA with a ventral bump and bearing a distal invagination, resulting in two subequal branches.

Description. See Kamura (1992).

Distribution. Japan, Korea and the Russian Federation.

Figures 5–8. European *Sernokorba* species; **5.** *Sernokorba tescorum*, male habitus, dorsal view; **6–8.** *Sernokorba betyar* sp. nov.; **6.** Female habitus, dorsal view; **7.** Male habitus, dorsal view; **8.** Male, gnathocoxae, ventral view. Scale bars: 1.0 mm.

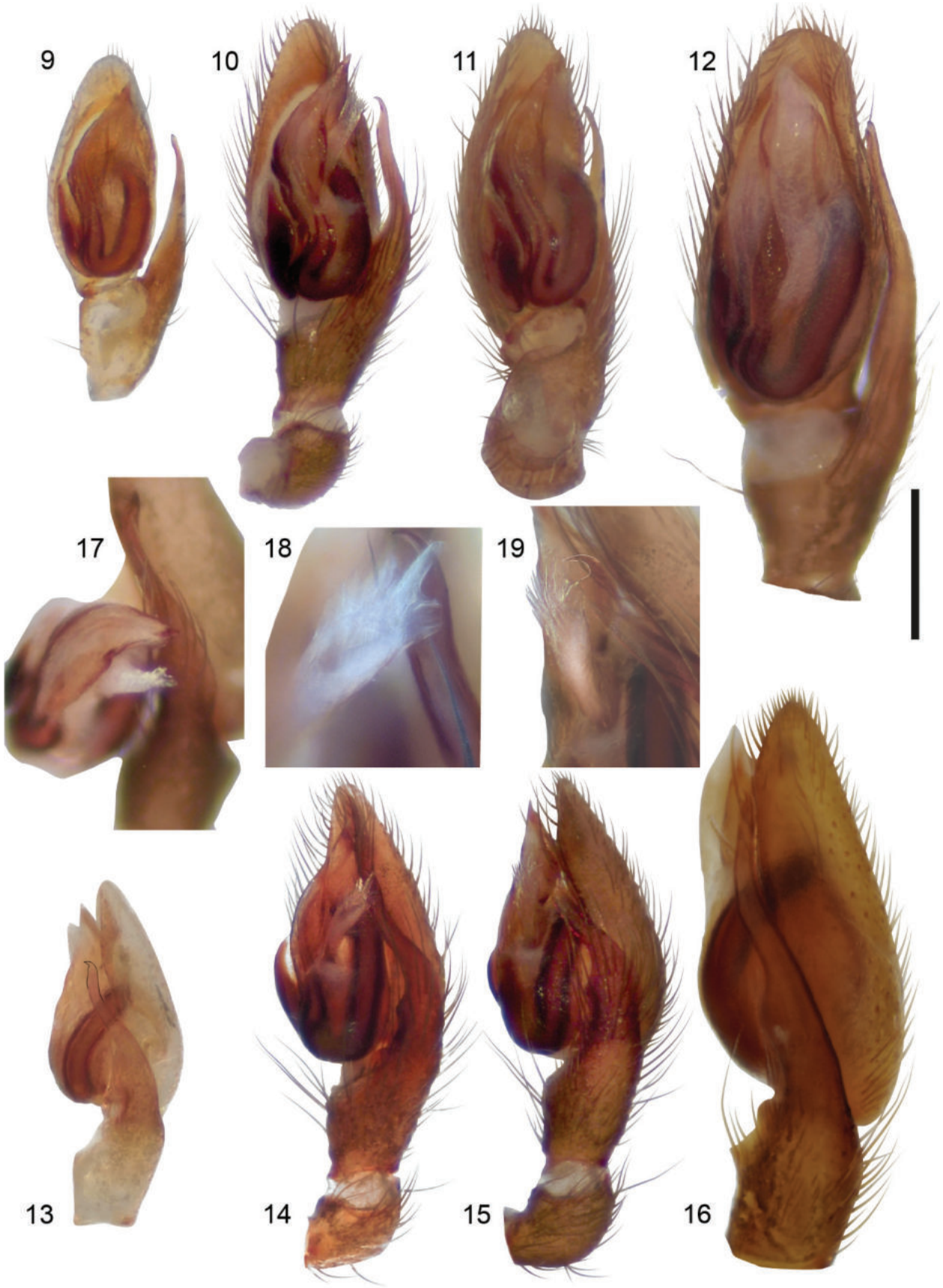

Figures 9–19. Palp comparison of the *Sernokorba* species; **9, 13.** *Sernokorba tescorum* **9.** Ventral view; **13.** Retrolateral view; **10, 11, 14, 15, 17–19.** *Sernokorba betyar* sp. nov. **10.** Ventral view; **11.** Proventral view; **14, 15.** Retrolateral view; **17.** Partially expanded palp, showing the conductor details, retrolateral view; **18.** Conductor closeup, retrolateral view; **19.** Slightly different angle; **12, 16.** *Sernokorba pallidipatellis*; **12.** Ventral view; **16.** Retrolateral view. Scale bar: 0.25 mm.

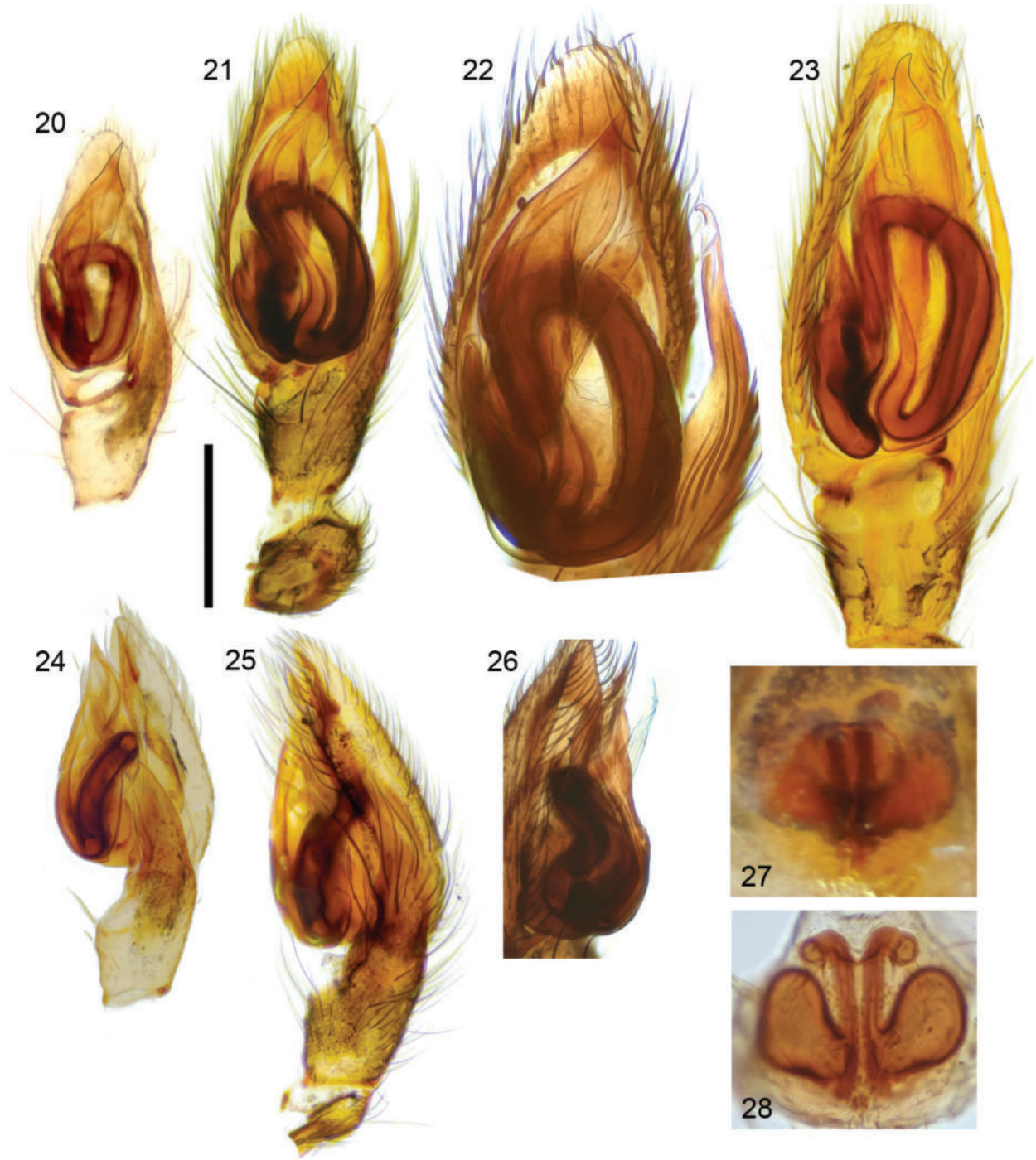

Figures 20–28. Cleared copulatory organs; **20, 24.** *Sernokorba tescorum*; **20.** Ventral view; **24.** Retrolateral view; **21, 22, 25–28.** *Sernokorba betyar* sp. nov.; **21, 22.** Ventral view; **25.** Retrolateral view; **26.** Prolateral view; **27.** Epigyne, ventral view; **28.** Vulva, dorsal view; **23.** *Sernokorba pallidipatellis*, ventral view. Scale bar: 0.25 mm.

***Sernokorba tescorum* (Simon, 1914)**

Figs 5, 9, 13, 20, 24, 29, 30, 35, 36, 42, 43

Remark. This species was recently reported from the Balkans, Bulgaria (Naumova et al. 2021). Fortunately, the record is accompanied with high quality images, and it is clear that the specimen shows some differences (i.e., in size of the cymbium, shape of the cymbium, the absence of clear finger–like extensions, and the coil shape of the spermophore) from the new species. However, we do not suggest any identification without examining the specimen itself.

Material examined. Spain: **Cantoblanco**: 1 male, Monte de Valdelatas Madrid. UTM: 30TVK4287, 40°32'11.5"N, 3°41'05.0"W, 700 m, 2002 May 27. A. Jiménez leg. (PCAM 5949).

Diagnosis. Abdominal pattern consists of three pairs of elongated white spots. Males have blunt conductor (Figs 9, 29, 35, 36). The female is very similar to that of the new species, but can be differentiated by the round spermathecae (Figs 42, 43).

Description. See Hernández-Corral et al. (2017) and Cornic and Ledoux (2013).

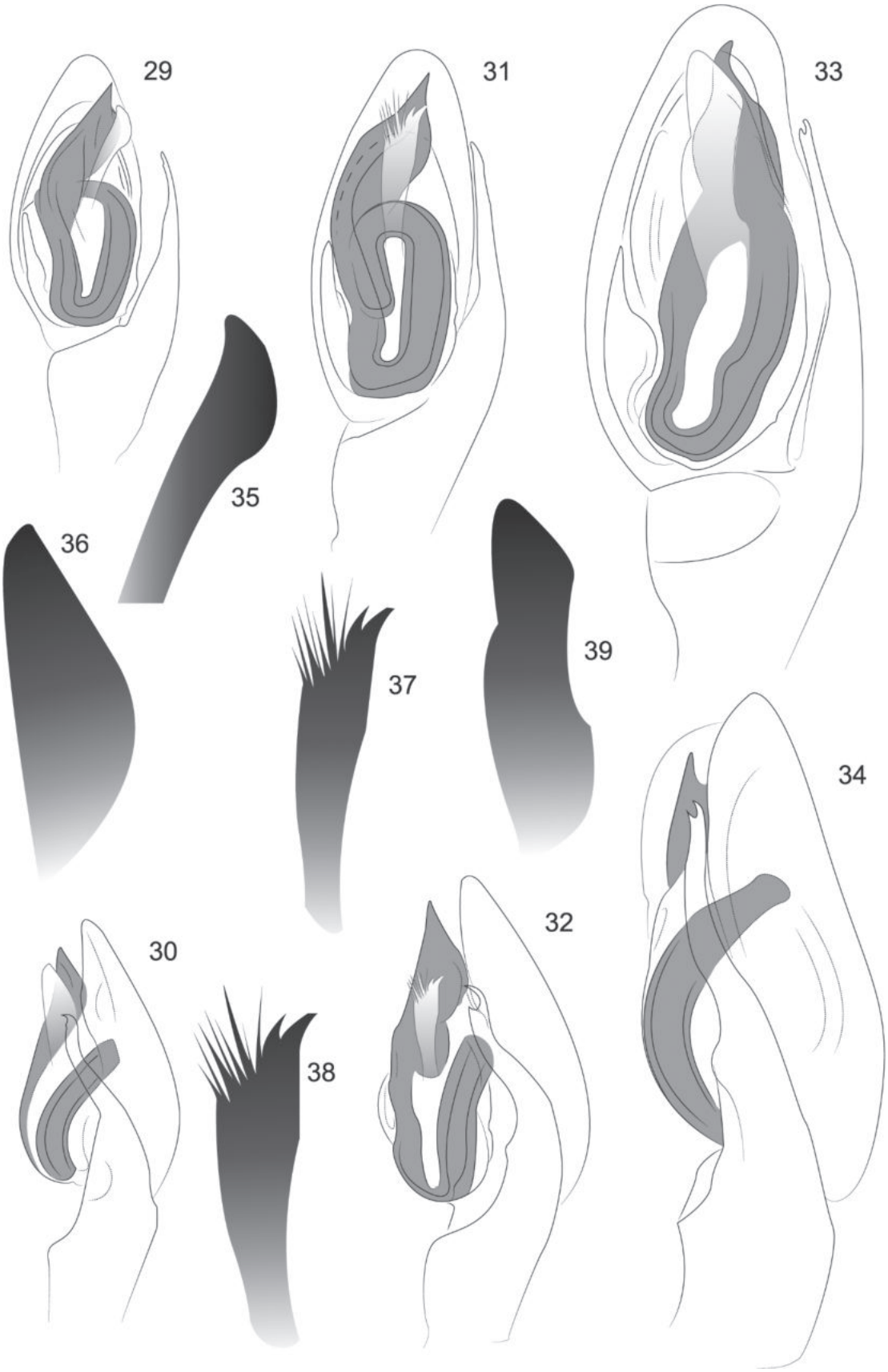

Figures 29–39. Illustrations of the male copulatory organs; **29, 30, 35, 36.** *Sernokorba tescorum*; **29.** Male copulatory organ ventral view; **30.** Male copulatory organ, retrolateral view; **35.** Conductor ventral view; **36.** Conductor retrolateral view; **31, 32, 37, 38.** *Sernokorba betyar* sp. nov.; **31.** Male copulatory organ ventral view; **32.** Male copulatory organ retrolateral view; **37.** Conductor ventral view; **38.** Conductor retrolateral view; **33, 34, 39.** *Sernokorba pallidipatellis*; **33.** Male copulatory organ ventral view; **34.** Male copulatory organ retrolateral view; **39.** Conductor ventral view.

Distribution. France, Spain and Bulgaria (Naumova et al. 2021; Nentwig et al. 2022). A combination of all the published occurrences until 2020 (Cornic and Ledoux 2013; Hernández-Corral et al. 2017; Breitling 2018) is shown in fig. 3.

Sernokorba betyar sp. nov.

https://zoobank.org/FD527ED0-2148-47D0-8E28-22B555FC37E3

Figs 6–8, 10, 11, 14, 15, 17–19, 21, 22, 25–28, 31, 32, 37, 38, 40, 41, 51, 52

Type material. ***Holotype*:** Hungary: **Fülöpháza:** male (46°51'55.00"N, 19°24'27.18"E) forest edge, pitfall trap, 1–10. June 2014, R. Gallé & N. Gallé-Szpisjak leg. (HNHM Araneae-9230).

***Paratypes*:** Hungary: **Tázlár:** 1 male, 46°30'27.62"N, 19°30'2.22"E, forest edge, pitfall trap, 1–10. June 2014, R. Gallé & N. Gallé-Szpisjak leg. (HNHM Araneae-9229); Hungary: **Fülöpháza:** 1 female 46°52'47.57"N, 19°24'17.36"E, forest edge, pitfall trap, 1–10. June 2014, R. Gallé & N. Gallé-Szpisjak leg. (HNHM Araneae-9228); Hungary: **Fülöpháza:** 2 male, 46°52'46.93"N, 19°24'43.59"E, forest edge, pitfall trap, 18–25. May 2014 R. Gallé & N. Gallé-Szpisjak leg. (HNHM Araneae-9231); Hungary: **Fülöpháza:** 1 female 46°53'13.61"N, 19°24'33.89"E, forest edge, pitfall trap, 18–25. May 2014 R. Gallé & N. Gallé-Szpisjak leg. (HNHM Araneae-9241); Hungary: **Fülöpháza:** 1 male, 46°52'9.10"N, 19°24'56.25"E, forest edge, pitfall trap, 18–25. May 2014 R. Gallé & N. Gallé-Szpisjak leg. (HNHM Araneae-9238).

Other material examined. Hungary: **Tázlár:** 1 male, 1 female, 46°31'7.83"N, 19°31'10.80"E, forest edge, pitfall trap 1–10. June 2014 R. Gallé & N. Gallé-Szpisjak leg.; Hungary: **Fülöpháza:** 1 male, 1 female, 46°52'15.25"N, 19°24'29.06"E, forest edge, pitfall trap, 18–25. May 2014 R. Gallé & N. Gallé-Szpisjak leg. (HNHM Araneae-9208).

Diagnosis. The male can be identified by the finger–like extensions on the tip of the conductor (Figs 37, 38), and by the almost straight spermophore as seen from the retrolateral side (Fig 25, 32). Also, the male has an apical ectal depression on the gnathocoxae (Fig. 8), similar to that of *S. tescorum*. The female can be distinguished by the edge of the spermathecae: the lateral edge is more or less straight (vs. rounded in *S. tescorum*) and the posterior edge is concave (vs. convex in *S. tescorum*). Also, it can be distinguished by the deep atrial pockets (Figs 27, 28, 40, 41) opposed to the shallow atrial pokets of the *S. tescorum*.

Description. Male (Holotype; HNHM Araneae-9230). Colour. Carapace light brown with pale brown radiating stripes, covered with white fine setae (Fig. 7); thoracic groove dark brown (Fig. 7). Chelicerae pale brown (Fig. 7). Gnathocoxae brown with a dark brown outline; terminal part in ventral view pale yellow. Labium brown (Fig. 8). Sternum brown with radial light brown spots, posterior end dark brown. Trochanter I brown, all other trochanters pale yellow. All femora dark brown; all other leg segments pale yellow. Abdomen dark greyish brown with a reddish scutum; an anterior transverse line and two pairs of whitish spots present in the area of the scutum; anterior pair of spots placed closer to the midline, posterior pair situated laterally. Venter light greyish yellow, with two thin longitudinal stripes starting at epigastric furrow and extending towards spinnerets. Epigastric area yellowish–brown. Sides of abdomen dark brown. Spinnerets' proximal segments dark brown/black, distal part pale yellow.

Carapace suboval, cephalic region much narrower (about 40% of maximal width), posterior region truncated (Fig. 7) and elevated, about twice as high as in front. Chelicerae thin, with one tooth on promargin and two teeth on retromargin. Gnathocoxae with an oblique depression on the lateral margin (Fig. 8). Sternum longer than wide. Labium as long as wide (Fig. 8), triangular. Clypeus low, about the diameter of AME high. Abdomen ovoid, longer than wide, truncated in front, with scutum covering 60% of the dorsum (Fig. 5). Total length, not including spinnerets, 4.32. Carapace 1.35 long, 0.98 wide, 0.41 high, highest at coxae III, widest at coxae II. Abdomen 2.72 long, 0.87 wide, with large bristles on proximal margin. Clypeus low, 0.10.

Leg measurements: I 3.05 (1.01, 0.42, 0.65, 0.51, 0.46); II 3.00 (0.99, 0.43, 0.63, 0.48, 0.47); III 2.89 (0.94, 0.39, 0.63, 0.47, 0.46); IV 3.99 (1.07, 0.57, 0.82, 1.0, 0.53). Leg formula IV-I-II-III.

Leg spination: I: femur d 1-1-1, p 0-0-1; tibia v 0-1-1. II: femur d 1-1-1, p 0-0-1; tibia v 0-1-1. III: femur d 1-1-1, p 0-0-1, r 0-0-1; patella p1, r1; tibia p 0-1-1 v 0-1-1, r 0-1-1; metatarsus p 0-1-2, r 0-0-2, v 0-0-1. IV: femur d 1-1-1, p 0-0-1, r 0-0-1; tibia d 0-1-0, p 1-1-1, v 1-1-1, r 0-1-1; metatarsus p 1-2-2, v 1-0-0, r 1-1-2.

Palp: Tibia longer than wide, RTA about 70% at cymbium's length (Figs 10, 11, 21, 22, 25), thin, bent in its middle and with an apical hook (Figs 14, 15, 32); spermophore U–shaped, proximal part of tegulum is tight (Figs 10, 11, 21, 22) (vs. loose in that of *S. tescorum*, as shown in Figs 9, 20). Spermophore bent slightly in retrolateral view (Figs 15, 25). Conductor membranous, with finger-like extensions (Figs 17–19, 31, 32, 37, 38).

Female (Paratype; HNHM 9241). Coloration as in male, except carapace and abdomen lighter (Fig. 6). Epigastric area yellowish–dark grey. Shape of carapace and abdomen (Fig. 6) as in males, except for absence of abdominal scutum. Total length, not including spinnerets, 4.04. Carapace 1.98 long, 1.50 wide, 0.57 high. Abdomen 3.58 long, 2.03 wide, 1.19.

Leg measurements: I 4.19 (1.45, 0.58, 0.82, 0.74, 0.60); II 4.13 (1.43, 0.57, 0.80, 0.75, 0.58); III 4.11 (1.30, 0.54, 0.81, 0.89, 0.57); IV 5.67 (1.65, 0.63, 1.21, 1.45, 0.73). Leg formula. IV-I-II-III.

Leg spination: I: femur d 1-1-1, p 0-0-1; tibia v 0-1-1. II: femur d 1-1-1, p 0-0-1; tibia v 0-1-1. III: femur d 1-1-1, p 0-0-1, r 0-0-1; patella p1, r1; tibia d 1-0-0, p 1-1-1 v 1-1-1, r 0-1-1; metatarsus d 0-1-1, p 0-1-1, r 0-1-1, v 1-0-1. IV: femur d 1-1-1, p 0-0-1, r 0-0-1; tibia d 1-0-0, p 1-1-1, v 1-1-2, r 0-1-1; metatarsus p 1-2-2, v 1-1-1, r 1-2-2.

Epigyne: copulatory openings positioned medially on anterior part; copulatory ducts short; spermathecae robust and pear-shaped.

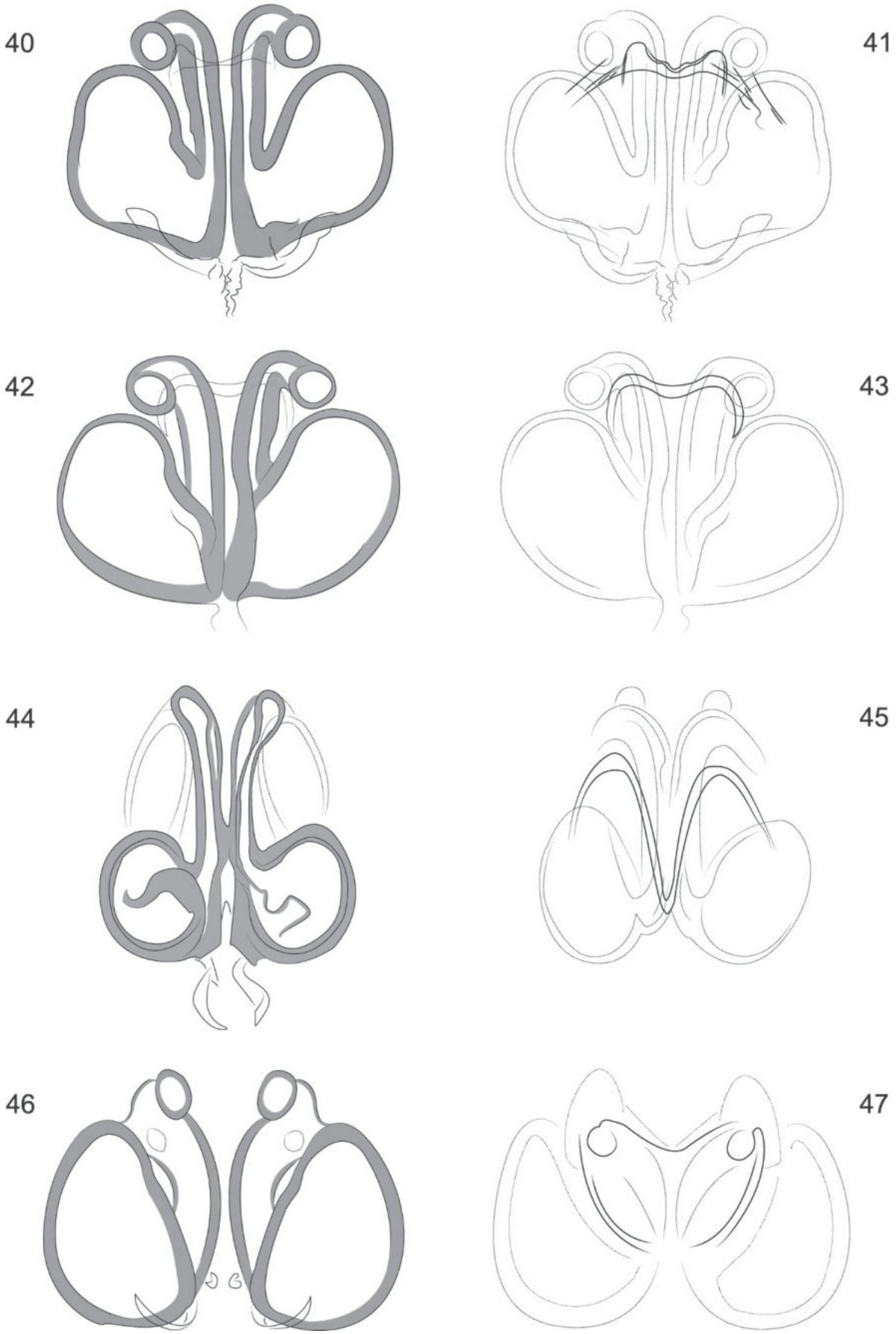

Figures 40–47. Illustrations of the female genitalia; **40, 41** *Sernokorba betyar* sp. nov.; **40.** Dorsal view; **41.** Ventral view; **42, 43.** *Sernokorba tescorum*; **42.** Dorsal view; **43.** Ventral view; **44, 45.** *Sernokorba pallidipatellis*; **44.** Dorsal view; **45.** Ventral view; **46, 47.** *Sernokorba fanjing*; **46.** Dorsal view; **47.** Ventral view.

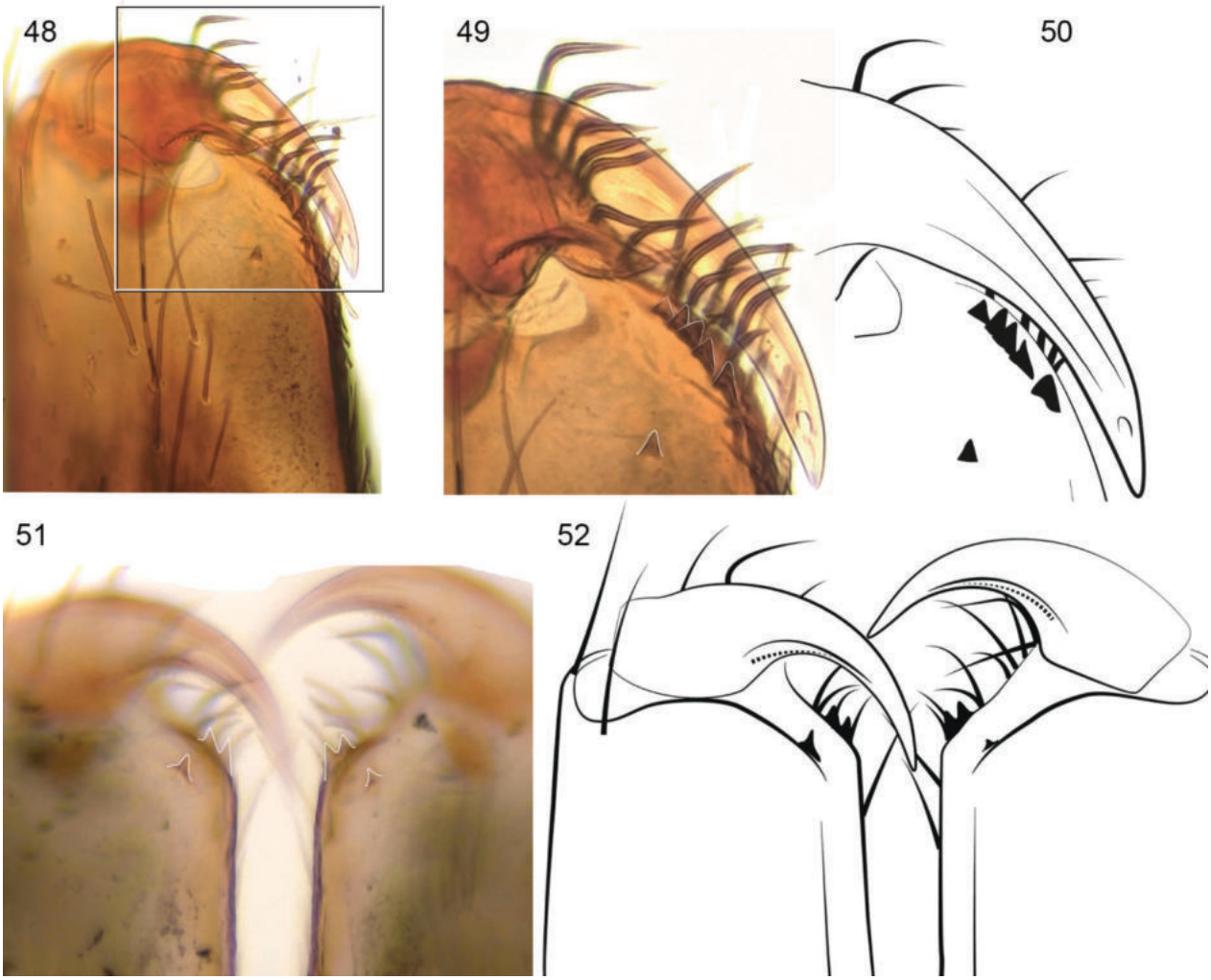

Figures 48–52. Male chelicerae; **48–50.** *Sernokorba pallidipatellis*; **51, 52.** *Sernokorba betyar* sp. nov.

Etymology. The specific name is a Hungarian noun in apposition and refers to the outlaws "betyár" found in hiding places on the Hungarian Great Plain, just as this species has been avoiding its discovery so far.

Distribution. Bács-Kiskun county, Forest steppes, Hungary.

Discussion

In the genus description of *Sernokorba*, Kamura (1992) mentioned concerning *S. pallidipatellis*: "I recognized that this species is unique in having a serrated carina on the promargin of fang furrow of chelicera", unequivocally illustrated (Kamura 1992: fig. 3), and used in this sense by subsequent authors (Song et al. 2004; Kim and Lee 2013) for *S. fanjing* and *S. pallidipatellis*. However, Cornic and Ledoux (2013) reports teeth, but only on the promargin: "Marge antérieure des chélicères garnie de trois dents, marge postérieure mutique". We compared the dentation of specimens of *S. pallidipatellis* (Figs 48–50) to both literature images and to that of *S. betyar* sp. nov. (Figs 51, 52). The cheliceral dentation of *S. pallidipatellis* (Figs 48–50) looks almost identical to literature sources (Kamura 1992: fig. 3). However, we also agree with Cornic and Ledoux (2013) and interpret it as teeth rather than a keel or carina. Azevedo et al. (2018) well illustrated the non-serrated cheliceral promargin (Azevedo et al. 2018: fig 20. e, g), which is diagnostic to the subfamily Herpyllinae. However, the keel on the promargin may not just "be a subtle projection or may appear as teeth with fused bases" (Kamura 1992). Despite Kamura's (1992) description and subsequent authors (Song et al. 2004; Kim and Lee 2013) implies the latter; we observed that the bases of the teeth are in fact separated as viewed from an oblique view (Figs 49, 50). We observed five teeth lumped together with a smaller one further placed, whereas there was one clear tooth on the retromargin. Such dentation has been observed (but not illustrated) in *Latonigena* Simon, 1893 by Ott et al. (2012), thus this character may require a second look with more genera involved. The dentation of *S. betyar* sp. nov. (i.e., two teeth on the promargin and one on the retromargin, Figs 51, 52) is different also from *S. tescorum* (i.e., three teeth on the promargin, none on the retromargin) which seems a good confirmation to separate the two species.

Species of the genus occur in a wide variety of habitats including lowland forests and grasslands, however,

specimens were collected mainly in mountainous regions (Kwon et al. 2014; Hernández-Corral et al. 2017; Naumova et al. 2021). According to our data, *S. betyar* sp. nov. is a typical member of the ground-dwelling spider fauna of lowland forest steppes. The relatively understudied forest steppes of Central Europe are among the most complex ecosystems in the region, and their nature conservation value is high. Forest steppes are important biodiversity hotspots (Gallé et al. 2022b) and listed in the Habitats Directive of the European Union. They harbour numerous endemic and rare plant and animal species, including several recently described spiders such as *Parasyrisca arrabonica* Szinetár & Eichardt, 2009 (Gnaphosidae) and *Alopecosa psammophila* Buchar, 2001 (Lycosidae). Although the abundance of *S. betyar* sp. nov. seems to be very low, this species presumably occurs in vast areas of forest steppes of Central and Eastern European forest steppes.

Acknowledgements

The study would have been impossible to carry out without the valuable help of colleagues who have sent comparative material of *S. pallidipatellis* (Takahide Kamura; Otemon Gakuin University), and *S. tescorum* (Antonio Melic; Sociedad Entomológica Aragonesa). This work was supported by the Hungarian National Research, Development and Innovation Office (Grant Id: NKFIH-FK-142926; NKFIH-KKP-133839). RG was supported by the János Bolyai Research Scholarship of the Hungarian Academy of Sciences.

References

Azevedo GHF, Griswold CE, Santos AJ (2018) Systematics and evolution of ground spiders revisited (Araneae, Dionycha, Gnaphosidae). Cladistics 34(6): 579–626. https://doi.org/10.1111/cla.12226

Bösenberg W, Strand E (1906) Japanische Spinnen. Abhandlungen der Senckenbergischen Naturforschenden Gesellschaft 30: 93–422.

Breitling R (2018) Eric Duffey's spider collection in the Manchester Museum – an update. Newsletter - British Arachnological Society 141: 5–9.

Coddington J (1983) A temporary slide mount allowing precise manipulation of small structures. Verhandlungen des naturwissenschaftlichen Vereins Hamburg 26: 291–292.

Cornic JF, Ledoux JC (2013) De araneis Galliae, III.1: *Sernokorba tescorum* (Simon, 1914). Revue Arachnologique 17(6): 83–85.

Császár P, Torma A, Gallé–Szpisjak N, Tölgyesi C, Gallé R (2018) Efficiency of pitfall traps with funnels and/or roofs in capturing ground–dwelling arthropods. European Journal of Entomology 115: 15–24. https://doi.org/10.14411/eje.2018.003

Gallé R, Tölgyesi C, Torma A, Bátori Z, Lörinczi G, Szilassi P, Gallé-Szpisjak N, Kaur H, Makra T, Módra G, Batáry P (2022a) Matrix quality and habitat type drive the diversity pattern of forest steppe fragments. Perspectives in Ecology and Conservation 20(1): 60–68. https://doi.org/10.1016/j.pecon.2021.11.004

Gallé R, Korányi D, Tölgyesi C, Lakatos T, Marcolin F, Török E, Révész K, Szabó ÁR, Torma A, Gallé-Szpijak N, Marja R, Szitár K, Deák B, Batáry P (2022b) Landscape-scale connectivity and fragment size determine species composition of grassland fragments. Basic and Applied Ecology 65: 39–49. https://doi.org/10.1016/j.baae.2022.10.001

Hernández-Corral J, Melic A, Micó E (2017) Primera cita del género *Sernokorba* Kamura, 1992 para la Península Ibérica con nuevos datos sobre *Sernokorba tescorum* (Simon, 1914) (Araneae: Gnaphosidae). Revista Iberica de Aracnologia 30: 167–169.

Kamura T (1992) Two new genera of the family Gnaphosidae (Araneae) from Japan. Acta Arachnologica 41(2): 119–132. https://doi.org/10.2476/asjaa.41.119

Kim ST, Lee SY (2013) Arthropoda: Arachnida: Araneae: Mimetidae, Uloboridae, Theridiosomatidae, Tetragnathidae, Nephilidae, Pisauridae, Gnaphosidae. Spiders. Invertebrate Fauna of Korea 21(23): 11–83.

Kwon TS, Lee CM, Kim TW, Kim SS, Sung JH (2014) Prediction of abundance of forest spiders according to climate warming in South Korea. Journal of Asia-Pacific Biodiversity 7(2): 133–155. https://doi.org/10.1016/j.japb.2014.04.002

Marusik YM (2009) A check–list of spiders (Aranei) from the Lazo Reserve, Maritime Province, Russia. Arthropoda Selecta 18: 95–109.

Murphy J (2007) Gnaphosid genera of the world. British Arachnological Society St Neots, Cambridgeshire, 605 pp.

Namkung J (2002) The spiders of Korea. Kyo-Hak Publishing Co., Seoul, 648 pp.

Naumova M, Blagoev G, Deltshev C (2021) Fifty spider species new to the Bulgarian fauna, with a review of some dubious species (Arachnida: Araneae). Zootaxa 4984(1): 228–257. https://doi.org/10.11646/zootaxa.4984.1.18

Nentwig W, Blick T, Bosmans R, Gloor D, Hänggi A, Kropf C (2022) Spiders of Europe. Version 11.2022. https://doi.org/10.24436/1

Ono H (1988) A revisional study of the spider family Thomisidae (Arachnida, Araneae) of Japan. National Science Museum, Tokyo, 252 pp.

Ott R, Rodrigues ENL, Brescovit AD (2012) Seven new species of *Latonigena* (Araneae, Gnaphosidae) from South America. Iheringia. Série Zoologia 102(2): 227–238. https://doi.org/10.1590/S0073-47212012000200016

Simon E (1914) Les arachnides de France. Synopsis générale et catalogue des espèces françaises de l'ordre des Araneae. Tome VI. 1re partie. Roret, Paris, 308 pp.

Song DX, Zhu M, Chen J (1999) The Spiders of China. Hebei Sci. Technol. Publ. House, Shijiazhuang, 640 pp.

Song DX, Zhu M, Zhang F (2004) Fauna Sinica: Invertebrata Vol. 39: Arachnida: Araneae: Gnaphosidae. Science Press, Beijing, 362 pp.

Tölgyesi C, Valkó O, Deák B, Kelemen A, Bragina TM, Gallé R, Erdős L, Bátori Z (2018) Tree–herb co–existence and community assembly in natural forest–steppe transitions. Plant Ecology & Diversity 11(4): 465–477. https://doi.org/10.1080/17550874.2018.1544674

Zoosyst. Evol. 99 (2) 2023, 337–344 | DOI 10.3897/zse.99.104613

PENSOFT

für Natur MUSEUM FÜR NATURKUNDE BERLIN

A survey of *Dysderella* Dunin, 1992 (Araneae, Dysderidae), with a new species from Iran

Alireza Zamani[1], Yuri M. Marusik[2,3], Tamás Szűts[4]

1 *Zoological Museum, Biodiversity Unit, FI-20014 University of Turku, Turku, Finland*
2 *Department of Zoology & Entomology, University of the Free State, Bloemfontein 9300, South Africa*
3 *Altai State University, Lenina Pr., 61, Barnaul, RF-656049, Russia*
4 *Department of Ecology, University of Veterinary Medicine Budapest, Rottenbiller u. 50, Budapest, 1077, Hungary*

https://zoobank.org/3A62C71E-EFF1-4D12-B7D2-15ED002A9D2E

Corresponding author: Alireza Zamani (zamani.alireza5@gmail.com)

Academic editor: Danilo Harms ♦ **Received** 5 April 2023 ♦ **Accepted** 25 May 2023 ♦ **Published** 7 June 2023

Abstract

The dysderid spider genus *Dysderella* Dunin, 1992 is surveyed. The genus currently comprises two species: *D. caspica* (Dunin, 1990) from Azerbaijan and North Caucasus and *D. transcaspica* (Dunin & Fet, 1985) from Turkmenistan and north-eastern Iran. Herein, *D. elburzica* **sp. nov.** is described based on male specimens collected in Tehran Province, northern Iran. All three species are illustrated and their distributions are mapped.

Key Words

Aranei, Caucasus, Dysderinae, Middle East, Turkmenistan, woodlouse spiders

Introduction

Dysderella Dunin, 1992, a small genus of dysderid spiders, is presently composed of only two known species, both of which were originally described in *Dysdera* Latreille, 1804. The first, *D. caspica* (Dunin, 1990), was described from Azerbaijan (Dunin 1990) and subsequently recorded from North Caucasus (Ponomarev and Alieva 2010). The second species, *D. transcaspica* (Dunin & Fet, 1985), was initially discovered in Turkmenistan (Dunin and Fet 1985) and later reported from north-eastern Iran (Zamani et al. 2015). In this study, we present a survey of this genus and describe a new species from Tehran Province of Iran. All three species are depicted with illustrations and their distribution records are mapped.

Material and method

Photographs of specimens and their copulatory organs were obtained using a Nikon D300S DSLR camera attached to a Nikon SMZ-800 stereomicroscope, a Tucsen TrueChrome Metrics microscope camera attached to a Nikon Eclipse E200 compound microscope and an Olympus E-520 camera attached to an Olympus SZX16 stereomicroscope or to the eye-piece of an Olympus BH2 transmission microscope. Digital images of different focal planes were stacked with Helicon Focus 8.1.1. Illustrations of the endogynes were made after digesting off tissues with a Neo PanPur commercial pancreatic enzyme cocktail pill, clearing the structures in wintergreen oil (methyl-salicylate), then mounting them on a temperate slide preparation (Coddington 1983). Lengths were measured without the chelicerae and the spinnerets. Leg segments were measured on the dorsal side and their measurements are listed as: total length (femur, patella, tibia, metatarsus, tarsus). All measurements are given in millimetres. Geographic coordinates of collection localities were obtained from the labels (given in parentheses) or georeferenced using Google Earth (given in square brackets). The distribution map was prepared using SimpleMappr (Shorthouse 2010).

Abbreviations: Eyes: AME – anterior median eye, **PLE** – posterior lateral eye, **PME** – posterior median eye. **Spination: Mt** – metatarsus, **pl** – prolateral, **Ti** – tibia, **v** – ventral.

Depositories: MMUE – Manchester Museum of the University of Manchester, United Kingdom (D.V. Logunov); **ZMFUM** – Zoological Museum of Ferdowsi University of Mashhad, Iran (O. Mirshamsi); **ZISP** – Zoological Institute, Russian Academy of Sciences, St. Petersburg, Russia (D.V. Logunov); **ZMMU** – Zoological Museum of Moscow State University, Russia (K.G. Mikhailov).

Taxonomy

Family Dysderidae C.L. Koch, 1837
Subfamily Dysderinae C.L. Koch, 1837

Genus *Dysderella* Dunin, 1992

Type species. *Dysdera transcaspica* Dunin & Fet, 1985, from Turkmenistan.

Diagnosis. The genus is most similar to *Dysdera* C.L. Koch, 1837, but can be distinguished from it by the smaller size (i.e. carapace < 2.1 mm vs. > 4 mm) and the spineless legs I and II (vs. spinose in most species).

Description. Small-sized (i.e. body length less than 5 mm). Pars cephalica very flat (Figs 1C, F, 4C, 6C). Interdistance of AMEs smaller than AME diameter. PMEs closely spaced. Legs with few spines; legs III and IV, if spinose, with only a few spines on tibiae and metatarsi. Gnathocoxae and tarsal claws as in *Dysdera*. Bulb with a hook-like posterior apophysis. Endogyne with Π-shaped anterior diverticulum and dumbbell-shaped 'spermatheca'.

Composition. Three species, including the new one described here (WSC 2023).

Distribution. From Northern Caucasus (Dagestan) southward to Tehran Province of Iran and eastward to southern Turkmenistan (Fig. 8).

Dysderella caspica (Dunin, 1990)

Figs 1A–F, 2A–C, 3A–F

Dysdera kollari: Dunin 1984: 53 (as per Dunin 1992: 71).
Dysdera caspica Dunin, 1990: 143, figs 4.1–4 (♂♀).
Dysderella caspica: Dunin 1992: 67, fig. 12 (♂♀); Ponomarev and Alieva 2010: 12.

Material. Azerbaijan: Baku Region: 1♂ (ZMMU), environs of Baku, Dyubendy, (40°29'N, 50°13'E), 18.05,

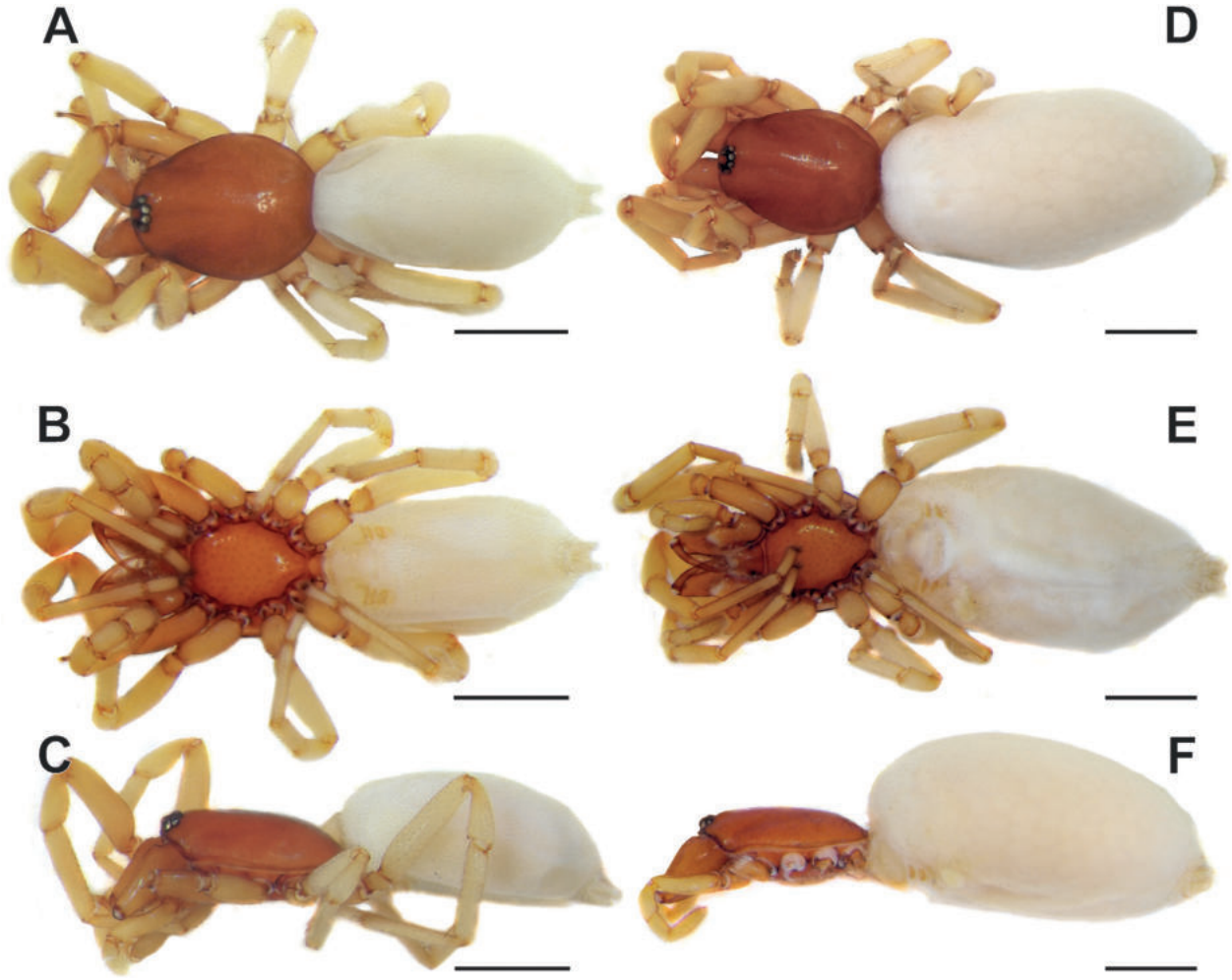

Figure 1. Male (**A–C**) and female (**D–F**) of *Dysderella caspica*: **A, D.** Habitus, dorsal view; **B, E.** Same, ventral view; **C, F.** Same, lateral view. Scale bars: 1.0 mm.

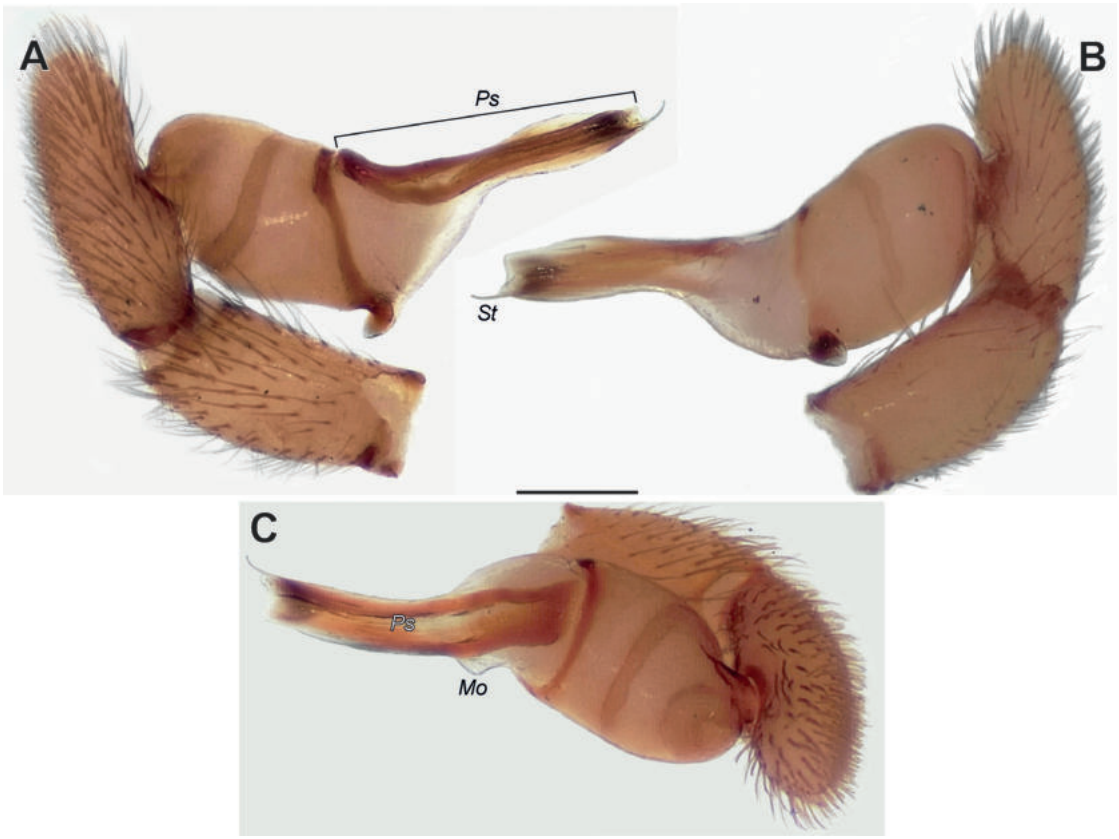

Figure 2. Male palp of *Dysderella caspica*: **A.** Prolateral view; **B.** Retrolateral view; **C.** Anterior view. Scale bar: 0.2 mm. Abbreviations: *Mo* – membranous outgrowth; *Ps* – psembolus; *St* – stylus.

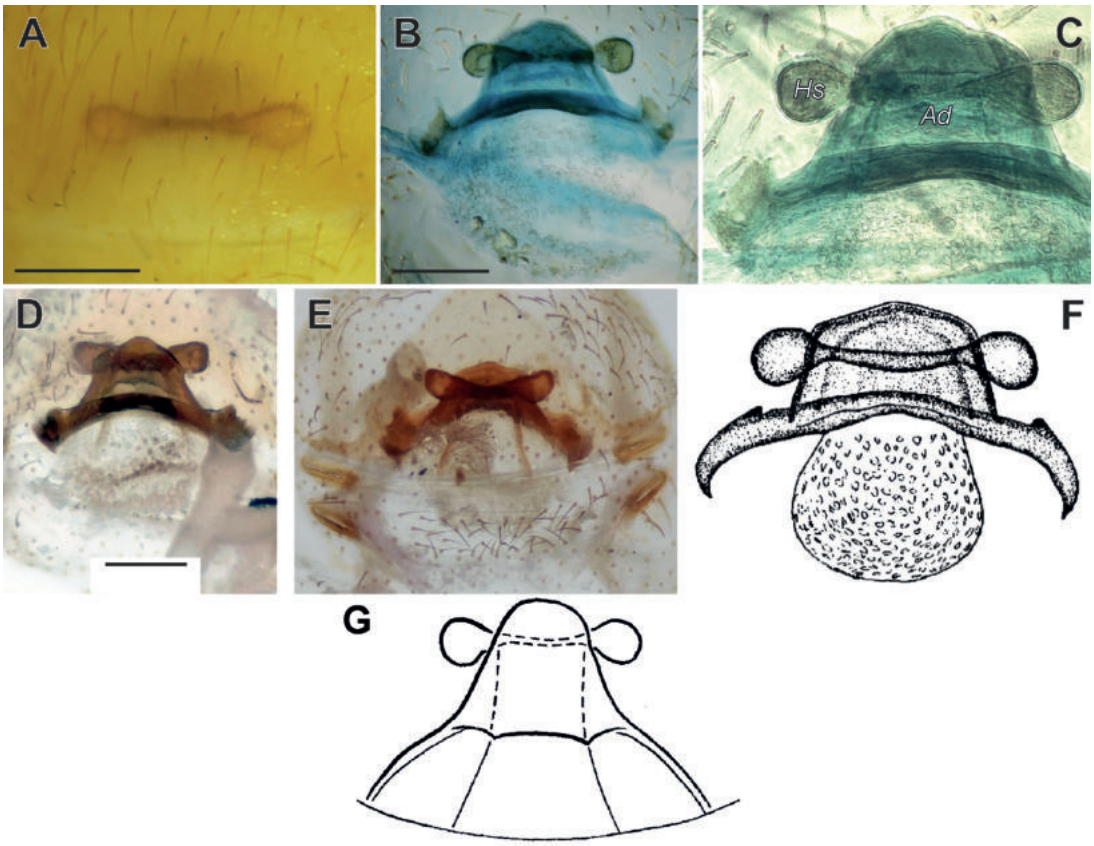

Figure 3. Endogynes of *Dysderella caspica* (**A–F**) and *D. transcaspica* (**G**): **A.** Intact, ventral view; **B–D, F, G.** Macerated, dorsal view; **E.** Same, ventral view; **F.** Reproduced from Dunin (1990); **G.** Reproduced from Dunin and Fet (1985). Scale bars: 0.2 mm. Abbreviations: *Ad* – anterior diverticulum; *Hs* – head of 'spermatheca'.

8.06.2003 (Y.M. Marusik); 1♂1♀2j. (ZMMU), Gobustan, (40°07'N, 49°23'E), 17–31.05.2003 (Y.M. Marusik).

Diagnosis. Male palp of *D. caspica* is most similar to that of *D. transcaspica*, but differs by the relatively shorter psembolus (*Ps*) (i.e. length/width ratio ca. 5, vs. 5.4) and the presence of a membranous outgrowth (*Mo*). Female of *D. caspica* differs from that of *D. transcaspica* by the relatively wider anterior diverticulum (*Ad*) (i.e. almost twice broader than long, vs. 1.5 times broader than long). Males of the two species differ also in spination (i.e. 1 spine on metatarsus III and 2 spines on leg IV in *D. caspica*, vs. 2 spines on metatarsus III and 3 spines on leg IV).

Description. Male. Habitus as in Fig. 1A–C. Total length 3.91. Carapace 1.62 long, 1.26 wide. Eye sizes: AME 0.07, PME 0.08, PLE 0.08. Carapace, sternum, chelicerae, labium and maxillae light reddish. Legs yellowish orange. Abdomen light beige, without any pattern. Spinnerets uniformly beige. Measurements of legs: I: 4.14 (1.23, 0.76, 0.89, 0.84, 0.42), II: 3.68 (1.10, 0.67, 0.78, 0.76, 0.37), III: 2.89 (0.81, 0.51, 0.53, 0.76, 0.28), IV: 3.90 (1.10, 0.61, 0.86, 0.97, 0.36). Spination: III: Ti: 1pl, 1v; Mt: 1pl. IV: Ti: 1pl; Mt: 1pl.

Palp as in Fig. 2A–C; tibia twice longer than wide, slightly shorter than cymbium; bulb ca. 3 times longer than wide, tegular part ca. 2 times longer than wide; psembolus ca. as long as tegular part, margins almost parallel, stylus short, shorter than width of psembolus; middle part of bulb with triangular membranous outgrowth (*Mo*).

Female. Habitus as in Fig. 1D–F. Total length 5.44. Carapace 1.83 long, 1.36 wide. Eye sizes: AME 0.11, PME 0.06, PLE 0.05. Colouration and spination as in male. Measurements of legs: I: 6.88 (1.96, 1.07, 1.53, 1.73, 0.59), II: 6.05 (1.69, 1.13, 1.34, 1.37, 0.52), III: 4.83 (1.38, 0.84, 0.84, 1.27, 0.50), IV: 6.69 (1.81, 1.29, 1.48, 1.53, 0.58).

Endogyne as in Fig. 3A–F; dumbbell-shaped 'spermatheca' well visible through integument; anterior diverticulum (*Ad*) almost 2 times broader than long, heads of spermatheca (*Hs*) globular, spaced by ca. 2.5 diameters.

Habitats. A xerophilous species that inhabits wormwood (*Artemisia absinthium* L.) and ephemeroid semi-deserts and can be found under stones, in soil cracks and within rodent burrows (Dunin 1992).

Distribution. Azerbaijan (Baku, Ganja and Goygol), North Caucasus (Dagestan) (Fig. 8).

Dysderella elburzica sp. nov.

https://zoobank.org/7DE212D7-1235-446D-BC53-46CB7BF1F41B

Figs 4A–C, 5A–F

Type material. ***Holotype*** ♂ (MMUE), Iran: Tehran Province: Latian Dam, (35°48'N, 51°08'E), 6–19.6.2000 (Y.M. Marusik). ***Paratype*:** 1♂ (MMUE), same data as for the holotype.

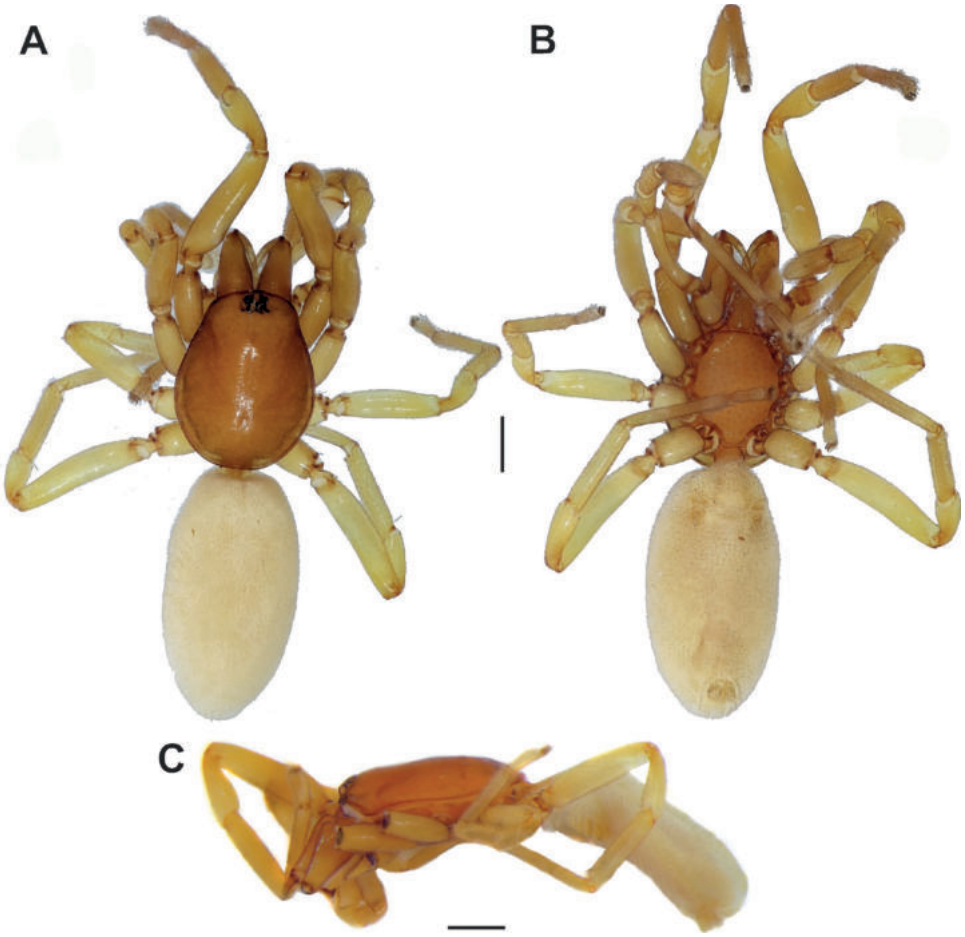

Figure 4. Male of *Dysderella elburzica* sp. nov.: **A.** Habitus, dorsal view; **B.** Same, ventral view; **C.** Same, lateral view. Scale bars: 0.5 mm.

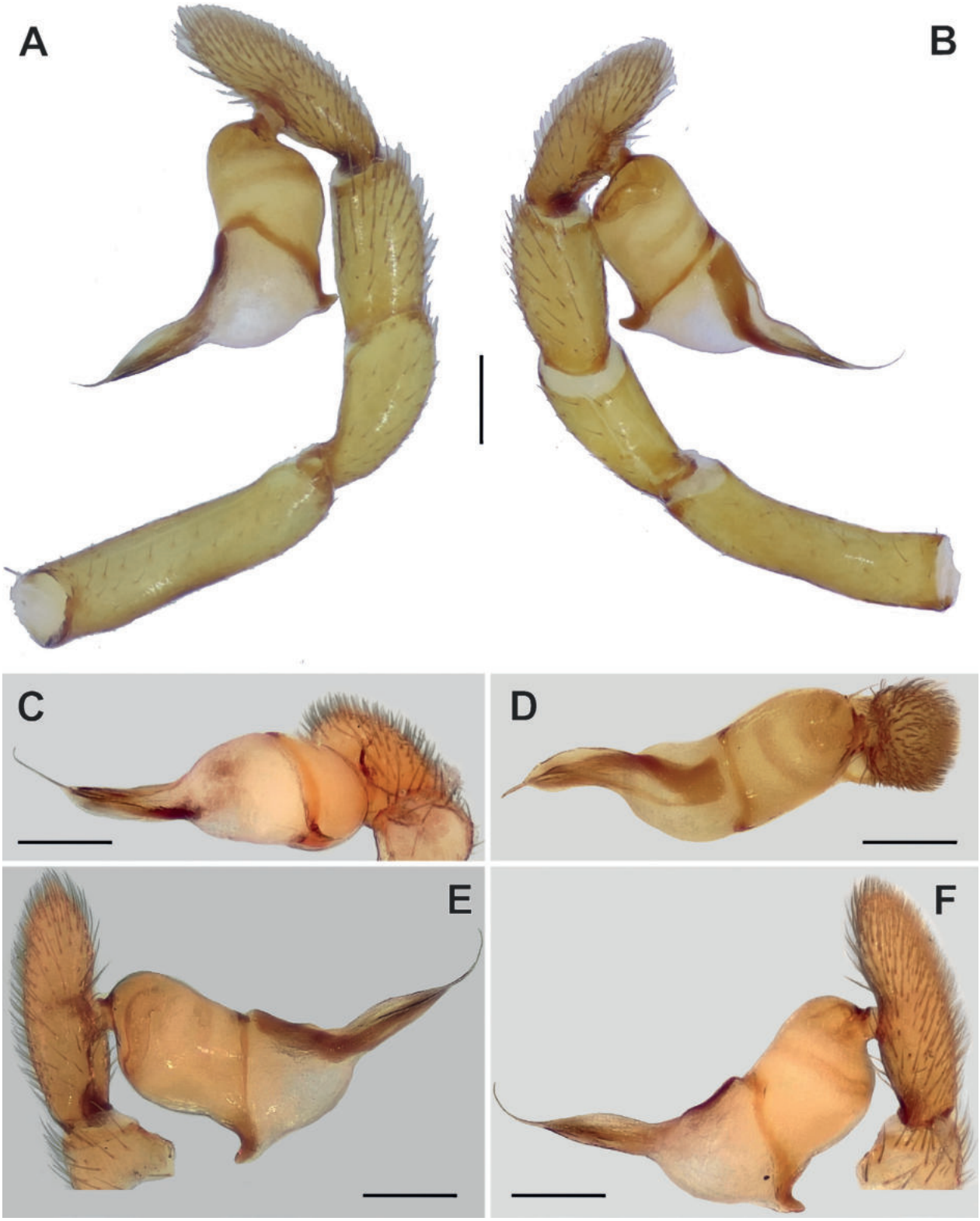

Figure 5. Male palp of *Dysderella elburzica* sp. nov.: **A.** Whole palp, retrolateral view; **B.** Same, prolateral view; **C.** Cymbium and bulb, posterior view; **D.** Same, anterior view; **E.** Same, prolateral view; **F.** Same, retrolateral view. Scale bars: 0.2 mm.

Etymology. The specific epithet is an adjective, referring to the Elburz Mountain Range in northern Iran.

Diagnosis. Male of the new species differs from its congeners by having tapering psembolus (vs. psembolus with subparallel margins).

Description. Male. Habitus as in Fig. 4A–C. Total length 3.63. Carapace 1.63 long, 1.19 wide. Eye sizes: AME 0.08, PME 0.08, PLE 0.06. Carapace, sternum, chelicerae, labium and maxillae light reddish. Legs yellowish orange. Abdomen light beige, without any pattern.

Spinnerets uniformly beige. Measurements of legs: I: 5.30 (1.35, 0.99, 1.27, 1.21, 0.48), II: 5.12 (1.51, 0.86, 1.16, 1.16, 0.43), III: 4.25 (1.22, 0.71, 0.77, 1.04, 0.51), IV: 5.32 (1.68, 0.69, 1.19, 1.37, 0.39). Spination: III: Ti: 1pl; Mt: 1pl. IV: Ti: 1pl; Mt: 1pl.

Palp as in Fig. 5A–F; femur 4 times longer than wide, almost as long as patella+tibia; patella and tibia subequal in length; bulb ca. 3.4 times longer than wide; psembolus ca. 1.7 times longer than tegulum (in prolateral view); psembolus gradually tapering, with long stylus.

Female. Unknown.

Distribution. Known only from the type locality in Tehran Province, northern Iran (Fig. 8).

Dysderella transcaspica (Dunin & Fet, 1985)

Figs 3G, 6A–C, 7A–J

Dysdera kollari: Ovtsharenko and Fet 1980: 443; Fet 1983: 837 (as per Dunin and Fet 1985: 298).

Dysdera transcaspica Dunin & Fet, 1985: 298, figs 1–4 (♂♀).

Dysdera transcaspica: Dunin 1985: 118, figs 5–7 (♂).

Dysderella transcaspica: Dunin 1992: 67; Zamani et al. 2015: 340, fig. 1a–g (♀).

Material. Turkmenistan: Balkan Province: 1♂1♀ (ZMMU), south-western Kopetdagh, Yoldere (= Eldere) Valley, [38°31'N, 56°23'E], under garland thorn, 25.05.1982 (N.S. Ustinova); 1 juv. (ZMMU), Aydere Valley, [38°24'N, 56°45'E], 27.05.1980 (V.Y. Fet). Iran: Razavi Khorasan Province: 1♂ (only palp) (ZMFUM), Torbat-e Jam, Ghader Abad, [35°16'N, 60°37'E], 05.2014 (B. Jannesar).

Note. Dunin and Fet (1985) stated that all type series (consisting of 16 males and 12 females) were deposited in ZISP. However, according to D.V. Logunov (personal communication), the material could not be located there. Three specimens were found in ZMMU, consisting of one male, one female without endogyne and a juvenile.

Diagnosis. See diagnosis for *D. caspica*.

Description. Male. Habitus as in Fig. 6A–C. Total length 4.00. Carapace 1.95 long, 1.45 wide. Eye sizes: AME 0.11, PME 0.10, PLE 0.11. Carapace, sternum, chelicerae, labium and maxillae reddish. Legs yellowish orange. Abdomen light beige, without any pattern. Spinnerets uniformly beige. Measurements of legs: I: 5.40 (1.45, 1.03, 1.26, 1.24, 0.42), II: 4.75 (1.17, 0.87, 1.13, 1.17, 0.41), III: 3.63 (1.07, 0.62, 0.68, 0.92, 0.34), IV: 5.00 (1.35, 0.83, 1.16, 1.21, 0.45). Spination: III: Ti: 1pl, 1v; Mt: 2v. IV: Ti: 1v; Mt: 2v.

Palp as in Fig. 7A–J; femur 4 times longer than wide and as long as patella+tibia; tibia almost as long as cymbium; psembolus almost straight, with subparallel margins, ca. 5.4 times longer than wide, with stylus (broken in the illustrated specimen).

Female. See Dunin and Fet (1985). Colouration and spination as in male; endogyne as in Fig. 3G.

Habitats. The habitats of this species range from foothills to low mountains. It can be found in various microhabitats, including under stones, within ground cracks and inside rodent burrows (Dunin 1985).

Distribution. Turkmenistan (Ahal, Ashgabat, Balkan, Mary), Iran (Razavi Khorasan) (Fig. 8).

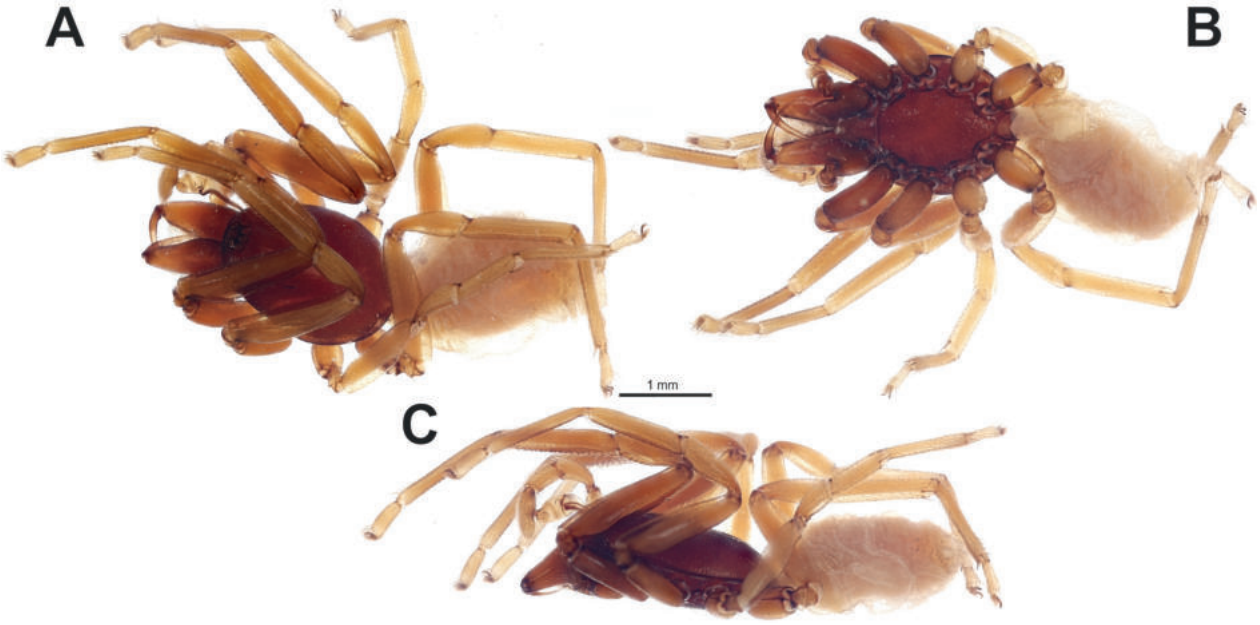

Figure 6. Male of *Dysderella transcaspica*: **A.** Habitus, dorsal view; **B.** Same, ventral view; **C.** Same, lateral view.

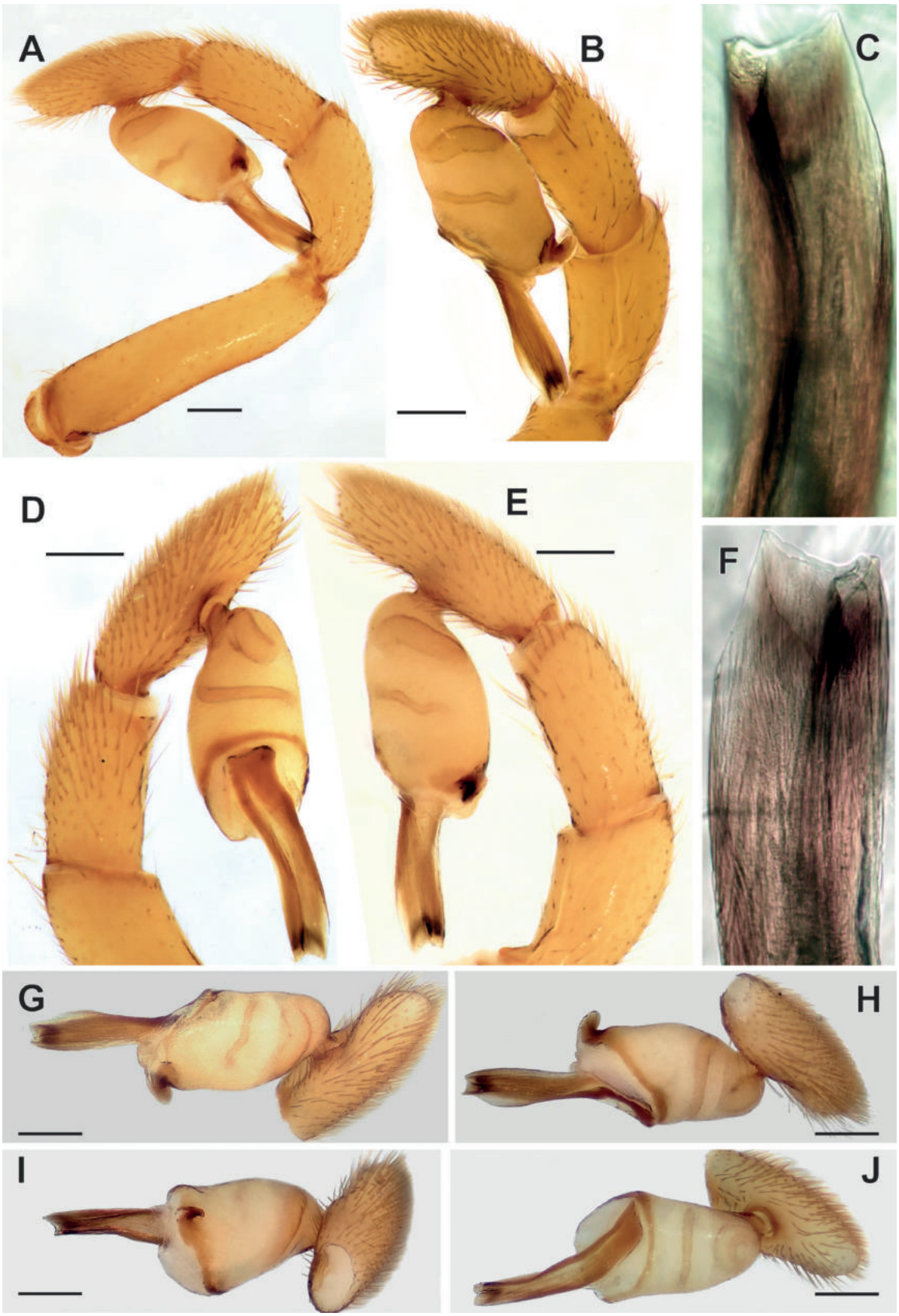

Figure 7. Male palp of *Dysderella transcaspica* (stylus broken): **A.** Whole palp, retrolateral view; **B, D, E.** Close-up, anteroretrolateral, prolateral and retrolateral views; **C, F.** Tip of psembolus, retrolateral and prolateral views; **G.** Cymbium and bulb, retrolateral view; **H.** Same, prolateral view; **I.** Same, posterior view; **J.** Same, anterior view. Scale bars: 0.2 mm.

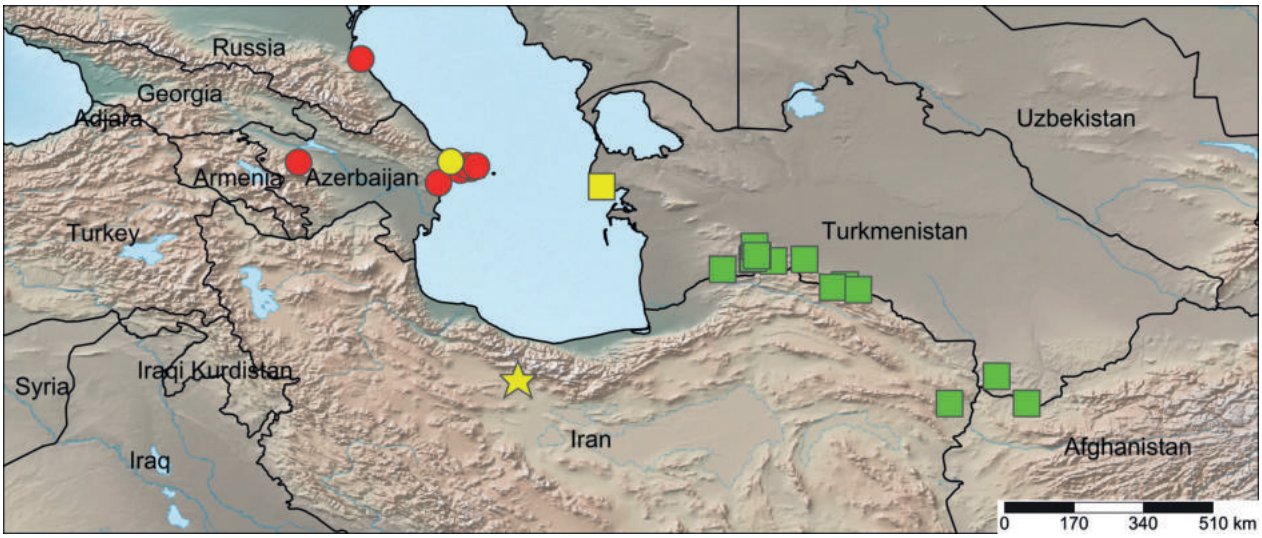

Figure 8. Distribution records of *Dysderella* spp.: circles – *D. caspica*; star – *D. elburzica* sp. nov.; square – *D. transcaspica*. Yellow symbols refer to the type localities.

Acknowledgements

We express our gratitude to Victor Fet for providing literature. We also wish to thank Kirill Y. Eskov and Kirill G. Mikhailov for their efforts in locating and providing a loan of the studied material of *D. transcaspica* deposited in ZMMU. Additionally, we would like to thank Dmitri V. Logunov for his effort in locating the apparently lost holotype and paratypes of this species in ZISP. We are thankful to the reviewers Mikhail Omelko, Maria Naumova and Anna Šestáková for their valuable comments and suggestions provided on the earlier version of the manuscript.

References

Coddington JA (1983) A temporary slide-mount allowing precise manipulation of small structures. Verhandlungen des Naturwissenschaftlichen Vereins in Hamburg 26: 291–292.

Dunin PM (1984) [Fauna and ecology of the spiders of the Apsheron Peninsula, Azerbaijan SSR]. In: Utochkin A (Ed.) Fauna and Ecology of Arachnids. University of Perm, 45–60. [in Russian]

Dunin PM (1985) [The spider family Dysderidae (Aranei, Haplogynae) in the Soviet Central Asia]. Trudy Zoologicheskogo Instituta Akademii Nauk SSSR, Leningrad 139: 114–120. [in Russian]

Dunin PM (1990) [Spiders of the genus *Dysdera* (Aranei, Haplogynae, Dysderidae) from Azerbaijan]. Zoologicheskiĭ Zhurnal 69(6): 141–147. [in Russian]

Dunin PM (1992) [The spider family Dysderidae of the Caucasian fauna (Arachnida Aranei Haplogynae)]. Arthropoda Selecta 1(3): 35–76. [in Russian]

Dunin PM, Fet VY (1985) [*Dysdera transcaspica* sp. n. (Aranei, Dysderidae) from Turkmenia]. Zoologicheskiĭ Zhurnal 64: 298–300. [in Russian]

Fet VY (1980) [Spider fauna (Aranei) of southwestern Kopetdag]. Entomologicheskoe Obozrenie 62(4): 835–845. [in Russian]

Ovtsharenko VI, Fet VY (1980) [Fauna and ecology of spiders (Aranei) of Badhyz (Turkmenian SSR)]. Entomologicheskoe Obozrenie 59(2): 442–447. [in Russian]

Ponomarev AV, Alieva SV (2010) [The new data on spiders (Aranei) fauna of Dagestan]. Vestnik Permskogo Universiteta: Seria Biologia 3: 12–16. [in Russian]

Shorthouse DP (2010) SimpleMappr, an online tool to produce publication-quality point maps. http://www.simplemappr.net [accessed 11.03.2023]

WSC (2023) World Spider Catalog. Version 23.5. Natural History Museum Bern. http://wsc.nmbe.ch [accessed on 05.04.2023]

Zamani A, Mirshamsi O, Jannesar B, Marusik YM, Esyunin SL (2015) New data on spider fauna of Iran (Arachnida: Araneae), Part II. Zoology and Ecology 25(4): 339–346. https://doi.org/10.1080/21658005.2015.1068508

Zoosyst. Evol. 99 (2) 2023, 345–361 | DOI 10.3897/zse.99.101943

PENSOFT

MUSEUM FÜR NATURKUNDE BERLIN

Diversity of Sand Snakes (Psammophiidae, *Psammophis*) in the Horn of Africa, with the description of a new species from Somalia

Jiří Šmíd[1,2], Sergio Matilla Fernández[1], Hassan Sh Abdirahman Elmi[2,3], Tomáš Mazuch[4]

1 *Department of Zoology, National Museum, Cirkusová 1740, Prague, Czech Republic*
2 *Department of Zoology, Faculty of Science, Charles University, Viničná 7, Prague, Czech Republic*
3 *Department of Biology, Amoud University, Boorama, Somaliland*
4 *Department of Forest Ecology, Mendel University, 61300 Brno, Czech Republic*

https://zoobank.org/216E01C8-8854-4763-BC82-9ACA678B697C

Corresponding author: Jiří Šmíd (jirismd@gmail.com)

Academic editor: Johannes Penner ♦ **Received** 14 February 2023 ♦ **Accepted** 19 May 2023 ♦ **Published** 27 June 2023

Abstract

The biological diversity of the Horn of Africa is one of the least studied in the world. Yet the Horn supports rich communities of species that are mostly endemic to the region. Here we study the diversity of Sand Snakes (*Psammophis*) in East Africa, their phylogeny and systematics. Previous studies have unveiled several cryptic and potentially undescribed species of *Psammophis* that occur in the Horn and their taxonomic status has remained unclear to this day. We used sequence data from two mitochondrial and one nuclear genes to reconstruct the phylogeny of the genus, in which we included newly obtained samples of six different *Psammophis* species from Somalia, Ethiopia, Eritrea, Sudan, and Egypt. Our aim was to assess the status of some of the undescribed species, examine the level of intraspecific genetic variation within individual species, improve our understanding of the species distributions, and contribute to the taxonomy of the genus. Our results confirm the existence of two undescribed species, one in eastern Somalia, which we formally describe as new, and one in southern Ethiopia that we refer to as *Psammophis* cf. *sudanensis* in accordance with previous studies. Further, we provide first genetic data for the nominotypical subspecies of *P. punctulatus* and confirm the species status for its subspecies *P. trivirgatus*. In addition, we provide new genetic data for *P. tanganicus* from Ethiopia and Somalia, and range extension records for *P. rukwae* from Eritrea and Ethiopia and for *P. aegyptius* from Somalia. Our findings contribute considerably to our understanding of the diversity and distribution of *Psammophis* in East Africa.

Key Words

East Africa, Eritrea, Ethiopia, phylogeny, reptilia, sand racers, Serpentes

Introduction

The Horn of Africa is the easternmost projection of the African continent that juts into the Indian Ocean. It supports a broad spectrum of habitats, from the Ethiopian Highlands that exceed 4500 m in elevation to the harsh lowland deserts of Somalia with barely any precipitation. The entire territory of the Horn is considered one of the global biodiversity hotspots, which are classified as regions of exceptionally high species richness and endemism while also suffering considerable habitat loss (Mittermeier et al. 2004). The Horn harbors a high diversity of squamate reptiles, of which snakes with narrow distribution ranges stand out the most (Lewin et al. 2016), implying that the snake fauna is mostly endemic to the region. At the same time, however, large parts of the Horn remain virtually unexplored for their difficult accessibility, and the fauna of the Horn is vastly understudied, especially from a genetic perspective (Šmíd 2022).

Sand Snakes of the genus *Psammophis* are distributed primarily in Africa where there are 27 out of 33 currently recognized species. Six additional species occur strictly in Asia, and one stretches broadly across both continents (Uetz et al. 2023). They are slender and swift diurnal

hunters, with long heads and large eyes with round pupils, and relatively large, grooved rear fangs. The genus is typified by the unusually small male copulatory organs (hemipenes), which are short and thin and lack any ornamentation characteristic of other snakes (Steehouder 1984; de Haan 2003). As a result, the sex is almost impossible to determine externally in *Psammophis*.

Thirteen species of *Psammophis* occur in and around the Horn of Africa. Five range broadly across the Horn; these are *P. biseriatus* Peters, 1881; *P. pulcher* Boulenger, 1895; *P. punctulatus* Duméril, Bibron & Duméril, 1854 with two subspecies - *punctulatus* and *trivirgatus* Peters, 1878; *P. sibilans* (Linnaeus, 1758); and *P. tanganicus* Loveridge, 1940, although the distribution of *P. pulcher* is very limited as the species is known only from a handful of specimens. *Psammophis aegyptius* Marx, 1958 and *P. schokari* (Forskål, 1775) are distributed by the Red Sea along which they penetrate south to Eritrea and northern Somalia. The more marginal species to the Horn, but otherwise generally widespread in other parts of Africa, are *P. angolensis* (Bocage, 1872), *P. lineatus* (Duméril, Bibron & Duméril, 1854), *P. mossambicus* Peters, 1882, *P. orientalis* Broadley, 1977, *P. rukwae* Broadley, 1966, and *P. sudanensis* Werner, 1919 (Figs 1, 2; Lanza 1990; Largen and Spawls 2010; Spawls et al. 2018). This list is, however, apparently far from complete. The existence of additional phylogenetic lineages that may deserve the rank of species has been confirmed in several phylogenetic studies of the genus. For instance, *P. sibilans* has been found to represent two independent lineages unrelated to each other, the nominotypical one distributed in Egypt and western Ethiopia, the other one in central Ethiopia, and termed in this paper *P.* sp. Ethiopia (Trape et al. 2019). Similarly, *P. sudanensis* contains two lineages separated phylogenetically by many other species in between, with samples of the real *P. sudanensis* originating from Chad and those referred here to as *P*. cf. *sudanensis* from Kenya and Tanzania (Kelly et al. 2008; Trape et al. 2019). Trape et al. (2019) also recovered an isolated evolutionary entity in western Ethiopia (sample MBUR 8346; termed here *P*. sp. Ethiopia 2) that is related to the western African *P. phillipsii* (Hallowell, 1844) and the southern and eastern African *P. mossambicus*. And lastly, Vidal et al. (2008) included in their analysis a sample of an undetermined species from extreme eastern Somalia. Its taxonomy has remained unsolved to date (Keates 2021).

In this study we analyze new material from the Horn of Africa and adjoining countries to provide further insight into the phylogenetic relationships, distribution, and taxonomy of the *Psammophis* snakes of the region. The newly analyzed material originated from targeted herpetological fieldtrips to the Horn countries that were carried out between 2010 and 2022. We assembled a genetic dataset of two mitochondrial and one nuclear gene that was based on published data and which included all known *Psammophis* species, and we supplemented it by 14 newly analyzed specimens, including specimens that could not be determined with certainty on the basis of morphology and which likely represented some of the putative new species. We inferred their phylogenetic position within the genus and investigated genetic variability of all *Psammophis* species to assess the taxonomic status of the putative new species in the context of a complete *Psammophis* phylogeny.

Methods

Data for genetic analyses

We assembled all genetic data that were available for the genus *Psammophis* on GenBank. To ensure sufficient overlap of loci we included only genes that were available for most of the Horn species. These were cytochrome b (cyt *b*) and NADH dehydrogenase subunit 4 (ND4) from the mitochondrial DNA, and oocyte maturation factor MOS (c-mos) from the nuclear DNA. Some species are represented in GenBank by many sequenced individuals. We pruned the dataset to contain only up to three samples per species, provided all the pruned species are monophyletic. It should be noted that the ND4 sequence of *P. biseriatus* (sample BK10724, GenBank accession DQ486284) and the c-mos sequence of *P. tanganicus* (sample CMRK87, GenBank accession DQ486183) contained too many ambiguous nucleotide positions to allow their inclusion in the dataset. Sequences of *Malpolon monspessulanus*, *Psammophylax variabilis*, *Psammophylax rhombeatus*, and *Rhamphiophis rostratus*, all of which belong to the Psammophiidae, were used to root the tree.

We de-novo sequenced 14 samples from different localities across the Horn of Africa and neighboring countries and belonging to *P. aegyptius* (seven samples from Egypt [2], Sudan [1], Somaliland [4]), *P. punctulatus punctulatus* (one sample from Ethiopia), *P. rukwae* (two samples from Ethiopia and Eritrea), *P. sudanensis* (one sample from Ethiopia), *P. tanganicus* (two samples from Ethiopia and Somaliland), and one sample from northern Somalia (central Somaliland) tentatively identified as *P.* cf. *tanganicus*. See Fig. 3 for the geographic origin of the samples and Suppl. material 1 for precise locality details.

DNA extraction, amplification, and sequencing

Genomic DNA was extracted from ethanol-preserved tissue samples using the DNA Mini Kit protocol. We PCR-amplified the three genes using primers and PCR conditions detailed in Šmíd et al. (2019). The PCR products were sequenced from both directions at Macrogen Europe (Amsterdam, the Netherlands). Quality of the raw sequences was inspected and contigs were assembled using the Geneious v. 11 software (Kearse et al. 2012). The tRNAs that flank the ND4 and that were amplified along with it were not included in the dataset because they may be problematic to align with certainty.

Figure 1. Sand Snakes of the Horn of Africa, part 1. **a.** *P. aegyptius* (Berbera, Somaliland); **b.** *P. angolensis* (South Africa); **c.** *P. biseriatus* (Voi, Kenya); **d.** *P. lineatus* (Nigeria); **e.** *P. mossambicus* (Baringo, Kenya); **f.** *P. orientalis* (Watamu, Kenya); **g.** *P. pulcher* (Bisanadi National Reserve, Kenya). Photo credit T. Mazuch (**a**); WR. Branch (**b**), S. Spawls (**c, e, f, g**), G. Dunger (**d**).

Figure 2. Sand Snakes of the Horn of Africa, part 2. **a.** *P. punctulatus* (Gewane, Ethiopia); **b.** *P. trivirgatus* (Mwingi, Kenya); **c.** *P. rukwae* (Asmara, Eritrea); **d.** *P. schokari* (Kasserine, Tunisia); **e.** *P. sibilans* (Debre Zeit, Ethiopia); **f.** *P.* cf. *sudanensis* (Yabelo, Ethiopia); **g.** *P. tanganicus* (Mado Gashi, Kenya). Photo credit T. Mazuch (**a, c, d, f, g**), S. Spawls (**b, e**).

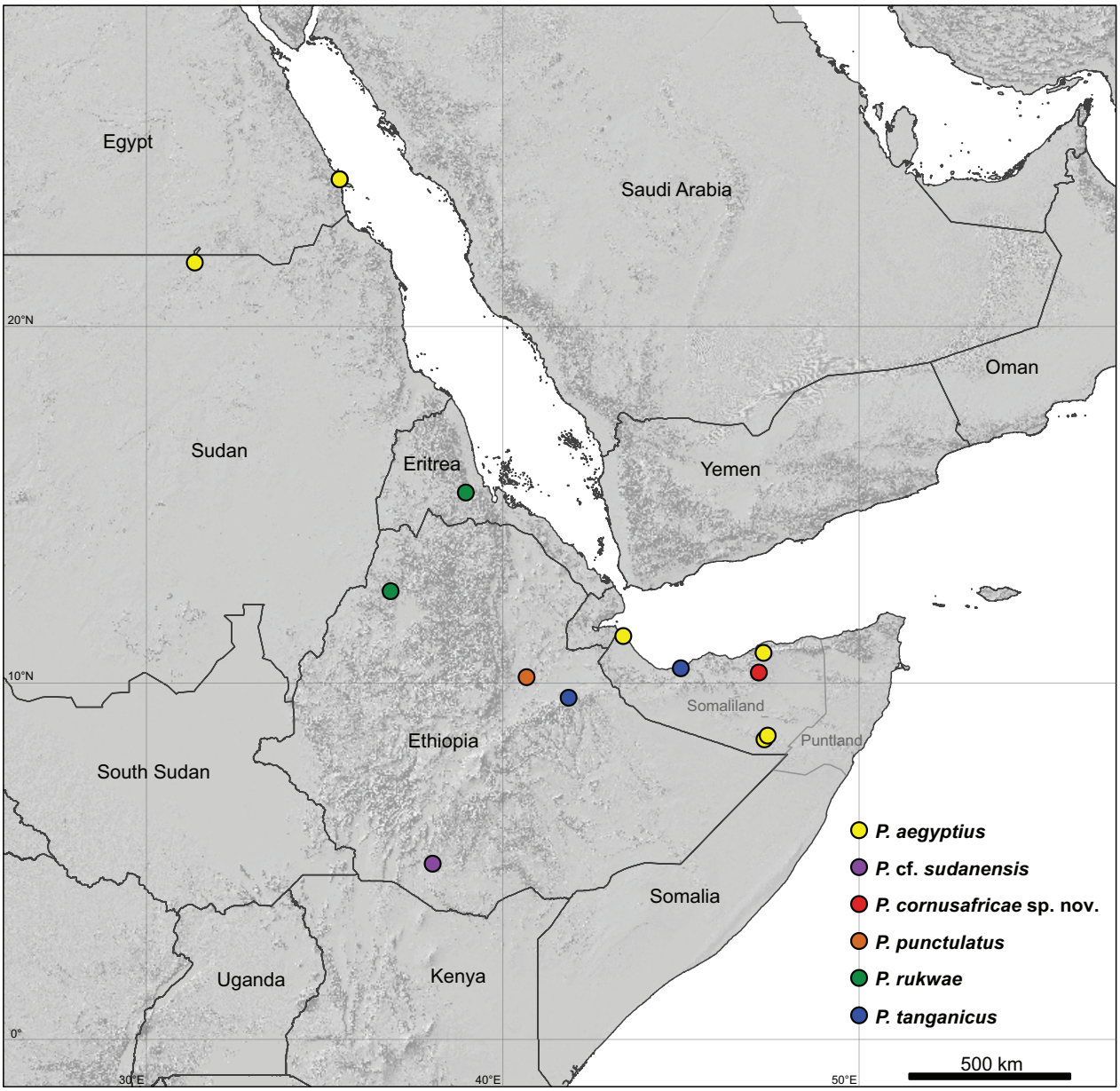

Figure 3. Geographic origin of the new material analyzed in this study. The background map shows the terrain surface. It was derived from the SRTM elevation data (Farr and Kobrick 2000) using the hillshade function of ArcMap.

All three genes were aligned with MAFFT (Katoh et al. 2019) using the auto strategy. The alignments were subsequently treated with Gblocks (Castresana 2000) to remove ragged ends. No stop codons were detected in the cyt *b* and ND4 alignments, indicating no nuclear mitochondrial pseudogenes were amplified. The final concatenated dataset contained 106 tips (102 ingroup + 4 outgroup) and was 2,149 base pairs (bp) long.

Phylogenetic analyses

The phylogenetic relationships within *Psammophis* were estimated by means of a Maximum Likelihood (ML) analysis and a Bayesian Inference (BI). The ML analysis was conducted in IQ-Tree (Nguyen et al. 2015) using the online interface (Trifinopoulos et al. 2016). The dataset was partitioned by gene and the best-fit model of nucleotide substitution was selected automatically for each partition during the analysis. Branch support was assessed with 1,000 replicates of the Shimodaira-Hasegawa-like approximate likelihood ratio test (SH-aLRT; Guindon et al. 2010), 1,000 replicates of ultrafast bootstrap (UFBoot; Hoang et al. 2018), and 100 standard bootstrap replicates (Felsenstein 1985).

The BI analysis was conducted in MrBayes v. 3.2 (Ronquist et al. 2012). The dataset was partitioned by gene and the best models were estimated by PartitionFinder v. 2.1 (Lanfear et al. 2017). The best models were as follows: GTR+I+G for the cyt *b* and ND4, HKY+G for the c-mos. The proportion of invariable sites parameter (+I) was not included as it is accounted for by the +G

parameter. We ran three independent runs for 10 million generations, sampling every 10,000 generations. Stationarity was determined by the sequentially calculated standard deviations of the split frequencies being lower than 0.01. We discarded the initial 10% of trees as burnin and generated a 50 percent majority rule consensus tree. Branches with SH-aLRT ≥ 80, UFBoot ≥ 95, standard bootstrap ≥ 70, and a Bayesian posterior probability (pp) ≥ 0.95 were considered strongly supported.

Comparisons of genetic distances

We assessed whether the genetic distances that separate the samples of the unidentified species from eastern Somalia from its sister species *P. tanganicus* are similar to or deviate from distances between other sister species across the *Psammophis* tree following the method of Šmíd et al. (2018). Pairwise genetic distances between all samples were obtained from the ML tree and were categorized in the following groups: within species, between sister species, between non-sister species, between *tanganicus* and the new species. Zero genetic distances between identical haplotypes were removed. Species were considered sister only when the sister relationship was strongly supported in all the phylogenetic analyses. The four outgroup species were pruned from the tree. We tested for significance between the four groups by means of one-way ANOVA with the Tukey HSD post hoc test for pairwise significance using R (R Core Team 2013). We also calculated uncorrected patristic distances (*p*-distances) for the two mitochondrial markers in MEGA X v. 10.2 (Kumar et al. 2018) with the pairwise deletion option.

Sex identification

We used the method of Laopichienpong et al. (2017) that allows the identification of sex by using molecular markers located on the gametologous genes. The psammophiids possess the ZZ/ZW sex determination system where males are the homogametic sex (ZZ), and females are heterogametic (ZW) (e.g., Augstenová et al. 2018). We amplified the CTNNB1 gametologous gene using the primers Eq-CTNNB1-11-F1 and Eq-CTNNB1-13-R (Matsubara et al. 2016; Laopichienpong et al. 2017) and PCR conditions detailed in the latter paper. Males were identified based on the presence of a single band on gel electrophoresis (both alleles on the Z sex chromosomes are of the same length), females had two bands present (the allele on the W sex chromosome is shorter than that on the Z chromosome; Laopichienpong et al. 2017).

Morphological analyses

For morphological comparisons, we examined the two specimens of *P. tanganicus* that were used in the genetic analysis (NMP-P6V 76371–2) and three specimens of the undescribed species from Somalia (NMP-P6V 76373, MVZ:Herp:242772, MVZ:Herp:242773), the former two of which were also included in the genetic analysis. Scale counts and color pattern of the *P. tanganicus* holotype (MCZ R-30380) were obtained from the photographs available at the MCZ collection database (https://mczbase.mcz.harvard.edu/guid/MCZ:Herp:R-30380). General morphological species characteristics of *P. biseriatus* and *P. tanganicus* were assembled from the literature (Largen and Spawls 2010; Spawls et al. 2018; Spawls et al. 2023). We measured snout-vent length (SVL), measured from the tip of the snout to the anterior margin of the cloaca, and tail length (TL), measured from the posterior margin of the cloaca to the tip of the tail. The following scale counts were recorded: supralabials; infralabials; dorsal scales at one head-length behind the head (termed anterior dorsals), at midbody (termed midbody dorsals), and one head-length anterior to the vent (termed posterior dorsals); ventrals; subcaudals. In addition, we collected data on the color and pattern of different body parts of all examined specimens. This dataset of color patterns was supplemented by photographs from throughout the distribution of *P. tanganicus* that were obtained from the literature (Bezy and Drewes 1985), provided by our colleagues (M. Berroneau, A. Childs, S. Kirchhoff, M. Menegon, D. Modrý, S. Spawls, A. Stein, E. Van Der Westhuizen) or downloaded from the iNaturalist online database (https://www.inaturalist.org/taxa/28961-Psammophis-tanganicus/browse_photos). Original high-resolution photographs of the examined specimens have been deposited in the MorphoBank (https://morphobank.org/) database where they are available for free download (346 photographs in total; Project No. 4527). MorphoBank accessions are provided in Suppl. material 1.

Due to a rather small number of specimens available for morphological examinations we did not carry out formal statistical analyses to compare the studied taxa. We nonetheless carried out informal comparisons between them to verify whether there are morphological differences consistent with the genetic results.

Museum acronyms

CAS – California Academy of Sciences, San Francisco, USA; **MCZ** – Museum of Comparative Zoology, Cambridge, USA; **MVZ** – Museum of Vertebrate Zoology, Berkeley, USA; **MSNG** – Museo Civico di Storia Naturale 'Giacomo Doria', Genova, Italy; **MZUF** – University di Firenze, Museo Zoologico 'La Specola', Firenze (Florence), Italy; **NHMUK** – Natural History Museum, London, UK; **NMP** – National Museum in Prague, Czech Republic; **TMHC** – Tomáš Mazuch herpetological collection, Dříteč, Czech Republic; **UniMoRe** – Collezione Franchini nella Sezione Musei Anatomici del Dipartimento del Museo di Paleobiologia e dell´Orto Botanico dell´Università di Modena e Reggio Emilia, Modena, Italy.

Results

Phylogenetic analyses

The ML and BI analyses resulted in identical topologies, although some branches were not statistically supported in either of the analysis (Fig. 4). Given that the dataset for the genetic analysis relied mostly on previously published sequences, the relationships between the *Psammophis* species remained largely congruent with other recent studies on the genus' phylogeny (Branch et al. 2019; Chen et al. 2021; Kurniawan et al. 2021; Taft et al. 2022). The subtle topological differences resulted either from different composition of taxa across different studies or from low branch support.

As for the newly analyzed samples, the sample of *P. punctulatus punctulatus* (JIR513) was recovered as sister to *P. punctulatus trivirgatus* with a robust branch support (SH-aLRT: 100/UFBoot: 100/Standard bootstrap: 100/MrBayes pp: 1.0; support values are shown in the same order hereafter). The genetic distances between the two taxa are 8.0% in the cytb *b* and 9.06% in the ND4.

The newly analyzed samples of *P. rukwae* (JIR511, TMHC2012.12.148) clustered within other samples of the species from Chad and Kenya (support 97.4/100/96/1.0), with *p*-distances within the species ranging between 1.48–5.17% in the cyt *b* and 0.76–5.74% in the ND4.

The new sample of *P. sudanensis* from Ethiopia (TMHC2013.07.250) did not cluster with the other samples of the species included in the analyses, but actually with a lineage termed *P.* cf. *sudanensis* from Kenya and Tanzania that was first discovered by Trape et al. (2019) (support 96.4/98/91/1.0). Our new sample was sister to all the other samples of this undescribed species (support 92.3/100/92/1.0), with *p*-distances between our and the other samples ranging between 5.0–5.49% in the ND4 (cyt *b* sequence is not available for TMHC2013.07.250).

The samples of *P. aegyptius* from Egypt and Sudan clustered with other samples of the species available on GenBank from Egypt and Niger (support 100/100/100/1.0), and the four samples from Somaliland were sister to this clade (support 97.5/99/97/1.0). Mean *p*-distances between the Somali samples and those from the north (Egypt, Sudan, Niger) were 8.03% in the cyt *b* (range 4.92–10.42%) and 9.24% in the ND4 (range 8.61–10.27%).

The two samples of *P. tanganicus* and that from central Somaliland that we tentatively identified as *P.* cf. *tanganicus* all clustered in a clade with *P. biseriatus* that was well supported in all analyses (support 100/100/100/1.0). In this clade, the two samples of *P. tanganicus* from Ethiopia and Somalia JIR508–509 (vouchers NMP-P6V 76371–2) were recovered to form a clade (support 100/100/100/1.0) that was sister to the remaining samples of *P. tanganicus* from Tanzania (support 95.9/99/95/1.0). The sample JIR510 (voucher NMP-P6V 76373) from central Somaliland was closely related to a sample of an undescribed *Psammophis* species from eastern Somalia sequenced by Vidal et al. (2008; sample and voucher codes TP28431 and MVZ:Herp:242772, respectively; support 100/100/100/1.0). *Psammophis biseriatus* was then sister to the group of *P. tanganicus* and the undescribed species (support 85.1/94/74/0.99). Uncorrected *p*-distances between *P. biseriatus*, *P. tanganicus* and the undescribed species are shown in Table 1.

Table 1. Mitochondrial genetic distances (uncorrected *p*-distances in %) between *P. biseriatus*, *P. tanganicus*, and *P. cornusafricae* sp. nov. Below the diagonal are values for the cyt *b* gene, above the diagonal for the ND4. For each comparison, the mean is shown with the min-max range in brackets.

	P. biseriatus	***P. tanganicus***	***P. cornusafricae* sp. nov.**
P. biseriatus		10.18 (9.52–10.57)	12.04 (11.99–12.08)
P. tanganicus	10.78 (10.33–11.04)		9.74 (9.26–10.77)
P. cornusafricae sp. nov.	9.90 (9.75–10.06)	7.79 (7.2–8.58)	

Comparisons of genetic distances

The genus showed clear genetic structuring with significant differences in the genetic distances found between the examined categories: within species, between sister species, between non-sister species, and the distance between the *P. tanganicus* and the undescribed species from Somalia (ANOVA $F_{(3,5152)} = 575.4$, $p < 0.001$). The post hoc tests confirmed pairwise differences between all categories ($p < 0.01$), except for the comparison between the categories 'between sister species' and '*tanganicus*-Somali species' ($p = 0.999$; Fig. 5), indicating that the genetic distance between *P. tanganicus* and this species is statistically comparable to the distance between other sister species pairs in the genus.

Taxonomic implications

Based on the combined evidence of the genetic and morphological differentiation we recognize the undescribed species from the northeastern Somali regions of Somaliland and Puntland as new and provide its formal description below.

Systematics

Psammophiidae Bourgeois, 1968
Psammophis Fitzinger, 1826

Psammophis cornusafricae sp. nov.

https://zoobank.org/F1E4DC4C-D816-47A9-B9E1-1DAB56323E56

English name: African Horn Sand Snake

Somali name: Subxaanyo [pronounced Subhanyo]; a term in the Somali language that refers to all *Psammophis* species that occur in the region. All Subxaanyo are believed to be harmless and friendly by the locals and are an important part of their folklore

Chresonymy. *Psammophis biseriatus* in Calabresi (1927; in part), Scortecci (1939a), Scortecci (1939b), Lanza (1983; in part), Regnoli et al. (2003; in part);

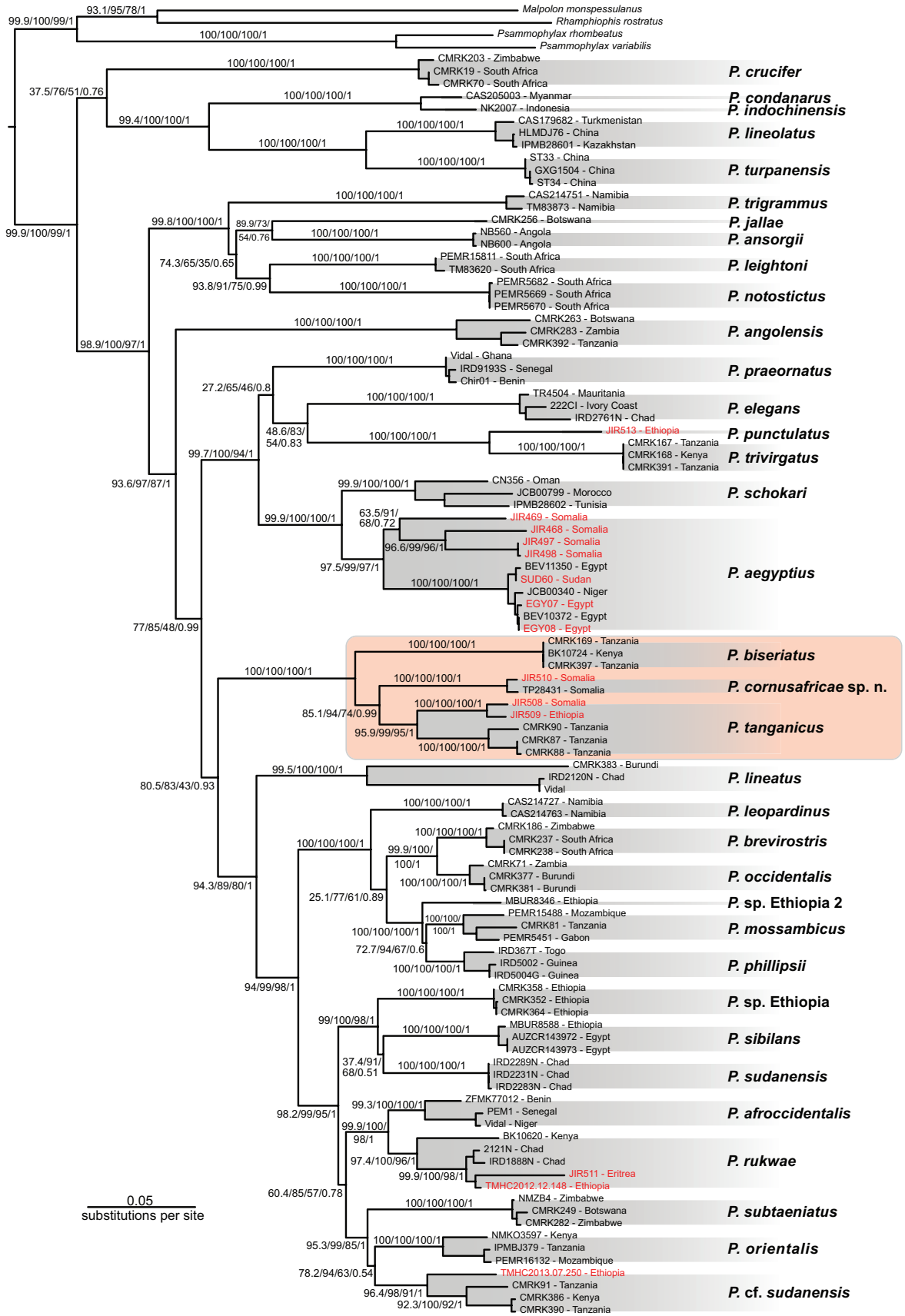

Figure 4. Maximum Likelihood phylogeny of the genus *Psammophis* based on a concatenated alignment of the cyt *b*, ND4 and c-mos genes (2,149 bp in total). The clade containing *P. biseriatus*, *P. tanganicus* and *P. cornusafricae* sp. nov. is highlighted in pink. Codes of samples newly sequenced for this study are in red. Locality details and original references of all samples are given in Suppl. material 1. Branch support is given in the order SH-aLRT/UFBoot/Standard bootstrap/MrBayes posterior probability.

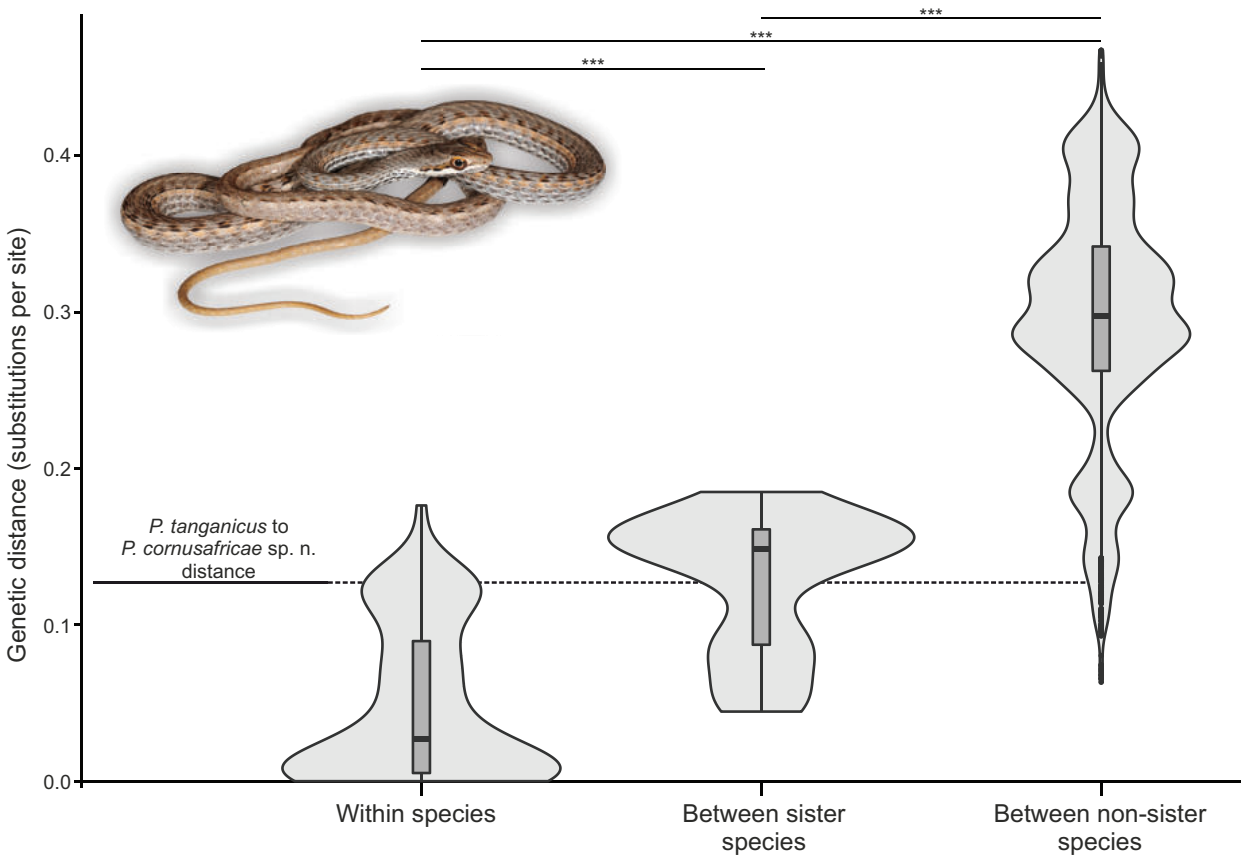

Figure 5. Comparison of genetic distances within the *Psammophis* species, between sister species pairs, between non-sister species. The distances (*y* axis) are based on the ML tree. Horizontal bars with asterisks on top of the graph indicate significant differences in the observed genetic distances ($p < 0.001$; tested by the Tukey HSD post hoc test of ANOVA). The average distance between *P. tanganicus* and *P. cornusafricae* sp. nov. (0.127 subst. per site) is shown by the dashed line. The animal depicted is specimen NMP-P6V 76373 (sample JIR510) of *P. cornusafricae* sp. nov.

Psammophis biseriatus tanganicus in Loveridge (1940; in part), Lanza (1990; in part);

Psammophis tanganicus Largen and Ramussen (1993; in part), Brandstätter (1996; in part), Largen and Spawls (2010; in part), Wallach et al. (2014; in part), Boundy (2020; in part);

Psammophis sp. in Vidal et al. (2008), Trape et al. (2019), Keates (2021).

Type material. *Holotype*: MVZ:Herp:242772 (sample code TP28431; Fig. 6), subadult, sex unknown; Somalia, Bari Region, Heela Spring, 11 km NW (by road) of Baargaal (11.371°N, 51.0412°E), elevation 77 m above sea level; collected by T. J. Papenfuss on June 29, 2003.

***Paratype*:** MVZ:Herp:242773, adult, sex unknown; same collection data as holotype.

Other material. NMP-P6V 76373 (sample JIR510; Fig. 7; MorphoBank accessions: M851260–M851339), subadult female (sex confirmed by genetics); Somaliland, 8.5 km S of Yuffleh (10.3°N, 47.182778°E), elevation 1758 m above sea level; collected by T. Mazuch on September 5, 2017.

Diagnosis. A *Psammophis* species sister to *P. tanganicus*, with the following combination of morphological characters: 11 infralabials; 9 supralabials, three of which are in contact with the eye; nostril pierced between two equal sized nasals; 15 anterior dorsals; 14–15 midbody dorsals; 11 posterior dorsals; 146–158 ventrals; 95–100 subcaudals. Body brown, grey or beige with only a faintly visible pale vertebral stripe but with well pronounced dorsolateral orange stripes on each side of the body. Tail with only a slight trace of or completely lacking any dark vertebral stripe; the posterior half of the tail uniformly pale yellow. Venter white to yellowish with a conspicuous stipple of irregular dark smears. Head dorsally with a symmetrical pattern of brown markings outlined by black margins which contrast with the grey or beige background coloration. Labials white with dark margins forming a black lip. Dark brown temporal stripe outlined by black blotches and stretching from the eye to the posterior end of the head.

Description of the holotype (Fig. 6). SVL 42.6 mm, TL 20.3 mm (the very tip of the tail is missing; the original tail was hence probably a few millimeters longer), total length 62.9 mm.

Head flattened dorsoventrally, separated from the body by a distinct neck; nostril pierced between two nasals, major sector-shaped (‘pac-man’-like shape); eyes large, with a round pupil; rostral roughly heptagonal, with a distinct groove at the base for flicking the tongue out; rostral visible from above and followed dorsally by one

Figure 6. Holotype of *Psammophis cornusafricae* sp. nov. (MVZ:Herp:242772).

pair of internasals, one pair of prefrontals, a long and narrow frontal with nearly equally as long supraoculars to its side; preoculars in narrow contact with the frontal and wedged between the prefrontals and supraoculars; large pair of parietals contacted laterally by large anterior temporals, posterior temporals and enlarged postparietals. The temporal formula of the anterior temporal + posterior temporal scales is 1+3. Laterally, rostral followed by two consecutive nasals, an elongated loreal and a large preocular that forms the anterior margin of the eye. Two postoculars at the posterior eye margin, the upper of which being contacted by the parietal and the lower by the anterior temporal. Nine supralabials, of which the 4th, 5th and 6th are in contact with the eye; 11 infralabials, five of which are in contact with the anterior pair of chin shields. Two pairs of chin shields. Four (right side) and five (left side) gulars in a longitudinal row between chin shields and preventrals. Anterior dorsals 15, midbody dorsals 14, posterior dorsals 11; 158 ventrals; 85 subcaudals.

Coloration in preservation: body brownish beige, dorsum darker than the flanks, with dark sets of three to five dorsolateral scales separated by two to three paler scale rows. The frontal and supraoculars with dark pigment patches at their anterior sides, posterior margins pale. Parietals with dark oblong blotches by the medial line and at the anterior margin of the scales. Internasals and prefrontals dark to the sides and paler medially, which forms a narrow white-yellowish stripe at the nose tip. Supralabials white with contrasting dark brown upper and lower margins. The white of the supralabials continues onto the sides of the neck. Throat with extensive dark spots arranged in longitudinal stripes – one on each side of the mouth on the lower side of the infralabials up to the 6th infralabial, one at the mid-line running through the chin shields and gulars further on the belly.

Comparisons. *Psammophis cornusafricae* sp. nov. can be differentiated from other congeners that occur in the Horn of Africa as follows: from its sister species *P. tanganicus* (character in brackets) by having 3–5 gulars in a longitudinal row between chin shields and preventrals (*versus* 2–3), posterior tip of the frontal moderately pointed (*versus* rounded), by lacking a clear orange or brownish dorsal stripe along the body and tail (*versus* orange vertebral stripe present), tail lacking a stripe, or having only a weakly developed dark vertebral stripe (*versus* tail with a clear dark vertebral stripe), having a clearly demarcated narrow temporal stripe on the head (*versus* broad stripe without clear demarcation), dark markings on the head dorsum paired and not fused (*versus* dark marking on the back of the head fused into a 'W' shape); from *P. biseriatus* (character in brackets) by having three supralabials in contact with the eye (*versus* two), usually one large anterior temporal (*versus* two), gular region strongly pigmented with dark longitudinal stripes (*versus* weakly pigmented with small dark spots), head ornately patterned above (*versus* uniformly colored), tail with

Figure 7. *Psammophis cornusafricae* sp. nov. in life (specimen NMP-P6V 76373, sample JIR510), with a close-up of the head in the upper left corner, and the habitat at the locality where the specimen was found (8.5 km S of Yuffleh, Somaliland) at the bottom.

absent or only a weakly developed dark vertebral stripe (*versus* tail with a clear dark vertebral stripe). Further morphological comparisons between *P. cornusafricae* sp. nov., *P. tanganicus*, and *P. biseriatus* are summarized in Table 2.

From the other Horn species *P. cornusafricae* sp. nov. differs by having a lower number of midbody dorsals (14–15 *versus* 17 or 19 in *P. aegyptius*, *P. lineatus*, *P. mossambicus*, *P. orientalis*, *P. punctulatus*, *P. rukwae*, *P. schokari*, *P. sudanensis* a *P.* cf. *sudanensis*, *P. trivirgatus*), or a higher number of midbody dorsals (11 in *P. angolensis*, 13 in *P. pulcher*).

Variation. The studied specimens of *P. cornusafricae* sp. nov. show some degree of morphological variation (Table 2). Namely, the number of infralabials varies between 10–11 and the number of supralabials between 8–9. The 3rd–5th supralabials are in contact with the eye in specimen NMP-P6V 76373 (the one with 8 supralabials); in the other two specimens it is the 4th–6th supralabials that touch the eye. Specimen NMP-P6V 76373 has three postoculars at the posterior eye margin and two anterior temporals (*versus* two postoculars and one anterior temporal in the other two specimens). Specimens MVZ:Herp:242773 and NMP-P6V 76373 (unilaterally) have two posterior tem-

Table 2. Morphological comparisons of *P. biseriatus*, *P. tanganicus* and *P. cornusafricae* sp. nov. Superscript letters refer to the original references from which the data was obtained as follows: [a] - Spawls et al. (2023); [b] - Largen and Spawls (2010); [c] - Bezy and Drewes (1985). *NA** indicates characters unavailable due to incomplete tail.

	P. biseriatus	***P. tanganicus***				***P. cornusafricae* sp. nov.**		
	General	**General**	**MCZ R-30380 Holotype**	**NMP-P6V 76371**	**NMP-P6V 76372**	**NMP-P6V 76373**	**MVZ:Herp:242772 Holotype**	**MVZ:Herp:242773 Paratype**
Total length (cm)	~ 50–80 (max 100)[a]	~ 50–80 (max 100)[a]	63	90.8	*NA* *	58.8	62.9	73.8
SVL (cm)			40.6	61.5	47.4	39.7	42.6	49.7
TL (cm)			22.4	29.3	*NA* *	19.1	20.3	24.1
SVL/Total length (×100)	61.7 (56–66)[c]	66.7 (64–81)[c]	64.4	67.7		67.5	67.7	67.3
Infralabials	10–11[c]	9–11	11	11	10	10/11 (right/left)	11	10
Supralabials	9[c]	9[c]	9	9	9	8	9	9
Supralabial in contact with eye	Two[b] (5th–6th)	Three (4th–6th)	Three (4th–6th)	Three (4th–6th)	Three (4th–6th)	Three (3rd–5th)	Three (4th–6th)	Three (4th–6th)
Midbody dorsals	15[a]	15[a]	15	15	15	15	14	15
Ventrals	138–168[a]	143–169[a]	151	159 (+2 preventrals)	150 (+1 preventral)	151 (+1 preventral)	158	146 (+1 preventral)
Subcaudals	97–134[a]	81–123[a]	114	110	*NA* *	95	85	100

porals (*versus* three in the holotype). There are 14 midbody dorsals in the holotype, while the other two specimens have 15. The number of ventrals and subcaudals varies between 146–158 and 85–100, respectively. The two specimens examined genetically are closely related (Fig. 4). They are 99.35% identical in the cyt *b* sequence (different in 7 out of 1087 bp), 98.63% identical in the ND4 (different in 9 out of 662 bp), and 99.75% identical in the c-mos (different in 1 out of 400 bp).

Etymology. The species epithet indicates the geographic origin of the species and translates as "The Sand Snake of the Africa's Horn". It is a noun in the genitive case that is derived from the Latin words for horn (*cornu-us*) and Africa (*Africa-ae*).

Distribution. Our knowledge on the distribution of *P. cornusafricae* sp. nov. is very limited because it has so far been confirmed only from two localities. They are both located in Somalia; the type locality is at the very tip of the Horn of Africa (Puntland), the locality of specimen NMP-P6V 76373 lies in central Somaliland, some 440 km west-southwest from the type locality (Fig. 8). Puntland and the eastern part of Somaliland are the driest parts of the Horn of Africa. They receive less than 200 mm of precipitation annually (Muchiri 2007), and are covered by sparse vegetation (ESA CCI Team 2017) and geologically formed by the so-called Karkar and Taleh formations that include limestones, dolomites, and gypsum (Schreiber 1993; Quiroga et al. 2022). We assume *P. cornusafricae* sp. nov. to roughly match the extent of the Karkar and Taleh formations and adjoin the range of *P. tanganicus* from the east. This distribution pattern with central Somaliland being a contact zone of closely related taxa has already been confirmed for other taxa, e.g. *Tomopterna* (Pyxicephalidae), *Hemidactylus* (Gekkonidae), *Heliobolus*, *Latastia*, *Pseuderemias* (Lacertidae), *Uromastyx*, *Xenagama* (Agamidae), *Echis* (Viperidae) (Arillo et al. 1965; Lanza 1990; Zimkus and Larson 2011; Wagner et al. 2013; Tamar et al. 2018; Spawls and Branch 2020; Šmíd et al. 2020; Spawls et al. 2023).

Discussion

Sand Snakes represent an important element of the snake fauna of Africa and Asia. Their diurnal habits, active foraging for prey and a relatively large size make them conspicuous and frequently encountered by naturalists (e.g., 2008 observations on iNaturalist as of April 27, 2023). This may be the reason why tissue samples are not that difficult to obtain for genetic analyses and why our understanding of their phylogenetic relationships is fairly complete, at least from the taxon sampling perspective. Of the 33 currently recognized species (Wallach et al. 2014; Uetz et al. 2023), 30 have been placed in the phylogenetic context. The phylogenetic studies have not only untangled the evolutionary history of the genus, but also identified several distinct genetic lineages that may represent yet undescribed species (Kelly et al. 2008; Branch et al. 2019; Chen et al. 2021; Keates 2021; Kurniawan et al. 2021; Taft et al. 2022). Coincidently, samples of all these undescribed species came from the Horn of Africa and the nearest adjacent regions, suggesting that the fauna of this forsaken region is still overlooked and that it needs further attention of researchers.

This study is the first to target the Sand Snakes of the Horn of Africa specifically. We analyze 14 newly obtained samples of six species and provide new insights into their distribution, genetic variability, and taxonomy. The phylogenetic reconstruction of the broader relationships between the *Psammophis* species confirmed previous findings (Kelly et al. 2008; Branch et al. 2019; Chen et al. 2021; Keates 2021; Taft et al. 2022), which is not surprising given their largely overlapping genetic data

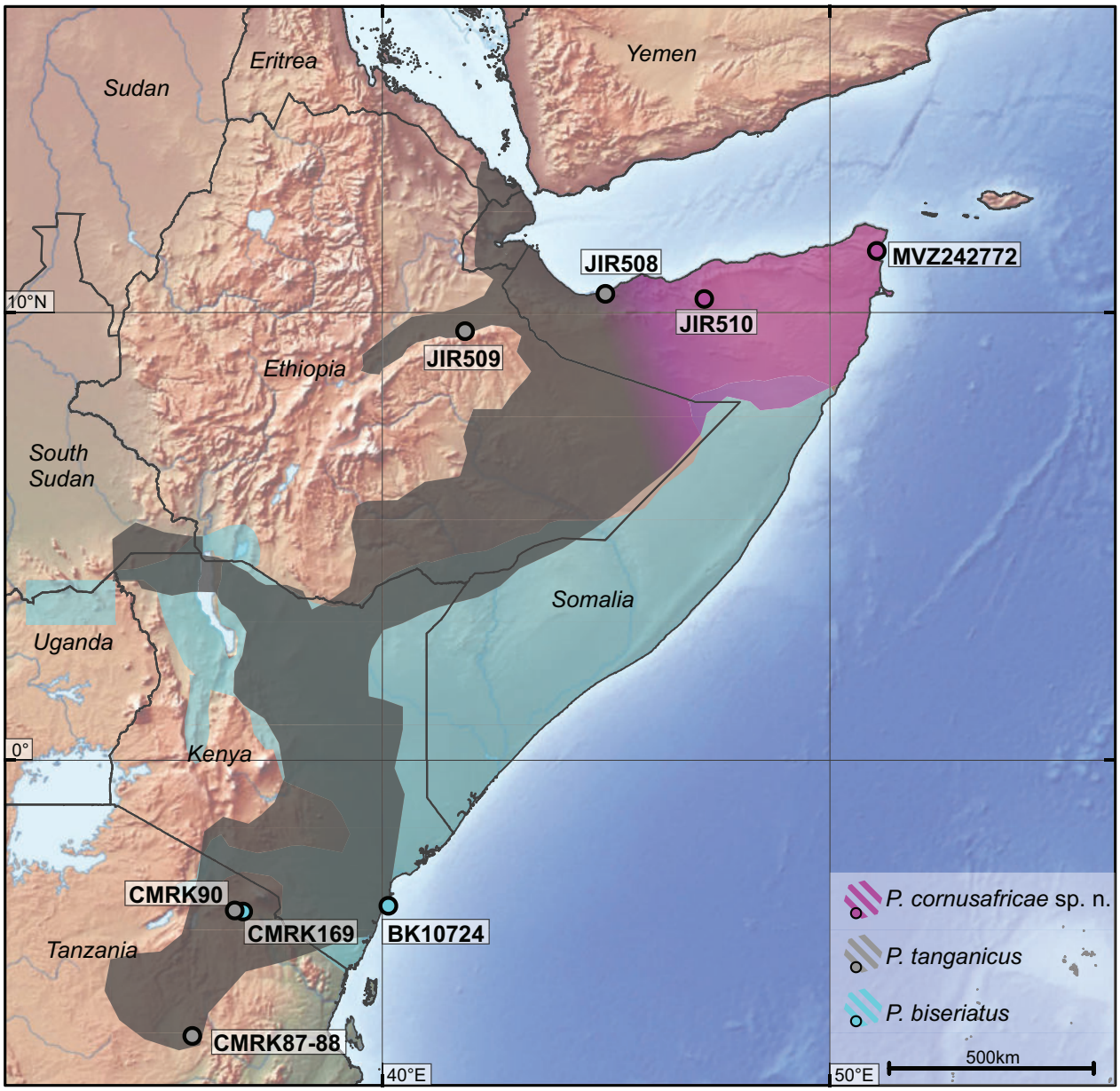

Figure 8. Distribution of *P. biseriatus*, *P. tanganicus* and *P. cornusafricae* sp. nov. in the Horn of Africa. Localities sampled for the genetic analysis are shown along with sample codes. The background layer shows shaded relief and water bodies and drainages and was made with Natural Earth (www.naturalearthdata.com). The species range maps were derived from Roll et al. (2017, 2021), Spawls et al. (2023), and the findings presented in this study.

matrices. The general structure of the tree and its potential implications for evolutionary origins of the genus are not new findings and we will not comment on them here. We will rather focus on the individual species analyzed by us, their intraspecific variation, closest phylogenetic relationships, and novel findings on their distribution.

The description of *P. cornusafricae* sp. nov. adds one more species to the list of snakes endemic to Puntland and eastern Somaliland (e.g., *Platyceps brevis* and *P. messanai* (Schätti and Lanza 1989; Schätti and Charvet 2003), *Spalerosophis josephscorteccii* (Lanza 1964), *Telescopus pulcher* (Mazuch et al. 2018), *Echis hughesi* (Cherlin 1990; Spawls et al. 2023), *Rhinotyphlops leucocephalus* (Roux-Estève 1974)). When first analyzed by Vidal et al. (2008), the phylogenetic relationships of this, at that time undescribed, species could not be inferred with certainty because there were only nine *Psammophis* species included in their study. Only more recent studies with a broader sampling of taxa enabled the identification of its closest relatives – *P. tanganicus* and *P. biseriatus*. *Psammophis tanganicus* has consistently been recovered as a sister species to *P. cornusafricae* sp. nov. (Trape et al. 2019; Keates 2021; this study). Precise delineation of the distribution ranges of *P. tanganicus* and *P. cornusafricae* sp. nov. and their potential contact zone is difficult to make at this point. The two closest confirmed localities of both species are in Somaliland and about 240 km apart. We assume the ranges of the two species meet some-

where in central Somaliland as observed in other taxa (see the Distribution section above). Ideally, other specimens from across Somaliland and Puntland that are deposited in herpetology collections worldwide and either catalogued as *P. tanganicus* or *P. biseriatus* (e.g., CAS, NHMUK, presumably MSNG, MZUF, UniMoRe; Calabresi 1927; Scortecci 1939b; Regnoli et al. 2003) and which were unfortunately not available to us should be examined to assess the distribution limits of both species. The new samples of *P. tanganicus* from Ethiopia and Somalia are slightly genetically different from those from Tanzania, which indicates that there is some level of intraspecific variation across its range. This genetic differentiation is, however, not mirrored by the morphological variation as the specimens from the northern part of the distribution are morphologically identical to other *P. tanganicus* populations from other parts of its range, including the holotype (MCZ R-30380) from central Tanzania.

Besides the description of the new species we also analyzed new specimens of other Horn taxa to shed light on their diversity and distributions. The two newly analyzed samples of *P. rukwae* from Ethiopia and Eritrea cluster with other samples of the species from Chad and Kenya. This broadly distributed species ranges from Senegal in the West through the Sahel to East Africa (Trape and Mané 2006; Spawls et al. 2018). *Psammophis rukwae* has only been confirmed recently from Ethiopia (Trape et al. 2019), and there are no records yet from Eritrea (Largen and Spawls 2010). The genotyped sample from Eritrea presented here is thus the first record of *P. rukwae* for the country.

The existence of the cryptic species referred to as *P*. cf. *sudanensis* that morphologically resembles *P. sudanensis* is well established (Trape et al. 2019; Keates 2021; Taft et al. 2022). Quite surprisingly, the two species are not closely related. While the real *P. sudanensis* forms a clade with *P. sibilans* and an undescribed species from Ethiopia (termed '*P*. sp. Ethiopia'), *P*. cf. *sudanensis* clusters with the East African *P. orientalis* and *P. subtaeniatus* from southern Africa. The new sample from Ethiopia included here that we originally identified as *P. sudanensis*, and which in fact turned out to belong to *P*. cf. *sudanensis*, proves that the two species are indeed phenotypically similar. Until detailed examinations of specimens of both species are carried out, and a formal description of the cryptic species is presented together with a differential diagnosis, it seems impossible to distinguish them without having to use DNA genotyping. We refrained from attempting to sort out the taxonomy of *P*. cf. *sudanensis* here due to the lack of comparative material.

The species with the most newly analyzed samples was *P. aegyptius*. The new samples from Egypt and Sudan are genetically very similar to other conspecific samples from the same region. The four samples from Somaliland, on the other hand, show marked genetic differences from the North African samples, as well as within themselves. The range of *P. aegyptius* covers the eastern part of the Sahara and has until now not been known to occur this far south (Largen and Spawls 2010; Geniez 2018). The new localities from Somaliland thus present a considerable range extension for the species.

Lastly, the sample of *P. punctulatus punctulatus* included in our analysis is the first of the taxon to have been analyzed. Previous material of the species belonged to the subspecies *P. p. trivirgatus* (Kelly et al. 2008) and the two taxa cluster together in the phylogeny. *Psammophis p. punctulatus* extends from southeastern Egypt to the extreme northwest of Somaliland; *P. p. trivirgatus* is distributed from northern Somaliland to Uganda, South Sudan (Ilemi Triangle) and Tanzania (Largen and Rasmussen 1993; Spawls et al. 2023). The two taxa show considerable and stable morphological differences, with *P. p. trivirgatus* having a lower number of subcaudals than *P. p. punctulatus* (143–163 in the former and 158–178 in the latter) and a bright orange head and three black dorsal stripes, compared to a grey head and one dorsal stripe in the latter (Fig. 2a, b). On the basis of their apparently partially overlapping ranges Lanza (1990) concluded that they represent different species. Based on the evidence of profound genetic diversification between the two taxa laid out here, in combination with the above mentioned morphological and geographical differences between them we follow Lanza's (1990) conclusion and recognize them as two distinct species, *Psammophis punctulatus* Duméril, Bibron & Duméril, 1854 and *Psammophis trivirgatus* Peters, 1878.

Sand Snakes rank among the most studied African snakes from the phylogenetic perspective. Yet, as evidenced by the number of cryptic or undescribed species, we are still far from fully comprehending their diversity. With the currently available sampling it is obvious that East Africa, and the Horn of Africa in particular, supports the highest diversity of undescribed species of *Psammophis*. Once their taxonomy is resolved, the diversity in the Horn may surpass that of the currently richest hotspot of the genus in southern Africa.

Acknowledgements

We are indebted to C. Spencer, J. Ho, and Natalie Ng (MVZ) for morphological examination and photographs of the MVZ specimens. Doubravka Velenská kindly helped with some of the lab work. We thank J. Lokvenc, F. Kovařík, P. Novák, V. Trailin, R. Štarha, A. I. Awale, M. Hiis, S. Musse, A. Shabele, and L. Wilson for field work assistance. We are indebted to A. A. Boqore (Vice President, Administration and Finance of Amoud University), M. M. Jibril (Vice President, Academic Affairs), S. A. Gulaid (President of Amoud University), M. Y. Muse (President of University of Hargeisa), and Shukri H. Ismail Bandare (Ministry of Environment and Climate Change, Republic of Somaliland) for issuing the collection and export permit (Ref. MOERD/M/I/251/2017, MOERD/M/I/721/2019, MOERD/M/I/230/2021). We thank W. Branch, G. Dunger and S. Spawls for providing photographs of life *Psammophis* specimens that we

used in Figs 1, 2. The editor J. Penner and reviewers W. Conradie, S. Spawls, J.-F. Trape, A. Tiutenko, and P. Wagner provided helpful feedback and fruitful comments on the first version of the manuscript. JŠ was supported by the Charles University Research Centre program No. 204069, and by the Ministry of Culture of the Czech Republic (DKRVO 2019–2023/6.VII.e, 00023272).

References

Arillo A, Balletto E, Spano' S (1965) II e III spedizione Scortecci in Migiurtinia: il genere *Eremias* Wiegmann (Reptilia, Lacertidae). Bollettino dei Musei di Zoologia e Anatomia Comparata della R Università di Genova 33: 85–109.

Augstenová B, Johnson Pokorná M, Altmanová M, Frynta D, Rovatsos M, Kratochvíl L (2018) ZW, XY, and yet ZW: Sex chromosome evolution in snakes even more complicated. Evolution 72(8): 1701–1707. https://doi.org/10.1111/evo.13543

Bezy RL, Drewes RC (1985) Specific status of the East African colubrid snake, *Psammophis tanganicus*. Journal of Herpetology 19(2): 246–253. https://doi.org/10.2307/1564178

Boundy J (2020) Snakes of the World: a supplement. CRC Press, 273 pp. https://doi.org/10.1201/9780429461354

Branch WR, Baptista N, Keates C, Edwards S (2019) Rediscovery, taxonomic status, and phylogenetic relationships of two rare and endemic snakes (Serpentes: Psammophiinae) from the southwestern Angolan plateau. Zootaxa 4590(3): 342–366. https://doi.org/10.11646/zootaxa.4590.3.2

Brandstätter F (1996) Sandrennattern. Westarp Wissenschaften, Magdeburg, 142 pp.

Calabresi E (1927) Anfibi e Rettili raccolti nella Somalia dai Proff. G. Stefanini e N. Puccioni (Gennaio-Luglio 1924). Atti della Società italiana di scienze naturali e del museo civico di storia naturale di Milano 66: 14–60.

Castresana J (2000) Selection of conserved blocks from multiple alignments for their use in phylogenetic analysis. Molecular Biology and Evolution 17(4): 540–552. https://doi.org/10.1093/oxfordjournals.molbev.a026334

Chen M, Liu J, Cai B, Li J, Wu N, Guo X (2021) A new species of *Psammophis* (Serpentes: Psammophiidae) from the Turpan Basin in northwest China. Zootaxa 4974(1): 116–134. https://doi.org/10.11646/zootaxa.4974.1.4

Cherlin V (1990) Taxonomic revision of the snake genus *Echis* (Viperidae) II. An analysis of taxonomy and description of new forms. Proceedings of the Zoological Institute, Leningrad 207: 193–223.

de Haan CC (2003) Extrabuccal infralabial secretion outlets in *Dromophis*, *Mimophis* and *Psammophis* species (Serpentes, Colubridae, Psammophiini). A probable substitute for 'self-rubbing'and cloacal scent gland functions, and a cue for a taxonomic account. Comptes Rendus Biologies 326(3): 275–286. https://doi.org/10.1016/S1631-0691(03)00073-8

ESA CCI Team 2017 (2017) S2 prototype LC map at 20m of Africa2016. http://2016africalandcover20m.esrin.esa.int/ [accessed Jan 7th, 2023]

Farr TG, Kobrick M (2000) Shuttle Radar Topography Mission produces a wealth of data. Eos (Washington, D.C.) 81(48): 583–585. https://doi.org/10.1029/EO081i048p00583

Felsenstein J (1985) Confidence limits on phylogenies: An approach using the bootstrap. Evolution; International Journal of Organic Evolution 39(4): 783–791. https://doi.org/10.2307/2408678

Geniez P (2018) Snakes of Europe, North Africa and the Middle East: A Photographic Guide. Princeton University Press, Princeton and Oxford, 379 pp.

Guindon S, Dufayard J-F, Lefort V, Anisimova M, Hordijk W, Gascuel O (2010) New algorithms and methods to estimate maximum-likelihood phylogenies: Assessing the performance of PhyML 3.0. Systematic Biology 59(3): 307–321. https://doi.org/10.1093/sysbio/syq010

Hoang DT, Chernomor O, Von Haeseler A, Minh BQ, Vinh LS (2018) UFBoot2: Improving the ultrafast bootstrap approximation. Molecular Biology and Evolution 35(2): 518–522. https://doi.org/10.1093/molbev/msx281

Katoh K, Rozewicki J, Yamada KD (2019) MAFFT online service: Multiple sequence alignment, interactive sequence choice and visualization. Briefings in Bioinformatics 20(4): 1160–1166. https://doi.org/10.1093/bib/bbx108

Kearse M, Moir R, Wilson A, Stones-Havas S, Cheung M, Sturrock S, Buxton S, Cooper A, Markowitz S, Duran C, Thierer T, Ashton B, Meintjes P, Drummond A (2012) Geneious Basic: An integrated and extendable desktop software platform for the organization and analysis of sequence data. Bioinformatics (Oxford, England) 28(12): 1647–1649. https://doi.org/10.1093/bioinformatics/bts199

Keates C (2021) Integrative systematic structuring of the widespread psammophiid snakes (Psammophiidae): a multi-evidence species delineation approach. Rhodes University, Grahamstown, South Africa, 219 pp.

Kelly CMR, Barker NP, Villet MH, Broadley DG, Branch WR (2008) The snake family Psammophiidae (Reptilia: Serpentes): Phylogenetics and species delimitation in the African sand snakes (*Psammophis* Boie, 1825) and allied genera. Molecular Phylogenetics and Evolution 47(3): 1045–1060. https://doi.org/10.1016/j.ympev.2008.03.025

Kumar S, Stecher G, Li M, Knyaz C, Tamura K (2018) MEGA X: Molecular evolutionary genetics analysis across computing platforms. Molecular Biology and Evolution 35(6): 1547–1549. https://doi.org/10.1093/molbev/msy096

Kurniawan N, Septiadi L, Fathoni M, Wibawa GS, Thammachoti P (2021) Out of Indochina: Confirmed specimen record and first molecular identification of *Psammophis indochinensis* Smith, 1943 (Squamata, Psammophiidae) from Bali, Indonesia. Check List 17(6): 1521–1531. https://doi.org/10.15560/17.6.1521

Lanfear R, Frandsen PB, Wright AM, Senfeld T, Calcott B (2017) PartitionFinder 2: New methods for selecting partitioned models of evolution for molecular and morphological phylogenetic analyses. Molecular Biology and Evolution 34: 772–773. https://doi.org/10.1093/molbev/msw260

Lanza B (1964) Il genere *Sphalerosophis* e descrizione di una nuova specie (Reptilia, Serpentes). Monitore Zoologico Italiano 72: 47–64.

Lanza B (1983) A list of the Somali amphibians and reptiles. Monitore Zoologico Italiano 8(1): 193–247. https://doi.org/10.1080/00269786.1983.11758573

Lanza B (1990) Amphibians and reptiles of the Somali Democratic Republic: Check list and biogeography. Biogeographia 14: 407–465. https://doi.org/10.21426/B614110318

Laopichienpong N, Tawichasri P, Chanhome L, Phatcharakullawarawat R, Singchat W, Kantachumpoo A, Muangmai N, Suntrarachun S, Matsubara K, Peyachoknagul S, Srikulnath K (2017) A novel method of caenophidian snake sex identification using molecular markers

based on two gametologous genes. Ecology and Evolution 7(13): 4661–4669. https://doi.org/10.1002/ece3.3057

Largen MJ, Rasmussen JB (1993) Catalogue of the snakes of Ethiopia (Reptilia Serpentes), including identification keys. Tropical Zoology 6(2): 313–434. https://doi.org/10.1080/03946975.1993.10539231

Largen MJ, Spawls S (2010) The Amphibians and Reptiles of Ethiopia and Eritrea. Edition Chimaira, Frankfurt am Main, 693 pp.

Lewin A, Feldman A, Bauer AM, Belmaker J, Broadley DG, Chirio L, Itescu Y, LeBreton M, Maza E, Meirte D, Meirte D, Nagy ZT, Novosolov M, Roll U, Tallowin O, Trape JF, Vidan E, Meiri S (2016) Patterns of species richness, endemism and environmental gradients of African reptiles. Journal of Biogeography 43(12): 2380–2390. https://doi.org/10.1111/jbi.12848

Loveridge A (1940) Revision of the African snakes of the genera *Dromophis* and *Psammophis*. Bulletin of the Museum of Comparative Zoology 87: 1–70.

Matsubara K, Nishida C, Matsuda Y, Kumazawa Y (2016) Sex chromosome evolution in snakes inferred from divergence patterns of two gametologous genes and chromosome distribution of sex chromosome-linked repetitive sequences. Zoological Letters 2(1): 1–16. https://doi.org/10.1186/s40851-016-0056-1

Mazuch T, Šmíd J, Price T, Frýdlová P, Awale AI, Elmi HSA, Frynta D (2018) New records of one of the least known snakes, *Telescopus pulcher* (Squamata: Colubridae) from the Horn of Africa. Zootaxa 4462(4): 483–496. https://doi.org/10.11646/zootaxa.4462.4.2

Mittermeier RA, Gil PR, Hoffmann M, Pilgrim J, Brooks T, Mittermeier CG, Lamoreux J, Fonseca GAB (2004) Hotspots revisited: Earth's biologically richest and most endangered terrestrial ecoregions. Conservation International, Washington, 392 pp.

Muchiri P (2007) Climate of Somalia. In: (SWALIM) TrW-SWaLIM (Ed), Nairobi, Kenya, 73 pp.

Nguyen L-T, Schmidt HA, Von Haeseler A, Minh BQ (2015) IQ-TREE: A fast and effective stochastic algorithm for estimating maximum-likelihood phylogenies. Molecular Biology and Evolution 32(1): 268–274. https://doi.org/10.1093/molbev/msu300

Quiroga E, Bertoni C, Van Goethem M, Blazevic LA, Ruden F (2022) A 3D geological model of the horn of Africa: New insights for hydrogeological simulations of deep groundwater systems. Journal of Hydrology. Regional Studies 42: 101166. https://doi.org/10.1016/j.ejrh.2022.101166

R Core Team (2013) R: A language and environment for statistical computing.

Regnoli L, Maramaldo R, Fratello B (2003) I "Colubridi" Opistoglifi della Collezione Franchini. Atti della Societa dei Naturalisti e Matematici di Modena 134: 167–215.

Roll U, Feldman A, Novosolov M, Allison A, Bauer AM, Bernard R, Böhm M, Castro-Herrera F, Chirio L, Collen B, Colli GR, Dabool L, Das I, Doan TM, Grismer LL, Hoogmoed MS, Itescu Y, Kraus F, LeBreton M, Lewin A, Martins M, Maza E, Meirte D, Nagy ZT, Nogueira CdC, Pauwels OSG, Pincheira Donoso D, Powney GD, Sindaco R, Tallowin OJS, Torres-Carvajal O, Trape J-F, Vidan E, Uetz P, Wagner P, Wang Y, Orme CDL, Grenyer R, Meiri S (2017) The global distribution of tetrapods reveals a need for targeted reptile conservation. Nature Ecology & Evolution 1: 1677–1682. https://doi.org/10.1038/s41559-017-0332-2

Roll U, Meiri S, Farrell M, Davies J, Gittleman J, Wiens J, Stephens P (2021) GARD 1.5 range shapefiles used in: Global diversity patterns are explained by diversification rates at ancient, not shallow, timescales. V1 ed. Scholars Portal Dataverse.

Ronquist F, Teslenko M, Van Der Mark P, Ayres DL, Darling A, Höhna S, Larget B, Liu L, Suchard MA, Huelsenbeck JP (2012) MrBayes 3.2: Efficient bayesian phylogenetic inference and model choice across a large model space. Systematic Biology 61(3): 539–542. https://doi.org/10.1093/sysbio/sys029

Roux-Estève R (1974) Révision systématique des Typhlopidae d'Afrique (Reptilia Serpentes). Mémoires du Muséum national d'Histoire naturelle 87: 1–313.

Schätti B, Charvet C (2003) Systematics of *Platyceps brevis* (Boulenger 1895) and related East African racers (Serpentes Colubrinae). Tropical Zoology 16(1): 93–111. https://doi.org/10.1080/03946975.2003.10531186

Schätti B, Lanza B (1989) *Coluber messanai*, a new species of snake from Northern Somalia. Bollettino del Museo regionale di Scienze naturali, Torino 7: 413–421.

Schreiber W (1993) Sedimentological and geochemical aspects of the Taleh Formation (Eocene) in North Somalia. In: Geoscientific Research in Northeast Africa. CRC Press, 449–454. https://doi.org/10.1201/9780203753392-82

Scortecci G (1939a) Gli ofidi velenosi dell'Africa Italiana. In. Istituto Sieroterapico Milanese, Milano, 292.

Scortecci G (1939b) Spedizione zoologica del Marchese Saverio Patrizi nel Basso Giuba e nell'Oltre Giuba. Giugno-Agosto 1934. XII. Rettili Ofidi. Annali del Museo Civico di Storia Naturale "G Doria", Genova 58: 263–291.

Šmíd J (2022) Geographic and taxonomic biases in the vertebrate tree of life. Journal of Biogeography 49(12): 2120–2129. https://doi.org/10.1111/jbi.14491

Šmíd J, Engelbrecht H, Taft JM, Telford NS, Makhubo BG, Bauer AM, Tolley KA (2018) A contribution to the phylogeny and taxonomy of the *Pachydactylus weberi* group (Squamata: Gekkonidae): a case of intraspecific colour polymorphism confounding taxonomy. African Journal of Herpetology 67(2): 113–126. https://doi.org/10.1080/21564574.2017.1398186

Šmíd J, Göçmen B, Crochet P-A, Trape J-F, Mazuch T, Uvizl M, Nagy ZT (2019) Ancient diversification, biogeography, and the role of climatic niche evolution in the Old World cat snakes (Colubridae, *Telescopus*). Molecular Phylogenetics and Evolution 134: 35–49. https://doi.org/10.1016/j.ympev.2019.01.015

Šmíd J, Mazuch T, Nováková L, Modrý D, Malonza PK, Elmi HSA, Carranza S, Moravec J (2020) Phylogeny and systematic revision of the gecko genus *Hemidactylus* from the Horn of Africa (Squamata: Gekkonidae). Herpetological Monograph 33(1): 26–47. https://doi.org/10.1655/HERPMONOGRAPHS-D-19-00010.1

Spawls S, Branch B (2020) The dangerous snakes of Africa. Bloomsbury, London, 336 pp.

Spawls S, Howell K, Hinkel H, Menegon M (2018) Field guide to the reptiles of East Africa. Bloomsbury, London, 624 pp.

Spawls S, Mazuch T, Abubakr M (2023) Handbook of Amphibians and Reptiles of Northeast Africa. Bloomsbury, London, 640 pp.

Steehouder A (1984) Repeated successful breeding of the red striped sand snake *Psammophis subtaeniatus sudanensis*, and some remarks on the 'polishing behaviour'of this species. Litteratura Serpentium 4: 90–103.

Taft JM, Maritz B, Tolley KA (2022) Stable climate corridors promote gene flow in the Cape sand snake species complex (Psammophiidae). Zoologica Scripta 51(1): 58–75. https://doi.org/10.1111/zsc.12514

Tamar K, Metallinou M, Wilms T, Schmitz A, Crochet PA, Geniez P, Carranza S (2018) Evolutionary history of spiny-tailed lizards (Agamidae: *Uromastyx*) from the Saharo-Arabian region. Zoologica Scripta 47(2): 159–173. https://doi.org/10.1111/zsc.12266

Trape J-F, Mané Y (2006) Guide des serpents d'Afrique occidentale. Savane et désert. IRD Éditions, Paris, 226 pp. https://doi.org/10.4000/books.irdeditions.37382

Trape J-F, Crochet P-A, Broadley DG, Sourouille P, Mané Y, Burger M, Böhme W, Saleh M, Karan A, Lanza B, Mediannikov O (2019) On the *Psammophis sibilans* group (Serpentes, Lamprophiidae, Psammophiinae) north of 12°S, with the description of a new species from West Africa. Bonn Zoological Bulletin 68: 61–91. https://doi.org/10.20363/BZB-2019.68.1.061

Trifinopoulos J, Nguyen L-T, von Haeseler A, Minh BQ (2016) W-IQ-TREE: A fast online phylogenetic tool for maximum likelihood analysis. Nucleic Acids Research 44(W1): W232–W235. https://doi.org/10.1093/nar/gkw256

Uetz P, Freed P, Hošek J (2023) The Reptile Database. http://www.reptile-database.org/ [accessed April 25th, 2023]

Vidal N, Branch WR, Pauwels OSG, Hedges SB, Broadley DG, Wink M, Cruaud C, Joger U, Nagy ZT (2008) Dissecting the major African snake radiation: A molecular phylogeny of the Lamprophiidae Fitzinger (Serpentes, Caenophidia). Zootaxa 1945(1): 51–66. https://doi.org/10.11646/zootaxa.1945.1.3

Wagner P, Mazuch T, Bauer AM (2013) An extraordinary tail – integrative review of the agamid genus *Xenagama*. Journal of Zoological Systematics and Evolutionary Research 51(2): 144–164. https://doi.org/10.1111/jzs.12016

Wallach V, Williams KL, Boundy J (2014) Snakes of the world: a catalogue of living and extinct species. CRC Press, Boca Raton, 1257 pp. https://doi.org/10.1201/b16901

Zimkus BM, Larson JG (2011) Examination of the molecular relationships of sand frogs (Anura: Pyxicephalidae: *Tomopterna*) and resurrection of two species from the Horn of Africa. Zootaxa 2933(1): 27–45. https://doi.org/10.11646/zootaxa.2933.1.2

Supplementary material 1

List of *Psammophis* species and samples included in the phylogenetic analysis

Authors: Jiří Šmíd, Sergio Matilla Fernández, Hassan Sh Abdirahman Elmi, Tomáš Mazuch

Data type: Genetic data matrix

Explanation note: List of *Psammophis* species and samples included in the phylogenetic analysis, with their sample/voucher number, country and locality of origin (datum WGS84), GenBank accession numbers, MorphoBank accessions (MorphoBank Project No. 4527), and original reference. Samples newly sequenced for this study are in bold. The GPS coordinates of *P. tanganicus* from Tanzania that are marked with asterisks are only approximate.

Link: https://doi.org/10.3897/zse.99.101943.suppl1

Zoosyst. Evol. 99 (2) 2023, 363–373 | DOI 10.3897/zse.99.102604

PENSOFT

für Natur MUSEUM FÜR NATURKUNDE BERLIN

A new species of slender flatworm in the genus *Eucestoplana* and a record of *E.* cf. *cuneata* (Platyhelminthes, Polycladida) from the Okinawa Islands, Japan, with an inference of their phylogenetic positions within Cestoplanidae

Aoi Tsuyuki[1,2], Yuki Oya[3], Hiroshi Kajihara[1]

1 *Department of Biological Sciences, Faculty of Science, Hokkaido University, Sapporo 060-0810, Japan*
2 *Creative Research Institute, Hokkaido University, Sapporo 001-0021, Japan*
3 *College of Arts and Sciences, J. F. Oberlin University, Machida 194-0294, Japan*

https://zoobank.org/D7ACA636-4B03-46F4-AF77-D5DEC8EB7084

Corresponding author: Aoi Tsuyuki (tykamsp0430@gmail.com)

Academic editor: Pavel Stoev ♦ **Received** 24 February 2023 ♦ **Accepted** 22 May 2023 ♦ **Published** 5 July 2023

Abstract

In this study, we describe a new species of elongated marine flatworm, *Eucestoplana ittanmomen* **sp. nov.**, collected from the intertidal zone of the Okinawa Islands, Japan. *Eucestoplana ittanmomen* **sp. nov.** is distinguished from other congeners based on the following characteristics: *i*) its translucent body lacking coloration, *ii*) its dome-shaped penis sheath, *iii*) the absence of cilia on the inner wall of the male atrium except outside the penis sheath, and *iv*) the presence of an adhesive organ at the posterior end of the body. Additionally, we report the occurrence of *E.* cf. *cuneata* (Sopott-Ehlers & Schmidt, 1975) in Japan; *E. cuneata* has previously been documented in the Galapagos and Fiji Islands. We conducted phylogenetic analyses to infer the positions of the two *Eucestoplana* species within Cestoplanidae using a concatenated dataset comprising partial 18S and 28S rDNA sequences from *E.* cf. *cuneata* and *E. ittanmomen* **sp. nov.** from Japan, as well as four known *Cestoplana* species with sequences available in public databases. Our phylogenetic analyses revealed that *Cestoplana* and *Eucestoplana* were reciprocally monophyletic. Furthermore, the genetic distance of the 16S rDNA sequences supported the genetic independence of the two sister species, *E.* cf. *cuneata* and *E. ittanmomen* **sp. nov.**

Key Words

Cotylea, histology, marine flatworms, marine invertebrates, molecular phylogeny, taxonomy

Introduction

Polyclad flatworms in the family Cestoplanidae Lang, 1884 are distinguishable from other flatworms by *i*) their slender bodies without tentacles, *ii*) ruffled pharynx located posterior to the center of the body, *iii*) male copulatory apparatus directed anteriorly, and *iv*) adhesive organ at the posterior end of the body (Faubel 1983; Prudhoe 1985). Currently this family comprises six genera: *Acestoplana* Faubel, 1983; *Cestoplana* Lang, 1884; *Cestoplanella* Faubel, 1983; *Cestoplanides* Faubel, 1983; *Cestoplanoida* Faubel, 1983; and *Eucestoplana* Faubel, 1983 (Faubel 1983).

The genus *Eucestoplana* currently includes two species, *Eucestoplana cuneata* (Sopott-Ehlers & Schmidt, 1975) and *Eucestoplana meridionalis* (Prudhoe, 1982a), which are distinguished from other cestoplanids by *i*) the presence of a tubular penis stylet housed in the male atrium and *ii*) the absence of a Lang's vesicle (Faubel 1983). These species have previously been reported in the Pacific

Ocean, including the Galapagos Islands, the Fiji Islands, and South Australia (Sopott-Ehlers and Schmidt 1975; Prudhoe 1982a; Tajika et al. 1991). During a faunal survey conducted as part of this study, we collected polyclad specimens of a new *Eucestoplana* species, along with *E.* cf. *cuneata*, from the intertidal zone of the Okinawa Islands, Japan. In this paper, we provide morphological descriptions of the new *Eucestoplana* species and *E.* cf. *cuneata*, based on the collected specimens. We calculated the genetic distances among the Japanese *Eucestoplana* specimens using partial 16S rDNA (16S) and cytochrome *c* oxidase subunit I (COI) sequences; the intraspecific genetic distances were also calculated based on partial 28S rDNA sequences among all cestoplanid species available in public databases. Additionally, we infer the phylogenetic positions of these two *Eucestoplana* species among other cestoplanids using molecular phylogenetic analyses of partial 18S and 28S rDNA sequences of all currently available cestoplanids in public databases.

Methods

Specimen collection and fixation

Specimens were collected from the Okinawa Islands, Japan, and processed using methods similar to those described in Tsuyuki et al. (2022, 2023). Gravel samples were collected at depths of about 20 cm from the water surface at low tide (down to about 15 cm from the sediment surface), then agitated in seawater to extract animals. The supernatant was filtered using a dip net with about 1-mm mesh, and the remaining residue was transferred into a bottle filled with fresh seawater. Before fixation, live worms were anesthetized in an $MgCl_2$ solution prepared with tap water to match the seawater salinity using an IS/Mill-E refractometer (AS ONE, Japan). Specimens were photographed using a Nikon D5600 digital camera with external strobe lightning provided by a pair of Morris Hikaru Komachi Di flash units. A portion of the body was preserved in 99.5% ethanol for DNA extraction, whereas the rest of the body was fixed in Bouin's solution for 24 h, then stored in 70% ethanol.

Morphological observation

For histological examination, specimens fixed in Bouin's solution were prestained with acid fuchsin, dehydrated in an ethanol series, cleared in xylene, embedded in paraffin wax, and sectioned serially at a thickness of 4 µm using a microtome. The sections were stained with hematoxylin and eosin, mounted on glass slides, and embedded in Entellan New (Merck, Germany) under coverslips. Specimens were observed and photographed using a Nikon D5600 digital camera under an Olympus BX51 compound microscope.

For comparison, we also examined the type series of *Eucestoplana cuneata* (as *Cestoplana cuneata*), which consists of the holotype ZMUG 25472 (3 slides) and the paratype ZMUG 25473 (5 slides), both of which have been deposited in the Biodiversity Museum Göttingen of the Georg-August-University Göttingen. In addition, we examined serial sagittal sections of *Eucestoplana cuneata* (as *Cestoplana cuneata*) collected from the Fiji Islands in Tajika et al. (1991).

DNA extraction, polymerase chain reaction, and sequencing

Total DNA was extracted using a DNeasy Blood & Tissue Kit (Qiagen, Germany). Prior to extraction, preserved tissues were incubated overnight in 180 µl of ATL buffer (Qiagen, Germany) with 20 µl of proteinase K (>700 U/ml; Kanto Chemical, Japan) at 55 °C. Four gene markers were used for the analysis: a partial sequence (677 bp) of the COI gene and the 16S (444–445 bp) for DNA barcoding, and fragments of the 18S rDNA (18S; 1,735 bp) and 28S rDNA (28S; 1,006 bp) for phylogenetic inference. Amplification of the four markers was performed using polymerase chain reaction (PCR) via a 2720 Thermal Cycler (Applied Biosystems, USA). The PCR reaction volume was 10 µl, including 1 µl of total DNA template, 1 µl of 10× ExTaq buffer (Takara Bio, Japan), 2 mM of each dNTP, 1 µM of each primer, and 0.25 U of Takara Ex Taq DNA polymerase (5 U/µl; Takara Bio, Japan) in deionized water.

Specific forward and reverse primer pairs were used for each marker: Acotylea_COI_F and Acotylea_COI_R (Oya and Kajihara 2017) for COI; 16SarL and 16SbrH (Palumbi et al. 1991) for 16S; hrms18S_F and hrms18S_R (Oya and Kajihara 2020) for 18S; and fw1 and rev4 (Sonnenberg et al. 2007) for 28S. The PCR amplification procedures were as follows: 94 °C for 1 min; 35 cycles of 94 °C for 30 s, 50 °C (COI, 16S, and 18S) or 52.5 °C (28S) for 30 s, and 72 °C for 2 min (18S), 1.5 min (28S), or 1 min (COI and 16S); and 72 °C for 7 min. PCR products were purified enzymatically using ExoSAP-IT reagent. Nucleotide sequences were determined by direct sequencing with a BigDye Terminator Kit ver. 3.1 and a 3730 Genetic Analyzer (Life Technologies, California, USA). Four internal primers were used for 18S: hrms18S_Fi1, hrms18S_Fi2, hrms18S_Ri1, and hrms18S_Ri2 (Oya and Kajihara 2020), and two internal primers were used for 28S: hrms_fw2 (Oya and Kajihara 2020) and rev4 (Sonnenberg et al. 2007). In addition to the specimens collected in the present study, a 1,735-bp partial sequence of 18S from the holotype of *Cestoplana nopperabo* Oya & Kajihara, 2019 was obtained using the same methods described above. Sequences were checked and edited using MEGA ver 7.0 (Kumar et al. 2016). The edited sequences were deposited in DDBJ/EMBL/GenBank, with accession numbers of LC740486–LC740495, LC745667, and LC745668.

Molecular phylogenetic analyses

For phylogenetic analyses, a concatenated dataset (2,834 bp) comprising partial 18S (1,735 bp) and 28S (1,099 bp) sequences was prepared (Table 1). Additional 18S and 28S sequences of three cotylean species, *Pericelis flavomarginata* Tsuyuki et al., 2020, *Prosthiostomum siphunculus* (Delle Chiaje, 1828) and *Theama mediterranea* Curini-Galletti et al., 2008, were used as outgroups (Table 1). Sequences were aligned using MAFFT ver. 7.427 (Katoh et al. 2017) with the L-INS-i strategy selected using the "Auto" option. Ambiguous sites were trimmed using Clipkit ver. 1.0 via the "kpic" option (Steenwyk et al. 2020). The optimal substitution models selected using PartitionFinder ver. 2.1.1 (Lanfear et al. 2016) according to the Akaike Information Criterion (Akaike 1974) with the greedy algorithm (Lanfear et al. 2012), were GTR + I + G for both the 18S and 28S partitions. A maximum likelihood (ML) analysis was performed using RAxML ver. 8.2.10 (Stamatakis 2014). A Bayesian phylogenetic inference (BI) was performed using MrBayes ver. 3.2.6 (Ronquist and Huelsenbeck 2003; Altekar et al. 2004) with two independent runs of Metropolis-coupled Markov chain Monte Carlo, each consisting of four chains of 2,000,000 generations. All parameters (*statefreq*, *revmat*, *shape*, and *pinvar*) were unlinked between each position; trees were sampled every 100 generations. The first 25% of trees were discarded as burn-in before a 50% majority-rule consensus tree was constructed. Convergence was confirmed based on an average standard deviation of split frequencies of 0.001138, potential scale reduction factors for all parameters of 1.000–1.025, and effective sample sizes for all parameters ≥ 404. Nodal support within the ML tree was assessed using an analysis of 1,000 bootstrap (BS) pseudoreplicates (Felsenstein 1985). ML BS values ≥70% and posterior probability values ≥90% were considered to indicate clade support. Genetic distances (uncorrected *p*-distances) were calculated using MEGA ver. X (Kumar et al. 2018) with gaps/missing data deleted completely.

Results

Molecular analyses

Molecular phylogeny

The resulting ML and BI trees were identical in terms of topology; all six examined species of Cestoplanidae formed a clade with full support (Fig. 1). Within the clade, *Eucestoplana* and *Cestoplana* were reciprocally monophyletic, each with support of 1.00PP/97% BS and 0.95PP/66% BS, respectively. Within *Cestoplana*, *C. nopperabo* was sister to the remaining three, *C. rubrocincta* (Grube, 1840), *C. salar* Marcus, 1949, and *C. techa* Du Bois-Reymond Marcus, 1957, which received full support. The latter two *C. salar* and *C. techa* were sisters with low support (0.67PP/62% BS).

Genetic distances between cestoplanid species

The interspecific genetic distances between our specimens representing *E.* cf. *cuneata* and *E. ittanmomen* sp. nov. were 3.153–3.378% for 16S and 1.107% for 28S, both of which were greater than the intraspecific ones (0.225% for 16S and 0.000% for 28S) observed within two specimens of *E.* cf. *cuneata*. We failed to amplify the COI sequence of the holotype of *E. ittanmomen* sp. nov. using the primer pair Acotylea_COI_F and Acotylea_COI_R whereas that of the Japanese specimens of *E.* cf. *cuneata* was successfully amplified with the same primers (LC740486–LC740488). The interspecific genetic distance for COI was 0.000–0.148% within three specimens of *E.* cf. *cuneata*.

The interspecific genetic distances for the 28S sequences among five species of Cestoplanidae available in public databases are shown in Table 2. The minimum value was 0.664% between *C. salar* and *C. techa* (both from Brazil), whereas the maximum value within this family was 6.977% between *C. rubrocincta* from Italy and *Eucestoplana ittanmomen* sp. nov. from Japan. Within the same genus, the maximum intraspecific genetic distance was 5.980% between *C. rubrocincta* and *C. nopperabo*.

Table 1. List of species used for the molecular phylogenetic analysis, GenBank accession numbers, and references, respectively.

Species	GenBank accession		Reference
	18S rDNA	28S rDNA	
Cestoplanidae			
Eucestoplana cf. *cuneata* (Sopott-Ehlers & Schmidt, 1975)	LC740491	LC740493	This study
Eucestoplana ittanmomen sp. nov.	LC740492	LC740495	This study
Cestoplana nopperabo Oya & Kajihara, 2019	LC745668	LC322284	Oya and Kajihara (2019); this study
Cestoplana rubrocincta (Grube, 1840)	MW376751	MW377504	Rodríguez et al. (2021)
Cestoplana salar Marcus, 1949	–	KY263653.2	Bahia et al. (2017)
Cestoplana techa Du Bois-Reymond Marcus, 1957	–	KY263654.2	Bahia et al. (2017)
Outgroup			
Pericelis flavomarginata Tsuyuki et al., 2020	LC672041	LC568535	Tsuyuki et al. (2020); Tsuyuki et al. (2021)
Prosthiostomum siphunculus (Delle Chiaje, 1828)	MZ292836	MZ292816	Rodríguez et al. (unpub.)
Theama mediterranea Curini-Galletti et al., 2008	MN384707	MN384705	Dittmann et al. (2019)

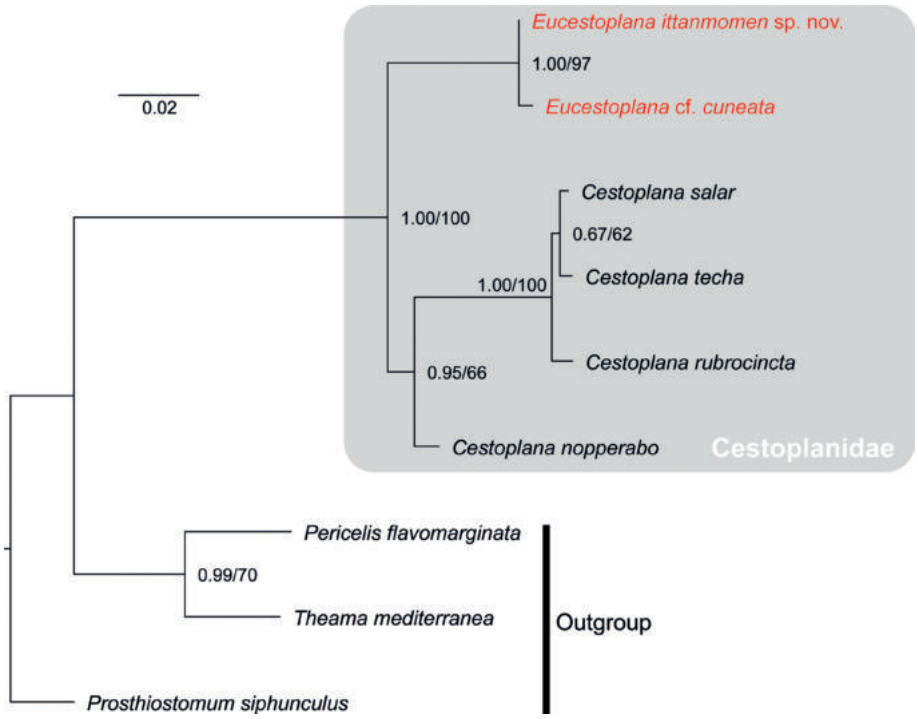

Figure 1. Maximum likelihood phylogenetic tree based on a concatenated dataset of partial 18S and 28S rDNA sequences. Numbers near nodes are posterior probabilities and bootstrap values. The species names of sequences which are newly determined in this study are indicated in the red.

Table 2. Interspecific uncorrected *p*-distances (%) for the 28S gene fragments between cestoplanid species of which sequences are available in public databases.

	C. nopperabo	***C. rubrocincta***	***C. salar***	***C. techa***	***E. ittanmomen* sp. nov.**
C. nopperabo LC322284.1	–	–	–	–	–
C. rubrocincta MW377504.1	5.980	–	–	–	–
C. salar KY263653.2	5.094	1.772	–	–	–
C. techa KY263654.2	4.873	1.883	0.664	–	–
E. ittanmomen sp. nov.	4.430	6.755	6.091	5.759	–
E. cf. *cuneata*	4.651	6.977	6.312	5.980	1.107

Taxonomy

Family Cestoplanidae Lang, 1884

Genus *Eucestoplana* Lang, 1884

Type species. *Cestoplana cuneata* Sopott-Ehlers & Schmidt, 1975.

Eucestoplana cf. *cuneata* (Sopott-Ehlers & Schmidt, 1975)

Figs 2, 3

?*Cestoplana cuneata* Sopott-Ehlers & Schmidt, 1975: 210–212, figs 9, 10; Tajika et al. 1991: 335.

?*Eucestoplana cuneata* (Sopott-Ehlers & Schmidt, 1975): Faubel 1983: 95.

Material examined. Japan •1; Okinawa Prefecture, the Okinawa Islands, Kouri Island, Tokei Beach; 26°42.86'N, 128°1.108'E; intertidal gravelly sediments; 7 Aug. 2021; A. Tsuyuki and Y. Oya leg.; sagittal sections (3 slides); GenBank: LC740488 (COI) and LC740489 (16S); ICHUM 8440. Japan •1; same data as above, except for the date (11 Aug. 2021); sagittal sections (4 slides); GenBank: LC740486 (COI), LC740491 (18S), LC740493 (28S); ICHUM 8441. Japan •1; Okinawa Prefecture, the Okinawa Islands, Okinawa Island, Nagahama Beach; 26°37.45'N, 128°11.06'E; under rocks; 9 Aug. 2021; A. Tsuyuki leg.; sagittal sections (4 slides); GenBank: LC740487 (COI), LC745667 (16S), LC740494 (28S); ICHUM 8442.

For comparison, we also examined eight serial sections of *Eucestoplana cuneata* (as *Cestoplana cuneata*) (ZMUG 25472 (holotype, three slides) and ZMUG 25473 (paratype, five slides)) and four serial sagittal sections of *Eucestoplana cuneata* (as *Cestoplana cuneata*) collected from the Fiji Island.

Description. Body slender and elongated, 24–30 mm long and 0.71–0.82 mm wide in living state (Fig. 2A). Pair of eyespot-clusters, each composed of 11–19 eyespots, distributed along midline in front of brain (Fig. 2B).

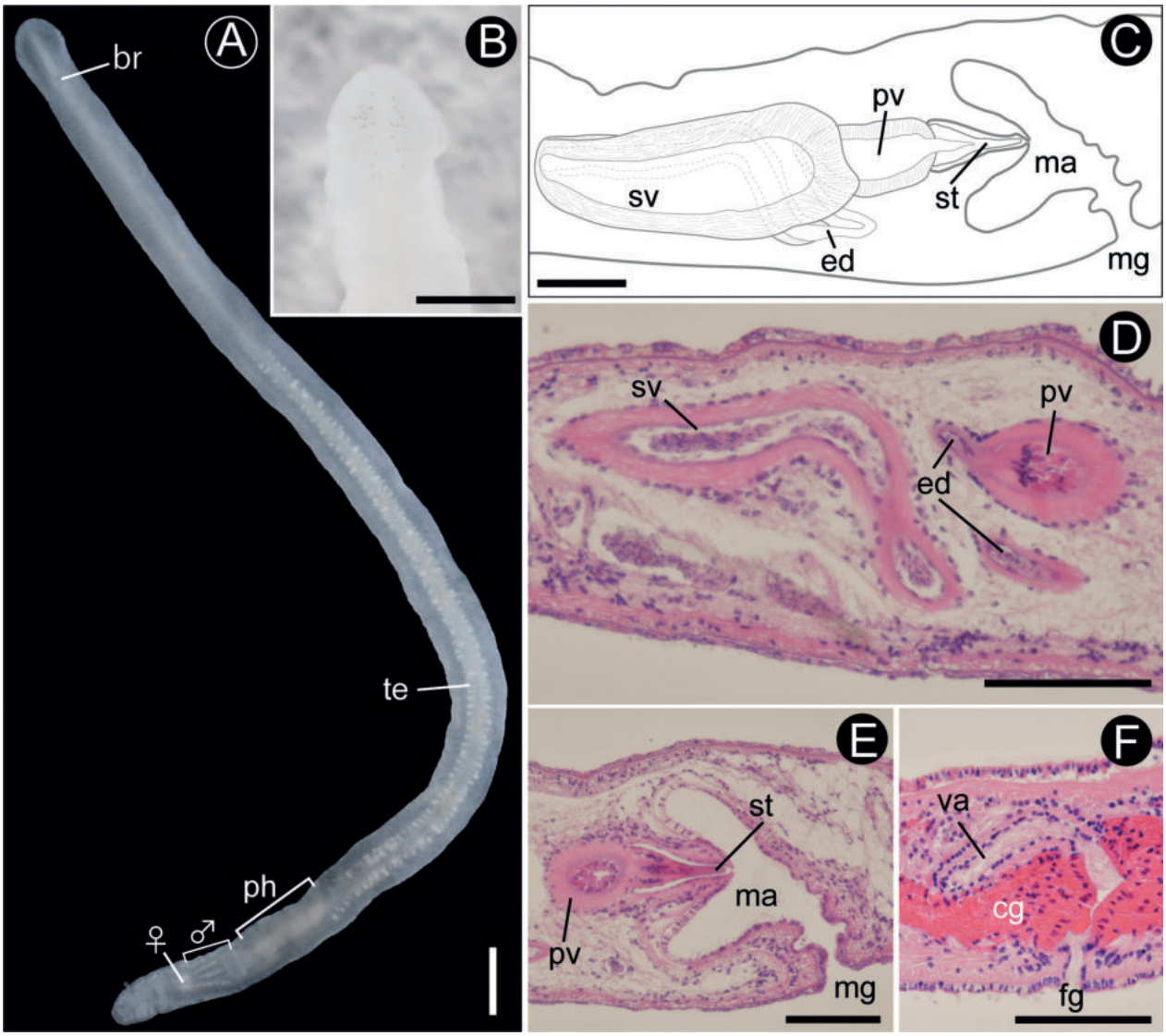

Figure 2. *Eucestoplana* cf. *cuneata* (Sopott-Ehlers & Schmidt, 1975). **A.** ICHUM 8442, whole animal in living state, dorsal view; **B.** ICHUM 8442, magnification of anterior body in living state, dorsal view, showing eyespot distribution; **C.** ICHUM 8440, schematic diagram of male copulatory apparatus in sagittal view, anterior to the right; **D, E.** ICHUM 8440, photomicrographs of sagittal sections, anterior to the right, showing male copulatory apparatus; **F.** ICHUM 8441, photomicrograph of sagittal section, showing female copulatory apparatus, anterior to the right. Abbreviations: **br** — brain; **cg** — cement glands; **ed** — ejaculatory duct; **fg** — female gonopore; **ma** — male atrium; **mg** — male gonopore; **ph** — pharynx; **pv** — prostatic vesicle; **st** — stylet; **sv** — seminal vesicle; **te** — testicular follicle; **va** — vagina; ♀ — female copulatory apparatus; ♂ — male copulatory apparatus. Scale bars: 1 mm (**A**, **B**); 100 µm (**C**–**F**).

Male copulatory apparatus composed of true seminal vesicle, interpolated prostatic vesicle, and penis papilla with stylet (Fig. 2C–E). Testicular follicles arranged in two lateral, longitudinal rows, about half length of body, running anteriorly from area in front of pharynx (Fig. 2A). Seminal vesicle antero-posteriorly elongated, posteriorly turning 180° right in front of female copulatory apparatus before running forward for short distance and then descending ventrally; thick muscular wall coating seminal vesicle, being thinner toward distal portion with forming ejaculatory duct seamlessly (Fig. 2C). Ejaculatory duct 942 µm long, extending from proximal end of prostatic vesicle to proximal end of seminal vesicle. Prostatic vesicle oval, with 19-µm thick muscular wall, lined with thick glandular epithelium (Fig. 2C–E). Penis papilla with wedged, strongly sclerotized stylet (about 60 µm long) (Fig. 2C, E). Penis sheath cone-shaped (Fig. 2C, E). Male atrium lined with cilia (Fig. 2E), opening to exterior via male gonopore with depth of about 67 µm (Fig. 2C, E). Pair of oviducts running posteriorly, then connecting to the proximal end of vagina independently. After receiving pair of oviducts, vagina curving dorsally and leading to female gonopore without evident cement pouch (Fig. 2F). Adhesive organ present at posterior end of body.

Redescription of holotype of *E. cuneata*. Male copulatory apparatus composed of true seminal vesicle, interpolated prostatic vesicle, and penis papilla with stylet (Fig. 3A). Seminal vesicle elongated, posteriorly turning 180° right, and then leading to ejaculatory duct; thick muscular wall coating seminal vesicle, being thinner

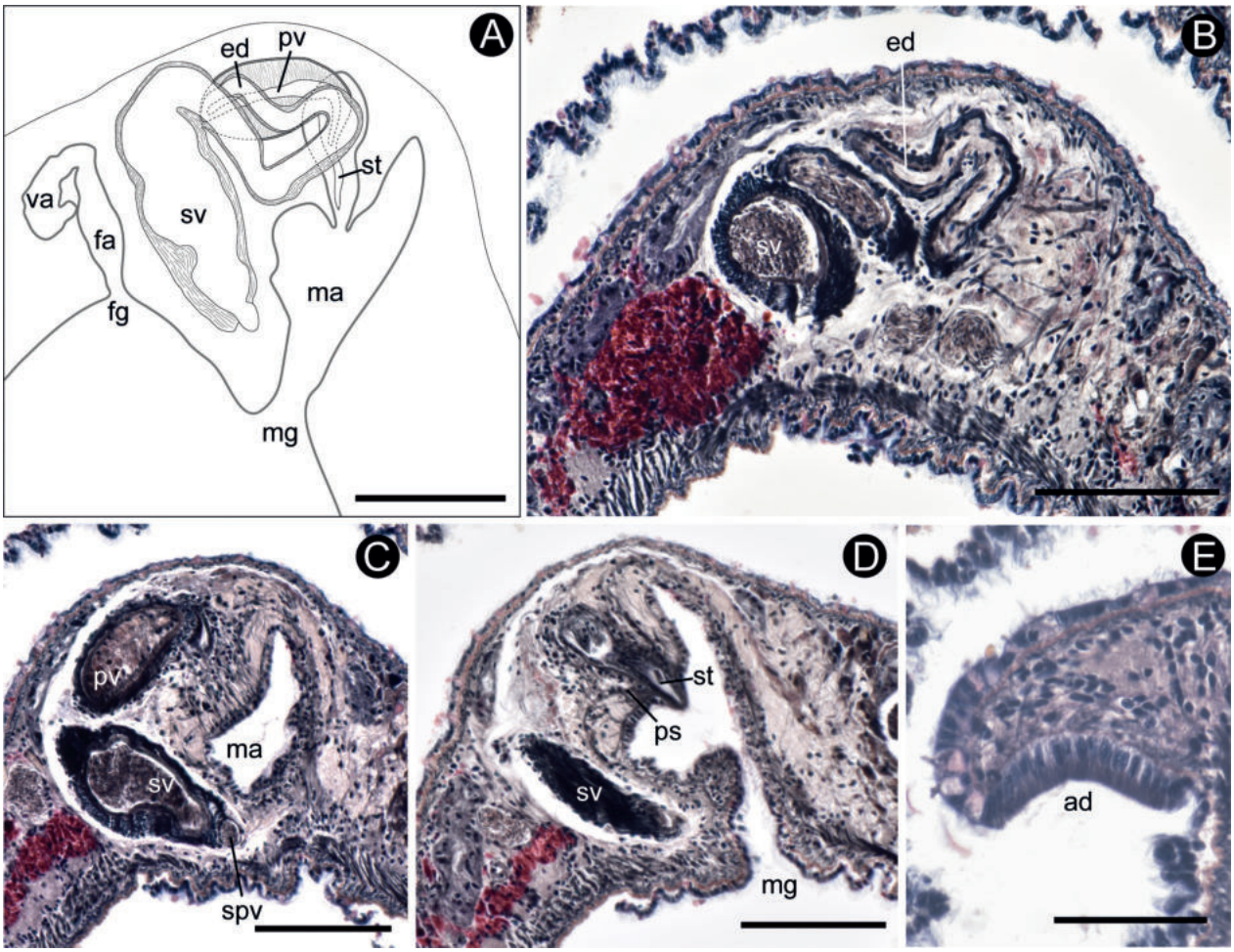

Figure 3. *Eucestoplana cuneata* (Sopott-Ehlers & Schmidt, 1975), holotype (ZMUG 25472), schematic diagram (**A**) and photomicrographs of sagittal sections (**B**–**E**) (anterior to the right). **A.** Male and female copulatory apparatuses; **B**–**D.** Male copulatory apparatus; **E.** Adhesive organ. Abbreviations: **ad** — adhesive organ; **ed** — ejaculatory duct; **fa** — female atrium; **fg** — female gonopore; **ma** — male atrium; **mg** — male gonopore; **ps** — penis sheath; **pv** — prostatic vesicle; **spv** — spermiducal vesicle; **st** —stylet; **sv** — seminal vesicle; **va** — vagina. Scale bars: 100 µm (**A**–**E**).

toward distal portion (Fig. 3A–D). Ejaculatory duct 455 µm long, extending from proximal end of prostatic vesicle to proximal end of seminal vesicle. Prostatic vesicle oval, with 13-µm thick muscular wall, lined with thick glandular epithelium (Fig. 3A, C). Penis papilla with sclerotized stylet (Fig. 3A, D). Penis sheath cone-shaped (Fig. 3A, D). Male atrium lined with cilia, opening to exterior via male gonopore with depth of about 95 µm (Fig. 3D). Pair of oviducts running posteriorly, then connecting to proximal end of vagina independently. Vagina curving dorsally after receiving oviducts. Adhesive organ present at posterior end of body (Fig. 3E).

Supplementary description of the specimen of *E. cuneata* from the Fiji Islands. Male copulatory apparatus composed of true seminal vesicle, interpolated prostatic vesicle, and penis papilla. Stylet not well observed possibly due to fixation state. Seminal vesicle elongated, posteriorly turning 180° right, and then leading to ejaculatory duct. Ejaculatory duct running to anterior, curving posteriorly behind male atrium, then connecting to proximal end of prostatic vesicle; part of ejaculatory duct from proximal end of seminal vesicle to proximal end of prostatic vesicle ca. 1 mm long. Prostatic vesicle oval; internal glandular epithelium not well observed possibly due to fixation state. Penis sheath cone-shaped. Male atrium lined with cilia, opening to exterior via male gonopore. Female reproductive organs and adhesive organ not available to be observed possibly due to fixation state.

Remarks. *Eucestoplana cuneata* was originally described from the Galapagos Islands. Our re-examination of the holotype revealed that the ejaculatory duct from proximal end of prostatic vesicle to proximal end of seminal vesicle was over twice as long as that in the original description (Sopott-Ehlers and Schmidt 1975, fig. 9).

We tentatively identified the present specimens from Kouri Island as *Eucestoplana* cf. *cuneata*. The specimens were consistent with the type specimens of *E. cuneata* in having: *i*) the eyespots distributed only anterior to the brain, *ii*) the wedged sclerotized stylet, *iii*) an adhesive organ at posterior end of body, *iv*) the conical penis sheath, and *v*) the fully ciliated inner wall of male atrium (Sopott-Ehlers and Schmidt 1975). The following morphological differences between the specimens from Japan and the Galapagos Islands should be tested by

genetic analyses if these are interspecific or intraspecific: *i*) body length (24–30 mm in our specimens; 10 mm in the original description), *ii*) eyespot number (about 30 in our specimens; 35–40 in the original description), and *iii*) length of ejaculatory duct from the proximal end of prostatic vesicle to proximal end of seminal vesicle (over 900 µm in our specimens; 455 µm in the holotype).

The wide range of distribution of *E. cuneata* needs to be verified in future studies. So far, this species has been collected from the Galapagos Islands (Sopott-Ehlers and Schmidt 1975) and the Fiji Islands (Tajika et al. 1991). Our re-examination of a specimen collected from the Fiji Islands suggested that it corresponded to the holotype of *E. cuneata* in having the *i*) conical shape of penis sheath and *ii*) the fully ciliated inner wall of male atrium. However, the Fiji specimen might be identical to *E.* cf. *cuneata* from the Okinawa Islands because it was more similar to Japanese specimens by having a long ejaculatory duct (about 1 mm). Future studies will resolve the doubt of the actual distribution of *E. cuneata* by comparing their morphology such as the body length, the eyespot number, and the male reproductive organs in more detail between different populations from the Galapagos Islands and the Fiji Islands.

Eucestoplana ittanmomen sp. nov.

https://zoobank.org/0D14C91F-156B-46C2-88C4-B1E63F94AC34

Figs 4, 5

Material examined. ***Holotype*: Japan** •1; Okinawa Prefecture, the Okinawa Islands, Kouri Island, Tokei Beach; 26°42.86'N, 128°1.108'E; intertidal gravelly sediments; 11 Aug. 2021; A. Tsuyuki and Y. Oya leg.; sagittal sections (6 slides); GenBank: LC740490 (16S), LC740492 (18S), and LC740495 (28S); ICHUM 8443. ***Paratype*: Japan** •1; same data as for holotype; sagittal sections (4 slides); ICHUM 8444.

Type locality. Japan, Okinawa Prefecture, Kunigami, Nakijin, Kouri Island, Tokei Beach (26°42.86'N, 128°1.108'E).

Diagnosis. Body slender and elongated; anterior margin rounded; dorsal surface translucent white without any color pattern; pair of eyespot-clusters distributed along midline in front of brain; penis papilla with heavily sclerotized stylet; penis sheath dome-shaped with external epithelium covered with cilia; cilia absent in inner wall of male atrium; adhesive organ present at posterior end of body.

Description of holotype. Body slender and elongated, 26 mm long and 0.75 mm wide in living state (Fig. 4A); anteriorly rounded, spreading like fan; posteriorly tapered. Dorsal surface smooth, translucent, without any color pattern. Ventral surface translucent. Tentacles absent. Pair of eyespot-clusters, each composed of 12–14 eyespots (12 on left; 14 on right), distributed along midline in front of brain (Fig. 4B), spreading out in fan shape anteriorly. Intestine highly branched without anastomosing, spreading throughout body, not reaching body margin. Pharynx ruffled, 1.94 mm long, situated on last fourth of body (Fig. 4A, C). Mouth opening at last third of pharyngeal pouch (Fig. 4C). Male gonopore opening at last ninth of body (Fig. 4A). Female gonopore situated posterior to male gonopore. Male copulatory apparatus consisting of true seminal vesicle, interpolated prostatic vesicle, and penis papilla with stylet (Fig. 4A). Testicular follicles arranged in single, lateral, longitudinal row on each side, about half length of body, running anteriorly from area in front of pharynx (Fig. 4A). Pair of sperm ducts separately entering proximal end of seminal vesicle; each duct forming spermiducal vesicle before entering seminal vesicle (Fig. 5A, B). Seminal vesicle extending posteriorly, about 700 µm long and 90 µm wide at its widest point, posteriorly turning 180° right in front of female copulatory apparatus before running anteriorly to lead to ejaculatory duct at position of proximal end of

Figure 4. *Eucestoplana ittanmomen* sp. nov., holotype (ICHUM 8443). **A.** Whole animal in living state, dorsal view; **B.** Magnification of anterior body, dorsal view, showing eyespot distribution; **C.** Photomicrograph of sagittal section (anterior to the right), showing pharynx and mouth. Abbreviations: **mo** — mouth; **ph** — pharynx; **te** — testicular follicle; ♀ — female copulatory apparatus; ♂ — male copulatory apparatus. Scale bars: 1 mm (**A**, **B**); 100 µm (**C**).

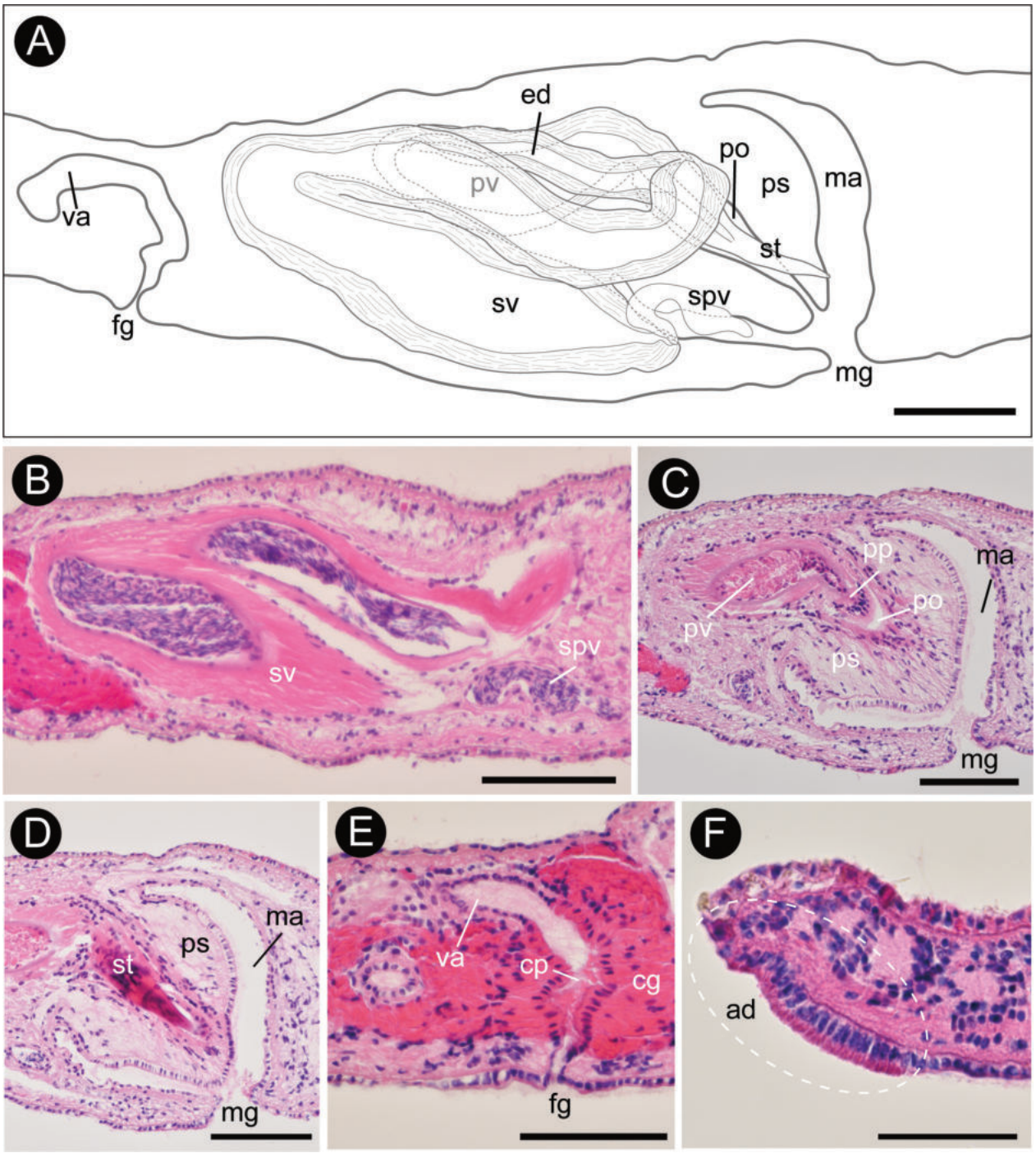

Figure 5. *Eucestoplana ittanmomen* sp. nov., schematic diagram (**A**) and photomicrographs of sagittal sections (**B**–**F**) (anterior to the right). **A.** ICHUM 8443 (holotype), male and female copulatory apparatuses; **B–D.** ICHUM 8443 (holotype), male copulatory apparatus; **E.** ICHUM 8443 (holotype), female copulatory apparatus; **F.** ICHUM 8444 (paratype), adhesive organ. Abbreviations: **ad** — adhesive organ; **cg** — cement glands; **cp** — cement pouch; **ed** — ejaculatory duct; **fg** — female gonopore; **ma** — male atrium; **mg** — male gonopore; **po** — penis pouch; **pp** — penis papilla; **ps** — penis sheath; **pv** — prostatic vesicle; **spv** — spermiducal vesicle; **st** —stylet; **sv** — seminal vesicle; **va** — vagina. Scale bars: 100 µm (**A**–**F**).

penis stylet; thick muscular wall, about 19 µm thickness, coating seminal vesicle and ejaculatory duct (Fig. 5A, B). Prostatic vesicle oval, elongated, with about 18-µm thick muscular wall, lined with thick glandular epithelium; distal end of prostatic vesicle forming penis papilla (Fig. 5A, C). Penis papilla with wedged, strongly sclerotized stylet (131 µm long), projecting into male gonopore (Fig. 5A, D). Penis sheath dome-shaped, about 184 µm wide at its widest point, housing penis stylet (Fig. 5A, C, D); external epithelium being exposed to male atrium, former being lined with cilia (Fig. 5C, D); penis pocket lined with non-ciliated epithelium. Male atrium lined with thin epithelium without cilia (Fig. 5C, D). Male gonopore about 27 µm deep. Female copulatory organ lacking Lang's

vesicle. Pair of oviducts running posteriorly, then connecting to proximal end of vagina independently. Vagina narrow, curved dorsoventrally, lined with ciliated epithelium, leading to female gonopore via narrow cement pouch (Fig. 5A, E). Numerous cement glands releasing their contents into cement pouch (Fig. 5E). Adhesive organ located at posterior end of body.

Description of paratype. Due to lack of anterior part of body, body length, width and eyespot arrangements unknown. Body coloration same as holotype. Pharynx ruffled, 1.27 mm in length; mouth opening at posterior region of pharyngeal pouch. Male copulatory apparatus composed of elongate seminal vesicle, interpolated prostatic vesicle, and penis papilla with wedged stylet (106 µm long); penis stylet slenderer than that of holotype. Penis sheath dome-shaped, with external epithelium ciliated; numerous eosinophilic glands piercing distal part of penis sheath. Male atrium covered with non-ciliated epithelium. Female copulatory apparatus same as holotype except for shape of cement pouch being more expanded than that of holotype. Adhesive organs present at posterior end of body (Fig. 5F).

Etymology. The specific name *ittanmomen* (Ittan-momen) is a Japanese noun, representing the name of one of the "yokai" (a class of supernatural entities and spirits in Japanese folklore). It is named after the long and narrow cloth-like white body of the flatworm, which evokes the similar-looking yokai, Ittan-momen.

Distribution. To date, only from the Okinawa Islands, Japan.

Remarks. Our specimens belong to *Eucestoplana* based on the following characteristics: *i*) the evident sclerotized penis stylet and *ii*) a female copulatory apparatus without any accessory ducts or Lang's vesicle. *Eucestoplana ittanmomen* sp. nov. can be easily distinguished from *E. meridionalis* by the following characteristics: *i*) translucent body, *ii*) fewer eyespots distributed only anterior to the brain, and *iii*) the presence of the adhesive organ (Table 3). Our new species is most similar to *E. cuneata* in having the following characteristics: *i*) around 30 eyespots distributed only anterior to the brain, *ii*) a wedge-shaped stylet, and *iii*) the adhesive organ located on the posterior end of the body. However, *E. ittanmomen* sp. nov. is differentiated from *E. cuneata* by the following characteristics: *i*) the shape of the penis sheath (dome-shaped in *E. ittanmomen* sp. nov.; cone-shaped in *E. cuneata*), *ii*) the arrangement of the cilia in the inner wall of the male atrium (only present along the outside of the penis sheath in *E. ittanmomen* sp. nov.; surrounding the whole male atrium in *E. cuneata*), and *iii*) the stylet length (106–131 µm in *E. ittanmomen* sp. nov.; 70 µm in *E. cuneata*). *Eucestoplana ittanmomen* sp. nov. can be also distinguished from *E.* cf. *cuneata* collected from the same locality by the same morphological differences as mentioned above. In addition, the genetic distance for 16S and 28S sequences between them could support that the two entities are likely to be genetically independent. The values for 16S (3.153%–3.378%) were much larger than the three interspecific values 0.5–1.8%, which were observed among three species of *Notocomplana* (*N. hagiyai*, *N. japonica*, and *N. koreana*) (Oya and Kajihara 2017). The *p*-distance between the 28S sequences of *E. ittanmomen* sp. nov. and *E.* cf. *cuneata* was also much larger than that between *C. salar* and *C. techa*, which are clearly different species because of their morphological difference (Table 2).

Discussion

The molecular phylogeny presented here reveals that the two *Eucestoplana* species, *E.* cf. *cuneata* and *E. ittanmomen* sp. nov., were most closely related to each other (Fig. 1). This phylogenetic closeness suggests synapomorphic traits within the cestoplanid lineage. Indeed, the *i*) heavily sclerotized penis stylet, *ii*) reduced number of eyespots, and *iii*) preference for gravelly interstitial habitats may be unique features of representatives

Table 3. Comparison of the selected characteristics among the known *Eucestoplana* species and our new species.

	E. cuneata	***E. ittanmomen* sp. nov.**	***E. meridionalis***
Body length (mm)	10[a]	26	20
Body width (mm)	?(slender, ribbon-shaped)	0.7	3
Anterior body shape	Rounded	Rounded	Slightly pointed
Eyespots	35–40[a], only anterior to the brain	About 20–30, only anterior to the brain	Numerous, distributed around brain
Dorsal coloration	? [a]; translucent white[b]	Translucent white	Chocolate-brown
Dorsal color pattern	? [a]	Absent	Absent
Mouth position	Near posterior end of pharynx	Near posterior end of pharynx	In posterior region of pharyngeal cavity
Seminal vesicle	Elongate, bending 180°	Elongated, bending 180° at position posterior to female reproductive organ	Elongate-oval
Stylet	70-µm long; wedge-shaped	106–131-µm long; wedge-shaped	Present
Penis sheath	Cone-shaped	Dome-shaped	Cone-shaped
Cilia along inner wall of male atrium	Surrounding the whole male atrium	Only present along the outside of the penis sheath	?
Adhesive organ	Present	Present	Absent
Distribution	The Galapagos Islands[a]; Fiji[b]	The Okinawa Islands, Japan	South Australia
Reference	[a]Sopott-Ehlers and Schmidt (1975); [b]Tajika et al. (1991)	This study	Prudhoe (1982a); Prudhoe (1982b)

of *Eucestoplana.* Although we were unable to include *Cestoplana nexa* Sopott-Ehlers & Schmidt, 1975 in our phylogenetic analyses, future studies may show that this species should affiliate with *Eucestoplana* rather than *Cestoplana* because the latter two characteristics of eyespot number and habitats are also found in this species. Further investigations involving more cestoplanid species are necessary to confirm the monophyly of *Cestoplana* and *Eucestoplana*. Additional species such as *E. meridionalis*, the other four species of *Cestoplana*, and representatives of the other four genera, viz. *Acestoplana*, *Cestoplanella*, *Cestoplanides*, and *Cestoplanoida* should be included in future studies to gain a more comprehensive understanding of the relationships within this family.

Acknowledgments

AT and HK are grateful to Prof. Maria Teresa Aguado Molina (Biodiversitätsmuseum Göttingen) for kindly allowing us to borrow the type specimens of *Eucestoplana cuneata* and to Dr. Jörn von Döhren (University of Bonn) for putting us in contact with Prof. Aguado Molina. The authors would like to thank Enago (www.enago.jp) for the English-language review. We thank four reviewers for giving us insightful comments to improve our manuscript. This study was funded by the Research Institute of Marine Invertebrates under Grant FY2019 No. 15 for AT and by the Japan Society for the Promotion of Science (JSPS) under KAKENHI grant number 20J11958 to YO.

References

Akaike H (1974) A new look at the statistical model identification. IEEE Transactions on Automatic Control 19(6): 716–723. https://doi.org/10.1109/TAC.1974.1100705

Altekar G, Dwarkadas S, Huelsenbeck JP, Ronquist F (2004) Parallel Metropolis coupled Markov chain Monte Carlo for Bayesian phylogenetic inference. Bioinformatics 20(3): 407–415. https://doi.org/10.1093/bioinformatics/btg427

Bahia J, Padula V, Schrödl M (2017) Polycladida phylogeny and evolution: Integrating evidence from 28S rDNA and morphology. Organisms, Diversity & Evolution 17(3): 653–678. https://doi.org/10.1007/s13127-017-0327-5

Curini-Galletti M, Campus P, Delogu V (2008) *Theama mediterranea* sp. nov. (Platyhelminthes, Polycladida), the first interstitial polyclad from the Mediterranean. The Italian Journal of Zoology 75(1): 77–83. https://doi.org/10.1080/11250000701690525

Delle Chiaje S (1828) Memorie sulla storia e notomia degli animali senza vertebre del regno di Napoli. Vol. III. Fratelli Fernandes, Napoli, 232 pp. https://doi.org/10.5962/bhl.title.10021

Dittmann IL, Cuadrado D, Aguado MT, Noreña C, Egger B (2019) Polyclad phylogeny persists to be problematic. Organisms, Diversity & Evolution 19(4): 585–608. https://doi.org/10.1007/s13127-019-00415-1

Du Bois-Reymond Marcus E (1957) On Turbellaria. Anais da Academia Brasileira de Ciências 29(1): 153–191.

Faubel A (1983) The Polycladida, Turbellaria. Proposal and establishment of a new system. Part I. The Acotylea. Mitteilungen aus dem Hamburgischen Zoologischen Museum und Institut 80: 17–121.

Felsenstein J (1985) Confidence limits on phylogenies: An approach using the bootstrap. Evolution; International Journal of Organic Evolution 39(4): 783–791. https://doi.org/10.2307/2408678

Grube E (1840) Actinien, Echinodermen und Würmer des adriatischen- und Mittelmeers, nach eigenen Sammlungen beschrieben. Verlag von J.H. Bon, Königsberg, 1–106. https://doi.org/10.5962/bhl.title.23025

Katoh K, Rozewicki J, Yamada KD (2017) MAFFT online service: Multiple sequence alignment, interactive sequence choice and visualization. Briefings in Bioinformatics 20(4): 1160–1166. https://doi.org/10.1093/bib/bbx108

Kumar S, Stecher G, Tamura K (2016) MEGA7: Molecular evolutionary genetics analysis version 7.0 for bigger datasets. Molecular Biology and Evolution 33(7): 1870–1874. https://doi.org/10.1093/molbev/msw054

Kumar S, Stecher G, Li M, Knyaz C, Tamura K (2018) MEGA X: Molecular evolutionary genetics analysis across computing platforms. Molecular Biology and Evolution 35(6): 1547–1549. https://doi.org/10.1093/molbev/msy096

Lanfear R, Calcott B, Ho SYW, Guindon S (2012) PartitionFinder: Combined selection of partitioning schemes and substitution models for phylogenetic analyses. Molecular Biology and Evolution 29(6): 1695–1701. https://doi.org/10.1093/molbev/mss020

Lanfear R, Frandsen PB, Wright AM, Senfeld T, Calcott B (2016) PartitionFinder 2: New methods for selecting partitioned models of evolution for molecular and morphological phylogenetic analyses. Molecular Biology and Evolution 34: 772–773. https://doi.org/10.1093/molbev/msw260

Lang A (1884) Die Polycladen (Seeplanarien) des Golfes von Neapel und der angrenzenden Meeresabschnitte. Eine Monographie. Wilhelm Engelmann, Leipzig, 1–172. https://doi.org/10.5962/bhl.title.10545

Marcus E (1949) Turbellaria Brasileiros (7). Boletim da Faculdade de Filosofia, Ciências e Letras, Universidade de São Paulo. Zoologia 14: 7–155. https://doi.org/10.11606/issn.2526-4877.bsffclzoologia.1949.129106

Oya Y, Kajihara H (2017) Description of a new *Notocomplana* species (Platyhelminthes: Acotylea), new combination and new records of Polycladida from the northeastern Sea of Japan, with a comparison of two different barcoding markers. Zootaxa 4282(3): 526–542. https://doi.org/10.11646/zootaxa.4282.3.6

Oya Y, Kajihara H (2019) A new bathyal species of *Cestoplana* (Polycladida: Cotylea) from the West Pacific Ocean. Marine Biodiversity 49(2): 905–911. https://doi.org/10.1007/s12526-018-0875-8

Oya Y, Kajihara H (2020) Molecular phylogenetic analysis of Acotylea (Platyhelminthes: Polycladida). Zoological Science 37(3): 271–279. https://doi.org/10.2108/zs190136

Palumbi S, Martin A, Romano S, McMillan WO, Stice L, Grabowski G (1991) The Simple Fools Guide to PCR. Ver. 2. Department of Zoology and Kewalo Marine Laboratory, University of Hawaii, Honolulu, 45 pp.

Prudhoe S (1982a) Polyclad flatworms. In: Shepherd SA, Thomas IM (Eds) Marine Invertebrates of Southern Australia. Handbook of the Flora and Fauna of South Australia. Part I: South Australian Government, Adelaide, 220–227.

Prudhoe S (1982b) Polyclad turbellarians from the southern coasts of Australia. Records of the South Australian Museum (Adelaide) 18: 361–384.

Prudhoe S (1985) A Monograph on Polyclad Turbellaria. Oxford University Press, Oxford, 259 pp.

Rodríguez J, Hutchings PA, Williamson JE (2021) Biodiversity of intertidal marine flatworms (Polycladida, Platyhelminthes) in southeastern Australia. Zootaxa 5024(1): 1–63. https://doi.org/10.11646/zootaxa.5024.1.1

Ronquist F, Huelsenbeck JP (2003) MrBayes 3: Bayesian phylogenetic inference under mixed models. Bioinformatics 19(12): 1572–1574. https://doi.org/10.1093/bioinformatics/btg180

Sonnenberg R, Nolte AW, Tautz D (2007) An evaluation of LSU rDNA D1-D2 sequences for their use in species identification. Frontiers in Zoology 4(1): 1–12. https://doi.org/10.1186/1742-9994-4-6

Sopott-Ehlers B, Schmidt P (1975) Interstitielle Fauna von Galapagos XIV. Polycladida (Turbellaria). Mikrofauna des Meeresbodens 54: 193–222.

Stamatakis A (2014) RAxML version 8: A tool for phylogenetic analysis and post-analysis of large phylogenies. Bioinformatics 30(9): 1312–1313. https://doi.org/10.1093/bioinformatics/btu033

Steenwyk JL, Buida TJ, Li Y, Shen X-X, Rokas A (2020) ClipKIT: A multiple sequence alignment trimming software for accurate phylogenomic inference. PLoS Biology 18(12): e3001007. https://doi.org/10.1371/journal.pbio.3001007

Tajika K-I, Raj U, Horiuchi S, Koshida Y (1991) Polyclad turbellarians collected on the Osaka University Expedition to Viti Levu, Fiji, in 1985, with remarks on distribution and phylogeny of the genus Discoplana. Hydrobiologia 227(1): 333–339. https://doi.org/10.1007/BF00027619

Tsuyuki A, Oya Y, Jimi N, Kajihara H (2020) Description of *Pericelis flavomarginata* sp. nov. (Polycladida: Cotylea) and its predatory behavior on a scaleworm. Zootaxa 4894(3): 403–412. https://doi.org/10.11646/zootaxa.4894.3.6

Tsuyuki A, Oya Y, Kajihara H (2021) Two new species of the marine flatworm *Pericelis* (Platyhelminthes: Polycladida) from southwestern Japan with an amendment of the generic diagnosis based on phylogenetic inference. Marine Biology Research 17(9–10): 946–959. https://doi.org/10.1080/17451000.2022.2048669

Tsuyuki A, Oya Y, Kajihara H (2022) Reversible shifts between interstitial and epibenthic habitats in evolutionary history: molecular phylogeny of the marine flatworm family Boniniidae (Platyhelminthes: Polycladida: Cotylea) with descriptions of two new species. PLoS ONE 17(11): e0276847. https://doi.org/10.1371/journal.pone.0276847

Tsuyuki A, Oya Y, Jimi N, Hookabe N, Fujimoto S, Kajihara H (2023) *Theama japonica* sp. nov., an interstitial polyclad flatworm showing a wide distribution along Japanese coasts. Zoological Science 40(3): 262–272. https://doi.org/10.2108/zs220105

Zoosyst. Evol. 99 (2) 2023, 375–389 | DOI 10.3897/zse.99.103682

PENSOFT

MUSEUM FÜR NATURKUNDE BERLIN

Illustrated catalogue of sphaeromatoid isopods (Crustacea, Malacostraca) in the Canadian Museum of Nature (CMN)

Valiallah Khalaji-Pirbalouty[1], Jean-Marc Gagnon[2]

1 *Department of Biology, Faculty of Basic science, Shahrekord University, Shahrekord, Iran*

2 *Beaty Centre for Species Discovery, Canadian Museum of Nature, Ottawa, Canada*

https://zoobank.org/551CBC3C-0F54-4634-9210-27E17A0A4E49

Corresponding author: Valiallah Khalaji-Pirbalouty (khalajiv@yahoo.com)

Academic editor: Luiz F. Andrade ♦ **Received** 17 March 2023 ♦ **Accepted** 8 June 2023 ♦ **Published** 5 July 2023

Abstract

Zoological collections are major treasures representing the history of animal biodiversity on Earth and are an important resource for biodiversity and conservation research. The Canadian Museum of Nature (CMN) has one of the oldest crustacean collections in North America.

Here, we provide an illustrated catalogue of the superfamily Sphaeromatoidea Latreille, 1825, deposited in the Canadian Museum of Nature's Crustacea Collection (CMNC). In this paper, we report 18 species, belonging to 3 families and 14 genera. The majority of species belong to the family Sphaeromatidae with 16 species, followed by the Ancinidae and the Tecticipitidae each with one species. We present a bibliography of the original description, current taxonomic status, the type locality, geographic distribution, and an updated illustration for all species.

Key Words

Canada, CMNC, Isopoda, Sphaeromatoidea, taxonomy

Introduction

The superfamily Sphaeromatoidea Latreille, 1825, comprising the Ancinidae, Sphaeromatidae and Tecticiptidae, with almost 111 genera and 649 known species, is one of the most frequently encountered and diverse isopod taxa (Boyko et al. 2008 onwards). Within the Sphaeromatoidea, the family Sphaeromatidae Latreille, 1825, is the largest family of free-living marine Isopoda, with 622 species belonging to 108 genera occurring in the shallow-water marine environments, and many as yet undescribed species and genera. The two small sphaeromatoid families are the Ancinidae Dana, 1852, with 15 described species distributed across two genera, and the Tecticipitidae Iverson, 1982, with one genus and 12 valid species (Boyko et al. 2008 onwards).

The history of isopod taxonomy in North America dates back to Say (1818), Dana (1853), Oscar Harger (1880) and Verrill et al. (1873), as well as the massive contributions of, among others, Harriet Richardson, culminating in her 1905 monograph. While many of the species described by these early authors are valid, the brief species descriptions provided at the time have resulted in difficulties in recognizing species and subsequent misidentifications by later authors. Many species in most families remain to be fully described. Furthermore, there is a need to review many of the genera and the placement of species within these. The Canadian Museum of Nature (CMN) holds large collections across all animal groups. Based on the Canadian Museum of Nature database, the museum's Invertebrate Collection contains more than seven million specimens in more than 1.9 million lots. Of these, Amphipoda, Isopoda and Mysidacea are the major groups found in the Crustacean Collection (CMNC). Most of the specimens were collected by Edward L. Bousfield, who joined the CMN in 1950. Bousfield was a world authority on the systematics of Amphipoda; he described more than 300

new species (Conlan et al. 2016). Besides his intensive focus on the Amphipoda, his collections cover all sorts of invertebrates (mostly marine), as well as isopod crustaceans. With more than 3200 isopod records in the CMN database, including about 80 genera and 190 species (about 85% of which are from marine and brackish water habitats), in addition to the many samples yet to be catalogued, this collection is amongst the most important natural history archives for this group in North America. The present catalogue is a comprehensive, up-to-date account of the 18 species of sphaeromatoid isopods represented in the Canadian Museum of Nature, with illustrations of the species. This catalogue is arranged alphabetically by genus and then by species names within families, followed by the original combination, author(s) name and year of publication. For each species, a current nomenclature (valid names or synonymy) is given.

Material and method

Sphaeromatoid isopods for this study are from the Crustacean Collection of the Canadian Museum of Nature (**CMNC**; located at its Natural Heritage Campus, in Gatineau, Quebec, Canada).

Specimens were examined using Zeiss Stereomicroscope (Stemi 508). Color images of the specimens were taken using a Zeiss AxioCam ERc5s digital camera mounted on a Zeiss (Stemi 508) stereomicroscope. Photographs were merged and edited using Adobe Photoshop CC v.20.0.6.

Results

Systematics
Alphabetical list of taxa

Family Ancinidae Dana, 1852
Genus *Bathycopea* Tattersall, 1905

***Bathycopea daltonae* (Menzies & Barnard, 1959)**
Fig. 1A, B

Ancinus daltonae Menzies & Barnard, 1959: 31, fig. 25; Schultz 1973: 270–272, fig. 1D, G.
Bathycopea daltonae.– Loyola e Silva, 1971: 217–222, figs 5–7; Kussakin 1979: 369, fig. 229; Shimomura 2008: 26.

Type locality. The shelf off San Miguel Island, California.

Material examined. Canada. 1 ovigerous ♀ (5.2 mm), 2 ♂♂ (up to 5.1 mm); British Columbia, Vancouver Island, Barclay Land District, Cape Beale; 2 Aug. 1975; E.L. Bousfield leg.; CMNC 1985-0633. 4 ♂♂ (up to 5 mm); British Columbia, Barclay Land District, Trevor Ch.; 29 Jul. 1975; E.L. Bousfield leg.; CMNC 1985-0630. 1 ovigerous ♀ (4 mm); British Columbia, Barclay Land District, Trevor Ch.; 30 May 1977; E.L. Bousfield leg.; CMNC 1985-0634. USA. 2 ovigerous ♀♀ (up to 4.9 mm), 1 ♂ (4.25 mm); Washington, Clallam Co., Makah Bay; 31 July 1966; E.L. Bousfield leg.; CMNC 1991-2557.

Distribution. San Miguel Islands, southern California to Vancouver Island.

Family Sphaeromatidae Latreille, 1825
Genus *Amphoroidea* H. Milne Edwards, 1840

***Amphoroidea typa* H. Milne Edwards, 1840**
Fig. 1C

Amphoroidea typa Milne Edwards, 1840: 22–23; Dana 1853: 783; Hansen 1905: 108–126; Menzies 1962a: 140–141, fig. 47D; Hurley and Jansen 1977: 27 (listed as type species).

Type locality. Chile.

Material examined. Chile. 30 ♀♀ (up to 19.5 mm), 1 ♂ (16.5 mm); Magallanes-Antarctica Region, Isla Lennox; 5 Feb.1970; E.L. Bousfield & J.W. Markham leg.; CMNC 1992-0567.

Distribution. Known only from Chile.

Genus *Cassidinidea* Hansen, 1905

***Cassidinidea ovalis* (Say, 1818)**
Fig. 1D

Naesa ovalis Say, 1818: 484–485.
Cassidena lunifrons Richardson, 1900: 222.
Naesa ovalis Richardson, 1900: 224.
Cassidina lunifrons.– Richardson 1901: 533, fig. 14.
Cassidisca lunifrons.– Richardson 1905: 273, figs 283–284.
Cassidisca ovali.– Richardson, 1905: 274, figs 283, 205.
Cassidinidea ovalis.– Hansen, 1905: 130; Menzies and Frankenberg 1966: 44 fig. 20; Schultz 1969: 115, fig. 158; Kussakin 1979: 336, figs 199–200; Heard 1982: 32, fig. 35; Kensley and Schotte 1989: 208, fig. 92; Bruce 1994: 1151, fig. 45; Camp et al. 1998: 136; Kensley and Schotte 1999: 701–702; Khalaji-Pirbalouty and Bruce 2021: 494–502, figs 2–5.

Type locality. St John's River in Florida.

Material examined. USA. 4 ♂♂ (up to 3 mm), 8 ♀♀ (up to 3.2 mm); South Carolina, Georgetown County; 26 Apr. 1965; E.L. Bousfield leg.; CMNC 1992-0582. 1 ♂ (2.8 mm), 6 ♀♀ (up to 3.2 mm); South Carolina, Charleston County, 25 Apr. 1965; E.L. Bousfield leg.; CMNC 1991-2575. 2 ♀♀ (up to 3 mm); North Carolina, Dare County; 11 Apr. 1975; E.L. Bousfield leg.; CMNC 1985-0643. 1 ♀ (3.1 mm); North Carolina, Tyrrell County, 11 Apr. 1975; E.L. Bousfield leg.; CMNC 1985-0644.

Distribution. Eastern coast of North America from New Jersey to Florida (Khalaji-Pirbalouty and Bruce 2021).

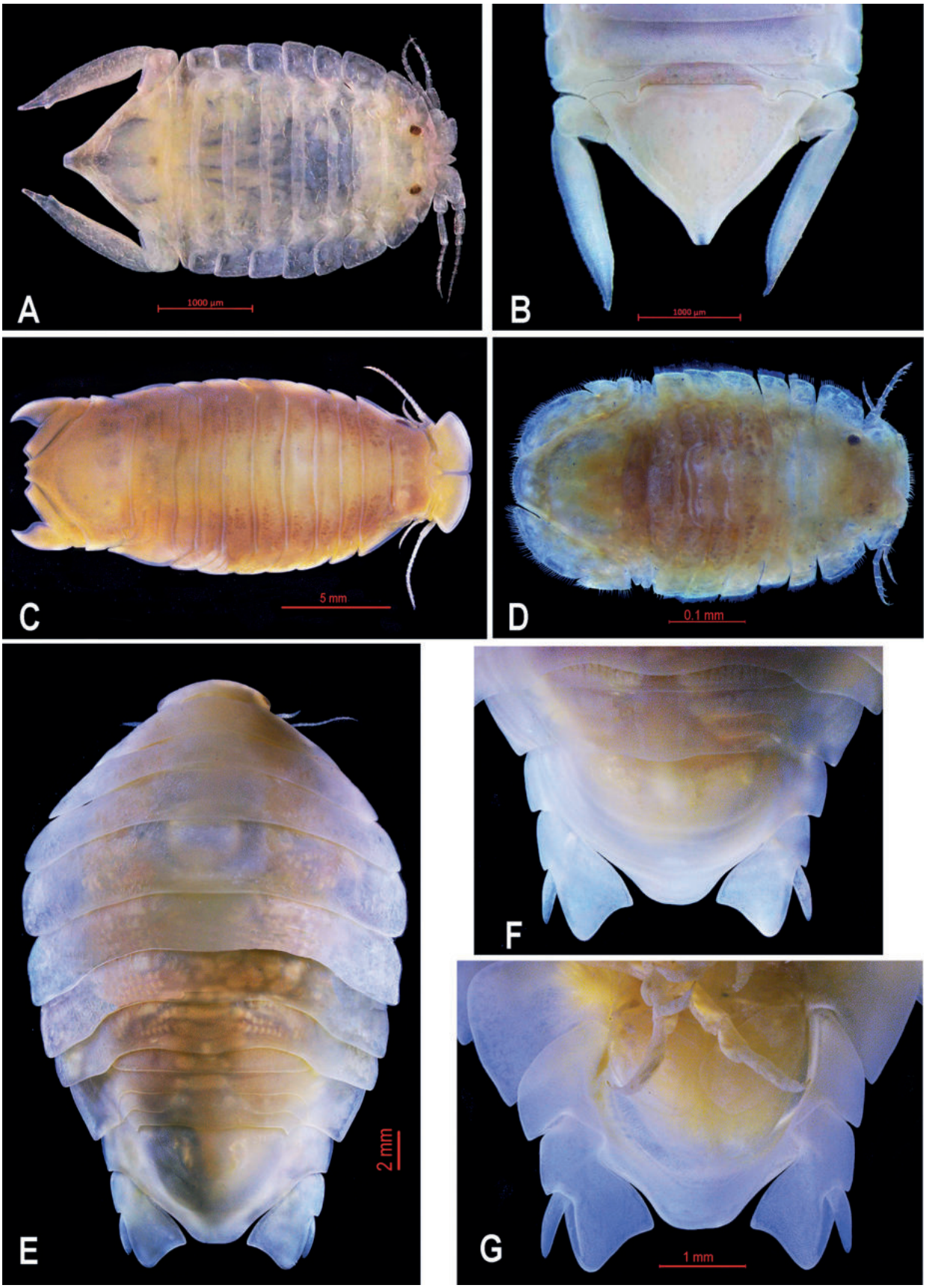

Figure 1. A. *Bathycopea daltonae* (Menzies & Barnard, 1959), male, (CMNC 1985-0633); **B.** Female, pleotelson; **C.** *Amphoroidea typa* Milne Edwards, 1840, female, (CMNC 1992-0567); **D.** *Cassidinidea ovalis* (Say, 1818) male, (CMNC 1992-0582); **E.** *Cassidinopsis emarginata* (Guérin-Méneville, 1843), male, (CMNC 1985-0636); **F.** Pleotelson dorsal view; **G.** Pleotelson ventral view.

Genus *Cassidinopsis* Hansen, 1905

Cassidinopsis emarginata (Guérin-Méneville, 1843)

Fig. 1, G

Cassidina emarginata Guérin-Méneville, 1843: 31; Cunningham 1871: 499, pl. 59, fig. 4; Miers 1879: 204; Studer 1883: 19; Pfeffer 1886: 63–69, pl. 2, figs 9–10, pl. 4, figs 23–30, pl. 6, figs 1–10; Dollfus 1891: 67, pl. 8, fig. 10; Stebbing 1900: 562; Ortmann 1911: 650.

Cassidinopsis emarginata – Hansen, 1905: 82, 87, 128; Hodgson 1910: 4; Tattersall, 1921: 223; Monod, 1931: 25–26; Stephensen 1947: 28; Vanhöffen 1914: 514; Menzies 1962a: 144, fig. 49; Carvacho, 1977: 177; Kussakin and Vasina1980: 356–360; Brandt 1998: 150, figs 9–11.

Cassidinopsis emarginatus.– Giambiagi, 1925: 233; Stebbing 1914: 351.

Type locality. Falkland Island. (Falkland Islands and the West coast of Patagonia).

Material examined. Chile. 1 ♂ (36 mm); Magallanes y de la Antártica Chilena Region, Isla Navarino, Punta Wulaia; 3 Feb. 1970; E.L. Bousfield leg.; CMNC 1985-0636. 18 ♂♂ and ♀♀ (up to 28 mm); Magallanes-Antarctica Region, Canal Beagle; 19 Feb. 1970; E.L. Bousfield leg.; CMNC 1985-0637. 1♀ (18 mm), 2 juveniles; Magallanes-Antarctica Region, Isla Lennox; 6 Feb. 1970; E.L. Bousfield leg.; CMNC 1985-0635.

Distribution. South Georgia Island, Falkland Islands to Southern coasts of Chile; Puerto Deseado, Argentina (Brandt 1998; Gomez Simes 1979).

Genus *Dynamene* Leach, 1814

Dynamene dilatata Richardson, 1899 (uncertain/ *incerta sedis*)

Fig. 2A, B

Dynamene dilatata Richardson, 1899: 882–883, fig. 8; Richardson 1905: 304, fig. 327; Schultz 1969: 122, fig. 171; Hatch 1947: 214, pl. 7, figs 85–86.

Dynamenella dilatata.– Kussakin, 1971: 450, fig. 298; Brusca et al. 2007: 521, 537, pl. 242.

Note. This species is retained in the genus *Dynamene* (in original combination) and listed as "taxon inquirendum" in WoRMS (Boyko et al. 2008 onwards). Thus, the correct generic status of this species is still in question. Since Richardson (1899; 1905) and subsequent authors provided only a brief description with a figure of the whole body, a morphological revision is required to correctly place this species.

Type locality. Monterey Bay, California.

Material examined. Canada. 3 ♀♀ (up to 6.5 mm); Oregon, Lincoln Co.; 12 Aug. 1966; E.L. Bousfield leg.; CMNC 1991-2567. 1 ovigerous ♀ (8.5 mm); British Columbia, Long Beach Unit, Long Beach; 5 Aug. 1955; E.L. Bousfield leg.; CMNC 1985-0648. 1 ♂ (5.5 mm); British Columbia, Long Beach Unit, Long Beach; 5 August 1955; E.L. Bousfield leg.; CMNC 1985-0660.

Genus *Dynamenella* Hansen, 1905

Dynamenella sheareri (Hatch, 1947)

Fig. 2C

Dynamene sheareri Hatch, 1947: 164, 262, fig. 173; George and Strömberg 1968: 246–248, pl. 2, fig. 9.

Dynamenella sheareri.– Schultz ,1969: 123, fig. 174; Harrison and Holdich 1982: 90.

Note. The true generic status of this species is still undetermined.

Type locality. Coos Bay, Oregon.

Material examined. Canada. 6 ♀♀ (up to 3 mm), 1 ♂ (3.8 mm); British Columbia, Renfrew Land Distr., Port Renfrew; 1 Aug. 1970; CMNC 1990-0069. 5 ♀♀ (up to 3.5 mm), 2 ♂♂ (4 mm), British Columbia, Vancouver Island, Barclay Land Distr., Bordelais Islets; 9 Aug. 1975; CMNC 1990-0070.

Remarks. *Dynamenella sheareri* cannot be a *Dynamenella* because of the following characters: having a single pleonal suture running to posterior margin (instead of two); penial process more fused, not basally swollen; appendix masculina is evenly slender and long, not "flask shaped."

Genus *Dynoides* Barnard, 1914

Dynoides canadensis Khalaji-Pirbalouty & Gagnon, 2021

Fig. 2D

Dynoides canadensis Khalaji-Pirbalouty & Gagnon, 2021: 12–20, figs 2–5.

Type locality. Canada, British Columbia.

Material examined. Canada. ***Holotype.*** ♂ (4.2 mm); British Columbia, Barclay Land District, Cape Beale; 19 July 1970; E.L. Bousfield leg.; CMNC 1985-0667.1. ***Paratypes.*** 4 ♂♂ (up to 4.2 mm), 18♀♀ (up to 4.3 mm), 1 ovigerous♀ (4.5 mm), same data as holotype; CMNC 1985-0667.2. 2 ♂♂ (up to 5 mm), 2 ovigerous ♀♀ (3.5 mm), 2 ♀♀ (3.5 mm); British Columbia, Sooke Land District, Whiffin Spit; 17 August 1955; E.L. Bousfield leg.; CMNC 1990-0064. 3 ♀♀ (up to 5 mm); British Columbia, Rupert Land Distr., Vancouver Island, Cape Scott; 18 July 1959; E.L. Bousfield leg.; CMNC 1990-0066. 20 ♂&♀; British Columbia, Renfrew Land Distr., Vancouver Island, Port Renfrew; 1 August 1970; E.L. Bousfield leg.; CMNC 1990-0068. 1♀ (3 mm); British Columbia, Queen Charlotte Islands Land Distr., Graham Island, 27 July 1957; E.L. Bousfield leg.; CMNC 1990-0067. 5 ♂♂ (up to 4.9), 6 ♀♀ (up to 4.2); British Columbia, Barclay Land District, Trevor Channel, Tzartus Island; 21 July 1970; E.L. Bousfield leg.; CMNC 1985-0664. 4 ♂♂ (up to 4.5 mm), 5 ♂♂ (up to 4.2 mm), British Columbia, Metchosin Land Distr., Sooke Basin, Becher Bay; 31 July 1970; E.L. Bousfield leg.; CMNC 1990-0057. 4♂♂ (up to 4.5 mm), 2 ♀♀ (3 mm), British

Columbia, Nootka Land Distr., Nootka Island; 20 August 1959; E.L. Bousfield leg.; CMNC 1990-0059. 1 ♂ (4.2 mm), 1 ♂ (3.5 mm), British Columbia, Rupert Land Distr., Hope Island; 22 August 1959; E.L. Bousfield leg.; CMNC 1990-0060. 1 ♂ (5.1 mm), 5 ♂♂ (up to 4 mm), 1 juvenile, British Columbia, Range 2 Coast Land Distr., Goose Island; 6 August 1964; E.L. Bousfield leg.; CMNC 1990-0061. 6 ♀♀ (up to 3 mm), British Columbia, Range 2 Coast Land Distr., Hunter Island; 8 August 1964; E.L. Bousfield leg.; CMNC 1990-0063. 8 ♂♂ (up to 5 mm), 20 ♀♀ (up to 4.1 mm), 10 juveniles, British Columbia, Range 3 Coast Land Distr., Princess Royal Island; 20 July 1964; E.L. Bousfield leg.; CMNC 1990-0065.

Distribution. Western coasts of British Columbia from Victoria area to Graham Island.

Genus *Exosphaeroma* Stebbing, 1900

Exosphaeroma gigas (Leach, 1818)

Fig. 2E, F

Sphaeroma gigas Leach, 1818: 346–347; Desmarest 1825: 301; Milne-Edwards 1840: 205; White 1847: 102; Dana 1853: 775; Miers 1879: 202–203; Haswell 1882: 287; Studer 1884: 17–18; Dollfus 1891: 62, pl. 8a, fig. 6.

Sphaeroma jurinii.– Krauss, 1843: 65.

Sphaeroma propinqua.– Nicolet, 1849: 277–278.

Sphaeroma chilensis.– Dana, 1853: 195–196.

Sphaeroma obtusa.– Hutton, 1879 (in Chilton 1906).

Exosphaeroma gigas.– Stebbing, 1900: 553–558, pl. 39; Chilton 1906: 271–272; Ortmann 1911: 646–647; Vanhöffen1914: 510–511; Tattersall 1921: 216; Giambiagi 1925: 235; Stephensen 1927: 362; Nierstrasz 1931: 194; Barnard 1940: 413, fig. 13; Hurley 1961: 269; Hale 1929: 275, fig. 273; Menzies 1962a: 132–134, fig. 43; Kussakin 1967: 235; Hurley and Jansen 1977: 58, fig. 52; Carvacho, 1977: 177–178; Kussakin and Vasina1980: 355–359; Brandt and Wägele 1989: 209–214. figs 5–9; Bruce 2003: 368.

Type locality. Unknown; The Natural History Museum, syntypes: 1941: 6:27: 5 (presented by Leach) and 1979: 420: 1, Sir Joseph Banks collection (Ellis 1981).

Material examined. Chile. 22 ♂♂ (up to 24 mm), 50 ♀♀ (up to 18 mm); Magallanes and Chilean Antarctica Region, Picton Island; 7 Feb. 1970; E.L. Bousfield leg.; CMNC 1990-0090. 46 ♂♂ and ♀♀; Magallanes and Chilean Antarctica Region, Navarino Island; 29 Jan. 1970; E.L. Bousfield leg.; CMNC 1990-0092. 300 ♂♂ and ♀♀; Magallanes and Chilean Antarctica Region, Canal Beagle; 19 Feb. 1970; E.L. Bousfield leg.; CMNC 1990-0094. FALKLAND. 1♀ (16 mm); Atlantic Ocean, Falkland Island, East Falkland; 1 Feb. 1969; S.W. Gorham leg.; CMNC 1992-0545. 9 ♂♂ and ♀♀ (up to 18 mm); East Falkland; 25 Jan. 1967; S.W. Gorham leg.; CMNC 1992-0552.

Distribution. Magallanes and Chilean Antarctica Region, Tierra del Fuego, Falkland Islands, Crozet Islands, Kerguelen Islands, Peru, South Africa, South Australia, New Zealand (Chatham Rise, Macquarie Island, Auckland Island, Campbell Island), Tasmania (Dana 1853; Vanhöffen 1914; Tattersall 1914; Kussakin 1967; Brandt and Wägele 1989).

Exosphaeroma rhomburum (Richardson, 1899)

Fig. 2G

Sphaeroma rhomburum Richardson, 1899: 835–836, fig. 12; 1900: 222.

Exosphaeroma rhomburum.– Richardson, 1905: 290, fig. 303; Nierstrasz 1931: 195; Schultz 1969: 135, fig. 197; Kussakin 1971: 402, fig. 257; Bruce 2003: 369.

Type locality. Monterey Bay, California.

Material examined. USA. 3 ♂♂ (up to 4.1 mm), 2 ovigerous ♀♀ (up to 4.2 mm); Washington, Clallam Co., Makah Bay; 31 July 1966; E.L. Bousfield leg.; CMNC 1991-2559. Canada. 4 ♂♂ (up to 4.5 mm), 4 ♀♀ (up to 5 mm); British Columbia, Range 5 Coast; 13 July 1964; E.L. Bousfield leg.; CMNC 1984-1535. 3 ♂♂ (up to 4.1 mm), 4 ♀♀ (up to 4.5 mm); British Columbia, Rupert Land Distr., Hope Island; 22 July 1959; E.L. Bousfield leg.; CMNC 1984-1537. 1 ♀ (4 mm); Alaska, Prince of Wales-Outer Ketchikan Census Area; 31 May 1961; E.L. Bousfield leg.; CMNC 1991-2501.

Distribution. Monterey Bay, California, Washington to British Columbia.

Exosphaeroma russellhansoni Wall, Bruce & Wetzer, 2015

Figs 2H, 3A, B

Exosphaeroma russellhansoni Wall, Bruce & Wetzer, 2015: 28–33, figs 9–12.

Type locality. Washington, Puget Sound, Seattle, Smith Cove.

Material examined. Canada. 15 ♂♂ (up to 6.2 mm); British Columbia, Esquimalt Land Distr., Esquimalt; 30 July 1970; E.L. Bousfield leg.; CMNC 1984-1465. 2 ♂♂ (5.1, 5.5 mm); British Columbia, Queen Charlotte Islands Land Distr., Yakan Pt.; 25 Aug. 1975; E.L. Bousfield leg.; CMNC 1984-1445. 3 ♂♂ (up to 6 mm); Land Distr., Graham Island; 11 Aug. 1975; E.L. Bousfield leg.; CMNC 1984-1447. 4 ♂♂ (up to 5.8 mm), 2 ♀♀ (up to 4.8 mm); British Columbia, Range 3 Coast Land Distr., Princess Royal Island; 20 July 1964; E.L. Bousfield leg.; CMNC 1984-1448. 5 ♂♂ (up to 6.5 mm), 2 ♀♀ (up to 4.8 mm); British Columbia, Metchosin Land Distr., Witty's Lagoon; 28 July 1964; E.L. Bousfield leg.; CMNC 1984-1449. 16 ♂♂ (up to 6 mm), 3 ♀♀ (up to 5 mm); British Columbia, Range 3 Coast Land Distr., Lady Douglas Island; 9 July 1964; E.L. Bousfield leg.; CMNC 1984-1452. 4 ♂♂ (up to 6.1 mm), 4 ♀♀ (up to 4.1 mm); British Columbia, Range 3 Coast Land Distr., Miles Island; 5 Aug. 1964; E.L. Bousfield leg.; CMNC 1984-1452. 2 ♂♂ (up to 6.5 mm); British Columbia, Range 5 Coast Land Distr., Stephens Island; 12 July 1964; E.L. Bousfield leg.; CMNC 1984-1455. 4 ♂♂ (up to 6.8 mm),

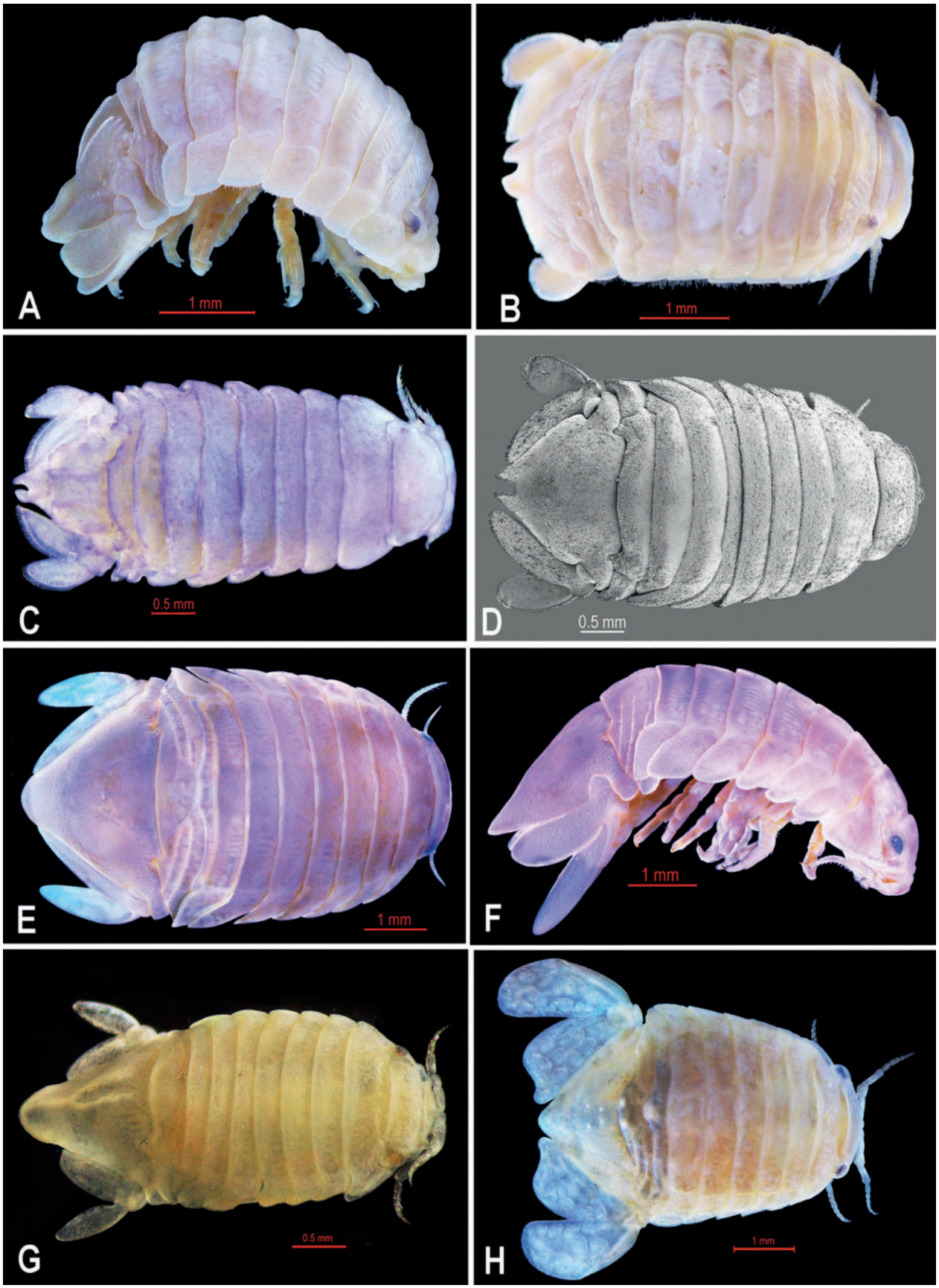

Figure 2. *Dynamene dilatata* Richardson, 1899, female, (CMNC 1991-2567). **A.** Lateral view; **B.** Dorsal view; **C.** *Dynamenella sheareri* (Hatch, 1947), male, (CMNC 1990-0070); **D.** *Dynoides canadensis* Khalaji-Pirbalouty & Gagnon, 2021, (CMNC 1985-0667b). *Exosphaeroma gigas* (Leach, 1818), male, (CMNC 1990-0090); **E.** Dorsal view; **F.** Lateral view. *Exosphaeroma rhomburum* (Richardson, 1899), male, (CMNC 1991-2559); **H.** *Exosphaeroma russellhansoni* Wall, Bruce & Wetzer, 2015, male, (CMNC 1984-1465).

1 ♀ (5.5 mm); British Columbia, Rupert Land Distr.; 7 Aug. 1959; E.L. Bousfield leg.; CMNC 1984-1461. 6 ♂♂ (up to 6.1 mm), 3 ♀♀ (up to 5 mm); British Columbia, Vancouver Island, Barclay Land Distr.; 8 September 1975; E.L. Bousfield leg.; CMNC 1984-1463. USA. 10 ♂♂ (up to 6.5 mm); Washington, Jefferson Co. (WA), Marrowstone Island; 26 July1966; E.L. Bousfield leg.; CMNC 1984-1456.

Exosphaeroma studeri Vanhöffen, 1914

Fig. 3C, D

Exosphaeroma studeri Vanhöffen, 1914: 510–511, fig. 44; Menzies 1962a: 132–133, fig. 43; Nierstrasz 1931: 195; Bruce 2003: 369.

Sphaeroma calcarea.– Dollfus 1891: 64, pl. 8, fig. 7. [Not *Sphaeroma calcarea* Dana, 1853; misidentification, according to Menzies 1962a].

Type locality. Punta Arenas, Chile.

Material examined. Chile. 1 ♂ (17.1 mm), 1 ovigerous ♀ (14.5 mm); Banco de las Taeas, Isla, Navarino; 5 Feb. 1970; E.L. Bousfield leg.; CMNC 2023-0242. 1 ♂ (18 mm) 5 ♀♀ (up to 12 mm); Canal Beagle; 19 Feb. 1970; E.L. Bousfield leg.; CMNC 2023-0243. 2 ♂♂ (9 mm), 3 ♀♀ (up to 6 mm); Isla Navarino; 5 Feb. 1970; E.L. Bousfield leg.; CMNC 2023-0244. 1 ♂ (9.8 mm); Peninsula Scott; W. Bank LW-HW; 20 Feb. 1970; E.L. Bousfield leg.; CMNC 2023-0245. 1 ♂ (15 mm), 2 subadult ♂♂ (13 mm), 3 ♀♀ (up to 13 mm); Islotes, Mamones, off Isla Lennox; 6 February 1970; E.L. Bousfield leg.; CMNC 2023-0246. 2 ♀♀ (up to 9.1 mm); Punta Robalo, Isla, Navarino; 29 Jan. 1970; E.L. Bousfield leg.; CMNC 2023-0247.

Distribution. Chile, Straits of Magellan (Menzies, 1962a).

Genus *Gnorimosphaeroma* Menzies, 1954

Gnorimosphaeroma oregonense (Dana, 1853)

Fig. 3E, F

Spheroma oregonensis Dana, 1853: 778, pl. 52x; Richardson 1899: 836; 1900: 223.

Sphaeroma olivacea.– Lockington, 1877: 45, pl. 1.

Exosphaeroma oregonensis.– Richardson, 1905: 296, figs 315, 316; Hatch, 1947: 213, Pl. 6, figs. 82, 83.

Neosphaeroma oregonense.– Monod, 1931: 76, fig. 74.

Gnorimosphaeroma oregonensis.– Miller, 1968: 12; Hoestlandt 1969: 325; Schultz 1969: 129, fig. 187; Kussakin 1971: 406–408, fig. 260–262; Hoestlandt 1975: 31; Brusca et al. 2007: 537, pl. 243; Wetzer et al. 2021: 32, figs 1–9 (Neotype designation).

Gnorimosphaeroma oregonensis lutea.– Menzies, 1954: 406, figs 1–4, 6A–P; Riegel 1959: 154–161, fig. 1A.

Gnorimosphaeroma oregonensis oregonensis.– Menzies, 1954: 406, figs 5, 7A–E, 12; Riegel 1959: 154–161, fig. 1B.

Note. Latest synonymies to the species can be found in Wetzer et al. (2021).

Material examined. Canada. 50 ♂♂ (up to 9.5 mm), 7 ♀♀ (up to 6 mm); British Columbia, Sayward Land Distr., Gowlland Island; 8 Jul. 1983; F. Rafi leg.; CMNC 1985-0715. 16 ♂♂ (up to 9.5 mm), 42 ♀♀ (up to 7 mm); British Columbia, Nootka Land Distr.; 13 June 1976; R.M. O'Clair leg.; CMNC 1987-0201. 75 ♂ & ♀; British Columbia, Sayward Land Distr.; 30 Aug. 1984; F. Rafi leg.; CMNC 1986-0206. 6 ♂♂ (up to 9 mm), 10 ♀♀ (up to 6 mm); British Columbia, Comox Land Distr.; 28 Jul. 1959; E. L. Bousfield leg.; CMNC 1987-0141. 97♂&♀; Alaska, Juneau Borough; 13 Jun. 1961; E. L. Bousfield leg.; CMNC 1987-0146. USA. 21♂&♀; Washington, Mason Co. (WA); 17 Jul. 1966; E. L. Bousfield leg.; CMNC 1991-2543.

Distribution. Widely distributed in North America from Alaska, British Columbia, and Vancouver to Washington (Kussakin 1979; Wetzer et al. 2021).

Genus *Ischyromene* Racovitza, 1908

Ischyromene menziesi (Sivertsen & Holthuis, 1980)

Fig. 3G, H

Dynamenella menziesi Sivertsen & Holthuis, 1980: 41–48, figs 6–8, pl. 1.

Ischyromene menziesi.– Harrison & Holdich, 1982: 86. [New combination]; Bruce 2006: 20; González et al. 2008: 174.

Dynamenella eatoni.– Menzies, 1962a: 135, fig. 44. [Not *Dynamene eatoni* Miers, 1875; misidentification, according to Harrison and Holdich 1982].

Type locality. Tristan da Cunha Island, south Atlantic Ocean.

Material examined. Chile. 1 ♂ (11 mm); Magallanes-Antarctica Region, Isla Lennox; 6 Feb.1970; E. L. Bousfield leg.; CMNC 1985-0652. 1 subadult ♂ (9 mm), 1 Ovi. ♀ (9 mm), 2 ♀♀ (10 mm, 19 mm); Magallanes-Antarctica Region, Isla Hoste; 4 Feb. 1970; E. L. Bousfield leg.; CMNC 1985-0653. 2 ♂♂ (10 mm), 2 ♀♀ (9 mm); 5 juveniles; Magallanes-Antarctica Region, Isla Picton; 7 Feb. 1970; E. L. Bousfield leg.; CMNC 1985-0655. 10 Juveniles; Magallanes-Antarctica Region, Canal Beagle; 19 Feb. 1970; E. L. Bousfield leg.; CMNC 1985-0656.

Distribution. Chile, South Atlantic Ocean (Tristan da Cunha, Nightingale, and Stoltenhoff Islands).

Genus *Paracerceis* Hansen, 1905

Paracerceis sculpta (Holmes, 1904)

Fig. 4A, B

Dynamene sculpta Holmes, 1904: 300–302, pl. 34, figs. 1–7.

Cilicaea sculpta.– Richardson, 1905: 318–319, fig. 349.

Paracerceis sculpta.– Richardson, 1905: 9; Menzies 1962b: 340, 341, fig. 2; Miller 1968: 14, fig. 3.; Brusca et al. 2007: 537, pl. 243.

Note. Latest synonymies to the species can be found in Martínez-Laiz et al. (2018).

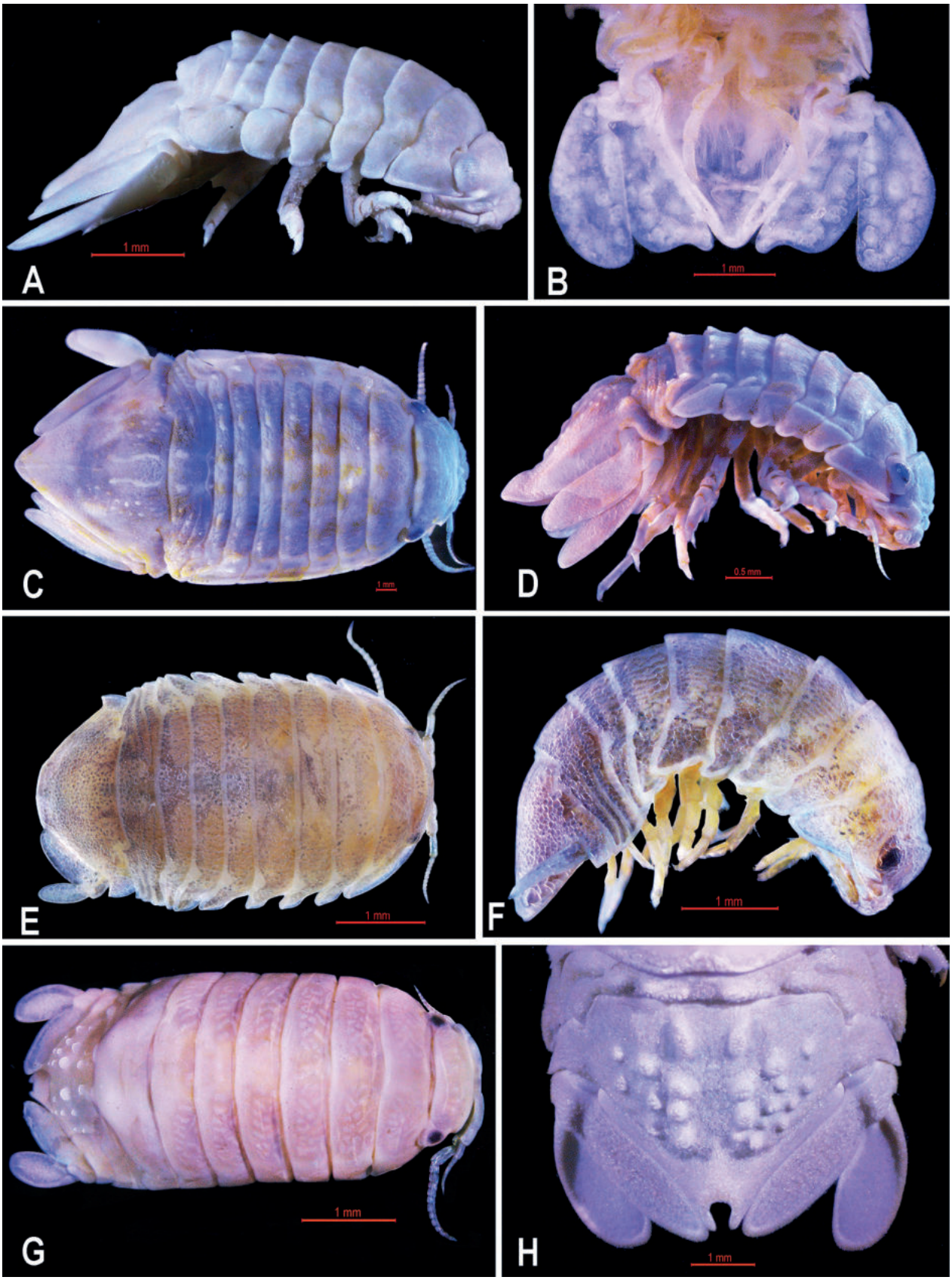

Figure 3. *Exosphaeroma russellhansoni* Wall, Bruce & Wetzer, 2015, male, (CMNC 1984-1465). **A.** Lateral view; **B.** Ventral view. *Exosphaeroma studeri* Vanhöffen, 1914, male, (CMNC 023-0242); **C.** Dorsal view; **D.** Lateral view. *Gnorimosphaeroma oregonense* (Dana, 1853), male, (CMNC 1985-0715); **E.** Dorsal view; **F.** Lateral view. *Ischyromene menziesi* (Sivertsen & Holthuis, 1980), male, (CMNC 1985-0652); **G.** Dorsal view; **H.** Pleotelson, dorsal view.

Type locality. San Clemente Island; San Diego, California.

Material examined. 1 ♂ (5.1 mm); Caribbean Sea; 15 Mar. 1968; N.A. Powell; CMNC 1992-0513. 2 ♂♂ (5 mm, 5.2 mm), 8 ♀♀ (up to 4.9 mm); Hawaiian Islands, Coconut Island; 1 Mar. 1962; D.C. Matthews leg.; CMNC 2023-0248. 3 ♀♀ (up to 4.5); Radio Island, North Carolina, 31 Mar. 1975; M.C. Govern leg.; CMNC 2023-0249.

Distribution. This species is widely distributed along the North American Pacific coast from southern California in San Diego to Mexico (Menzies 1962b); Pakistan, in the Indian Ocean (Yasmeen and Javed 2001); Hawaii, Hong Kong, Japan, Australia, Argentina, Brazil and the Azores (mid –Atlantic Ocean); in the Mediterranean Sea from Tunisia, Italy, Greece, France, Malta, Cyprus and Turkey. The wide distribution is most likely correct and results from ship-borne translocations. (Ulman et al. 2017; Martínez-Laiz et al. 2018; Rumbold et al. 2018).

Genus *Paradella* Harrison & Holdich, 1982

Paradella dianae (Menzies, 1962)

Fig. 4C, D

Dynamenopsis dianae Menzies, 1962b: 341, fig. 3.
Dynamenella dianae.– Menzies & Glynn, 1968: 63, 113, fig. 3.
Paradella dianae.– Harrison & Holdich, 1982: 104, fig. 6.
Paradella quadripunctata.– Van Dolah et al. 1984: 52.

Note. A comprehensive synonymy to the species can be found in Martínez-Laiz et al. (2018: 8–10).

Type locality. The Bay of San Quintin, Baja California.

Material examined. USA. 4 ♂♂ (up to 7.5 mm); 3 ♀♀ (up to 5 mm); Carteret County, North Carolina; 8 Apr. 1975; E. L. Bousfield leg.; CMNC 1990-0073.

Distribution. Baja California (Menzies 1962b), Italy, Egypt, Spain, Cyprus, Turkey, Libya Pakistan (Arabian Sea); Cádiz Bay, Caleta Vélez, Motril, Barbate (Spain), Australia (Menzies 1962b; Ulman et al. 2017; Martínez-Laiz et al. 2018). Its presence in different parts of the world, especially port cities, indicates a transport via shipping.

Genus *Sphaeroma* Bosc, 1802

Sphaeroma quadridentatum (Say, 1818)

Fig. 4E

Sphaeroma quadridentata Say, 1818: 400–401; De kay 1844: 44; White 1847: 102; Harger 1873 in Verrill, Smith and Harger 1873: 275, pl.5, fig. 21; Kensley and Schotte 1989: 234, fig. 10.
Sphaeroma quadridentatum.– Harger 1880: 368–370, pl. 9, figs. 53, 54; Smith 1964: 103, pl. 15, fig. 27; Miller 1968: 8, fig. 3; Schultz 1969: 128, fig. 183; Kussakin 1971: 394, fig. 248;

Type locality. Saint Catherine's Island, Georgia.

Material examined. USA. 4 ♂♂ (up to 6 mm); 2 ♀♀ (up to 5 mm); Virginia, Gloucester; 17 Apr. 1975; E. L. Bousfield leg.; CMNC 1992-0583. 4 ♂♂ (up to 6 mm); 8 ♀♀ (up to 5 mm); Pawley's Greek, Carolina; 17 Mar. 1915; E. L. Bousfield leg.; CMNC 2023-0250. 2 ♂♂ (up to 6 mm); 3 ♀♀ (up to 5.5 mm); South Carolina; 16 May 1975; D.R. Calder leg.; CMNC 2023-0251.

Distribution. Georgia, Florida, Long Island Sound, Connecticut, New Haven County, West Haven, Savin Rock. It is common on the southern shore of New England (Harger 1880; Kensley and Schotte 1989).

Sphaeroma terebrans Bate, 1866

Fig. 4F

Sphaeroma terebrans Bate, 1866: 28, pl. 2, fig. 5; Stebbing 1904: 16; Richardson 1905: 282–286, figs. 294–298; Calman 1921: 217–218; Baker 1926: 247–278; Nierstrasz 1931: 192; Van Name 1936: 447–449, fig. 279; Barnard 1940: 405; Pillai 1954: 9; Pillai 1955: 129–131, Pl. 6, figs 1–11; Loyola e Silva 1960: 14–28, figs 1, 2; John 1968: 1–73, pl. 1, figs 1–36; Miller 1968: 11, fig. 3; Harrison and Holdich 1984: 287–292, fig. 4; Kensley and Schotte 1989: 234, fig. 10; Wilkinson 2004: 1; Baratti et al. 2005: 225–234; Li et al. 2016: 307, fig. 2.
Sphaeroma destructor Richardson, 1897: 105–107.

Type locality. India.

Material examined. USA. 3 ♂♂ (up to 9 mm); South Carolina, Charleston Co.; 25 Apr. 1965; E. L. Bousfield leg.; CMNC 1991-2576. NIGERIA. 15 ♂♂ (up to 9 mm); 30 ♀♀ (up to 7 mm); Mayuku Creek; 5 Oct. 1975; C. Powell leg.; CMNC 2023-0252.

Distribution. Virginia to Louisiana; Belize; Cuba; Venezuela to Brazil; Gulf of Mexico; Kenya, Nigeria, Tanzania, Zanzibar, east coast of southern Africa, Pakistan, India, Sri Lanka, Thailand, Indonesia, Philippines, Australia, China (Kensley and Schotte 1989; Wilkinson 2004; Li et al. 2016).

Family Tecticipitidae Iverson, 1982
Genus *Tecticeps* Richardson, 1897

Tecticeps convexus Richardson, 1899

Fig. 4G, H

Tecticeps convexus Richardson, 1899: 837–838, fig. 15; Richardson 1905: 278–280, figs 290–291; Richardson 1906: 4, figs 6–9; Schultz 1969: 116, fig. 161; Kussakin 1971: 347, figs 210, 211; Brusca et al. 2007: 538.

Type locality. Monterey Bay, California.

Material examined. ALASKA. 10 ♂♂ (up to 9 mm); 25 ♀♀ (up to 10.5 mm); Sitka Borough, Chichagof Island; 30 Jul. 1980; G. Peter & G. Ronald leg.; CMNC 1992-0541. Canada. 15 ♂&♀; British Columbia, Range 4 Coast Land Distr., Banks Island;18 Jul. 1964; E. L. Bousfield leg.; CMNC 1991-2583. 19 ♂&♀; British Columbia, Range 2 Coast Land Distr., Goose Island; 5 Aug. 1964; E. L. Bousfield leg.; CMNC 1991-2584. 2 ♂&♀;

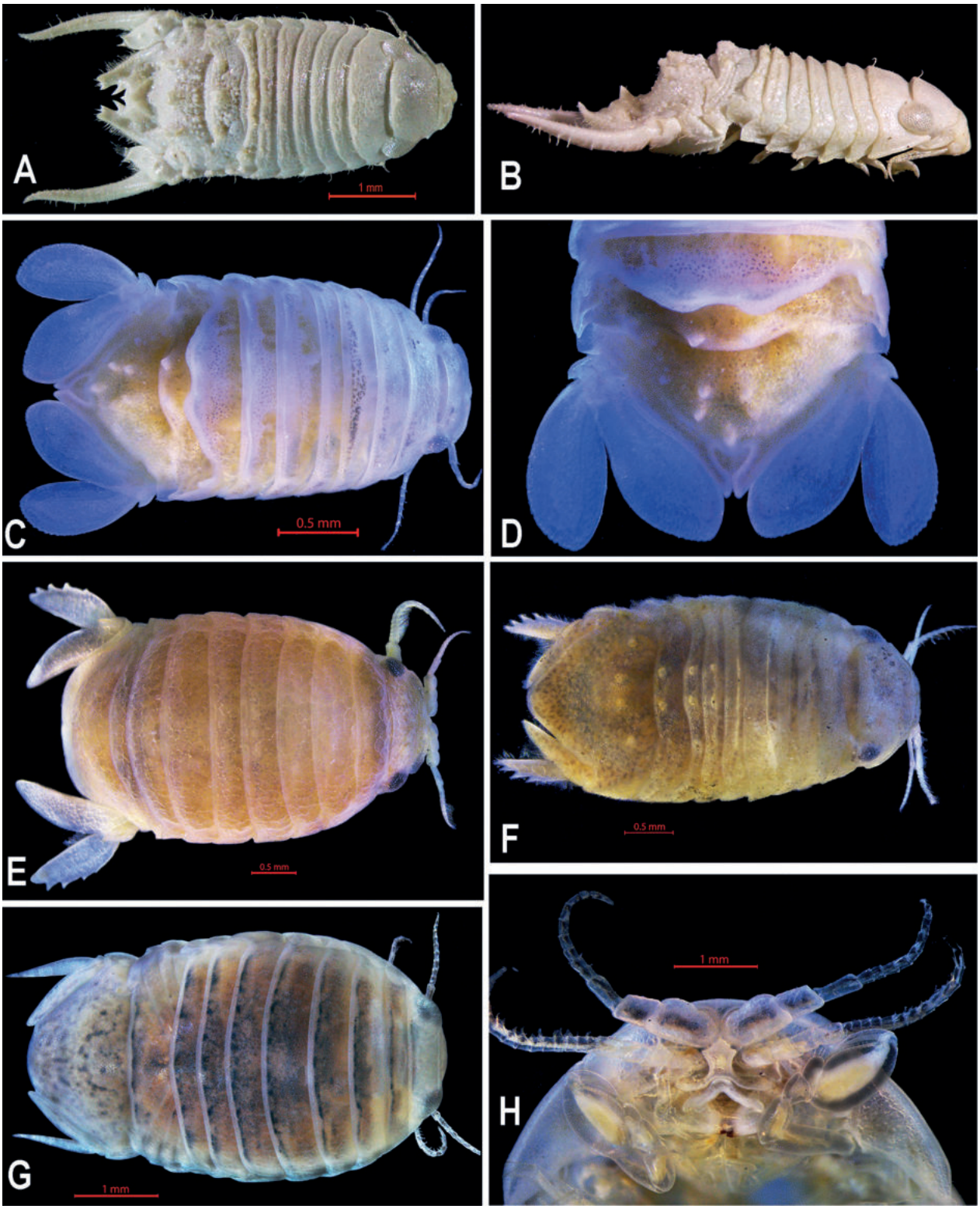

Figure 4. *Paracerceis sculpta* (Holmes, 1904), male, (CMNC 1992-0513). **A.** Dorsal view; **B.** Lateral view. *Paradella dianae* (Menzies, 1962), male, (CMNC 1990-0073); **C.** Dorsal view; **D.** Pleotelson, dorsal view; **E.** *Sphaeroma quadridentatum* (Say, 1818); **F.** *Sphaeroma terebrans*, Bate 1866. *Tecticeps convexus* Richardson, 1899, male, (CMNC 1992-0541); **G.** Dorsal view; **H.** Head ventral view.

British Columbia, Vancouver Island, Barclay Land Distr., Pachena Bay; 22 Jul. 1975; E. L. Bousfield leg.; CMNC 1991-2590. USA. 33 ♂&♀; Washington, Clallam Co., Crescent Bay; 27 Jul. 1966; E. L. Bousfield leg.; CMNC 1991-2550. 7 ♂&♀; Washington, Clallam Co., Shipwreck Pt.; 1 Aug. 1966; E. L. Bousfield leg.; CMNC 1991-2562. 2 ♀♀; Oregon, Tillamook Co., Cape Kiwanda; 16 Aug. 1966; E. L. Bousfield leg.; CMNC 1991-2574.

Distribution. Eastern Pacific, British Columbia, Oregon to California (Espinosa-Pérez and Hendrickx 2006).

Discussion

The first contribution to the knowledge of isopod taxonomy of North America was Say (1818), who described *Naesa depressus* and *N. ovalis* from the east Coast of North America; these species were later placed in the genus *Ancinus* and *Cassidinidea* by H. Milne Edwards (1840) and Hansen (1905), respectively. A third sphaeromatid isopod, *Sphaeroma quadridentatum*, was described by Say (1818) from Georgia and East Florida. Dana (1853) described *Spheroma oregonensis* from the Pacific Coast of North America; this species being transferred to the combination *Gnorimosphaeroma oregonense* (Dana, 1853) by Wetzer et al. (2021). Harger (1873) reported *Sphaeroma quadridentatum* (Say, 1818) to occur from Massachusetts to Florida. Historically, the major period of isopod documentation in North America was from Richardson's first major (1899) contribution to Kensley and Schotte's (1989) field guide. Prior to 1899, 75 isopod species had been recorded for North America. When Richardson (1899) worked on the North American Pacific Coast, she added 22 new species to the isopod fauna, including seven new sphaeromatids.

At the turn of the 20th century, in 1905, Harriet Richardson published her significant monograph on the isopod fauna of North America in the Bulletin of the U.S. National Museum. This contribution included all terrestrial, freshwater, and marine isopods and Tanaidacea. Out of about 240 marine isopod species, 31 species (≈13%) were from the family Sphaeromatidae. The next comprehensive account was given by Hatch (1947), who gave a systematic account of the Pacific Northwest crustacean isopods, reporting 70 species, most of them (51 species) being marine isopods, of which seven species (≈14%) were sphaeromatids. Schultz (1969), in "*How to know the marine isopod crustaceans*", listed 444 marine species known from the waters off the coasts of North America, of which 45 (≈10%) are sphaeromatid isopods. Finally, Kensley and Schotte (1989) reported about 280 shallow-water species from the Caribbean, of which 30 species (≈11%) were sphaeromatid isopods.

There are now 110 accepted genera and close to 650 named species of the sphaeromatoid isopods worldwide (Boyko et al. 2008 onwards). Given that there are approximately 6250 species of marine and estuarine isopods (Poore and Bruce 2012), sphaeromatoid isopods account for approximately 10% of the marine species. The ratio of North American sphaeromatids to the other marine isopods appears to be around 10% as well.

In recent decades, a few taxonomic studies of the North American marine isopod fauna have described or reported new species. For instance, *Paradella tiffany* Bruce & Wetzer, 2004, and *P. garsonorum* Wetzer & Bruce, 2007, are both described from Baja California, Mexico. Later, Bruce and Wetzer (2008) reported a *Pseudosphaeroma* Chilton, 1909 species from the Pacific coast of North America.

Wall et al. (2015) added three new north-eastern Pacific species, *Exosphaeroma paydenae*, *E. russellhansoni*, and *E. pentche*. Recently, Wetzer et al. (2021) revised *Gnorimosphaeroma oregonense* (Dana, 1852) from the north-eastern Pacific. Furthermore, Khalaji-Pirbalouty and Gagnon (2021) described *Dynoides canadensis* from the south-western coast of British Columbia, and *Cassidinidea ovalis*, a common species along the Atlantic Coast of North America, was redescribed by Khalaji-Pirbalouty and Bruce (2021). At last count, 70 species of sphaeromatid isopods have been reported from North America (Wall et al. 2015; Khalaji-Pirbalouty and Gagnon 2021; Wetzer et al. 2021). This accounts for roughly 10% of all reported sphaeromatid isopods worldwide. In comparison, Australia, with the length of its coastline approximately 15% of that of North America, has a rich sphaeromatid fauna with 203 recorded species, which are nearly 30% of all sphaeromatid species known worldwide (Poore et al. 2002; Bruce 2003, 2009; Poore 2005). Yet, it is estimated that the species number for this family in Australia is still about 50% of the expected total (Poore et al. 2002; Bruce 2003).

The relatively low number of North American sphaeromatid species may be, in part, related to the lower-diversity trends observed for most taxa in higher-latitude regions, particularly in the Northern Hemisphere. The number of known sphaeromatid species reported from Australia is about three times that of North America; it appears that temperate regions are more favorable for sphaeromatid isopods, as previously mentioned by Poore and Bruce (2012). There are clearly other major factors at play, such as the age of the crust around Australia, and also that the family may have primarily evolved and radiated largely in the Southern Hemisphere (unpublished results).

Taxonomic diversity at the family level and above, as reported here, would greatly benefit from the addition of new, fresh material from the field (particularly from under-collected regions and using finer scale methods that capture small crustaceans) which, beyond morphological examination, would provide the additional opportunity to run genetic analyses. There is, however, still lots of material to be examined in collections such as that of the CMN. Work by isopod taxonomists in these collections will likely result in the description of many new species (for instance, see Khalaji-Pirbalouty and Gagnon 2021), especially where there are lots of unexamined samples with unidentified species, or where previous identifications have not been reviewed by experts.

Acknowledgements

We express our gratitude to the Canadian Museum of Nature, Ottawa (Visiting Scientist Awards 2019) and Shahrekord University, for providing financial support for this project. Special thanks to Philippe Ste-Marie (Assistant Collections Manager, Invertebrate Collections, Zoology) for his assistance during the first author's visit to the Canadian Museum of Nature. We deeply appreciate the constructive comments and helpful suggestions from Wolfgang Wägele (Zoological Research Museum

Alexander Koenig, Bonn), Niel Bruce (Queensland Museum), and Brenda Doti (Universidad de Buenos Aires, Argentina) that helped improve the manuscript.

References

Baker WH (1926) Species of the isopod family Sphaeromidae from the eastern, southern and western coasts of Australia. Transactions and Proceedings of the Royal Society of South Australia 50: 247–279.

Baratti M, Goti E, Messana G (2005) High level of genetic differentiation in the marine isopod *Sphaeroma terebrans* (Crustacea Isopoda Sphaeromatidae) as inferred by mitochondrial DNA analysis. Journal of Experimental Marine Biology and Ecology 315(2): 225–234. https://doi.org/10.1016/j.jembe.2004.09.020

Barnard KH (1940) Contributions to the crustacean fauna of South Africa. XII. Further additions to the Tanaidacea, Isopoda and Amphipoda, together with keys for the identification of the hitherto recorded marine and freshwater species. Annals of the South African Museum 32: 381–543.

Bate CS (1866) Carcinological gleanings. No. II. Annals and Magazine of Natural History, series 3 17(97): 24–31. https://doi.org/10.1080/00222936608679472

Boyko CB, Bruce NL, Hadfield KA, Merrin KL, Ota Y, Poore GCB, Taiti S [Eds] (2008 [onwards]) World Marine, Freshwater and Terrestrial Isopod Crustaceans database. Sphaeromatoidea Latreille, 1825. World Register of Marine Species. https://www.marinespecies.org/aphia.php?p=taxdetails&id=292950 [on 2023-03-15]

Brandt A (1998) Sphaeromatidae (Crustacea, Isopdoda) of the Beagle Channel and description of *Cymodopsis beageli* n. sp. Beaufortia 48(7): 137–161.

Brandt A, Wägele JW (1989) Redescriptions of *Cymodocella tubicauda* Pfeffer, 1887 and *Exosphaeroma gigas* (Leach, 1818) (Crustacea, Isopoda, Sphaeromatidae). Antarctic Science 1(3): 205–214. https://doi.org/10.1017/S0954102089000325

Bruce NL (2003) New genera and species of sphaeromatid isopod crustaceans from Australian marine coastal waters. Memoirs of the Museum of Victoria 60(2): 309–369. https://doi.org/10.24199/j.mmv.2003.60.28

Bruce NL (2006) A new species of *Ischyromene* Racovitza, 1908 (Sphaeromatidae: Isopoda: Crustacea) from intertidal marine habitats in New Zealand. Zootaxa 1220(1): 19–34. https://doi.org/10.11646/zootaxa.1220.1.2

Bruce NL (2009) A new genus and new species of Sphaeromatidae (Crustacea: Isopoda) from the Great Barrier Reef, Australia. Memoirs of the Museum of Victoria 66(1): 35–42. https://doi.org/10.24199/j.mmv.2009.66.5

Bruce NL, Wetzer R (2004) *Paradella tiffany* sp. nov., a distinctive sphaeromatid isopod (Crustacea: Isopoda: Sphaeromatidea) from Baja California, Mexico. Zootaxa 623(1): 1–12. https://doi.org/10.11646/zootaxa.623.1.1

Bruce NL, Wetzer R (2008) New Zealand exports: *Pseudosphaeroma* Chilton, 1909 (Isopoda: Sphaeromatidae), a Southern Hemisphere genus introduced to the Pacific coast of North America. Zootaxa 1908(1): 51–56. https://doi.org/10.11646/zootaxa.1908.1.4

Brusca RC, Coelho VR, Taiti S (2007) Isopoda. In: Carlton JT (Ed.) The Light and Smith Manual: Intertidal Invertebrates from Central California to Oregon (4th edn.). University of California Press, Berkeley, 503–542.

Calman WT (1921) Notes on marine boring animals: Crustacea. Proceedings of the General Meetings for Scientific Business of the Zoological Society of London 1921(2): 215–220. https://doi.org/10.1111/j.1096-3642.1921.tb03260.x

Carvacho A (1977) Sur une importante collection d'isopodes des îles Kerguelen. Comité National Français des Recherches Antarctiques 42: 173–191.

Chilton C (1906) List of Crustacea from the Chatham Islands. Transactions of the N.Z. Institute 38: 269–73.

Conlan KE, Bousfield MA, Hendrycks EDA, Mills EL, Cook FR, Gruchy CG (2016) A tribute to Dr. Edward Lloyd Bousfield, 1926–2016. Canadian Field Naturalist 130(4): 359–372. https://doi.org/10.22621/cfn.v130i4.1932

Cunningham RO (1871) Notes on the reptiles, Amphibia, fishes, Mollusca, and Crustacea obtained during the voyage of H.M.S. Nassau in the years 1866–1869. Transactions of the Linnean Society of London 27(4): 465–502. https://doi.org/10.1111/j.1096-3642.1871.tb00219.x

Dana JD (1853) Crustacea. Part II. In: Wilkes C (Ed.) United States Exploring Expedition. During the years 1838, 1839, 1840, 1841, 1842. Under the command of Charles Wilkes. U. S. N. C. Sherman. Philadelphia, 689–1618.

De Kay JE (1844) Crustacea. Zoology of New-York or the New-York Fauna; comprising detailed descriptions of all the animals hitherto observed within the State of New-York, with brief notices of those occasionally found near its borders, and accompanied by appropriate illustrations (Vol. 1, Part 6). Carrol and Cook, Albany, 70 pp.

Desmarest AG (1825) Considérations générales sur la classe des crustacés, et description des espèces de ces animaux, qui vivent dans la mer, sur les côtes, ou dans les eaux douces de la France, Paris, 446 pp. https://doi.org/10.5962/bhl.title.6869

Dollfus A (1891) Crustacés isopodes, 55–76. Mission Scientifique de Cape Horn 1882–1883, Tome VI, Zoologie 55–76. Gauthier-Villars, Paris.

Ellis JP (1981) Some type specimens of Isopoda (Flabellifera) in the British Museum (Natural History), and the isopods in the Linnaean Collection. Bulletin of the British Museum (Natural History). Historical Series 40(4): 121–128. https://doi.org/10.5962/p.271708

Espinosa-Pérez MC, Hendrickx ME (2006) A comparative analysis of biodiversity and distribution of shallow-water marine isopods (Crustacea: Isopoda) from polar and temperate water in the East Pacific. Belgian Journal of Zoology 136: 219–247.

Giambiagi DC (1925) Resultado de la primera expedición a Tierra del Fuego (1921). Enviada por la Facultad de Ciencias Exactas, Físicas y Naturales de la Universidad Nacional de Buenos Aires. Crustáceos, Isópodos. Anales de la Sociedad Científica Argentina 1925: 229–246.

Gomez Simes E (1979) Algunos isopodos de la Ria Deseado (Santa Cruz, Argentina). Contribuciones Científica Centro de Investigación de Biología Marina. Estación Puerto Deseado, Buenos Aires 166: 5–16.

González ER, Haye PA, Balanda MJ, Thiel M (2008) Systematic list of species of peracarids from Chile (Crustacea, Eumalacostraca). Gayana (Concepción) 72(2): 157–177. https://doi.org/10.4067/S0717-65382008000200006

Guérin-Méneville FE (1843) Crustacès. In: Cuvier G (Ed.) Iconographie du Règne animal de G. Cuvier, ou représentation d'après nature de l'une des espèces les plus remarquable et souvent non encore figurées de chaque genre d'animaux (Vol. 3). Baillière, Paris.

Hale HM (1929) The Crustaceans of South Australia. Part 2. Handbooks of the Flora and Fauna of South Australia, issued by the British Science Guild (South Australia Branch). Adelaide: British Science Guild (South Australian Branch), 201–380.

Hansen HJ (1905) On the propagation, structure and classification of the family Sphaeromidae. The Quarterly Journal of Microscopical Science 49: 69–135. https://doi.org/10.1242/jcs.s2-49.193.69

Harger O (1880) Report on the marine Isopoda of New England and adjacent waters. Report of the United States Commission of Fish and Fisheries. For 1878(6): 297–462. https://doi.org/10.5962/bhl.title.1391

Harrison K, Holdich DM (1982) Revision of the genera *Dynamenella*, *Ischyromene*, *Dynamenopsis*, *Cymodocella* (Crustacea: Isopoda), including a new genus and five new species of eubranchiate Sphaeromatids from Queensland waters. Journal of Crustacean Biology 2(1): 84–119. https://doi.org/10.2307/1548115

Harrison K, Holdich DM (1984) Hemibranchiate sphaeromatids (Crustacea: Isopoda) from Queensland, Australia, with a world-wide review of the genera discussed. Zoological Journal of the Linnean Society 81(4): 275–387. https://doi.org/10.1111/j.1096-3642.1984.tb01175.x

Haswell WA (1882) Catalogue of the Australian stalk- and sessile-eyed Crustacea. Sydney, Australian Museum, 324 pp. https://doi.org/10.5962/bhl.title.1948

Hatch MH (1947) The Chelifera and Isopoda of Washington and adjacent regions. University of Washington Publications in Biology 10(5): 155–274.

Hodgson TV (1910) Crustacea IX. Isopoda. In: Harmer SF (Ed.) National Antarctic Expedition 1901–1904. Natural History (Vol. 5) (Zoology and Botany). British Museum (Natural History), London, 77 pp.

Hoestlandt H (1969) Sur un sphérome nouveau de la côte pacifique américaine, *Gnorimosphaeroma rayi* n. sp. (isopode flabellifère). Comptes rendus hebdomadaires des Séances de l' Académie de Sciences, Paris, 268D: 325–327.

Hoestlandt H (1975) Occurrences of the Isopoda Flabellifera *Gnorimosphaeroma rayi* Hoestlandt on the coast of Japan, eastern Siberia and Hawaii, with a brief note on its genetic polychromatism. Publications of the Seto Marine Biological Laboratory 22(1/4): 31–46. https://doi.org/10.5134/175891

Holmes S (1904) Remarks on the sexes of Sphaeromids, with a description of a new species of *Dynamene*. Proceedings of the California Academy of Sciences (3). Zoology 3: 295–306.

Hurley DE (1961) A checklist and key to the Crustacea Isopoda of New Zealand and Subantartic Islands. Transactions of the Royal Society of New Zealand (Zoology) 1: 259–292.

Hurley DE, Jansen KP (1977) The marine fauna of New Zealand: Family Sphaeromatidae (Crustacea Isopoda Flabellifera). New Zealand Oceanographic Institute Memoir 63: 1–80.

John PA (1968) Habits, structure and development of *Sphaeroma terebrans* (a wood-boring isopod). University of Kerala Publications 1: 1–73.

Kensley B, Schotte M (1989) Guide to the Marine Isopod Crustaceans of the Carribean. Smithsonian Institution Press, Washington D.C. and London, 114 pp. [204, 232, and 234.] https://doi.org/10.5962/bhl.title.10375

Khalaji-Pirbalouty V, Bruce NL (2021) Redescription of the type species of the genus *Cassidinidea* Hansen, 1905 (Crustacea: Isopoda: Sphaeromatidae) with notes on geographic distribution of the New World species. Marine Biology Research 17(5–6): 494–502. https://doi.org/10.1080/17451000.2021.1990958

Khalaji-Pirbalouty V, Gagnon JM (2021) A new species of *Dynoides* Barnard, 1914 (Crustacea, Isopoda, Sphaeromatidae) from Canada, with notes on geographic distribution of the north-eastern Pacific Ocean species. Marine Biology Research 17(1): 12–20. https://doi.org/10.1080/17451000.2021.1892766

Krauss CFF (1843) Die Südafrikanischen Crustaceen. Eine Zusammenstellung aller bekannten Malacostraca, Bemerkungen über deren Lebensweise und geographische Verbreitung, nebst Beschreibung und Abbildung mehrerer neuen Arten, Stuttgart, 68 pp. https://doi.org/10.5962/bhl.title.4825

Kussakin OG (1967) Isopoda and Tanaidacea from the coastal zones of the Antarctic and subantarctic. In Biological Results of the Soviet Antarctic Expedition (1955–1958), 3. Isseldovaniia Fauny Morei 4(12): 220–380. https://doi.org/10.2307/1442262

Kussakin OG (1979) Marine and brackish-water Isopoda of cold and temperate (boreal) waters of the Northern Hemisphere. Part 1. Flabellifera, Valvifera, and Tyloidea). National Academy of Sciences, USSR, Zoology [Opredeliteli po Faune SSR, Akademiya Nauk, SSSR] 122: 1–470.

Kussakin OG, Vasina GS (1980) Additions to the marine Isopoda and Gnathiida of Kerguelen Islands (Southern Indian Ocean). Tethys 9(4): 355–369.

Leach WE (1818) Cymothoadées. In: Cuvier F (Ed.) Dictionnaire des Sciences Naturelles 12: 338–354.

Li X-F, Chong H, Zhong C-R, Xu J-Q, Huang J-R (2016) Identification of *Sphaeroma terebrans* via morphology and the mitochondrial cytochrome c oxidase subunit I (COI) gene. Zoological Research 37(5): 307–312. https://doi.org/10.13918/j.issn.2095-8137.2016.5.307

Lockington WN (1877) Remarks on the Crustacea of the Pacific coast, with descriptions of some new species. Proceedings of the California Academy of Sciences 7: 28–36. https://doi.org/10.5962/bhl.part.27534

Loyola e Silva J (1960) Sphaeromatidae do litoral Brasiliero (Isopoda-Crustacea). Boletim da Universidade do Parana. Zoologia 4: 1–182.

Loyola e Silva Jde (1971) Sôbre os gêneros *Ancinus* Milne Edwards, 1840e *Bathycopea* Tattersall, 1909, da coleção U.S. Nat. Mus. (Isopoda-Crustacea). Arquivos do Museu Nacional, Rio de Janeiro 54: 209–223.

Martínez-Laiz G, Ros M, Guerra-García JM (2018) Marine exotic isopods from the Iberian Peninsula and nearby waters. PeerJ 6e4408. https://doi.org/10.7717/peerj.4408

Menzies RJ (1954) A review of the systematics and ecology of the genus "*Exosphaeroma*," with the description of a new genus, a new species, and new subspecies (Crustacea, Isopoda, Sphaeromatidae). American Novitates 1683: 1–24.

Menzies RJ (1962a) The zoogeography, ecology and systematics of the Chilean marine isopods. Lunds Universitets Arsskrift A vd. 2, 57(11): 1–162.

Menzies RJ (1962b) The marina isopod fauna of Bahia de San Quintin, Baja California, Mexico. Pacific Naturalist 3(11): 331–348.

Menzies RJ, Barnard JL (1959) Marine Isopoda on coastal shelf bottoms of southern California: Systematics and ecology. Pacific Naturalist 1(11–12): 1–35.

Menzies RJ, Glynn PW (1968) The common marine isopod crustacea of Puerto Rico. A handbook for marine biologists. In: Hummelinck W

(Ed.) Studies on the Fauna of Curaçaoand other Caribbean Islands (Vol. XXVII). The Hague Martinus Nijhoff, Leiden, 133 pp.

Miers EJ (1875) Descriptions of new species of Crustacea collected at Kerguelen's Island by the Rev. A. E. Eaton. Annals and Magazine of Natural History (ser. 4) 16: 73–76. https://doi.org/10.1080/00222937508681124

Miers EJ (1879) Crustacea. In: Eaton AE (Ed.) An Account of the Petrological, Botanical, and Zoological Collections Made in Kerguelen's Land and Rodriguez During the Transit of Venus Expeditions in the Years 1874–75. Philosophical Transactions of the Royal Society of London 168: 200–214.

Miller MA (1968) Isopoda and Tanaidacea from buoys in coastal waters of the continental United States, Hawaii, and the Bahamas (Crustacea). Proceedings of the United States National Museum 125(3652): 1–53. https://doi.org/10.5479/si.00963801.125-3652.1

Milne Edwards H (1834–1840) Histoire Naturelle des Crustacés, Comprenant l´Anatomie, la Physiologie et la Classification de ces Animaux (Vol. III). Librairie Encyclopédique de Roret, Paris, 638 pp. https://doi.org/10.5962/bhl.title.16170

Monod T (1931) Tanaidaces et Isopodes Aquatiques de l'Afrique Occidentales et Septentrional 3e Partie. Sphaeromatidae. Mémoires de la Société des sciences naturelles de Neuchâtel 29: 1–91.

Nierstrasz HF (1931) Die Isopoden der Siboga-Expedition III. In: Max Weber (Ed.) Isopoda Genuina, II. Flabellifera. Siboga Expéditie (Vol. 32c). E. J. Brill, Leiden, 16–227.

Ortmann AE (1911) Crustacea of Southern Patagonia. Reports of the Princeton University Expeditions to Patagonia, 1896–1899 (Zoology), 635–667. https://doi.org/10.5962/bhl.title.10517

Pfeffer G (1886) Die Krebse von Süd-Georgien nach der Ausbeute der Deutschen Station 1882–83. Jahrbuch der Hamburgischen Wissenschaftlichen Anstalten 4: 43–150. https://doi.org/10.5962/bhl.title.10084

Pillai NK (1954) A preliminary note on the Tanaidacea and Isopoda of Travancore. Bulletin of the Central Research Institute. University of Tranvancore, Trivandrum 3(1): 1–21.

Pillai NK (1955) Wood boring Crustacea of Travancore. I. Sphaeromatidae. Bulletin of the Central Research Institute of the University of Travancore, Series C. Nature and Science 4(1): 127–139.

Poore GCB (2005) Supplement to the 2002 catalogue of Australian Crustacea: Malacostraca – Syncarida and Peracarida (Vol. 19.2A): 2002–2004. Museum Victoria Science Reports 7: 1–15. https://doi.org/10.24199/j.mvsr.2005.07

Poore GCB, Bruce NL (2012) Global Diversity of Marine Isopods (Except Asellota and Crustacean Symbionts). PLoS ONE 7(8): e43529. https://doi.org/10.1371/journal.pone.0043529

Poore GCB, Lew Ton HM, Bruce NL (2002) Sphaeromatidae Latreille, 1825. 221–252. In: Houston WWK, Beesley P (Eds) Crustacea: Malacostraca: Syncarida, Peracarida: Isopoda, Tanaidacea, Mictacea, Thermosbaenacea, Spelaeogriphacea. Zoological Catalogue of Australia. CSIRO Publishing, Melbourne, 433 pp.

Richardson H (1897) Description of a new species of *Sphaeroma.* Proceedings of the Biological Society of Washington 11: 105–107.

Richardson H (1899) Key to the isopods of the Pacific Coast of North America, with descriptions of twenty-two new species. Proceedings of the United States National Museum 21(1175): 815–869. https://doi.org/10.5479/si.00963801.21-1175.815

Richardson H (1905) A monograph on the isopods of North America. Bulletin of the United States National Museum 54, 727 pp. https://doi.org/10.5479/si.03629236.54.i

Richardson H (1906) Descriptions of new isopod crustaceans of the family Sphaeromidae. Proceedings of the United States National Museum 31(1479): 1–22. https://doi.org/10.5479/si.00963801.31-1479.1

Riegel JA (1959) A revision in the sphaeromid genus *Gnoriomosphaeroma* Menzies (Crustacea: Isopoda) on the basis of morphological, physical, and ecological studies on two of its "subspecies". The Biological Bulletin 117(1): 151–162. https://doi.org/10.2307/1539047

Rumbold C, Meloni M, Doti B, Correa N, Albano M, Sylvester F, Obenat S (2018) Two new nonindigenous isopods in the Southwestern Atlantic: Simultaneous assessment of population status and shipping transport vector. Journal of Sea Research 138: 1–7. https://doi.org/10.1016/j.seares.2018.04.008

Say T (1818) An account of the Crustacea of the United States, part 7. Journal of the Academy of Natural Sciences of Philadelphia 1: 374–401.

Schultz GA (1969) How to Know the Marine Isopod Crustaceans. W.M. C. Brown Company Publishers, Iowa, 359 pp.

Schultz GA (1973) *Ancinus* H. Milne Edwards in the new world (Isopoda, Flabellifera). Crustaceana 25(3): 267–275. https://doi.org/10.1163/156854073X00254

Shimomura M (2008) *Bathycopea* (Isopoda: Sphaeromatidea: Ancinidae) from Japan, with descriptions of two new species and redescription of *B. parallela* Birstein. Zootaxa 1678(1): 25–49. https://doi.org/10.11646/zootaxa.1678.1.2

Sivertsen E, Holthuis LB (1980) The marine Isopod Crustacea of the Tristan da Cunha archipelago. Gunneria 35: 1–128.

Smith RI (1964) Keys to marine invertebrates of the Woods Hole Region. Contribution No. 11, Systematics-Ecology Program, Marine Biological Laboratory, Woods Hole, Massachusetts, 208 pp.

Stebbing TRR (1900) On some crustaceans from the Falkland Islands, collected by Mr. Rupert Vallentin. Proceedings of the General Meetings for Scientific Business of the Zoological Society of London 1900: 517–568. https://doi.org/10.5962/bhl.title.10309

Stebbing TRR (1904) Gregarious Crustacea from Ceylon. Spolia Zeylanica, Bulletin of the National Museum. Ceylon 2: 1–29.

Stebbing TRR (1914) Crustacea from the Falkland Islands collected by Mr Rupert Vallentin, FLS. Part II. Proceedings of the General Meetings for Scientific Business of the Zoological Society of London 84(2): 341–378. https://doi.org/10.1111/j.1469-7998.1914.tb07042.x

Stephensen K (1927) Papers from Dr. Th. Mortensen's Pacific expedition 1914–16. XL. Crustacea from the Auckland and Campbell Islands. Videnskabelige Meddelelser fra Dansk naturhistorisk Forening i Kobenhaven 83: 289–390.

Stephensen K (1947) Tanaidacea, Isopoda, Amphipoda, and Pycnogonida. In: Norske videnskaps-akademi i Oslo (Eds) Scientific Results of the Norwegian Antarctic Expedition 1927–1928. Oslo, 90 pp.

Studer T (1884) Isopoden, gesammelt während der reise SMS Gazelle um die erde 1874–76. Kurfürstlich Akademie der Wissenschaften, Berlin, 27 pp.

Tattersall WM (1905) The marine fauna of the coast of Ireland. Part V. Isopoda. Reports of the Department of Agriculture and Technical Instruction for Ireland. Scientific Investigations of the Fisheries Branch 1904(2): 1–90.

Tattersall WM (1914) Order Isopoda: Tribe Flabellifera. Transactions of the Royal Society of Edinburgh 49: 880–890. https://doi.org/10.1017/S0080456800017178

Tattersall WM (1921) Crustacea. Part VI-Tanaidacea and Isopoda. Natural History Report. British Antarctic Terra Nova Expedition, 1910. Zoology 3: 191–258. https://doi.org/10.5962/bhl.title.1679

Ulman A, Ferrario J, Occhipinti-Ambrogi A, Arvanitidis C, Bandi A, Bertolino M, Bogi C, Chatzigeorgiou G, Çiçek BA, Deidun A, Ramos-Esplá A, Koçak C, Lorenti M, Martínez-Laiz G, Merlo G, Princisgh E, Scribano G, Marchini A (2017) A massive update of non-indigenous species records in Mediterranean marinas. PeerJ 5: e3954. https://doi.org/10.7717/peerj.3954

Van Dolah RF, Knott DM, Calder DR (1984) Ecological effects of rubble weir jetty construction at Murrells Inlet, South Carolina–Vol. I: colonization and community development on new jetties. Technical Report EL-84-4. Prepared by Marine Resources Research Institute, Charleston, SC, for Coastal Engineering Research Center. Vicksburg, U.S. Army Engineer Waterways Experiment Station, 138 pp. https://doi.org/10.5962/bhl.title.48315

Vanhöffen E (1914) Die Isopoden der deutschen Südpolar-Expedition 1901–1903. Deutsche Südpolar-Expedition. Zoologie 15: 447–598. https://doi.org/10.5962/bhl.title.10649

Verrill AE, Smith SI, Harger O (1873) Catalogue of the marine invertebrate animals of the southern coast of New England, and adjacent waters. In: Verrill AE, Smith SI (Eds) Report upon the invertebrate animals of Vineyard Sound and adjacent waters, with an account of the physical features of the region. Extracted from: Report of Professor S.F. Baird, Commissioner of Fish and Fisheries, on the condition of the sea-fisheries of the south coast of New England in 1871 and 1872. Government Printing Office, Washington, 243 pp. https://doi.org/10.5962/bhl.title.31963

Wall A, Bruce N, Wetzer R (2015) Status of *Exosphaeroma amplicauda* (Stimpson, 1857), *E. aphrodita* (Boone, 1923) and description of three new species (Crustacea, Isopoda, Sphaeromatidae) from the north-eastern Pacific. ZooKeys 504: 11–58. https://doi.org/10.3897/zookeys.504.8049

Wetzer R, Bruce NL (2007) A new species of *Paradella* Harrison & Holdich, 1982 (Crustacea: Isopoda: Sphaeromatidae) from Baja California, Mexico, with a key to East Pacific species. Zootaxa 1512(1): 39–49. https://doi.org/10.11646/zootaxa.1512.1.2

Wetzer R, Wall A, Bruce NL (2021) Redescription of *Gnorimosphaeroma oregonense* (Dana, 1853) (Crustacea, Isopoda, Sphaeromatidae), designation of neotype, and 16S-rDNA molecular phylogeny of the north-eastern Pacific species. ZooKeys 1037: 23–56. https://doi.org/10.3897/zookeys.1037.63017

White A (1847) List of the Specimens of Crustacea in the Collection of the British Museum. Natural History Museum, London, 143 pp.

Wilkinson LL (2004) The Biology of *Spaeroma Terebrans* in Lake Pontchartrain, Louisiana with Emphasis on Burrowing. PhD Dissertation, University of New Orleans, New Orleans, 205 pp. https://scholarworks.uno.edu/td/205

Yasmeen R, Javed W (2001) A new record of *Paracerceis sculpta* (Holmes, 1904) (Sphaeromatidae: Isopoda) from Pakistan, northern Arabian Sea. Pakistan Journal of Marine Sciences 10: 43–48. https://www.pakjmsuok.com/index.php/pjms/article/view/45

Zoosyst. Evol. 99 (2) 2023, 391–397 | DOI 10.3897/zse.99.105770

PENSOFT

für Natur MUSEUM FÜR NATURKUNDE BERLIN

First report of a histozoic *Henneguya* (Cnidaria, Endocnidozoa) infecting a synbranchid potamodromous fish from South America: Morphostructural and biological data

Patrick D. Mathews[1,2], Omar Mertins[2], Luis L. Espinoza[3], Julio C. Aguiar[1], Tiago Milanin[4]

1 *Department of Parasitology, Institute of Biosciences, São Paulo State University, 18618-689 Botucatu, Brazil*

2 *Laboratory of Nano Bio Materials, Department of Biophysics, Paulista Medical School, Federal University of Sao Paulo, 04023-062 São Paulo, Brazil*

3 *Laboratory of Biology and Molecular Genetics, Faculty of Veterinary Medicine, Universidad Nacional Mayor de San Marcos, Lima 15021, Peru*

4 *Department of Basic Sciences, Faculty of Animal Science and Food Technology, University of São Paulo, 13635-900, Pirassununga, Brazil*

https://zoobank.org/7D9E1775-A6FC-49D0-9B89-EBF51D3DC912

Corresponding author: Patrick D. Mathews (patrickmathews83@gmail.com)

Academic editor: Pavel Stoev ♦ **Received** 1 May 2023 ♦ **Accepted** 12 June 2023 ♦ **Published** 5 July 2023

Abstract

In this study, a *Henneguya* myxosporean species is described to infect an ecological, biological, and evolutionary important fish from Amazon biome. The myxosporean was found in the skin of only one specimen of marbled swamp eel, *Synbranchus marmoratus* caught in a small stream from Peruvian Amazon floodplain. Mature myxospores have ovoid shape from the valvular view, measuring 32.2 ± 0.6 µm (31.6–32.8) in total length, 21.5 ± 0.3 µm (21.2–21.8) in spore body length, 11.7 ± 0.5 µm (11.2–12.2) in width and 10.6 ± 0.9 µm (9.7–11.5) in thickness. Non-bifurcate caudal appendage, measuring 10.7 ± 0.4 µm (10.3–11.1) in length. Two polar capsules elongated aubergine in shape, equal in size and measuring 4.9 ± 0.2 µm (4.7–5.1) in length and 3.1 ± 0.5 µm (2.6–3.6) in width. Polar tubules coiled in 7–8 turns. This is the first report of a *Henneguya* species parasitizing a fish of the order Synbranchiformes from Amazon basin and the first to describe this parasite infecting a potamodromous fish from South America.

Key Words

Henneguya, myxosporean, marbled swamp eel, skin, Peru

Introduction

Myxosporean are a biologically diverse group of microscopic cnidarians of wide distribution around the world (Atkinson et al. 2018). They mostly innocuous parasites with complex life cycles that involve invertebrate and vertebrate hosts (Okamura et al. 2015). Although, most myxosporean species have fish hosts, they have radiated sporadically into other groups of vertebrates, including amphibians, reptiles, waterfowl and small mammals (Okamura et al. 2015). Within myxosporean, *Henneguya* Thélohan, 1892 is one of the most species rich genera with more than 250 species described taxonomically (Eiras 2002; Rangel et al. 2023). Although the Amazon basin is one of the main biodiversity hotspots, the myxosporean fauna is poorly known. To date only 19 *Henneguya* species have been reported in fish from this geographic region with almost all reported data so far coming from the Brazilian part of the Amazon basin (Eiras and Adriano 2012; Mathews et al. 2016; Naldoni et al. 2018). In the Peruvian Amazon, despite a recording of over 650 fish species, there is a gap in the knowledge of myxosporean diversity. Indeed, only three *Henneguya* species have been described (Mathews et al. 2017, 2018, 2020).

The marbled swamp eel *Synbranchus marmoratus* Bloch, 1795 is considered a potential predator and it can be found throughout flooded forests, small streams and associated swamps subject to water level changes, between the rainy season and the dry period (Heisler 1982; Favorito et al. 2005;

Junges et al. 2010). This species of fish is a protogynous diandric, meaning that females will change their sex and become males (Allsop and West 2003). It is a potamodromous species which is capable of switching from exclusive water breathing to exclusive air breathing (Heisler 1982). Despite, the ecological, biological, and evolutive importance of the marbled swamp eel, little is known about its parasitic fauna, particularly the ones concerning myxosporean parasites.

This study aims to contribute to the increase of knowledge of diversity cnidarian myxosporean and their interaction with fishes from Amazon biome. Thus, spore morphology features using light, scanning and transmission electron microscopy as well as other important biological characters such as tissue tropism and host-specificity are provided.

Materials and methods

Six specimens of *S. marmoratus* (ranging from 18.1 to 21.6 cm in length) that died during transport were donated by local fishers for ornamental fishes in March 2018. According to the fishers, these fish were caught in a small stream near of the Village Oran (3°21'0"S, 72°31'0"W), Omagua Region, Department of Loreto, Peru.

Morphometric analysis was performed following the criteria outlined by Lom and Arthur (1989). Measurements and photographs were taken from 30 randomly selected formalin-fixed mature myxospores, using a computer equipped with Axiovision 4.1 image capture software coupled to an Axioplan 2 Zeiss microscope (Carl Zeiss AG, Oberkochen, Germany). Spore length, thickness, polar capsule length, width, and caudal appendage length were measured and given in micrometers (µm) and expressed as a mean ± standard deviation, followed by the range in parentheses where appropriate. Permanent slides containing mature myxospores stained with Giemsa were mounted and deposited in the cnidarian collection of the Zoology Museum at the University of São Paulo – MZUSP, São Paulo, Brazil (Hapantotype MZUSP 8733).

Histological analysis was performed on fresh tissue fragments containing plasmodium. Infected tissue was fixed in 10% buffered formalin solution, then dehydrated with increasing series of ethanol, diaphanized, embedded in paraffin, cut into serial sections 5 µm thick using an HM 340E electron microtome (Thermo ScientificTM, Massachusetts, USA), and stained with haematoxylin/eosin. A light microscope DM1000 (Leica, Washington, USA) coupled to a computer and using the Leica Application Suite software version 1.6.0 was used for image capture.

Surface ultrastructure observation was performed in leaked myxospores from ruptured plasmodium using a glass slide previously treated with poly-L-lysine. Samples were processed as described in Mathews et al. (2022a). Samples were visualized with a DSM 940 scanning electron microscope (Carl Zeiss, Hamburg, Germany) operating at 15 kV. For internal structural analyses, a whole intact plasmodium was fixed in 2.5% glutaraldehyde with 0.1 M buffered cacodylate (pH 7.4) for 24 h and processed routinely according to standard transmission electron microscope methods. Samples were examined under a JEOL 1200 EX II transmission electron microscope at 60 kV and micrographs were captured with a GATAN 791 camera.

For molecular diagnostic, extraction of genomic DNA (gDNA) was performed in a single plasmodium dissected from the skin and fixed in absolute ethanol. The gDNA was extracted using a DNeasy Blood & Tissue Kit (Qiagen Inc., California, USA), in accordance with the manufacturer's instructions for animal tissue protocol. Polymerase chain reactions (PCRs) were conducted in a final volume reaction of 25 µL, which comprised 10–50 ng of extracted DNA, 0.2 pmol for each primer, 12.5 µL of Dream Taq Green PCR Master Mix (Thermo Scientific) and nuclease-free water. Partial 18S rDNA sequence was amplified using routinely chosen primers paired as follows ERIB1 with ACT1r and Myxgen4F with ERIB10 (Barta et al. 1997, Kent et al. 2000, Hallett and Diamant 2001). PCRs were performed in an AG22331 Hamburg Thermocycler (Eppendorf, Hamburg, Germany) and amplification thermal cycling consisted of 95 °C for 5 min, followed by 35 cycles at 95 °C for 1 min, 58 °C for 1 min, 72 °C for 2 min, and then final elongation at 72 °C for 5 min. Amplification PCR products were electrophoresed in 2.0% agarose gel in a Tris-Acetate EDTA buffer, stained with Sybr Safe DNA gel stain (Invitrogen by Life Technologies, Carlsbad, USA), and analyzed under a Stratagene 2020E trans illuminator (Stratagene California, San Diego, USA). Band sizes of the amplicons was estimated by comparison with the concurrently run molecular weight marker 1 Kb Plus DNA Ladder (Invitrogen by Life Technologies). PCR products were purified using USB ExoSap-IT (Thermo Fisher Scientific, Waltham, USA) in accordance to the manufacturer's instructions. Purified PCR amplicons were sequenced using the same PCR primers and performed with a BigDye Terminator v3.1 cycle sequencing kit (Applied Biosystems Inc., California, USA) in an ABI 3730 DNA sequencing analyzer.

Results

Of six wild specimens of *S. marmoratus*, a single wild specimens of *S. marmoratus* examined, was infected in the skin by an unknown cnidarian myxosporean species. Based on the phenotypic characters of the mature myxospores, this species was assigned to the genus *Henneguya*. The fish presented five plasmodia distributed in the body skin. The same were not found in any other organ.

Taxonomic summary

Phylum: Cnidaria Verrill, 1865.
Subphylum: Endocnidozoa Schuchert, 1996.
Class: Myxosporea Bütschli, 1881.
Order: Bivalvulida Shulman, 1959.
Family: Myxobolidae Thélohan, 1892.

Genus *Henneguya* Thélohan, 1892

Species. *Henneguya* sp. (We suggest that this isolate, after determination by molecular phylogenetic data, be named as (*H. atingae*) based on host species common name in Peru.

Type host. *Symbranchus marmoratus* (Teleostei: Symbranchidae).

Site of infection. Stratus corneum of epidermis layer of the skin.

Type locality. Small stream, adjacent area of Oran Village, Loreto Department, Peru (3°21'0"S, 72°31'0"W).

Description. Morphological observations by light microscopic showed mature myxospores have ovoid shape from the valvular view, measuring 32.2 ± 0.6 µm (31.6–32.8) in total length, 21.5 ± 0.3 µm (21.2–21.8) in spore body length, 11.7 ± 0.5 µm (11.2–12.2) in width and 10.6 ± 0.9 µm (9.7–11.5) in thickness (Fig. 1a, c). Non-bifurcate caudal appendage, measuring 10.7 ± 0.4 µm (10.3–11.1) in length (Fig. 1a, c). Two polar capsules elongated aubergine in shape, equal in size and measuring 4.9 ± 0.2 µm (4.7–5.1) in length and 3.1 ± 0.5 µm (2.6–3.6) in width (Fig. 1b, c). Sporoplasm evidenced two nuclei in valvular view and sutural line was noticeable in side view (Fig. 1b, c).

Surface topography analyses of mature myxospores in valvular view revealed smooth valve cell with presence of mucous in a small area (Fig. 2a). In sutural view myxospore evidence a conspicuous sutural line (Fig. 2c). The density of caudal appendage is likely be identical to that of its valve (Fig. 2b). Internal ultrastructural observations showed binucleated sporoplasm contained sev-

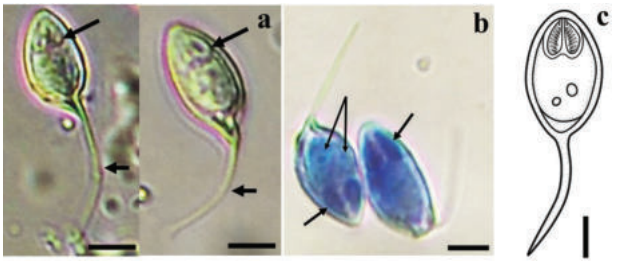

Figure 1. *Henneguya* sp. parasite from the skin of *Synbranchus marmoratus*. **a**: formalin-fixed myxospores in valvular view showing appendage caudal (large arrows) and two polar capsules in the anterior pole of spore occupied only the anterior third of the myxospore body (small blue arrows). **b**: mature myxospores stained with Giemsa with noticeable binucleate sporoplasm (double arrow) and polar capsules with aubergine shape (large arrow). **c**: schematic illustration of mature myxospore with polar tubule inside of polar capsule. Scale bars: 5 µm.

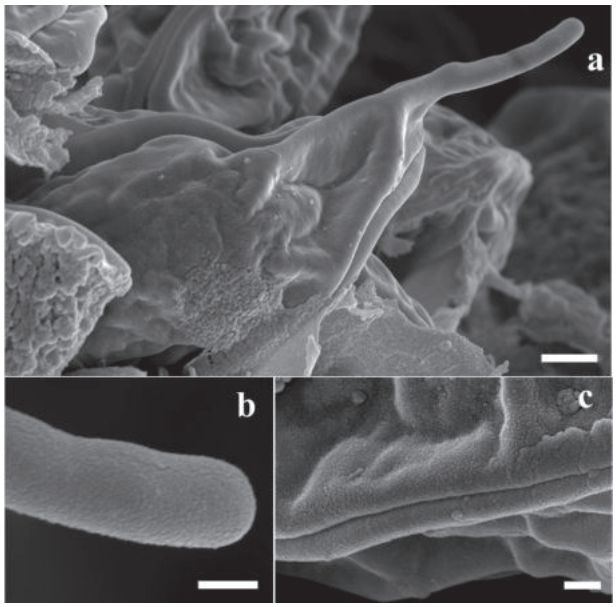

Figure 2. Surface topography by SEM of *Henneguya* sp. infecting skin of *Synbranchus marmoratus*. **a**: mature myxospore in valvular view showing smooth valve cell with presence of mucous (white star) in a small area and caudal appendage. Scale bar. 1 µm. **b**: amplified area of the caudal appendage evidencing density of caudal appendage likely to be identical to that of its valve. Scale bar. 200 nm **c**: myxospore evidence a conspicuous sutural line in sutural view. Scale bar: 100 nm.

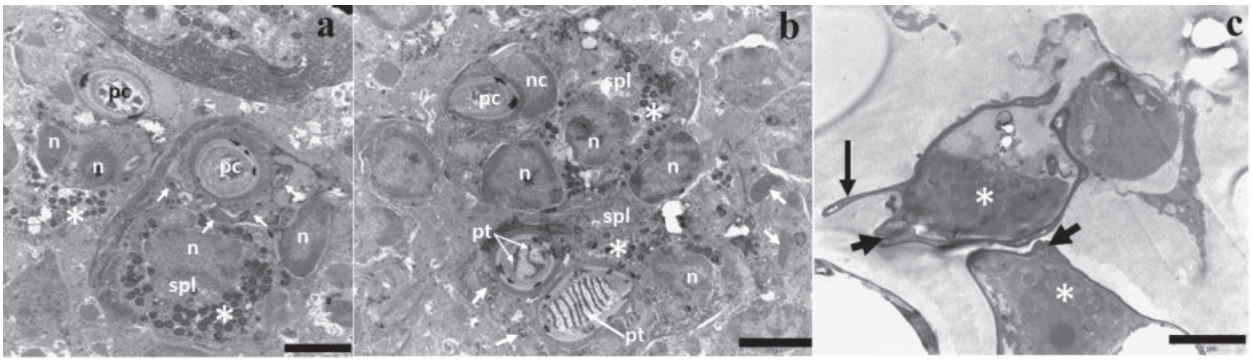

Figure 3. Internal ultrastructure by TEM of myxospore of *Henneguya* sp. infecting skin of *Synbranchus marmoratus*. **a**: sporoblast in young developmental stage showing binucleated sporoplasm (n) contained several sporoplasmosomes (asterisk), valve-forming materials (white arrow) and polar capsules (pc) with absence of polar tubule. **b**: polar capsule (pc) with capsular nuclei, polar tubule internalized contained seven to eight coils (pt), sporoplasm binucleated (spl/n) and contained sporoplasmosomes (asterisk) at a more advanced sporoblast developmental stage. **c**: Spores with sutural lines (small arrows), sporoplasm with numerous sporoplasmosomes (asterisk) and caudal appendage (large arrow). Scale bars: 2 µm.

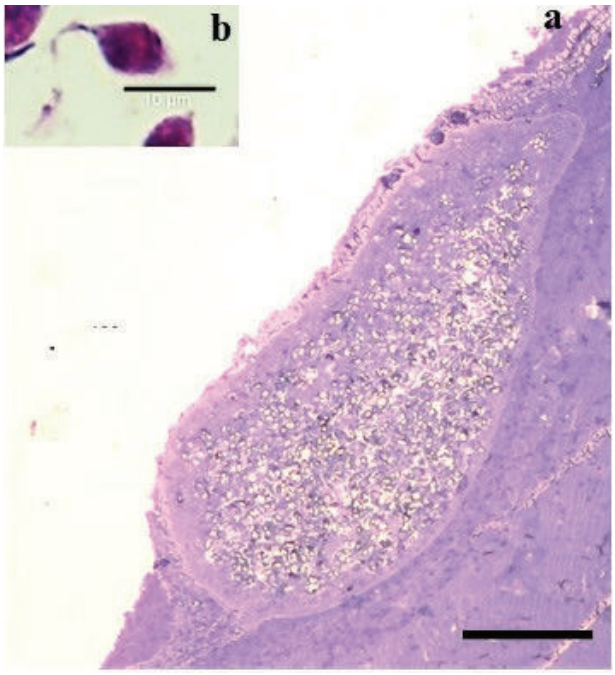

Figure 4. Histological sections of the host-tissue infected of *Synbranchus marmoratus* with *Henneguya* sp. **a**: Intact plasmodium located in the stratus corneum of epidermis layer of the skin. Scale bar. 50 µm. **b**: mature myxospore in sutural view with noticeable caudal appendage. Scale bar. 10 µm.

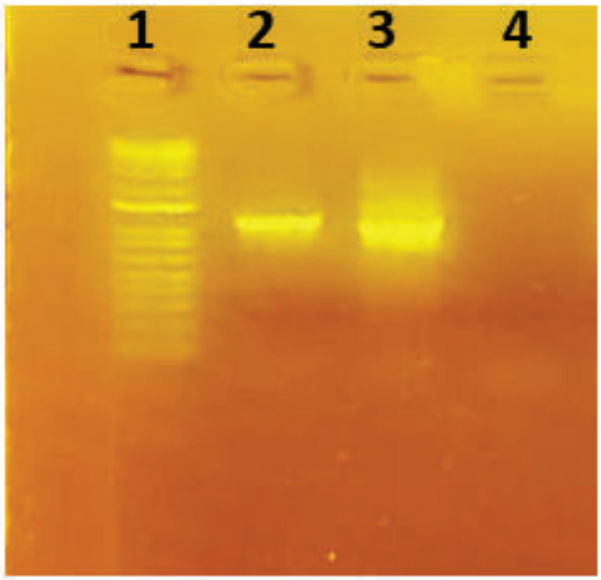

Figure 5. Agarose gel showing 18S rDNA gene PCR amplification of *Henneguya* sp. from skin infected of *S. marmoratus*. Lane 1: DNA ladder marker, Lane 2: amplicon 1000 pb approx. (ERIB1/ACT1r), Lane 3: amplicon 1100 pb approx. (Myxgen4F/ ERIB10), Lane 4: Negative Control.

eral sporoplasmosomes and valve-forming materials in young sporoblast developmental myxospore stage (Fig. 3a). Polar capsule with polar tubule internalized and contained seven to eight coils at a more advanced sporoblast developmental stage (Fig. 3b). Caudal appendage and conspicuous sutural line in mature spores. (Fig. 3c).

Histologic evidenced tissue tropism of the myxosporean under study, occurring in the stratus corneum of epidermis layer of the skin (Figure 4). The parasites induced no apparent tissue destruction, ulcerations, necrosis or inflammatory response. For molecular procedures, partial 18S rDNA gene was successfully amplified by PCR (Fig. 5), however, sequencing failed.

Discussion

Despite the growing description of myxosporean infecting South American fishes (Sousa et al. 2021; Adriano and Oliveira 2022), the diversity of these ancient metazoans in this neotropical realm remains largely unknown (Okamura et al. 2018; Mathews et al. 2022b). In this context, our study describes a histozoic myxosporean species of *Henneguya*, infecting skin of the Amazonian potamodromous fish *S. marmoratus*. In the Amazon biome, *Henneguya* encompasses 22 recognized species (Table 1), reported infecting Characiform, Perciform, Cichliform, Gymnotiform and Siluriform fishes (Mathews et al. 2017, 2018; Adriano and Oliveira 2022; Rangel et al. 2023). However, to the best of our knowledge, this is the first report of a *Henneguya* species parasitizing a fish of the order Synbranchiformes from Amazon basin and the first to describe this parasite infecting a potamodromous fish from South America. Thus, our results contribute to freshwater myxobolids taxonomy and to increasing our knowledge of cnidarian myxosporean diversity.

The morphological data of the mature myxospore isolated were first compared considering *Henneguya* species previously described from Peruvian Amazon freshwater fishes. Nevertheless, these differ from the new isolated in myxospore body length (18.7 ± 0.9 µm in length for *H. multiradiatus*, 14.3 ± 0.1 µm for *H. loretoensis*, 13.4 ± 0.9 µm for *H. peruviensis* and 21.5 ± 0.3 µm to the new isolated), polar capsule length (9.1 ± 0.1 µm in *H. multiradiatus*, 5.1 ± 0.2 µm in *H. loretoensis*, 3.3 ± 0.2 µm in *H. peruviensis* and 4.9 ± 0.2 µm in the new isolated), number of coils of the polar tubule (10–11 in *H. multiradiatus*, five in *H. loretoensis*, four to five in *H. peruviensis* and seven to eight in the new isolated) and in the length of the caudal appendage (25.8 ± 0.6 µm in *H. multiradiatus*, 21.9 ± 0.1µm in *H. loretoensis*, 10.7 ± 0.1 in *H. peruviensis* and 10.7 ± 1.2 µm in the new isolated). Compared with the all other freshwater *Henneguya* species reported to infect Amazonian fishes, the new isolated differed in at least one characteristic (shape of spore, size of spore or polar capsule, presence or absence or number of valve striations, size of caudal appendage and number of polar tubules turns), tissue and host preference as showed in the Table 1.

According to Molnár and Eszterbauer (2015), for freshwater histozoic myxosporean particularly for *Henneguya* and *Myxobolus* species, the site of infection is considered an important taxonomic key for identification due to high organ and/or tissue specificity of these group of parasites. Accordingly, differences are observed because plasmodia

Table 1. Comparative data of *Henneguya* sp. with other *Henneguya* species parasites of Amazon fish. Spore dimensions, infection sites, and fish host are given. TL: total length; BL: body length; APCL: caudal appendage length; SW: spore width; ST: spore thickness; PCL: polar capsule length; PCW: polar capsule width; NCT: number of coils of polar tubules, *: Peru. All measurements are in μm and/or means ± SD. Source: Rangel et al. 2023, Eiras, 2002.

Species	TL	BL	APCL	SW	ST	PCL	PCW	NCT	Site of infection	Fish species
**Henneguya sp.*	32.2 ± 0.6	21.5 ± 0.3	10.7 ± 0.4	11.7 ± 0.5	10.6 ± 0.9	4.9 ± 0.2	3.1 ± 0.5	7–8	skin	*Synbranchus marmoratus*
Henneguya longisporoplasma	53.4 ± 2.9	12.6 ± 0.6	40.7 ± 2.8	5.7 ± 0.5	5.3 ± 0.5	3.5 ± 0.3	1.9 ± 0.2	4–5	gill filaments, fins	*Plagioscion squamosissimus*
**Henneguya multiradiatus*	44.5 ± 0.6	18.7 ± 0.9	25.8 ± 0.6	7.1 ± 0.2	5.5 ± 0.3	9.1 ± 0.1	1.7 ± 0.1	10–11	Abdominal cavity serosa	*Brochis multiradiatus*
**Henneguya peruviensis*	24.2 ± 1.3	13.4 ± 0.9	10.7 ± 1.2	3.9 ± 0.1	–	3.3 ± 0.2	1.6 ± 0.2	4–5	Gill filaments	*Hyphessobrycon loretoensis*
**Henneguya loretoensis*	36. 2 ± 0.2	14.3 ± 0.1	21.9 ± 0.1	5.1 ± 0.2	–	5.1 ± 0.2	2.4 ± 0.3	5	Gill filaments	*Corydoras leucomelas*
Henneguya tucunarei	43.8 ± 4.1	14 ± 0.8	28.1 ± 4.3	6.1 ± 0.7	–	3.4 ± 0.5	1.98 ± 0.3	3–4	Gill filaments	*Cichla monoculus*
Henneguya tapajoensis	54.6 ± 3.9	16.4 ± 1.2	39 ± 3.9	7 ± 0.4	5 ± 0.1	4.2 ± 0.5	2.1 ± 0.4	4–5	Gill filaments	*Cichla pinima*
Henneguya jariensis	46.7 ± 1.5	13.4 ± 0.7	33.1 ± 1.7	6.5 ± 0.5	–	4 ± 0.3	2 ± 0.1	4	Fins	*Cichla monoculus*
Henneguya paraensis	42.3 ± 0.3	12.8 ± 0.42	29.5 ± 0.73	8.6 ± 0.3	–	7.4 ± 0.1	2.6 ± 0.1	5–7	Gill filaments	*Cichla temensis*
Henneguya melini	40.8 ± 0.3	15.5 ± 0.2	25.3 ± 0.1	4.7 ± 0.1	–	4.8 ± 0.5	1.7 ± 0.3	5–6	Gill filaments	*Corydoras melini*
Henneguya aequidens	41 ± 1.5	15 ± 0.9	27 ± 0.6	6 ± 0.8	–	3 ± 0.3	3 ± 0.3	4–6	Gill filaments	*Aequidens plagiozonatus*
Henneguya torpedo	48.62 ±0.5	28.53 ± 0.3	19.64 ±0.4	7.25 ± 0.31	3.06 ± 0.2	6.41 ± 0.2	1.84 ± 0.1	5–6	Brain and spinal cord	*Brachyhypopomus pinnicaudatus*
Henneguya arapaima	51.6 ± 3.4	14.2 ± 0.8	38.3 ± 2.9	5.7 ± 0.5	4.9 ± 0.2	6.5 ± 0.2	6.3 ± 0.1	5	Gill arch	*Arapaima gigas*
Henneguya rondoni	17.7	7	10.7	3.6	2.5	2.5	0.85	6–7	Lateral nerves	*Gymnorhamphichthys rondoni*
Henneguya rhamdia	50 ± 1.8	13.1 ± 1.1	36.9 ± 1.6	5.2 ± 0.5	–	4.7 ± 0.4	1.1 ± 0.2	10–11	Gill filaments	*Rhamdia quelen*
Henneguya schtzodon	28.9	13.1	16.3	3.3	–	5.4	1.3	8–10	Kidney	*Schtzodon fasciatum*
Henneguya friderici	33.8	10.4	23.3	5.7	4.9	4.9	2.1	7–8	Gut, gill, kidney and liver	*Leporinus friderici*
Henneguya astyanax	47.8 ± 0.71	15.2 ± 0.77	32.6 ± 1.11	5.7 ± 0.71	4.2 ± 0.3	5.0 ± 0.13	1.5 ± 0.07	8–9	Gill filaments	*Astyanax bimaculatus*
Henneguya curimata	35.4	16.6	19.1	6.2	–	3.3 ± 0.02	1.5 ± 0.04	10–11	Kidney	*Curimata inormata*
Henneguya testicularis	27.5	14	13.5	6.5	–	9	2	12–13	Testicle	*Moenkhausia oligolepis*
Henneguya malabarica	28.3	12.6	17.1	4.8	–	3.7	1.8	6–7	Gill filaments	*Hoplias malabaricus*
Henneguya adherens	32.3	12.4	20.5	5.8	–	3.1	1.2	3–4	Gill filaments	*Acestrorhynchus falcatus*
Henneguya amazonica	59.3 ± 0.5	13.9 ± 0.1	45.4 ± 0.6	5.7 ± 0.06	–	3.3 ± 0.02	1.5 ± 0.04	6	Gill lamellae	*Crenlcichla lepldota*

of the new species were located in the skin, whereas *H. peruviensis* and *H. loretoensis* plasmodia are found in the gill filaments and *H. multiradiatus* plasmodia in the abdominal cavity serosa. To our knowledge no *Henneguya* species have been reported from the skin of a fish from Amazon biome (Table 1). In the same vein, fish host represent an indispensable trait for accurately distinguishing new freshwater histozoic *Henneguya*/*Myxobolus* species since these parasites tend to cluster largely based on host phylogenies (Carriero et al. 2013; Mathews et al. 2021; Milanin et al. 2021). This is the first report of a *Henneguya* species parasitizing a synbranchid fish. Thus, considering the fine-scale of the host-specificity, we consider our finding to be important for this isolate as an unknown species.

Regarding molecular data, from South America of the around hundred recognized species, large number of species lack molecular data (Milanin et al. 2017). Indeed, for much of the myxosporean described myxospore morphology was used by ichthyopathologist researchers for species discrimination, because myxo-

spore is a unique structure possessing many characters important for classification (Lom and Dyková 1992). In our study, the partial 18S rDNA gene was successfully amplified by PCR using general eukaryotic and specific primers to myxosporean parasites (Fig. 5). However, after the amplification process, sequencing failed so it was not possible to carry out phylogenetic analysis. In addition, to the few samples with only five plasmodia to perform morphological, ultrastructural, histological and molecular analysis and limitations in accessing new samples of the same region. Although, we were not able to provide the phylogenetic data, the new isolate was strongly characterized based on spore morphometrically features as well as biological traits such as tissue preference and host specificity both important taxonomic keys for classification of freshwater histozoic myxobolids. Future molecular phylogenetic studies are highly recommended, since this would permit stronger taxonomic comparison.

Acknowledgements

The authors thank the São Paulo Research Foundation, FAPESP, for Post-Doc fellowship awarded to P.D. Mathews. The authors are grateful to A.H. Aguillera, P.A. Cortez and Prof. R. Sinigaglia-Coimbra from the Electron Microscopy Center (CEME) at UNIFESP for supporting the SEM and TEM analysis. The authors thank Dr. Christopher George Berger from Occidental College, Los Angeles for revision of the English language.

References

Adriano EA, Oliveira OMP (2022) Myxobolidae in Catálogo Taxonômico da Fauna do Brasil. PNUD. http://fauna.jbrj.gov.br/fauna/faunadobrasil/152860 [Accessed 18 Jan 2022]

Allsop DJ, West SA (2003) Constant relative age and size at sex change for sequentially hermaphroditic fish. Journal of Evolutionary Biology 16(5): 921–929. https://doi.org/10.1046/j.1420-9101.2003.00590.x

Atkinson SD, Bartholomew JL, Lotan T (2018) Myxozoans: Ancient metazoan parasites find a home in phylum Cnidaria. Zoology (Jena, Germany) 129: 66–68. https://doi.org/10.1016/j.zool.2018.06.005

Barta JR, Martin DS, Liberator PA, Dashkevicz M, Anderson JW, Feighner SD, Elbrecht A, Perkins-Barrow A, Jenkins MC, Danforth D, Ruff MD, Profous-Juchelka H (1997) Phylogenetic relationships among eight *Eimeria* species infecting domestic fowl inferred using complete small subunit ribosomal DNA sequences. The Journal of Parasitology 83(2): 262–271. https://doi.org/10.2307/3284453

Carriero MM, Adriano EA, Silva MRM, Ceccarelli PS, Maia AAM (2013) Molecular phylogeny of the *Myxobolus* and *Henneguya* genera with several new South American species. PLoS ONE 8: e73713. https://doi.org/10.1371/journal.pone.0073713

Eiras JC (2002) Synopsis of the species of the genus *Henneguya* Thelohan, 1892 (Myxozoa: Myxosporea: Myxobolidae. Systematic Parasitology 52(1): 43–54. https://doi.org/10.1023/A:1015016312195

Eiras JC, Adriano EA (2012) Checklist of the species of the genus *Henneguya* Thélohan, 1892 (Myxozoa, Myxosporea, Myxobolidae) described between 2002 and 2012. Systematic Parasitology 83(2): 95–104. https://doi.org/10.1007/s11230-012-9374-7

Favorito SE, Zanata AM, Assumpção MI (2005) A new *Synbranchus* (Teleostei: Synjbranchidae) from Ilha de Marajó, Pará, Brazil, with notes on its reproductive biology and larval development. Neotropical Ichthyology 3: 319–328. https://doi.org/10.1590/S1679-62252005000300001

Hallett SL, Diamant A (2001) Ultrastructure and small-subunit ribosomal DNA sequence of *Henneguya lesteri* n. sp. (Myxosporea), a parasite of sand whiting *Sillago analis* (Sillaginidae) from the coast of Queensland, Australia. Diseases of Aquatic Organisms 46: 197–212. https://doi.org/10.3354/dao046197

Heisler N (1982) Intracellular and extracellular acid-base regulation in the tropical fresh-water teleost fish *Synbranchus marmoratus* in response to the transition from water breathing to air breathing. The Journal of Experimental Biology 99(1): 9–28. https://doi.org/10.1242/jeb.99.1.9

Junges CM, Lajmanovich RC, Peltzer PM, Attademo AM, Bassó A (2010) Interactions between *Synbranchus marmoratus* (Teleostei: Synbranchidae) and *Hypsiboas pulchellus* tadpoles (Amphibia: Hylidae): importance of lateral line in nocturnal predation and effects of fenitrothion exposure. Chemosphere 81(10): 1233–1238. https://doi.org/10.1016/j.chemosphere.2010.09.035

Kent ML, Khattra J, Hedrick RP, Devlin RH (2000) *Tetracapsula renicola* n. sp. (Myxozoa: Saccosporidae); the PKX myxozoan: the cause of proliferative kidney disease of salmonid fishes. The Journal of Parasitology 86: 103–111. https://doi.org/10.1645/0022-3395(2000)086[0103:TRNSMS]2.0.CO;2

Lom J, Arthur JR (1989) A guideline for the preparation of species descriptions in Myxosporea. Journal of Fish Diseases 12(2): 151–156. https://doi.org/10.1111/j.1365-2761.1989.tb00287.x

Lom J, Dyková I (1992) Myxosporidia (Phylum Myxozoa). In: Lom J, Dyková I (Eds) Protozoan parasites of fishes. Developments in aquaculture and fisheries sciences Elsevier, Amsterdam, 159–235.

Mathews PD, Maia AAM, Adriano EA (2016) *Henneguya melini* n. sp. (Myxosporea: myxobolidae), a parasite of *Corydoras melini* (Teleostei: siluriformes) in the Amazon region: morphological and ultrastructural aspects. Parasitology Research 115(9): 3599–3604. https://doi.org/10.1007/s00436-016-5125-z

Mathews PD, Naldoni J, Adriano EA (2017) Morphology and small subunit rDNA- based phylogeny of a new *Henneguya* species, infecting the ornamental fish *Corydoras leucomelas* from the Peruvian Amazon. Acta Tropica 176: 51–57. https://doi.org/10.1016/j.actatropica.2017.07.017

Mathews PD, Mertins O, Pereira JOL, Maia AAM, Adriano EA (2018) Morphology and 18S rDNA sequencing of *Henneguya peruviensis* n. sp. (Cnidaria: Myxosporea), a parasite of the Amazonian ornamental fish *Hyphessobrycon loretoensis* from Peru: A myxosporean dispersal approach. Acta Tropica 187: 207–213. https://doi.org/10.1016/j.actatropica.2018.08.012

Mathews PM, Mertins O, Milanin T, Espinoza LL, Alama-Bermejo G, Audebert F, Morandini AC (2020) Taxonomy and 18S rDNA-based phylogeny of *Henneguya multiradiatus* n. sp. (Cnidaria: Myxobolidae) a parasite of *Brochis multiradiatus* from Peruvian Amazon. Microbial Pathogenesis 147: 104372. https://doi.org/10.1016/j.micpath.2020.104372

Mathews PD, Bonillo C, Rabet, N, Lord C, Causse R, Keith P, Audebert F (2021) Phylogenetic analysis and characterization of a new parasitic cnidarian (Myxosporea: Myxobolidae) parasitizing skin of the giant mottled eel from the Solomon Islands. Infection Genetics and Evolution 94: 104986. https://doi.org/10.1016/j.meegid.2021.104986

Mathews PD, Mertins O, Milanin T, Aguiar JC, Gonzales-Flores APP, Tavares LER, Morandini AC (2022a) Ultrastructure, surface topography, morphology and histological observations of a new parasitic cnidarian of the marbled swamp eel from the world's largest tropical wetland area, Pantanal, Brazil. Tissue & Cell 79: 101909. https://doi.org/10.1016/j.tice.2022.101909

Mathews PD, Mertins O, Flores-Gonzales APP, Espinoza LL, Aguiar JC, Milanin T (2022b) Host–Parasite Interaction and Phylogenetic of a new Cnidarian myxosporean (Endocnidozoa: Myxobolidae) Infecting a valuative commercialized ornamental fish from Pantanal wetland biome, Brazil. Pathogens (Basel, Switzerland) 11(10): 1119. https://doi.org/10.3390/pathogens11101119

Milanin T, Atkinson SD, Silva MR, Alves RG, Maia AA, Adriano EA (2017) Occurrence of two novel actinospore types (Cnidaria: Myxosporea) in Brazilian fish farms, and the creation of a novel actinospore collective group. Seisactinomyxon. Acta Parasitologica 62(1): 121–128. https://doi.org/10.1515/ap-2017-0014

Milanin T, Mathews PD, Morandini AC, Mertins O, Audebert F, Pereira JOL, Maia AA M (2021) Morphostructural data and phylogenetic relationships of a new cnidarian myxosporean infecting spleen of an economic and ecological important bryconid fish from Brazil. Microbial Pathogenesis 150: 104718. https://doi.org/10.1016/j.micpath.2020.104718

Molnár K, Eszterbauer E (2015) Specificity of Infection Sites in Vertebrate Hosts. In: Okamura B, Gruhl A, Bartholomew JL (Eds) Myxozoan Evolution, Ecology and Development. Springer, Switzerland, 295–313. https://doi.org/10.1007/978-3-319-14753-6_16

Naldoni J, Maia AAM, Correa LL, Da Silva MRM, Adriano EA (2018) New myxosporeans parasitizing *Phractocephalus hemioliopterus* from Brazil: Morphology, ultrastructure and SSU-rDNA sequencing. Diseases of Aquatic Organisms 128(1): 37–49. https://doi.org/10.3354/dao03210

Okamura B, Gruhl A, Bartholomew JL (2015) An introduction to Myxozoan evolution, ecology and development. In: Okamura B, Gruhl A, Bartholomew JL (Eds) Myxozoan Evolution, Ecology and Development, Springer, Switzerland, 1–20. https://doi.org/10.3354/dao03210

Okamura B, Hartigan A, Naldoni J (2018) Extensive uncharted biodiversity: The parasite dimension. Integrative and Comparative Biology 58: 1132–1145. https://doi.org/10.1093/icb/icy039

Rangel LF, Santos MJ, Rocha S (2023) Synopsis of the species of *Henneguya* Thélohan, 1892 (Cnidaria: Myxosporea: Myxobolidae) described since 2012. Systematic Parasitology 100(3): 291–305. https://doi.org/10.1007/s11230-023-10088-2

Sousa FB, Milanin T, Morandini AC, Espinoza LL, Flores-Gonzales A, Gomes ALS, Matoso DA, Mathews PD (2021) Molecular diagnostic based on 18S rDNA and supplemental taxonomic data of the cnidarian coelozoic *Ceratomyxa* (Cnidaria, Myxosporea) and comments on the intraspecific morphological variation. Zoosystematics and Evolution 97(2): 307–314. https://doi.org/10.3897/zse.97.64769

Zoosyst. Evol. 99 (2) 2023, 399–422 | DOI 10.3897/zse.99.105511

PENSOFT

für Natur MUSEUM FÜR NATURKUNDE BERLIN

Diversity of the genus *Tropodiaptomus* Kiefer, 1932 (Crustacea, Copepoda, Calanoida, Diaptomidae) in Thailand, with the description of two new species

Thanida Saetang[1,2], Supiyanit Maiphae[1,2]

1 *Animal Systematics and Ecology Speciality Research Unit (ASESRU), Department of Zoology, Faculty of Science, Kasetsart University, Bangkok 10900, Thailand*

2 *Biodiversity Center Kasetsart University, Bangkok 10900, Thailand*

https://zoobank.org/F8AA89A2-56BC-4A96-9835-C16AAE2744C1

Corresponding author: Supiyanit Maiphae (supiyanit.m@ku.th)

Academic editor: Kay Van Damme ♦ **Received** 26 April 2023 ♦ **Accepted** 16 June 2023 ♦ **Published** 5 July 2023

Abstract

Tropodiaptomus is a genus of diaptomid copepods with 10 species currently recorded in Thailand. A recent study on DNA taxonomy revealed putative new species among specimens collected from freshwater habitats throughout Thailand. This study examined the morphological characteristics and confirmed the taxonomic status of the two putative new species of *Tropodiaptomus*. Results showed that the two new taxa were different from other species in the genus *Tropodiaptomus*. These two new species, *T. pedecrassum* **sp. nov.** and *T. longiprocessus* **sp. nov.**, were described and illustrated based on material collected from a swamp in northern Thailand and a pond in western Thailand, respectively. They were distinguished from their congeners by the length of the spinous process on the antepenultimate segment of the adult male right antennule, the number of lobes and serration pattern on the inner margin of the adult male left P5, and the shape and supplementary process on the surface structures of basis and distal exopod segments of the adult male right P5. These discoveries increased the number of records of this genus in Thailand to 12 species. A pictorial key to all species is provided, and their ecological and biogeographical distributions are updated and discussed.

Key Words

habitat preference, new species, Thailand, *Tropodiaptomus longiprocessus*, *Tropodiaptomus pedecrassum*

Introduction

To date, 170 copepod species have been recorded from freshwater habitats in Thailand (Saetang et al. 2020; Sanoamuang and Dabseepai 2021). The diaptomid family in the calanoid group is highly diverse, comprising 42 species in Thailand, with 14 new species added during the last 20 years. *Mongolodiaptomus* and *Tropodiaptomus* are the two most diverse genera, each containing 10 species (Saetang et al. 2020; Sanoamuang and Dabseepai 2021). Interestingly, *Tropodiaptomus* has the highest number of 63 species in the family Diaptomidae worldwide (Walter and Boxshall 2023). Most species in this genus are restricted to one or a few biogeographic regions, with 21 species distributed in Asia (Saetang et al. 2020; Walter and Boxshall 2023). In Thailand, undiscovered species are postulated to exist within specific habitats such as temporary ponds and this genus remains underexplored. Saetang et al. (2020) investigated 468 samples collected from 190 freshwater habitats throughout Thailand. Eight species were reported with one new to science. Later, Saetang (2021) and Saetang et al. (2022) conducted extensive morphological and DNA taxonomy studies on *Tropodiaptomus*, with results determining at least 12 species recorded in Thailand. These integrative methods indicated a high level of genetic diversity in some *Tropodiaptomus* species, with the possibility of cryptic species. Based on genetic data, three more putative new species await morphological study and description (Saetang et al. 2022).

Our study proposes *Tropodiaptomus* sp. 1 and *Tropodiaptomus* sp. 2 mentioned in Saetang et al. (2022) as new species with detailed descriptions and illustrations of both males and females. A pictorial key for practical use to identify members of this genus was presented and the present diversity and species distribution were updated.

Materials and methods

Samples were qualitatively collected from swamp in Dok Kham Tai District, Phayao Province, northern Thailand (19°13'57.6"N, 100°02'56.5"E) in January 2018 and Thong Phaphum District, Kanchanaburi Province (14°39'09.1"N, 98°33'27.5"E) in June 2019 using a plankton net of 60 µm mesh and immediately preserved in 70% ethanol. All adult males and females were sorted using an Olympus SZ40 stereo microscope, and each specimen was dissected and mounted on a slide in glycerine and then sealed using nail varnish.

The morphological characteristics were examined and identified using an Olympus CH2 compound microscope, and drawings were made from both complete and dissected specimens using a camera lucida connected to the microscope. The final versions of the drawings were made using Adobe Illustrator CS5 program (version 15.0). The specimens were identified to species level according to Lai et al. (1979), Lai and Fernando (1981), Kiefer (1982), and Sanoamuang (2002). The descriptive terminology proposed by Huys and Boxshall (1991) was adopted. Abbreviations used in the text and figures are: **A1** = antennule, **ae** = aesthetasc, **s** = spine, **sp** = spinous process, **A2** = antenna, **P1–P5** = swimming legs 1–5, **exp-1 (2, 3)** = first (second and third) segment of exopod, **enp-1 (2, 3)** = first (second and third) segment of endopod.

All type specimens were deposited in the reference collection of the Princess Maha Chakri Sirindhorn National History Museum, Prince of Songkla University, Songkhla, Thailand (**PSUNHM**).

Results

Systematics

Order CALANOIDA Sars, 1903
Family DIAPTOMIDAE Baird, 1850

Genus *Tropodiaptomus* Kiefer, 1932

Type species. *Tropodiaptomus orientalis* (Brady, 1886).

***Tropodiaptomus pedecrassum* sp. nov.**
https://zoobank.org/D922BBEE-6472-4B19-AF44-540A34C93DB4

Type locality. Swamp near rice field, Dok Kham Tai District, Phayao Province, northern Thailand (19°13'57.6"N, 100°02'56.5"E). Temporary habitat without macrophytes.

Material examined. *Holotype*. One adult male, dissected and mounted onto five slides, Dok Kham Tai, Phayao province, northern Thailand (19°13'57.6"N, 100°02'56.5"E), 31 January 2018, Thanida Saetang and Supiyanit Maiphae; PSUZC-PK2008-01–PSUZC-PK2008-05. ***Allotype*.** One adult female, collected with holotype; PSUZC-PK2008-06–PSUZC-PK2008-08. ***Paratype*.** One adult male, collected with holotype; PSUZC-PK2008-09–PSUZC-PK2008-11.

Description of the adult male. *Body* (Figs 1A, 2A). Total body length about 1,145 µm (1.1 mm) (measured from anterior margin of rostrum to posterior margin of caudal rami). Prosome length about 2 times as long as urosome (including caudal rami). Fourth and fifth pedigers separated by distinct septum. Fifth pediger produced into small asymmetrical posterolateral wings (left wing shorter than right wing), each distal end with spine. Urosome 5-segmented. Genital somite with dorsolateral sensilla on right and left side, fourth somite with expanded right corner. Anal somite with deep cleft, length about 0.8 times as long as wide. Caudal rami parallel, symmetrical, length about 1.8 times as long as wide, with setules on inner margin. Each ramus with six setae.

Rostrum (Fig. 3A). Two rostral elements on anterior margin with suture in the middle.

A1 (Figs 1B, C, 3B–D). Asymmetrical. ***Left A1*** non-geniculate, 25-segmented, reaching beyond the end of caudal rami. Armature formula of each segment as follows: 1+ae, 3+ae, 1+ae, 1, 1+ae, 1, 1+ae, 1+s, 2+ae, 1, 1, 1+ae+s, 1, 1+ae, 1, 1+ae, 1, 1, 1+ae, 1, 1, 2, 2, 2, 5+ae. ***Right A1*** transformed and geniculate, 22-segmented. Strongly dilated between segment 13and segment 18. Spinous process on segment 20 (antepenultimate) straight and bent at distal end, reaching 3/4 next segment, and with longitudinal hyaline membrane on outer margin (Fig. 7A–G, arrowhead). Armature formula of each segment as follows: 1+ae, 3+ae, 1+ae, 1, 1+ae, 1, 1+ae, 1+s, 2+ae, 1+sp, 1+sp, 1+ae+s, 1+ae+sp, 2+ae, 2+ae+sp, 2+ae+sp, 1+s, s, 1+3s, 4+sp, 2, 5+ae.

A2 (Fig. 4A). Coxa with one inner seta on distal corner. Basis with two inner setae on distal corner. Exopod 7-segmented, exp-1–6 with 1, 3, 1, 1, 1, and 1 inner setae, respectively, and exp-7 with one inner and three apical setae. Endopod 2-segmented, enp-1 with two inner setae and one longitudinal row of outer spinules, enp-2 with nine inner and seven apical setae; and one group of outer spinules.

Mandible (Fig. 4B). Coxa with eight strongly chitinised teeth and one seta on gnathobase. Basis with four inner setae. Exopod 4-segmented with 1, 1, 1, and 3 setae, respectively. Endopod 2-segmented, enp-1 with four inner setae, enp-2 with nine apical setae and one longitudinal row of outer spinules.

Maxillule (Fig. 4C). Precoxal arthrite with four plumose setae and eleven bipinnate spines.

Coxal endite with three plumose setae, and coxal epipodite with seven plumose setae and two bipinnate spines. Basis with two endites; the proximal with four

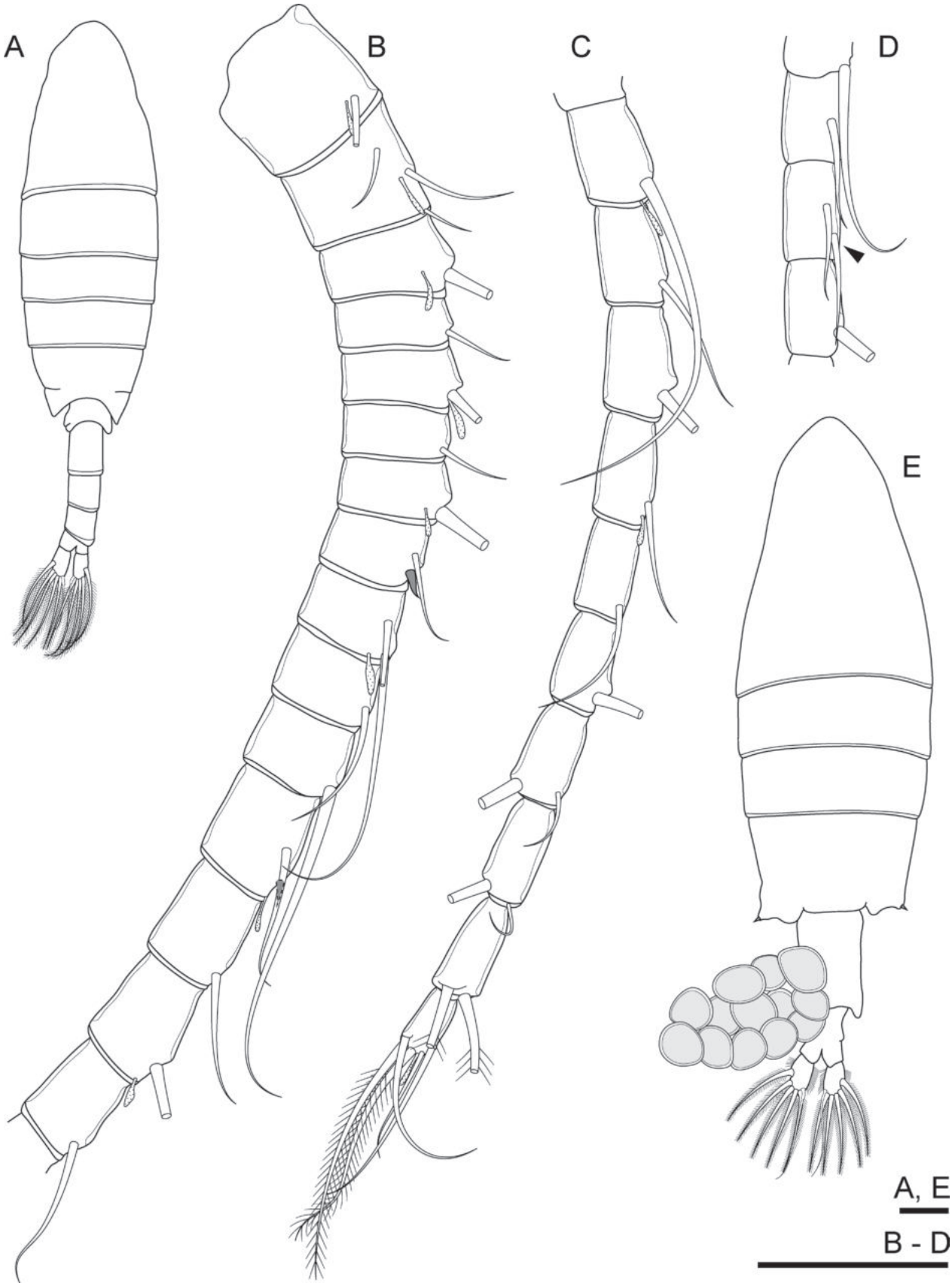

Figure 1. *Tropodiaptomus pedecrassum* sp. nov., male holotype. **A.** Habitus, dorsal view; **B.** Segment 1–15 of left antennule (gray color indicates spine); **C.** Segment 16–25 of left antennule; **D.** Segment 12–14 of left antennule of the adult male specimen from the same population of holotype, (arrowhead indicates variation of setae on segment 13); female allotype; **E.** Habitus, dorsal view. Scale bars: 100 µm.

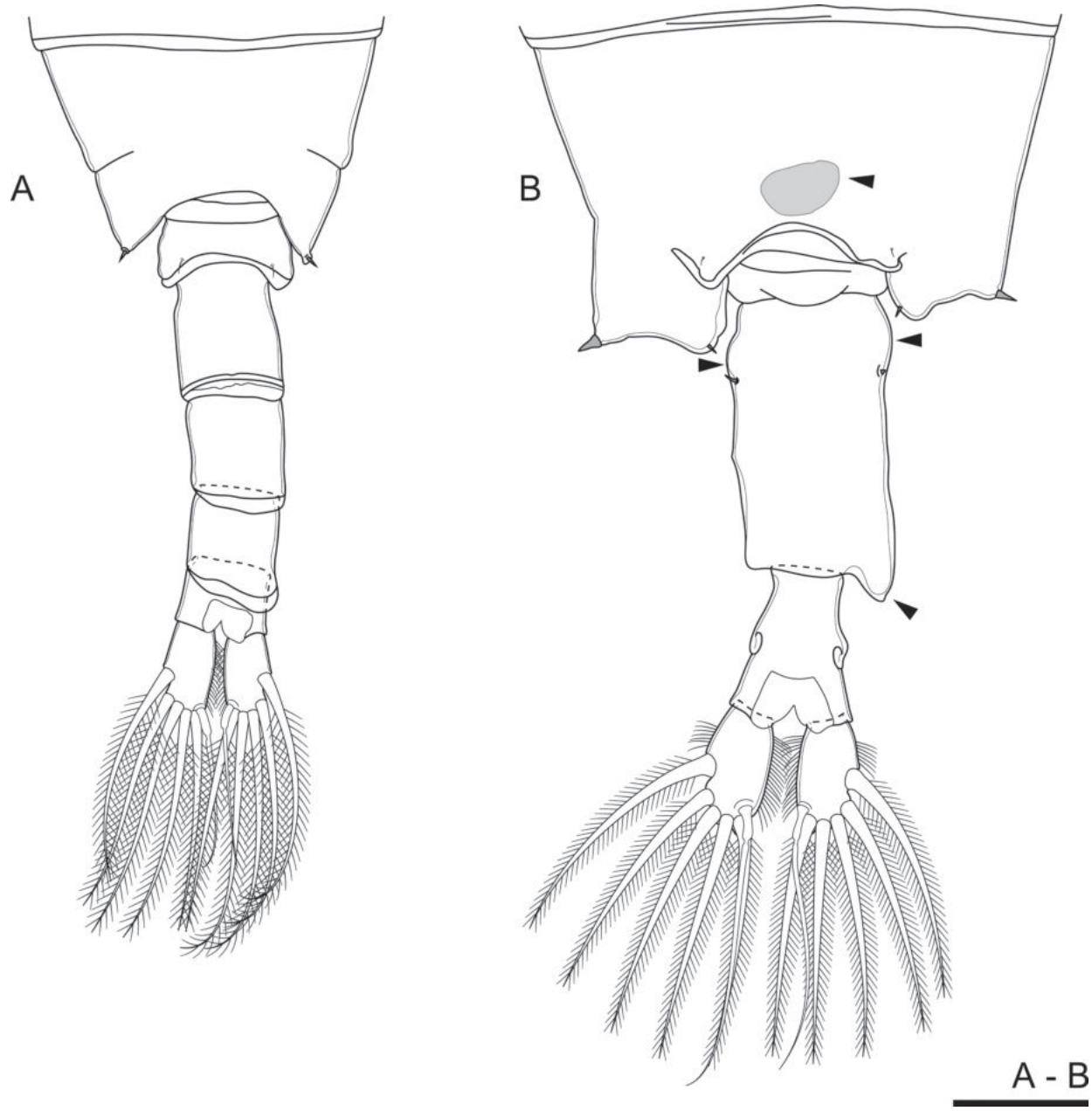

Figure 2. *Tropodiaptomus pedecrassum* sp. nov., male holotype. **A.** Pediger 5 and urosome, dorsal view; female allotype; **B.** Pediger 5 and urosome, dorsal view (arrowhead indicates anterior part swollen in both sides and triangular-like lobe, and grey ellipse indicates dorsal prominence). Scale bar: 100 μm.

plumose setae and the distal with eight plumose setae, and basal exite with one bipinnate spines. Exopod 1-segmented with six plumose setae, one longitudinal row of setules on inner margin of segment. Endopod 1-segmented with four plumose setae.

Maxilla (Fig. 4D). Proximal praecoxal endite with four setae, distal praecoxal endite with three setae. Proximal and distal coxal endites with three setae each. Allobasis protruding into endite with five setae. Endopod reduced to two segments, enp-1 with two setae and enp-2 with three setae.

Maxilliped (Fig. 4E). Praecoxal endite with one seta. Coxal endites with 2, 3, and 3 setae, respectively. Distal corner of coxa produced into rounded lobe with spinules on inner margin. Basis with three setae on distal third, and one row of setules and one row of spinules on inner margin. Endopod 6-segmented; with 2, 3, 2, 2, 1+1, and 4 setae, respectively.

P1–P4 (Fig. 5A–D). Biramous. Intercoxal sclerite naked. Coxa with one inner seta. Basis without seta except P4 with one seta on outer distal margin. P1 with 3-segmented exopod and 2-segmented endopod, P2–P4 with 3-segmented exopod and endopod, endopod reaching proximal of exp-3. ***P1*** (Fig. 5A). Exp-1 with one longitudinal row of inner setules. Exp-2 and exp-3 with one longitudinal row of outer setules. Enp-2 with one row of spinules close

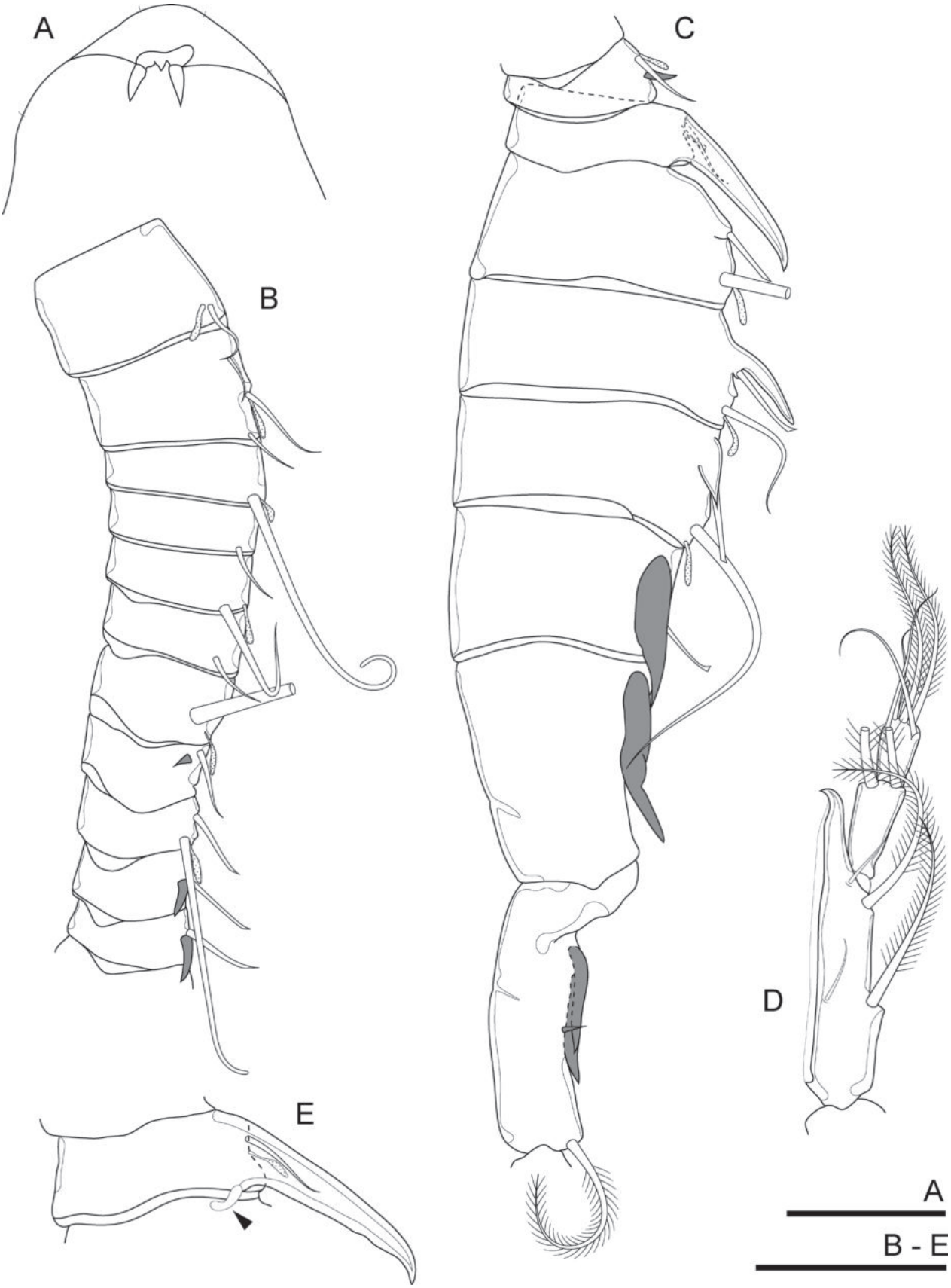

Figure 3. *Tropodiaptomus pedecrassum* sp. nov., male holotype. **A.** Rostrum; **B.** Segment 1–11 of right antennule; **C.** Segment 12–19 of right antennule (gray color indicate spine); **D.** Segment 20–22 of right antennule; **E.** Segment 13 of right antennule of the adult male specimen from the same population of holotype (arrowhead indicates hyaline knob). Scale bars: 100 µm.

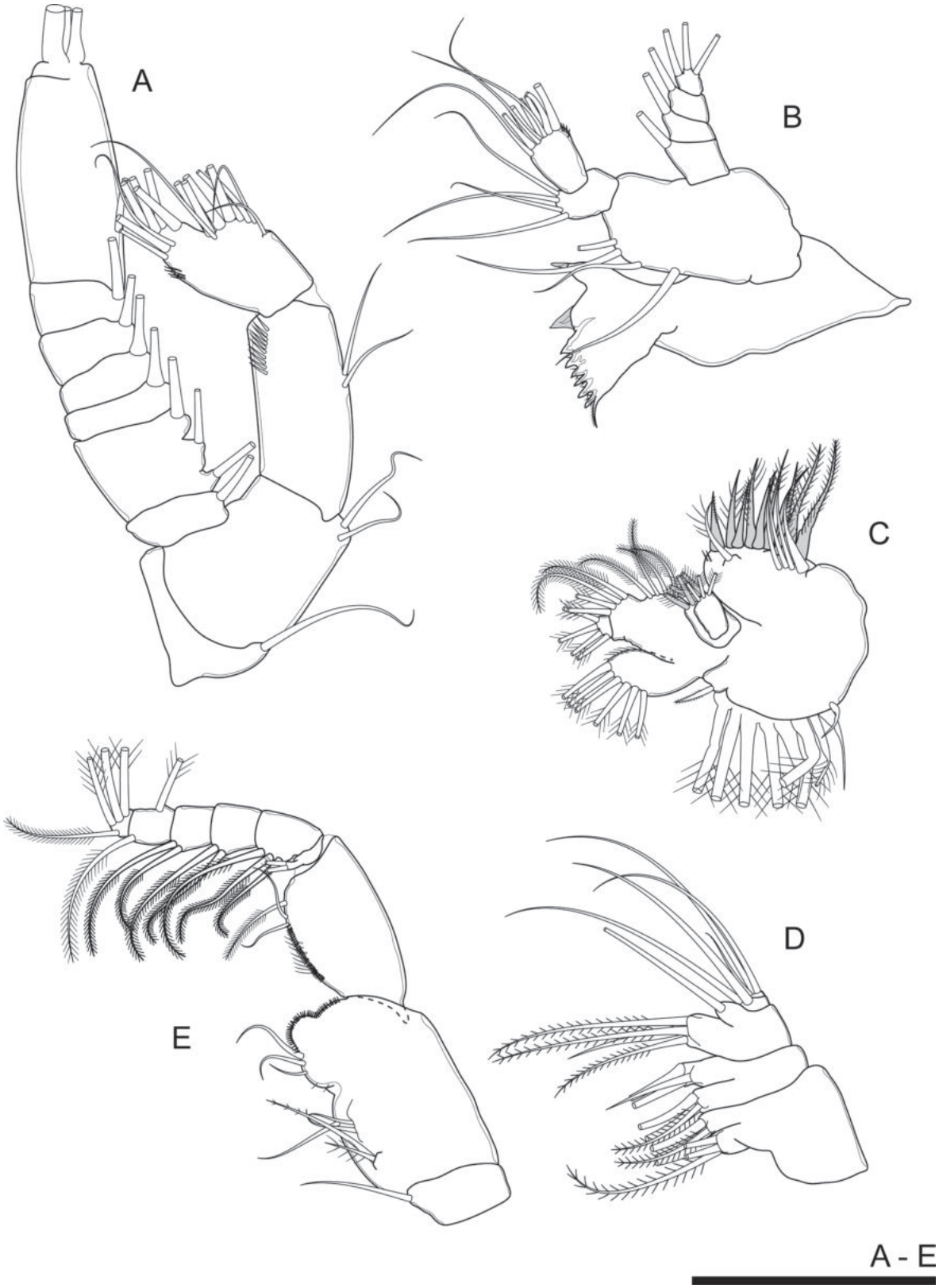

Figure 4. *Tropodiaptomus pedecrassum* sp. nov., male holotype. **A.** Antenna; **B.** Mandible; **C.** Maxillule; **D.** Maxilla; **E.** Maxilliped. Scale bar: 100 μm.

to distal end. ***P2–P4*** (Fig. 5B–D). Exp-1 with one longitudinal row of inner setules. Exp-2 and exp-3 with one longitudinal row of outer and inner setules. Enp-1 with one longitudinal row of outer setules in P2 and P4. Enp-2 with one longitudinal row of outer setules in P2–P4, enp-2 of P2 with Schmeil's organ. Enp-3 with one longitudinal row of outer setules in P2, one longitudinal row of outer and inner setules in P4. Exp-3 and enp-3 with one and two

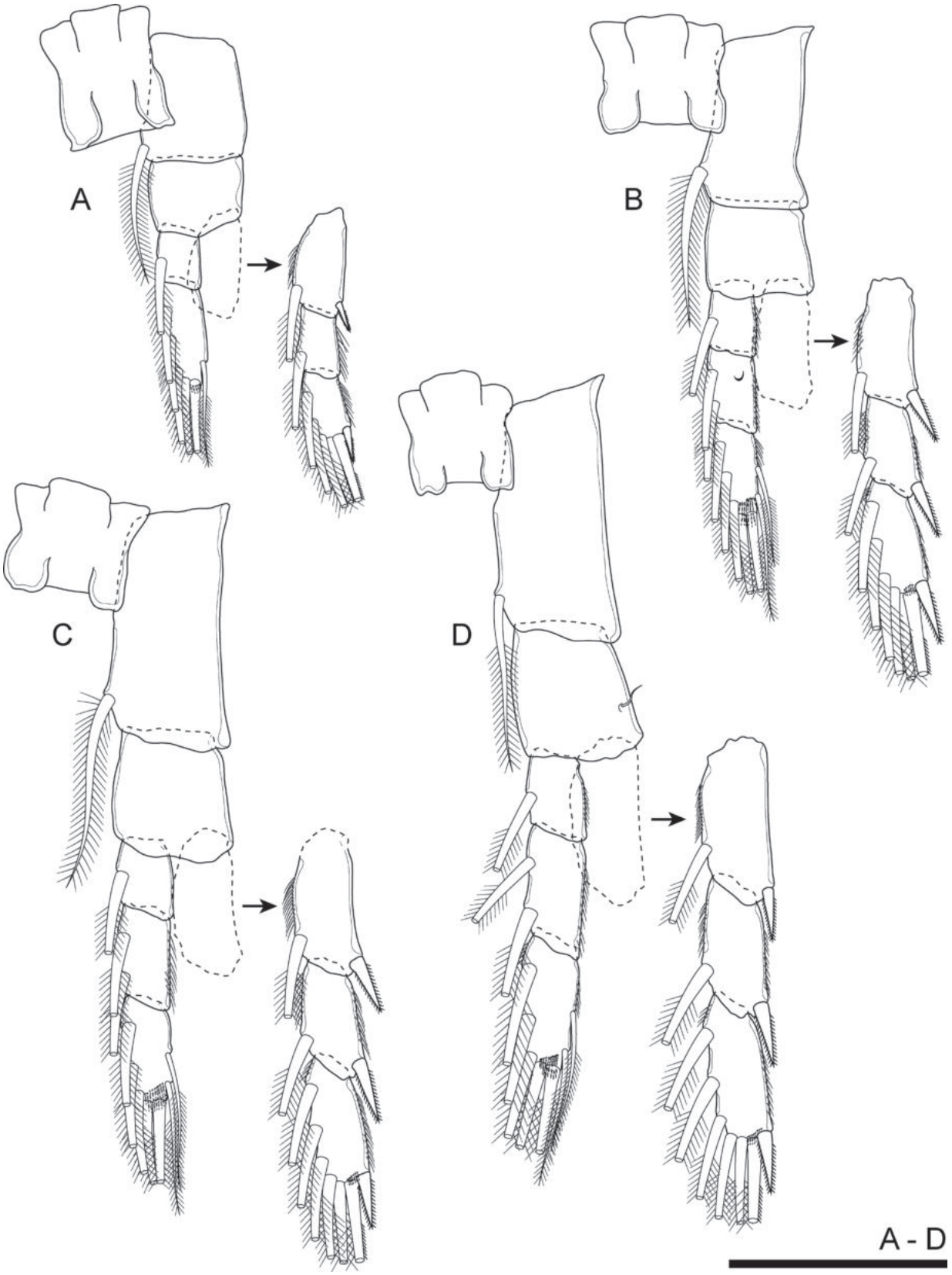

Figure 5. *Tropodiaptomus pedecrassum* sp. nov., male holotype. **A.** P1; **B.** P2; **C.** P3; **D.** P4. Scale bar: 100 µm.

rows of outer spinules close to distal end in P2–P4, respectively. Armature formula of P1–P4 as in Table 1.

P5 (Figs 6A, 8A–D). Asymmetrical. ***Left leg*** (Figs 6A, 8A–D), reaching slightly beyond proximal margin of exp-2 of right P5. Coxa as long as wide, with spine inserted on outer lobe. Basis cylindrical, about 1.4 times as long as wide, with one distal outer smooth seta. Exopod flattened, about 1.7 times as long as wide, inner margin one lobe, the

serration gradually decreases in size from the proximal to distal end (Fig. 8C, arrowhead). Apex of exopod with usual 'finger-and-thumb' combination, 'finger' slim, and set with radiant, hair-like 'thumb' sphere, ventral surface of exopod with 2 hairy pads. Endopod 2-segmented with incomplete separation of segments (Fig. 8D, arrowhead), conical, reaching beyond middle of exp-1, rounded distally with two parallel rows of setules. ***Right leg*** (Figs 6A, 8A, B), coxa as long as wide, with spine inserted on outer lobe. Basis cylindrical, about 1.3 times as long as wide, four structures occurring on dorsal surface: (i) one round process on proximal third close to inner margin, (ii) one triangular process in middle close to inner margin, (iii) one longitudinal hyaline lamella inserted near inner margin, and (iv) one distal outer smooth seta. Exopod 2-segmented. Exp-1 small, about 0.6 times as long as wide, with triangular lobe on inner margin, distal outer corner produced into acute spinous process, nearly as long as its segment. Exp-2 rhomboid, about 2.7 times as long as wide, dorsal surface with one semicircular hyaline knob on proximal outer margin, one semicircular hyaline lamella on distal inner margin, and one triangular process in middle of segment (Figs 6A, 8A, B (arrowhead)), and distal end of segment with one round hyaline prominence inserted between end claw and lateral spine (Fig. 8A, B (arrowhead)). Lateral spine nearly straight, acutely pointed, about as long as exp-2, inserted on distal corner of exp-2, with spinules on its inner margin. End claw curved and gradually tapering to acuminate tip, about 2.6 times as long as exp-2, inner margin with spinules distally. Endopod 1-segmented, conical, reaching distal end of exp-1, distal end with two rows of setules.

Description of the adult female. ***Body*** (Figs 1E, 2B, 6B, 8E, F). Total body length about 1,626 µm (1.6 mm) (measured from anterior margin of rostrum to posterior margin of caudal rami). Prosome length about 2.6 times as long as urosome (including caudal rami). Fourth and fifth pedigers completely fused, fusion being indicated by indentation on each side (Figs 1E, 2B). Fifth pediger produced into asymmetrical posterolateral wings (right wing shorter than left wing), each distal end with posterior spine, and each wing with one dorsal spine on inner margin (right spine smaller than left spine) (Figs 1E, 2B). Dorsal surface of fifth pediger with prominence (Figs 2B (grey ellipse), 8E (arrowhead)). Urosome2-segmented. Genital double-somite asymmetrical, about 1.8 times as long as wide, both sides of anterior part swollen (Fig. 2B (arrowhead)), with two unequal dorsolateral spines (right spine smaller than left spine) in anterior third (Figs 1E, 2B, 8F). Right distal corner of genital double-somite one triangular-like lobe (Figs 2B (arrowhead), 8F (arrowhead)). Genital area on ventral surface shows opercular pad protecting gonopores, characterised by rectangular and semicircular expansions (Fig. 6B). Anal somite about 1.6 times as long as wide (Figs 1E, 2B, 8F). Caudal rami parallel (Figs 1E, 2B, 8F), symmetrical, about 1.9 times as long as wide, with setules on outer and inner margins (Figs 1E, 2B, 8F (arrowhead)). Each ramus with six setae.

A1, A2, mandible, maxillule, maxilla, maxilliped, P1–P4 and rostrum (not shown) same as male.

P5 (Figs 6C, 8G–I). Symmetrical. Coxal spine on posterior lobe on caudal surface. Basis with one smooth outer seta on distolateral margin. Exopod 3-segmented. Exp-1 cylindrical, length about 2.2 time as long as wide. Exp-2 tapering into long claw, each side with one row of spinules starting in middle of segment. Exp-3 fused with exp-2 (Figs 6C (arrowhead), 8I (arrowhead)), with two unequal spines; inner spine about 3.6 times as long as outer spine, and with short spine laterally. Endopod 1-segmented, cylindrical, length about 0.6 time as long as exp-1, two unequal strong smooth spiniform setae distally (Figs 6C, 8G, H (arrowhead)), outer seta longer than inner seta, two parallel rows of spinules on distal end.

Variability. Morphological variability has been observed in: (i) the total body length (except of caudal setae) which ranged from 1,145–1,380 µm (mean 1,283 µm, n = 6) in the adult males and 1,520–1,626 µm (mean 1,575 µm, n = 5) in the adult females; (ii) the length of the spinous process on antepenultimate segment of the adult male right A1 is 3/4 to equal of segment 21 (Fig. 7A–G; see Table 2 in Saetang et al. 2022); (iii) segment 13 of the adult male right antennule with one hyaline knob (Fig. 3E (arrowhead)); and (iv) the number of setae on segment 13 of the adult male left A1 has one seta (n = 10) or two setae (n = 2) (Fig. 1D (arrowhead); see Table 2 in Saetang et al. 2022)

Etymology. The specific name '*pedecrassum*' is derived from the chubby shape of the adult male P5 that is clearly different from the more rectangular shape in other species of the genus.

Co-occurring species. In our samples, the new taxon co-occurred with one other copepod species, *Mongolodiaptomus botulifer* (Kiefer, 1974).

Distribution and ecology. *Tropodiaptomus pedecrassum* sp. nov. was found only in its type locality so far. It was recorded in two out of 471 samples collected from 206 freshwater habitats throughout Thailand between September 2017 and July 2019. Water temperature 19.6 °C, conductivity 620 µs cm-1, salinity

Table 1. Armature formula of P1–P4 in *T. pedecrassum* sp. nov. and *T. longiprocessus* sp. nov. (Arabic numerals representing setae and Roman numerals representing spine from outer-inner or outer-apical-inner margins).

Swimming legs	Coxa	Basis	Exp			Enp		
			1	2	3	1	2	3
P1	0–1	0–0	I–1	0–1	I,3,2	0–1	1,2,3	–
P2	0–1	0–0	I–1	I–1	I,3,3	0–1	0–2	2,2,3
P3	0–1	0–0	I–1	I–1	I,3,3	0–1	0–2	2,2,3
P4	0–1	1–0	I–1	I–1	I,3,3	0–1	0–2	2,2,3

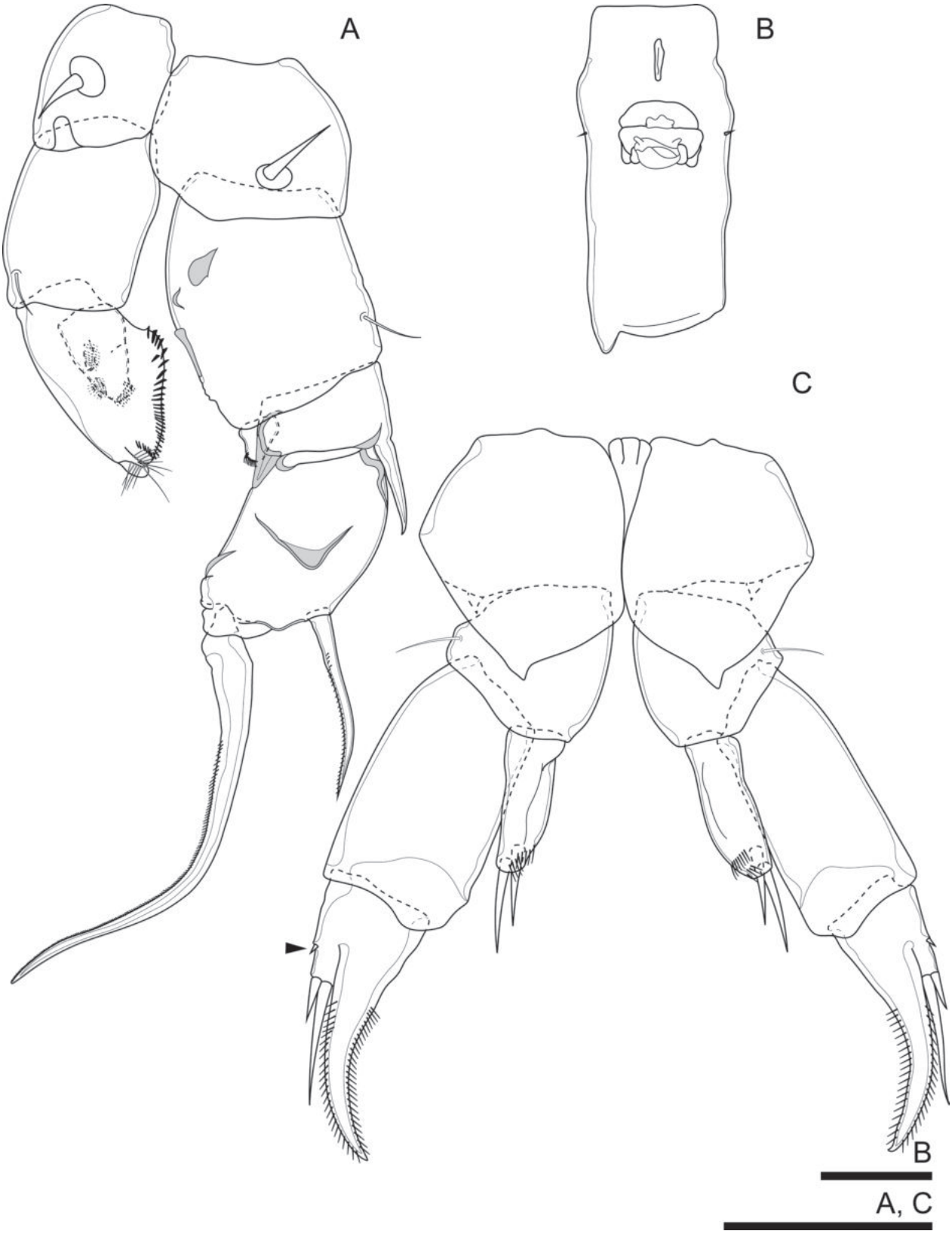

Figure 6. *Tropodiaptomus pedecrassum* sp. nov., male holotype. **A.** P5, dorsal view; *Tropodiaptomus pedecrassum* sp. nov., female allotype; **B.** genital double-somite, ventral view; **C.** P5, dorsal view (arrowhead indicates exp-3). Scale bars: 100 μm.

0.3 ppt, total dissolved solids 450 mg L-1, dissolved oxygen 3.3 mg L-1, pH 7.1, and water depth 30–40 cm, substrate with mud.

Differential diagnosis. *Tropodiaptomus pedecrassum* sp. nov. is confirmed to belong to the genus *Tropodiaptomus* based on the combination of characteristics men-

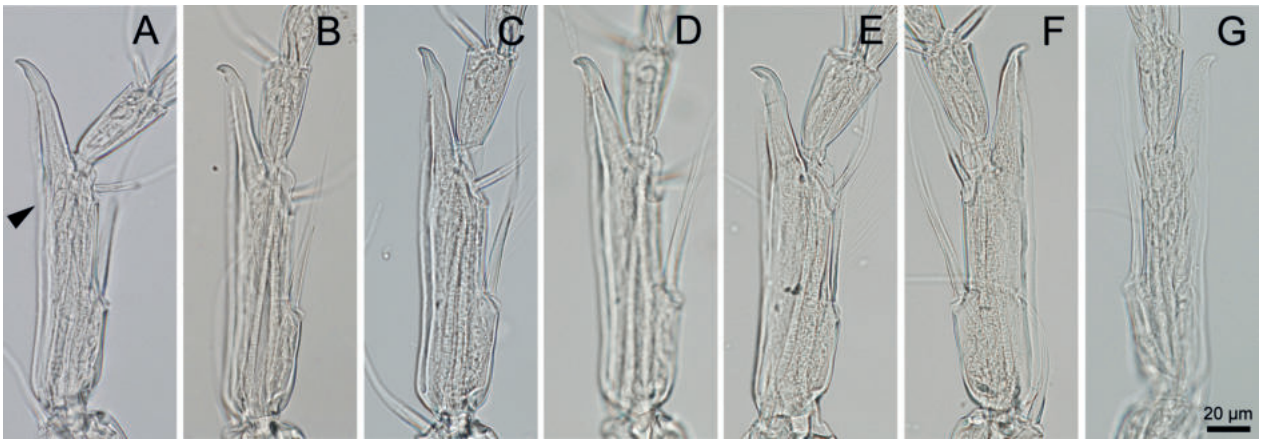

Figure 7. *Tropodiaptomus pedecrassum* sp. nov.; morphological variation of antepenultimate segment of the male right antennule (arrowhead indicates longitudinal hyaline membrane).

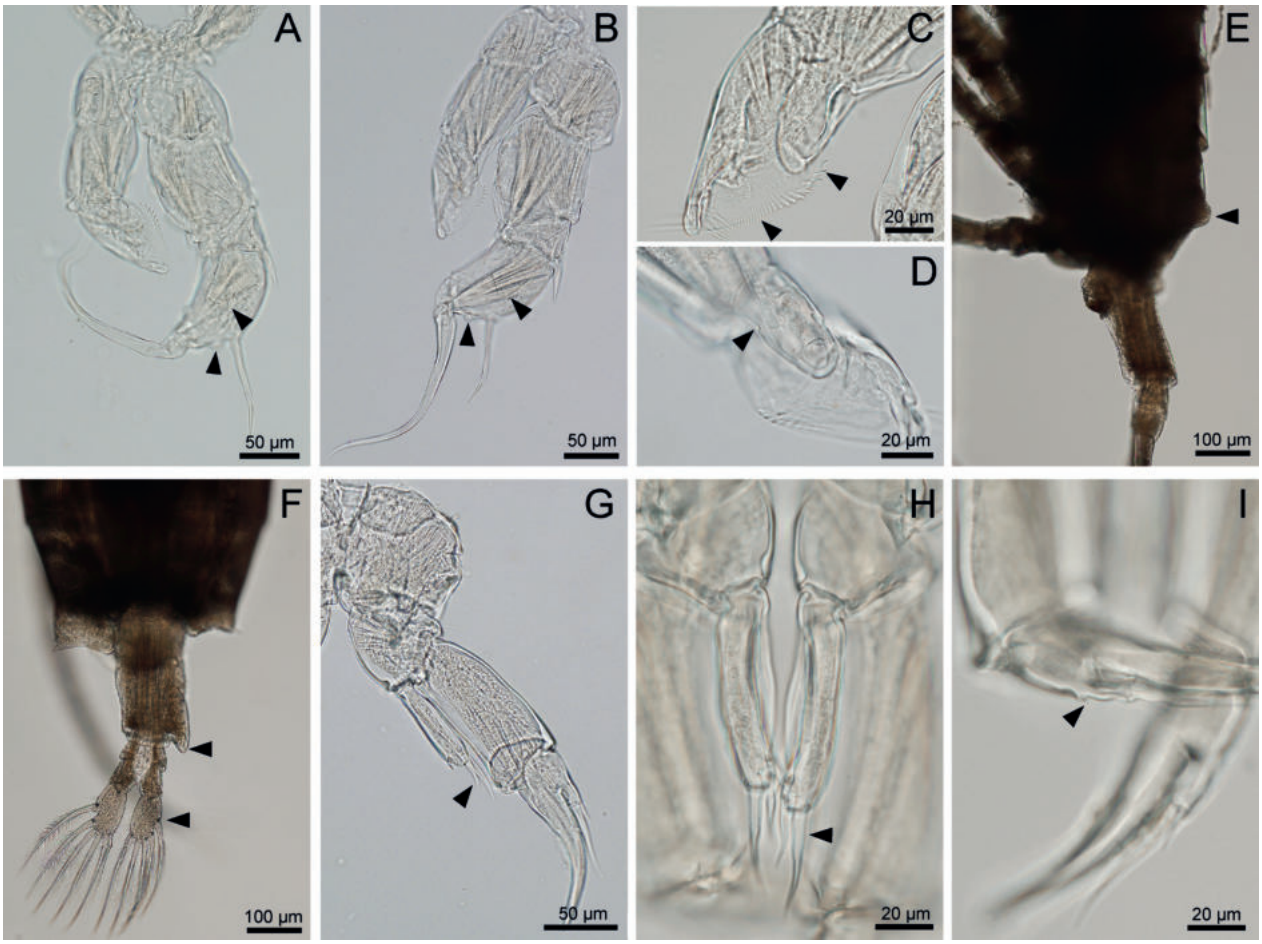

Figure 8. *Tropodiaptomus pedecrassum* sp. nov., male. **A, B.** P5, dorsal view; **c, d.** Exopodal and endopodal segment of left P5; female. **E.** Pediger 5 and urosome, lateral view; **F.** Pediger 5 and urosome, dorsal view; **g.** P5, dorsal view; **h.** Endopod of P5; **i.** Exp-2 and exp-3 of P5. Arrowheads show structures discussed in the description.

tioned by Lai and Fernando (1979a, 1979b), Sanoamuang (2002), Saetang et al. (2020): (i) the process on the antepenultimate segment of the adult male right antennule is always smooth; (ii) the exopod of the adult male left P5 fused into a single flattened piece and its inner margin is denticulate or serrate; (iii) the inner margin on the basis of the adult male right P5 has a hyaline lobe; (iv) the urosome of the adult female comprises two somites; and (v) the endopod segment of the adult female P5 has slender setae at the distal end.

This species differs from the congeneric species by the following characters: (i) antepenultimate segment of the male right antennule with straight spinous process reaching 3/4 or equal of next segment; (ii) inner margin of

Table 2. Comparison of four morphologically similar species of *Tropodiaptomus* (after Kiefer 1930; 1982 and this study).

Morphological characters	*T. pedecrassum* sp. nov.	*T. longiprocessus* sp. nov.	*T. hebereri*	*T. lanaonus*
The adult male				
Body length, except caudal satae (μm)	1,145–1,380	1,490–1,545	1,350–1,400	1,120–1,150
Right A1: segment-16 with spinous process	Yes	Yes	No	No
Right A1: relative length of the spinous process of segment 20	3/4 of or equal to segment 21	Longer than segment 21	1/2 of segment 21	Longer than segment 21
Left A1: number of setae on segment-13	1 or 2	1	1	1
Right P5: basis, supplementary process and surface structures	One round process, one semicircular process and one longitudinal hyaline lamella	One triangular process and one longitudinal hyaline lamella	One triangular process, one semicircular process and one semicircular hyaline lamella	One triangular process and one longitudinal hyaline lamella
Right P5: exp-1, length of spinous process on outer distal margin/ segment length	Equal	Shorter	Shorter	Shorter
Right P5: exp-2, shape	Rhomboid	Rectangular	Trapezoidal	Rectangular
Right P5: exp-2, supplementary process	Triangular-shape process, large	Large and long process	Triangular process	Semicircular process
Right P5: lateral spine of the exp-2	Short	Long	Short	Long
Right P5: exp-2, one round hyaline prominence inserted between end claw and lateral spine	Present	Absent	Present	Absent
Right P5: length of enp vs exp-1 length	Shorter	Longer	Longer	Longer
Left P5: exp, inner margin	1 lobe, the serration gradually decreasing in size from proximal to distal end	2 lobes, shallow, uniform serration	1 lobe, the serrate of the proximal part larger than the distal part	2 lobes, shallow, uniform serration
Left P5: enp (number of segment)	2 (yet incompletely separated)	2	1	2
Left P5: length of finger vs thumb length	Equal	Equal	3/4	Equal
The adult female				
Body length, except caudal satae (μm)	1,520–1,626	1,570–1,700	1,500–1,600	1,200–1,250
Fifth pediger: lateral wings	Asymmetrical	Asymmetrical	Asymmetrical	Symmetrical
Fifth pediger: dorsal prominence	Present	Absent	Present	Absent
Genital double-somite	Asymmetrical, dilate on proximal both sides	Asymmetrical, dilate on proximal right side	Asymmetrical, dilate on proximal both sides	Symmetrical
Genital double-somite: outer distal corner with lobe	Triangular lobe	Absent	Large round lobe	Small round lobe
Caudal rami: outer margin with setules	Present	Present	Absent	Present
P5: exp-3 fused with exp-2	Yes	Yes	No	No data
P5: end claw, outer margin with setules	Present	Present	Present	No data
P5: enp, elements on distal end	Spiniform smooth setae	Spiniform smooth setae	Slender smooth seta	Slender smooth seta

exopodal segment of the male left P5 with single lobe and the serration gradually decreases in size from the proximal to distal end; (iii) basis of the male right P5 with two processes and one longitudinal hyaline lamella; (iv) exp-1 of the male right P5 with triangular lobe on inner margin, distal outer corner produced into acute spinous process, length about as long as its segment; and (v) exp-2 of the male right P5 with rhomboid shape, dorsal surface with one semicircular hyaline knob on proximal outer margin, one semicircular hyaline lamella on distal inner margin, and one triangular process in middle of segment.

According to the identification key given by Saetang et al. (2020), *Tropodiaptomus pedecrassum* sp. nov. is most similar to *T. hebereri*. However, it distinctly differs from *T. hebereri* in the following characters: (i) inner margin of the basis of the adult male right P5 has one round process, one semicircular process, and one longitudinal hyaline lamella; (ii) length of spinous process of the outer corner of exp-1 of the adult male right P5 is as long as exp-1; (iii) inner margin of the exopod of the adult male left P5 has one lobe, and the serration gradually decreases in size from the proximal to the distal end; (iv) dorsal surface of exp-2 of the adult male right P5 has one semicircular hyaline knob, one semi-circular hyaline lamella, and one triangular process; and (v) caudal rami of the adult female have outer and inner setules (Table 2).

Tropodiaptomus longiprocessus sp. nov.

https://zoobank.org/F33BE672-BC19-4644-8477-D4C6F817D397

Type locality. Nong Ping swamp (NP2), Thong Phaphum district, Kanchanaburi province, western Thailand (14°38'49.1"N, 98°33'48.8"E). Temporary habitat without macrophytes.

Other localities. Nong Ping swamp (NP3) Thong Phaphum District, Kanchanaburi Province, Western Thailand (14°39'00.4"N, 98°34'33.7"E). Temporary habitat without macrophytes.

Material examined. ***Holotype.*** Adult male, dissected and mounted onto one slide, Thong Phaphum District, Kanchanaburi province, western Thailand (14°38'49.1"N, 98°33'48.8"E), 22 June 2019, Thanida Saetang and Supiyanit Maiphae; PSUZC-PK2009-01. ***Allotype.*** One adult female, collected with holotype; PSUZC-PK2009-02.

***Paratype*.** One adult male, collected with holotype; PSU-ZC-PK2009-03.

Description of the adult male. ***Body*** (Fig. 9A, B). Total body length about 1,500 µm (measured from anterior margin of rostrum to posterior margin of caudal rami). Prosome length about 2.4 times as long as urosome (including caudal rami). Fourth and fifth pedigers separated by distinct septum. Fifth pediger produced into small symmetrical posterolateral wings, each distal end with spine. Urosome 5-segmented. Genital somite with dorsolateral sensillum on right side, fourth somite with expanded right corner. Anal somite with deep cleft, length as long as wide. Caudal rami parallel, symmetrical, length about 1.9 times as long as wide, with setules on inner margin. Each ramus with six setae.

Rostrum (Fig. 9C). Two rostral elements on anterior margin with suture in the middle.

A1 (Figs 10A–C, 11A, B, 16H). Asymmetrical. ***Left A1*** non-geniculate, 25-segmented, reaching beyond the end of caudal rami. Armature formula of each segment as follows: 1+ae, 3+ae, 1+ae, 1, 1+ae, 1, 1+ae, 1+s, 2+ae, 1, 1, 1+ae+s, 1, 1+ae, 1, 1+ae, 1, 1, 1+ae, 1, 1, 2, 2, 2, 5+ae. ***Right A1*** transformed and geniculate, 22-segmented. Strongly dilated between segment 13 and segment 18. Spinous process on segment 20 (antepenultimate) straight and bent at distal end, reaching longer than next segment, and with longitudinal hyaline membrane on outer margin (Fig. 10D). Armature formula of each segment as follows: 1+ae, 3+ae, 1+ae, 1, 1+ae, 1, 1+ae, 1 +s, 2+ae, 1+sp, 1+sp, 1+ae+s, 1+ae+sp, 2+ae, 2+ae+sp, 2+ae+sp, 1+s, s, 1+3s, 4+sp, 2, 5+ae.

A2 (Fig. 9D). Coxa with one inner seta on distal corner. Basis with two inner setae on distal corner. Exopod 7-segmented, exp-1–6 with 1, 3, 1, 1, 1, and 1 inner setae, respectively, and exp-7 with one inner and three apical setae. Endopod 2-segmented, enp-1 with two inner setae and one longitudinal row of outer spinules, enp-2 with nine inner and seven apical setae; and one group of outer spinules.

Mandible (Fig. 12A). Coxa with eight strongly chitinised teeth and one seta on gnathobase. Basis with four inner setae. Exopod 4-segmented with 1, 1, 1, and 3 setae, respectively. Endopod 2-segmented, enp-1 with four inner setae, enp-2 with nine apical setae and three horizontal rows of outer spinules.

Maxillule (Fig. 12B–E). Precoxal arthrite with three plumose setae and twelve bipinnate spines. Coxal endite with four plumose setae, and coxal epipodite with seven plumose setae and two bipinnate spines. Basis with two endites; the proximal with four plumose setae and the distal with eight plumose setae, and basal exite with one bipinnate spine. Exopod 1-segmented with six plumose setae, one longitudinal row of inner setules. Endopod 1-segmented with four plumose setae and one horizontal row of outer setules.

Maxilla (Fig. 12F). Proximal praecoxal endite with six setae, distal praecoxal endite with three setae. Proximal and distal coxal endites with three setae each. Allobasis protruding into endite with four setae. Endopod reduced to two segments, each with three setae.

Maxilliped (Fig. 12G). Praecoxa completely fused to coxa; endites with 1, 2, 3, and 3 setae, respectively. Distal corner of coxa produced into rounded lobe with spinules on inner margin. Basis with three setae in distal third, one row of setules and one row of spinules in proximal half. Endopod 6-segmented; with 2, 3, 2, 2, 1+1, and 4 setae, respectively.

P1–P4 (Figs 13A–D, 16I). Biramous. Intercoxal sclerite naked. Coxa with one inner seta. Basis without seta except P4 with one seta on outer distal margin. P1 with 3-segmented exopod and 2-segmented endopod, P2–P4 with 3-segmented exopod and endopod, endopod reaching proximal of exp-3. P1 (Figs 13A, 16I). Basis with lateral setules close to outer margin. Exp-2, exp-3, enp-1 and enp-2 with one longitudinal row of outer setules. Exp-3 and enp-2 with one row of spinules close to distal end. P2–P4 (Fig. 13B–D). Exp-1 with one longitudinal row of inner setules. Exp-2 and exp-3 with one longitudinal row of outer and inner setules in P2 and P4, and one longitudinal row of inner setules in P3. Enp-1 with one longitudinal row of outer setules in P3 and P4. Enp-2 and enp-3 with one longitudinal row of outer setules in P2, one longitudinal row of outer and inner setules in P3 and P4, enp-2 of P2 with Schmeil's organ. Exp-3 and enp-3 with one and two rows of outer spinules close to distal end in P2–P4, respectively. Armature formula of P1–P4 as same as *Tropodiaptomus pedecrassum* sp. nov. (Table 1).

P5 (Figs 14A, E, 16A, E). Asymmetrical. ***Left leg***, reaching beyond middle of exp-2 of right P5. Coxa as long as wide, with spine inserted on outer lobe. Basis cylindrical, about 1.9 times as long as wide, with one distal outer smooth seta. Exopod flattened, about 2.2 times as long as wide, inner margin two lobes with uniform serration (Figs 14A, 16A, E). Apex of exopod with usual 'finger-and-thumb' combination, 'finger' slim, and set with radiant, hair-like 'thumb' sphere, ventral surface of exopod with two hairy pads. Endopod 2-segmented (Fig. 16G), conical, reaching beyond middle of exp-1, rounded distally with two parallel rows of setules. ***Right leg***, coxa as long as wide, with spine inserted on outer lobe. Basis cylindrical, about 1.7 times as long as wide, three structures occurring on dorsal surface: (i) one triangular process in proximal third close to inner margin, (ii) one longitudinal hyaline lamella inserted near inner margin in middle, and (iii) one laterodistal smooth seta. Exopod 2-segmented. Exp-1 small, about 0.5 times as long as wide, with triangular lobe on inner margin, laterodistal corner produced into acute spinous process. Exp-2 rectangular, about 1.5 times as long as wide, dorsal surface with two longitudinal hyaline lamellae in middle and distal inner margin and one large and long process in middle near outer margin. Lateral spine nearly straight, acutely pointed, about 1.3 times as long as exp-2, inserted in laterodistal corner of exp-2, with spinules on its inner margin. End claw curved and gradually tapering to acuminate tip, about 2.5 times

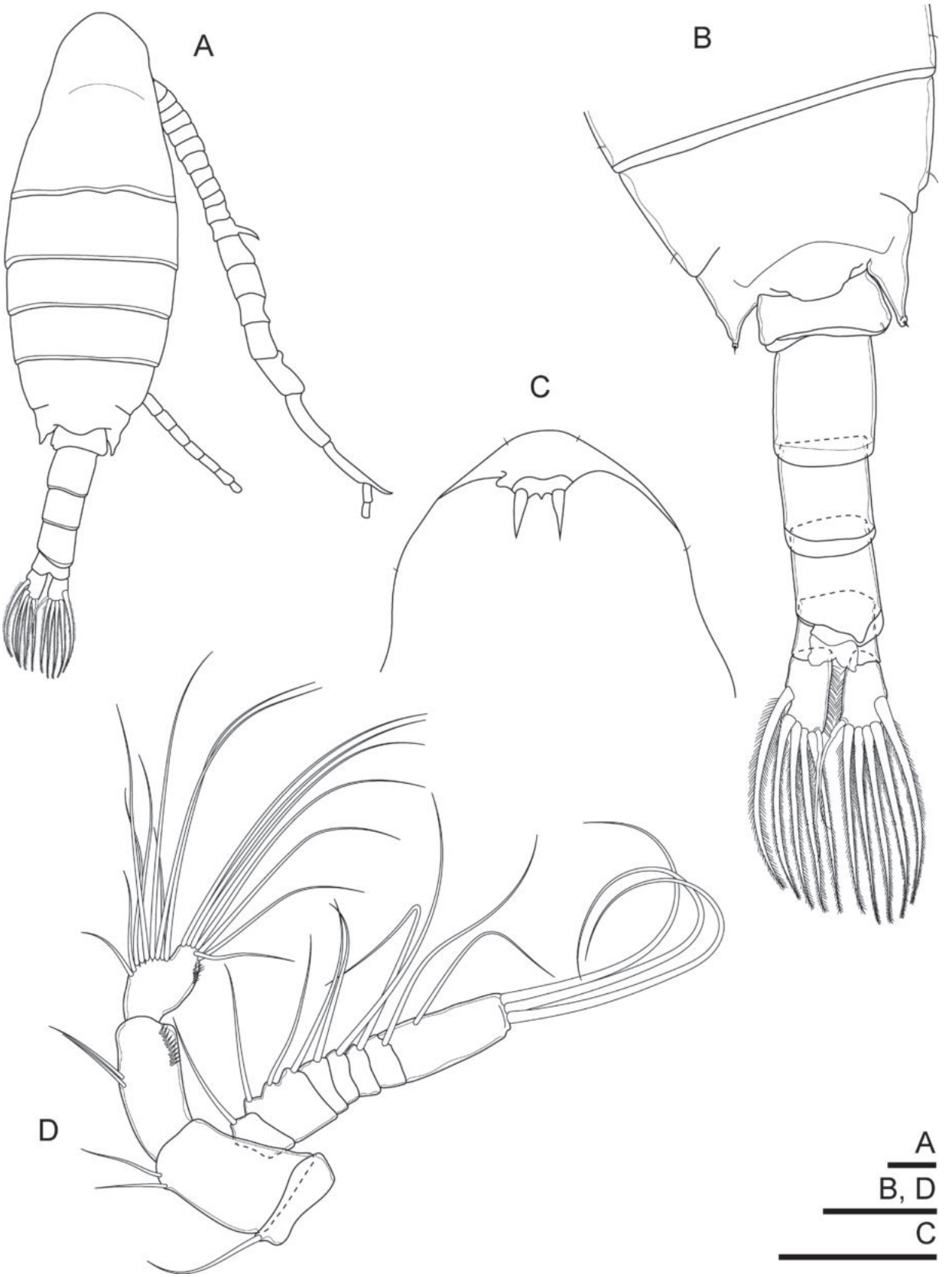

Figure 9. *Tropodiaptomus longiprocessus* sp. nov., male holotype. **A.** habitus, dorsal view; **B.** pediger 5 and urosome, dorsal view; **C.** rostrum; **D.** antenna. Scale bars: 100 μm.

as long as exp-2, inner margin with spinules distally. Endopod 1-segmented, conical, reaching beyond proximal margin of exp-2, distal end with two rows of setules.

Description of the adult female. ***Body*** (Figs 15A–C, 16J, K). Total body length about 1,640 μm (1.6 mm) (measured from anterior margin of rostrum to posterior

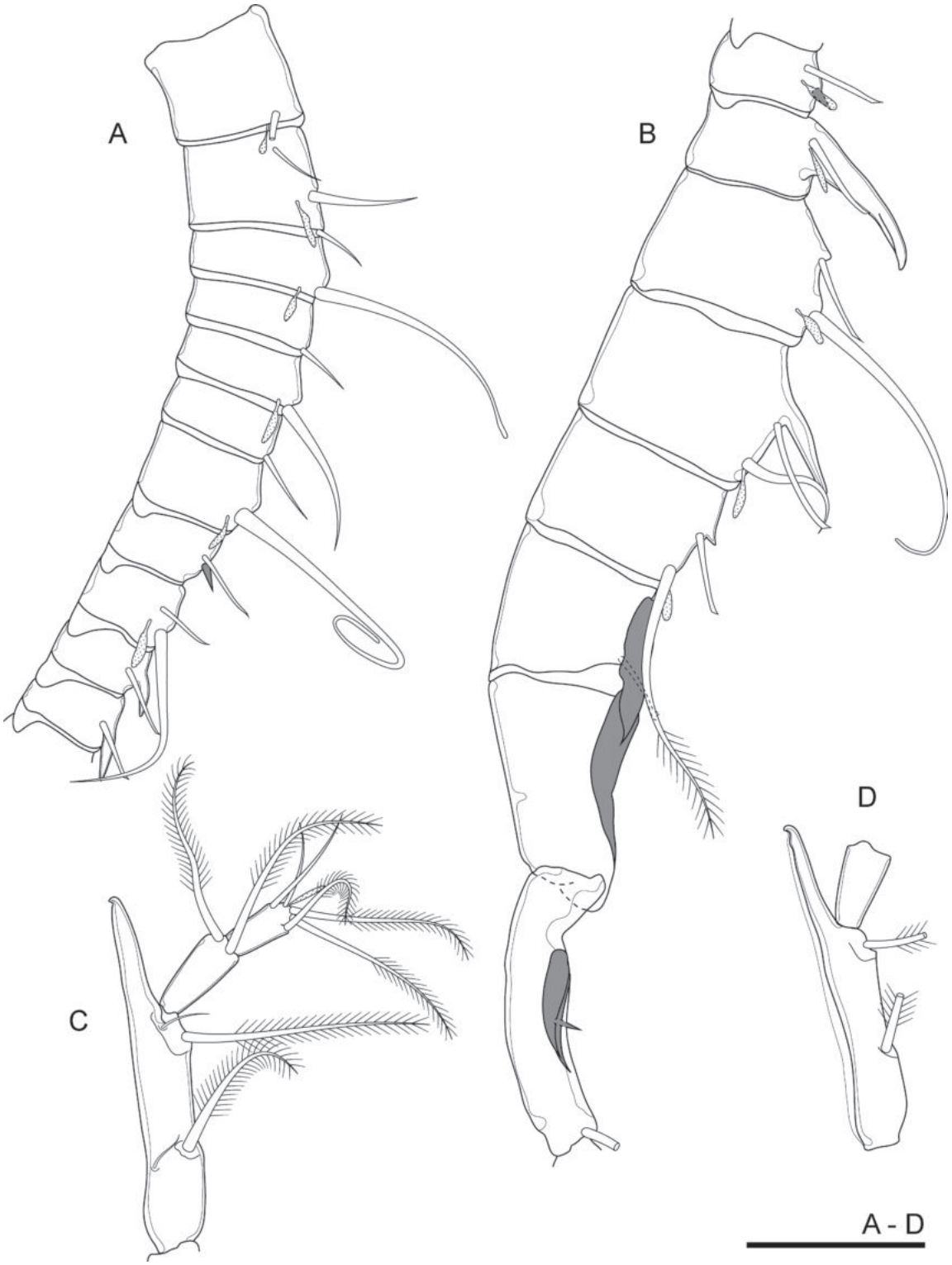

Figure 10. *Tropodiaptomus longiprocessus* sp. nov., male holotype. **A.** Segment 1–11 of right antennule; **B.** Segment 12–19 of right antennule (gray color indicates spine); **C.** Segment 20–22 of right antennule; **D.** Segment 20 and 21 of right antennule of the adult male specimen from the same population of holotype. Scale bar: 100 μm.

margin of caudal rami). Prosome length about 3.1 times as long as urosome (including caudal rami). Fourth and fifth pedigers completely fused, fusion being indicated by indentation on each side. Fifth pediger produced into asymmetrical posterolateral wings (right wing shorter than left wing), each distal end with posterior spine, and each wing with one dorsal spine on inner margin (right spine smaller than left spine) (Fig. 16K). Dorsal surface of fifth pediger without prominence (Fig. 16J). Urosome 2-segmented. Genital double-somite asymmetrical, about twice times as long as wide, right sides of anterior part swollen (Figs 15B (arrowhead), 16K), with two

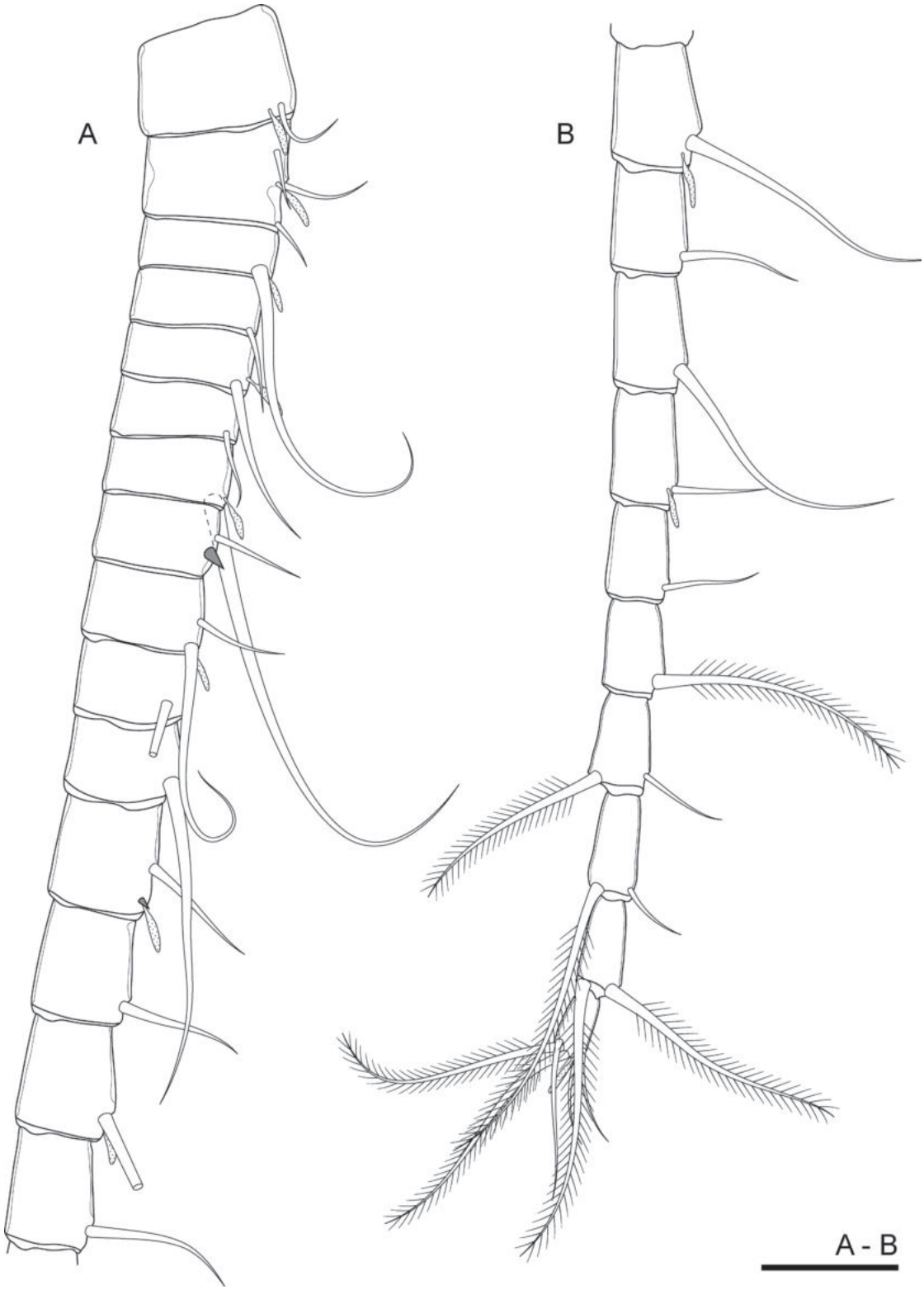

Figure 11. *Tropodiaptomus longiprocessus* sp. nov., male holotype. **A.** Left antennule, segment 1–15; **B.** Left antennule, segment 16–25 (gray color indicates spine). Scale bar: 100 µm.

unequal dorsolateral spines (right spine smaller than left spine) in anterior third (Fig. 15B). Right distal corner of genital double-somite without lobe (Figs 15B, 16K (arrowhead)). Genital area on ventral surface shows opercular pad protecting gonopores, characterised by rectangular and semicircular expansions (Fig. 15C). Anal somite about 1.2 times as long as wide. Caudal rami parallel, symmetrical, about 1.5 times as long as wide, with setules on outer and inner margins (Fig. 15B). Each ramus with six setae.

A1, A2, mandible, maxillule, maxilla, maxilliped, P1–P4 (not shown) and rostrum (Fig. 15D) same as male.

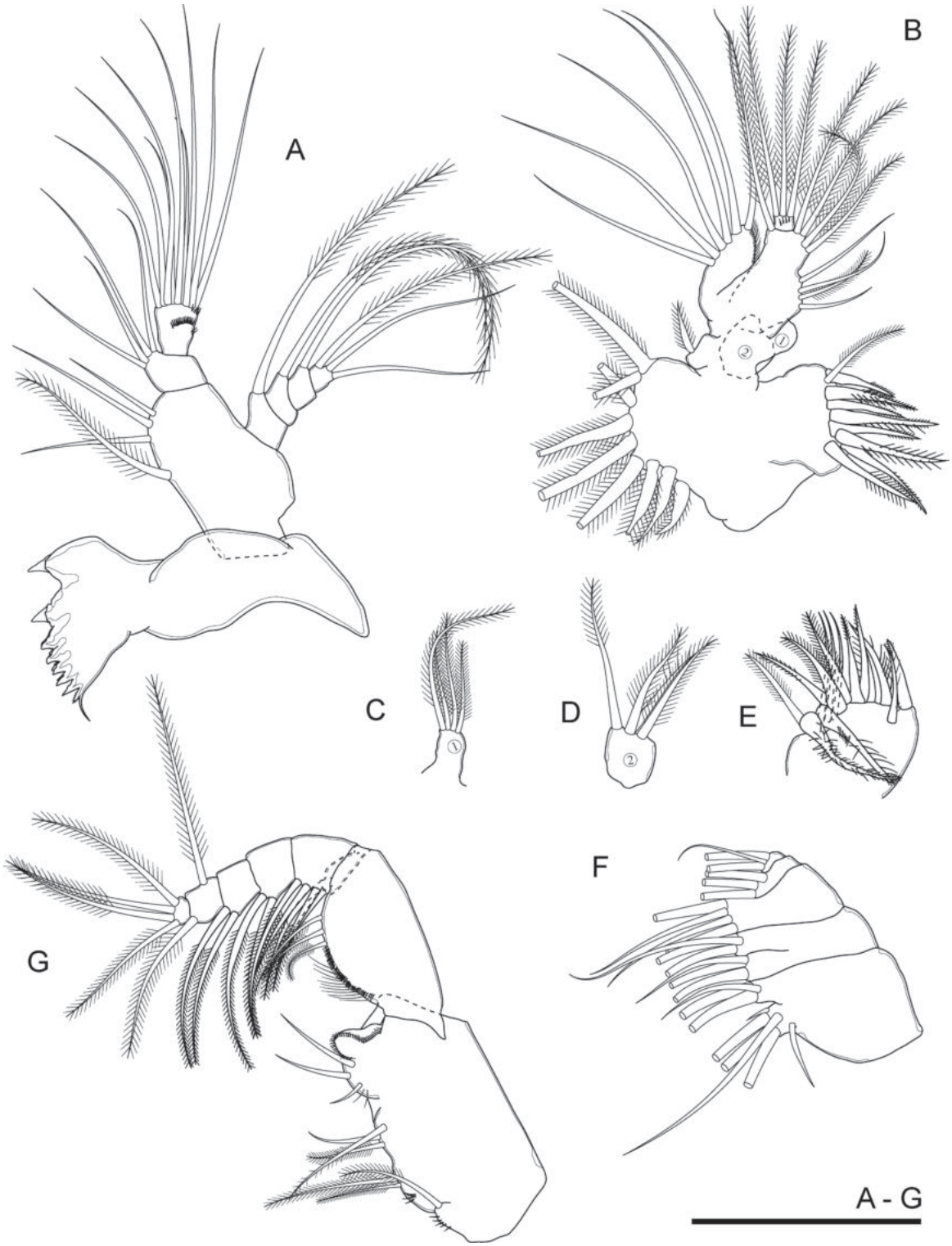

Figure 12. *Tropodiaptomus longiprocessus* sp. nov., male holotype. **A.** Mandible; **B.** Maxillule; **C–E.** Maxillule; **F.** Maxilla; **G.** Maxilliped. Scale bar: 100 μm.

P5 (Figs 14F, 16L). Symmetrical. Coxa spine on posterior lobe on caudal surface. Basis with one smooth outer seta on distolateral margin. Exopod 3-segmented. Exp-1 cylindrical, length about 1.9 time as long as wide. Exp-2 tapering into long claw, each side with one row of spinules starting in middle of segment. Exp-3 fused with exp-2 (Figs 14F, 16L (arrowhead)), with two unequal spines, inner spine about 4.9 times as long as outer spine, and with short spine laterally. Endopod 1-segmented, cylindrical, length about 0.7 time as long as exp-1, two strong smooth spiniform setae distally (Figs 14F, 16L (arrowhead)), outer seta longer than inner seta, two parallel rows of spinules on distal end.

Variability. Morphological variability has been observed in: (i) the total body length (except of cau-

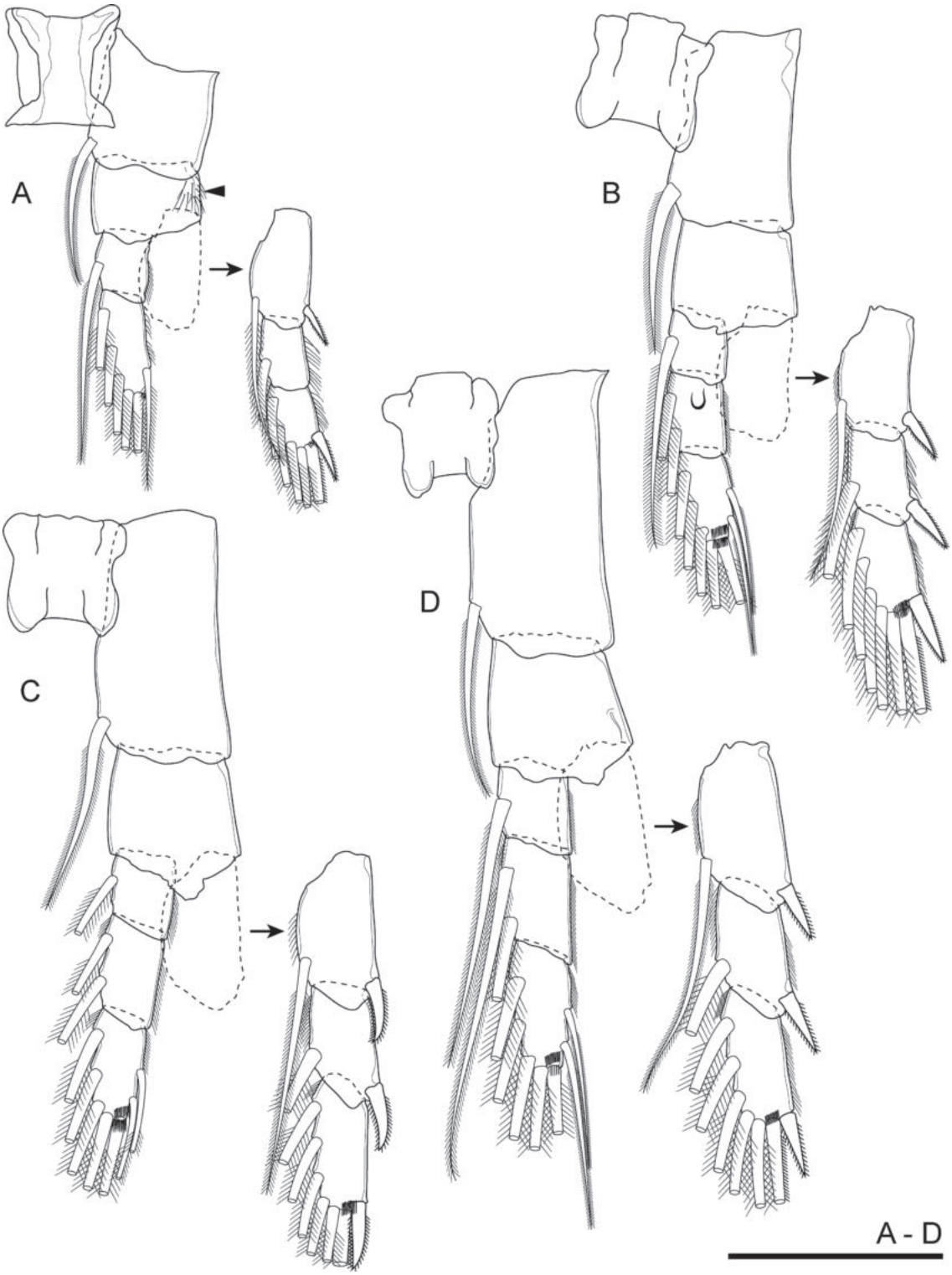

Figure 13. *Tropodiaptomus longiprocessus* sp. nov., male holotype. **A.** P1 (arrowhead indicates lateral setules close to outer margin); **B.** P2; **C.** P3; **D.** P4. Scale bar: 100 µm.

dal setae) which ranged from 1,490 –1,545 µm (mean 1,510 µm, n = 4) in the adult males and 1,570–1,700 µm (mean 1,646 µm, n = 6) in the adult females; and (ii) shape and length of large and long process on exp-2 of the adult male right P5 (Figs 14B–D, 16B–D). Moreover, it needs to be noted that the inner margin of exopod of the adult male left P5 appeared single lobe in positions other than dorsal which can lead to misidentification (Fig. 16F).

Etymology. The specific name '*longiprocessus*' is derived from the presence of a long process on exp-2 of the right P5 in the adult male.

Co-occurring species. There were no other diaptomid copepods in these samples.

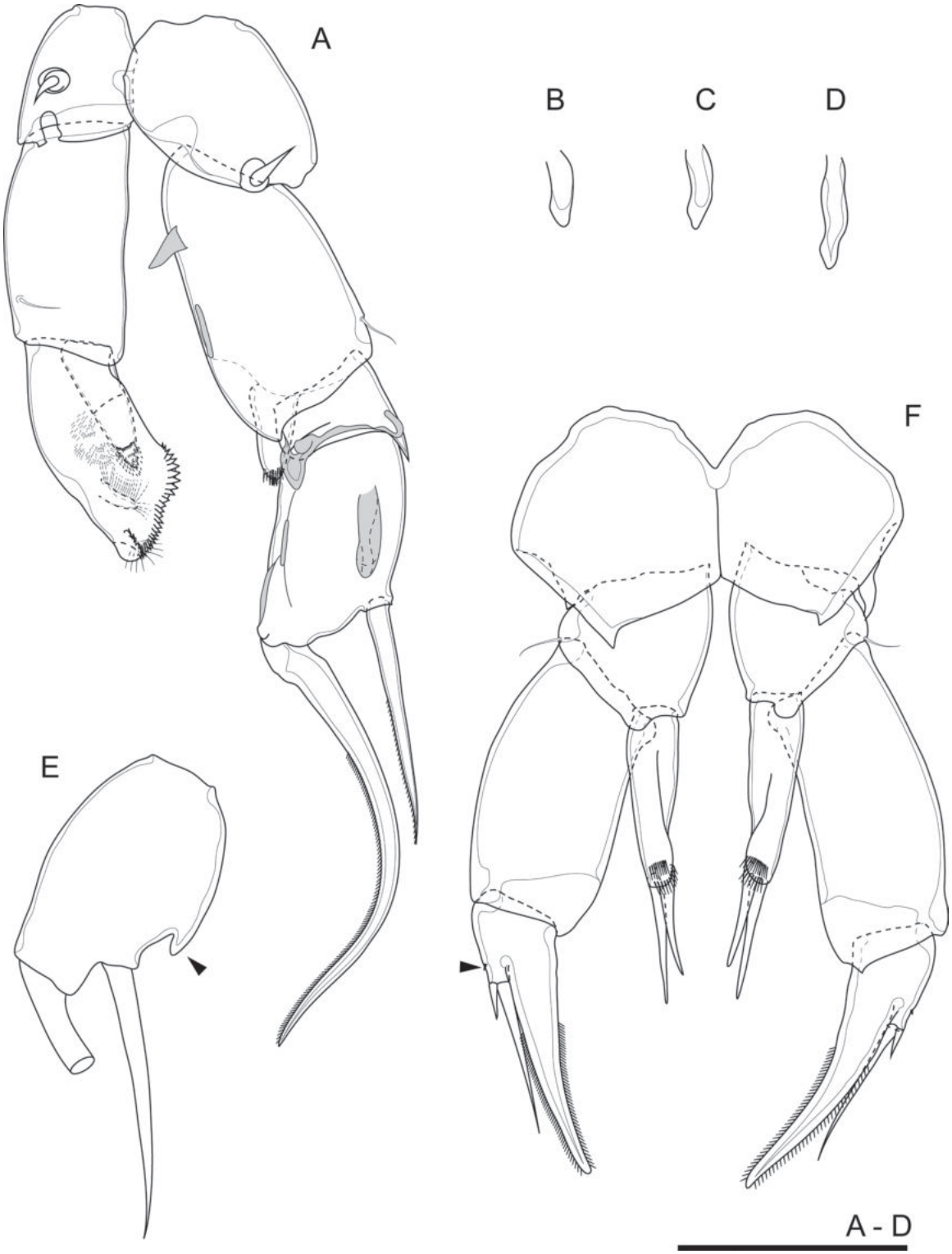

Figure 14. *Tropodiaptomus longiprocessus* sp. nov., male holotype. **A.** P5, dorsal view; **B–D.** Shape variation of hyaline lamella on exp-2 of right P5 in adult male, dorsal surface; **E.** Exp-2 of right P5 of the adult male specimen from the same population of holotype, lateral view (arrowhead indicates hyaline lamella); *Tropodiaptomus longiprocessus* sp. nov., female allotype: **F.** P5 (arrowhead indicates exp-3). Scale bar: 100 µm.

Distribution and ecology. *Tropodiaptomus longiprocessus* sp. nov. was found only in its type locality. It is rare because it was found only in two of 471 samples collected from 206 freshwater habitats throughout Thailand between September 2017 and July 2019. Water temperature 26.6–28.0 °C, conductivity 623.3–672.7 µs cm-1, salinity 0.3 ppt, total dissolved solids 385–424 mg L-1, dissolved oxygen 2.5–6.0 mg L-1, pH 7.2–7.3, and water depth 0.2–0.3 m, substrate with mud. However, in order to understand more in their habitat preference, the whole year samples are needed to be examined.

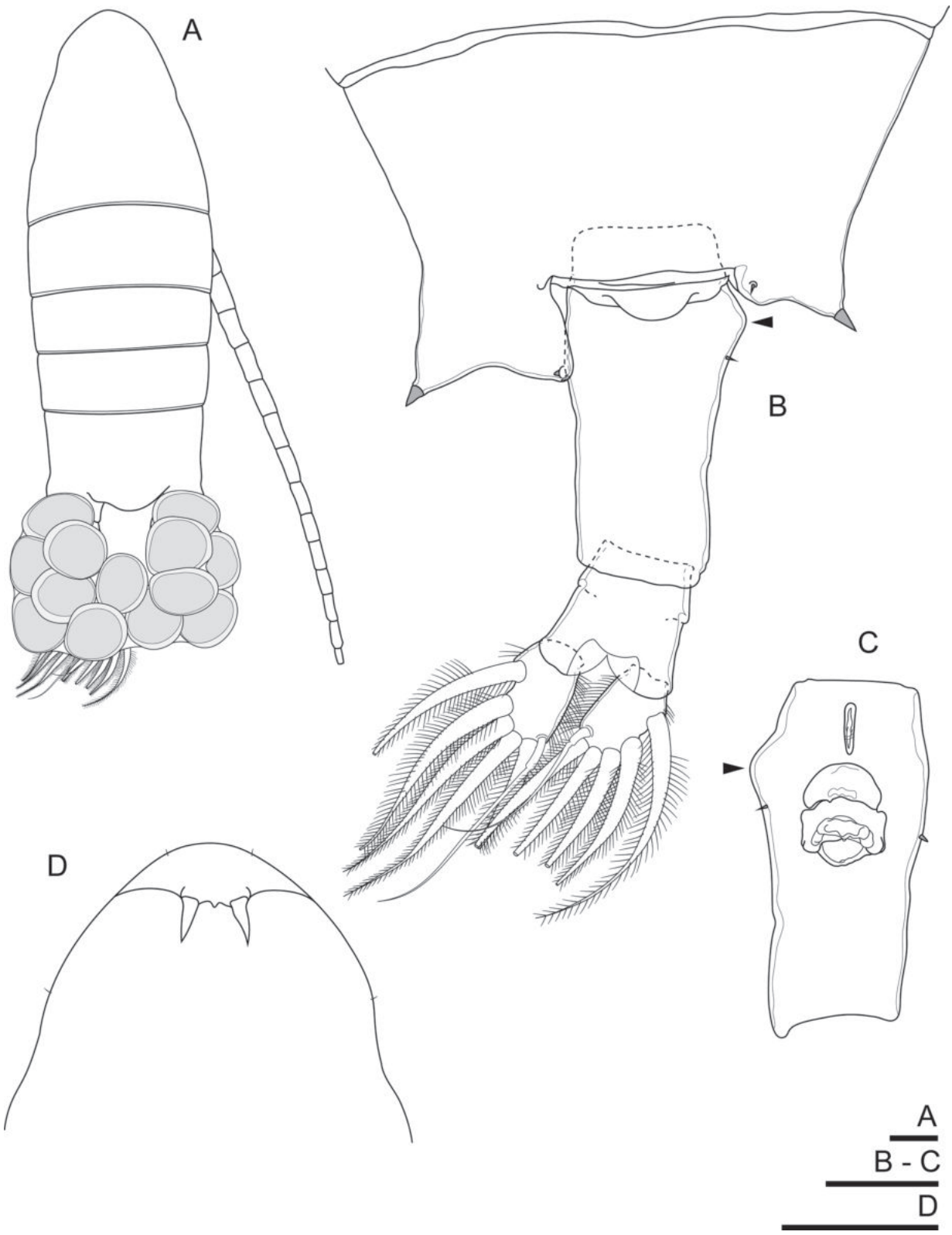

Figure 15. *Tropodiaptomus longiprocessus* sp. nov., female allotype. **A.** Habitus, dorsal view; **B.** Pediger 5 and urosome, dorsal view; **C.** Genital double-somite, ventral view; **D.** Rostrum. Scale bars: 100 μm.

Differential diagnosis. *Tropodiaptomus longiprocessus* sp. nov. differs from the congeneric species by the following respects: (i) antepenultimate segment of the male right antennule with straight spinous process reaching beyond the distal margin of next segment; (ii) inner margin of exopodal segment of the male left P5 with two lobes, and with uniform serration; (iii) basis of the male right P5 with one triangular process and one longitudinal hyaline lamella; (iv) exp-1 of the male right P5 with triangular lobe on inner margin, distal outer corner produced into acute spinous process; and (v) exp-2 of the male right P5 rectangular, dorsal surface with two longitudinal hyaline

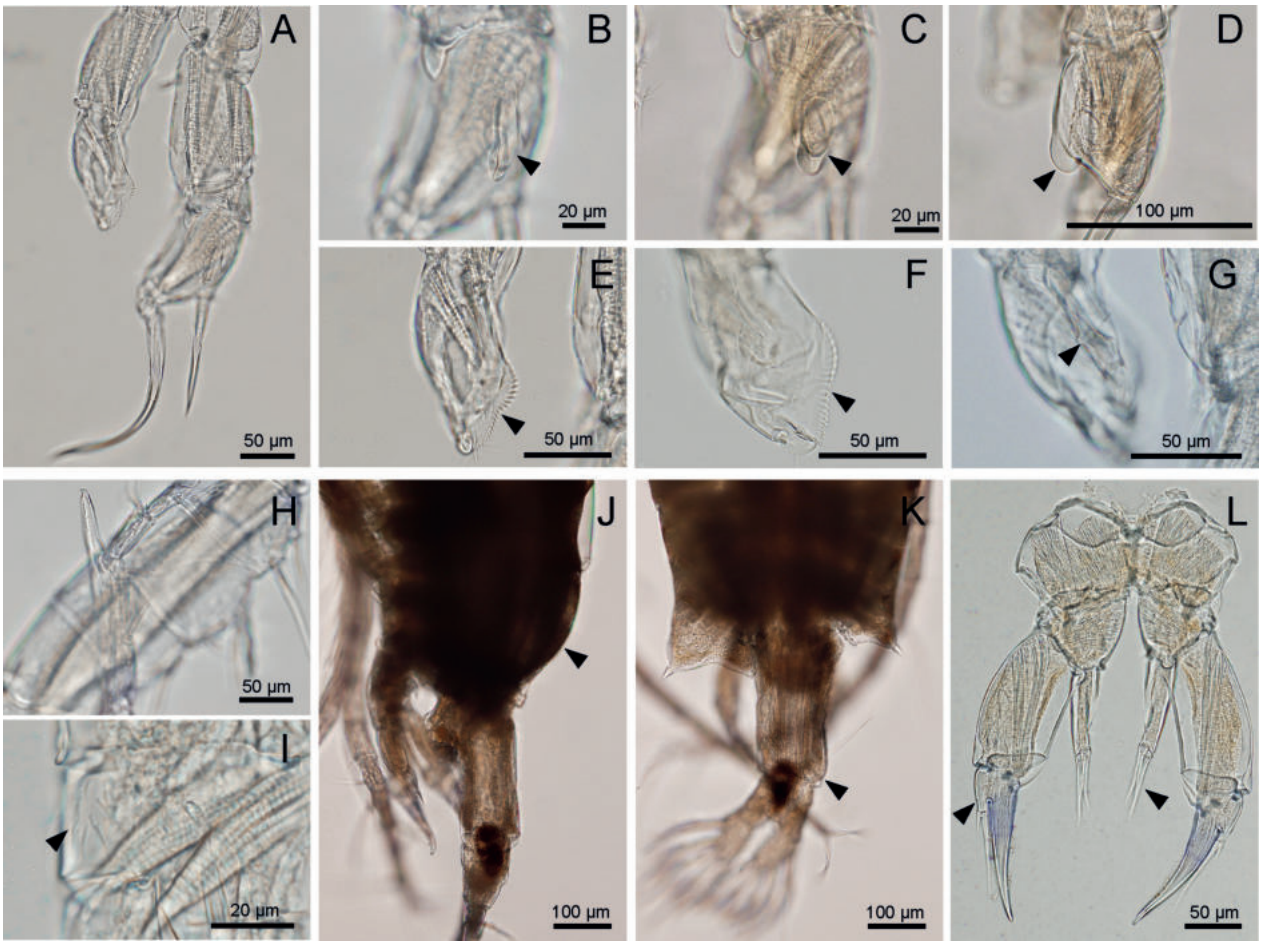

Figure 16. *Tropodiaptomus longiprocessus*sp. nov; male. **A.** P5, dorsal view; **B, C.** Hyaline lamella on exp-2 of right P5, dorsal surface; **D.** Hyaline lamella on exp-2 of right P5, lateral surface; **E, F.** Exopodal segment of the male left antennule,dorsal surface; **G.** Exopodal segment of the male left antennule,ventral surface; **H.** Antepenultimate segment of right antennule; **I.** Lateral part of P1 basis; female: **J.** Pediger 5 and urosome, lateral view; **K.** Pediger 5 and urosome, dorsal view; **L.** P5. Arrowheads show the characters discussed in the description.

lamellae in middle and distal inner margin and one large and long process in middle in lateral third.

Tropodiaptomus longiprocessus sp. nov. is the most similar to *T. lanaonus*, but it differs distinctively in the following characters: (i) the dorsal surface of exp-2 of the adult male right P5 has two longitudinal hyaline lamellae and one large and long process; (ii) lateral wings of the fifth pediger of adult female are asymmetrical; (iii) anterior part of the genital double-somite of the adult female is dilated on the right side; (iv) right posterior corner of the genital double-somite of the adult female does not have a round lobe; and (v) distal end of the endopodal segment of the adult female P5 has smooth spiniform setae (Table 2).

The diversity of *Tropodiaptomus* in Thailand is presented as a pictorial key in Fig. 17 to facilitate easy and quick identification.

Tropodiaptomus species diversity and distribution in Thai water bodies

Tropodiaptomus species have been recorded from various ponds, lakes, streams, roadside canals and rice field habitats in Thailand (Sanoamuang 2002; Saetang et al. 2020, 2022), with 12 species now recorded (Table 3) (Saetang et al. 2020, 2022; Sanoamuang and Dabseepai 2021). However, the status of some species remains unclear. Molecular data have confirmed that *T.* cf. *lanaonus* and *T. lanaonus* s. str. are different species (Saetang et al. 2022) but thorough morphological comparisons of numerous specimens are still needed to confirm species-level separation of *T.* cf. *lanaonus*. The validity of *T. doriai* is also in serious doubt, with no further reports on this species in Thailand since it was first reported by Daday in 1906 from a freshwater habitat close to Bangkok (Lai and Fernando 1981; Sanoamuang 2002).

Each species of *Tropodiaptomus* can be found in various types of freshwater habitats, while most occur in both temporary and permanent water bodies with a limited geographical distribution range (Fig. 18). Only *Tropodiaptomus vicinus* is widely distributed throughout Thailand, except in the north, while *T. oryzanus* is common but restricted to the northeastern region and *T. hebereri*, *T. megahyaline*, *Tropodiaptomus* sp. 1 and *Tropodiaptomus* sp. 2 have restricted distributions in one region in a few localities. Most species can be found

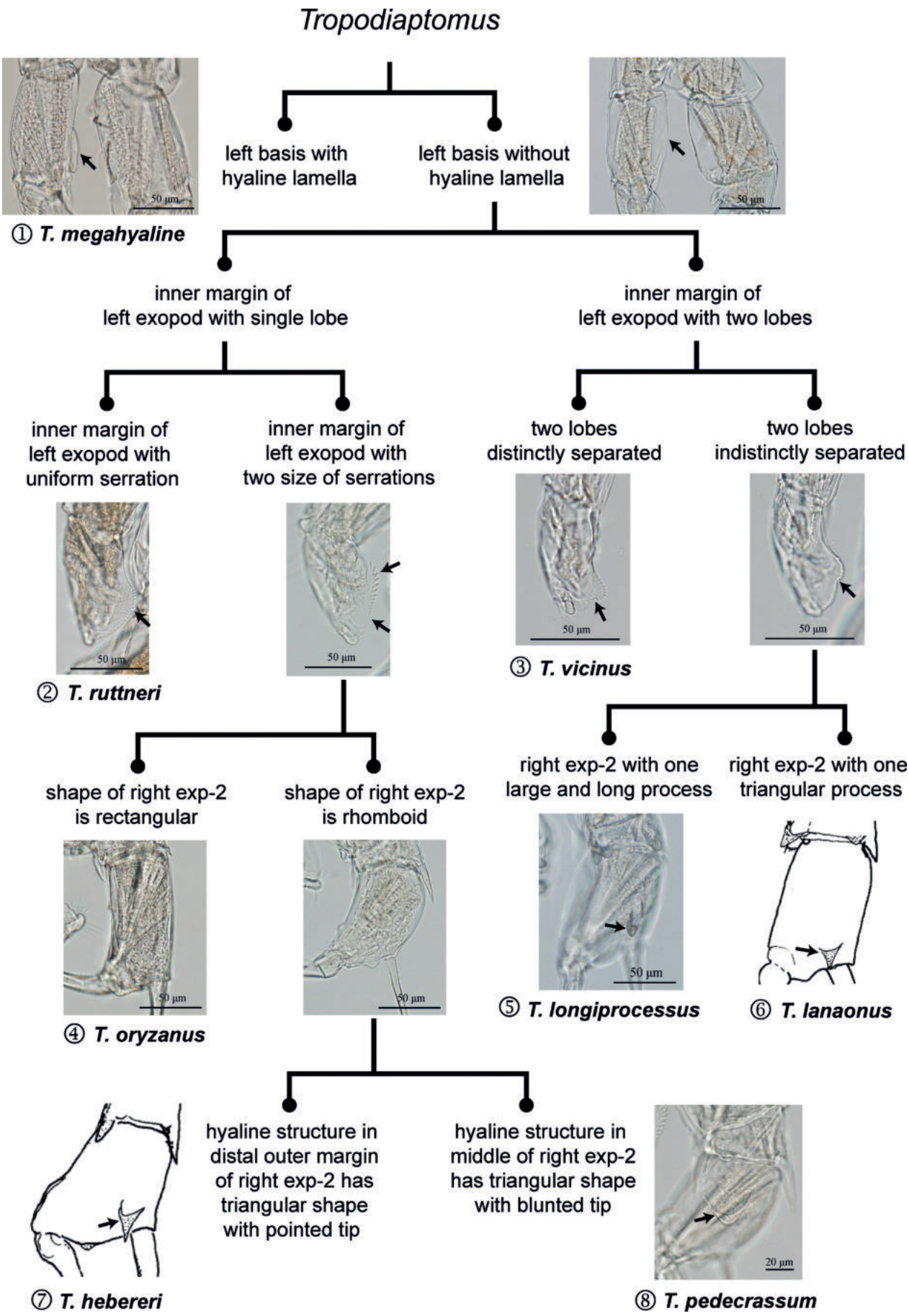

Figure 17. Pictorial key of the adult male P5 of *Tropodiaptomus* species found in Thailand. Right exp-2 of P5 of *Tropodiaptomus lanaonus* and *T. hebereri* were modified from Kiefer (1982).

during all seasons in Thailand. *T. oryzanus* and *T. vicinus* can be found all year round, in both rainy and dry seasons, including during low temperature periods in Northern Thailand. Some species are seasonal, with *T. pedecrassum* found only during low temperature periods in the north and *T. longiprocessus* and *Tropodiaptomus* sp.1 found only during the rainy season, with distribution restricted to temporary pools (Table 3).

Discussion

This study assessed the morphological characteristics and molecular data recorded by Saetang et al. (2020) and confirmed the species status of *Tropodiaptomus pedecrassum* sp. nov. and *Tropodiaptomus longiprocessus* sp. nov. These two species clearly differ from their congeners: (i) the inner margin of the adult male left P5 had a single lobe and serration gradually decreased in size from the proximal to distal end in *Tropodiaptomus pedecrassum* sp. nov. with two lobes and uniform serration in *Tropodiaptomus longiprocessus* sp. nov. and (ii) exp-2 of the adult male right P5 was rhomboid-shaped, with one triangular-shaped process on the frontal surface in *Tropodiaptomus pedecrassum* sp. nov., and a rectangular shaped large and long process in the middle third lateral in *Tropodiaptomus longiprocessus* sp. nov.

The discovery of these two new species increases the number of *Tropodiaptomus* species recorded in Thailand from 10 to 12, thus accounting for 19% of species diversity worldwide. Based on the large number of samples taken throughout Thailand, most *Tropodiaptomus* species

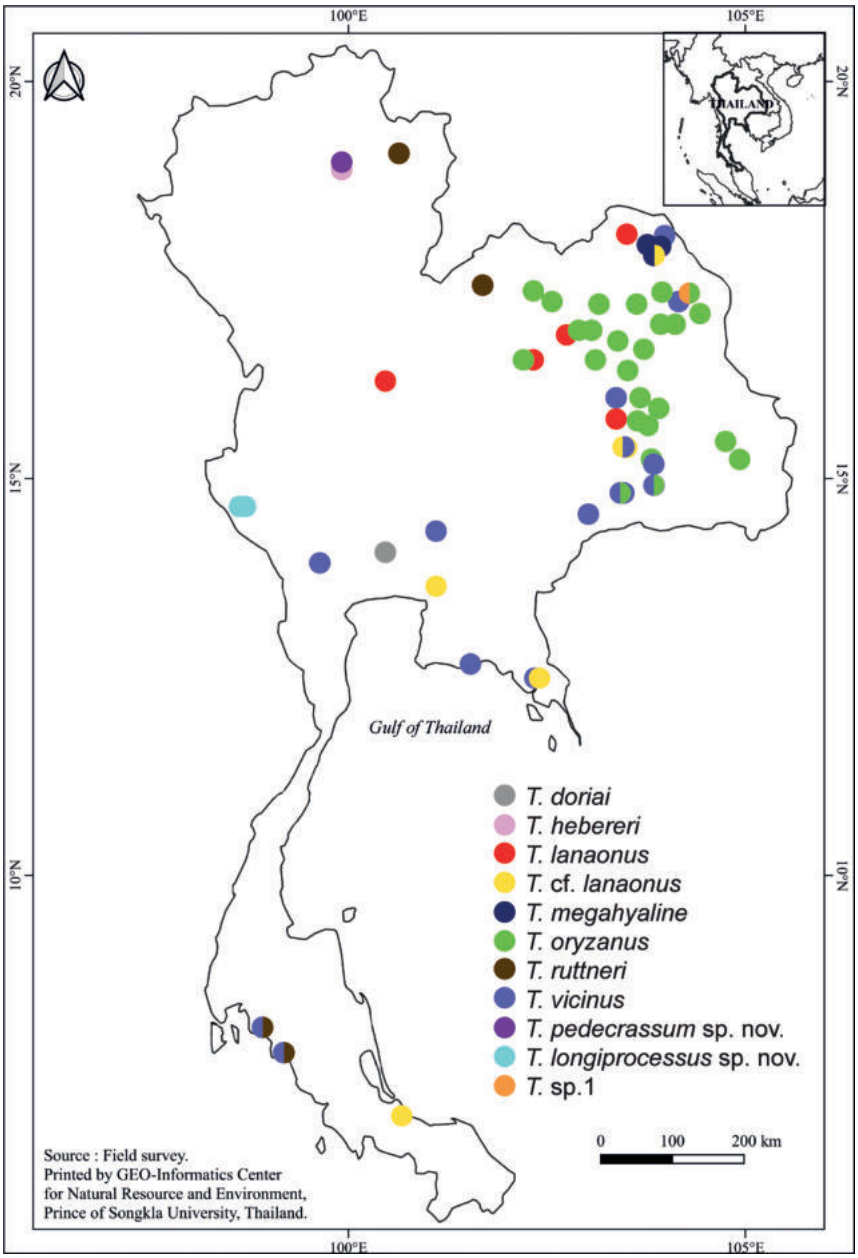

Figure 18. Distribution of *Tropodiaptomus* found in Thailand (*Tropodiaptomus* sp. 2 is not included in this figure because no distribution data are available).

Table 3. Geographic distribution of *Tropodiaptomus* species in Thai water bodies and remarks on their status.

Species	Distribution in Thai water bodies	Co-occurring species in Thai water bodies	Wider Distribution	Notes
1. *T. doriai*	Freshwater habitat close to Bangkok, central Thailand	No data	India, Indonesia and Sri Lanka (Kiefer 1982; Ambedkar 2012)	It was recorded only once in Thailand (Lai and Fernando 1981 referred to Daday 1906) and has never been found again. Therefore, its occurrence status is still doubtful.
2. *T. hebereri*	Cold season (January), in a roadside canal in northern Thailand	None	China, India, Indonesia and Malaysia (Kiefer 1930, 1982; Hsiao 1950; Ambedkar 2012)	
3. *T. lanaonus*	Floodplain, lake and pond in both dry (March) and rainy seasons (August) in central and northeastern Thailand	No data	Philippines (Kiefer 1982)	
4. *T.* cf. *lanaonus*	Rice field, river, roadside canal, swamp in both dry (May) and rainy seasons (June, September, October, November) in eastern, northeastern and southern Thailand	*Dentodiaptomus javanus*, *Eodiaptomus phuphanensis*, *Heliodiaptomus elegans*, *Mongolodiaptomus botulifer*, *M. dumonti*, *M. malaindosinensis*, *M. pectinidactylus*, *Phyllodiaptomus christineae*, *P. roietensis*, *P. surinensis*, *Phyllodiaptomus* sp., *Tropodiaptomus megahyaline*, *T. vicinus*, *Vietodiaptomus blachei*	–	This species does not agree with the original description of *T. lanaonus* in (i) the length of the spinous process in the antepenultimate segment of adult male right antennule is 1/2 to 3/4 of segment 21, and (ii) the ornamentation on the basis of adult male right P5 has one hyaline lamella and one apophysis or one hyaline lamella and no apophysis (Saetang et al. 2022)
5. *T. megahyaline*	Pond and rice field in both dry (May) and rainy season (June) in northeastern Thailand	*Heliodiaptomus elegans*, *Mongolodiaptomus malaindosinensis*, *M. pectinidactylus*, *Neodiaptomus songkhramensis*, *Tropodiaptomus* cf. *lanaonus*, *Vietodiaptomus blachei*	Endemic in Thailand (Saetang et al. 2020)	
6. *T. oryzanus*	Several types of habitats including canal, floodplain, lake, man-made pond, pond, rice field and roadside canal in dry (April, May), rainy (June, August, October) and cold season (December) in northeastern Thailand	*Dentodiaptomus javanus*, *Neodipatomus laii*, *Mongolodiaptomus botulifer*, *M. malaindosinensis*, *Tropodiaptomus vicinus*	Cambodia, China, Japan, Korea, Malaysia, Taiwan and Vietnam (Kiefer 1937, 1982)	
7. *T. ruttneri*	Peat swamp, swamp roadside canal and pond in both dry (March) and rainy seasons (August, November) in north, northeastern and southern Thailand	*Mongolodiaptomus botulifer*	China and Malaysia (Kiefer 1982)	
8. *T. vicinus*	Several types of habitats including canal, fish pond, floodplain, lake, man-made pond, marsh, peat swamp, pond, rice field, river, swamp and roadside canal in dry (April, May), rainy (June, August, October, November) and cold season (December) in the central, eastern, northeastern, southern and western Thailand	*Dentodiaptomus javanus*, *Eodiaptomus phuphanensis*, *Heliodiaptomus elegans*, *Mongolodiaptomus botulifer*, *M. malaindosinensis*, *Neodipatomus laii*, *N.yangtsekiangensis*, *Phyllodiaptomus christineae*, *P. roietensis*, *P. surinensis*, *Tropodiaptomus oryzanus*, *T.* cf. *lanaonus*	Cambodia, India, Indonesia, Laos, Malaysia, Philippines and Vietnam (Lai et al. 1979; Kiefer 1982; Ambedkar 2012)	
9. *T. pedecrassum* sp. nov.	Swamp in cold season (January, February) in northern Thailand	*Mongolodiaptomus botulifer*		Recorded as *Tropodiaptomus* sp.1 in Saetang et al. (2022).
10. *T. longiprocessus* sp. nov.	Swamp in rainy season (June) in western Thailand	None		Recorded as *Tropodiaptomus* sp.2 in Saetang et al. (2022).
11. *Tropodiaptomus* sp. 1	Pond in rainy season (October) in northeastern Thailand	None		Recorded as *Tropodiaptomus* sp.3 in Saetang et al. (2022). Although the molecular data suggested that is a putative new species, more specimens are needed to prove its status.
12. *Tropodiaptomus* sp. 2	Pond in northern Thailand no information available on temporal distribution	No data		Recorded as *Tropodiaptomus* sp. in Sanoamuang and Dabseepai (2021).

have a limited distribution at one site or one region, with only *T. vicinus* having a wide distribution. Moreover, *Tropodiaptomus* is distributed in a specific habitat, temporary pools without vegetation and the occurrences of this genus are seasonal. This type of habitat is undersampled in SE Asia, however it is important for our understanding of the diversity of this genus. However, recent findings of new records in Southeast Asia (Defaye 2002; Ambedkar and Elia 2014; Saetang et al. 2020), including the present discovery of two new species, indicate that this genus may have a wider geographical distribution than recorded previously (Lai and Fernando 1979b; Lai and Fernando1981; Ambedkar and Elia 2014).

Saetang et al. (2022) considered that more undiscovered species exist in this genus in SE Asia. Further intensive study is required, in terms of intensive sampling year-round as well as the use of efficient tools such as molecular systematics together with morphological

examinations. This will clarify the taxonomic status of currently confusing data and more accurately estimate the species richness and ecological and biogeographical distribution of members of this genus in Thailand.

Acknowledgements

We would like to thank the editor and the reviewer for taking the time and effort to review the manuscript. We sincerely appreciate all the valuable comments and suggestions that helped us improve the quality of the manuscript. This research was approved by the Institutional Animal Care and Use Committee, Kasetsart University, Thailand (approval no. ACKU61-SCI-004). The authors would like to thank Kasetsart University for providing post-master research scholarship through the Biodiversity Center Kasetsart University. Dr. Rapeepan Jaturapruek is thankful for assistance in field sampling.

References

Ambedkar D (2012) Morpho-taxonomy and biogeography of diaptomid copepods of India, with descriptions of four new species of the genus *Tropodiaptomus* Kiefer, 1932 (Crustacea: Calanoida). PhD Thesis, Acharya Nagarjuna University, Guntur.

Ambedkar D, Elia B (2014) A new species of the genus *Tropodiaptomus* (Copepoda: Diaptomidae). Crustaceana 87(4): 430–447. https://doi.org/10.1163/15685403-00003299

Daday EV (1906) Untersuchungen über die Copepodenfauna von Hinterindien, Sumatra und Java, nebst einem Beitrag zurb Copepoden kenntnis der Hawaii-Inseln. Zoologische Jahrbucher 24: 175–206.

Defaye D (2002) A new *Tropodiaptomus* (Copepoda, Calanoida, Diaptomidae, Diaptominae) from Vietnam. Crustaceana 75(3–4): 341–350. https://doi.org/10.1163/156854002760095417

Hsiao SC (1950) Copepods from Lake Erh Hai, China. Proceedings of the United States National Museum 100(3261): 161–200. https://doi.org/10.5479/si.00963801.100-3261.161

Huys R, Boxshall GA (1991) Copepod evolution. The Ray Society, 468 pp.

Kiefer F (1930) Neue Ruderfußkrebse von den Sunda-Inseln. Zoologischer Anzeiger 86: 185–189.

Kiefer F (1937) Sÿßwassercopoden aus Ostasien. II. Neue Diaptomiden und Cyclopiden von der Insel Formosa. Zoologischer Anzeiger 119: 58–64.

Kiefer F (1982) Comparative studies on morphology, taxonomy and geographical distribution of the species of the genus *Tropodiaptomus* Kiefer from Asiatic inland waters. Hydrobiologia 93(3): 223–253. https://doi.org/10.1007/BF00012334

Lai HC, Fernando CH (1979a) The malaysian *Tropodiaptomus* (Copepoda: Calanoida) and its distribution. Hydrobiologia 65(1): 75–81. https://doi.org/10.1007/BF00032722

Lai HC, Fernando CH (1979b) Zoogeographical and distribution of Southeast Asian freshwater Calanoida. Hydrobiologia 74(1): 53–66. https://doi.org/10.1007/BF00009015

Lai HC, Fernando CH (1981) The freshwater Calanoida (Crustacea: Copepoda) of Thailand. Hydrobiologia 76(1–2): 161–178. https://doi.org/10.1007/BF00014047

Lai HC, Mamaril A, Fernando CH (1979) The freshwater Calanoida (Copepoda) of the Philippines. Crustaceana 37(3): 225–240. https://doi.org/10.1163/156854079X00546

Saetang T (2021) Systematics of genus *Tropodiaptomus* Kiefer, 1932 (Copepoda, Calanoida, Diaptomidae) in Thailand. PhD Thesis, Kasetsart University, Bangkok, Thailand. https://doi.org/10.1080/00222933.2020.1843726

Saetang T, Sanoamuang L, Maiphae S (2020) A new species of genus *Tropodiaptomus* Kiefer, 1932 (Crustacea: Copepoda: Calanoida: Diaptomidae) from Thailand. Journal of Natural History 54(35–36): 2297–2322. https://doi.org/10.1080/00222933.2020.1843726

Saetang T, Marrone F, Vecchioni L, Maiphae S (2022) Morphological and molecular diversity patterns of the genus *Tropodiaptomus* Kiefer, 1932 (Copepoda, Calanoida, Diaptomidae) in Thailand. Scientific Reports 12(1): e2218. https://doi.org/10.1038/s41598-022-06295-4

Sanoamuang L (2002) Freshwater Zooplankton in Thailand: Calanoid Copepod. Klangnana Publisher, Khon Kaen, 159 pp.

Sanoamuang L, Dabseepai P (2021) Diversity, distribution, and habitat occurrence of the diaptomid copepods (Crustacea: Copepoda: Diaptomidae) in freshwater ecosystems of Thailand. Water 13(17): e2381. https://doi.org/10.3390/w13172381

Walter TC, Boxshall G (2023) World of Copepods database. *Tropodiaptomus* Kiefer, 1932. https://www.marinespecies.org/aphia.php?p=taxdetails&id=348143

Zoosyst. Evol. 99 (2) 2023, 423–437 | DOI 10.3897/zse.99.103003

PENSOFT

für Natur MUSEUM FÜR NATURKUNDE BERLIN

Stenotanais (Crustacea, Tanaidacea) from the Santos Basin: the first described species of the family Akanthophoreidae off the Brazilian coast

Juliana Lopes Segadilha[1], Graham Bird[2], Marcos Tavares[1]

1 *Museu de Zoologia, Universidade de São Paulo, São Paulo-SP, 04263-000, Brazil*

2 *Waikanae, Kâpiti, New Zealand*

https://zoobank.org/CFCE08BC-6C73-47EA-807D-EB9C3F2547E5

Corresponding author: Juliana Lopes Segadilha (julianasegadilha@gmail.com)

Academic editor: Luiz F. Andrade ♦ **Received** 8 March 2023 ♦ **Accepted** 31 May 2023 ♦ **Published** 4 October 2023

Abstract

Benthic samples collected from depths ranging between 686 and 2410 m along the Brazilian continental upper slope from Rio de Janeiro State to Santa Catarina State (23°S to 27°S) yielded a wealth of tanaidacean material, including two new species of *Stenotanais*. This is the first described species of the family Akanthophoreidae from Brazilian waters. *Stenotanais leonardoi* **sp. nov.** has a combination of unique characters including the uropod basal article longer than the pleotelson and the exopod somewhat wider than the endopod, longer than the endopod article-1 (0.7 times endopod length) and supporting two flat and wide terminal setae. *Stenotanais uropedon* **sp. nov.** is recognisable by its oar-shaped uropod endopod, with article-2 large, broad and flattened and the short exopod, only 0.3 times the endopod length. An identification key to the species of *Stenotanais* is given. These two species bring the total number of described akanthophoreids to 56 species and that of all tanaidaceans in Brazilian waters to 66 species.

Key Words

continental margin, Peracarida, south-western Atlantic, Tanaidomorpha, taxonomy, upper slope

Introduction

The family Akanthophoreidae Sieg, 1986 currently includes 54 species classified into ten genera (WoRMS 2023) and encompasses small and slender tanaidacean species known to occur in all oceans, but is best investigated in the Northeast Atlantic Basin (Bird and Holdich 1984; Guerrero-Kommritz 2005; Bamber et al. 2009; Błażewicz-Paszkowycz and Bamber 2011; Bamber 2014; Jóźwiak et al. 2018a, b). In the South Atlantic, akanthophoreid species have been described from the Southeast Atlantic (SE): Angola Basin (Guerrero-Kommritz 2004, 2005) and Subantarctic: South Georgia, South Sandwich Islands and Beagle Channel (Sieg 1986; Schmidt and Brandt 2001; Guerrero-Kommritz 2005; Błażewicz-Paszkowycz 2014), whilst the waters off the south-western Atlantic remained a blank space on the world map of akanthophoreid distribution. Recently, surveys of the benthic macrofauna of the Brazilian continental shelf and slope revealed that akanthophoreids are actually one of the five most abundant and diverse families of Tanaidacea (Lavrado et al. 2017a, b; Guimarães et al. 2020; Lavrado HP, pers. comm.).

Amongst this family, the genus *Stenotanais* Bird & Holdich, 1984 was erected by Bird & Holdich to distinguish these species from all other leptognathiid genera (as then defined) mainly by the extreme length of the pereonites 1–5, a very robust cheliped carpus and propodus with strong ventral spines and the presence of very robust uropodal setae. Currently, it is included in the family Akanthophoreidae after the Larsen and Araújo-Silva (2014) phylogenetic analysis of the group and there are four described species accommodated within the genus: *Stenotanais arenasi* Larsen, 2011; *S. crassiseta* Bird & Holdich, 1984; *S. hamicauda* Bird & Holdich, 1984; *S. macrodactylus* Larsen, 2005 (WoRMS 2023).

Amongst the akanthophoreid material obtained from the Santos Basin, off the south-eastern coast of Brazil, collect-

ed during the Santos Project – Santos Basin Environmental Characterization (Brazil), coordinated by PETROBRAS/CENPES, was a wealth of specimens of *Stenotanais* belonging to two undescribed species. Both species are described and illustrated herein and a key to all *Stenotanais* species is provided. These two new species bring the total diversity of tanaidaceans in Brazilian waters to 66 species.

Materials and methods

Study area and collection

A total of 277 akanthophoreids was collected along the Brazilian continental margin (between 23°S and 27°S) of the SW Atlantic, during the scientific expedition Santos Project (PCR-BS) – Santos Basin Environmental Characterization (Brazil), coordinated by PETROBRAS/CENPES, in 2019 on board the R/V Ocean Stalwart. A list of the sampling stations is given in the Suppl. material 1.

Sediment samples were taken using a box corer, with three replicate samples at each station (stn) and subsequently stratified into three sediment layers, 0–2, 2–6 and 6–10 cm. Samples were washed through a 300-µm-mesh sieve. The material retained was fixed in 4% borax-buffered formalin (making molecular data unfeasible) and subsequently preserved in 70% ethanol and then tanaidaceans were sorted and identified.

Taxonomy

Selected specimens were dissected using chemically-sharpened tungsten-wire needles and appendages, mounted on slides using glycerine and then sealed. Careful examination and drawings of external morphology of the studied material was performed using a microscope Zeiss, equipped with a camera lucida and then digitalised with WACOM Tablet using the graphic programme Adobe Illustrator CC 2017 for producing taxonomic plates. The morphological terminology follows the literature related to the family Akanthophoreidae (Bird and Holdich 1984; Larsen 2003, 2005, 2011; Guerrero-Kommritz and Brandt 2005). The term "neuter" was used for post-manca stages that are not immediately categorisable as females or sub-adult (preparatory) males, although the majority are probably non-ovigerous females (Bird 2004). All setae are simple unless stated otherwise and the term 'PSS' is used for 'pinnate sensory setae' and 'L:W' for 'length to width ratio/as long as wide'. 'Spine' is used as a descriptor of stout or rigid setae (i.e. in its correct etymological sense) and the two are homologous in general structure/development.

Total body length (TBL) was measured from the tip of the rostrum to the tip of the pleotelson and pereonite width at the broadest part on whole specimens. The length/width ratio was calculated from the measurement made at mid-length and width of an article. To simplify species descriptions, the expression 'Nx' replaces 'N times as long as'. The diagnostic characters to distinguish between species are given in Table 1.

Holotypes were chosen from the best-preserved individuals. The type-material is deposited at Museu de Zoologia, Universidade de São Paulo (MZUSP) (São Paulo, Brazil).

Results

Systematics

Order Tanaidacea Dana, 1849
Suborder Tanaidomorpha Sieg, 1980
Superfamily Paratanaoidea Lang, 1949
Family Akanthophoreidae Sieg, 1986

Genus *Stenotanais* Bird & Holdich, 1984

Diagnosis (Modified from Larsen 2005, 2011). Female. Body elongate (11.5–13× L:W). Pereonites longer than wide, with straight lateral edges. Pleon short (15–20% of TBL). Antennule shorter than carapace, four-articled. Antenna six-articled. Mandibular molar tapering, with terminal spines. Maxillule with eight to ten terminal spines. Maxilliped endite with rounded cusps, spiniform lateral corners and distal seta. Cheliped carpus robust with large distoventral shield; chela robust, fixed finger with two robust ventral spines. Pereopods 1–3 basis wider than on pereopods 4–6; merus and carpus with spine. Pereopods 4–6 without coxae. Pereopods 4–6 dactylus and unguis not fused; dactylus with double-row of small spines. Pleopods short and broad, with plumose or simple setae. Uropods prominent, often as long as antennae: endopod two-articled; exopod one- or two-articled; specialised setae with a wide and flat basis present on either exopod or endopod.

Male. Immature (preparatory) male with antennule thicker than in female, functional mouthparts present (see remarks on genus). Sexually mature 'swimming' type: cephalothorax as long as first three pereonites; pereon shorter than in female; pleon well developed, as long as pereon, caudally pointed; multi-articulate antennule with multiple aesthetascs, distal article longer than preceding article; no functional mouthparts; uropod biramous, endopod and exopod two-articled.

Type species. *Stenotanais crassiseta* Bird & Holdich, 1984, by original designation. Gender: feminine.

Species included. *Stenotanais arenasi* Larsen, 2011; *S. crassiseta* Bird & Holdich, 1984; *S. hamicauda* Bird & Holdich, 1984; *S. macrodactylus* Larsen, 2005; *S. leonardoi* sp. nov.; *S. uropedon* sp. nov.

Remarks. The rather infrequently-recorded *Stenotanais* is similar to akanthophoreid genera such as *Pseudakanthophoreus* Lubinevsky, Tom & Bird, 2022 and *Parakanthophoreus* Larsen & Araújo-Silva, 2014, by having chelipeds without extensive surface ornamentation and the absence of spurs on pleonite-5, pleotelson and the uropod basal article or endopod article-1. However, *Stenotanais* can be distinguished mainly by having the basis of pereopods 1–3 thicker than the basis of pereopods 4–6

Table 1. Diagnostic characters of *Stenotanais* species. Abbreviations: A1 = antennule; Car. = carpus; Che. = cheliped; Endo. = endopod; Exo. = exopod; Mer. = merus; P = pereopod; Prop. = propodus; Uro. = uropod.

Species	***Stenotanais leonardoi* sp. nov.**	***S. uropedon* sp. nov.**	***S. arenasi* Larsen, 2011**	***S. crassiseta* Bird & Holdich, 1984**	***S. hamicauda* Bird & Holdich, 1984**	***S. macrodactylus* Larsen, 2005**
Type locality	Brazil (SW Atlantic)	Brazil (SW Atlantic)	Manganese Nodule Province (Central Pacific)	Rockall Trough (NE Atlantic)	Feni Ridge (NE Atlantic)	Gulf of Mexico (NW Atlantic)
Depth (m)	686–2410	991–1974	4954	2070–2916	1600–4829	1320–2387
Holotype sex	female	female	male	female	female	female
A1 length/ cephalothorax length	0.6×	0.6×	0.7×	0.6×	0.6×	0.8×
Che. basis (L:W)	3.6×	3.9×	2.4×	2.9×	3.8×	2.5×
Che. carpal shield	present	present	absent	present	present	present
Che. fixed finger, cutting edge setation	two simple setae	two simple setae and one spine	three robust setae	three simple setae	three simple setae	two robust setae
P1–6 mer. and carp. ventral spines type	simple spines	serrate spines	simple spines (= spiniform setae)	simple spines	simple spines	simple and bi-serrate (P5) spines
P2–3 carp. spine length/ prop. length	long spine (longer than half)	long spine (longer than half)	long spine (longer than half)	short spine (about one third)	long spine (about half)	long spine (P2: longer than half; P3: about half)
P2–3 prop. inferior margin	convex	convex	straight	convex	convex	straight
P2–3 prop. ventral setation	spine, microtrichia and spinules	spine, microtrichia and spinules	spine (= spiniform seta) and setules (= microtrichia)	spine and spinules	spine and spinules	spine
P1 dactylus length/ unguis length	1.0×	1.3×	0.9×	0.8×	0.9×	1.3×
P2 dactylus length/ unguis length	0.7×	1.1×	0.9×	0.8×	0.9×	> 2.0×
P3 dactylus length/ unguis length	-	1.4×	0.7×	0.9×	1.0×	1.4×
P4–6 carp. bone-shaped seta	absent	absent	present	absent	absent	absent
Uro. basis length/ pleotelson length	longer than (1.1×)	shorter than (0.6×)	shorter than (0.5×)	shorter than (Bird and Holdich (1984) text)	shorter than (0.4×)	longer than (1.4×)
Uro. exo. length/ endo. article-1 length	longer than (1.8×)	as long as	shorter than (0.8×)	as long as	longer than (1.7×)	longer than (2.2×)
Uro. exo. length/ endo. length	long, 0.7×	short, 0.3×	short, 0.4×	short, 0.4×	long, about 0.8×	long, about 0.8×
Uro. endo. shape	subparallel margins	oar-shaped (article-2 broad and flattened)	subparallel margins	subparallel margins	subparallel margins	subparallel margins
Uro. exo. shape	somewhat wider than endopod	subparallel margins	subparallel margins	subparallel margins	oar-shaped (broader distally)	subparallel margins
Uro. endo. seta type	simple setae	simple setae	simple setae	one flat and wide distal seta	one flat and wide distal seta	simple setae
Uro. exo. seta type	two flat and wide distal setae	two flat and wide distal setae	one specialised distal seta with flat and wide basis	simple setae	simple setae	one flat and wide medial seta and two articulated wide distal setae

and the presence of specialised setae with a wide and flat basal attachment on the uropod (Bird and Holdich 1984; Larsen 2011).

Larsen (2011) described *S. arenasi*, based on a single specimen and expressed uncertainty as to whether it really belongs to *Stenotanais*, so that its generic affiliation should be considered tentative. We agree that this species may belong to a different genus as its cheliped lacks a strong carpal shield, the shape of the antennule articles 3–4 does not conform to other *Stenotanais* species (article-3 not rectangular and article-4 minute, as long as wide; which can be a sexually dimorphic character) and the uropods are not ventrally deflexed (i.e. not folded back on themselves). Although not an impediment for supporting the exclusion of *S. arenasi* from *Stenotanais*, it is of note that it is so far the only species of the genus reported from the Pacific Ocean (Fig. 8). Despite these considerations, we adhere to the current classification until more evidence is available.

The single available specimen of *S. arenasi* may be a preparatory male, based on characters of the antennule articles 1–2 (as suggested by Larsen 2011) and has functional mouthparts. Here, we record the first sexually mature 'swimming' male of *S. leonardoi* sp. nov. (see below), the first to have been noticed in *Stenotanais*, although it would have been desirable to confirm the link between male and female forms of the same species using molecular analysis.

Another character in the original generic diagnosis of Bird and Holdich (1984) is the pereopods 1–3 propodus having a distinct convex inferior margin armed with small strong spinules. This needs further investigation as it is true for *S. crassiseta*, *S. hamicauda* and both new species described here, but not for *S. arenasi* and *S. macrodactylus*.

Stenotanais leonardoi sp. nov.

https://zoobank.org/4148D462-1E56-49B4-A4EE-A8023D18C47F

Figs 1–4

Material examined. ***Holotype*:** Brazil – Santa Catarina State • neuter, length 1.9 mm; stn A8 R2, 0–2 cm; MZUSP 43545.

***Paratypes*:** Brazil – São Paulo State • 1 neuter (dissected), length 2.1 mm; stn E8 R3, 5–10 cm; MZUSP 43547 – Santa Catarina State• 1 male, length 0.9 mm; stn A8 R3, 2–5 cm; MZUSP 43546 • 3 neuters; stn A8 R1, 2–5 cm (1 dissected); MZUSP 43548 • 2 neuters; stn A8 R2, 2–5 cm; MZUSP 43549 • 2 neuters; stn A8 R3, 0–2 cm; MZUSP 43550 • 1 neuter; stn A10 R2, 2–5 cm; MZUSP 43551 • 1 neuter; stn A11 R3, 0–2 cm; MZUSP 43552 – Paraná State • 1 neuter; stn B7 R1, 0–2 cm; MZUSP 43553 • 2 neuters; stn B7 R2, 2–5 cm; MZUSP 43554 • 1 neuter; stn B7 R3, 2–5 cm; MZUSP 43555 • 1 neuter; stn B8 R2, 2–5 cm; MZUSP 43556 • 1 neuter; stn B9 R2, 5–10 cm; MZUSP 43557 – São Paulo State • 2 neuters; stn C7 R1, 2–5 cm; MZUSP 43558 • 1 neuter; stn C7 R2, 2–5 cm; MZUSP 43559 • 1 neuter; stn C7 R3, 2–5 cm; MZUSP 43560 • 1 neuter; stn C7 R3, 5–10 cm; MZUSP 43561 • 1 neuter; stn C8 R1, 2–5 cm; MZUSP 43562 • 2 neuters and 1 juvenile; stn C8 R2, 2–5 cm; MZUSP 43563 • 2 neuters; stn C9 R1, 2–5 cm; MZUSP 43564 • 1 neuter; stn C9 R1, 5–10 cm; MZUSP 43565 • 1 neuter; stn C11 R1, 2–5 cm; MZUSP 43566 • 1 neuter; stn C11 R2, 2–5 cm; MZUSP 43567 • 1 neuter; stn D8 R1, 0–2 cm; MZUSP 43568 • 2 neuters; stn E7 R3, 2–5 cm; MZUSP 43569 • 1 neuter; stn E8 R1, 5–10 cm; MZUSP 43570 • 2 neuters; stn E8 R3, 2–5 cm; MZUSP 43571 • 2 neuters; stn E9 R1, 5–10 cm; MZUSP 43572 – Rio de Janeiro State • 1 neuter; stn F7 R1, 2–5 cm; MZUSP 43573 • 1 neuter; stn F7 R2, 2–5 cm; MZUSP 43574 • 1 neuter; stn F7 R2, 5–10 cm; MZUSP 43575 • 1 neuter; stn F7 R3, 2–5 cm; MZUSP 43576 • 1 neuter; stn H7 R2, 2–5 cm; MZUSP 43577 • 1 neuter; stn H10 R2, 2–5 cm; MZUSP 43578 • 1 neuter; stn H10 R2, 5–10 cm; MZUSP 43579 • 1 neuter; stn P5 R3, 2–5 cm; MZUSP 43580.

Diagnosis. Neuter. Cheliped fixed finger with two simple setae on cutting edge. Pereopods 2–3 carpus with long spine, longer than half length of propodus. Uropod basal article longer than pleotelson; exopod and endopod with subparallel margins; exopod slightly wider than endopod, longer than endopod article-1 (0.7× endopod), with two flat and wide terminal setae.

Etymology. The species is dedicated to the first author's life partner, Leonardo Santos de Souza, who has supported and encouraged this author in her academic career.

Description. Based on neuter holotype (MZUSP 43545) length 1.9 mm, dissected neuter paratype (MZUSP 43547) length 2.1 mm and male (MZUSP 43546) length 0.9 mm. Body (Fig. 1A) very slender, about 14× L:W. Cephalothorax elongate 1.7× L:W, 1.5× pereonite-1, straight-sided, naked. Pereonites 1–6. All pereonites rectangular, longer than wide, parallel-sided; pereonite-1 1.3× L:W; pereonite-2 2.3× L:W; pereonite-3 2.4× L:W; pereonites 4–5 2.0× L:W; pereonite-6 shortest, 1.3× L:W. Pleon (Fig. 1A) short, 0.2× TBL, about as long as pereonites 5 and 6 combined, with five subequal pleonites. Pleotelson short, trapezoidal 0.6× L:W, less than half-length of pleon.

Antennule (Fig. 2A) 0.6× cephalothorax; article-1 about 0.4× TL, 1.6× L:W, with one simple seta and three distal PSS; article-2 1.8× L:W, 0.8× article-1, with two simple setae and one distal PSS; article-3 0.9× L:W, 0.3× article-2, with simple subdistal seta; article-4 2.6× L:W, 1.9× article-3, with simple subdistal seta and with aesthetasc, three simple and minute terminal setae. Antenna (Fig. 2B) article-1 fused with body; article-2 as long as wide, with one simple distal seta; article-3 1.5× L:W, naked; article-4 2.8× L:W, 2.2× article-3, with three medial PSS and three simple distal setae; article-5 3.0× L:W, 0.7× article-4, with a distal seta; article-6 minute with five simple terminal setae.

Labrum (Fig. 2C) elongate, hood-shaped, covered by minute setae. Mandible (Fig. 2D–G) with acuminate molar process with three or four terminal spines; left mandible (Fig. 2D, E) incisor smooth, with five unequal teeth and smooth lacinia mobilis (separated from incisor by wide gap); right mandible (Fig. 2F, G) with three strong teeth on incisor process, molar broken off during dissection. Maxillule (Fig. 2H) endite with nine terminal spines (at least two serrate), outer margin with setule; palp broken off during dissection. Maxilla (Fig. 2I) ovoid and stout, but large relative to maxilliped.

Maxilliped (Fig. 2J) basis with one simple seta near articulation with palps, not reaching distal margin of endites; endites unfused, with rounded distal cusps and a short seta on distal edge; palp article-1 naked; article-2 with three inner and one outer setae; article-3 with three (two long) inner setae; article-4 with four inner setae and one subdistal outer seta. Labium and epignath not observed.

Cheliped (Fig. 2K) and sclerite calcified; basis with one minute dorsodistal seta and long posterior projection (lobe), not reaching pereonite-1; 3.6× L:W; merus subtriangular, with ventral seta; carpus stout 1.4× L:W, with ventral seta and one proximal and one dorsodistal setae, carpal shield large, well developed; propodus stout 0.9× carpus, 1.5× L:W, with two setae near dactylus insertion on inner side (one long and one short); fixed finger with two strong serrate ventral spines and one spine on distolateral margin; cutting edge with two simple setae, dactylus slightly shorter than fixed finger.

Pereopod-1 (Fig. 3A) stout; coxa annular, seta not observed; basis broad 2.2× L:W, naked; ischium with seta (not drawn); merus short 0.8× L:W, with one ventrodistal seta and long spine reaching carpus distal margin; carpus short 0.6× L:W, about as long as merus, with ventrodistal spine and one spinule (microtrichial), dorsodistal with long spine and microtrichia; propodus short 1.9× L:W, 2.3× carpus, with convex inferior margin with ventrodistal spine, microtrichia and two spinules and dorsodistal minute seta; dactylus as long as unguis, together 0.8× propodus.

Pereopod-2 (Fig. 3B) stout; basis broad 2.0× L:W, with large dorsal PSS; ischium with one seta; merus 1.1× L:W, with ventrodistal long spine reaching carpus distal margin; carpus short as long as wide, as long as merus, with ventral spinules and microtrichia, two unequal ventrodistal spines (one longer than half length of propodus) and dorsodistal spine; propodus short 2.0× L:W, 1.7× carpus, with convex inferior margin with ventrodistal spine,

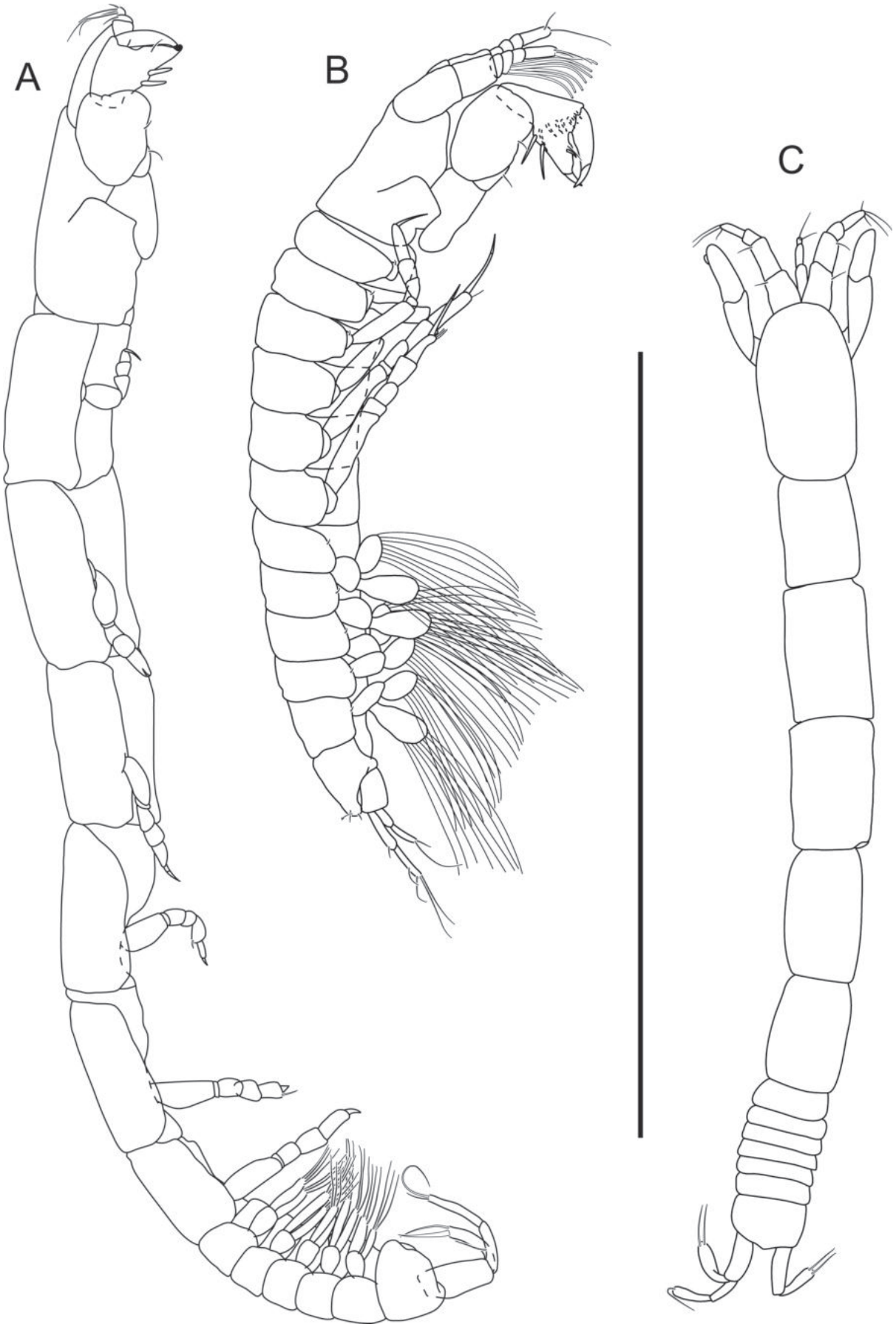

Figure 1. *Stenotanais leonardoi* sp. nov. **A.** Holotype, neuter (MZUSP 43545), lateral view; **B.** Paratype, male (MZUSP 43546), lateral view; **C.** Paratype, juvenile (MZUSP 43563), dorsal view. Scale bars: 1.0 mm.

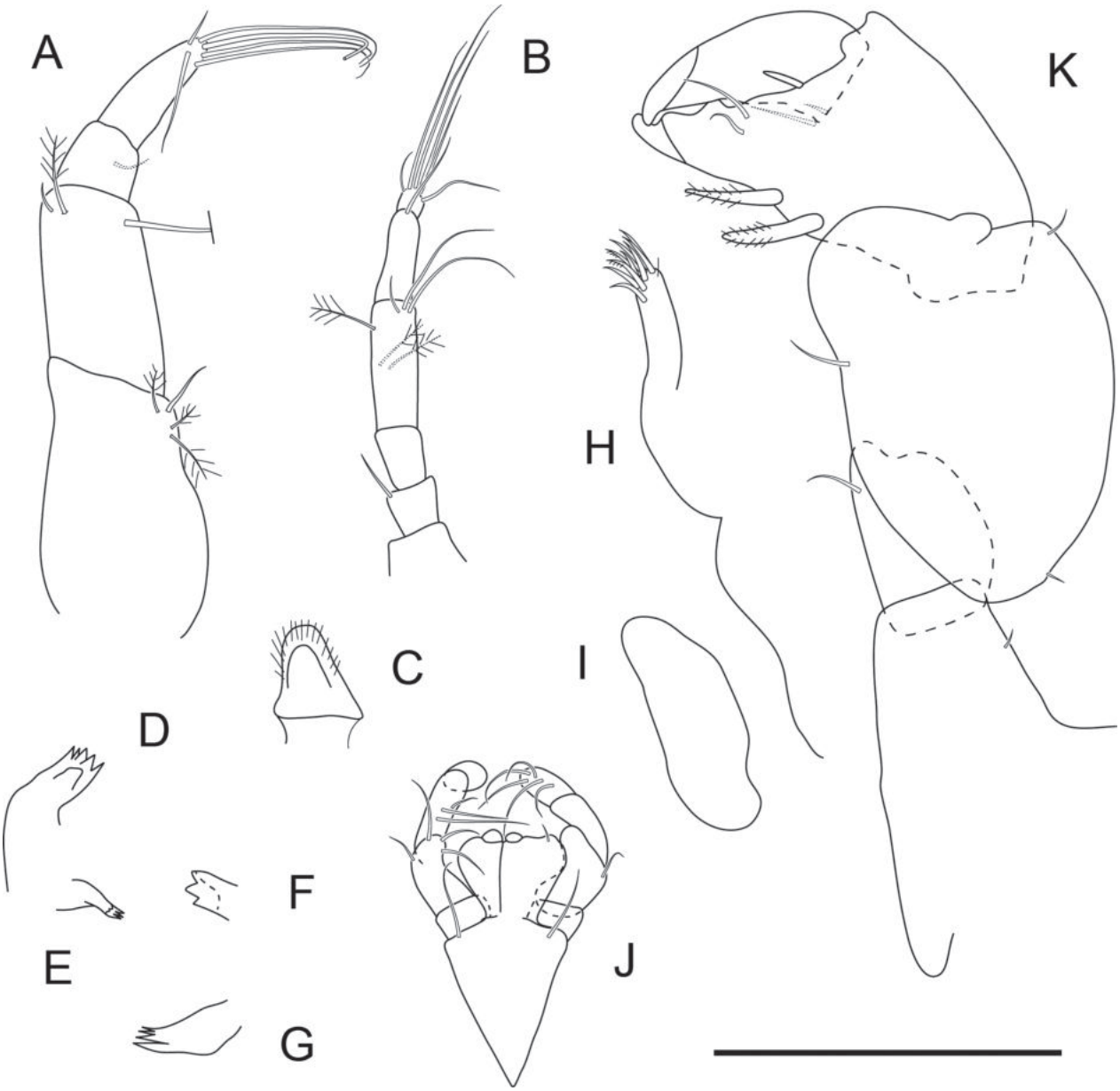

Figure 2. *Stenotanais leonardoi* sp. nov. Paratype, neuter dissected (MZUSP 43547). **A.** Antennule; **B.** Antenna; **C.** Labrum; **D.** Left mandible (incisor); **E.** Left mandible (molar); **F.** Right mandible (incisor); **G.** Right mandible (molar); **H.** Maxillule; **I.** Maxilla; **J.** Maxilliped; **K.** Cheliped. Scale bars: 0.1 mm.

microtrichia and two spinules, dorsodistal minute seta; dactylus 0.7× unguis, together 0.8× propodus.

Pereopod-3 (Fig. 3C) similar to pereopod-2, except basis naked.

Pereopod-4 (Fig. 3D) basis broken during dissection, naked; ischium with two long seta (only one drawn); merus 1.2× L:W, with two ventrodistal spines; carpus 1.6× L:W, with one seta and three distal spines; propodus stout 2.8× L:W, with two ventrodistal spines and robust dorsodistal seta; dactylus with double row of ventral spines, 1.9× unguis, together as long as propodus.

Pereopod-5 (Fig. 3E) similar to pereopod-4, except basis 2.4× L:W; 2.3× L:W, with dorsodistal minute and robust setae; dactylus and unguis together 1.2× propodus.

Pereopod-6 (Fig. 3F) similar to pereopod-5, except basis 1.9× L:W; ischium with two long seta (only one drawn); propodus short 1.6× L:W, with three robust dorsodistal setae (one long and two short); dactylus with larger ventral spines, 3.2× unguis, together 0.9× propodus.

Pleopod (Fig. 3G) basal article naked; exopod with at least four plumose setae on outer margin and one seta on inner margin; endopod with at least ten plumose setae on outer margin, large gap between most proximal.

Uropod (Fig. 3H) reflexed; basis long 2.3× L:W, about 1.1× pleotelson, naked; exopod (Fig. 3H") one-articled, somewhat wider than endopod, 0.7× endopod, with long medial seta and tipped by two specialised stout setae; endopod (Fig. 3H') two-articled; article-1 with distal seta; article-2 with long medial seta, two PSS and two simple distal setae.

Male (Figs 1B, 4A–C). The only specimen of a putative 'swimming male' of this species has a pereon short-

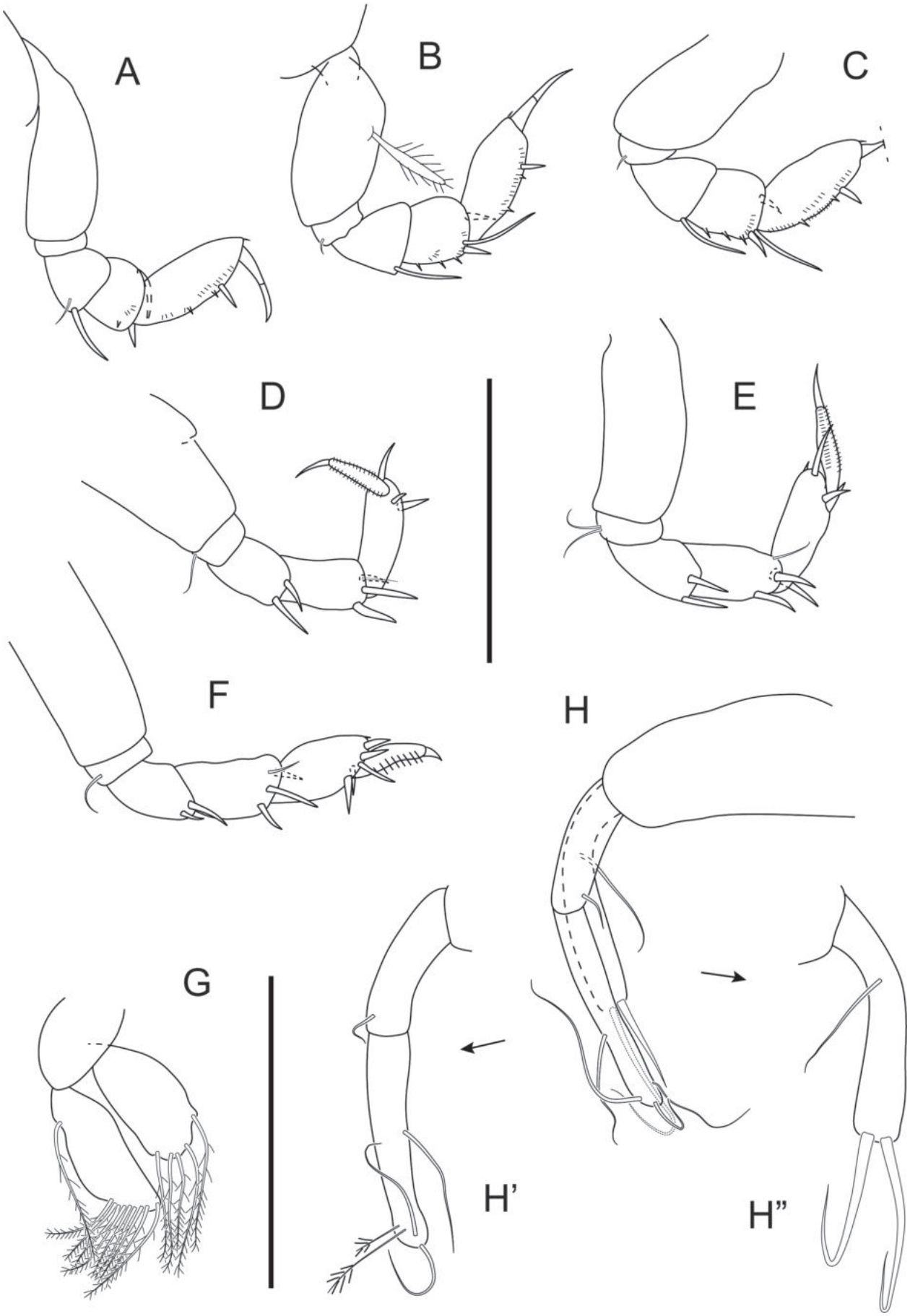

Figure 3. *Stenotanais leonardoi* sp. nov. Paratype, neuter dissected (MZUSP 43547). **A–F.** Pereopods 1–6; **G.** Pleopod; **H.** Uropod; **H'.** Uropod endopod; **H".** Uropod exopod. Scale bar: 0.1 mm.

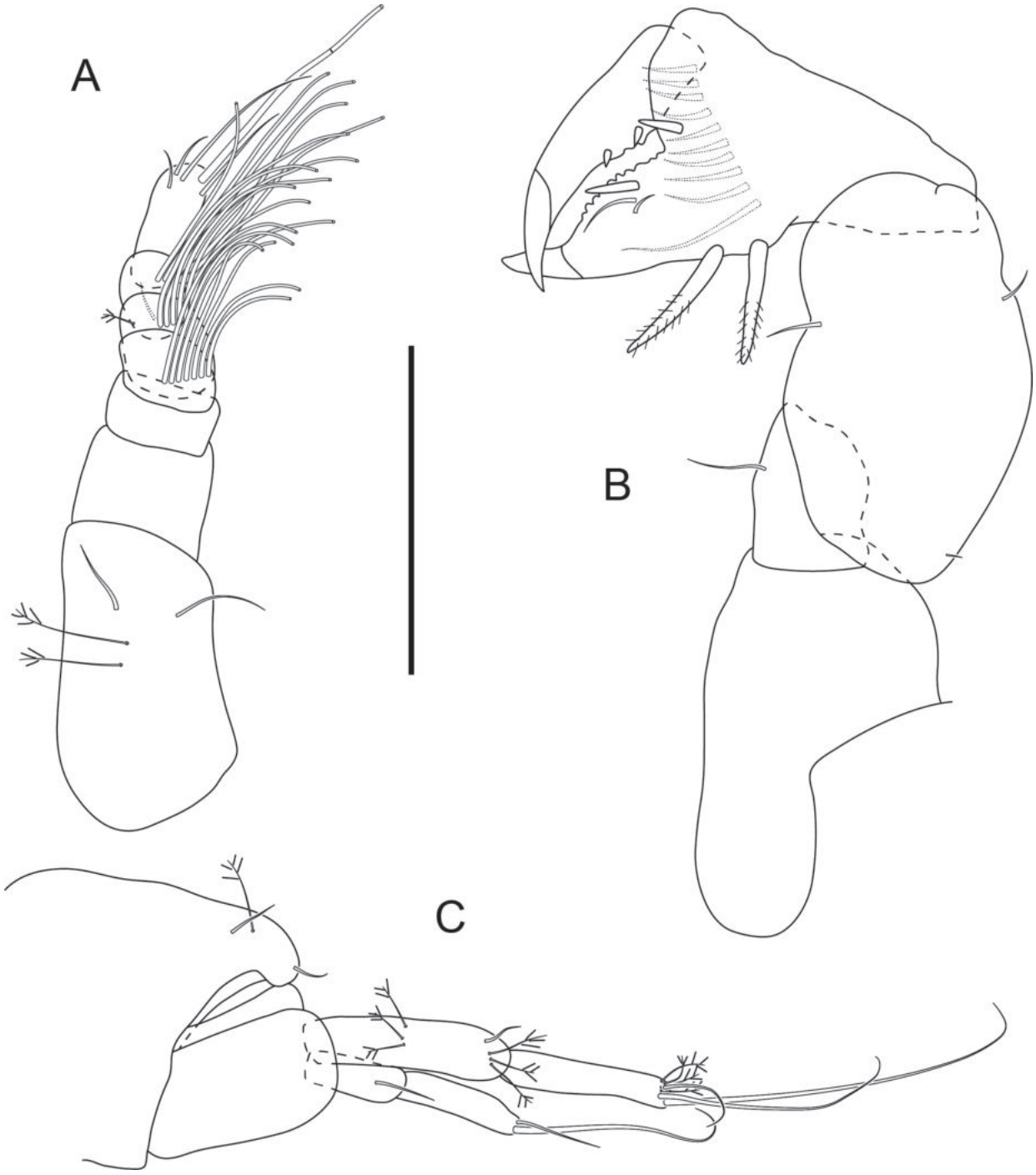

Figure 4. *Stenotanais leonardoi* sp. nov. Paratype, male (MZUSP 43546). **A.** Antennule; **B.** Cheliped; **C.** Uropod. Scale bar: 0.1 mm.

er than in female and a well-developed pleon (Fig. 1B), larger than in female, as long as the pereon. Antennule seven-articled (Fig. 4A), broader than female, with numerous aesthetascs. No functional mouthparts. Cheliped thinner than in female (Fig. 4B), propodus fixed finger and dactylus with sharp point. Pleopods strong, supported with long plumose setae (with more setae than female). Uropod biramous (Fig. 4C), endopod and exopod of two articles.

Type locality. Santa Catarina State, Brazil; stn A8 R2, -27,29679714, -46,62516071 (1045 m).

Distribution. Brazil: Santos Basin (Rio de Janeiro, São Paulo, Paraná and Santa Catarina States). Occurring on the lower slope and the São Paulo Plateau area, ranging from depths of 686 to 2410 m. This species was the most abundant (51 individuals), with 71% of the specimens found at 2–5 cm sediment layer (i.e. up to 25× their body length).

Remarks. This new species is similar to *S. crassiseta* from the NE Atlantic in having the propodus of pereopods 1–3 with a convex inferior margin bearing many spinules and the general shape of the uropod endopod, but is distinguished by: (1) the cheliped basis more slender 3.6× L:W (2.9× in *S. crassiseta*); (2) the cheliped fixed finger with two simple setae on cutting edge (three in *S. crassiseta*); (3) the pereopod-1 dactylus as long as

unguis (0.8× in *S. crassiseta*); (4) the pereopods 2–3 carpus with long spine, longer than half length of propodus (about one third in *S. crassiseta*); and (5) the uropod exopod one-articled and much longer than endopod article-1, 0.7× endopod (exopod two-articled and as long as endopod article-1, 0.4× in *S. crassiseta*).

Stenotanais leonardoi sp. nov. also resembles *S. macrodactylus* from the Gulf of Mexico (NW Atlantic) mainly by the shape of uropod; however, it differs by a combination of characters including: (1) antennule 0.6× cephalothorax (slightly shorter 0.8× in *S. macrodactylus*); (2) cheliped fixed finger with two simple setae on cutting edge (two 'spiniform setae' in *S. macrodactylus*); (3) pereopod-2 dactylus 0.7× unguis (more than twice in *S. macrodactylus*); and (4) pereopods 2–3 propodus with convex inferior margin with ventrodistal spine, microtrichia and spinules (only with ventrodistal spine in *S. macrodactylus*). The new species has the cheliped fixed finger with strong serrate spines ventrally, which could have been overlooked by other authors (e.g. as 'strong spines', Bird and Holdich (1984) or as 'robust spiniform setae', Larsen (2005, 2011)).

The male is of the 'swimming' type with no functional mouthparts, shortened pereon and multi-articulate antennule with multiple aesthetascs. This specimen was found in the same sample as an individual of *S. leonardoi* (a neuter) and was identified as this species by chelipedal features, such as the basis with a long posterior lobe, a carpal shield and well-developed fixed finger with two strong serrate ventral spines and uropod rami with subparallel margins (not oar-shaped as in *S. uropedon* sp. nov.). Only one male specimen was sampled while 50 neuters were collected, demonstrating how "unbalanced" the sexual ratio can be in tanaidacean species. However, as with all 'swimming males' and the rare matching of sexes, only with a molecular analysis can conspecificity be absolutely confirmed (Błażewicz-Paszkowycz et al. 2014).

Stenotanais uropedon sp. nov.

https://zoobank.org/0EA50F8D-E7F1-434D-A5A1-ED2E28B86E43
Figs 5–7

Material examined. ***Holotype*:** Brazil – São Paulo State • neuter, length 1.7 mm; stn D10 R3, 5–10 cm; MZUSP 43581.

***Paratypes*:** Brazil – Rio de Janeiro State • 1 neuter (dissected), length 1.7 mm; stn P10 R3, 5–10 cm; MZUSP 43582 – Santa Catarina State • 1 neuter; stn A8 R1, 0–2 cm; MZUSP 43583 – Paraná State • 1 neuter; stn B9 R1, 5–10 cm; MZUSP 43584 • 1 neuter; stn B9 R3, 5–10 cm; MZUSP 43585 – São Paulo State • 1 neuter; stn C8 R1, 2–5 cm (dissected); MZUSP 43586 • 1 neuter; stn E8 R1, 0–2 cm; MZUSP 43587 • 1 neuter; stn E8 R3, 2–5 cm; MZUSP 43588 • 1 neuter; stn E10 R2, 2–5 cm; MZUSP 43589 • 1 neuter; stn E10 R3, 5–10 cm; MZUSP 43590. – Rio de Janeiro State • 1 juvenile; stn F8 R2, 0–2 cm; MZUSP 43591 • 1 neuter; stn F8 R2, 2–5 cm; MZUSP 43592 • 1 neuter; stn F9 R3, 2–5 cm; MZUSP 43593 • 2 neuters; stn G9 R1, 0–2 cm; MZUSP 43594 • 1 juvenile; stn P3 R2, 2–5 cm; MZUSP 43595.

Diagnosis. Neuter. Cheliped fixed finger with two simple setae and one spine on cutting edge and a nearby spine on the distolateral margin of the propodal palm. Pereopods 2–3 carpus with long spine, longer than half length of propodus. Uropod endopod oar-shaped, with article-2 broad and flattened; exopod short, 0.3× of endopod length; both rami without specialised articulated setae.

Etymology. From the Greek 'pedon' (noun), meaning 'oar, rudder'; alluding to the shape of uropod endopod. The name is a noun in apposition with the generic name.

Description. Based on neuter holotype (MZUSP 43581) length 1.7 mm and dissected neuter paratype (MZUSP 43582) length 1.7 mm. Body (Fig. 5A) slender, about 8.5× L:W. Cephalothorax elongate 1.7× L:W, 1.7× pereonite-1, straight-sided, naked. Pereonites 1–6. All pereonites rectangular, parallel-sided; pereonite-1 0.8× L:W; pereonite-2 1.3× L:W; pereonites 3–4 1.2× L:W; pereonite-5 square, as long as wide; pereonite-6 shortest, 0.5× L:W. Pleon (Fig. 5A, B) short, 0.1× TBL, about as long as pereonites 5 and 6 combined, with five subequal pleonites, with one minute seta on lateral margins. Pleotelson (Fig. 5B) trapezoidal about 0.7× L:W, 0.4× pleon, with pointed posterior margin bearing two pairs of simple setae and one of PSS distally.

Antennule (Fig. 5C) 0.6× cephalothorax; article-1 0.5× TL, 1.9× L:W, with three middle PSS and one simple and two PSS distally; article-2 1.6× L:W, 0.6× article-1, with two simple (one long and one minute) and two distal PSS; article-3 1.1× L:W, 0.5× article-2, with simple subdistal seta; article-4 2.4× L:W, 1.5× article-3, with aesthetasc and six simple terminal setae. Antenna (Fig. 5D) article-1 fused with body; article-2 0.8× L:W, with one simple distal seta; article-3 1.3× L:W, naked; article-4 2.7× L:W, 1.9× article-3, with one simple medial seta and three simple setae and two distal PSS; article-5 3.0× L:W, 0.7× article-4, with one distal seta; article-6 minute with five simple terminal setae.

Labrum (Fig. 5E) large, hood-shaped, covered by minute setae on lateral and distal margins. Mandible (Figs. 5F, G) broken during dissection; left mandible (Fig. 5F) with incisor smooth; right mandible (Fig. 5G) with at least two teeth on incisor process, molar broken off during dissection. Maxillule (Fig. 5H) endite with eight terminal spines (at least two serrate), outer margin with setules; palp broken off during dissection. Maxilla (Fig. 5I) ovoid and stout, with one side wider, but large relative to maxilliped. Labium (Fig. 5J) with distal corner finely setose.

Maxilliped (Fig. 6A) basis with simple seta near articulation with palps, not reaching distal margin of endites; endites unfused, divided into three lobe-like structures, with one seta on distal edge; palp article-1 naked; article-2 with three inner (at least one serrate) and one outer setae; article-3 with three (two long, at least one serrate) inner setae; article-4 with four inner setae and one subdistal outer seta. Epignath not observed.

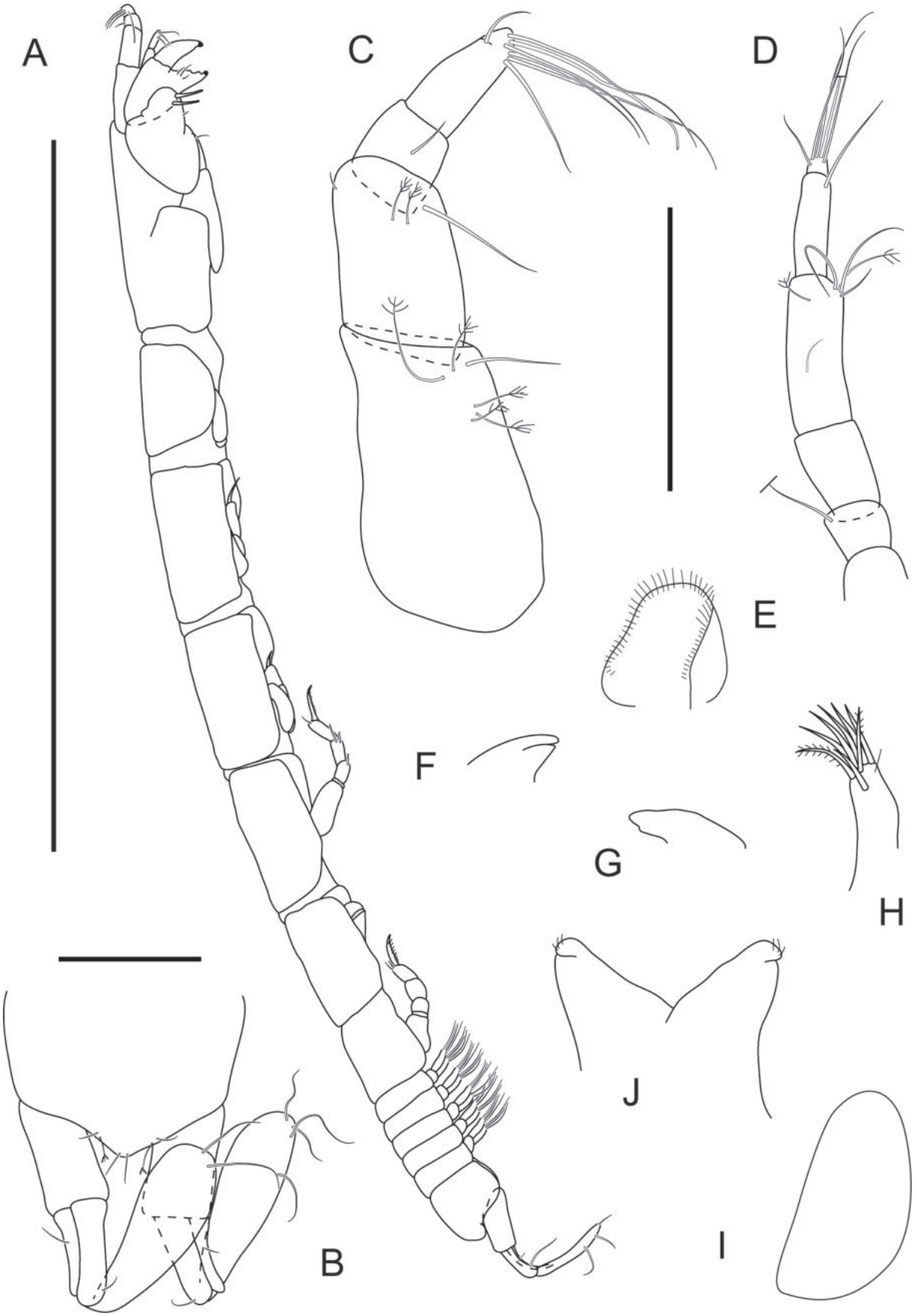

Figure 5. *Stenotanais uropedon* sp. nov. **A.** Holotype, neuter (MZUSP 43581), lateral view; **B.** Pleotelson and uropods, dorsal view; **C.** Antennule; **D.** Antenna; **E.** Labrum; **F.** Left mandible (incisor); **G.** Right mandible (incisor); **H.** Maxillule; **I.** Maxilla; **J.** Labium. Scale bars: 1.0 mm (**A**); 0.1 mm (**B–J**).

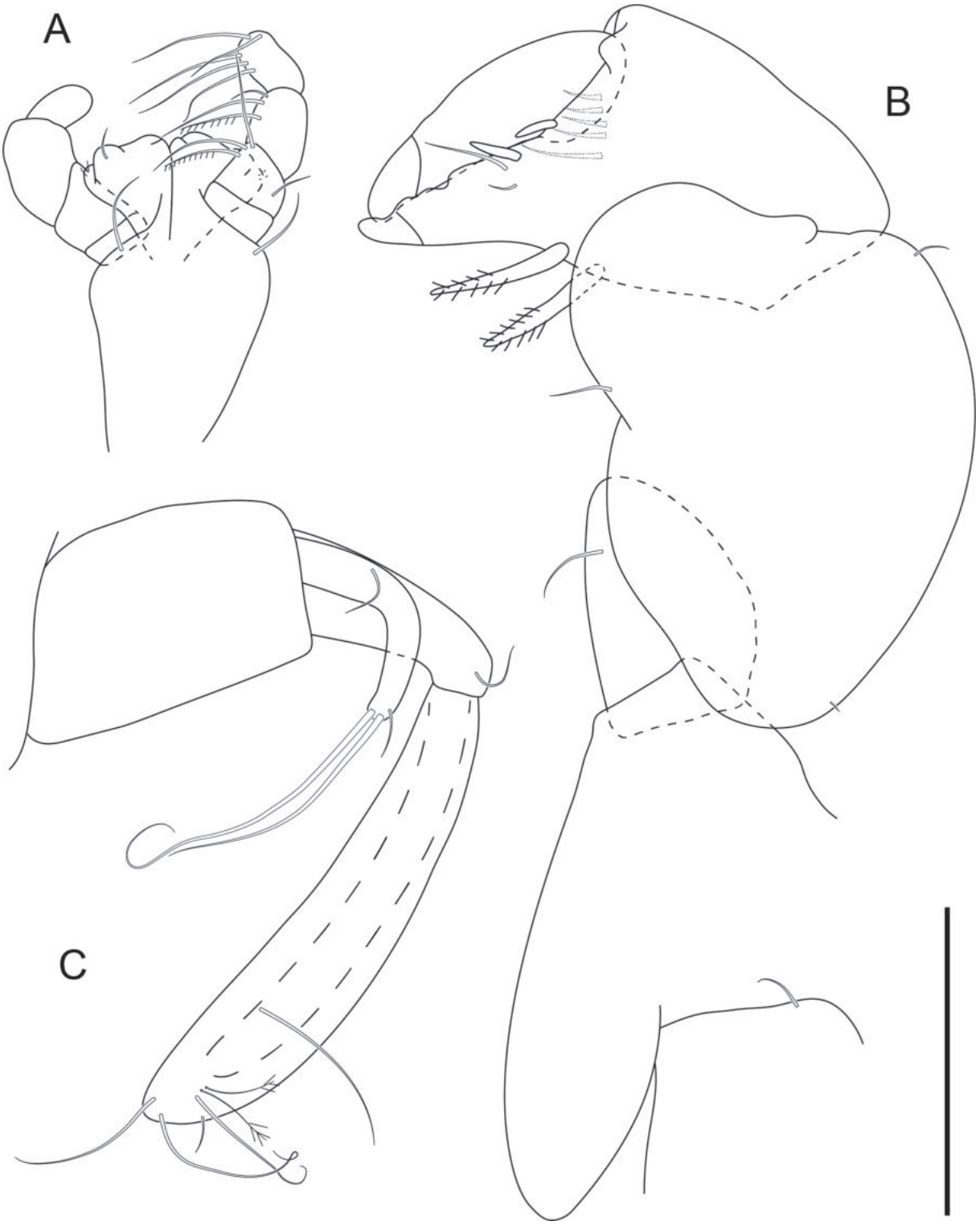

Figure 6. *Stenotanais uropedon* sp. nov. Paratype, neuter dissected (MZUSP 43582). **A.** Maxilliped; **B.** Cheliped; **C.** Uropod. Scale bars: 0.1 mm.

Cheliped (Fig. 6B) calcified; basis attached to cephalothorax by large sclerite with dorsodistal setae; basis with long posterior lobe, not reaching pereonite-1, 3.9× L:W; merus subtriangular, with one ventral seta; carpus stout 1.4× L:W, with one ventral seta and one proximal and one dorsodistal setae, carpal shield well developed; propodus stout 0.9× carpus, 1.6× L:W, with an outer spine and five setae near dactylus insertion on inner side; fixed finger with two strong serrate spines ventrally; cutting edge with two simple setae and one spine; dactylus slightly shorter than fixed finger.

Pereopod-1 (Fig. 7A) coxa with small seta; basis broad 1.8× L:W, naked; ischium with seta; merus 1.3× L:W, with ventrodistal seta and long serrate spine not

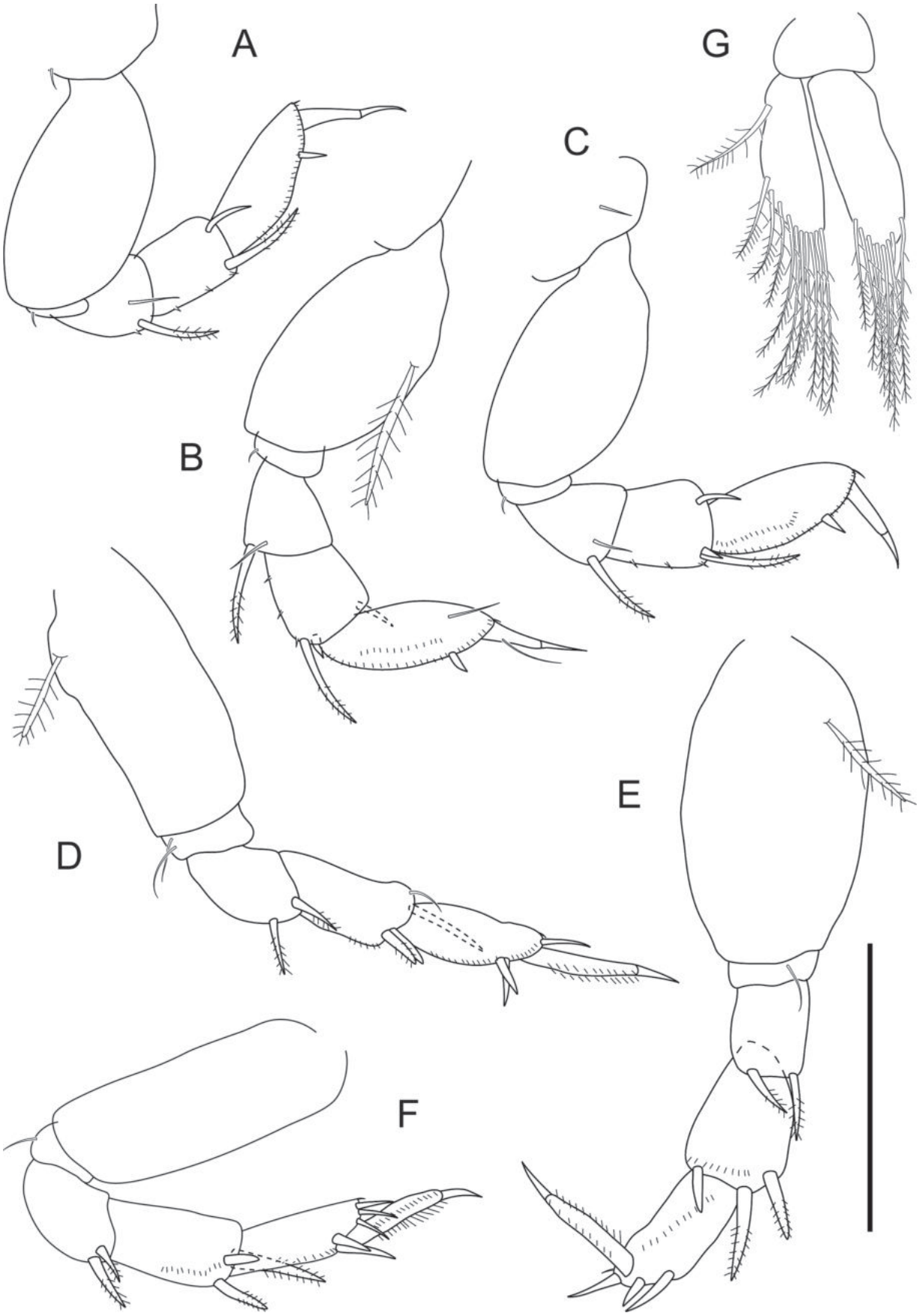

Figure 7. *Stenotanais uropedon* sp. nov. Paratype, neuter dissected (MZUSP 43582). **A–F.** Pereopods 1–6; **G.** Pleopod. Scale bars: 0.1 mm.

reaching carpus distal margin; carpus 1.2× L:W, about as long as merus, with ventrodistal long serrate spine, dorsodistal spine and ventral spinules; propodus 2.2× L:W, 1.6× carpus, with convex inferior margin with ventrodistal spine and microtrichia, one dorsodistal minute seta; dactylus 1.3× unguis; together 0.8× propodus.

Pereopod-2 (Fig. 7B) coxa with a small seta (not drawn); basis broad 1.7× L:W, with large dorsal PSS; ischium with one seta; merus 1.1× L:W, with a ventrodistal seta and long serrate spine almost reaching carpus distal margin; carpus about as long as wide, about as long as merus, with ventral spinules, two unequal ventrodistal spines (one about half length of propodus) and dorsodistal spine; propodus 2.1× L:W, 1.6× carpus, with convex inferior margin with ventrodistal spine and microtrichia, one mid-dorsal simple seta and one dorsodistal minute seta; dactylus 1.1× unguis, with one seta; together 0.7× propodus.

Pereopod-3 (Fig. 7C) similar to pereopod-2, except basis 1.9× L:W, naked; dactylus 1.4× unguis, naked.

Pereopod-4 (Fig. 7D) basis about 2.3× L:W, with large ventral PSS; ischium with two long setae; merus 1.3× L:W, with two ventrodistal serrate spines; carpus 1.8× L:W, with one seta and three (one long and two short) distal spines; propodus stout 2.4× L:W, with two ventrodistal spines and one robust and one minute dorsodistal setae; dactylus long with double row of ventral spines, 2.4× unguis, together 1.1× propodus.

Pereopod-5 (Fig. 7E) similar to pereopod-4, except basis 1.8× L:W; ischium with two long setae (only one drawn); carpus 1.2× L:W, with three distal spines; propodus 2.2× L:W.

Pereopod-6 (Fig. 7F) similar to pereopod-5, except basis 2.7× L:W, naked; merus 1.4× L:W; carpus 1.7× L:W; propodus 2.6× L:W, with three robust dorsodistal setae; dactylus with larger ventral spines, 2.6× unguis.

Pleopod (Fig. 7G) basal article naked; exopod with at least seven plumose setae on outer margin and one seta on inner margin; endopod with at least ten plumose setae and one more robust proximal seta on outer margin, large gap between most proximal.

Uropod (Fig. 6C) rami reflexed; basis 1.4× L:W, 0.6× pleotelson, naked; exopod one-articled, 0.3× endopod, with medial seta and tipped by two stout and one simple setae; endopod two-articled; article-1 with one distal seta; article-2 oar-shaped, with one long medial seta and two PSS and four simple distal setae.

Type locality. São Paulo State, Brazil; stn D10 R3, -25,94725395, -44,83425777 (1906 m).

Distribution. Brazil: Santos Basin (Rio de Janeiro, São Paulo, Paraná and Santa Catarina States). Occurring on the lower slopes and the São Paulo Plateau area, ranging from depths of 991–1974 m. Twenty-two individuals of this species were collected, with 41% of them found in the 5–10 cm sediment layer (i.e. up to 50–60× their body length) and 32% at a depth of 2–5 cm.

Remarks. This new species resembles *S. hamicauda* from the NE Atlantic by the oar-shaped uropod, but is different from it by: (1) cheliped fixed finger with two simple setae and one spine on cutting edge (three simple setae in *S. hamicauda*); (2) pereopods 1–3 dactylus 1.3× unguis (about as long as in *S. hamicauda*); (3) uropod endopod oar-shaped (in *S. hamicauda* the exopod is oar-shaped); and (4) exopod short, 0.3× endopod length (in *S. hamicauda* exopod reaching about 0.8× endopod length).

Stenotanais uropedon sp. nov. differs from *S. leonardoi* by its oar-shaped uropod endopod, with the article-2 broad and flattened (with short exopod, 0.3× endopod), whereas in *S. leonardoi*, the exopod is slightly wider than the endopod (0.7× endopod). Additionally, *S. uropedon* has pereopods with the merus and carpus having long serrate distoventral spines, which are different from those of *S. leonardoi* (with simple spines); however, these different forms could have been overlooked by previous authors in other congeneric species.

Key to the *Stenotanais* species

Modified from Larsen (2005, 2011)

1	Cheliped carpus without large ventrodistal shield	*S. arenasi*
–	Cheliped carpus with large ventrodistal shield	2
2	Uropod exopod or endopod distinctly oar-shaped (broader distally)	3
–	Uropod exopod or endopod slender/subparallel-sided	4
3	Uropod exopod oar-shaped, reaching at least to 0.75× of entire endopod length; exopod with two specialised flattened setae	*S. hamicauda*
–	Uropod endopod oar-shaped, with article-2 broad and flattened; exopod 0.3× of entire endopod length; exopod with two flat and wide setae	*S. uropedon* sp. nov.
4	Uropod basal article longer than pleotelson; exopod one-articled	5
–	Uropod basal article shorter than pleotelson; endopod with one flat and wide seta distally; exopod two-articled without flat and wide setae	*S. crassiseta*
5	Uropod exopod with one flat and wide seta at mid-length and two articulated wide terminal setae	*S. macrodactylus*
–	Uropod exopod with two flat and wide terminal setae	*S. leonardoi* sp. nov.

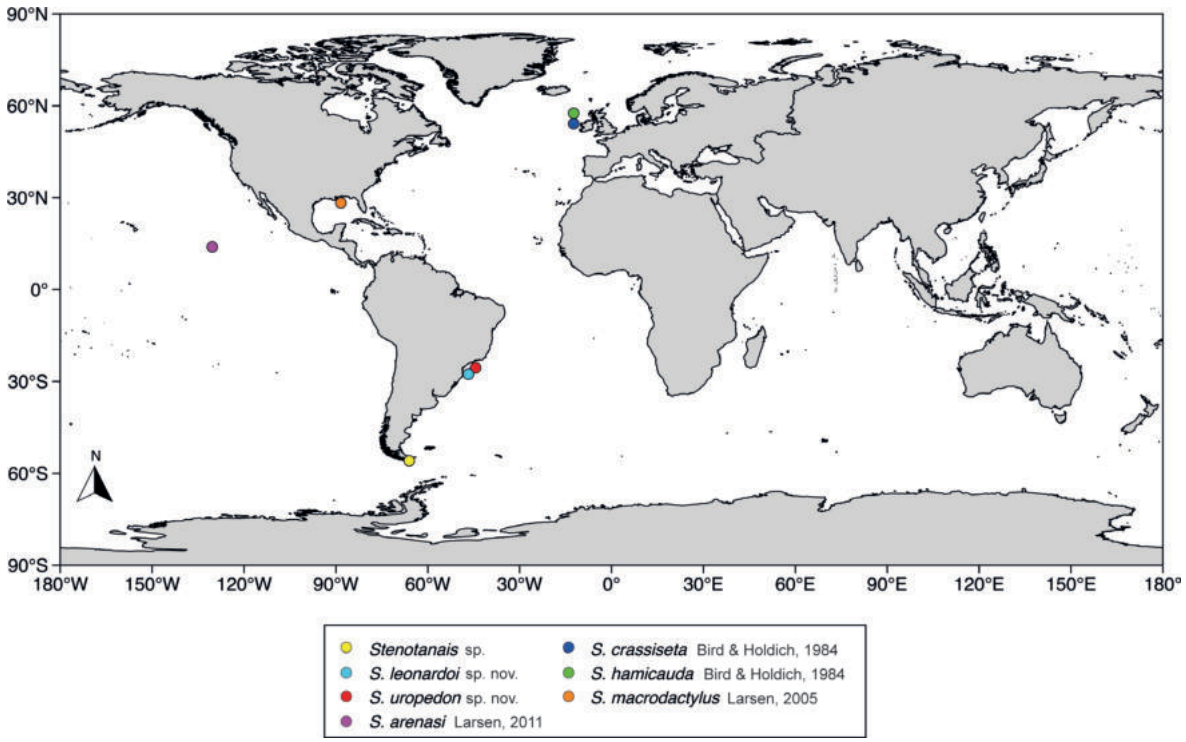

Figure 8. Geographic distribution of *Stenotanais* species based on the present study and literature data (Bird and Holdich 1984; Schmidt and Brandt 2001; Larsen 2005, 2011).

Discussion

This is the first Brazilian species described of the family Akanthophoreidae and the second record of the genus *Stenotanais* in the Southern Hemisphere. *Stenotanais* was first reported from the Southern Hemisphere on the continental slope of Magellan Region (Beagle Channel; 1279 m) (Schmidt and Brandt 2001), but the species was not identified and could not be compared to the two new species presented herein; this record was included on the distribution map of the genus as *Stenotanais* sp. (Fig. 8) for future studies to establish if this Subantarctic taxon refers to a different species. *Stenotanais* is now composed of six species, five of them distributed in the Atlantic Ocean (Fig. 8): two in the NE Atlantic – *S. crassiseta* and *S. hamicauda*, one in the NW Atlantic – *S. macrodactylus* and the two new species from Brazil, SW Atlantic. Only *S. arenasi* was recorded from the Pacific Ocean, but this classification should be further investigated (see genus remarks).

The two new deep-burrowing species of *Stenotanais* described here bring the total number of akanthophoreids to 56 species and that of all tanaidaceans in Brazilian waters to 66 species. Although many papers on Tanaidacea off Brazilian waters have been published in recent years, we are still discovering new taxa in this region, with plenty of new species to be discovered in the future. Taxonomic works from understudied areas, such as the Brazilian deep-waters, provide a basis for future studies in fields such as biogeography, ecology and evolution and, although several papers have been published in the last decade, there is still much to be investigated regarding the tanaidaceans of Brazil.

Acknowledgements

The authors are grateful to the PETROBRAS/CENPES, which coordinated the fieldworks and made available the material examined. The first author also would like to thank Fundação de Apoio à Universidade de São Paulo (FUSP) for providing the postdoctoral fellowship (PIPD) during the course of this study. We also would like to thank the contribution of David Drumm and anonymous referees for their helpful comments and suggestions on the manuscript.

JLS and MT contributed to designing the study; JLS received funds for this work, identified the material, worked on illustrations, prepared the tables and wrote the manuscript; GB and MT reviewed the text; GB reviewed the English language. All authors read and approved the final manuscript and consent to publication.

References

Bamber RN (2014) Interstitial Tanaidaceans (Crustacea: Peracarida) from São Miguel, Açores, with description of five new species. Acoreana 10: 17–56.

Bamber RN, Bird GJ, Błażewicz-Paszkowycz M, Galil B (2009) Tanaidaceans (Crustacea: Malacostraca: Peracarida) from soft-sediment habitats off Israel, eastern Mediterranean. Zootaxa 2109(1): 1–44. https://doi.org/10.11646/zootaxa.2109.1.1

Bird GJ (2004) The Tanaidacea (Crustacea, Peracarida) of the North-East Atlantic: The shelf and bathyal Paratyphlotanais of the "Atlantic Margin.". Journal of Natural History 38: 1359–1384. https://doi.org/10.1080/0022293031000155359

Bird GJ, Holdich DM (1984) New Deep-sea Leptognathiid Tanaids (Crustacea, Tanaidacea) from the North-east Atlantic. Zoologica Scripta 13(4): 285–315. https://doi.org/10.1111/j.1463-6409.1984.tb00044.x

Błażewicz-Paszkowycz M (2014) Crustacea: Tanaidacea. In: Broyer C De, Koubbi P, Griffiths H, Raymond B, D'Acoz C d'Udekem, Putte A Van de, Danis B, David R, Grant S, Gutt J, Held C, Hosie G, Huettmann F, Post A, Ropert-Coudert Y (Eds) The Biogeographic Atlas of The Southern Ocean. The Scientific Committee on Antarctic Research, Scott Polar Research Institute, Cambridge, 173–180.

Błażewicz-Paszkowycz M, Bamber RN (2011) Tanaidomorph tanaidacea (crustacea: Peracarida) from mud-volcano and seep sites on the Norwegian Margin. Zootaxa 3061(1): 1–35. https://doi.org/10.11646/zootaxa.3061.1.1

Błażewicz-Paszkowycz M, Jennings RM, Jeskulke K, Brix S (2014) Discovery of swimming males of Paratanaoidea (Tanaidacea). Polish Polar Research 35(2): 415–453. https://doi.org/10.2478/popore-2014-0022

Guerrero-Kommritz J (2004) A revision of the genus *Paraleptognathia* Kudinova-Pasternak, 1981 (Crustacea: Tanaidacea) and description of four new species. Zootaxa 481(1): 1–63. https://doi.org/10.11646/zootaxa.481.1.1

Guerrero-Kommritz J (2005) Review of the genus *Chauliopleona* Dojiri and Sieg, 1997 (Crustacea, Peracarida, Tanaidacea) and description of three new species. Journal of Natural History 39(16): 1177–1210. https://doi.org/10.1080/00222930420001975 86

Guerrero-Kommritz J, Brandt A (2005) Phylogenetic analysis of genera of "Akanthophoreinae" (Crustacea: Tanaidacea). Organisms, Diversity & Evolution 5(4): 285–296. https://doi.org/10.1016/j.ode.2004.12.005

Guimarães CPG, de Carvalho MAO, Guimarães DA de O (2020) Macrofauna do sistema bentônico do talude continental de Sergipe e sul de Alagoas. In: Arguelho M de LP de M, Carneiro MER (Eds) Geoquímica e Bentos do Talude Continental de Sergipe-Alagoas. Editora UFS, São Cristovão, 203–250.

Jóźwiak P, Drumm DT, Błażewicz M (2018a) A new genus of family Akanthophoreidae and new species of genus *Parakanthophoreus* Larsen & Araújo-Silva, 2014 (Crustacea: Tanaidacea: Tanaidomorpha) from the North Atlantic. Marine Biodiversity 48(2): 897–914. https://doi.org/10.1007/s12526-018-0866-9 [BIODIVERSITY]

Jóźwiak P, Janicka M, Dębiec P, Stępiński A, Mielczarz K, Serigstad B, Błażewicz M (2018b) New Tanaidacea (Crustacea: Peracarida) from the Gulf of Guinea. Marine Biodiversity 48(4): 1715–1730. https://doi.org/10.1007/s12526-017-0646-y

Larsen K (2003) Proposed new standardized anatomical terminology for the Tanaidacea (Peracarida). Journal of Crustacean Biology 23(3): 644–661. https://doi.org/10.1651/C-2363

Larsen K (2005) Deep-Sea Tanaidacea (Peracarida) from the Gulf of Mexico. Brill, Leiden, 381 pp. https://doi.org/10.1163/9789047416883

Larsen K (2011) The tanaidacean assemblage from the Central Pacific Manganese Nodule Province. II. The genera Stenotanais and Typhlotanais (Crustacea). Zootaxa 3088(1): 39–53. https://doi.org/10.11646/zootaxa.3088.1.4

Larsen K, Araújo-Silva CL (2014) The ANDEEP Tanaidacea (Crustacea: Peracarida) revisited III: The family Akanthophoreidae. Zootaxa 3796: 237–264. https://doi.org/10.11646/zootaxa.3796.2.2

Lavrado HP, Disaró ST, Esteves AM, da Fonsêca-Genevois V, Mello e Sousa SH de, Omena EP, Paranhos R, Sallorenzo IA, Veloso VG, Ribeiro-Ferreira VP, Curbelo-fernandez MP, Falcão AP da C (2017a) Comunidades bentônicas dos substratos inconsolidados da Plataforma continental e Talude continental da Bacia de Campos: uma visão integrada entre seus componentes e suas relações com o ambiente. In: Falcão AP da C, Lavrado HP (Eds) Ambiente Bentônico: caracterização ambiental regional da Bacia de Campos, Atlântico Sudoeste. Elsevier Ltd., Rio de Janeiro, 307–352. https://doi.org/10.1016/B978-85-352-7263-5.50010-2

Lavrado HP, Omena EP, Bernardino AF (2017b) Macrofauna bentônica do Talude continental e cânions da Bacia de Campos. In: Falcão AP da C, Lavrado HP (Eds) Ambiente Bentônico: caracterização ambiental regional da Bacia de Campos, Atlântico Sudoeste. Elsevier Ltd., Rio de Janeiro, 259–306. https://doi.org/10.1016/B978-85-352-7263-5.50009-6

Schmidt A, Brandt A (2001) The tanaidacean fauna of the Beagle Channel (southern Chile) and its relationship to the fauna of the Antarctic continental shelf. Antarctic Science 13(4): 420–429. https://doi.org/10.1017/S095410200100058X

Sieg J (1986) Tanaidacea (Crustacea) von der Antarktis und Subantarktis. Mitteilungen aus der Zoologischen Museum der Universität Kiel 2: 1–80.

WoRMS (2023) Tanaidacea. http://www.marinespecies.org/aphia.php?p=taxdetails&id=1133 [March 3, 2023]

Supplementary material 1

Benthic samples with *Stenotanais* specimens obtained during Santos Project (PCR-BS) – Santos Basin Environmental Characterization (Brazil).

Authors: Juliana Lopes Segadilha, Graham Bird, Marcos Tavares

Data type: Table (word file).

Link: https://doi.org/10.3897/zse.99.103003.suppl1

Zoosyst. Evol. 99 (2) 2023, 439–455 | DOI 10.3897/zse.99.102575

PENSOFT

MUSEUM FÜR NATURKUNDE BERLIN

Two new *Oxynoemacheilus* species in western Anatolia (Teleostei, Nemacheilidae)

Davut Turan[1], Sadi Aksu[2], Gökhan Kalayci[1]

1 *Recep Tayyip Erdogan University, Faculty of Fisheries, 53100 Rize, Türkiye*

2 *Eskişehir Osmangazi University, Vocational School of Health Services, 26700 Eskişehir, Türkiye*

https://zoobank.org/8D151C12-8994-4338-BFFA-48F4DE5DA4A0

Corresponding author: Gökhan Kalayci (gokhan.kalayci@erdogan.edu.tr)

Academic editor: Nicolas Hubert ♦ **Received** 23 February 2023 ♦ **Accepted** 9 June 2023 ♦ **Published** 4 October 2023

Abstract

Oxynoemacheilus sakaryaensis **sp. nov.**, is restricted to the Sakarya River basin, and *O. melenicus* **sp. nov.**, is distributed in both the Sakarya River and Büyükmelen Stream. *Oxynoemacheilus sakaryaensis* is distinguished by having a flank plain or with numerous irregularly shaped pale brownish bars and a caudal-peduncle depth 2.8–3.2 times in its length. *Oxynoemacheilus melenicus* is distinguished by having a flank with 10–13 irregular shaped brownish bars or blotches and the caudal peduncle depth 1.9–2.8 times in its length. *Oxynoemacheilus banarescui*, *O. samanticus*, *O. simavicus*, *O. fatsaensis*, *O. sakaryaensis*, and *O. melenicus* are valid, which belong to the *O. bergianus* species group. *O. melenicus* and *O. sakaryaensis* were differentiated from all other *Oxynoemacheilus* species in western Anatolia by two diagnostic and unique nucleotide substitution sites in the COI barcoding region. Also, species delineation tests (ABGD, GMYC, ASAP) and phylogenetic analyses support the validity of *O. melenicus* and *O. sakaryaensis* as distinct species.

Key Words

Cytochrome oxidase I, freshwater fish, molecular identification, Northwestern Anatolia, species delineation, taxonomy

Introduction

Nemacheilid loaches of the genus *Oxynoemacheilus* are widespread fishes all over the Eastern Mediterranean, the southern Caucasus, Anatolia, Mesopotamia, and Central Iran (Freyhof et al. 2011, 2022; Kottelat 2012). Freyhof et al. (2011) list 41 species as valid in that genus, and Kottelat (2012) also included *O. oxianus* from the Central Asian Amu-Darya drainage. Since, Çiçek et al. (2018); Erk`akan (2012); Freyhof (2016); Freyhof et al. (2017, 2019, 2021a, 2021b, 2022); Freyhof and Abdullah (2017); Freyhof and Geiger (2021); Freyhof and Özuluğ (2017); Kamangar et al. (2014); Kaya et al. (2020, 2021); Saygun et al. (2021); Sayyadzadeh et al. (2016); Sungur et al. (2017); Turan et al. (2019); Yoğurtçuoğlu et al., (2021a, 2021b); Yoğurtçuoğlu et al. (2022) described and re-validated additional species and we recognize 62 species of *Oxynoemacheilus* as valid. *Oxynoemacheilus* is one of the largest genera of freshwater fishes in the Western Palearctic. It has been reviewed comprehensively in the global distribution zone due to the many species. Indeed, most *Oxynoemacheilus* species are distributed in small ranges except *O. bergianus*, which lives in both the Caspian Sea basin and the Persian Gulf basin (Freyhof 2016; Freyhof and Abdullah 2017; Freyhof and Özuluğ 2017; Freyhof et al. 2017; Freyhof et al. 2022). In recent years, new species (*O. veyseli*, *O. elsae*, *O. ciceki*) have been discovered from stretching Anatolia and nearby basins (Çiçek et al. 2018; Eagderi et al. 2018; Sungur et al. 2017; Freyhof et al. 2022).

Freyhof et al. (2022) treated four species within *O. bergianus* species group as valid, corresponding to *O. banarescui*, *O. bergianus*, *O. fatsaensis*, and *O. simavicus*. Bektaş et. al (2022) reported *O. bergianus*, *O. samanticus*, *O. fatsaensis*, *O. banarescui* and O. *simavicus* as valid species. Freyhof et al. (2022) reported O. *simavicus*

from drainages in the southern shores of the Marmara Sea, as well as the Sakarya and Büyükmelen Stream. In this study, these populations of the species in Sakarya and Büyükmelen rivers are described as new species as *O. sakaryaensis* and *O. melenicus*. These two species are included in the *O. bergianus* species group, which has a slender caudal peduncle and lack the two distinct black or dark-brown spots on the caudal fin base and the presence of suborbital flap or groove.

Material and methods

The care of experimental animals was consistent with the Republic of Turkey's animal welfare laws, guidelines, and policies. After anesthesia, fishes were fixed in 5% formaldehyde stored in 70% ethanol or directly fixed in 99% ethanol. Measurements were made with a dial caliper and recorded to 0.1 mm. All measurements were made point-to-point, never by projections. Methods for counts and measurements followed Kottelat and Freyhof (2007) and the terminology of head canals followed Kottelat (1990). Standard length (SL) was measured from the tip of the snout to the end of the hypural complex. The length of the caudal peduncle was measured from behind the base of the last anal-fin ray to the end of the hypural complex, at mid-height of the caudal-fin base. The last two branched rays articulating on a single pterygiophore in the dorsal and anal fins are counted as "1½". Simple rays of dorsal and anal fins were not counted as they were deeply embedded. The holotype was included in the calculation of means and SD. Males of several *Oxynoemacheilus* show an exposed lachrymal bone, which is often called a suborbital flap or groove. We distinguish between a suborbital flap and a suborbital groove. In the present study, all *Oxynoemacheilus* having an exposed lachrymal bone possess a suborbital groove.

We see no application in developing identification keys for several species in large geographic areas. Therefore, we provide keys for western Anatolia only. Differential species diagnoses are given against related species as derived by the COI molecular analysis presented here and against geographically adjacent species. No differential diagnosis is provided against largely unrelated and/or geographically distant species.

Abbreviations used: **SL**, standard length; **K2P**, Kimura 2-parameter. Collection codes: **FFR**, Recep Tayyip Erdogan University Zoology Museum of the Faculty of Fisheries, Rize. Materials examined are listed at the end of the study.

DNA extraction, PCR and sequencing

Total DNA was extracted from fin clips via Qiacube automated DNA/RNA purification system using Qiagen DNeasy Blood & Tissue Kits (Qiagen, Hilden, Germany). DNA quality and quantity were checked on a NanoDrop 2000/c spectrophotometer (Thermo Scientific, Rockford, IL, USA) and 0.8% agarose gel electrophoresis. The standard vertebrate DNA barcode region of *COI* gene (645 bp) was amplified using a universal *COI* barcoding primer pair, the FishF1 (5'-TCAACCAACCACAAAGACATTGGCAC-3') and FishR1 (5'-TAGACTTCTGGGTGGCCAAAGAATCA-3') (Ward et al. 2005). PCR reactions were performed in a 50 µL reaction volume containing 5 µL 10× PCR buffer, 100 ng template DNA, 0.5 mM dNTPs mix, 3 mM $MgCl_2$, 0.5 mM of each primer, and 1 µL Taq DNA polymerase (New England Biolabs). The polymerization was carried out under the following conditions: initial denaturation at 95 °C for 30 s, denaturation at 95 °C for 30 s, annealing at 58 °C for 45 s, extension at 68 °C for 1 min through 35 cycles, and a final extension at 68 °C for 5 min using Biorad T100 (Bio-Rad, Hercules, CA, USA) thermal cycler. The PCR products were also run and visualized under UV Quantum–Capt ST4 system (Vilber Lourmat, France), purified, and sequenced at Macrogen Europa Inc. (Amsterdam, Netherlands).

Molecular data analysis

We have used the newly generated 30 DNA barcodes from the present study and included additional 42 specimens from earlier studies deposited to NCBI GenBank (Geiger et al. 2014, Geiger 2019, Turan et al. 2019, Bektas et al. 2022, Freyhof et al. 2022) (Table 1). The dataset also consisted of DNA barcodes from individuals *Seminemacheilus lendlii* and *Oxynoemacheilus cemali* as outgroup taxon. Clustal W algorithm (Thompson et al. 1994) in Bioedit v7.2.5 (Hall 1999) was used to align COI barcode sequences, and the sequences were submitted to NCBI GenBank with accession numbers OQ332806–OQ332835. Phylogenetic relationships among species were carried out using both maximum likelihood (ML) and Neighboor Joining (NJ) analysis using MEGA 11 (Tamura et al. 2021). TrN+G model (Kimura 1980) was chosen as the best nucleotide substitution model according to the Bayesian information criterion (BIC) in jModeltest v. 0.0.1 (Posada 2008). The K2P distance model (Kimura 1980) in MEGA 11 was used to estimate pairwise genetic distances among species. POPART (1.7) (Leigh and Bryant 2015) was used to generate and display the haplotype network. We used three single-locus species delimitation methods relying on different operational criteria for species delimitation being implemented: ABGD, Automatic Barcode Gap Discovery (Puillandre et al. 2012), Assemble Species by Automatic Partitioning (ASAP) (Puillandre et al. 2021) and GMYC, the General Mixed Yule Coalescent method, single-threshold version (Fujisawa and Barraclough 2013). All species delimitation methods were performed using the COI sequences (not haplotypes). The ABGD species delimitation was performed via the ABGD web server with default settings (https://bioinfo.mnhn.fr/abi/public/abgd/abgdweb.html, accessed on 1 May 2023) and ASAP species delimitation was performed via the ASAP web server (https://bioinfo.mnhn.fr/abi/public/asap/asapweb.html, accessed on 1 May 2023) and the following parameters:

Table 1. List of COI sequences downloaded from NCBI GenBank with information on drainage and country of origin.

Species	Accession N.	Drainage	Reference
O. melenicus	OK316642	Asar stream, Büyükmelen River	Freyhof et. al. 2022
O. melenicus	MH018854	Büyükmelen drainage	Turan et. al. 2019
O. melenicus	MH018856	Büyükmelen drainage	Turan et. al. 2019
O. melenicus	OK316651	Asar stream, Büyükmelen	Freyhof et. al. 2022
O. melenicus	OK316688	Doğançay, Sakarya River	Freyhof et. al. 2022
O. melenicus	MH018855	Büyükmelen drainage	Turan et. al. 2019
O. melenicus	OK316739	Asar stream, Büyükmelen River	Freyhof et. al. 2022
O. melenicus	OK316620	Allıkova stream, Sakarya River	Freyhof et. al. 2022
O. melenicus	OK316798	Allıkova stream, Sakarya River	Freyhof et. al. 2022
O. sakaryaensis	OK316616	Bayındır stream, Sakarya River	Freyhof et. al. 2022
O. sakaryaensis	OK316622	Bayındır stream, Sakarya River	Freyhof et. al. 2022
O. sakaryaensis	OK316635	Bayındır stream, Sakarya River	Freyhof et. al. 2022
O. sakaryaensis	OK316735	Bayındır stream, Sakarya River	Freyhof et. al. 2022
O. sakaryaensis	OK316743	Bayındır stream, Sakarya River	Freyhof et. al. 2022
O. sakaryaensis	OK316796	Bayındır stream, Sakarya River	Freyhof et. al. 2022
O. simavicus	KJ553724	Simav stream	Geiger et. al. 2014
O. simavicus	KJ553970	Simav stream	Geiger et. al. 2014
O. fatsaensis	OL855789	Tersakan stream, Yesilirmak	Bektaş et. al. 2022
O. fatsaensis	OL855790	Tersakan stream, Yesilirmak	Bektaş et. al. 2022
O. fatsaensis	OL855791	Tersakan stream, Yesilirmak	Bektaş et. al. 2022
O. banarescui	OK316694	Yenice River	Freyhof et. al. 2022
O. banarescui	MH469261	Devrekani stream	Turan et. al. 2019
O. banarescui	MH469262	Devrekani stream	Turan et. al. 2019
O. samanticus	MH018861	Terme stream, Kızılırmak River	Turan et. al. 2019
O. samanticus	OK316652	Kızılırmak River	Freyhof et. al. 2022
O. samanticus	MH018863	Vezirkoprü stream, Kızılırmak River	Turan et. al. 2019
O. bergianus	MH469265	Murat River	Turan et. al. 2019
O. bergianus	MH469266	Murat River	Turan et. al. 2019
O. bergianus	OL855763	Murat River	Bektaş et. al. 2022
O. bergianus	OL855764	Merziman stream, Euphrates	Bektaş et. al. 2022
O. bergianus	OL855765	Goksu river, Euphrates	Bektaş et. al. 2022
O. bergianus	OL855766	Sogutlucay stream, Euphrates	Bektaş et. al. 2022
O. bergianus	OL855767	Sogutlucay stream, Euphrates	Bektaş et. al. 2022
O. bergianus	OK316672	Yalekhlou, Caspian sea basin	Freyhof et. al. 2022
O. bergianus	OK316691	Murat River	Freyhof et. al. 2022
O. bergianus	MK546446	Caspian sea basin	Geiger 2019
O. bergianus	MK546447	Euphrates	Geiger 2019
O. bergianus	MK546448	Euphrates	Geiger 2019
O. bergianus	MK546449	Şerhan stream, Euphrates	Geiger 2019
O. angorae	OL855744	Karasu stream, Iznik lake	Bektaş et. al. 2022
O. angorae	OL855745	Purtek stream, Sakarya	Bektaş et. al. 2022
O. angorae	OL855747	Zamanti stream, Seyhan	Bektaş et. al. 2022

Pmin = 0.001, Pmax = 0.1, 1000 replicates, and the Kimura evolutionary model, with TS/TV = 2.0. The same parameters were applied under ABGD analysis. GMYC analysis was applied by the single-threshold version of the method, which usually outperforms the multiple-threshold version (Fujisawa and Barraclough 2013). The input ultrametric phylogenetic tree was made in BEAST v.1.8.4 (Drummond et al. 2012) with the following parameters: strict clock, Speciation:Yule process as the tree prior with 5 million generations, and sampling frequency of 1000. The resulting ultrametric tree was imported into R 3.1.3 (R Core Team 2013), and the single threshold ST-GMYC analysis was carried out using the R packages (Splits; Ezard et al. (2009) and Ape libraries; Paradis et al. (2004). In the concordant outcome of these methods, the resulting delimitation appears more logical (Dellicour and Flot 2018).

Results

Key to *Oxynoemacheilus bergianus* species group in the Anatolia

1 Snout length equal or greater than postorbital length ..... *O. samanticus*
– Snout length equal or smaller than postorbital length 2
2 Flank with marmalade pattern or with numerous irregularly shaped dark brown blotches as two or three horizontal rows..... *O. fatsaensis*
– The flank plain or with two to numerous irregularly shaped dark brown blotches 3
3 The flank with plain yellowish or with numerous irregularly shaped pale brown bars in most individuals..... *O. sakaryaensis*
– The flank dark brownish with 2–13 irregular shaped dark brownish bars or blotches 4
4 Maxillary barbells approximately equal or greater outer rostral barbells ..... *O. banarescui*
– Maxillary barbells always shorter than outer rostral barbells 5
5 The flank dark brownish with 10–13 irregular shaped dark brownish bars or blotches ..... *O. melenicus*
– The flank with 2–9 irregularly shaped brown bars or blotches..... 6
6 Interorbital width 15–24% HL..... *O. simavicus*
– Interorbital width 26–34% HL..... *O. bergianus*

***Oxynoemacheilus sakaryaensis* sp. nov.**

https://zoobank.org/6006326D-484D-435C-BD03-AFAE9A84DEE3

Figs 1, 2

Type material. *Holotype*. FFR15629, 1, 58 mm SL; Turkey: Ankara prov.: stream Kirmir 3 km north of Güdül, a tributary of Sakarya River, 40.236°N, 32.606°E.

Examined materials. *Paratypes*. FFR15514, 20, 51–62 mm SL; same data holotype. – FFR01527, 17, 50–62 mm SL; Turkey: Ankara prov.: stream Kirmir about 3 km north of Güdül, 40.236°N, 32.261°E. – FFR01387, 9, 39–58 mm SL; Turkey: Ankara prov.: stream İlhan at İlhan Village, 40.093°N, 32.245°E. – FFR15621, 27, 37–65 mm SL; Turkey: Ankara prov.: stream İlhan at İlhan Village, 40.097°N, 32.250°E. – FFR15623, 21, 49–60 mm SL; Turkey: Ankara prov.: stream Kirmir about 6 km north of Güdül 40.259°N, 32.268°E.– FFR15624, 14, 47–60 mm SL; Turkey: Ankara prov.: stream Bayındır at Gümele Village, 40.314°N, 32.466°E. –FFR 1364, 16, 25–64 mm SL; Turkey: Ankara prov: stream Kirmir at Kızılcahamam, 40.483°N, 32.653°E.–FFR 1386, 13, 49–62 mm SL; FFR 15515, 1, 62 mm SL; Turkey: Ankara prov: stream Öz at Kızılcahamam, 40.463°N, 32.653°E.–FFR 1387, 9, 39–58 mm SL; FFR 1527, 17, 50–62 mm SL; Turkey: Ankara prov: stream İlhan 5 km west of Gökçebağ, 40.093°N, 32.245°E. – FFR 15514, 1, 59 mm SL; Turkey: Ankara prov: stream Kirmir 3 km north of Güdül, 40.236°N, 32.261°E.

Material used in molecular genetic analysis. FFR DNA 15623, 4, Turkey: Ankara prov.: stream Kirmir about 6 km north of Güdül, 40.259°N, 32.268°E. (GenBank accession numbers OQ332822–OQ332825) – FFR DNA 15629, 3, Turkey: Ankara prov: stream Kirmir about 3 km north of Güdül 40.236°N, 32.606°E. (GenBank accession numbers OQ332826–OQ332828) – FFR DNA 15621, 3, Turkey: Ankara prov: stream İlhan at İlhan Village, 40.097°N, 32.250°E. (GenBank accession numbers OQ332829–OQ332831) – FFR DNA 1527, 2, Turkey: Ankara prov: stream Kirmir about 3 km north of Güdül, 40.236°N, 32.261°E. (GenBank accession numbers OQ332820–OQ332821)

Diagnosis. *Oxynoemacheilus sakaryaensis* is distinguished from *O. melenicus* by having the flank plain yellowish or numerous irregularly shaped pale brownish bars (vs. the flank with 10–13 irregular shaped dark brownish bars or blotches, 0–2 irregularly shaped brownish saddle in front of dorsal-fin origin (vs. 3–4) and caudal peduncle depth 2.8–3.2 times in its length (vs. 1.9–2.8). *Oxynoemacheilus sakaryaensis* is distinguished from *O. angorae* by having a caudal-peduncle depth 2.8–3.2 times in its length (vs.1.4–1.8), the flank with plain yellowish or with numerous irregularly shaped brown bars in most individuals (vs. showing a dark-brown mid lateral stripe or a series of fused, dark-brown blotches interrupted by a whitish or pale-brown lateral line (Fig. 3), a groove in upper lip in males (vs. absent), an axillary lobe at the base of pelvic fin (vs. absent) and the caudal-fin moderately forked (vs. emarginated) *Oxynoemacheilus sakaryaensis* is distinguished from *O. banarescui* by the flank with plain yellowish or with numerous irregularly shaped brown bars in most individuals (vs. 7–9 brownish blotches on flank (Fig. 4), the caudal peduncle depth 2.8–3.2 times in its length (vs. 1.9–2.8) and maxillary barbells always shorter than outer rostral barbells (vs. equal or shorter) *Oxynoemacheilus sakaryaensis* is distinguished from *O. simavicus* by the flank with plain yellowish or with numerous irregularly shaped pale brown bars in most individuals (vs. flank with 2–8 dark brownish blotches (Fig. 5) and 7–9 small and very pale brownish saddles on back (vs. 4–5 large dark brownish saddles on back). *Oxynoemacheilus sakaryaensis* is distinguished from *O. samanticus* by having a snout length smaller than postorbital length (vs. the snout length longer than the postorbital length), more slender caudal peduncle (caudal peduncle depth 2.8–3.2 times in its length, vs. 2.2–2.7) and the flank with plain yellowish or with numerous irregularly shaped brown bars in most individuals (vs. 5–10 black or dark brown bars or blocks on flank (Fig. 6). *Oxynoemacheilus sakaryaensis* is distinguished from *O. fatsaensis* by the flank with plain yellowish or with numerous irregularly shaped brown bars in most individuals (vs. the flank with marmalade pattern or with numerous irregularly shaped dark brown blotches as two or three horizontal rows (Fig. 7) and more slender caudal peduncle (caudal peduncle length 2.8–3.2 times greater than its length (vs. 2.0–2.6). *Oxynoemacheilus sakaryaensis* is distinguished from *O. bergianus* by the flank with plain yellowish or with numerous irregularly shaped brown bars in most individuals (vs. 4–9 black or dark brown bars or blocks on flank (Fig. 8) and a greater distance between anus and anal-fin origin (3–5% SL, vs. 2–3).

Oxynoemacheilus sakaryaensis is distinguished from *O. seyhanensis* by having the caudal-peduncle length 2.8–3.2 times greater than its depth (vs.1.2–1.4), the flank with plain yellowish or with numerous irregularly shaped brown bars in most individuals (vs. the body with marmorate pattern or numerous small irregularly shaped and spaced dark-brown bars on flank (Fig. 9), a suborbital groove in males (vs. absent), an axillary lobe at base of pelvic fin (vs. absent), a forked caudal fin (vs. slightly emarginate), lacking dorsal and ventral adipose crest on caudal peduncle (vs. present) and a more slender caudal peduncle (depth 2.7–3.5 times in its length, vs. 2.0–2.6, vs. 1.2–1.4). *Oxynoemacheilus sakaryaensis* is distinguished from *O. cemali* by having the flank with plain yellowish or with numerous irregularly shaped brown bars in most individuals (vs. 9–15 irregularly shaped dark-gray bars on the flank), a forked caudal-fin (vs. slightly forked), and having a slender caudal peduncle (the caudal-peduncle length 2.8–3.2 times greater than its depth (vs.1.4–2.0).

Description. See Figs 1, 2 for general appearance and Table 2 for morphometric data. Adult size large (maximum 65 mm SL). Body slender, compressed at caudal peduncle, greatest depth about midline between nape and dorsal-fin origin, slightly decreasing towards caudal-fin base. No hump at nape. Greatest body width at pectoral-fin base. Head pointed, upper head profile slightly convex on snout,

Figure 1. *Oxynoemacheilus sakaryaensis*, FFR15629 holotype, 58 mm SL; Turkey: stream Kirmir.

Figure 2. *Oxynoemacheilus sakaryaensis*, FFR 15623 paratypes, top to bottom 56 mm SL, 61 mm SL; Turkey: stream Kirmir.

Figure 3. *Oxynoemacheilus angorae*, FFR01513, 55 mm SL, Turkey: stream Berçin, FFR01526, 64 mm SL; Turkey: stream Kirmir.

Table 2. Morphometric data of *Oxynoemacheilus sakaryaensis* (holotype, FFR15629, paratypes, FFR 15514; n = 20).

	Holotype	paratypes			
		mean	min	max	SD
Standard length (mm)	58		51	62	
In percent of standard length					
Head length	23.8	23.1	20.4	24.8	1.1
Body depth at dorsal–fin origin	14.2	16.5	14.2	17.7	0.8
Predorsal length	52.7	50.3	47.7	53.0	1.7
Postdorsal length	35.9	35.6	32.0	39.7	2.0
Preanal length	74.2	71.0	68.4	74.2	1.5
Prepelvic length	52.4	49.5	46.6	52.4	1.4
Distance between pectoral and pelvic-fin origins	32.0	29.6	27.0	32.0	1.1
Distance between pelvic and anal-fin origins	22.0	21.1	18.0	27.5	1.9
Distance between vent and anal-fin origin	3.8	4.0	3.2	5.1	0.5
Depth of caudal peduncle	6.3	7.2	6.4	7.9	0.4
Length of caudal peduncle	23.1	21.4	19.7	23.7	1.3
Dorsal-fin depth	17.6	18.8	16.6	20.7	1.2
Anal-fin depth	15.0	16.3	14.5	18.2	0.9
Pectoral-fin length	20.0	22.2	18.3	26.3	1.7
Pelvic-fin length	17.8	16.8	14.6	17.9	0.9
In percent of head length					
Head depth at eye	46.5	49.3	45.4	58.1	3.2
Snout length	33.6	42.2	35.6	37.9	3.1
Eye diameter	19.4	20.6	17.3	24.5	1.9
Postorbital distance	45.7	46.9	42.5	55.3	3.2
Maximum head width	61.6	62.0	54.6	69.5	3.3
Interorbital width	25.3	28.0	23.1	35.8	3.2
Length of inner rostral barbel	23.9	25.9	20.5	32.7	2.8
Length of outer rostral barbel	28.3	30.6	24.8	37.6	3.4
Length of maxillary barbel	26.7	26.6	22.4	34.1	2.7
Caudal peduncle length/depth	3.0	2.9	2.8	3.2	0.1

flattened on ventral surface. Snout slightly pointed at tip. Mouth narrow and arched, lips well developed. A narrower median interruption in lower lip. A narrower median incision in upper lip a very shallow groove. A suborbital groove in males. Barbels short, inner rostral barbel not reaching to base of maxillary barbel; outer almost not reaching to vertical through anterior eye margin. Maxillary barbell not reaching to posterior eye-margin in most individuals. Caudal peduncle slender, compressed laterally, length 2.8–3.2 times longer than deep. Axillary lobe presents at pelvic-fin base, fully attached to body. Pelvic-fin origin below first or second branched dorsal-fin ray. Anal-fin origin at vertically equal to dorsal-fin tip. The pectoral fin almost reaching vertical through tip of dorsal-fin origin in males. No dorsal or ventral adipose crest on caudal peduncle.

Lateral line complete, reaching caudal-fin base. Body covered by embedded scales on flank, back, and belly. Dorsal fin with 8½ branched rays, its outer margin straight or slightly concave. Anal fin with 5½ branched rays, its outer margin straight or slightly concave. Pectoral fin with 10–12 rays, outer margin straight. Pelvic fin with 7–8 rays, outer margin slightly convex. Caudal fin with 8+8, 8+9, and 9+9 branched rays, outer margin moderately forked and lopes slightly pointed.

Coloration. Body yellowish or brownish in life and preserved individuals. Head and cheek with small, plain brown mottling on top and cheeks, without color pattern ventrally. No pigmentation below a line from pectoral-fin base to anus. A large, irregularly shaped, dark-brown blotch at dorsal fin-origin. Flank plain yellowish with numerous irregularly shaped brown bars in most

Figure 4. *Oxynoemacheilus banarescui*, IUSHM 2018-1403, 62 mm SL, 46 mm SL; Turkey: stream Davulga.

Figure 5. *Oxynoemacheilus simavicus*, FFR 01544, mm SL, 52 mm SL; Turkey: stream Nilüfer.

Figure 6. *Oxynoemacheilus samanticus*, FFR015518, 64 mm SL, 62 mm SL; Turkey: stream Soruk.

Figure 7. *Oxynoemacheilus fatsaensis*, FFR 01566 paratypes, 74 mm SL, 67 mm SL; Turkey: stream Tersakan.

Figure 8. *Oxynoemacheilus bergianus*, FFR015506, 59 mm SL, 57 mm SL; Turkey, Murat River at Ballıbostan.

Figure 9. *Oxynoemacheilus seyhanensis*, FFR01577, 53 mm SL, 54 mm SL; Turkey: stream Soruk.

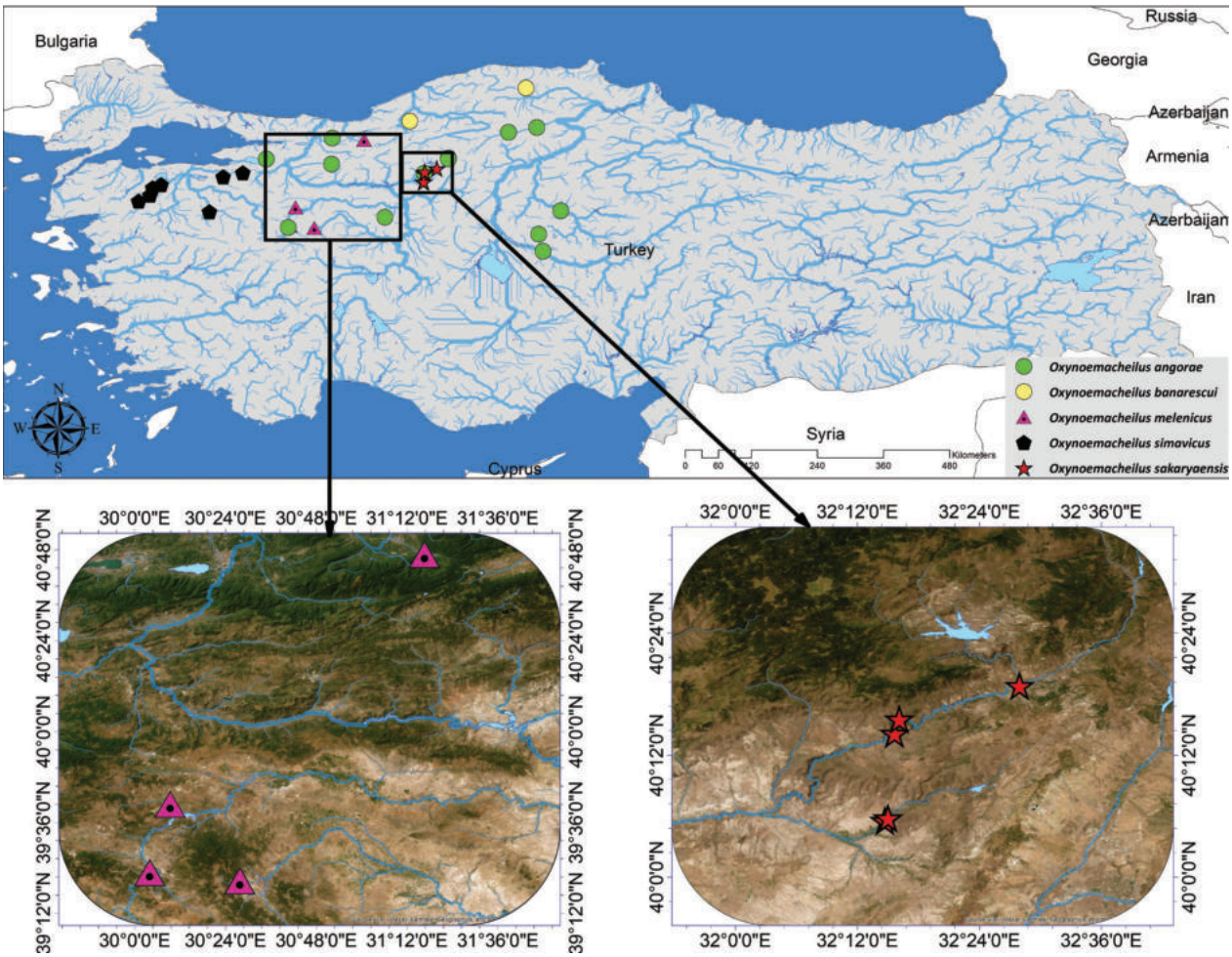

Figure 10. Distribution of *Oxynoemacheilus* species in the western Anatolia.

individuals. Back with zero to 2 pale blotches anterior to dorsal-fin origin. The dorsal part of caudal peduncle with 3–4 irregularly shaped pale saddle, not fused with mid-lateral blotches. One or two irregular shaped small black spots on caudal-fin base. Dorsal-fin with 1–2 and caudal fin with 2–3 fine, irregularly shapes black bands on rays. Anal, pectoral and pelvic fins greyish to yellowish, with numerous small black spots on rays.

Distribution. *Oxynoemacheilus sakaryaensis* was found in the Sakarya drainage in western Anatolia (Fig. 10).

Etymology. The name of the species is derived from the Sakarya River.

Oxynoemacheilus melenicus sp. nov.

https://zoobank.org/F530199C-A29C-4A1B-A3F1-493CDF0390CF

Figs 11, 12

Type material. ***Holotype***. FFR15627, 1, 65 mm SL; Turkey: Eskişehir prov.: stream Yarılgan at Gemiç Village, 39.343°N, 30.463°E.

Examined materials. ***Paratypes***. FFR15626, 39, 50–69 mm SL; same data holotype. FFR01378, 2, 45–57 mm SL; Turkey: Kütahya prov.: stream Porsuk at Kütahya 39.380°N, 30.067°E. – FFR01525, 1, 55 mm SL; Turkey: Kütahya prov.: stream Porsuk about 9 km south of Kütahya, 39.349°N, 30.038°E. – FFR15625, 4, 32–49 mm SL; Turkey: Kütahya prov: stream Porsuk at Porsuk Village, 39.348°N, 30.036°E. –FFR15630, 5, 61–63 mm SL; Turkey: Eskişehir prov.: stream Allıkova about 3km south of Kümbet, 39.681°N, 30.157°E. –FFR 01564, 10, 45–61 mm SL; Turkey: Düzce prov: stream Asar about 2 km west of Kaynaşlı a tributary of Büyükmelen drainage, 40.781°N, 31.277°E.

Material used in the molecular genetic analysis. FFR DNA 15630, 2, Turkey: Eskişehir prov.: stream Allıkova about 3km south of Kümbet, 39.681°N, 30.157°E (GenBank accession numbers OQ332806, OQ332808). – FFR DNA 15625, 3, Turkey: Kütahya prov.: stream Porsuk at Porsuk Village, 39.348°N, 30.036°E. (GenBank accession numbers OQ332809–OQ332811). – FFR DNA 15627, 4, Turkey: Eskişehir prov.: stream Yarılgan at Gemiç Village 39.343°N, 30.463°E. (GenBank accession numbers OQ332812–OQ332815). –FFR DNA 15631, 4, Turkey: Eskişehir prov.: a tributary of Sakarya River about 9 km northeast of Nasreddi Hoca Village, 39.553°N, 31.757°E. (GenBank accession numbers OQ332816–OQ332819). – FFR DNA 01524, 1, Turkey: Kütahya prov.: stream Porsuk at Porsuk Village 39.350°N, 30.038°E. (GenBank accession number OQ332807).

Figure 11. *Oxynoemacheilus melenicus*, FFR15627 holotype, 65 mm SL; Turkey: stream Yarılgan.

Diagnosis. *Oxynoemacheilus melenicus* is distinguished from *O. angorae* by having a more slender caudal pedincle (caudal pedinuncle depth 1.9–2.8 times in its length, vs.1.4–1.8), the flank with 6–13 irregular shaped brownish bars or blotches (a dark-brown midlateral stripe or a series of fused, dark-brown blotches interrupted by a whitish or pale-brown lateral line (Fig. 3), a suborbital groove in males (vs. absent), an axillary lobe at pelvic fin base (vs. absent), a forked caudal fin (vs. slightly emarginate), a more slender caudal peduncle (depth .5 times in its length, vs. 2.4–1.8).). *Oxynoemacheilus melenicus* is distinguished from *O. banarescui* by having the flank with 10–13 irregular shaped brownish bars or blotches (vs. the flank with 7–10 large, irregularly shaped dark-brown, vertically elongated blotches or bars along lateral midline behind dorsal-fin origin (Fig. 4) and maxillary barbells always shorter than outer rostral barbells (vs. equal or longer). *Oxynoemacheilus melenicus* is distinguished from *O. simavicus* by having the flank with 10–13 irregularly shaped brown bars or blotches (vs. 2–8 blotches (Fig. 5) and 6–8 irregularly shaped dark brown saddle on back (vs. 4–6) and a longer head (head length 22–26% SL, vs. 19–22). *Oxynoemacheilus melenicus* is distinguished from *O. samanticus* by having the with 10–13 irregular shaped brownish bars or blotches (vs. the flank with 5–10 irregular shaped brownish blotches along lateral line (Fig. 6) and the snout length smaller than postorbital length (vs. the snout length longer than postorbital length) and the pelvic-fin origin below first or second unbranched dorsal-fin ray (vs. equal with dorsal fin origin). *Oxynoemacheilus melenicus* is distinguished from *O. fatsaensis* by having the flank plain brownish or with 10–13 irregular shaped brownish bars or blotches (vs. flank marmalade pattern or with numerous irregularly shaped dark brown blotches as one or two horizontal rows (Fig. 7) and the pelvic-fin origin below the last unbranched dorsal-fin ray (vs. first or second branched dorsal-fin ray).

Oxynoemacheilus melenicus is distinguished from *O. bergianus* the flank with 10–13 dark brownish bars on flank (vs. 4–9 bars or blotches (Fig. 8) and the presence prominent bars or blotches in front of dorsal fin (vs. mostly absent or slightly prominent) and a greater distance between anus and anal-fin origin (4–6% SL, vs. 2–3). *Oxynoemacheilus melenicus* is distinguished from *O. seyhanensis* by having the with 10–13 irregular shaped brownish bars or blotches (vs. the body with marmorate pattern or numerous small irregularly shaped and spaced dark-brown bars on flank (Fig. 9), a suborbital groove in males (vs. absent), an axil-

Figure 12. *Oxynoemacheilus melenicus*, FFR15626 paratypes, top to bottom 60 mm SL, 63 mm SL; Turkey: stream Yarılgan.

lary lobe at pelvic fin base (vs. absent), a forked caudal fin (vs. slightly truncate) and a more slender caudal peduncle (caudal peduncle length 1.9–2.7 times its depth, vs. 1.1–1.4). *Oxynoemacheilus melenicus* is distinguished from *O. cemali* by having a forked caudal-fin (vs. slightly forked) and a more slender caudal peduncle (depth 1.9–2.6 times in its length, vs. 1.4–2.0).

Description. See Figs 11, 12 for general appearance and Table 3 for morphometric data. Adult size large (maximum 69 mm Ls). Body slender, compressed at caudal peduncle, greatest depth about midline between nape and dorsal-fin origin, slightly decreasing towards caudal-fin base. No hump at nape. Greatest body width at pectoral-fin base. Head pointed, upper head profile slightly convex on snout, flattened on ventral surface. Snout slightly pointed at tip. Mouth narrow and arched, lips well developed. A narrower median interruption in lower lip. A suborbital groove in males. No median incision in upper lip. Barbels short, inner rostral barbel not reaching to base of maxillary barbel; outer almost not reaching to vertical through anterior eye margin. Maxillary barbel, not reaching to posterior eye-margin in most individuals. Caudal peduncle slender, compressed laterally, length 1.9–2.7 times longer than deep. Axillary lobe present at pelvic-fin base, fully attached to body. Pelvic-fin origin below first or second branched dorsal-fin ray. Anal-fin origin at vertically equal to dorsal-fin tip. Pectoral fin not reaching vertical through tip of dorsal-fin origin in males. No dorsal or ventral adipose crest on caudal peduncle. Pelvic fin not reaching vertical of dorsal-fin tip, almost reaching to anus. Anal fin not reaching caudal-fin base. Caudal fin moderately forked.

Lateral line complete, reaching caudal-fin base. Body covered by embedded scales on flank, back, and belly.

Table 3. Morphometric data of *Oxynoemacheilus melenicus* (holotype, FFR15627; paratypes, FFR 15626; n = 20).

	Holotype	paratypes			
		mean	min	max	SD
Standard length (mm)	65		51	69	
In percent of standard length					
Head length	23.4	23.4	22.0	25.4	0.9
Body depth at dorsal–fin origin	15.5	15.7	14.3	17.0	0.8
Predorsal length	52.1	50.9	47.4	53.2	1.7
Postdorsal length	36.4	36.8	34.6	39.8	1.1
Preanal length	71.8	71.4	67.3	74.8	1.9
Prepelvic length	49.5	50.5	47.4	53.7	1.7
Distance between pectoral and pelvic-fin origins	27.5	29.4	27.2	31.9	1.4
Distance between pelvic and anal-fin origins	22.0	20.5	18.6	23.2	1.2
Distance between vent and anal-fin origin	4.4	4.6	3.7	4.6	0.7
Depth of caudal peduncle	7.8	7.3	6.2	8.3	0.4
Length of caudal peduncle	17.2	19.1	17.2	20.5	0.5
Dorsal-fin depth	18.1	18.3	16.8	20.3	0.9
Anal-fin depth	15.8	15.9	14.2	18.4	1.0
Pectoral-fin length	20.2	21.6	19.0	23.9	1.4
Pelvic-fin length	15.4	16.0	14.7	17.2	0.7
In percent of head length					
Head depth at eye	46.7	44.7	39.4	48.6	2.2
Snout length	44.7	43.2	36.0	37.5	2.8
Eye diameter	16.0	18.2	14.3	20.9	1.7
Postorbital distance	50.3	45.0	38.3	50.8	3.8
Maximum head width	67.3	59.2	53.3	67.3	2.6
Interorbital width	24.7	24.3	19.6	29.8	2.7
Length of inner rostral barbel	20.4	24.2	19.5	29.7	3.0
Length of outer rostral barbel	34.1	29.3	21.1	34.1	3.3
Length of maxillary barbel	26.5	27.2	21.3	35.4	3.6
Caudal peduncle length/depth	2.3	2.6	2.3	2.8	0.2

Table 4. Pairwise distance Kimura's two parameters (K2P) values based on cytochrome oxidase sequences of *Oxynoemacheilus* species.

	O. melenicus	*O. sakaryaensis*	*O. simavicus*	*O. fatsaensis*	*O. banarescui*	*O. samanticus*	*O. bergianus*
O. melenicus							
O. sakaryaensis	0,017						
O. simavicus	0,024	0,027					
O. fatsaensis	0,032	0,042	0,044				
O. banarescui	0,034	0,037	0,035	0,040			
O. samanticus	0,032	0,038	0,041	0,039	0,027		
O. bergianus	0,036	0,038	0,045	0,041	0,032	0,024	
O. angorae	0,076	0,079	0,092	0,076	0,075	0,076	0,080

Table 5. List of the variable nucleotide substitutions in the 645 base pairs long mt DNA COI barcode region.

Species	Variable nucleotide positions			
	111122	2222222233	3334444444	556
	2489078900	0133478915	6891267899	292
	1063670214	7314365451	0161387308	247
O. melenicus	CCTYATGGGY	RCAGGCGTGR	GTTRGYGAYC	RCC
O. sakaryaensis	T..T..WAR.	..R..T....	RC..R..GCG	..T
O. simavicus	TYW.WC.A..	.A.R.TACC.	..C...A.C.	SA.

(Y= C/T, R= A/G, W= A/T, S= C/G)

Dorsal fin with 7–8½ branched rays, its outer margin straight or slightly concave. Anal fin with 5½ branched rays, its outer margin straight. Pectoral fin with 10–11 rays, outer margin straight. Pelvic fin with 7–8 rays, outer margin slightly convex. Caudal fin with 8+8, 8+9, and 9+9 branched rays, outer margin forked, and lopes slightly pointed.

Coloration. Body yellowish in life and light brown in preserved individuals. Head and cheek plain or with small, plain brown mottling on top and cheeks, without color pattern ventrally. Numerous pigmentations below a line from pectoral-fin base to anus. A dark brown blotch at dorsal fin-origin. Flank plain brownish or with 10–13 irregular shaped brownish bars or blotches. Back in front of dorsal-fin with zero or four dark brownish blotch. Upper part of caudal peduncle with 3–4 irregularly shaped dark brownish blotches, not fused with midlateral bars or blotches in most individuals. One irregular shaped small black spots on caudal-fin base. Dorsal fin with 1–2 and caudal fin with 2–3 fine, irregularly shapes black bands on rays. Anal, pectoral and pelvic fins plain yellowish, and pectoral fin with few small black spots on rays.

Distribution. *Oxynoemacheilus melenicus* was found in the Büyükmelen Stream and Sakarya River drainage in western Anatolia (Fig. 10).

Etymology. The name of the species is derived from the Stream Büyükmelen.

Phylogenetic positions *of Oxynoemacheilus melenicus* and *Oxynoemacheilus sakaryaensis*

COI barcode region sequences were analyzed in seven *Oxynoemacheilus* species in western Anatolia. *Oxynoemcaheilus* species were divided into three main clades in the all phylogenetic analysis supported by high bootstrap values. The first clade consisted of *O. bergianus* group species which are *O. melenicus*, *O. sakaryaensis and O. simavicus O. banarescui*, *O. bergianus*, *O. samanticus*. The second and third clades included *O. fatsaensis* and *O. angorae*, respectively. *O. melenicus*, constituted a highly supported clade sister to *O. sakaryaensis* (Fig. 13). Intrageneric K2P distances between species ranged from 1.7% (*O. melenicus*, *O. sakaryaensis*) to 8.0% (*O. angorae and O. bergianus*). K2P distance is 1.7% between *O. melenicus* and its closest relative, *O. sakaryaensis* and, 2.4% between *O. melenicus and O. simavicus* (Table 4). Also, the K2P distance is 2.7% between *O. sakaryaensis* and *O. simavicus*. *O. melenicus* differs from its most closely related congeners, *O. sakaryaensis*, and *O. simavicus*, by 9 and 12 nucleotide substitution sites and *O. sakaryaensis* differs from *O. simavicus*, by 13 nucleotide substitution sites. *O. melenicus* and *O. sakaryaensis* were differentiated from all other *Oxynoemacheilus* species in western Anatolia by two diagnostic and unique nucleotide substitution sites in the COI barcoding region (Table 5). In the haplotype network analysis, the 32 distinct haplotypes were determined. The most common haplotype was H9, shared by many populations belonging to *O. sakaryaensis*. All species have unique haplotypes, as distinctly illustrated in the haplotype network (Fig. 14).

We found eight OTUs according to ABGD and GMYC analysis. The ASAP determined nine clusters for studied species of *Oxynoemacheilus*. The likelihoods of GMYC and null models were 600.9632 and 595.6004, respectively. The GMYC analysis was represented by eight ML entities (CI: 8–11). ASAP's best partition (score = 1.50) results from a p-distance threshold of 0.009 and both recursive and initial partition predicts ten subsets. ABGD analysis determined that the barcode gap is 0.012.

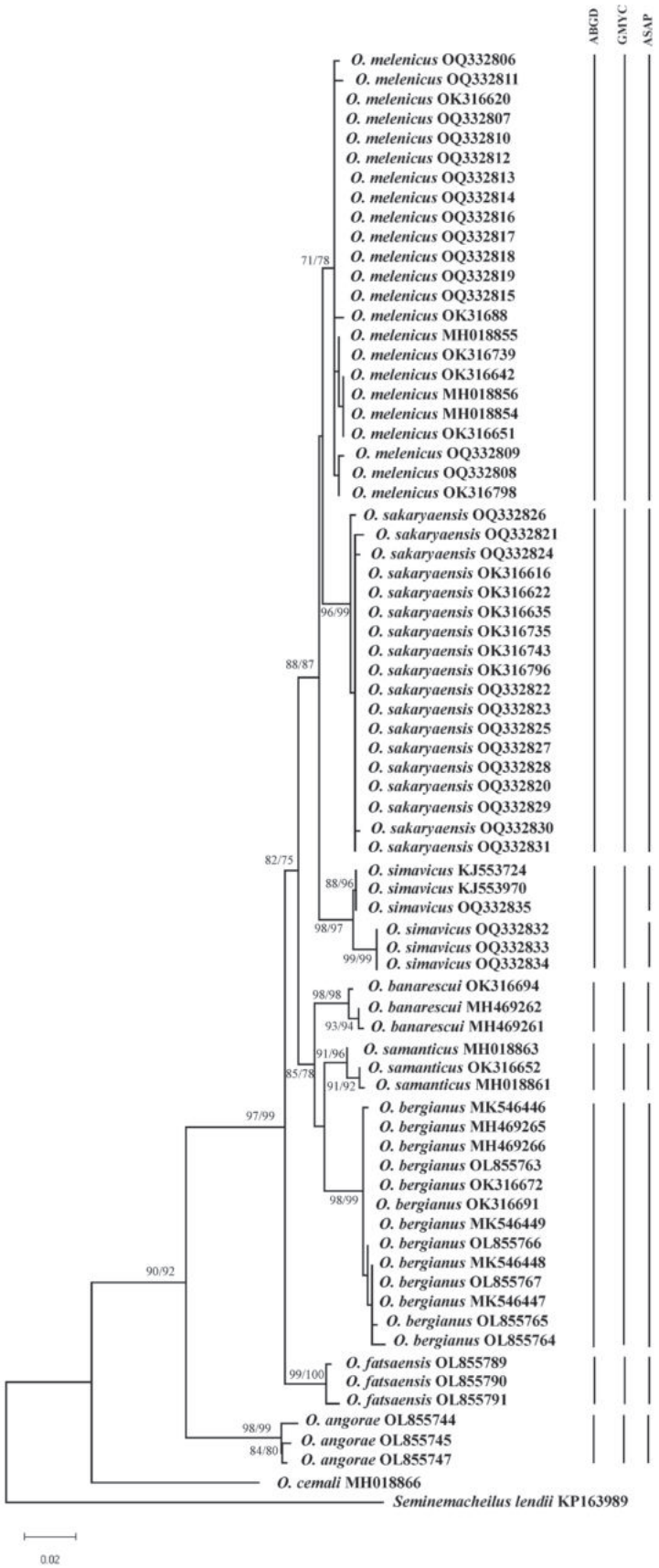

Figure 13. Maximum likelihood tree based on mitochondrial cytochrome oxidase subunit I (COI; 645 bp) gene sequences of *Oxynoemacheilus spp*. Maximum likelihood and Neighboor Joining analyses resulted in congruent trees. Bootstrap and posterior probability values are shown above nodes on tree if 70% or higher. ABGD, GMYC and ASAP clusters were indicated in vertical bars.

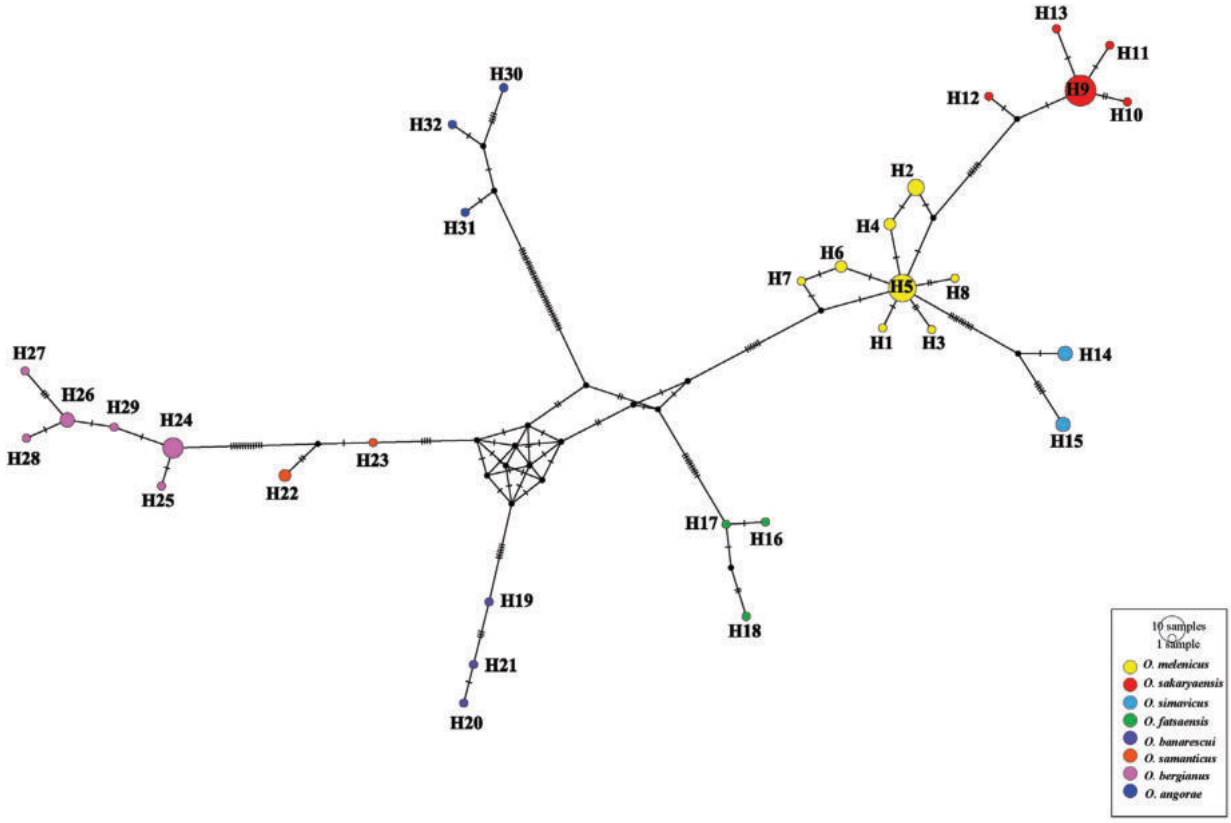

Figure 14. Median-joining network of the COI haplotypes. Circle size corresponds to sample size; one bar indicates an additional mutational step. Small black circles represent median vectors. Each small lines represent one nucleotide difference.

Discussion

Oxynoemacheilus melenicus and *O. sakaryaensis* were genetically identified in *O. bergianus* species group. Similar to this study Freyhof et al. 2022 revealed two unnamed molecular clades in the Western Black Sea (Büyükmelen and Sakarya River drainage), which could represent candidate species. However, they could not describe these species because morphological differences could not be found. In this study, besides morphological differences, the results from the species delineation tests (ABGD, GMYC, ASAP) and phylogenetic analyses support the validity of *O. melenicus* and *O. sakaryaensis* as distinct species.

Freyhof et al. 2022 detected 15 entities in the PTP analysis, while mPTP detected four entities representing putative species, and ASAP predicted 15 entities, which are mainly congruent to the PTP result. According to their results, *O. banarescui*, *O. fatsaensis*, *O. samanticus*, *O. simavicus*, and specimens from Sakarya and Büyük Melen were determined as different clusters, and *O. bergianus* was divided into two clusters. In our ABGD and GMYC analysis, eight entities were defined, which are *O. melenicus*, *O. sakaryaensis*, *O. simavicus*, *O. banarescui*, *O. bergianus*, *O. samanticus*. *O. fatsaensis* and *O. angorae*. Unlike ABGD and GMYC, *O. simavicus* was divided into two clusters in the ASAP analysis. In this regard, this study reflected that the species delineation tests agree with the previous research. Freyhof et.al. (2022) reported that *Oxynoemacheilus bergianus* group comprises ten molecular clades following congruently well-supported NJ, MP, and ML based entities. Species described as *O. bergianus*, *O. banarescui*, *O. fatsaensis*, and *O. simavicus* from Turkey, *O. lenkoranensis* from Azerbaijan, and *O. longipinnis* and *O. parvinae* from Iran belong to this species group. In addition to these, it also includes four unnamed molecular clades. We did not have the opportunity to examine *O. lenkoranensis*, *O. longipinnis*, *O. parvinae*, and four unnamed groups due to the lack of specimens from their localities. However, we examined many specimens from their distribution area from *Oxynoemacheilus bergianus*, *O. banarescui*, *O. fatsaensis*, *O. samanticus*. We concluded that *O. bergianus*, *O. banarescui*, *O. fatsaensis*, *O. samanticus*, and *O. simavicus*, together with *O. sakaryaensis* and *O. melenicus* are valid species.

Freyhof et al. (2022) did not make a detailed comparison, considering that the Sakarya and Büyükmelen populations are *O. simavicus*. They gave only brief information about the color and pattern characteristics of the *O. simavicus*. Freyhof et al. 2022 stated that *O. simavicus* with mottled and blotched individuals are common, including those from the Simav, Büyükmelen, and Sakarya River drainages. According to our results, *Oxynoemacheilus sakaryaensis* is characterized by having a flank with plain or with numerous irregularly shaped pale brownish bars and *O. melenicus* with a flank with 10–13 irregularly shaped brownish bars or blotches. However, *O. simavicus* is characterized by a flank with 2–8 dark brownish blotches.

Comparative material

***Oxynoemacheilus angorae*:** FFR001389, 2, 49–63 mm SL; Turkey: Ankara prov.: stream Berçin at Kızılcahamam, 40.471N 32.655E. – FFR01506, 5, 37–63 mm SL; Turkey: Bolu prov.: stream Uludere at Hendek, 40.809°N, 30.758°E. – FFR01513, 14, 41–60 mm SL; Turkey: Ankara prov.: stream Berçin at Kızılcahamam, 40.482°N, 32.653°E. – FFR01521, 6, 60–77 mm SL; Turkey: Bilecik prov.: stream Göynük 4 km west of Göynük, 40.386°N, 30.746°E. – FFR01524, 4, 51–63 mm SL; Turkey: Kütahya prov.: stream Porsuk on road from Kütahya to Uşak, 39.350°N, 30.038°E. – FFR01526, 6, 45–63 mm SL; Turkey: Ankara prov.: stream Kirmir 3 km north of Güdül, 40.236°N, 32.261°E. – FFR01547, 9, 46–54 mm SL; Turkey: İznik prov.: stream Karasu 6 km southeast of İznik, 40.468°N, 29.681°E. – FFR01549, 50, 20–59 mm SL; Turkey: Ankara prov.: stream Peçenek 7 km east of Şereflikoçhisar, 40.471°N, 32.655°E. – FFR01550, 2, 34–51 mm SL; Turkey: Yozgat prov.: stream Delice at 2 km southeast of Yerköy, 39.622°N, 34.490°E. – FFR01554,116, 32–62 mm SL; Turkey: Kastamonu prov.: stream Devrez 6 km southeast of Tosya, 40.984°N, 34.099°E. – FFR01557, 14, 29–43 mm SL; Turkey: Kırşehir prov.: Kızılırmak River at Kesikköprü, 38.961°N, 34.199°E. – FFR01558, 43, 20–67 mm SL; Turkey: Kırşehir prov.: stream Kılıçözü Kızılcahamam 2 km north of Özbağ, 39.241°N, 34.128°E. – FFR01559, 4, 51–61 mm SL; Turkey: Çankırı prov.: stream Devrez 2 km south of Ilgaz, 40.904°N, 33.638°E. – FFR01571, 5, 52–67 mm SL; Turkey: Eskişehir prov.: stream Pürtek 11 km southeast of Sivrihisar, 39.518°N, 31.618°E.

***Oxynoemacheilus banarescui*:** FFR15511, 4, 43–77 mm SL; Turkey: Kastamonu prov.: stream Devrekanı 8 km northeast of Devrekanı, 41.627°N, 33.922°E. – IUSHM 2018-1403, 10, 50 –62 mm SL; Turkey: Karabük prov.: stream Davulga at 15 km north of Mengen, 41.087°N, 32.023°E.

***Oxynoemacheilus cemali*:** FFR01359, 4, 53–73 mm SL; Turkey: Giresun prov: stream Dereli at Dereli, 40.740°N, 38.450°E. – FFR01440, 7, 31–64 mm SL; Turkey: Erzincan prov: stream Köroğlu 2 km south of Kürelik, 39.932°N, 38.749°E. – FFR01441, 12, 52–95 mm SL; Turkey: Gümüşhane prov: stream Değirmen at Yukarıözlüce village, 39.986°N, 39.540°E. – FFR01470, 16, 47–72 mm SL; Turkey: Erzincan prov: stream Köroğlu 2 km north of Refahiye, 39.920°N, 38.760°E. – FFR01515, 12, 30–83 mm SL; Turkey: Samsun prov: stream Tersakan 5 km northeast of Havza, 40.989°N, 35.717°E. – FFR01582, 26, 49–70 mm SL; Turkey: Erzurum prov: Çoruh River 500 m northwest of Adabaşı, 40.380°N, 40.320°E.– FFR 01583, 19, 68–88 mm SL; Turkey: Erzurum prov: stream Yağlı at 2 km southeast of İncesu, 40.308°N, 41.007°E. – FFR01584, 22, 36–88 mm SL; Turkey: Erzurum prov: stream Tortum 4 km west of Demirciler, 40.379°N, 40.320°E. – FFR01585, 3, 70–81 mm SL; Turkey: Erzurum prov: stream Tortum 600 m west of Engüzek Kapı Castle, 40.510°N, 41.523°E. – FFR01586, 16, 36–64 mm SL; Turkey: Erzurum prov: stream Tortum 2 km west of Altınçanak, 40.568°N, 41.596°E. – FFR01587, 27, 51–75 mm SL; Turkey: Erzurum prov: stream Oltu 2 km west of Ayvalı, 40.753°N, 41.854°E. – FFR01588, 8, 60–86 mm SL; Turkey: Artvin prov: stream Oltu 3 km southwestern of İşhanı, 40.774°N, 41.713°E. – FFR01589, 18, 48–72 mm SL; Turkey: Artvin prov: Çoruh River at 1 km north of Bademli, 40.445°N, 40.901°E. – FFR01590, 33, 67–78 mm SL; Turkey: Artvin prov: stream Ekşinar 1 km north of Ekşinar, 41.116°N, 42.056°E. – FFR01591, 4, 66–68 mm SL; Turkey: Artvin prov: stream Köprüler 3 km northwest of Ardanuç, 41.137°N, 42.038°E. – FFR01592, 14, 41–84 mm SL Turkey: Artvin prov: stream Okçular 2 km south of Eskikale, 41.263°N, 42.191°E. – FFR01593, 27, 49–83 mm SL; Turkey: Artvin prov: stream Göknar 1 km north of Çayağzı, 41.284°N, 42.232°E. – FFR01594, 54, 46–74 mm SL; Turkey: Gümüşhane prov: stream Şiran 15 km northwest of Şiran, 40.310°N, 39.031°E. – FFR01596, 17, 60–70 mm SL; Turkey: Giresun prov: stream Bağırsak Alucra, 40.310°N, 38.773°E.

Oxynoemacheilus fatsaensis: FFR15513, 1, 55 mm SL; Turkey: Samsun prov: stream Tersakan 5 km east of Havza 40.990°N, 35.717°E. – FFR01361, 5, 46–58 mm SL; Turkey: Samsun prov: stream İlhanlı at Ayvacık 40.990°N, 36.634°E. – FFR01362, 10, 37–64 mm SL; Turkey: Giresun prov: stream Aksu at Dereli 40.731°N, 38.460°E. – FFR01362, 10, 37–64 mm SL; Turkey: Tokat prov: stream Kelkit 9 km north of Erba 40.759°N, 36.515°E. – FFR01516, 31, 38–75 mm SL; same data as holotype.

Oxynoemacheilus seyhanensis: FFR01433, 9, 38–78 mm SL; Turkey: Sivas prov.: Kızılırmak River at Zara, 39.902°N, 37.763°E. – FFR01474, 32, 32 –79 mm SL; Turkey: Sivas prov.: Kızılırmak River 7 km north of Zara, 39.961°N, 37.739°E. – FFR01545, 20, 51–78 mm SL; Turkey: Çankırı prov.: stream Ulusu at Çerkeş, 40.820°N, 32.800°E. – FFR01551, 1, 69 mm SL; Turkey: Yozgat prov.: stream Delice 11 km northwest of Yerköy, 39.698°N, 34.362°E. – FFR01552, 7, 38–77 mm SL; Turkey: Yozgat prov.: stream Delice 2 km southeast of Yerköy, 39.622°N, 34.490°E. – FFR01578, 8, 50–67 mm SL; Turkey: Çankırı prov.: stream Ulusu at Çerkeş, 40.800°N, 32.883°E.

Oxynoemacheilus bergianus: FFR01457, 11, 64–72 mm SL; Turkey: Malatya prov.: stream Sultansuyu 8 km east of Akçadağ, 38.339°N, 38.064°E. – FFR01467, 28, 54–64 mm SL; Turkey: Erzurum prov.: stream Baş 10 km east of Aşkale, 39.948°N, 40.804°E.–FFR 1457, 11, 64 –72 mm SL; Turkey: Malatya prov.: stream Sultansuyu 8 km east of Akçadağ, 38.3388°N, 38.0620°E. –FFR 15506, 25, 33–59 mm SL; Turkey: Ağrı prov.: Murat River 17 km west of Taşlıçay, 39.6785°N, 43.1887°E.

Oxynoemacheilus samanticus: FFR01553, 2, 55–62 mm SL; Turkey: Yozgat prov.: stream Delice, 2 km southeast of Yerköy, 39.622°N, 34.490°E. – FFR01556, 3, 37–55 mm SL; Turkey: Sinop prov.: stream Gökırmak at Çarşak 11 km east of Boyabat, 41.453°N, 34.889°E. –FFR015518, 19, 54–62 mm SL; Turkey: Samsun prov.: stream Soruk 20 km east of Vezirköprü, 41.119°N, 35.227°E.

Oxynoemacheilus simavicus: FFR01380, 12, 38–50 mm SL; Turkey: Balıkesir prov: stream Koca at Manyas. –FFR01505, 28, 32–56 mm SL; Turkey: Balıkesir prov:

stream Sakar at Manyas 40.050°N, 27.962°E. – FFR01518, 8, 44–74 mm SL; Turkey: Balıkesir prov: stream Koca 4 km north of Balya 39.782°N, 27.596°E. – FFR01520, 8, 47–55 mm SL; Turkey: Balıkesir prov: stream Değirmenboğazı 13 km west of Manyas 40.000°N, 27.828°E. – FFR01522, 4, 47–51 mm SL; Turkey: Balıkesir prov: stream Koca at Ilıca 39.878°N, 27.780°E. – FFR01542, 4, 48–49 mm SL; Turkey: Bursa prov: stream Nilüfer at Narlıdere 40.244°N, 29.298°E. – FFR01544, 4, 48–49 mm SL; Turkey: Bursa prov: stream Nilüfer at Misi 40.180N 28.974E.

Material used in the molecular genetic analysis

Oxynoemacheilus simavicus

FFR DNA 01505, 1, Turkey: Balıkesir prov: stream Sakar at Manyas 40.050°N, 27.962°E. (GenBank accession number OQ332835) – FFR DNA 01512, 3, Turkey: Balıkesir prov: stream Dursunbey 4 km south of Adaören 39.609°N, 28.751°E. (GenBank accession numbers OQ332832–OQ332834)

Acknowledgments

We thank Jörg Freyhof for his contribution to the manuscript. We thank Esra Bayçelebi for taking photos of some specimens, and fieldwork. Also, we are pleased to thank Cüneyt Kaya, İsmail Aksu, Züleyha Akpınar, and Yusuf Bektaş for their great help during fieldwork in the studied area. Many thanks also to Baran Yoğurtçuoğlu (Ankara), Müfit Özuluğ (İstanbul), and Mahmut Elp (Kastamonu) for providing material and editor and reviewers, who took the burden to read the manuscript for valuable comments. This study was supported by the Scientific Research Project Coordination Unit of Recep Tayyip Erdogan University (Project No: FBA-2022-1419).

References

Bektas Y, Aksu İ, Kaya C, Bayçelebi E, Turan D (2022) DNA barcoding and species delimitation of the genus *Oxynoemacheilus* (Teleostei: Nemacheilidae) in Anatolia. Journal of Fish Biology 101: 505–514. https://doi.org/10.1111/jfb.15114

Çiçek E, Eagderi S, Sungur S (2018) *Oxynoemacheilus veyseli*, a new nemacheilid species from the upper aras river drainage of Turkey (Teleostei: Nemacheilidae). Iranian Journal of Ichthyology 5: 232–242. https://doi.org/10.22034/iji.v5i3.302

Dellicour S, Flot J-F (2018) The hitchhiker's guide to single-locus species delimitation. Molecular Ecology Resources 18(6): 1234–1246. https://doi.org/10.1111/1755-0998.12908

Drummond AJ, Suchard MA, Xie D, Rambaut A (2012) Bayesian phylogenetics with BEAUti and the BEAST 1.7. Molecular Biology and Evolution 29(8): 1969–1973. https://doi.org/10.1093/molbev/mss075

Eagderi S, Jalili P, Çiçek E (2018) *Oxynoemacheilus elsae*, a new species from the Urmia Lake basin of Iran (Teleostei: Nemacheilidae). FishTaxa 3: 453–459.

Erk'akan F (2012) Two New Oxynoemacheilus (Teleostei: Nemacheilidae) Species from Western Turkey. Research Journal of Biological Sciences 7(2): 97–101. https://doi.org/10.3923/rjbsci.2012.97.101

Ezard T, Fujisawa T, Barraclough TG (2009) SPlits: SPecies' LImits by Threshold Statistics. http://r-forge.r-project.org/projects/splits/ [R Package version 1 1: r29]

Freyhof J (2016) *Oxynoemacheilus karunensis*, a new species from the Persian Gulf basin (Teleostei: Nemacheilidae). Zootaxa 4175(1): 94–100. https://doi.org/10.11646/zootaxa.4175.1.9

Freyhof J, Abdullah YS (2017) Two new species of *Oxynoemacheilus* from the Tigris drainage in Iraqi Kurdistan (Teleostei: Nemacheilidae). Zootaxa 4238(1): 73–87. https://doi.org/10.11646/zootaxa.4238.1.5

Freyhof J, Geiger MF (2021) *Oxynoemacheilus shehabi*, a new nemacheilid loach from the upper Orontes in southern Syria (Teleostei: Nemacheilidae). Zootaxa 4908(4): 571–583. https://doi.org/10.11646/zootaxa.4908.4.9

Freyhof J, Özuluğ M (2017) *Oxynoemacheilus hazarensis*, a new species from Lake Hazar in Turkey, with remarks on *O. Euphraticus* (Teleostei: Nemacheilidae). Zootaxa 4247(4): 378–390. https://doi.org/10.11646/zootaxa.4247.4.2

Freyhof J, Erk'akan F, Özeren C, Perdices A (2011) An overview of the western Palaearctic loach genus *Oxynoemacheilus* (Teleostei: Nemacheilidae). Ichthyological Exploration of Freshwaters 22: 301–312.

Freyhof J, Kaya C, Turan D (2017) *Oxynoemacheilus kentritensis*, a new species from the upper Tigris drainage in Turkey with remarks on *O. frenatus* (Teleostei: Nemacheilidae). Zootaxa 4258(6): 551–560. https://doi.org/10.11646/zootaxa.4258.6.4

Freyhof J, Kaya C, Turan D, Geiger M (2019) Review of the *Oxynoemacheilus tigris* group with the description of two new species from the Euphrates drainage (Teleostei: Nemacheilidae). Zootaxa 4612(1): 29–57. https://doi.org/10.11646/zootaxa.4612.1.2

Freyhof J, Yoğurtçuoğlu B, Kaya C (2021a) *Oxynoemacheilus sarus*, a new nemacheilid loach from the lower Ceyhan and Seyhan in southern Anatolia (Teleostei: Nemacheilidae). Zootaxa 4964(1): 123–139. https://doi.org/10.11646/zootaxa.4964.1.6

Freyhof J, Kaya C, Epitashvili G, Geiger MF (2021b) *Oxynoemacheilus phasicus*, a new nemacheilid loach from the eastern Black Sea basin with some remarks on other Caucasian Oxynoemacheilus (Teleostei: Nemacheilidae). Zootaxa 4952(1): 135–151. https://doi.org/10.11646/zootaxa.4952.1.8

Freyhof J, Kaya C, Geiger M (2022) A practical approach to revise the *Oxynoemacheilus bergianus* species group (Teleostei: Nemacheilidae). Zootaxa 5128(2): 151–194. https://doi.org/10.11646/zootaxa.5128.2.1

Fujisawa T, Barraclough TG (2013) Delimiting species using single-locus data and the generalized mixed yule coalescent approach: A revised method and evaluation on simulated data sets. Systematic Biology 62(5): 707–724. https://doi.org/10.1093/sysbio/syt033

Geiger MF, Herder F, Monaghan MT, Almada V, Barbieri R, Bariche M, Berrebi P, Bohlen J, Casal-Lopez M, Delmastro GB, Denys GPJJ, Dettai A, Doadrio I, Kalogianni E, Kärst H, Kottelat M, Kovačić M, Laporte M, Lorenzoni M, Marčić Z, Özuluğ M, Perdices A, Perea S, Persat H, Porcelotti S, Puzzi C, Robalo J, Šanda R, Schneider M, Šlechtová V, Stoumboudi M, Walter S, Freyhof J (2014) Spatial het-

erogeneity in the mediterranean biodiversity hotspot affects barcoding accuracy of its freshwater fishes. Molecular Ecology Resources 14: 1210–1221. https://doi.org/10.1111/1755-0998.12257

Geiger MF (2019) FREDIE – Freshwater Diversity Identification for Europe (unpublished). https://www.ncbi.nlm.nih.gov/ [downloaded from NCBI Genbank]

Hall TA (1999) BioEdit a user-friendly biological sequence alignment editor and analysis program for Windows 95/98/NT. Nucleic Acids Symposium Series 41: 95–98.

Kamangar BB, Prokofiev AM, Ghaderi E, Nalbant TT (2014) Stone loaches of Choman River system, Kurdistan, Iran (Teleostei: Cypriniformes: Nemacheilidae). Zootaxa 3755(1): 33–61. https://doi.org/10.11646/zootaxa.3755.1.2

Kaya C, Turan D, Bayçelebi E, Kalayci G, Freyhof J (2020) *Oxynoemacheilus cilicicus*, a new nemacheilid loach from the Göksu River in southern Anatolia (Teleostei: Nemacheilidae). Zootaxa 4808(2): 284–300. https://doi.org/10.11646/zootaxa.4808.2.3

Kaya C, Yoğurtçuoğlu B, Freyhof J (2021) *Oxynoemacheilus amanos*, a new nemacheilid loach from the Orontes River drainage (Teleostei: Nemacheilidae). Zootaxa 4938(5): 559–570. https://doi.org/10.11646/zootaxa.4938.5.3

Kimura M (1980) A simple method for estimating evolutionary rates of base substitutions through comparative studies of nucleotide sequences. Journal of Molecular Evolution 16(2): 111–120. https://doi.org/10.1007/BF01731581

Kottelat M (1990) F. Pfeil, München Indochinese nemacheilines. A revision of nemacheiline loaches (Pisces: Cypriniformes) of Thailand, Burma, Laos, Cambodia and southern Viet Nam, 262 pp. https://doi.org/10.2307/1446613

Kottelat M (2012) Conspectus cobitidum*: An inventory of the loaches of the world (Teleostei: Cypriniformes: Cobitoidei). The Raffles Bulletin of Zoology 26: 1–199.

Leigh JW, Bryant D (2015) POPART: Full-feature software for haplotype network construction. Methods in Ecology and Evolution 6(9): 1110–1116. https://doi.org/10.1111/2041-210X.12410

Paradis E, Claude J, Strimmer K (2004) APE: Analyses of phylogenetics and evolution in R language. Bioinformatics (Oxford, England) 20(2): 289–290. https://doi.org/10.1093/bioinformatics/btg412

Posada D (2008) jModelTest: Phylogenetic model averaging. Molecular Biology and Evolution 25(7): 1253–1256. https://doi.org/10.1093/molbev/msn083

Puillandre N, Lambert A, Brouillet S, Achaz G (2012) ABGD, Automatic Barcode Gap Discovery for primary species delimitation. Molecular Ecology 21(8): 1864–1877. https://doi.org/10.1111/j.1365-294X.2011.05239.x

Puillandre N, Brouillet S, Achaz G (2021) ASAP: Assemble species by automatic partitioning. Molecular Ecology Resources 21(2): 609–620. https://doi.org/10.1111/1755-0998.13281

R Core Team (2013) R: A language and environment for statistical computing [Internet]. Vienna, Austria, 201.

Saygun S, Ağdamar S, Özuluğ M (2021) *Oxynoemacheilus fatsaensis*, a new nemacheilid loach from the Elekçi Stream in Northern Anatolia (Teleostei: Nemacheilidae). Zoologischer Anzeiger 294: 39–49. https://doi.org/10.1016/j.jcz.2021.07.011

Sayyadzadeh G, Eagderi S, Esmaeili HR (2016) A new loach of the genus *Oxynoemacheilus* from the Tigris River drainage and its phylogenetic relationships among the nemacheilid. Iranian Journal of Ichthyology 3: 236–250.

Sungur S, Jalili P, Eagderi S (2017) *Oxynoemacheilus ciceki*, new nemacheilid species (Teleostei, Nemacheilidae) from the Sultan Marsh, Kayseri province, Turkey. Iranian Journal of Ichthyology 4: 375–383.

Tamura K, Stecher G, Kumar S (2021) MEGA11: Molecular Evolutionary Genetics Analysis Version 11. Molecular Biology and Evolution 38(7): 3022–3027. https://doi.org/10.1093/molbev/msab120

Thompson JD, Higgins DG, Gibson TJ (1994) CLUSTAL W: Improving the sensitivity of progressive multiple sequence alignment through sequence weighting, position-specific gap penalties and weight matrix choice. Nucleic Acids Research 22(22): 4673–4680. https://doi.org/10.1093/nar/22.22.4673

Turan D, Kaya C, Kalayci G, Bayçelebi E, Aksu İ (2019) *Oxynoemacheilus cemali*, a new species of stone loach (Teleostei: Nemacheilidae) from the Çoruh River drainage, Turkey. Journal of Fish Biology 94(3): 458–468. https://doi.org/10.1111/jfb.13909

Ward RD, Zemlak TS, Innes BH, Last PR, Hebert PDNN (2005) DNA barcoding Australia's fish species. Philosophical Transactions of the Royal Society of London, Series B, Biological Sciences 360(1462): 1847–1857. https://doi.org/10.1098/rstb.2005.1716

Yoğurtçuoğlu B, Kaya C, Freyhof J (2021a) *Oxynoemacheilus nasreddini*, a new nemacheilid loach from Central Anatolia (Teleostei: Nemacheilidae). Zootaxa 4974(1): 135–150. https://doi.org/10.11646/zootaxa.4974.1.5

Yoğurtçuoğlu B, Kaya C, Özuluğ M, Freyhof J (2021b) *Oxynoemacheilus isauricus*, a new nemacheilid loach from Central Anatolia (Teleostei: Nemacheilidae). Zootaxa 4975(2): 369–378. https://doi.org/10.11646/zootaxa.4975.2.7

Yoğurtçuoğlu B, Kaya C, Freyhof J (2022) Revision of the *Oxynoemacheilus angorae* group with the description of two new species (Teleostei: Nemacheilidae). Zootaxa 5133(4): 451–485. https://doi.org/10.11646/zootaxa.5133.4.1

Zoosyst. Evol. 99 (2) 2023, 457–472 | DOI 10.3897/zse.99.106667

PENSOFT

für Natur MUSEUM FÜR NATURKUNDE BERLIN

Revision of the genus *Oxyarcturus* (Isopoda, Valvifera, Antarcturidae), with a description of a new deep-sea species from Argentina

Emanuel Pereira[1,2], Daniel Roccatagliata[1,2], Brenda L. Doti[1,2]

1 *CONICET-Universidad de Buenos Aires, Instituto de Biodiversidad y Biología Experimental y Aplicada (IBBEA), Buenos Aires, Argentina*

2 *Universidad de Buenos Aires, Facultad de Ciencias Exactas y Naturales, Departamento de Biodiversidad y Biología Experimental (DBBE), Buenos Aires, Argentina*

https://zoobank.org/A22910A6-C10B-4D15-AE6A-2AA91A92A6CC

Corresponding author: Emanuel Pereira (emanuelp@bg.fcen.uba.ar, emanuel.mito@gmail.com)

Academic editor: Luiz F. Andrade ♦ **Received** 19 May 2023 ♦ **Accepted** 28 June 2023 ♦ **Published** 4 October 2023

Abstract

A new antarcturid isopod, *Oxyarcturus holoacanthus* **sp. nov.**, is fully described based on seven specimens collected in the Mar del Plata submarine canyon at 2950 m depth, during the "Talud Continental III" expedition on board the Argentinian RV "Puerto Deseado". *Oxyarcturus holoacanthus* **sp. nov.** is closely related to *O. spinosus* (Beddard, 1886), from which it can be distinguished by the body spine pattern. The penial plate, a novel character for the genus *Oxyarcturus*, as well as for the family Antarcturidae, is described in detail. The species *O. dubius* (Kussakin, 1967) and *O. beliaevi* (Kussakin, 1967) are considered as *incertae sedis* until further morphological and molecular data can clarify their taxonomic position. An update of the geographic and bathymetric records of the genus *Oxyarcturus* is provided.

Key Words

Mar del Plata submarine canyon, *Oxyarcturus beliaevi* (Kussakin, 1967), *Oxyarcturus dubius* (Kussakin, 1967), *Oxyarcturus holoacanthus* sp. nov., Southwest Atlantic

Introduction

The valviferan isopod family Antarcturidae Poore, 2001 is one of the most diverse families of the suborder in the deep-sea (Poore and Bruce 2012). Currently, it contains approximately 100 nominal species, assigned to 17 genera, most of them distributed in the Southern Hemisphere (Poore 2001; Boyko et al. 2008; Pereira et al. 2019). In particular, the genus *Oxyarcturus*, which is herein studied, was erected by Brandt (1990) to include three species from the Subantarctic Region and off South Africa (Beddard 1886; Kussakin 1967; Kensley 1977, 1978; Brandt 1990).

The deep-sea fauna off the Argentine coast is still scarcely known. Ten species of Antarcturidae were reported from this area during the 19th and 20th centuries; all these species were collected by foreign surveys, and each one reported from a single station (Beddard 1886; Kussakin 1967; Kussakin and Vasina 1998; Doti et al. 2020). In 2012 and 2013 the Argentine RV "Puerto Deseado" carried out three expeditions to the Mar del Plata submarine canyon (Talud Continental I–III). These surveys resulted in a remarkable improvement in our knowledge of the benthic invertebrates from this area, i.e., cold-water corals, echinoderms, crustaceans, etc. (Martinez et al. 2014; Doti 2017; Pereira and Doti 2017; Bernal et al. 2018; Risaro et al. 2020; Flores et al. 2021; Pereira et al. 2021; Roccatagliata 2023; among others). In particular, for the family Antarcturidae, three species collected by the above mentioned surveys were recently described: *Xiphoarcturus kussakini* Pereira, Roccatagliata & Doti, 2019, *X. carinatus* Pereira, Roccatagliata & Doti, 2019, and *Fissarcturus argentinensis* Pereira, Roccatagliata & Doti, 2020, bringing to 13 the number of species of Antarcturidae recorded off Argentina (Pereira et al. 2019, 2020).

In the current contribution a new deep-sea species of the family Antarcturidae, *Oxyarcturus holoacanthus* sp. nov.

is fully described and illustrated based on seven specimens collected in the Mar del Plata submarine canyon. In addition, *O. dubius* (Kussakin, 1967) and *O. beliaevi* (Kussakin, 1967) are considered as *incertae sedis* until their taxonomic status is resolved. Finally, the geographic and bathymetric distributions of the genus are updated.

Material and method

The specimens were obtained with a bottom otter trawl during the "Talud Continental III" expedition on board the RV "Puerto Deseado", in 2013. Afterwards, the material was fixed in 96% ethanol.

The described specimens were stained with Chlorazol Black E, and the appendages were dissected and temporarily mounted in glycerol. Drawings of the whole animal were prepared with a Leica MZ8 stereoscopic microscope, those of the dissected appendages were prepared using a Carl Zeiss (Axioskop) compound microscope, both equipped with a camera lucida. Line drawings were rendered in a digital format using a Wacom tablet and the Adobe Illustrator program (Coleman 2003).

For the sake of clarity, in those appendages with a large number of setae, some of them were omitted in the figures. Therefore, the number of setae drawn may not match with the numbers mentioned in the text.

Habitus photographs were taken with a digital camera Nikon D7500 equipped with a macro lens Sigma 105 mm f2.8 EX. Appendages' photographs were taken with a digital camera Sony Cyber-shot DSC-WX1 mounted on the compound microscope.

Total body length was measured in dorsal view from the frontal margin of head to the tip of the pleotelson (in flexed specimens, total length was estimated by the sum of individual body parts). Appendage lengths were measured after Hessler (1970). For the terminology of the body parts, spines and setae, see Pereira et al. (2019). The eye size was estimated by the ratio between the eye diameter (e) and the distance between the eye and the anterior margin of the head (d) following Pereira et al. (2020).

The geographic distribution of the *Oxyarcturus* species was charted using the PanMap software v.0.9.6 (Diepenbroek et al. 2002), on a map generated by the GeoMapApp software v.3.6.15 (www.geomapapp.org) / CC BY (Ryan et al. 2009).

The type material is deposited in the Invertebrate collection of the Museo Argentino de Ciencias Naturales "Bernardino Rivadavia" (**MACN**), Buenos Aires.

Results

Suborder Valvifera Sars, 1883
Family Antarcturidae Poore, 2001

Genus *Oxyarcturus* Brandt, 1990

Oxyarcturus Brandt, 1990: 73–74;– Wägele 1991: 138;– Poore 2001: 224.

Type species. *Arcturus spinosus* Beddard, 1886.

Diagnosis (modified from Brandt 1990). Body slender and geniculate; dorsal surface covered with many spines. Head with two long supraocular spines, followed by two (or more) long posterior supraocular spines. Eyes well developed, lateral, rounded or rather oval. All pleonites fused with pleotelson, pleonites 1–3 separated by transverse grooves. Pleotelson with two long caudolateral spines, and a single subterminal medial spine in between. Antenna longer than body, flagellum multiarticulate with at least 8 articles. Pereopod I developed into a strong subchela, dactylus not swollen. Pereopods II–IV, dactylus without filter setae.

Remarks. Brandt (1990) in a comprehensive work of the Antarctic Valvifera revised the old genus *Antarcturus* zur Strassen, 1902, and transferred 17 of the species previously placed in this genus to *Acantharcturus* Schultz, 1981, *Chaetarcturus* Brandt, 1990, *Litarcturus* Brandt, 1990, *Tuberarcturus* Brandt, 1990 and *Oxyarcturus* Brandt, 1990. Brandt (1990) erected the genus *Oxyarcturus* to include three species: *O. spinosus* (Beddard, 1886), *O. dubius* (Kussakin, 1967) and *O. beliaevi* (Kussakin, 1967); and stated that members of this genus have "caudal margin of pleotelson with 3 acute spines, two long laterocaudal ones and one shorter medial spine"; being this the only feature characterizing the genus. Although this medial spine is evident in *O. spinosus* (type species) and *O. holoacanthus* sp. nov. (see Beddard (1886); current study Figs 1A, B, 2C), the presence of this spine in *O. dubius* and *O. beliaevi* is uncertain. Unfortunately, Kussakin (1967) did not include figures in dorsal view of *O. dubius* and *O. beliaevi*. However, he wrote that *O. dubius* has "very small, weakly expressed spinules, largest of which were disposed in midline near posterior margin of pleotelson". Regarding *O. beliaevi*, although Kussakin (1967) did not mention the presence of a medial spine in this species, Kensley (1977, 1978) reported this spine in specimens from South Africa. However, Wägele (1991) and Kussakin and Vasina (1995) questioned Kensley's identification.

In addition, Kussakin (1967) stated that *O. dubius* has numerous long setae on the internal margin of the five distal articles (ischium to dactylus) on the pereopods II–IV. Within Antarcturidae, the presence of filter setae on the dactyli of the pereopods II–IV is characteristic of the species of the genera *Chaetarcturus* Brandt, 1990, *Mixarcturus* Brandt, 1990, *Caecarturus* Schultz, 1981 and *Glaberarcturus* Kussakin & Vasina, 1998 (Schultz 1981; Brandt 1990; Kussakin and Vasina 1998).

O. dubius (Kussakin, 1967) is clearly not a member of *Oxyarcturus*, and *O. beliaevi* (Kussakin, 1967) probably neither. Therefore, these two species are herein removed from the genus *Oxyarcturus* and placed as *incertae sedis*, until further morphological and molecular data can clarify their taxonomic position.

On the other hand, the specimens from South Africa identified by Kensley (1977) as *Antarcturus beliaevi* most probably belong to a new species of *Oxyarcturus*. If confirmed to be a new species, its description should be

completed, one specimen should be designated as holotype, and a formal name should be adopted.

Species included. *O. spinosus* (Beddard, 1886); *O. holoacanthus* sp. nov., and probably *Antarcturus beliaevi* Kussakin, 1967 *sensu* Kensley 1977.

Oxyarcturus holoacanthus sp. nov.

https://zoobank.org/D7DE7D4E-1C60-4CD8-A180-808C9317B91F

Figs 1–10

Type material. ***Holotype*** adult ♂ (30.7 mm). "Talud Continental III" expedition, Sta. 47 (38°06.58'S, 53°42.83'W), 2950 m, bottom otter trawl, 06 Sep. 2013, RV "Puerto Deseado", I. Chiesa & A. Martinez leg. MACN-In 44318.

Paratypes 4 adult ♂♂ (31.3–35.4 mm); 1 adult ♂ broken; 1 ovigerous ♀ (38.9 mm). Same data as holotype. MACN-In 44319.

Diagnosis. Head with 2 long supraocular spines and 6 posterior supraocular spines. Eyes large (e/d ratio = 1.6). Pereonite 1 with 6 submedial, 2 sublateral and 4 lateral long spines. Pereonites 2–4 with 4 submedial, 2 sublateral and 2 lateral long spines. All four pereonites with additional small spines. Pereonites 5–7 with 2 submedial spines, and sublateral and lateral spines. All pleonites fused with the pleotelson, pleonite 1 indicated by transverse groove. Pleonites 1–3 with 2 submedial spines, and sublateral and lateral spines. Pleotelson, dorsal surface and lateral margins with long spines. Uropod, external surface of protopod with many short spines.

Description. Adult male (habitus based on the holotype MACN-In 44318; appendages based on the paratype MACN-In 44319-a).

Body (Figs 1A, B, 2A, B) cylindrical and geniculate. Head with 2 long supraocular spines, 6 long posterior supraocular spines, 2 long lateral spines. Eyes large (e/d ratio = 1.6). Pereonite 1 with 6 submedial, 2 sublateral and 4 lateral long spines. Pereonites 2–4 with 4 submedial, 2 sublateral and 2 lateral long spines. All four pereonites with additional small spines. Pereonites 5–7 with 2 submedial spines, and sublateral and lateral spines. All pleonites fused with pleotelson, pleonite 1 indicated by transverse groove. Pleonites 1–3 with 2 submedial spines, and sublateral and lateral spines; pleonite 3 with 2 long lateral spines. Pleotelson with 2 long caudolateral spines, and 1 short subterminal medial spine in between; dorsal surface with long spines; lateral margins with spines.

Antennula (Fig. 3A, B) peduncle of 3 articles; article 1 widest, with 1 feather-like seta distally, setules on both margins, and cuticular combs; article 2 longest, with 8 feather-like setae (some of them broken); article 3 0.79× article 2 length, with 2 simple setae (broken). Flagellum of 3 articles; article 1 very short, ring-like and glabrous; article 2 longest, with 22 groups of 1–3 aesthetascs and 0–2 long simple setae each; article 3 minute, knob like, with 1 aesthetasc and 3 simple setae.

Antenna (Figs 1A, C, 2A, B, 3C) peduncle of 5 articles; article 1 short and wide, glabrous; article 2 subequal in width to article 1, with 3 distal spines and 5 simple setae on ventral margin; article 3 0.38× article 5 length, with 2 distal spines and 8 simple setae; article 4 0.88× article 5 length, with 2 distal spines; article 5 longest, with 1 distal spine. Flagellum of 8 articles, last article minute, claw-like (flagellum broken in the paratype drawn).

Mandibles (Fig. 3D, E) asymmetrical, without palp. Incisor processes with 4 strong sclerotized teeth. Molar processes with grinding surface and indented margins; right molar process narrower than left one, and with 9 setae on lower surface. Left *lacinia mobilis* with 3 rounded teeth and 1 stout serrate seta; right *lacinia mobilis* with 4 acute teeth and a few small setae.

Maxillula (Fig. 4A) lateral lobe with 10 stout setae distally. Mesial lobe with 3 setulate long setae distally (1 of them broken). Both lobes with simple setae marginally.

Maxilla (Fig. 4B) outer lobe with 6 serrate setae distally. Mesial lobe with 4 serrate setae distally. Inner lobe with 22–23 setulate setae distally. Surface and margins of outer, mesial and inner lobes covered with setules.

Maxilliped (Fig. 4C) basal endite short and broad, with 18 setulate setae on distal and lateral margins. Palp of 5 articles; article 1 0.4× article 3 length, with 11 simple setae; article 2 0.6× article 3 length, with 24–25 simple setae; article 3 longest, with 40 simple and serrulate setae on inner margin, and 4 long setae (3 of them broken) on outer distal angle; article 4 0.9× article 3 length, with 30 simple and serrulate setae on inner margin, and 8 long simple and serrulate setae along outer margin; article 5 shortest, with 12 simple and serrulate setae. Epipod long, oval, surpassing distal margin of palp article 1, with few simple setae on ventral surface and inner margin. Basis and epipod, ventral surfaces with small setae and cuticular combs.

Pereopod I (Fig. 4D) shorter and stouter than pereopods II–IV. Basis short, with 1 short proximal spine (broken); ischium, merus and carpus 0.6, 0.4 and 0.3× propodus length, respectively; propodus longest article; dactylus 0.6× propodus length (excluding claws), with 2 distal claws, ventral claw 0.4× dorsal claw length. Distal corner of basis and flexor margin of ischium with long simple setae. Flexor margins of merus to dactylus, and mesial face of propodus with serrulate setae (for sake of clarity, these latter setae were not drawn in Fig. 4D).

Pereopods II–IV (Fig. 5) alike, pereopod IV longest. Bases gradually changing from short and smooth (pereopod II) to long and with spines (pereopod IV). Note: spines are broken or worn out in the specimen drawn. These spines are better preserved in the holotype (see Figs 1A, 2A). Ischium, merus and carpus with 1 long distal spine (except on carpus of pereopod IV). Distal corner of flexor margin of basis and flexor margins of ischium to propodus with two rows of filter setae. Dactylus (excluding claws) 0.2–0.3× propodus length, with 2 distal claws, ventral claw 0.4–0.6× dorsal claw length (see Fig. 5C).

Pereopods V–VII (Fig. 6) alike, shorter than pereopods II–IV, pereopod V longest (pereopod VI broken at merus level). Bases longest article, with spines and 0–4 feather-like setae on extensor margin.

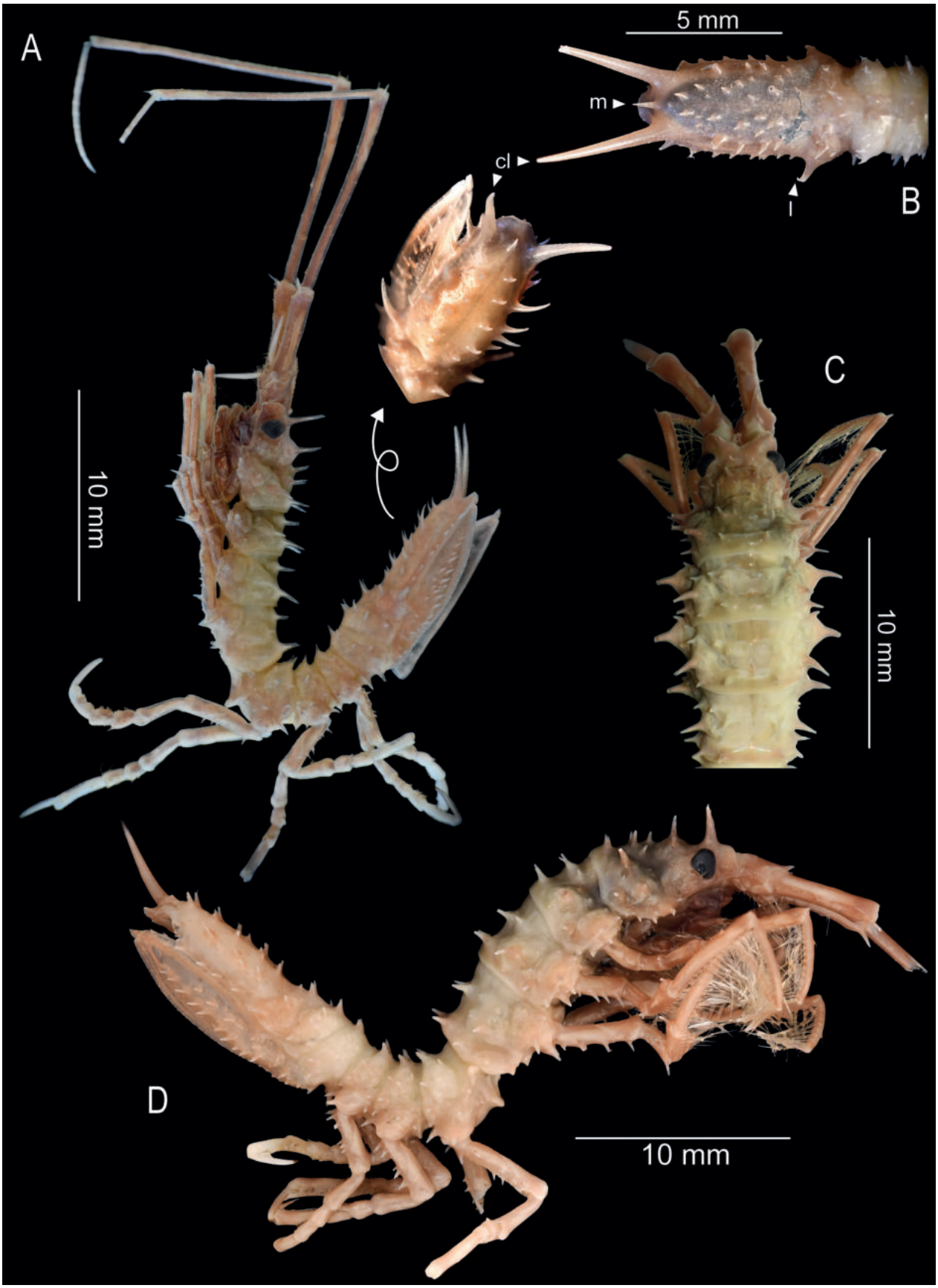

Figure 1. *Oxyarcturus holoacanthus* sp. nov. Photographs. Holotype male (MACN-In 44318). **A.** Habitus, lateral view. Paratype male (MACN-In 44319-a); **B.** Pleon, dorsal view. Paratype female (MACN-In 44319-b); **C.** Head and pereonites 1–4, dorsal view; **D.** Habitus, lateral view. **cl** – caudolateral spine; **m** – medial spine; **l** – lateral spine.

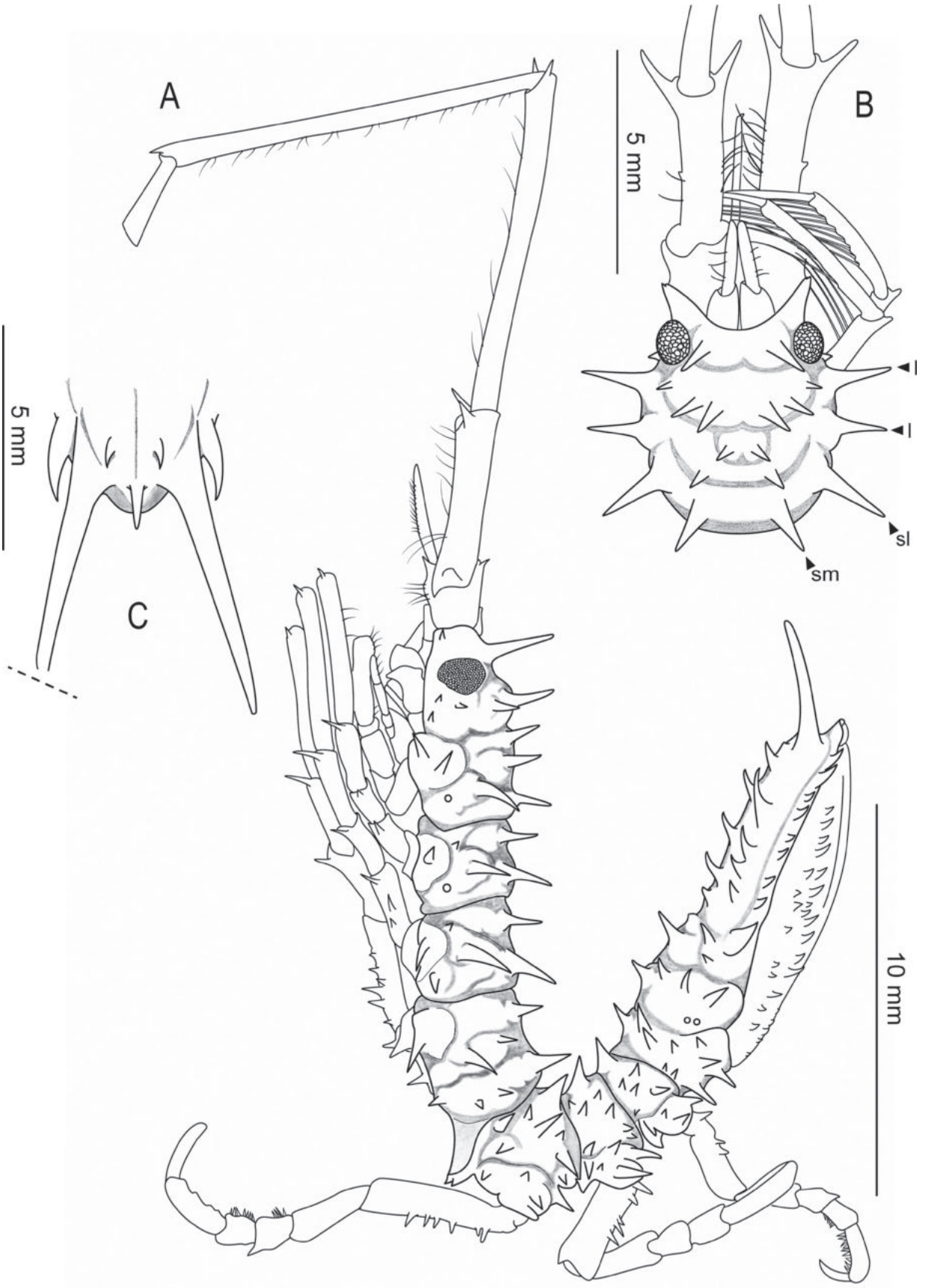

Figure 2. *Oxyarcturus holoacanthus* sp. nov. Holotype male (MACN-In 44318). **A.** Habitus, lateral view; **B.** Head and pereonite 1dorsal view (arrowhead point pereonite 1 spines). Paratype male (MACN-In 44319-a); **C.** Tip of pleotelson, dorsal view. **sm** – submedial spine; **sl** – sublateral spine; **l** – lateral spine.

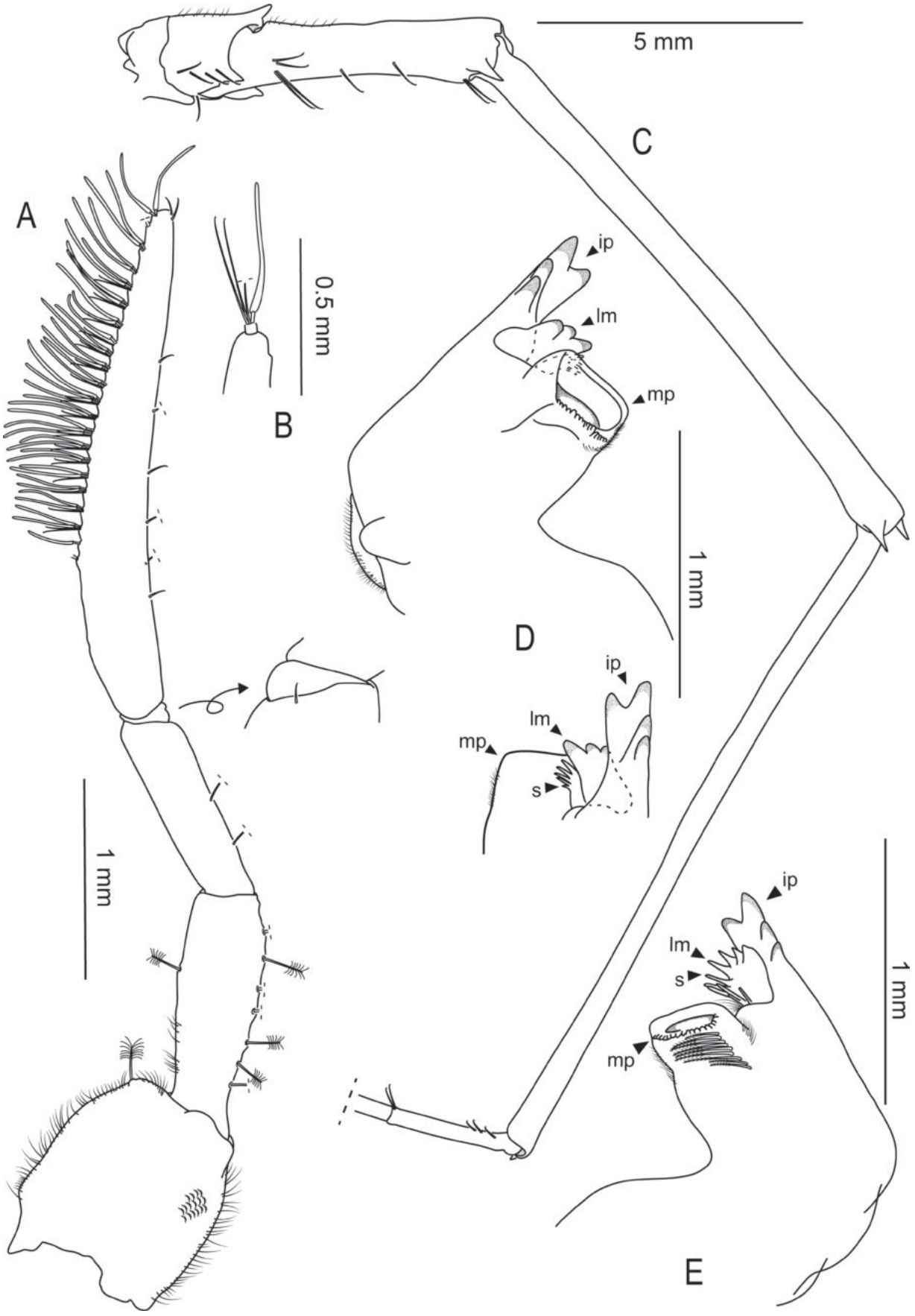

Figure 3. *Oxyarcturus holoacanthus* sp. nov. Paratype male (MACN-In 44319-a). **A**. Left antennula (last article missing), with detail of first flagellar article; **B.** Right antennula, last article; **C.** Left antenna; **D.** Left mandible, different views; **E.** Right mandible. **ip** – incisor process; **lm** – *lacinia mobilis*; **mp** – molar process; **s** – seta.

Figure 4. *Oxyarcturus holoacanthus* sp. nov. Paratype male (MACN-In 44319-a). **A.** Left maxillula; **B.** Left maxilla, with detail of setulate seta; **C.** Left maxilliped, with detail of endite and serrulate seta; **D.** Left pereopod I, with details of dactylus and a serrulate seta.

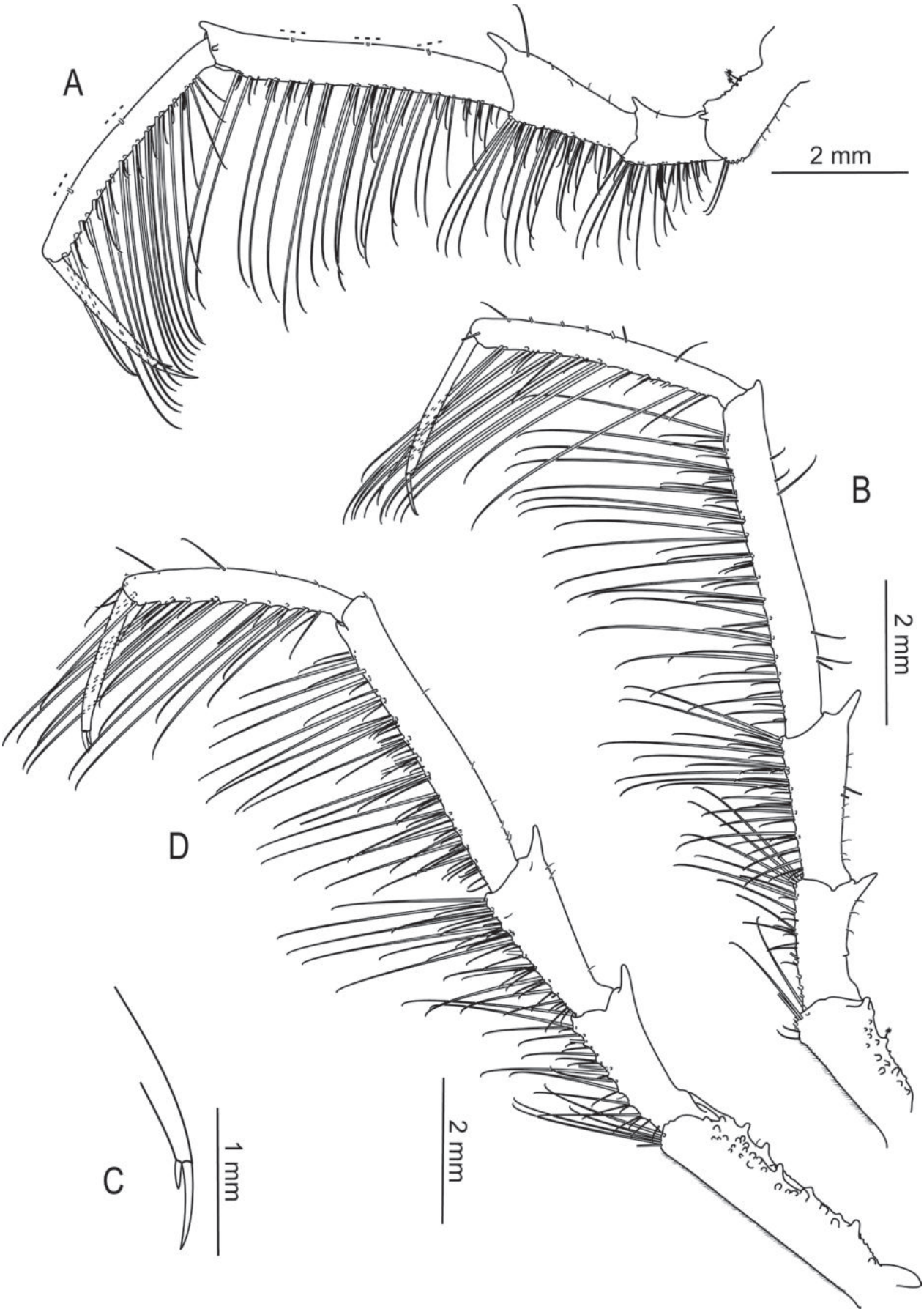

Figure 5. *Oxyarcturus holoacanthus* sp. nov. Paratype male (MACN-In 44319-a). **A.** Left pereopod II; **B.** Left pereopod III; **C.** Distal claws of right pereopod III; **D.** Left pereopod IV.

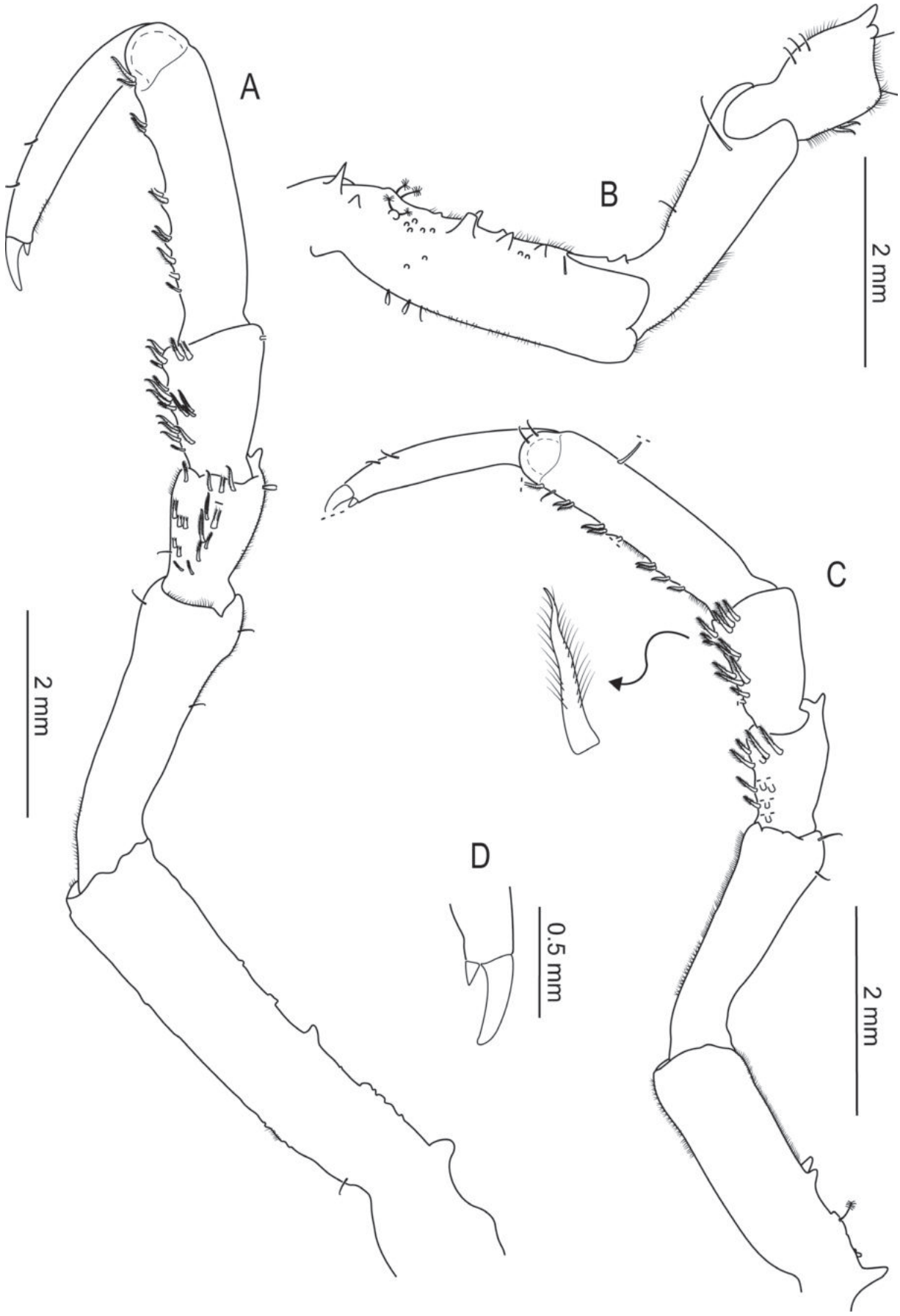

Figure 6. *Oxyarcturus holoacanthus* sp. nov. Paratype male (MACN-In 44319-a). **A.** Left pereopod V; **B.** Left pereopod VI, basis to merus only (remaining articles broken); **C.** Left pereopod VII, with detail of a spine-like seta; **D.** Distal claws of right pereopod VII.

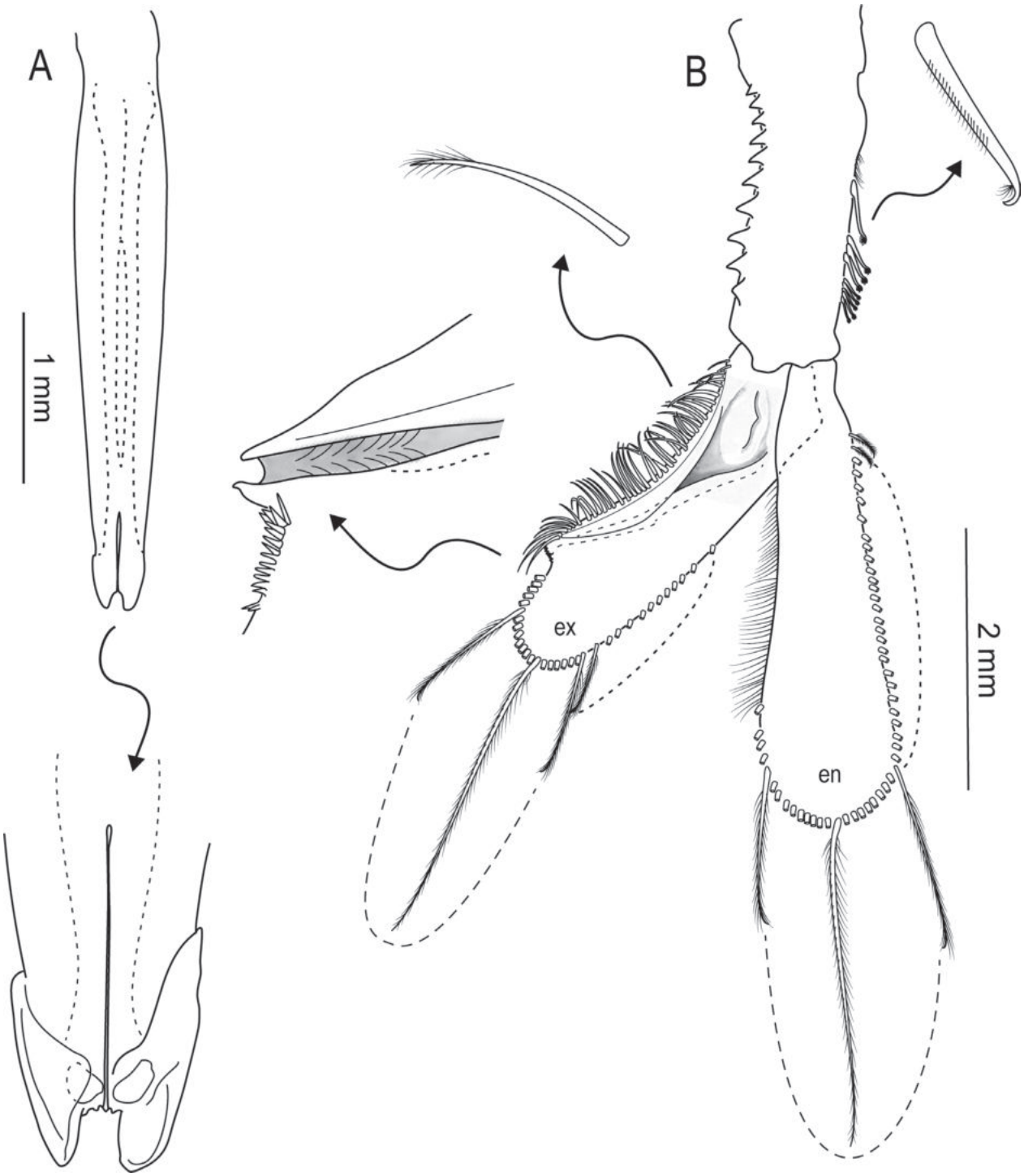

Figure 7. *Oxyarcturus holoacanthus* sp. nov. Paratype male (MACN-In 44319-a). **A.** Penial plate, with detail of distal tip; **B.** Left pleopod I, with details of distal end of groove, curved distal-plumose seta and coupling seta. **en** – endopod; **ex** – exopod.

Note: spines are broken or worn out in the specimen drawn. These spines are better preserved in the holotype (see Figs 1A, 2A). Ischium subequal in length to propodus; merus 0.4× propodus length, with 1 distal spine and 10–16 spine-like setae on flexor margin; carpus 0.5× propodus length, with 13–18 spine-like setae on flexor margin; propodus with 10 spine-like setae on flexor margin; dactylus (excluding claws) 0.8× propodus length, with 2 simple setae on extensor margin and 2 distal claws, ventral claw 0.3× dorsal claw length (see Fig. 6D). All articles with small setae scattered on extensor and flexor margins.

Penial plate (Figs 7A, 8A) fused and elongated, tapering distally; distal end barely slit, with two lateral spoon-like projections (see details).

Pleopod I (Figs 7B, 8B) protopod longer than those of remaining pleopods, with 9 coupling setae on inner margin, and 10 stout spines along outer margin. Endopod 1.1× exopod length, inner and distal margins with 55 plumose setae; outer margin with many setules. Exopod,

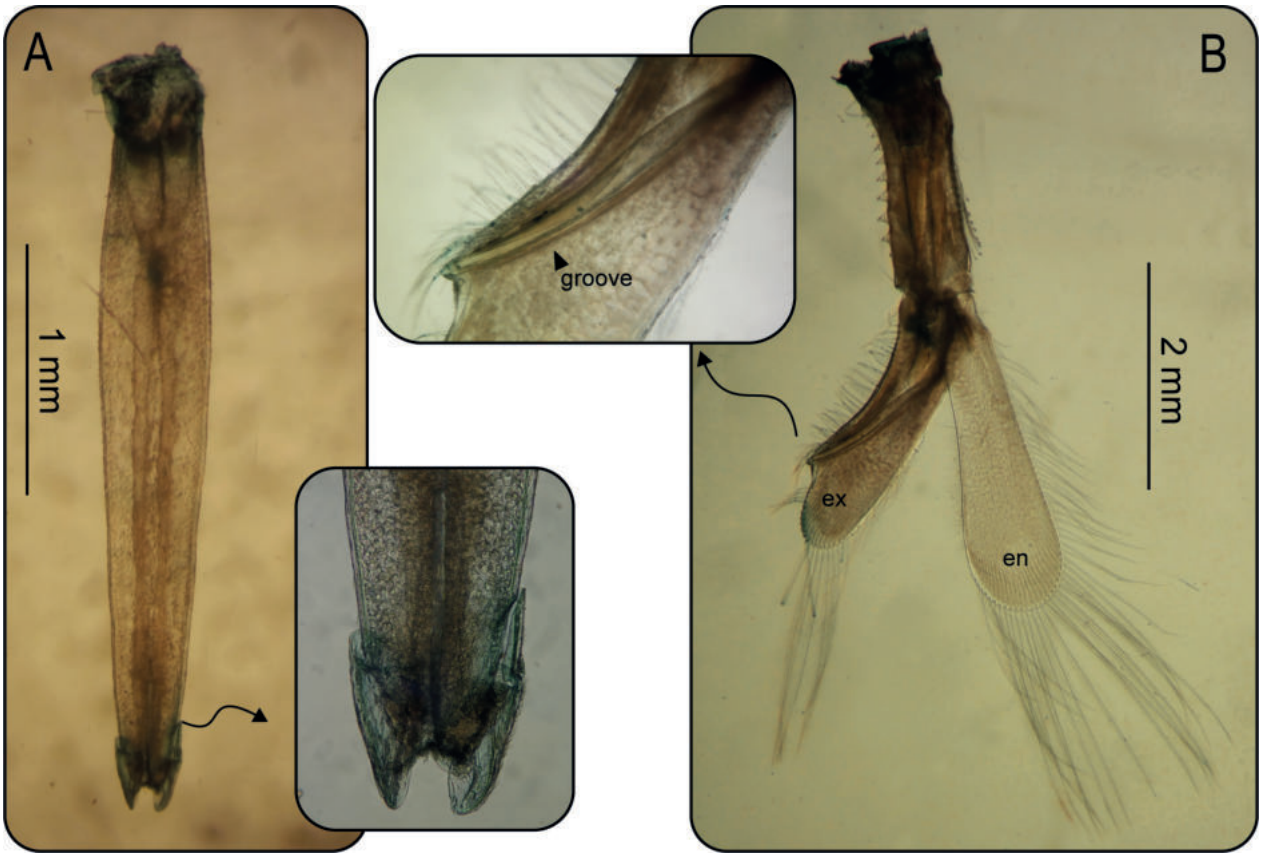

Figure 8. *Oxyarcturus holoacanthus* sp. nov. Light microscope photographs. Paratype male (MACN-In 44319-a). **A.** Penial plate, with detail of distal tip; **B.** Left pleopod I, with detail of posterior groove. **en** – endopod; **ex** – exopod.

inner and distal margins with 33 plumose setae; outer margin with 49–50 short distally plumose setae (some of them arranged in a second row on posterior surface). Posterior surface groove narrowing distally, and ending on lateral margin, overlapped by a thin layer; groove slightly projected distally, followed by a group of tiny setae (see detail). All plumose setae shorter than rami.

Pleopod II (Fig. 9A) protopod quadrangular, with 6 coupling setae on inner margin. Endopod with 63 plumose setae marginally. *Appendix masculina* subequal in length to endopod, tapering distally, with a small, rounded expansion close to distal end (see detail). Exopod subequal in length to endopod, with 90 plumose setae marginally. All plumose setae shorter than rami.

Pleopods III–V (Fig. 9B–D) protopod with 0–2 plumose setae on inner margin. Endopod 0.8–1.0× exopod length, with 2–30 plumose setae and some short simple setae. Exopod with distal setules.

Uropod (Fig. 9E, F) biramous. Protopod, external surface with 16 spines and many stunt tubercles; inner margin with 20 plumose setae (some broken). Endopod with 2 distal setae (both broken). Exopod 0.7× endopod length, glabrous.

Adult female description (habitus and appendages based on paratype MACN-In 44319-b).

As adult male, except for:

Antennula (Fig. 10A) flagellum: article 1 with 3 feather-like setae; article 2 with 16 groups of 1–3 aesthetascs and 2 long simple setae each; article 3 with 2 aesthetascs, 1 feather-like seta (broken) and 2 simple setae.

Pleopod I (Fig. 10B) protopod longer than those of remaining pleopods, with 11 coupling setae on inner margin, and 10 stout spines on outer margin. Rami subequal in length. Endopod with 62 plumose setae marginally. Exopod with 79 plumose setae marginally. All plumose setae shorter than rami.

Pleopod II (Fig. 10C) protopod quadrangular, with 7 coupling setae on inner margin, and 4 plumose setae on outer margin (broken). Rami subequal. Endopod with 78 plumose setae marginally. Exopod with 86 plumose setae marginally. All plumose setae shorter than rami.

Etymology. The specific epithet combines two Greek words *holos* = "entire, complete" and *akantha* = "spine", referring to the many long and acute spines that cover the body surface of this species.

Distribution. Only known from the Mar del Plata submarine canyon, off Buenos Aires Province, Argentina, at 2950 m depth (Fig. 11).

Remarks. *Oxyarcturus holoacanthus* sp. nov. is most similar to *O. spinosus*. Both species have a large number of long spines on body surface. *Oxyarcturus holoacanthus* sp. nov. can be distinguished from *O. spinosus* as follows: head with 6 posterior supraocular spines (2–4 posterior supraocular spines in *O. spinosus*), pereonites 1–4 with 4–6 submedial spines (only 2 submedial spines in *O. spinosus*), pereonites 5–7

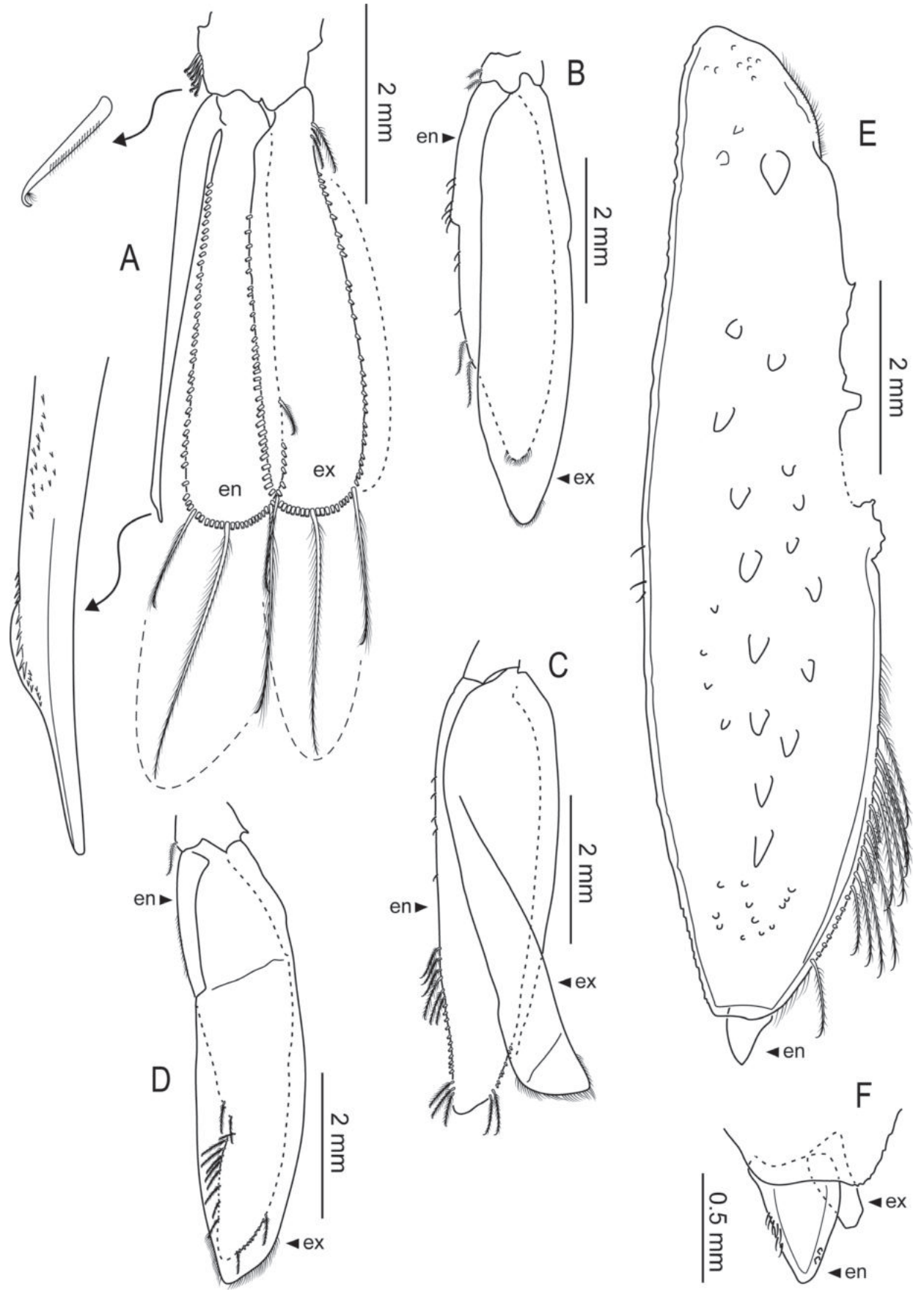

Figure 9. *Oxyarcturus holoacanthus* sp. nov. Paratype male (MACN-In 44319-a). **A.** Left pleopod II, with detail of tip of *appendix masculina* and coupling seta; **B–D.** Left pleopods III–V, respectively; **E.** Left uropod, external view; **F.** Right uropod, detail of rami, external view. **en** – endopod; **ex** – exopod.

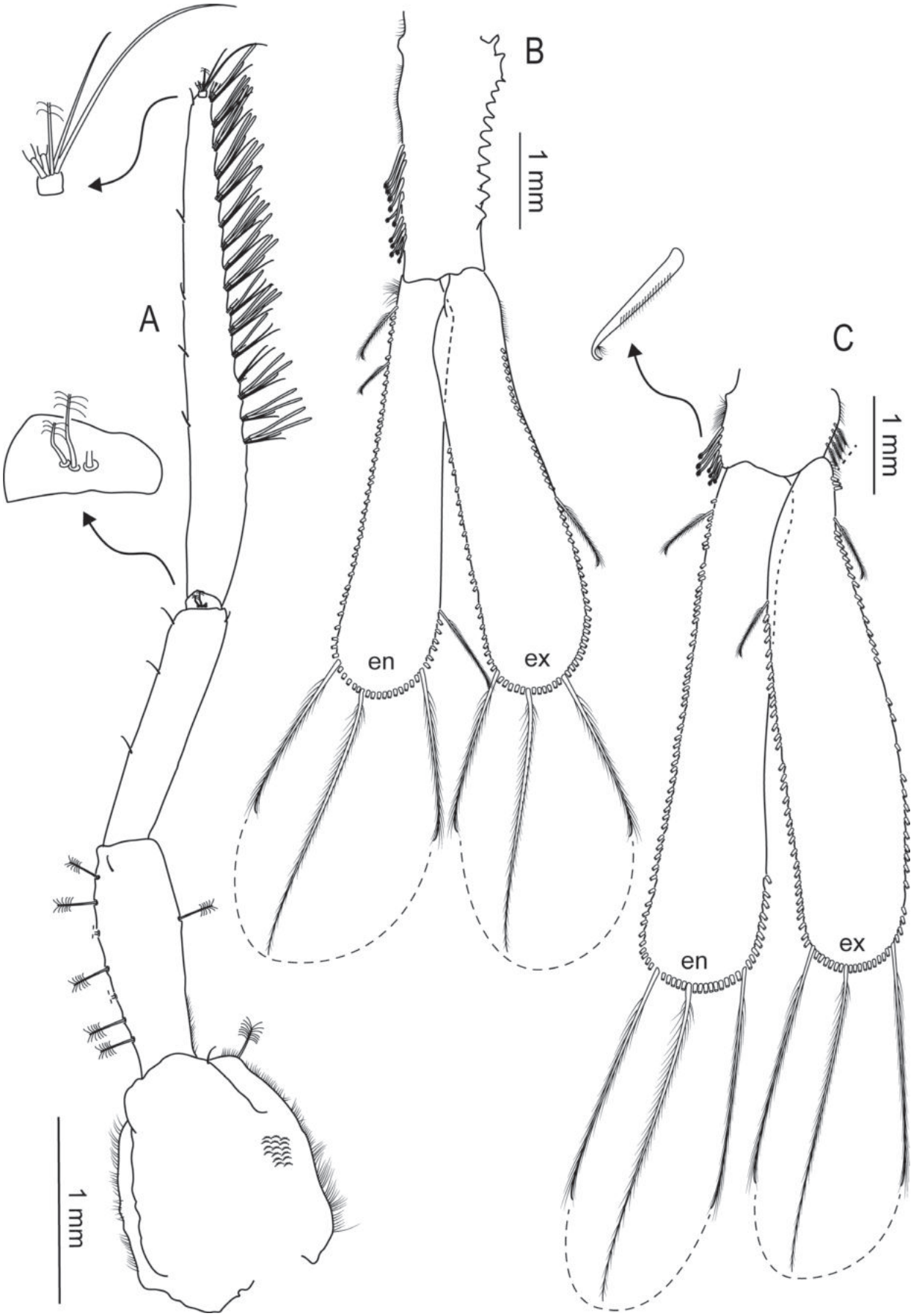

Figure 10. *Oxyarcturus holoacanthus* sp. nov. Paratype female (MACN-In 44319-b). **A.** Antennula, with details of first and third flagellar articles; **B.** Pleopod I; **C.** Pleopod II, with detail of coupling seta. **en** – endopod; **ex** – exopod.

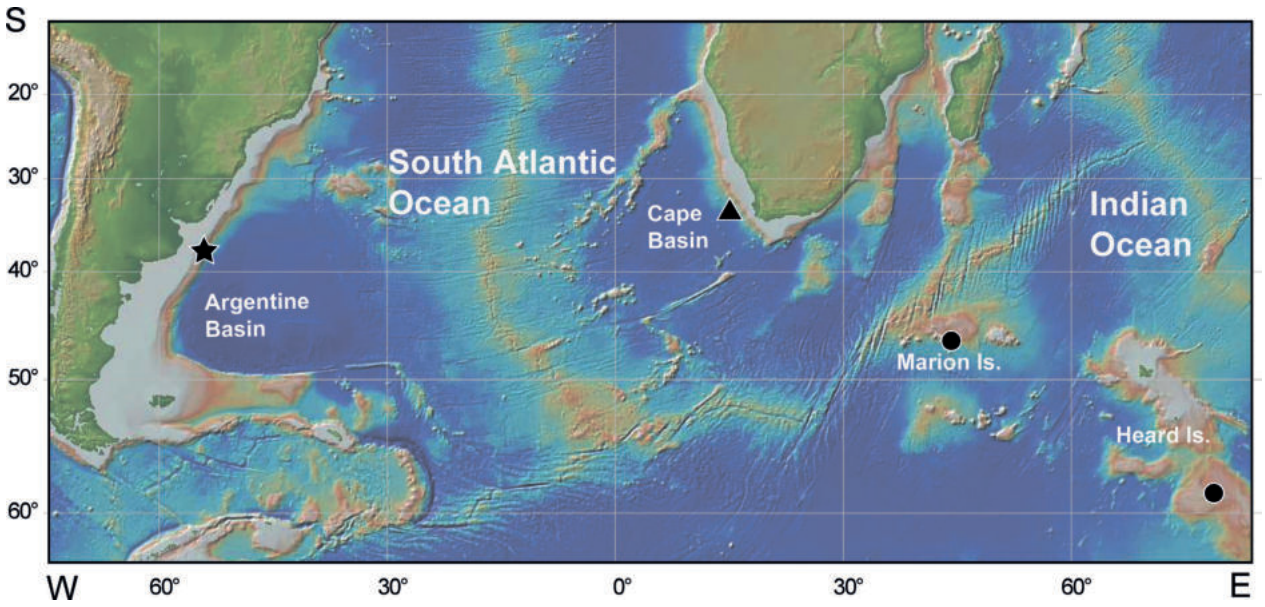

Figure 11. Distribution of *Oxyarcturus* species. (**star**) *O. holoacanthus* sp. nov.; (**circle**) *O. spinosus* (Beddard, 1886); (**triangle**) *Antarcturus beliaevi* Kussakin, 1967 *sensu* Kensley, 1977.

and pleon with many long dorsal spines on both sexes (male with small tubercles and female with small spines in *O. spinosus*).

Discussion

Oxyarcturus is one of the most poorly known genera of the family Antarcturidae. Currently, this deep-sea genus is composed of two nominal species and one probable new species from South Africa, each one with few records and few specimens reported (Beddard 1886; Kensley 1977, 1978; present study). This is also true for the new species herein studied, which was described based on only seven specimens obtained in a single station at the Mar del Plata submarine canyon.

Valviferans occur in 34 of 41 samples examined from the Talud Continental I–III expeditions (Pereira et al., in prep.). The single record of *Oxyarcturus holoacanthus* sp. nov. herein reported may reflect a patchy distribution of this species rather than an artifact of the sampling methods. It is worth noting that among the isopod species, singletons (species recorded only once) have also been reported from other deep-sea areas (Brandt et al. 2005; 2007a, b, 2015; Brix et al. 2018).

Although just a few specimens of *Oxyarcturus holoacanthus* sp. nov. were collected, it was possible to perform a detailed description of the body and appendages. The penial plate, which appears to be atypical for the family, is herein also described (Figs 7A, 8A). Pereira et al. (2020) described the penial plate of *Fissarcturus patagonicus* (Ohlin, 1901) as well, and discussed the importance of this character in the systematics of the family Antarcturidae. These findings suggest that the morphology of the penial plate should be included in future descriptions and phylogenetic studies. However, we are aware that this is not at all times possible, since deep-sea species are usually collected in low numbers of specimens, and adult males are not always available.

The spine pattern of *Oxyarcturus holoacanthus* sp. nov. showed slight variations among the specimens examined. However, since we have few specimens and some of them are damaged, we are not able to confirm whether these differences are related to size and/or sex. It is worth noticing that intraspecific variations in the spine pattern have been reported to some species of Antarcturidae (Nordenstam 1933; Kussakin 1967). Beddard (1886) mentioned that females of *O. spinosus* show more abundant and longer spines than males. Furthermore, sexual variation in the spine pattern has also been reported for other antarcturids, mainly in the genus *Fissarcturus* Brandt, 1990 (Brandt 1990, 2007; Pereira et al. 2020).

The members of the genus *Oxyarcturus* are known only from the Southern Hemisphere (Fig. 11, Table 1) i.e., *O. spinosus* was recorded off Marion Island and off Heard Island, *O. holoacanthus* sp. nov. off Argentina (Mar del Plata submarine canyon, ca. 38°S, 53°W), and *Antarcturus beliaevi sensu* Kensley, 1977 off South Africa. Regarding the bathymetric distribution (Table 1)

Table 1. Geographic and bathymetric distributions of *Oxyarcturus* species.

Species	Localities	Depths (m)	References
O. spinosus	Off Marion Is., between Heard Is. and Davis Sea	1580–2514	Beddard (1886), Kussakin (1967)
O. holoacanthus sp. nov.	Off Argentina (Mar del Plata submarine canyon)	2950	Current study
Antarcturus beliaevi sensu Kensley, 1977	Off South Africa	2500–3000	Kensley (1977, 1978)

all the species of *Oxyarcturus* were collected at deep waters between 1580–3000 m. Thus, the members of *Oxyarcturus* seem to be restricted to the lower slope.

Acknowledgments

We are grateful to Guido Pastorino (MACN) for leading the expedition "Talud Continental III"; and the crew of the RV "Puerto Deseado" for their assistance on board. We are particularly indebted to Ignacio Chiesa (CADIC) and Alejandro Martinez (INFIP) who collected the specimens studied in this contribution. To Sofía Calderón López (IBBEA) for her assistance with the photographs. Angelika Brandt (Senckenberg) and Gary Poore (Museums Victoria) whose comments helped us to improve this manuscript are also thanked. This research was funded by the National Scientific and Technical Research Council (CONICET, PIP 11220200102070CO).

References

Beddard FE (1886) Report on the Isopoda collected by H.M.S. Challenger during the years 1873–76. Part II. Report of the Voyage of the HMS Challenger 17: 1–175.

Bernal MC, Cairns SD, Penchaszadeh PE, Lauretta D (2018) *Errina argentina* sp. nov., a new stylasterid (Hydrozoa: Stylasteridae) from Mar del Plata submarine canyon (Southwest Atlantic). Marine Biodiversity 49(2): 833–839. https://doi.org/10.1007/s12526-018-0861-1

Boyko CB, Bruce NL, Hadfield KA, Merrin KL, Ota Y, Poore GCB, Taiti S [Eds] (2008 [onwards]) World Marine, Freshwater and Terrestrial Isopod Crustaceans database. Antarcturidae Poore, 2001. World Register of Marine Species. https://www.marinespecies.org/aphia.php?p=taxdetails&id=174627 on 2023-06-19

Brandt A (1990) Antarctic Valviferans (Crustacea, Isopoda, Valvifera). New Genera, New Species and Redescriptions. E.J. Brill, Leiden, 176 pp.

Brandt A (2007) Three new species of *Fissarcturus* (Isopoda, Antarcturidae) from the Southern Ocean. Zoological Journal of the Linnean Society 149(2): 263–290. https://doi.org/10.1111/j.1096-3642.2007.00247.x

Brandt A, Brenke N, Andres HG, Brix S, Guerrero-Kommritz E, Mühlenhardt-Siegel U, Wägele JW (2005) Diversity of peracarid crustaceans (Malacostraca) from the abyssal plain of the Angola Basin. Organisms, Diversity & Evolution 5: 105–112. https://doi.org/10.1016/j.ode.2004.10.007

Brandt A, Brix S, Brökeland W, Choudhury M, Kaiser S, Malyutina M (2007a) Deep-sea isopod biodiversity, abundance, and endemism in the Atlantic sector of the Southern Ocean—Results from the ANDEEP I–III expeditions. Deep-sea Research. Part II, Topical Studies in Oceanography 54(16–17): 1760–1775. https://doi.org/10.1016/j.dsr2.2007.07.015

Brandt A, Gooday AJ, Brandão SN, Brix S, Brökeland W, Cedhagen T, Choudhury M, Cornelius N, Danis B, DeMesel I, Diaz RJ, Gillan DC, Ebbe B, Howe JA, Janussen D, Kaiser S, Linse K, Malyutina M, Pawlowski J, Raupach M, Vanreusel A (2007b) First insights into the biodiversity and biogeography of the Southern Ocean deep sea. Nature 447(7142): 307–311. https://doi.org/10.1038/nature05827

Brandt A, Elsner NO, Malyutina MV, Brenke N, Golovan OA, Lavrenteva AV, Riehl T (2015) Abyssal macrofauna of the Kuril–Kamchatka Trench area (Northwest Pacific) collected by means of a camera-epibenthic sledge. Deep-sea Research. Part II, Topical Studies in Oceanography 111: 175–187. https://doi.org/10.1016/j.dsr2.2014.11.002

Brix S, Stransky B, Malyutina M, Pabis K, Svavarsson J, Riehl T (2018) Distributional patterns of isopods (Crustacea) in Icelandic and adjacent waters. Marine Biodiversity 48(2): 783–811. https://doi.org/10.1007/s12526-018-0871-z

Coleman CO (2003) "Digital inking": How to make the perfect line drawings on computers. Organisms, Diversity & Evolution 3(4): 1–14. https://doi.org/10.1078/1439-6092-00081

Diepenbroek M, Grobe H, Reinke M, Schindler U, Schlitzer R, Sieger R, Wefer G (2002) PANGAEA–An information system for environmental sciences. Computers & Geosciences 28(10): 1201–1210. https://doi.org/10.1016/S0098-3004(02)00039-0

Doti BL (2017) Three new paramunnids (Isopoda: Asellota: Paramunnidae) from the Argentine Sea, South-west Atlantic. Journal of the Marine Biological Association of the United Kingdom 97(8): 1695–1709. https://doi.org/10.1017/S0025315416001016

Doti BL, Chiesa IL, Roccatagliata D (2020) Biodiversity of the Deep-Sea Isopods, Cumaceans, and Amphipods (Crustacea: Peracarida) Recorded off the Argentine Coast. In: Hendrickx ME (Ed.) Deep-Sea Pycnogonids and Crustaceans of the Americas. Springer Nature, Switzerland, 157–191. https://doi.org/https//doi.org/10.1007/978-3-030-58410-8

Flores JN, Penchaszadeh PE, Brogger MI (2021) Heart urchins from the depths: *Corparva lyrida* gen. et sp. nov. (Palaeotropidae), and new records for the southwestern Atlantic Ocean. Revista de Biología Tropical 69(Suppl. 1): 14–34. https://doi.org/10.15517/rbt.v69iSuppl.1.46320

Hessler RR (1970) The Desmosomatidae (Isopoda, Asellota) of the Gay Head-Bermuda Transect. Bulletin of the Scripps Institution of Oceanography 15: 1–185.

Kensley B (1977) New records of marine Crustacea Isopoda from South Africa. Annals of the South African Museum 72: 239–265.

Kensley B (1978) Guide to the Marine Isopods of Southern Africa. South African Museum & The Rustica Press, Wynberg, Cape Town, 173 pp.

Kussakin OG (1967) Fauna of Isopoda and Tanaidacea in the coastal zones of the Antarctic and subantarctic water. Biological Reports of the Soviet Antarctic Expedition 3(1955–1958): 220–389.

Kussakin OG, Vasina GS (1995) Antarctic hadal arcturids, with descriptions of a new genus and five new species (Isopoda: Valvifera: Arcturidae). Zoosystematica Rossica 3: 207–228.

Kussakin OG, Vasina GS (1998) New bathyal and abyssal arcturids from the western Antarctic and Subantarctic (Crustacea: Isopoda: Arcturidae). Zoosystematica Rossica 7: 55–75.

Martinez MI, Solís-Marín FA, Penchaszadeh PE (2014) *Benthodytes violeta*, a new species of a deep-sea holothuroid (Elasipodida: Psychropotidae) from Mar del Plata Canyon (south-western Atlantic Ocean). Zootaxa 3760: 89–95. https://doi.org/10.11646/zootaxa.3760.1.6

Nordenstam Å (1933) Marine Isopoda of the families Serolidae, Idotheidae, Pseudidotheidae, Arcturidae, Parasellidae and Stenetriidae mainly from the South Atlantic. Further Zoological Results of the Swedish Antarctic Expedition 1901–1903(3): 1–284.

Ohlin A (1901) Isopoda from Tierra del Fuego and Patagonia. Svenska Expeditionen Till Magellansländerna 2: 261–306.

Pereira E, Doti B (2017) *Edotia abyssalis* n. sp. from the Southwest Atlantic Ocean, first record of the genus (Isopoda, Valvifera, Idoteidae) in the deep sea. Zoologischer Anzeiger 268: 19–31. https://doi.org/10.1016/j.jcz.2017.04.007

Pereira E, Roccatagliata D, Doti BL (2019) *Xiphoarcturus* – a new genus and two new species of the family Antarcturidae (Isopoda: Valvifera) from the Mar del Plata submarine canyon and its phylogenetic relationships. Arthropod Systematics & Phylogeny 77: 303–323. https://doi.org/10.26049/ASP77-2-2019-07

Pereira E, Roccatagliata D, Doti BL (2020) On the antarcturid genus *Fissarcturus* (Isopoda: Valvifera): Description of *Fissarcturus argentinensis* n. sp., first description of the male of *Fissarcturus patagonicus* (Ohlin, 1901), and biogeographic remarks on the genus. Zoologischer Anzeiger 288: 168–189. https://doi.org/10.1016/j.jcz.2020.08.002

Pereira E, Doti BL, Roccatagliata D (2021) A new species of *Pseudione sensu lato* (Isopoda: Bopyridae) on a squat lobster host from the deep South-West Atlantic. Zootaxa 4996(2): 363–373. https://doi.org/10.11646/zootaxa.4996.2.10

Poore GCB (2001) Isopoda Valvifera: Diagnoses and relationships of the families. Journal of Crustacean Biology 21(1): 205–230. https://doi.org/10.1163/20021975-99990118

Poore GC, Bruce NL (2012) Global diversity of marine isopods (except Asellota and crustacean symbionts). PLoS ONE 7(8): e43529. https://doi.org/10.1371/journal.pone.0043529

Risaro J, Williams GC, Pereyra D, Lauretta D (2020) *Umbellula pomona* sp. nov., a new sea pen from Mar del Plata Submarine Canyon (Cnidaria: Octocorallia: Pennatulacea). European Journal of Taxonomy 720: 121–143. https://doi.org/10.5852/ejt.2020.720.1121

Roccatagliata D (2023) The genus *Platytyphlops* (Cumacea: Crustacea): A new species from Argentina, taxonomic status of *Platytyphlops orbicularis* (Calman, 1905), and remarks on the genus. Zoologischer Anzeiger 302: 284–292. https://doi.org/10.1016/j.jcz.2022.12.008

Ryan WBF, Carbotte SM, Coplan JO, O'Hara S, Melkonian A, Arko R, Weissel RA, Ferrini V, Goodwillie A, Nitsche F, Bonczkowski J, Zemsky R (2009) Global Multi-Resolution Topography synthesis. Geochemistry, Geophysics, Geosystems 10(3). https://doi.org/10.1029/2008gc002332

Sars GO (1883) Oversigt af Norges Crustaceer med forelúbige Bemaerkninger over de nye eller mindre bekjendte Arter. I. (Podophthalmata-Cumacea-Isopoda-Amphipoda). Forhandlinger I Videnskabs-Selskabet I Kristiania 1882: 1–124.

Schultz GA (1981) Arcturidae from the Antarctic and Southern Seas (Isopoda,Valvifera) Part I. Antarctic Research Series 32: 63–94. https://doi.org/10.1029/AR032p0063

Wägele J-W (1991) Antarctic Isopoda Valvifera (Vol. 2). Koeltz Scientific Books, Koenigstein, 213 pp.

zur Strassen O (1902) Über die Gattung Arcturus und die Arcturiden der deuschen Tiefsee-Expedition. Zoologischer Anzeiger 25: 682–689.

Zoosyst. Evol. 99 (2) 2023, 473–487 | DOI 10.3897/zse.99.108048

PENSOFT

für Natur MUSEUM FÜR NATURKUNDE BERLIN

A new freshwater amphipod (Amphipoda, Gammaridae) from the Fakıllı Cave, Düzce Türkiye: *Gammarus kunti* sp. nov.

Murat Özbek[1], Hazel Baytaşoğlu[2], İsmail Aksu[2]

1 *Department of Hydrobiology, Faculty of Fisheries, Ege University, TR-35100 Bornova - Izmir, Türkiye*

2 *Recep Tayyip Erdogan University, Faculty of Fisheries and Aquatic Sciences, 53100 Rize, Türkiye*

https://zoobank.org/EF4B3FAB-3E50-481E-98DE-8F4B6E07F382

Corresponding author: Murat Özbek (murat.ozbek@ege.edu.tr)

Academic editor: Luiz F. Andrade ♦ **Received** 15 June 2023 ♦ **Accepted** 8 August 2023 ♦ **Published** 4 October 2023

Abstract

Aquatic species (such as fish, amphipods, isopods, hirudineans etc.) adapted to environmental conditions can live in caves connected to groundwater. The species of *Niphargus* and *Gammarus* are the most commonly encountered amphipods in caves. Türkiye is very rich in terms of karst areas and is home to more than 2000 known caves. Fakıllı Cave, located in Düzce Province in the Western Anatolian Region, has a length of 1071 m. A new amphipod species belonging to the *Gammarus* genus has been identified from the cave and named as *Gammarus kunti* **sp. nov.** Some of the characteristic features of the newly-identified species can be listed as "Medium-large size; smooth body, well-developed and reniform eyes; non-prolonged extremities; antennal gland cone is straight and long; second antenna with setose peduncular and flagellar segments; medial palmar spine present; posterior margin of pereopod 3 densely setose; anterior margins of pereopods 6 and 7 armed with spines only; epimeral plates not pointed". Although the mentioned features are generally seen in epigean species, the members of this species were sampled from the dark zone of the Fakıllı Cave. The partial sequences of the COI (573 bp) and 28S (914 bp) genes of the newly-described species, *Gammarus kunti* **sp. nov.**, were generated. The pairwise genetic distances between the new species, *Gammarus kunti* sp. nov. and other species ranged from a minimum of 16.23% (*G. tumaf*) to a maximum of 28.27% (*G. roeselii*) for the COI gene and a minimum of 0.88% (*G. tumaf*) to a maximum of 6.81% (*G. balcanicus*) for the 28S gene. Phylogenies generated by the NJ and ML methods, based on the combined data, assigned the new species as an independent lineage with high support values. In addition, the ASAP method identified the new species as a single MOTU independent of other species. *G. tumaf* and *G. baysali* are the sister taxa of *G. kunti* **sp. nov.** Detailed descriptions and drawings of the extremities of the male holotype and the female allotype are given and the morphology of the newly-identified species is compared with its relatives.

Key Words

benthos, cave, identification key, invertebrate, molecular identification, new species

Introduction

Caves, mid-ocean islands, deep seas, remote lakes and extremely cold and/or hot habitats are typical examples of extreme environments. Extreme conditions can lead to more effective functioning of organisms' adaptation and evolution mechanisms resulting in morphological changes that can be associated not only with the absence of light in caves, but also with the presence of different microhabitats. In addition, morphological changes may be niche-based and related to the presence of various micro-habitats (Trontelj et al. 2012).

Gammarus, the most widely distributed epigean freshwater genus of the Amphipoda order, has spread from the Western Palearctic to China and North America (Vainola et al. 2008). The representatives of the genus generally live in epigean habitats, but are also distributed in hypogean habitats, such as caves and wells (Karaman and Pinkster 1977). Reduced or vestigial eyes, elongated antennae and extremities and a non-pigmented body are

some of the morphological features frequently encountered in *Gammarus* species adapted to living in hypogean habitats (Pinkster and Karaman 1978; Fišer 2009; Özbek et al. 2013).

Türkiye is located between the Eurasian, African and Arabian plates and is situated on the Alpine-Himalayan Mountain Belt. As a result, it is a karst-rich country with more than 2000 known caves (Nazik et al. 2019; Yamaç et al. 2021). Studies on the amphipod fauna of Türkiye's inland waters, which started with the identification of *Gammarus argaeus* from Mount Erciyes (Vávra 1905), have increased over time and with a total of 51 *Gammarus* species reported. A total of 20 amphipod species belonging to the genus *Niphargus* Schiödte, 1849; *Gammarus* Fabricius, 1775; *Parhadzia* Vigna Taglianti, 1988 and *Bogidiella* Hertzog, 1933 have been reported from the caves and wells of Türkiye (İpek and Özbek 2022). In a recent study, this number increased by one more and *Gammarus tumaf* was identified from Gökgöl Cave, Zonguldak Province (Özbek et al. 2023).

The study aims to examine the individuals collected from Fakıllı Cave, Düzce Province, Türkiye, in terms of morphological and molecular features. Detailed descriptions and drawings of the extremities of the male holotype and female allotype are given and the morphology of the newly-identified species is compared with its relatives.

Materials and methods

Sampling area

Fakıllı Cave is located in Fakıllı Village, 8 km southeast of Akçakoca Town, Düzce Province, NW Türkiye. The total length of the cave is 1071 m and 350 m from the cave entrance is open for visitors. The entrance of the cave, which is 100 ms above sea level, has a width of 5–10 m and a ceiling height of 5–6 m. From the entrance of the cave, the sections are passed through long narrow corridors. There are many natural features including galleries, stalactites and stalagmites going in various directions inside the cave, which was registered as a first-degree protected area by the Ministry of Culture and Tourism's Regional Board of Protection of Cultural and Natural Assets (Zengin and Eker 2020).

Morphological identification

Individuals were collected with a hand aspirator from the dark zone of the cave, fixed in 70% ethanol in the field and transported to the laboratory for taxonomic identification. Specimens were dissected under a stereomicroscope, straightened with forceps and body length was measured from the base of the first antennae to the base of the telson. Permanent slides of the male holotype individual were prepared using the high-viscosity mount, CMCP-10. Photographs of the extremities were taken with a digital camera connected to an Olympus CX41. A digitiser board (Wacom PTH-451) and a standard pen connected to a PC were used for detailed drawings of the extremities. Scaled drawings of the extremities were made on the photographs (Coleman 2003). The geographical location of the cave is shown in Fig. 1. The collected samples are kept in the Museum of the Faculty of Fisheries, Ege University (ESFM).

Molecular identification

DNA extraction, PCR amplification and Sequencing

Total DNA was extracted on the Automated DNA isolation device (QIAcube Qiagen, Germany) according to the DNeasy Blood & Tissue Kit (Qiagen, Hilden, Germany) protocol. Mitochondrial cytochrome c oxidase subunit I gene (COI) and the nuclear large subunit ribosomal RNA gene (28S) were amplified from the extracted DNA. Amplification of the COI marker was performed with the primers UCOIF (5'- TAWACTTCDGGRTGRCCRAAAAAYCA-3') and UCOIR (5'- ACWAAYCAYAAAGAYATYGG-3') according to the PCR protocol of Costa et al. (2009). Amplification of the 28S marker was performed with the primers 28F (5'- TTAGTAGGGGCGACCGAACAGGGAT-3') and 28R (5'- GTCTTCGCCCCTATGCCCAACTGA-3') according to the PCR protocol of Hou et al. (2007).

PCR products of the COI and 28S genes were purified by using the QIAquick PCR Purification Kit (Qiagen). Bidirectional sequencing of both PCR products was performed with an ABI PRISM 3730x1 Genetic Analyser using a BigDye Terminator 3.1 cycle sequencing ready reaction kit (Applied Biosystem) according to the Sanger method at Macrogen Europe.

Molecular data analyses

We sequenced the partial sequences of the COI and 28S genes from one individual to perform molecular analyses and generate the genetic record of the new species. In addition, we downloaded a total of 27 reference sequences (COI and 28S sequences for each species) from the GenBank (NCBI: National Centre for Biotechnology Information) for use in molecular analyses. Detailed information on the sequences used in molecular analyses is given in Table 1.

The raw COI and 28S sequences of the new species were corrected by checking their chromatograms in Bioedit 7.2.5 programme (Hall 1999). All sequences were then aligned with the Clustal W method (Thompson et al. 1994), trimmed at the ends and converted to a FASTA format file. The pairwise genetic distances were calculated separately for both genes according to the uncorrected *p*-distance in MEGA X software (Kumar et al. 2018).

Figure 1. The habitus of the male holotype (up) and the type locality of *Gammarus kunti* sp. nov. (down).

To perform the phylogenetic analyses, the COI and 28S sequences, both newly-generated and downloaded from GenBank, were added end-to-end to obtain a concatenated dataset (28S+COI) for each species. Phylogeny of *Gammarus* species was estimated by using Neighbour-Joining (NJ) and Maximum Likelihood (ML) methods in *MEGA X* software. The NJ tree was generated according to the *p*-distance parameter. The ML tree was generated according to the General Reversible Time (GTR) with gamma-distributed invariant sites (G+I) model (Tavaré 1986) and the best-fit substitution model was selected with the lowest Akaike Information Criterion (AIC) score in jModelTest 0.1.1 (Posada 2008). The nodal support of the NJ and ML analyses was computed with the bootstrap test (Felsenstein 1985) using 1000 pseudoreplicates. To root the *Gammarus* phylogeny, *Pontogammarus robustoides* (also see Table 1) was used as an outgroup in the analyses.

The species delimitation analysis was carried out using the ASAP (Assemble Species by Automatic Partitioning) method, based on COI data. To implement the ASAP method, we used the Kimura 2-parameter (K2P) distances and transition/transversion ratio (R:1.4) settings at the web address https://bioinfo.mnhn.fr/abi/public/asap/. The transition/transversion ratio (R) for the COI data was calculated in MEGA X software.

Table 1. Information of sequences used in molecular analyses.

Species	Locality	28S	COI	References
Gammarus kunti sp. nov. (T)	Fakıllı Cave, Türkiye	OP650556	OP642558	This study
G. tumaf (T)	Gökgöl Cave, Türkiye	ON751931	ON749780	Özbek et al. (2023)
G. baysali (T)	Cumayanı Cave, Türkiye	ON751932	ON749781	Özbek et al. (2023)
G. kesslerianus (T)	Simferopol, Crimea, Ukraine	JF965721	JF965909	Hou et al. (2011)
G. komareki (T)	Ca. 200.km SE Sofia, Bulgaria	JF965725	JF965913	Hou et al. (2011)
G. komareki	Mazandaran, Iran	JF965723	JF965911	Hou et al. (2011)
G. rambouseki (T)	Bitola, Macedonia	JF965770	JF965946	Hou et al. (2011)
G. roeselii	Netherlands	JF965771	JF965947	Hou et al. (2011)
G. fossarum (T)	Regensburg, Germany	JF965696	JF965886	Hou et al. (2011)
G. plaitisi	Tinos, Komi, Greece	MT999102	MT999049	Hupało et al. (2020)
G. uludagi	Evia, Greece	JF965817	JF965986	Hou et al. (2011)
G. monspeliensis (T)	Montpellier, France	JF965738	JF965923	Hou et al. (2011)
G. ibericus	Lascaux, France	JF965713	JF965901	Hou et al. (2011)
G. pulex (T)	Slovenia	JF965767	JF965943	Hou et al. (2011)
G. lacustris	Bled, Slovenia	JF965728	JF965915	Hou et al. (2011)
G. italicus	Rieti, Lazio, Italy	JF965716	JF965904	Hou et al. (2011)
G. varsoviensis (T)	Secymin, Poland	JF965818	JF965987	Hou et al. (2011)
G. kischineffensis (T)	Targu Bujor, Romania	MG987529	MG987571	Copilaș-Ciocianu et al. (2018)
G. spelaeus (T)	Simferopol, Crimea, Ukraine	JF965801	JF965971	Hou et al. (2011)
G. balcanicus (T)	Kolašin, Montenegro	JF965640	JF965834	Hou et al. (2011)
G. bosniacus (T)	Sarajevo, Bosnia and Herzegovina	JF965680	JF965872	Hou et al. (2011)
G. leopoliensis (T)	Vistula, Poland	JF965734	JF965919	Hou et al. (2011)
G. stojicevici (T)	Bela Palanka, Serbia	JF965808	JF965978	Hou et al. (2011)
G. halilicae (T)	Lazaropole, Macedonia	JF965711	JF965900	Hou et al. (2011)
G. pljakici	Galicica planina, Macedonia	JF965758	JF965936	Hou et al. (2011)
G. stankokaramani (T)	Ohrid, Macedonia	JF965806	JF965976	Hou et al. (2011)
G. salemaai	Gradište, Macedonia	JF965780	JF965955	Hou et al. (2011)
Pontogammarus robustoides	Delta Volgi, Russia	JF965822	JF965990	Hou et al. (2011)

Note: (T) Topotype samples of nominal taxa.

Results

Gammarus kunti sp. nov.

https://zoobank.org/25D58B26-4577-460C-AF00-0D20B1D04397

Figs 1–7

Type material. ***Holotype.*** Male, 11.5 mm (ESFM-MA-LI/20–15), Akçakoca District, Düzce Province, Türkiye (41°3'7.01"N, 31°10'38.70"E), 16.xiii.2020; collected by M. Elverici.

Paratypes. 3 males and 5 females, (ESFM-MA-LI/20–16), same data as holotype.

Diagnosis. A medium-large species. Body smooth, pigmentation weak; eyes well-developed, ovoid; extremities not prolonged; second antenna with setose peduncular and flagellar segments; antennal gland cone long; medial palmar spine present; posterior margin of pereopod 3 densely setose; anterior margins of pereopods 5 to 7 armed with spines and a few short setae; epimeral plates not pointed; inner ramus of uropod 3 longer than 0.75 of the outer one; telson weakly armed.

Description of male holotype. ***Head*****:** Rostrum absent, inferior antennal sinus deep, rounded. Eyes kidney-shaped; shorter than the diameter of the first peduncular segment of antenna 1 (Figs 1, 5G).

Antennae**:** Antenna 1 is as long as half of the body length; the length ratio of the peduncular segments is 1:0.67:0.4; peduncle segments bear a few groups of minute setae; the length of the setae is much shorter than the segment where they are implanted; the main flagellum with 32 segments; each segment bears a few short setae in distal side; aesthetasc absent; accessory flagellum 6 segmented (Fig. 3A). Antenna 2 is shorter than antenna 1 (ratio 1:0.67); the antennal gland cone is straight, reaches to the distal end of the third peduncular segment; setation is rich both on peduncular and flagellar segments; peduncular segments 4 and 5 bear many groups of setae; the setae on the ventral part of the peduncle segments are longer than the dorsal ones and can be up to 1.5 times longer than the diameter of the segment; flagellum consists of 15 segments; flagellar segments are setose and swollen; each segment bears many long setae on both dorsal and ventral sides; calceoli absent (Fig. 3B).

Mouthparts**:** Left mandible (Fig. 2A) with 5-toothed incisor, lacinia mobilis with 3 dentitions, molar triturative. The first article of palp without setae, the second one bears 12 setae; the setae become shorter from distal to proximal. The third segment has 28 D-setae, 4–5 E-setae, one group of A-setae and one group of B-setae. C-setae absent.

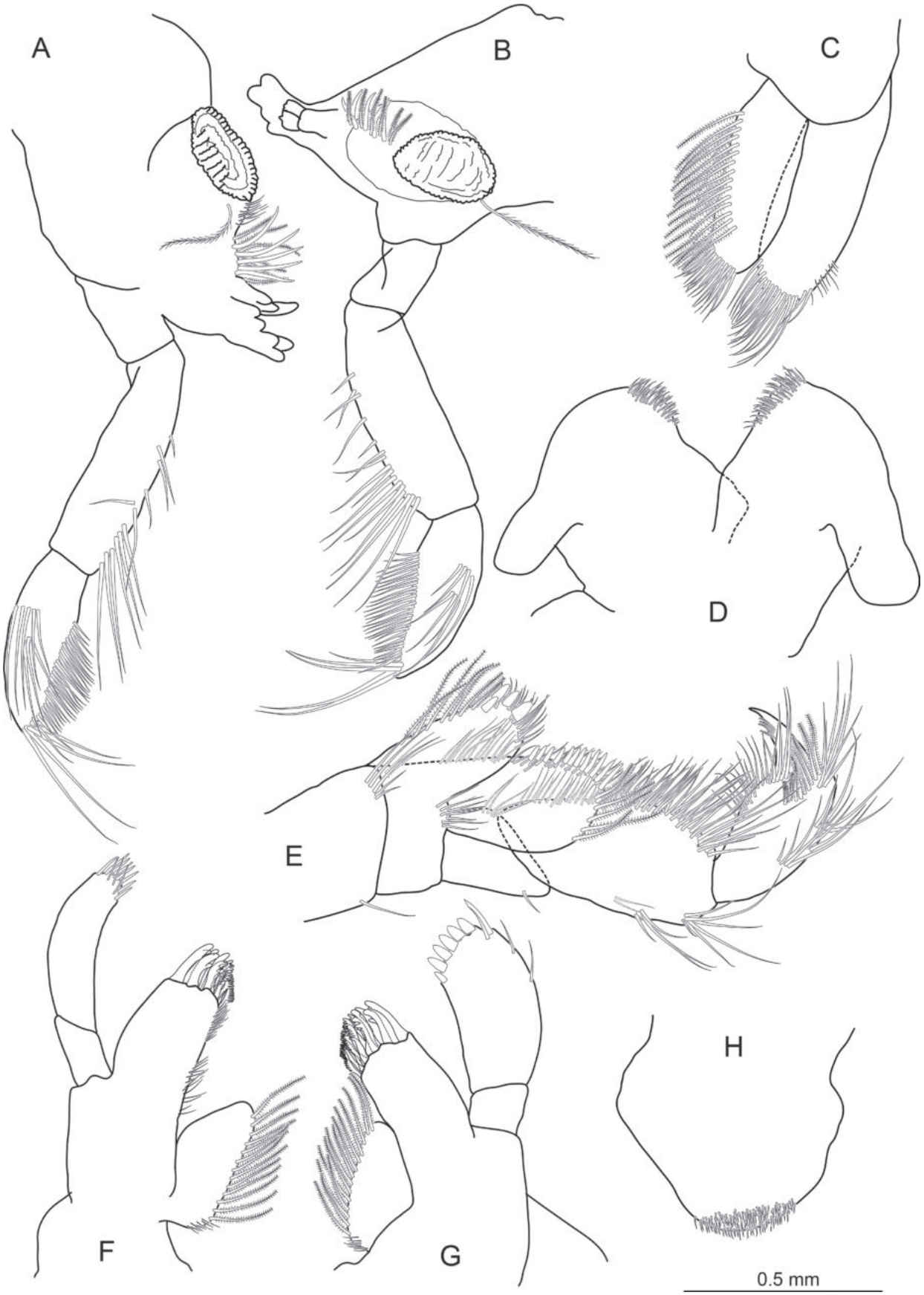

Figure 2. *Gammarus kunti* sp. nov., (male holotype). **A.** Left mandible; **B.** Right mandible; **C.** Maxilla 2; **D.** Lower lip 1; **E.** Maxilliped; **F.** Left maxilla 1; **G.** Right maxilla 1; **H.** Upper lip.

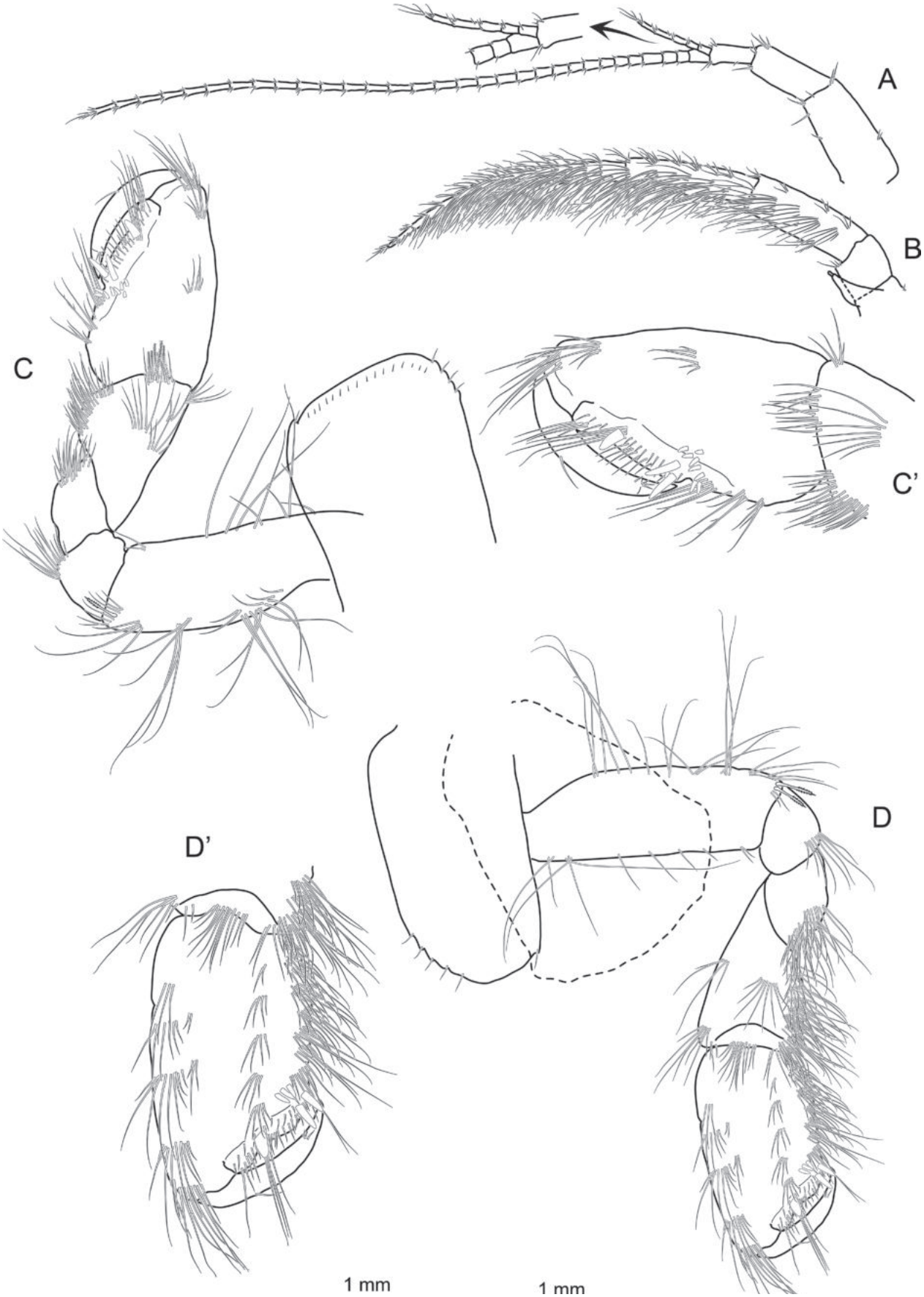

Figure 3. *Gammarus kunti* sp. nov., (male holotype). **A.** Antenna 1; **B.** Antenna 2; **C.** Gnathopod 1; **C'.** Palm of gnathopod 1; **D.** Gnathopod 2; **D'.** Palm of gnathopod 2.

Right mandible (Fig. 2B) has a 4-toothed incisor and bifurcate lacinia mobilis.

Right maxilla I (Fig. 2G) is asymmetric to the left, it has 14 plumose setae along the inner margin of the inner lobe. The outer lobe bears 11 distal stout serrate spines and some tiny setules on the inner margin. Palp of the outer lobe with no setae in the first segment and six stout spines and two simple setae on the distal part of the second segment, in addition to two marginal setae along the outer margin. The second article of left palp elongated and bears 8 spines and 3 simple setae on its distal part and no setae along the outer margin (Fig. 2F).

Lower lip (Fig. 2D) has no inner lobe and bears numerous small simple setae along the distal margins of both lobes.

Upper lip (Fig. 2H) with numerous minute setules in the distal part.

Maxilla II (Fig. 2C) has 20–25 simple setae in the distal part of the outer lobe and a few tiny hairs along the outer margin. The inner lobe also has 8–10 simple setae in the distal part in addition to 15 plumose setae located in a diagonal row along the inner margin. There are also a few tiny hairs in the proximal part of the inner margin of the lobe.

Maxilliped (Fig. 2E) inner plate has 3 tooth-like spines and a spine in the distal part and the distal corner, respectively. Additionally, there are 7 plumose setae along the inner margin of the lobe. Outer plate armed with 5–6 serrate stout setae in the distal part and 12 spines along its inner margin.

Coxal plates**:** Coxal plate 1 is rectangular, the distal part slightly widened, the ventral margin slightly convex and bears 4 antero-distal setae and one postero-distal seta in addition to some tiny setules along the ventral margin (Fig. 3C). Coxal plate 2 is in the shape of an elongated rectangle, distal part narrower than the proximal, the ventral margin is highly convex, antero-distal part with 5 setae and postero-distal part with one seta (Fig. 3D). Coxal plate 3 is similar to coxal plate 2 in shape, with 3 and 1 setae in the antero- and postero-distal ends, respectively (Fig. 4A). The ventral edge of the fourth coxal plate is slightly convex and bears 3 and 6 setae along the anteroventral and posterior margins, respectively (Fig. 4B). Coxal plate 5 (Fig. 5A) and Coxal plate 6 exhibit a bilobate structure (Fig. 5B), each having one seta in the anterior lobes and four and one setae in the posterior lobes, respectively. Coxal plate 7 is characterised by the presence of five setae on the postero-ventral margin (Fig. 5C).

Gnathopods**:** Basal segment of gnathopod 1 bears many long setae along both margins, the length of the setae can be as long as twice the diameter of the segment. Ischium bears a group of setae in the postero-ventral corner. Carpus is triangular and bears four groups of setae along the anterior margin in addition to many setae groups on both ventral and posterior sides. Propodus pyriform, the length/width ratio is 1: 0.57, anterior margin with two groups of setae, medial palmar spine is present, postero-distal corner armed with two strong spines in addition to some small spines, posterior margin bears 4–5 groups of setae. Dactylus reaches the postero-distal corner and bears a simple seta along the outer margin in addition to a small setule around the distal part of the inner margin (Fig. 3C, C').

Basis and ischium of gnathopod 2 have a similar setation to that of gnathopod 1. Merus and carpus are more setose than those of gnathopod 1. Carpus triangular, densely setose along the posterior margin in addition to two groups of setae along the anterior margin. Propodus is densely setose and has a sub-rectangular shape, the length/width ratio is 1: 0.53, anterior margin bears 6 groups of setae, posterior margin with many groups of setae, medial palmar spine is present, the postero-distal corner is armed with two strong spines in addition to some small spines. Dactylus reaches the postero-distal corner and bears a simple seta along the outer margin in addition to a small setule around the distal part of the inner margin (Fig. 3D, D').

Pereopods**:** Anterior and posterior margins of the basal segment of pereopod 3 bear long setae, the setae along the posterior margin are much longer than those in the anterior margin, posterior margins of the merus, carpus and propodus bear long setae, the setae can be more than three times the diameter of the segment where they are implanted. Dactylus slim, a minute plumose seta occurs on the outer margin; the inner margin with two small setules (Fig. 4A).

The basal segment of pereopod 4 has a similar setation to that of pereopod 3. Ischium, merus, carpus and propodus have groups of setae along their posterior margins, but they are much shorter and less than those in pereopod 3, the length of the setae can be as long as (or slightly longer) than the diameter of the segment where they are implanted. Dactylus slim, a minute plumose seta occurs on the outer margin; the inner margin with two small setules (Fig. 4B).

Posterior margins of the basal segments of pereopods 5 to 7 are more or less convex and bear many short setae, anterior margins with 5–7 small spines and no setae present on the inner surfaces of the basal segments; no spine exists in the postero-ventral corner of the basal segment of pereopod 7. Pereopods 6 and 7 bear no setae along the anterior margins of ischium, merus and carpus, while pereopod 5 has a few setae longer than the accompanying spines along with the mentioned segments. Propodus of pereopods 5 to 7 with 2–3 groups of long setae groups along their outer margins in addition to 5–6 groups of small spines along their inner margins. Dactylus slim, a minute plumose seta occurs on the outer margin; the inner margin with two small setules (Fig. 5A–C).

Epimeral plates**:** They are neither curved nor sharply pointed. Epimeral plate 1 bears 2 long setae in addition to 4–5 setules along the anterior margin, the postero-ventral corner is angular (Fig. 5D). Epimeral plate 2 bears 5–6 setae in the antero-ventral corner, the ventral margin is armed with 1 spine and two short setae, the posterior margin with 4–5 setules, the postero-ventral corner is angular (Fig. 5E). Epimeral plate 3 is slightly pointed; the antero-ventral corner bears 3–4 setae; the ventral margin is armed with 3 spines; the posterior margin bears 6–7 setules (Fig. 5F).

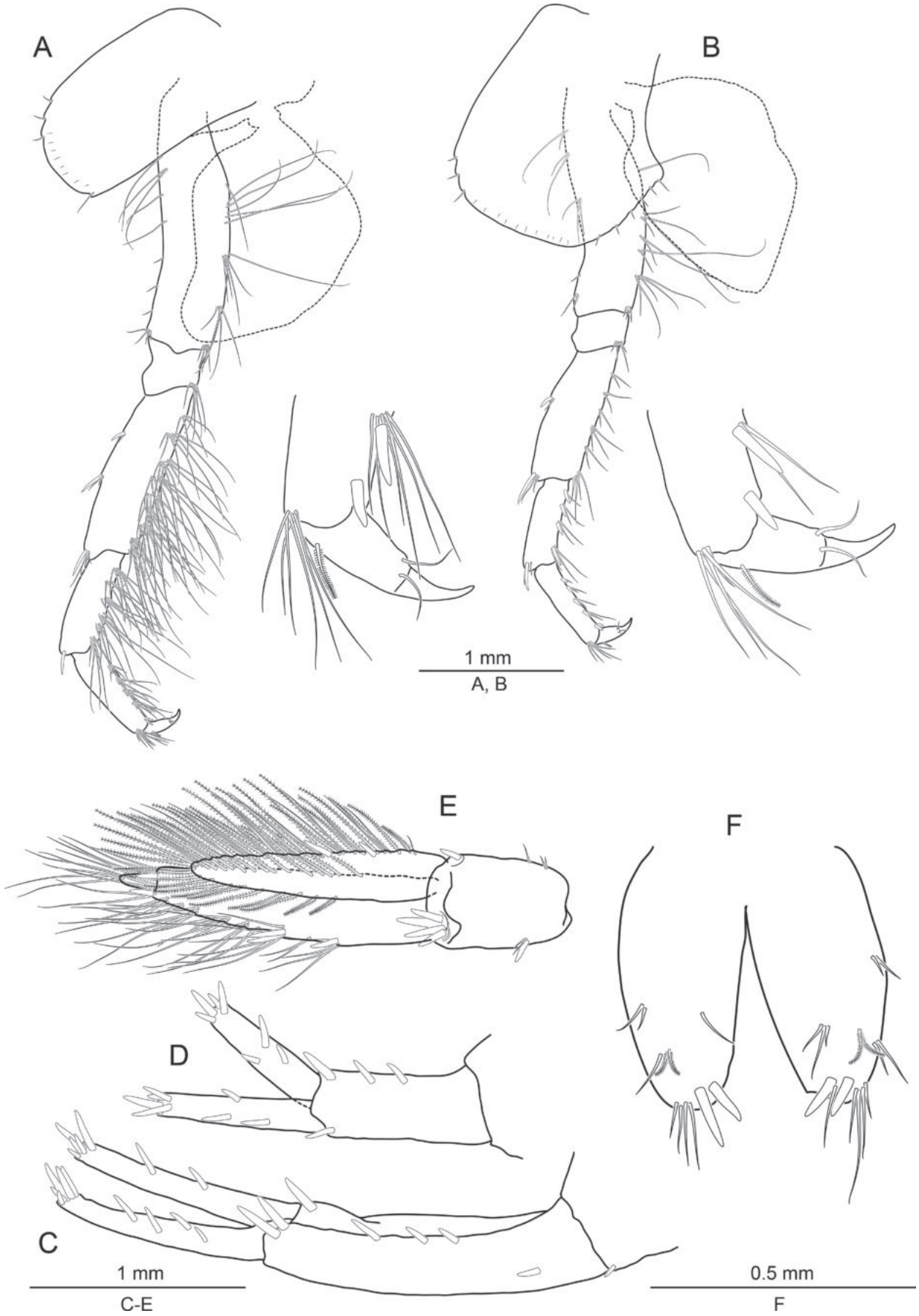

Figure 4. *Gammarus kunti* sp. nov., (male holotype). **A.** Pereopod 3; **B.** Pereopod 4; **C.** Uropod 1, **D.** Uropod 2; **E.** Uropod 3; **F.** Telson.

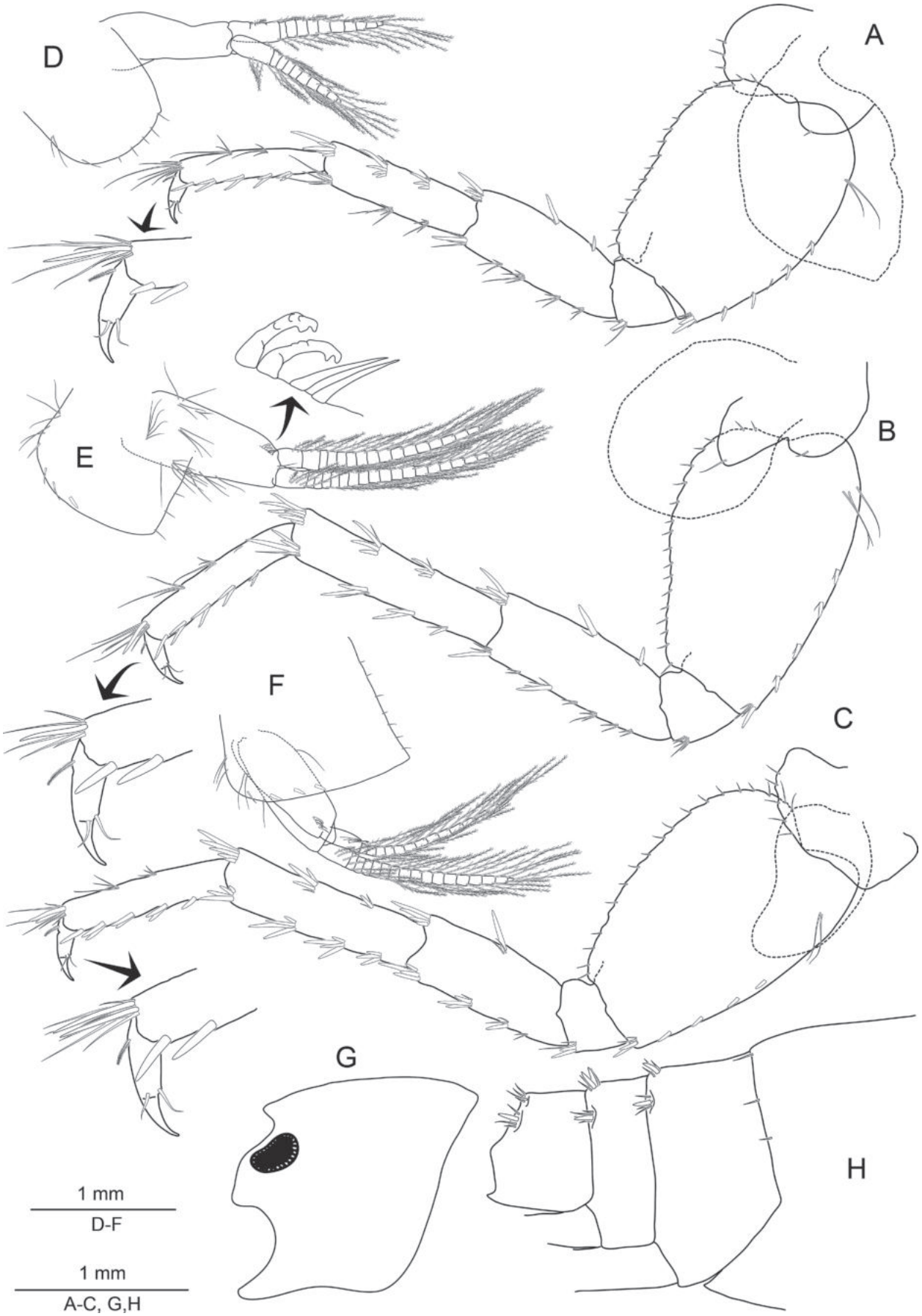

Figure 5. *Gammarus kunti* sp. nov., (male holotype). **A.** Pereopod 5; **B.** Pereopod 6; **C.** Pereopod 7; **D.** Pleopod 1; **E.** Pleopod 2; **F.** Pleopod 3; **G.** Head; **H.** Urosomites.

***Urosomites*:** Not elevated. Each segment bears a median and two dorsolateral groups of armaments; each of them consists of 1–2 spines and 3–4 accompanying setae (Fig. 5H).

***Uropods*:** Uropod 1 has a spine in the disto-ventral corner of the base; the peduncle is longer than the rami; the length ratio is about 1:0.7. Peduncle with a spine in the outer margin of the proximal part in addition to 3 spines along the inner margin and 3 spines in the distal part. The inner ramus is slightly longer than the outer ramus and bears 3–4 spines along their inferior margin in addition to 4–5 distal spines. The outer ramus with 2 spines along the inferior margin in addition to 4–5 distal spines (Fig. 4C).

Uropod 2 is smaller than the first one; the length ratio is about 1:0.6; the peduncle segment is slightly longer than the rami and bears 2+2 spines along the inner margin and the distal part, respectively. The outer margin is bare. The length and armaments of both rami are similar to each other, bearing 2–3 spines along their inner and outer margins in addition to 4–5 longer spines on their distal tips (Fig. 4D).

Uropod 3 is setose and bears simple and plumose setae. The peduncle segment is much shorter than the outer ramus and the length ratio is about 1:0.41. The outer ramus is two articulated and densely setose along both margins; the outer margin bears 2 groups of spines accompanied by groups of long simple setae; the inner margin with plumose setae; the second article is well developed and longer than the surrounding distal spines. The inner ramus is about 0.77× the length of the outer ramus. It bears two spines along the outer margin in addition to groups of simple and plumose setae; the inner margin bears both simple and plumose setae (Fig. 4E).

***Telson*:** Telson lobes cleft, each lobe bears 2 spines and 2–3 simple setae in their distal parts. The setae are longer than the spines. There are 2–3 groups of short setae on the dorsal surface of the lobes in addition to two plumose setules. The length/width ratio of each lobe is about 1:0.5 (Fig. 4F).

Etymology. The species epithet is derived from the name of scientist Dr. Kadir Boğaç Kunt, who has valuable contributions to the Arachnida species of Türkiye and sent the materials for this study.

Description of females. Smaller than males. Except for the sexual dimorphism indicated for the genus *Gammarus*, females do not show obvious differences from males. At first glance, the morphological differences between the female allotype and the male holotype can be listed as follows: less setose antenna 2, not swollen flagellar segments of antenna 2, less setose gnathopod 2 and more setose pereopods 4–7 (Figs 6, 7).

***Variability*:** Some of the paratypes are immature. The eyes are kidney-shaped or slightly oval. The number of flagella segments in antenna 1 varies between 26 and 29. Similarly, there are 10–11 flagellar segments in antenna 2.

Molecular data analyses

We generated the partial sequences of the COI (573 bp) and 28S (914 bp) genes of the newly-described species, *Gammarus kunti*. After all sequences were aligned, the total length is 1489 bp including gaps. While no stop codon, insertion, deletion and a gap was detected in the protein-coding mtDNA COI gene, there were insertions and deletions in the nuclear 28S gene. Additionally, newly-generated sequences are deposited in GenBank accession numbers, for COI; OP642558 and 28S; OP650556. Thus, the first genetic record of the newly-described species was created. We performed the genetic comparison of the new species with the reference sequences of the topotype samples of the nominal taxa in GenBank. In the absence of sequences of topotype samples, correct sequences considered representative of the species were preferred (Table 1).

For the COI gene, the pairwise genetic distance amongst the species ranged from a minimum of 5.24% (*G. stankokaramani* - *G. salemaai*) to a maximum of 28.62% (*G. kesslerianus* - *G. plaitisi*). The pairwise genetic distances between the new species *Gammarus kunti* sp. nov. and the other species ranged from a minimum of 16.23% (*G. tumaf*) to a maximum of 28.27% (*G. roeselii*). For the 28S gene, the pairwise genetic distance amongst the species ranged from a minimum of 0.11% (*G. halilicae* - *G. pljakici*) to a maximum of 7.84% (*G. rambouseki* - *G. stojicevici*).

The pairwise genetic distances between the new species *Gammarus kunti* sp. nov. and the other species ranged from a minimum of 0.88% (*G. tumaf*) to a maximum of 6.81% (*G. balcanicus*). The genetic distance of the new species to the nearest species is approximately three times greater for the COI gene and eight times greater for the 28S gene than the minimum genetic distance between valid *Gammarus* species. This indicates that the new species is well differentiated genetically. All pairwise genetic distance values amongst *Gammarus* species are given in Suppl. material 1.

Phylogenies generated by the NJ and ML methods, based on the concatenated data, yielded fully compatible trees. Except for a few branches (ML:16–67%; NJ:25–69%), the other branches (ML: 82–100%; NJ: 83–100%) in the phylogenies were generally resolved and supported with high bootstrap values. *G. tumaf* Özbek et al., 2023 and *G. baysali* Özbek et al., 2013 are the sister taxa of *G. kunti* sp. nov. The phylogenetic position of the new species, *Gammarus kunti* sp. nov., indicates an independent lineage supported by high bootstrapping values (for NJ: 95%, for ML: 91%; Fig. 8).

The species delimitation analysis we implemented according to the ASAP method, based on COI data, identified 26 MOTUs (molecular operational taxonomic units) for 27 *Gammarus* species. The best ASAP score had 1.5 ($p=0.01$) at a threshold distance of 0.079053. The analysis identified species *G. stankokaramani* and *G. salemaai* as a single MOTU. The new species formed a single MOTU independent of other species.

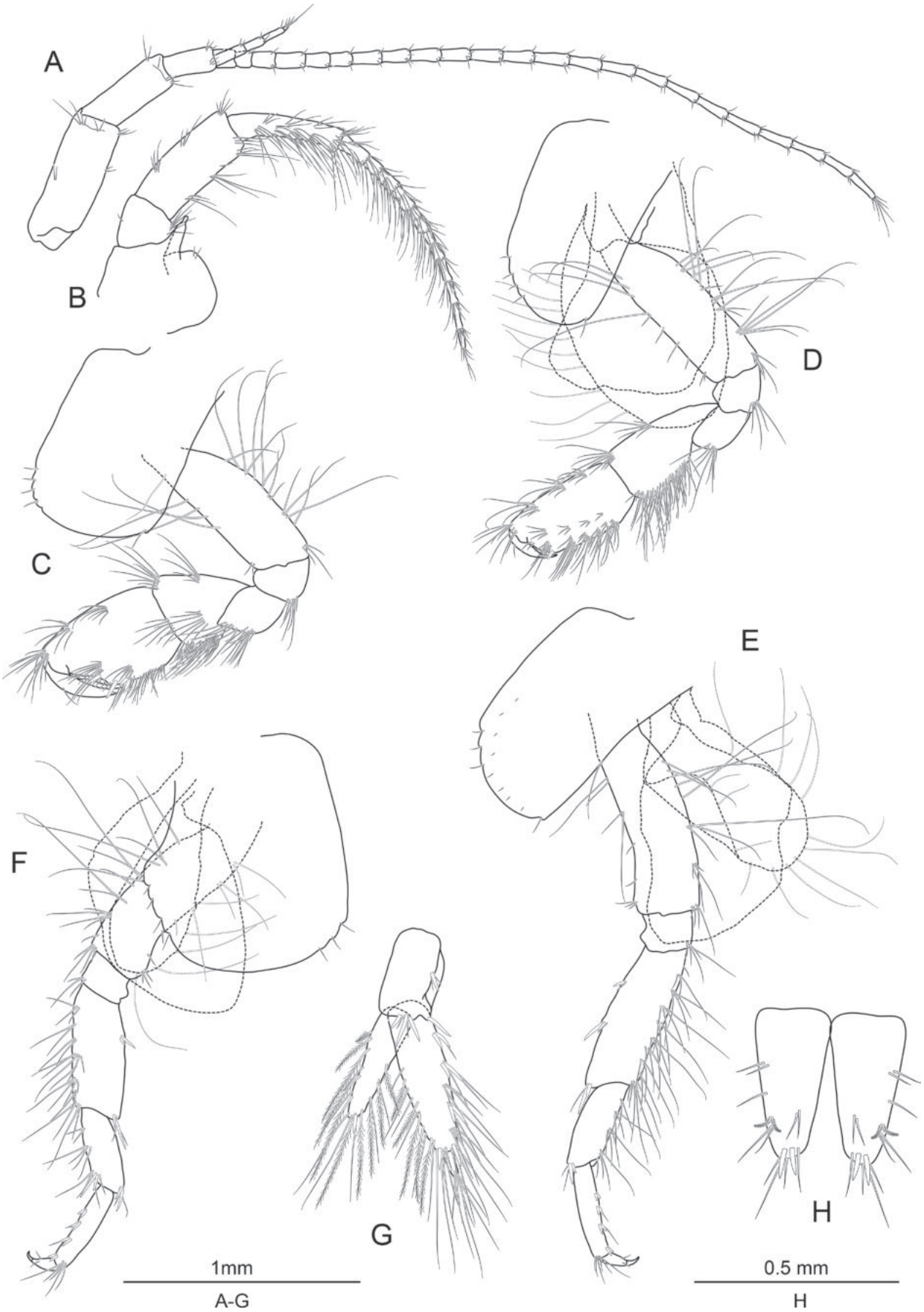

Figure 6. *Gammarus kunti* sp. nov., (female allotype). **A.** Antenna 1; **B.** Antenna 2; **C.** Gnathopod 1; **D.** Gnathopod 2; **E.** Pereopod 3; **F.** Pereopod 4; **G.** Uropod 3; **H.** Telson.

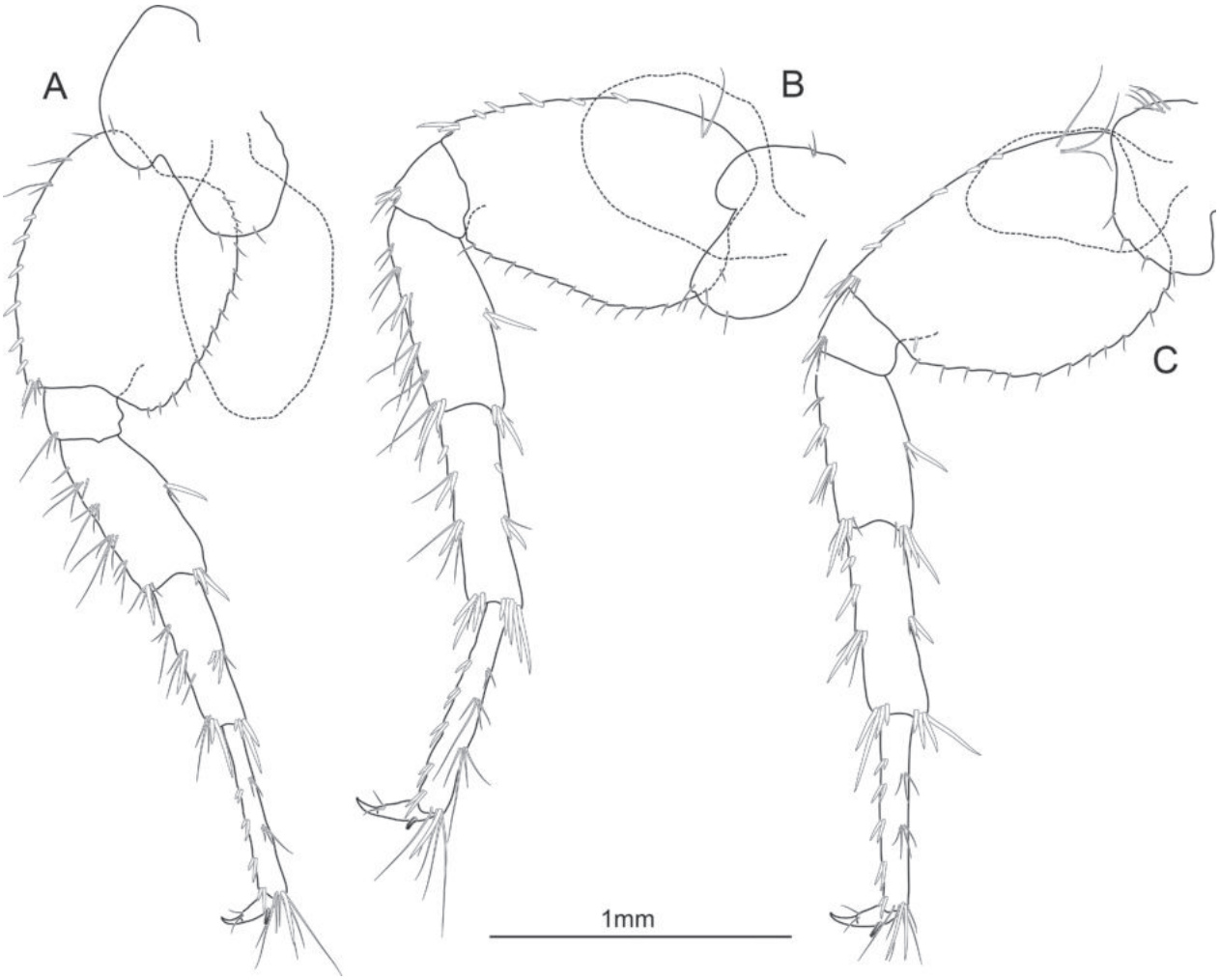

Figure 7. *Gammarus kunti* sp. nov., (female allotype). **A.** Pereopod 5; **B.** Pereopod 6; **C.** Pereopod 7.

Discussion

Gammarus kunti sp. nov. is a species belonging to the *Gammarus pulex*-group due to the setation of the posterior part of pereopods 3 and 4 and the setation of uropod 3 (Karaman and Pinkster 1977). *Gammarus kunti* sp. nov. shows close proximity to *G. baysali* and *G. tumaf*, considering the genetic analysis results (Fig. 8). In addition, the newly-described species show some similarities with *G. kesslerianus* and *G. komareki* (Schäferna, 1922). *G. kesslerianus* has not been recorded from Türkiye, while *G. komareki* has been reported from the entire Black Sea Region of Turkey, including the Thrace Region (İpek and Özbek 2022).

Although *Gammarus kunti* sp. nov. is genetically and morphologically close to *G. baysali*, it differs from *G. baysali* in having several morphological features. The newly-identified species is smaller than *G. baysali*. Additionally, having well-developed eyes, shorter antenna 1, more setose antenna 2, not elongated extremities and not setose anterior margins of pereopods 5–7 are some of the discriminant characteristics of *G. kunti* (Table 2).

G. kunti sp. nov. also resembles *G. tumaf* which is reported from the Gökgöl Cave, Zonguldak Province by the same authors of the present study in 2023. The newly-identified species differs from it by having reniform eyes, while eyes are minute in *G. tumaf*. Inner lobe of right maxilla 1 bears 14 and 20 plumose setae in *G. kunti* and *G. tumaf*, respectively. *G. kunti* has six stout spines in the palp of right maxilla 1, while the number of the stout spines is five in *G. tumaf*. In addition, the newly-identified species has 15 plumose setae in the inner lobe of maxilla 2, while *G. tumaf* has 20 plumose setae (Table 2).

The new species is also similar to *Gammarus obruki* Özbek, 2012 by having kidney-shaped eyes, setose antenna 2 and armaments and setation of pereopods 5–6, but differs from it by being smaller and having much shorter antenna 1 and shorter inner/outer lobe ratio of uropod 3. In addition, *G. kunti* has 14 plumose setae in the inner lobe of right maxilla 1, while it has 18 in *G. obruki.* Similarly, the new species has two setae along the outer margin of the palp of the right maxilla 1, while *G. obruki* has three setae in the mentioned part of maxilla 1. Inner lobe of maxilla 2 bears 15 plumose setae in the newly-identified species and the number is 21 in *G. obruki*. Similarly, the number of D-setae in the palp of the mandible in *G. kunti* and G. *obruki* differs from each other (28 vs. 37, respectively) (Table 2).

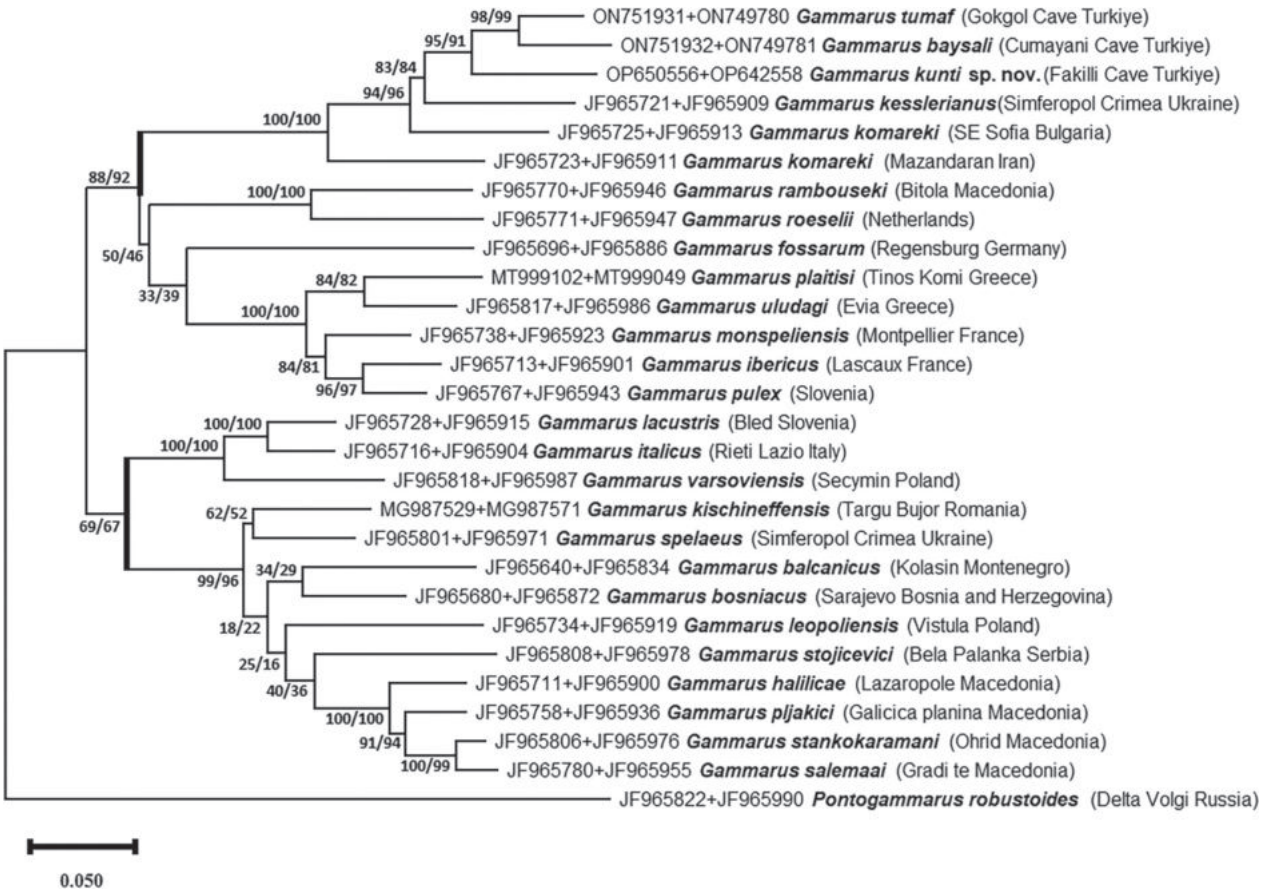

Figure 8. Maximum Likelihood (ML) phylogenetic tree generated, based on the concatenated dataset (28S+COI). ML and NJ methods yielded the same topologies and, therefore, only the ML tree is shown. The bootstrap values of NJ and ML are shown on nodes (NJ/ML).

Table 2. Some of the morphological features of *Gammarus kunti* sp. nov., *G. baysali*, *G. tumaf* and *G. obruki*.

Characters	Gammarus kunti sp. nov.	*G. baysali*	*G. tumaf*	*G. obruki*
Body length	11.5 mm	18.1 mm	12.6 mm	21.0 mm
Eyes	Kidney-shaped	eyeless	minute	Kidney-shaped
Body colour	whitish	colourless, whitish	whitish	yellowish
Antenna 1	32+6 flagellar segments	41+6 flagellar segments	30+5 flagellar segments	52+6 flagellar segments
Antenna 2	peduncular and flagellar segments densely setose	peduncular and flagellar segments setose	peduncular and flagellar segments densely setose	fifth peduncular and flagellar segments densely setose
Antennal gland cone	straight, reaches to the distal end of the third peduncular segment	straight, reaches to the distal end of the third peduncular segment	straight, reaches to the distal end of the third peduncular segment	straight, not reaching to the distal end of the third peduncular segment
Inner lobe of right maxilla 1	with 14 plumose setae	with 19 plumose setae	with 20 plumose setae	with 18 plumose setae
Palp of right maxilla 1	6 stout spines, 2 setae along the anterior margin	6 stout spines, 4 setae along the anterior margin	5 stout spines, 2 setae along the anterior margin	6 stout spines, 3 setae along the anterior margin
Maxilla 2	inner lobe with 15 plumose setae	inner lobe with 21 plumose setae	inner lobe with 20 plumose setae	inner lobe with 21 plumose setae
Number of D-setae	28	34	28	37
Pereopods	not elongated	elongated	not elongated	slightly elongated
Pereopods 6–7	anterior margins without setae	anterior margins with setae	anterior margins without setae	anterior margins without setae
Uropod 3	setose, inner/outer lobe ratio: 0.77	setose, inner/outer lobe ratio: 0.9	setose, inner/outer lobe ratio: 0.75	setose, inner/outer lobe ratio: 0.9

At first glance, the newly-identified species looks similar to *G. komareki* by the setation of the antennae, by the presence and the shape of the eyes, uropod 3 and telson, but the following characters are different. In *G. kunti* sp. nov., the antennal gland cone reaches to the distal end of the third peduncular segment, but it is shorter (roughly halfway) in *G. komareki*. Similarly, *G. kunti* sp. nov. has less D-setae in the third segment of the mandible palp (28 in *G. kunti*; 40 in *G. komareki*), less setose pereopod 4 and not setose anterior margins of pereopods 6–7. Another important differentiation is that, in males, the setation on the carpus and merus posterior margin of the 4th pereiopod is significantly shorter in *G. kunti* (subequal to the diameter of underlying segment) than in *G. komareki* (longer than the diameter of underlying segment).

G. kunti sp. nov. also resembles *Gammarus komareki aznavensis* Özbek & Rasouli, 2014 in terms of setation of antenna 2, pereopods 3 and 4, but the newly-identified species differs from *G. komareki aznavensis* by its larger size, by having smaller eyes, longer antenna 1, by absence setae along the anterior margins of pereopod 6 and by the shorter setation of the telson (Özbek and Rasouli 2014).

The newly-identified species differs from *G. kesslerianus* by the body length (smaller), having fewer flagellar segments in antenna 2 and shorter endopod of uropod 3.

Gammarus kesslerianus werneri S. Karaman 1934 was identified from Iznik Lake, NW Anatolia. After S. Karaman's record, the subspecies has been never re-described and collected again until G.S. Karaman's re-description (Karaman 2018). He elevated the subspecies to the specific rank as *Gammarus werneri* and transferred it into the *Gammarus balcanicus*-group. So, *Gammarus kunti* sp. nov. distinctly differs from *G. werneri* because the newly-identified species belong to the *Gammarus pulex*-group.

Gammarus kunti sp. nov. differs from *Gammarus rambouseki* (S. Karaman, 1931) by having reniform eyes, by the absence of long setae on the peduncular segments of antenna 1, by the absence of long setae along the anterior margins of pereopod 5 to 7 and by the presence of plumose setae on uropod 3. Additionally, *G. rambouseki* has less setose antenna 2 and more setose urosomites and telson (Karaman and Pinkster 1977).

Gammarus kunti sp. nov. is similar to *Gammarus fossarum* Koch, 1836 by having reniform eyes, a setose posterior margin of pereopod 3 and the armaments of pereopods 5 to 7. However, the newly-identified species differ from *G. fossarum* by having much more setose antenna 2 and by having a more elongated inner lobe of the uropod 3.

Studies conducted in recent years suggest that the western Black Sea Region of Türkiye is quite rich in terms of freshwater amphipods. Many new and endemic species have been identified from the caves and water bodies in the region (Andreev and Kenderov 2012; Karaman 2012; Özbek 2012; Özbek et al. 2013, 2023). To reveal the biodiversity of Turkish inland waters, studies supported by molecular analyses should be increased.

Acknowledgements

The authors would like to thank Mert Elverici and Kadir Boğaç Kunt (collectors and biologist experts); Barış Kaymaz, Hilmi Umut Demiriz, Özlem Kaya, Burak Gezer (support access to caves and aquatic habitats and sportive caving within the Turkish Caving Federation); Gökhan Eren Çankaya, Ertuğrul Kulaksızoğlu (support at various stages within the scope of the project, within the body of Kaşif Consulting, Reporting, Organisation Company); Mustafa Uzun (the director of the Natural Assets branch of the Turkish Ministry of Environment, Urbanisation and Climate Change, General Directorate of Conservation of Natural Assets). The samples studied in the present study were collected during the "Research Project for Some Caves in the Western and Eastern Black Sea Regions and Central Anatolia Region" carried out within the scope of the Turkish Ministry of Environment, Urbanisation and Climate Change. The authors would like to thank the referees, especially D. Copilaş-Ciocianu, who contributed significantly to the development of the article. The study was financially supported by Ege University Research Fund (BAP No: 24046).

References

Andreev S, Kenderov L (2012) Sur une nouvelle espèce du genre *Niphargus* de la Turquie – *Niphargus turcicus* n. sp. (Amphipoda, Niphargidae). Historia Naturalis Bulgarica 20(2001): 47–56.

Coleman CO (2003) "Digital inking": How to make perfect line drawings on computers. Organisms, Diversity & Evolution 3(4): 303–304. https://doi.org/10.1078/1439-6092-00081

Copilaş-Ciocianu D, Zimţa AA, Grabowski M, Petrusek A (2018) Survival in northern microrefugia in an endemic Carpathian gammarid (Crustacea: Amphipoda). Zoologica Scripta 47(3): 357–372. https://doi.org/10.1111/zsc.12285

Costa F, Henzler CM, Lunt DH, Whiteley NM, Rock J (2009) Probing Marine *Gammarus* (Amphipoda) Taxonomy with DNA Barcodes. Systematics and Biodiversity 7(4): 365–379. https://doi.org/10.1017/S1477200009990120

Felsenstein J (1985) Confidence limits on phylogenies: An approach using the bootstrap. Evolution; International Journal of Organic Evolution 39(4): 783–791. https://doi.org/10.2307/2408678

Fišer C (2009) The subterranean genus *Niphargus* (Crustacea, Amphipoda) in the Middle East: A faunistic overview with descriptions of two new species. Zoologischer Anzeiger 248(2): 137–150. https://doi.org/10.1016/j.jcz.2009.03.003

Hall TA (1999) BioEdit: A user-friendly biological sequence alignment editor and analysis program for Windows 95/96/NT. Nucleic Acids Symposium Series 41: 95–98.

Hou Z, Fu J, Li S (2007) A molecular phylogeny of the genus *Gammarus* (Crustacea: Amphipoda) based on mitochondrial and nuclear gene sequences. Molecular Phylogenetics and Evolution 45(2): 596–611. https://doi.org/10.1016/j.ympev.2007.06.006

Hou Z, Sket, B, Fiser C, Li S (2011) Eocene habitat shift from saline to freshwater promoted Tethyan amphipod diversification. Proceedings of the National Academy of Sciences (PNAS) 108(35): 14533–14538. https://doi.org/10.1073/pnas.1104636108

Hupało K, Karaouzas I, Mamos T, Grabowski M (2020) Molecular data suggest multiple origins and diversification times of freshwater gammarids on the Aegean archipelago. Scientific Reports 10(1): 19813. https://doi.org/10.1038/s41598-020-75802-2

İpek M, Özbek M (2022) An updated and annotated checklist of the Malacostraca (Crustacea) species inhabited Turkish inland waters. Turkish Journal of Zoology 46(1): 14–66. https://doi.org/10.3906/zoo-2109-12

Karaman GS (2012) New species *Niphargus religiosus*, sp. n. (Fam. Niphargidae), with remarks to *Amathillina cristata* G.O. Sars, 1894 (Fam. Gammaridae) in Turkey (Contribution to the Knowledge of the Amphipoda 257). Poljoprivreda i Sumarstvo 53(07): 49–76.

Karaman GS (2018) On two partially known species of the genus *Gammarus* Leach 1813/14 (Fam. Gammaridae) from Asia Minor (Turkey) (Contribution to the Knowledge of the Amphipoda 304). Ecologica Montenegrina 19: 110–124. https://doi.org/10.37828/em.2018.19.12

Karaman GS, Pinkster S (1977) Freshwater *Gammarus* species from Europe, North Africa and adjacent regions of Asia (Crustacea-Amphipoda). Part I. *Gammarus pulex*-group and related species. BIijdragen Tot de Dierkunde 47(1): 1–97. https://doi.org/10.1163/26660644-04701001

Kumar S, Stecher G, Li M, Knyaz C, Tamura K (2018) MEGA X: Molecular evolutionary genetics analysis across computing platforms. Molecular Biology and Evolution 35(6): 1547–1549. https://doi.org/10.1093/molbev/msy096

Nazik L, Poyraz M, Karabıyıkoğlu M (2019) Karstic landscapes and landforms in Turkey. In: Migon P (Ed.) World Geomorphological Landscapes. Springer, 181–196. https://doi.org/10.1007/978-3-030-03515-0_5

Özbek M (2012) A new freshwater amphipod species, *Gammarus obruki* sp. nov., from Turkey (Amphipoda: Gammaridae). Turkish Journal of Zoology 36(5): 567–575. https://doi.org/10.3906/zoo-1112-2

Özbek M, Rasouli H (2014) *Gammarus komareki aznavensis* subsp. nov., a new amphipod subspecies from Iran (Amphipoda: Gammaridae). Turkish Journal of Zoology 38(3): 326–333. https://doi.org/10.3906/zoo-1306-1

Özbek M, Yurga L, Külköylüoğlu O (2013) *Gammarus baysali* sp. nov., a new freshwater amphipod species from Turkey (Amphipoda: Gammaridae). Turkish Journal of Zoology 37: 163–171. https://doi.org/10.3906/zoo-1209-14

Özbek M, Aksu İ, Baytaşoğlu H (2023) A new freshwater amphipod (Amphipoda, Gammaridae), *Gammarus tumaf* sp. nov. from the Gökgöl Cave, Türkiye. Zoosystematics and Evolution 99(1): 15–27. https://doi.org/10.3897/zse.99.89957

Pinkster S, Karaman GS (1978) A new blind *Gammarus* species from Asia Minor, *Gammarus vignai* n. sp. (Crustacea, Amphipoda). Quaderni Di Speleologia. Circolo Speleologico Romano 3: 27–36.

Posada D (2008) jModelTest: Phylogenetic model averaging. Molecular Biology and Evolution 25(7): 1253–1256. https://doi.org/10.1093/molbev/msn083

Tavaré S (1986) Some probabilistic and statistical problems in the analysis of DNA sequences. Lectures on Mathematics in the Life Sciences 17: 57–86.

Thompson JD, Higgins DG, Gibson TJ (1994) CLUSTAL W: Improving the sensitivity of progressive multiple sequence alignment through sequence weighting, position-specific gap penalties and weight matrix choice. Nucleic Acids Research 22(22): 4673–4680. https://doi.org/10.1093/nar/22.22.4673

Trontelj P, Blejec A, Fišer C (2012) Ecomorphological convergence of cave communities. Evolution 66(12): 3852–3865. https://doi.org/10.1111/j.1558-5646.2012.01734.x

Vainola R, Witt JDS, Grabowski M, Bradbury JH, Jazdzewki K, Sket B (2008) Global diversity of amphipods (Amphipoda; Crustacea) in Freshwater. Hydrobiologia 595(1): 241–255. https://doi.org/10.1007/s10750-007-9020-6

Vávra V (1905) Rotatorien und Crustaceen. Annalen Des K. K. Naturhistorischen Hofmuseums in Wien 20: 106–113.

Yamaç A, Gilli E, Tok E, Törk K (2021) Cave and karst systems of the world (Vol. 1). Springer, 1–10. https://doi.org/10.1007/978-3-030-65501-3_1

Zengin B, Eker M (2020) The effects of cave tourism on Akçakoca tourism: Fakıllı Cave example. Journal of Turkish Tourism Research 4(1): 220–233. https://doi.org/10.26677/TR1010.2020.309

Supplementary material 1

The pairwise genetic distance values amongst the Gammarus species, based on the COI dataset (below the diagonal) and 28S dataset (above the diagonal)

Authors: Murat Özbek, Hazel Baytaşoğlu, İsmail Aksu
Data type: xls

Link: https://doi.org/10.3897/zse.99.108048.suppl1

Zoosyst. Evol. 99 (2) 2023, 489–501 | DOI 10.3897/zse.99.102345

PENSOFT

für Natur MUSEUM FÜR NATURKUNDE BERLIN

Identification of the rare deep-dwelling goby *Suruga fundicola* Jordan & Snyder, 1901 (Gobiiformes, Gobiidae) from the Yellow Sea

Changting An[1,2], Ang Li[1,2], Huan Wang[1,2], Busu Li[1,2], Kaiying Liu[1], Hongyue Sun[1], Shufang Liu[1,2], Zhimeng Zhuang[1], Richard van der Laan[3]

1 *National Key Laboratory of Mariculture Biobreeding and Sustainable Goods, Yellow Sea Fisheries Research Institute, Chinese Academy of Fishery Sciences, 106 Nanjing Road, Qingdao, Shandong, China*

2 *Laboratory for Marine Fisheries Science and Food Production Processes, Laoshan Laboratory, Qingdao, China*

3 *Grasmeent 80, 1357JJ Almere, Netherlands*

https://zoobank.org/BED03B87-4DB0-4940-BC16-A1886CC92EF7

Corresponding author: Shufang Liu (liusf@ysfri.ac.cn)

Academic editor: Nalani Schnell ♦ **Received** 19 February 2023 ♦ **Accepted** 13 September 2023 ♦ **Published** 5 October 2023

Abstract

During the 2022 R/V cruises in the Yellow Sea, four goby specimens (51.2–63.5 mm) were captured by using an Agassiz trawl at a water depth of about 70 meters. These specimens were identified as *Suruga fundicola*, mainly by the morphometric characters. Their identification was further confirmed by a molecular phylogenetic analysis based on *12S* and *COI* mtDNA genes. Considering that the four specimens were in good condition and that the original description is brief, a detailed description of the specimens is given. Moreover, the present study presents a preliminary analysis of its phylogenetic position within the *Acanthogobius*-lineage (Gobiidae). The discovery of this goby in the Yellow Sea enriches our knowledge of the fish diversity and distribution of this region, and sheds some light on the ecological habitat of these gobies.

Key Words

Acanthogobius-lineage, distribution, morphology, mtDNA genes, species identification, taxonomy

Introduction

The gobies (order Gobiiformes) include about 2400 species divided into about 320 genera, which are widely distributed throughout the tropical, subtropical, and temperate regions of the world (Parenti 2021; Fricke et al. 2023). These goby species are known from the deep see waters (at a depth of over 300 meters) to elevated mountain streams (at an altitude of over 1000 meters) (Iwata et al. 2000; Shibukawa and Aonuma 2007; Parenti 2021). About 90% of them dwell in marine water, and generally live at the bottom of the sea with a depth of no more than 30 m (Wu and Zhong 2008; Akihito et al. 2013). Only a few species of goby inhabit deep waters; examples from the Western Pacific are species of the genera *Obliquogobius* Koumans, 1941 and *Suruga* Jordan & Snyder, 1901 (Shibukawa and Aonuma 2007; Fujiwara and Shibukawa 2022). According to the record, *Suruga fundicola* Jordan & Snyder, 1901 can inhabit the bottom of deep water off the coast (depth about 40–400 meters; Akihito et al 2013; Choi and Lee 2019).

The goby genus *Suruga* Jordan & Snyder, 1901 of the family Gobiidae comprises only one species, *Suruga fundicola* Jordan & Snyder, 1901 (Akihito et al 2013; Fricke et al. 2023). Based on axial skeletal features, *Suruga* was placed in the *Acanthogobius*-group (sometimes denoted as the tribe Acanthogobiini Parenti 2021) with 7 other genera, *Acanthogobius* Gill, 1859, *Amblychaeturichthys* Bleeker, 1853, *Chaeturichthys* Richardson 1844, *Lophiogobius* Günther, 1873, *Pterogobius* Gill, 1863, *Sagamia* Jordan & Snyder, 1901 and *Siphonogobius* Shibukawa & Iwata, 1998 (Birdsong et al. 1988; Shibukawa 1997).

These eight genera including 18 species, are defined by a unique pattern of the dorsal-pterygiophore formula 3/ I II II I I I 0 (indicating the relationship between the pterygiophores of the dorsal fins and the corresponding spines of the vertebrae), and these genera are regarded as a putative monophyletic assemblage (Akihito et al. 1984; Shibukawa and Iwata 2013a). Mainly based on molecular evidence, the monophyly was only partially confirmed based on few species sequences of this group, and the assemblage was confirmed to be part of the *Acanthogobius*-lineage (a monophyletic lineage of the family Gobiidae comprises about 29 genera) (Agorreta et al. 2013; Thacker and Dawn 2013). The phylogenetic position of *S. fundicola* remained unknown up until now, for the sequence from *S. fundicola* was not included in these molecular studies.

Since its original description, *S. fundicola* has occasionally been found in marine surveys (Kuroda 1957; Yamamuta et al. 1993; Shinohara et al. 2001; Shinohara et al. 2005; Iwatsuki et al. 2017; Choi and Lee 2019; Sonoyama et al. 2020). So far, *S. fundicola* is mainly known from temperate regions of Japan, including off the Pacific coast from Matsushima Bay to Tosa Bay (Fig. 1, black arrows 2 and 3), Japan Sea coast from Aomori Prefecture to Yamaguchi Prefecture (Fig. 1, black arrows 4 and 5), and the Okinawa Trough (black full circle 6) (Akihito et al. 2013). This species is also reported off Tongyeong, South Korea (Fig. 1 blue full circle 7) (Choi and Lee 2019). Although Okiyama (2014) recorded juveniles as *S. fundicola* from two stations of the East China Sea in 1956 (Fig. 1, orange full circle 8 and 9), this species identification was not accepted by subsequent authors (Akihito et al 1984; Wu and Zhong 2008; Akihito et al 2013; Wu and Zhong 2021). So far, there is no record of this species from the Yellow Sea. According to the historical records, there are about 50 goby species known to occur in the Yellow Sea, all of which live in shallow coastal waters (Wu and Zhong 2008; Liu et al. 2015; Parenti 2021).

Two R/V cruises, conducted during 2022, yielded four goby specimens from stations H27 (35°59.69'N, 123°07.63'E) and H12 (33°59.55'N, 123°22.99'E) in the Yellow Sea (see Fig. 1, green triangles). These specimens have notably large eyes, and combined with other morphometric characters these four gobies would conform to *Suruga fundicola* Jordan & Snyder, 1901. But there were a few inconsistent descriptive features, which hampered a definite identification. In order to confirm this morphology-based species identification, *COI* and *12S* genes of mitochondrial DNA of these four specimens were amplified. Phylogenetic analyses of the obtained sequences and the literature available sequences of other *Acanthogobius*-lineage gobies (also including one GenBank-retrieved *12S* sequence of *S. fundicola* from Jogashima Island, Japan, accession number LC069781), showed that the specimens belong to the species *S. fundicola*.

This is the first report on the occurrence of *S. fundicola* in the Yellow Sea based on available specimens.

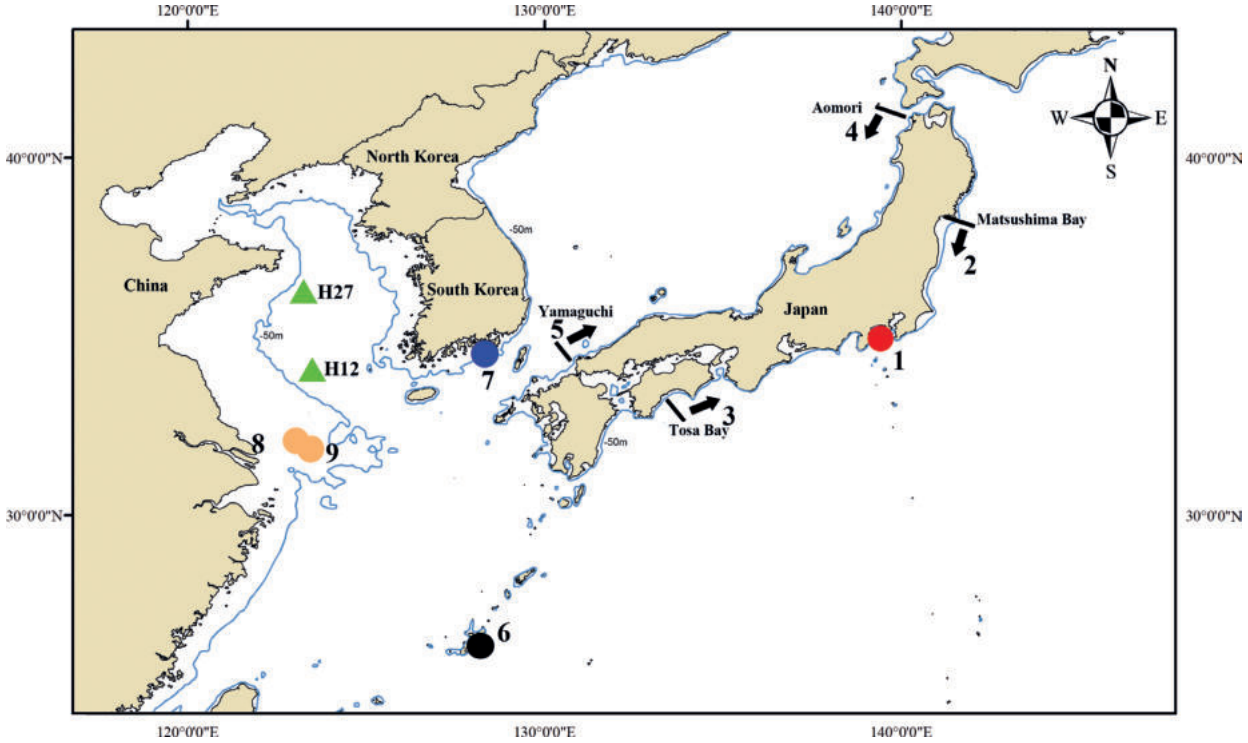

Figure 1. Historical distributional records of *S. fundicola* and the sampling stations. The red full circle 1 indicates the type locality: Sagami Bay (Jordan and Snyder 1901); black arrows 2 and 3 indicate the distribution from Matsushima Bay to Tosa Bay, and black arrows 4 and 5 indicate the distribution from Aomori Prefecture to Yamaguchi Prefectural, black full circle 6 indicates Okinawa Trough (Akihito et al. 2013); blue full circle 7 indicates the records of Tongyeong of South Korea (Choi and Lee 2019); orange full circle 8 and 9 indicate the records in the East China Sea (Okiyama 2014); the green triangles H27 and H12 point to the locations of the survey stations where the four goby specimens were caught.

Materials and methods

Specimen sampling and preservation

The fisheries resources survey vessel Lanhai 101 carried out two R/V cruises conducted by the Yellow Sea Fisheries Research Institute (YSFRI) in spring (April) and summer (July) 2022. A small Agassiz trawl (with a mouth of 1.8 m in width and 0.6 m in height) was employed during each cruise, at an average speed of 3 n mile/h (=5556 m/h) for 20 minutes. Four specimens of *S. fundicola* were collected, two in the spring (at H27 on 15 April) and two in the summer (one at H12 on 16 July and one at H12 on 20 July). The environmental parameters were obtained by the CTD measurements (SBE 911). Immediately after the capture of these specimens, the digital photographs were taken for each of them in a special glass tank with a Canon 5DSR, equipped with a micro lens (Canon), see Fig. 2. The muscle of the right lateral body was removed and stored in 95% ethanol for further molecular analysis. The voucher specimens were then fixed in 10% formalin preservative and then transformed to 75% alcohol for morphological examination and permanent curation, and deposited in the National Marine Fishery Biological Germplasm Resource Bank, China.

Morphological analysis

Meristic counts and morphometric measurements followed the methods used by Choi and Lee (2019). Additionally, two other counts (Pelvic fin rays and Dorsal fin pterygiophore formula) and one morphometric measurement (Caudal peduncle length) were used. Thus, ten meristic and twenty-one morphometric measurements were taken for each individual in this study (Table 1). Measurements and counts were taken on the left side of the specimens whenever possible. Measurements were made point

Table 1. Comparison of meristic and morphometric data of *S. fundicola* with the literature values. The numbers in bold point to the observed differences. Dorsal-fin pterygiophore formula is expressed as "3/I II II I I I 0 i/12", where "3" shows the number of vertebrae before the 1st dorsal fin is inserted, the Roman numerals in uppercase show the number of the dorsal pterygiophores inserted between the neural spines, the Roman numeral in lowercase shows the number of the interdorsal pterygiophores, and "12" shows that the two pterygiophore of the 1st ray of the second dorsal fin are mounted over the 12th vertebrae (Akihito et al. 1984; Shibukawa and Iwata 2013).

Characteristic	Present study		Original description		Choi and Lee (2019)	
	Range	Mean	Range	Mean	Range	Mean
Standard length (mm)	51.8–63.5	58.7	50.0–63.0	55.3	44.3–51.8	
Meristic counts						
First dorsal fin rays	VIII	VIII	VIII	VIII	VIII	VIII
Second dorsal fin rays	I, 16	I, 16	17–19	17.8	I, 16–17	
Anal fin rays	I, 15–16	I, 15.8	16–18	17	I, 15–16	
Pectoral fin rays	20–21	20.3			20–22	
Pelvic fin rays	I–5	I–5				
Lateral line scales	39–41	40	38–44	40.5	37–42	
Transverse scales	8–10	9.0			10–11	
Predorsal scales	10–11	10.8	10–12	10.7	8–11	
Vertebral number	14+21	14+21			14+21–22	
Dorsal-fin pterygiophore formula	3/I II II I I I 0 i/12					
Morphometric data						
Percentage against SL (%)						
Head length	24.5–28.0	26.1	26.0–27.0	26.3	25.9–29.7	27.8
Head depth	13.1–17.6	15.4			14.6–17.6	16.1
Head width	13.2–14.2	13.6			15.1–18.3	16.8
Snout length	4.5–5.7	5.5	5.0–7.0	6.0	5.4–7.8	6.4
Eye diameter	8.1–9.7	8.7	9.5–11.0	10.1	9.2–11.4	10.0
Interorbital width	0.9–1.9	1.4	1.0	1.0	0.7–2.1	1.5
Jaw length	8.3–10.3	9.0	10.0–11.0	10.3	8.6–11.9	10.5
Body width	10.6–10.3	11.8			10.9–14.7	12.6
Body depth at origin of first dorsal fin	15.3–22.4	18.9			15.3–19.0	16.9
Body depth at origin of anal fin	16.0–18.3	16.9			12.1–15.1	13.4
Snout to origin of first dorsal fin	31.5–33.4	32.5	32.0–36.0	33.5	28.6–36.0	33.4
Snout to origin of second dorsal fin	53.3–58.7	55.1	52.0–54.0	52.5	51.4–55.7	53.7
Snout to origin of anal fin	55.7–61.1	59.1	56.0–58.0	57.5	53.0–58.6	55.9
Caudal peduncle length	10.7–13.5	11.7	10.0–14.0	11.8		
Caudal peduncle depth	6.9–8.8	8.0	7.0–7.5	7.1	6.7–9.1	8.2
Pectoral fin length	19.5–21.8	20.6	21	21	17.7–20.9	19.0
Base of dorsal fin	13.8–14.7	14.3			13.4–16.3	14.7
Base of second dorsal fin	33.7–36.6	35.4			30.8–38.3	35.6
Base of anal fin	30.2–37.7	32.4			30.6–37.0	32.4
Caudal fin length	19.8 –23.3	21.4			18.6–27.2	22.3

to point with a digital caliper linked directly to a data-recording computer and the data were recorded to the nearest 0.1 mm. The measurements of the body were given as percentages (%) of the standard length (SL). Detailed information about the meristic and morphometric measurements is provided in Table 1. Osteological features were observed with the help of micro-CT radiographs (Bruker, skyskan-1276) or from X-rays (Aolong, version 90). Cephalic sensory canals and papillae were recorded from specimens stained with cyanine blue following Akihito et al. (1984), the notations following Sanzo (1911); Shibukawa and Aizawa (2013); Shibukawa and Iwata (2013).

DNA extraction, amplification and sequencing

DNA was extracted by using TIANamp Genomic DNA Kit (Tiangen Biotech, Beijing) according to the manufacturer's recommended protocol, and the quality was estimated at wave-length 260/280 nm by a Nano-300 micro-spectrophotometer (Allsheng, Hangzhou, China). The obtained DNA solutions were stored at -20 °C until used.

The mitochondrial *12S* rRNA (*12S*) and the *cytochrome c oxidase I* (*COI*) genes were amplified by PCR with different primer combinations. For *12S*, we used MiFish-U-F and MiFish-U-R designed by Miya et al. (2015). Primers reported by Ward et al. (2005) were used for the amplification of *COI*. PCR was conducted in 25 µl volumes, including 12.5 µl Master mix Taq, 1 µl of each primer, 1 µl template DNA, adding double distilled water to adjust the volume. Thermocycling conditions were as follows: initial denaturation for 4 min at 94 °C, denaturation for 50 s at 94 °C, annealing for 50 s at 55 °C for *COI* and 59 °C for *12S*, and extension 1 min for *COI* and 30 s for *12S* at 72 °C. After 35 cycles, the final extension was done at 72 °C for 10 min. The PCR products were bidirectional sequenced by BGI Genomics Co., Ltd.. In this study, four specimens of *S. fundicola* and three specimens of *Amblychaeturichthys hexanema* (Bleeker, 1853) were sequenced for phylogenetic analysis, and all amplified *COI* and *12S* sequences were submitted to GenBank (for the accession numbers, see Table 2).

Molecular sequence analysis

All amplified sequences of the two mtDNA genes were concatenated and used for molecular phylogenetic analysis, along with 37 GenBank-retrieved sequences from 19 related species of 14 genera belonging to the *Acanthogobius*-lineage. In addition, *Odontobutis haifengensis* Chen, 1985 (Odontobutidae) was used as an outgroup (Table 3). Multiple alignments were prepared for *COI* and *12S* sequences using the program MUSCLE in MEGA X (Edgar

Table 2. The detailed information of specimens analyzed in this study.

Species	Specimen catalog	GenBank no.		Sampling location	Resource
		COI	***12S* rRNA**		
Suruga fundicola 1	YSFRI27216	OP824753	OP837791	Yellow Sea station H27	Present study
S. fundicola 2	YSFRI27217	OP824754	OP837792	Yellow Sea station H27	Present study
S. fundicola 3	YSFRI36942	OP824752	OP837789	Yellow Sea station H12	Present study
S. fundicola 4	YSFRI36943	OP824755	OP837790	Yellow Sea station H27	Present study
S. fundicola 5	CBM:ZF:15688	/	LC069781	Japan: off west of Jogashima Island	GenBank
Amblychaeturichthys hexanema 1	YSFR27208	OP824756	OP837786	North Yellow Sea	Present study
Am. hexanema 2	YSFR27209	OP824757	OP837787	North Yellow Sea	Present study
Am. hexanema 3	YSFR27210	OP824758	OP837788	North Yellow Sea	Present study
Am. hexanema 4	Uncatalogued	KT781104	KT781104	China: Qingdao, Shandong Prov.	GenBank
Acanthogobius flavimanus	Uncatalogued	MW271007	MW271007	Uncatalogued (Maybe from China)	GenBank
Ac. hasta	Uncatalogued	MK253669	MK253669	China: Lianyungang City, Jiangsu Prov.	GenBank
Chaeturichthys stigmatias	Uncatalogued	MN038166	MN038166	China: Qingdao, Shandong Prov.	GenBank
Lophiogobius ocellicauda	Uncatalogued	KR815520	KR815520	China: Zhoushan, Zhejiang Prov.	GenBank
Lepidogobius lepidus	UW:151092	KF918879	LC092050	USA: Washington, Puget Sound	GenBank
Chaenogobius gulosus	JM120726-11	KP696748	KP696748	Korea: coastal area of Jangmok	GenBank
Chaenogobius annularis	Uncatalogued	OM830225	OM830225	China	GenBank
Gymnogobius urotaenia	Uncatalogued	KT601093	KT601093	Uncatalogued (Maybe from South Korea)	GenBank
Parachaeturichthys polynema	ECSFRI-NMW01	OK012405	OK012405	China: East China Sea	GenBank
Eucyclogobius newberryi	LodgeLab Enewberryi_1	KP013101	KP013101	Uncatalogued	GenBank
Gillichthys mirabilis	Uncatalogued	FJ211845	FJ211845	China: Nantong city, Jiangsu Prov.	GenBank
Gymnogobius petschiliensis	20131115NA05	AY525784	AY525784	China: Qingdao, Shandong Prov.	GenBank
Luciogobius platycephalus	Uncatalogued	JX971538	JX971538	China: Zhoushan, Jiangsu Prov.	GenBank
L. pallidus	Uncatalogued	KF040451	KF040451	South Korea: Jeju Island	GenBank
Tridentiger bifasciatus	Uncatalogued	JN244650	JN244650	China: Zhoushan fishing ground Zhejiang Prov.	GenBank
T. trigonocephalus	Uncatalogued	KT282115	KT282115	Uncatalogued (Maybe from China)	GenBank
Rhinogobius similis	Uncatalogued	KF371534	KF371534	China: Liangzi Lake in the middle reaches of the Yangtze River	GenBank
Odontobutis haifengensis (Odontobutidae)	Uncatalogued	MF383619	MF383619	China: Fengshun, Guanggong	GenBank

Table 3. The depth (D), temperature (T), and salinity (S) of H12 and H27.

Data	Station	Bottom layer			Surface layer		
		D (m)	T (°C)	S(‰)	D (m)	T (°C)	S(‰)
April 18, 2022	H12	69.0	10.5	33.0	3.2	12.1	32.6
April 15, 2022	H27	74.0	9.5	32.8	2.8	10.5	32.6
July 16, 2022	H12	69.0	10.8	33.1	2.0	26.9	30.8
July 20, 2022	H27	74.0	9.2	32.8	2.8	25.6	30.8

2004). Genes were concatenated with the help of SequenceMatrix 1.8 (Vaidya et al. 2011). The genetic distance was calculated in MEGA X, based on Kimura 2-parameter (K2P) (Kimura 1980), and the base composition was calculated with the same software, based on K2P (Sudhir et al. 2018). The optimal evolution model was GTR selected in MEGA X based on Akaike's information criterion (AIC), and the maximum likelihood tree (ML tree) was constructed with the same software (Kumar et al. 2018), with 1,000 bootstrap replications.

Results

Suruga fundicola Jordan & Snyder, 1901

Figs 2, 3, Table 1

Suruga fundicola Jordan & Snyder, 1901: 96, fig. 20 (original description, type locality: Sagami Sea, Japan); Akihito et al. 1984: 279 (in English), fig. 253-H; Akihito et al. 2002: 1207 (in Japanese); Akihito et al. 2013: 58 (in Japanese); Shibukawa and Iwata 2013a: 45; Matsui et al. 2014: 6; Choi and Lee 2019:255, fig. 1.

Diagnosis. Distinct from all other gobies (Gobiidae), members of the *Acanthogobius*-group share a unique dominant pattern of the dorsal-pterygiophore formula, 3/I II II I I I 0 (Akihito et al. 1984). In the *Acanthogobius*-group, *S. fundicola* can be distinguished from the species of *Sagamia*, *Siphonogobius* and *Pterogobius* by possessing no free rays in the upper part of the pectoral fin and the posterior margin of the pelvic frenum indented. *S. fundicola* can be distinguished from the species of *Lophiogobius*, *Amblychaeturichthys*, and *Chaeturichthys* by the lack of barbels or flaps on the ventral surface of the head (except for the mental frenum). From species of *Acanthogobius*, *S. fundicola* can be distinguished by the large eye, its diameter greater than the snout length (vs. usually less); each cephalic sensory papilla formed into a minute skin flap (vs. not), the posterior oculoscapular canal absent (vs. posterior oculoscapular canal and its terminal pores K' and L' present).

Description of Yellow Sea specimens. The counts and measurements are given in Table 1. Dorsal-fin rays VIII-I, 16; anal-fin rays I, 15 (1), I, 16 (3); pectoral-fin rays 20 (3), 21 (1); pelvic fin rays I, 5 (4); longitudinal scales 39 (1), 40 (2), 41 (1); pre-dorsal mid-line scales 10 (1), 11 (3); transverse scales 8 (1), 9 (2); 10 (1); vertebral count 14+21 = 35 (4); dorsal-pterygiophore formula 3/I II II I I I 0 i/12; epural 2; anal-fin pterygiophores anterior to first haemal spine 2.

The following measurements are in % SL: head length 24.5–28.0 (mean 26.1); head depth 13.1–17.6 (15.4); head width 13.2–14.2 (13.6); snout length 4.5–5.7 (5.5); eye diameter 8.1–9.7 (8.7); interorbital width 0.9–1.9 (1.4); jaw length 8.3–10.3 (9.0); body width 10.6–10.3 (11.8); body depth at origin of first dorsal fin 15.3–22.4 (18.9); body depth at origin of anal fin 16.0–18.3 (16.9); snout to origin of first dorsal fin 31.5 –33.4 (32.5); snout to origin of second dorsal fin 53.3–58.7 (55.1); snout to origin of anal fin 55.7–61.1 (59.1); caudal peduncle length 10.7–13.5 (11.7); caudal peduncle depth 6.9–8.8 (8.0); pectoral fin length 19.5–21.8 (20.6); base of dorsal fin 13.8–14.7 (14.3); base of second dorsal fin 33.7–36.6 (35.4); base of anal fin 30.2–37.7 (32.4); caudal fin length 19.8–23.3 (21.4).

General body appearance was shown in Figs 2, 3. Body small, moderately elongated; predorsal body profile slightly convex; ventral profile slightly concave, especially from pectoral-fin insertion to anal-fin origin. Head large, not depressed, short but longer than wide, depth and width less than those of the body. Snout short, obtuse in lateral and dorsal view, shorter than eye diameter and postorbital head length. Eyes notably large, situated dorsolateral in upper half of the head, with very narrow interorbital space, eyes nearly meeting, diameter larger than interorbital space or snout length. Mouth almost terminal, but upper jaw slightly protruding. Maxillary concealed except at its posterior end. Tongue thick, rather broad, round anteriorly. Gill openings broad, extending anteriorly to the vertical line of the posterior margin of the eye; upper edge of the gill opening on fleshy pectoral-fin base, slightly above the upper margin. No barbels. Body covered with cycloid scales, anterior small, posterior large and the scales are rather loosely attached. Head naked.

Fins flexible, without spinous rays. First dorsal fin with 8 slender spines, reaching origin of second dorsal when depressed; dorsal-pterygiophore formula 3/I II II I I I 0 i/12. Second dorsal fin with 1 simple and 16 branched rays, shorter than the first spines. Origin of first dorsal fin posterior to a vertical through base of pectoral fins, first dorsal fin without filamentous spines. The distal margin of the first dorsal fin is convex, when adpressed, the distal tip touches the base of the spine of the second dorsal fin. Dorsal fins discontinuous. Origin of second dorsal fin somewhat at vertical through the anus, and anterior to the anal fin. When adpressed, the distal tips of the second dorsal fin and the anal fins do not reach the procurrent rays of the caudal fin. Pectoral fins rounded, with 20 rays. The pectoral fin extends posteriorly to the vertical line through the posterior margin of the base of the first dorsal fin. Pelvic fin fused into a disc, each with 1 simple and 5 branched rays. Anal fin with 15–16 rays, the anterior of the anal fin below the third branched dorsal ray of the second dorsal fin. Segmented caudal-fin rays 7+7, upper unsegmented caudal fin rays about 12 and lower unsegmented caudal fin rays about 11.

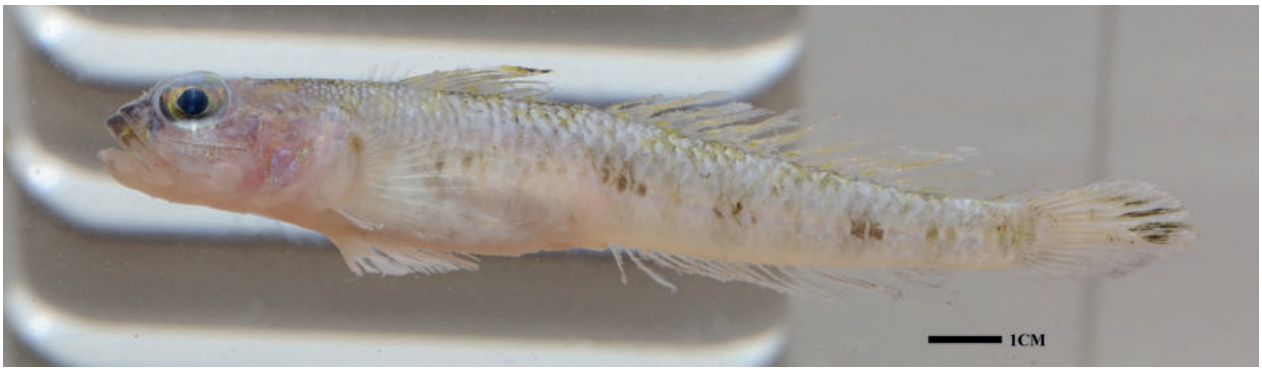

Figure 2. Lateral view of *S. fundicola*: YSFRI27216, 63.5 mm SL, photographed alive immediately upon capture.

Figure 3. Lateral (**a**), dorsal (**b**), and ventral (**c**) views of *S. fundicola*: YSFRI27216, 63.5 mm SL.

Cephalic canals are variably developed and are shown in Fig. 4: anterior oculoscapular canal (AOC) with B′, D (S), F, H’; posterior oculoscapular canal (POC) absent; preopercular canal (PC) with pores M′ and O’; four short longitudinal sensory papillae (SSP) rows (=rows r, u, s, t) on snout; four SSP rows (=rows g, j, k, and l) close behind the eye; two SSP rows (=rows h, i) before dorsal fin; two transverse sensory papillae (TSP) rows (=rows n and o) on snout and behind the eye, respectively; four longitudinal sensory papillae (LSP) rows (=rows a, b, c, and d) on the cheek; anterior end of row a approaches the anterior margin of the eye; rows b and c very close together;

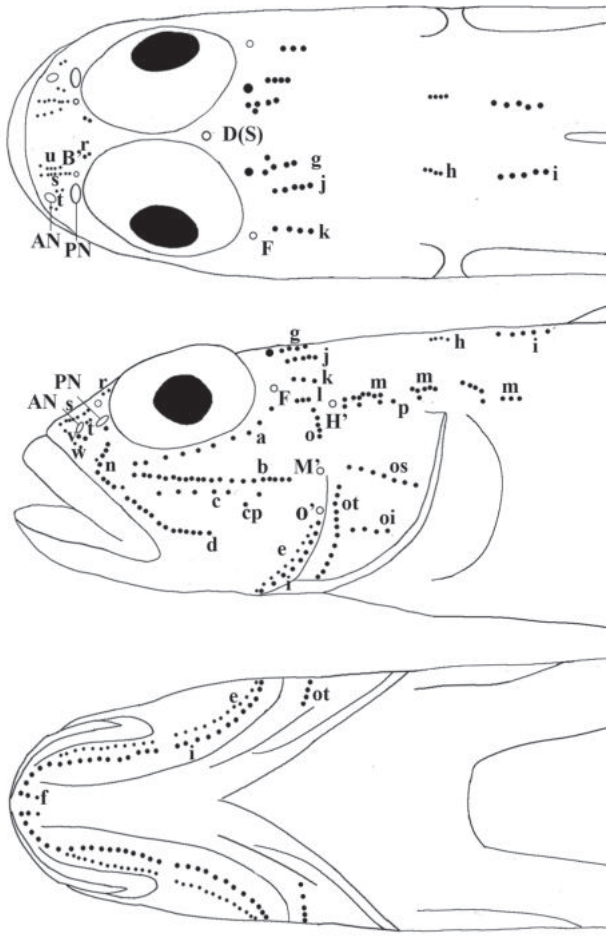

Figure 4. Dorsal (top), lateral (middle), and ventral (bottom) views of the head of *S. fundicola*: YSFRI27216, 63.5 mm SL female), showing cephalic sensory canal pores (indicated by roman uppercase letters, except for AN and PN) and papillae (indicated by roman lowercase letters). AN and PN, indicated anterior and posterior nares, respectively.

row cp with a single sensory papilla; row d arc-shaped, extending posteriorly to the vertical line through the posterior margin of the pupil; two long parallel longitudinal rows of sensory papillae just behind the chin (=row f), and ending on both sides at the opercles, one TSP row (=row ot) and two LSP rows (=rows os and oi) on the opercles, row ot extends to the ventral side.

Cranium flat, frontals extremely narrow (Fig. 5a, e). No suborbital bone. Five branchiostegal rays, the first one thin, and last one strong (Fig. 5f). Four pairs of ceratobranchials (Fig. 5g). Well-developed teeth on upper and lower pharyngeal. Three pairs of otoliths, sagittae, lapillus and asteriscus (Fig. 5e). Vertebral count 35, 14 abdominal vertebrae (av) and 21 caudal vertebrae (cv), 14 pairs of ribs appending on parapophysis (Fig. 5a, b). Three hypurals (HY), respectively HY1+2 (HY1 and HY2 fused into one), HY3+4 (HY3 and HY4 fused into one), and HY5; two epurals, EP1 and EP2.

Coloration. In freshly collected specimens (Fig. 2), head and dorsum of body dusky, darker on snout, with several irregular light-yellow blotches on the lateral body, ventral body lighter, abdomen almost white. Pupil of the eye black, iris golden gray. A light sapphirine blotch present on the gill cover. Six or seven large dark spots scattered along middle of the side from the gill opening to the caudal-fin base; 2 or 3 light orange stripes on gray dorsal and caudal fins, the anterior margin of first dorsal fin with dusky spots, the upper posterior of caudal fin with a black stripe, anal fin somewhat gray.

Coloration changed after 2 months of preservation (10% formalin preservative and then transformed to 75% alcohol), the yellow and orange pigment disappeared from body and fins, and the body of the fish became dark-yellowish, covered with tiny black spots, back darker and belly lighter, snout black, lateral dark spots not clear. Pupil of the eye white, iris golden black. Dorsal, pectoral, pelvic and anal fins light greyish.

Distribution. Northwest Pacific: off Pacific coasts from Miyagi Prefecture to Tosa Bay, Japan Sea from Aomori to Yamaguchi Prefecture, Okinawa Trough (Akihito et al. 2013), Southern Sea of Korea (Choi and Lee 2019), East China Sea (Okiyama 2014) and Yellow Sea (present study).

Habitat and ecology. The four specimens were collected at depths between 69 and 74 meters (Fig. 1). The two stations maintained a relatively low temperature of about 10 °C and a high salinity of about 33‰ in April and July 2022 (Table 3). This species is considered as one of the deepest dwelling goby in Japan, known from depths of 40 to 400 meters (Akihito et al. 2013; Choi and Lee 2019).

The catch at the stations mainly consists of ophiuroids, molluscs, jellyfishes, fishes and so on, most common species of which are the brittle stars *Ophiura sarsii vadicola* Djakonov, 1954 (Ophiuroidea) and *Stegophiura sladeni* (Duncan, 1879) (Ophiuroidea) (Fig. 6). Examples of the co-existing fish species are *Jaydia lineata* (Temminck & Schlegel, 1843) (Apogonidae), *Cleisthenes pinetorum* Jordan & Starks, 1904 (Pleuronectidae), *Liparis tanakae* (Gilbert & Burke, 1912) (Liparidae), *Pholis fangi* (Wang & Wang, 1935) (Pholidae), and *Hexagrammos otakii* Jordan & Starks, 1895 (Hexagrammidae).

Sequence characteristics and phylogenetic placement. The concatenated *COI* and *12S* sequences from 22 species were 704 bp in length (after trimming, except LC069781), including 400 conserved sites, 307 variable sites, 278 parsimony informative sites, and 24 singleton sites. The mean four nucleotide frequency of *S. fundicola* was A=26.1%, T=28.8%, C=27.3% and G =17.8%, slightly A-T rich (54.9%). The intragroup sequence divergence of *S. fundicola* was 0.5%; the genetic distance between samples of the Yellow Sea and the sequence (LC069781) of *S. fundicola* from west of Jogashima Island of Japan was 0.2%. This species has a genetic distance of 19.2% (*C. stigmatias*) to 26.3% (*E. newberryi*) to the other 20 species we used (see Table 4). The ML tree based on the concatenated sequences is shown in Fig. 7. In the tree topology, all species from the same genus clustered in one lineage; the four sequences of *S. fundicola* clustered into a highly supported (94% bootstrap P value) lineage and

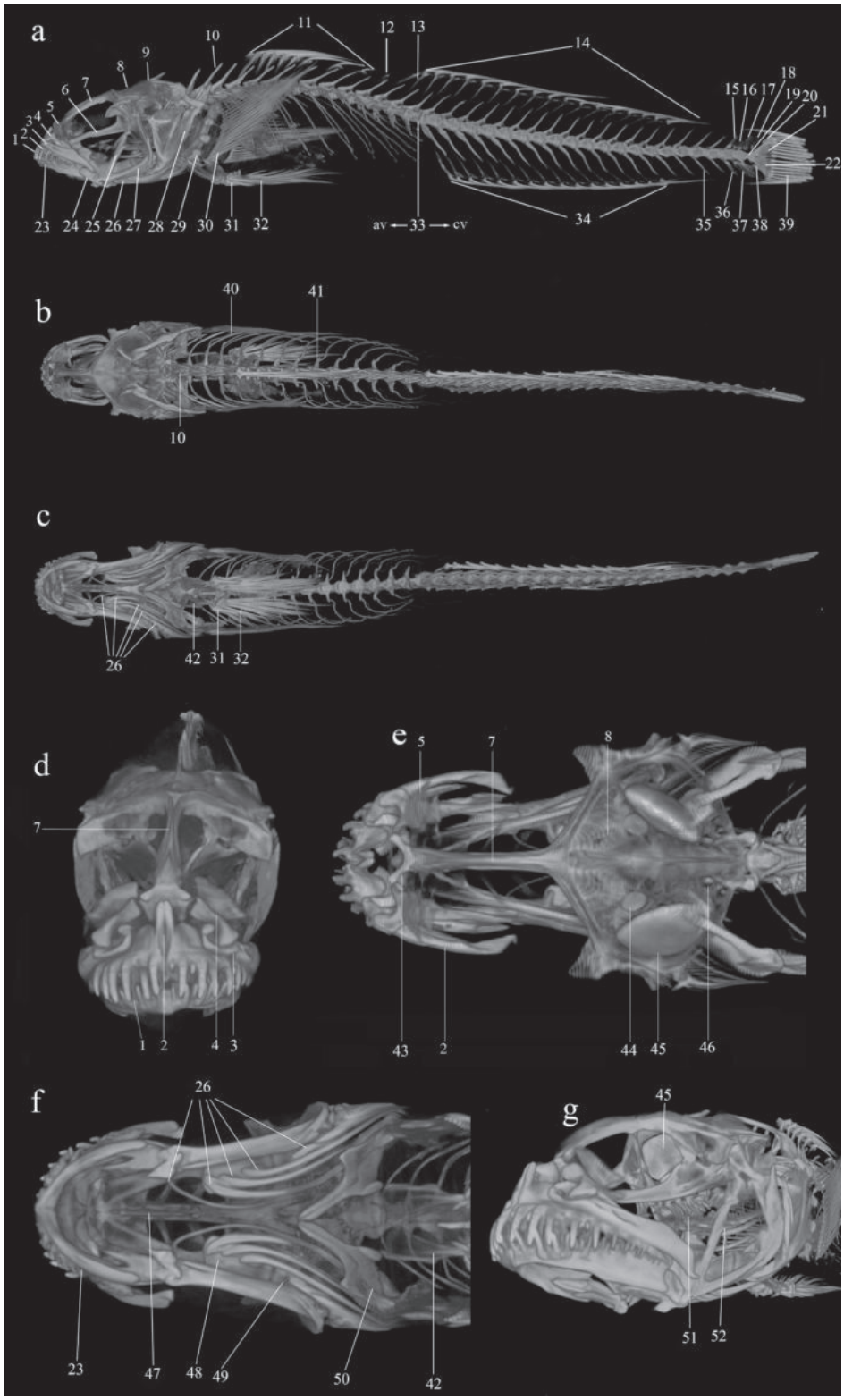

Figure 5. Micro-CT images of right (**a**), dorsal (**b**), and ventral (**c**) views of specimen YSFRI27216; front (**d**) dorsal (**e**), ventral (**f**), and oblique view (**g**) of the head of specimen YSFRI27216. 1. teeth, 2. premaxilla, 3. maxilla, 4. palatine, 5. ectethmoid, 6. parasphenoid, 7. frontal, 8. parietal, 9. supraoccipital, 10. neural spine, 11. first dorsal fin spines, 12. interdorsal pterygiophores, 13. pterygiophore, 14. second dorsal fin rays, 15. neural spine of preural centrum 3(NPU3), 16. neural spine of preural centrum 2(NPU2), 17. epural 1 (EP1), 18. epural 2 (EP2), 19. urostyle, 20. hypural 5 (HY5), 21. hypural 3+4 (HY3+4), 22. hypural 1+2 (HY1+2), 23. dental, 24. articular, 25. sympletic, 26. branchiostegal rays, 27. preopercular, 28. subopercular, 29. proximal radials, 30. pectoral fin soft rays, 31. pelvic fin spine, 32. vertebral canal, 33. boundary of abdominal vertebra and candal vertebrae, 34. anal fin rays, 35. ventrispinales, 36. haemal spine of preural centrum 3 (HPU 3), 37. haemal spine of preural centrum 2 (HPU 2), 38. parhypural (PH), 39. caudal fin ray, 40. rib, 41. parapophysis, 42. pelvic bone, 43. ethmoid, 44. lapillus 3+4 (HY3+4), 45. sagittae, 46. asteriscus, 47. basihyal, 48. ceratohyal, 3 (HPU 3). 49. epihyal, 50. cleithrum, 51. pharyngeal tooth, 52. ceratobranchial.

Figure 6. The catch of A: H27 (15 April), B: H12 (15 July), and C: H27 (20 July).

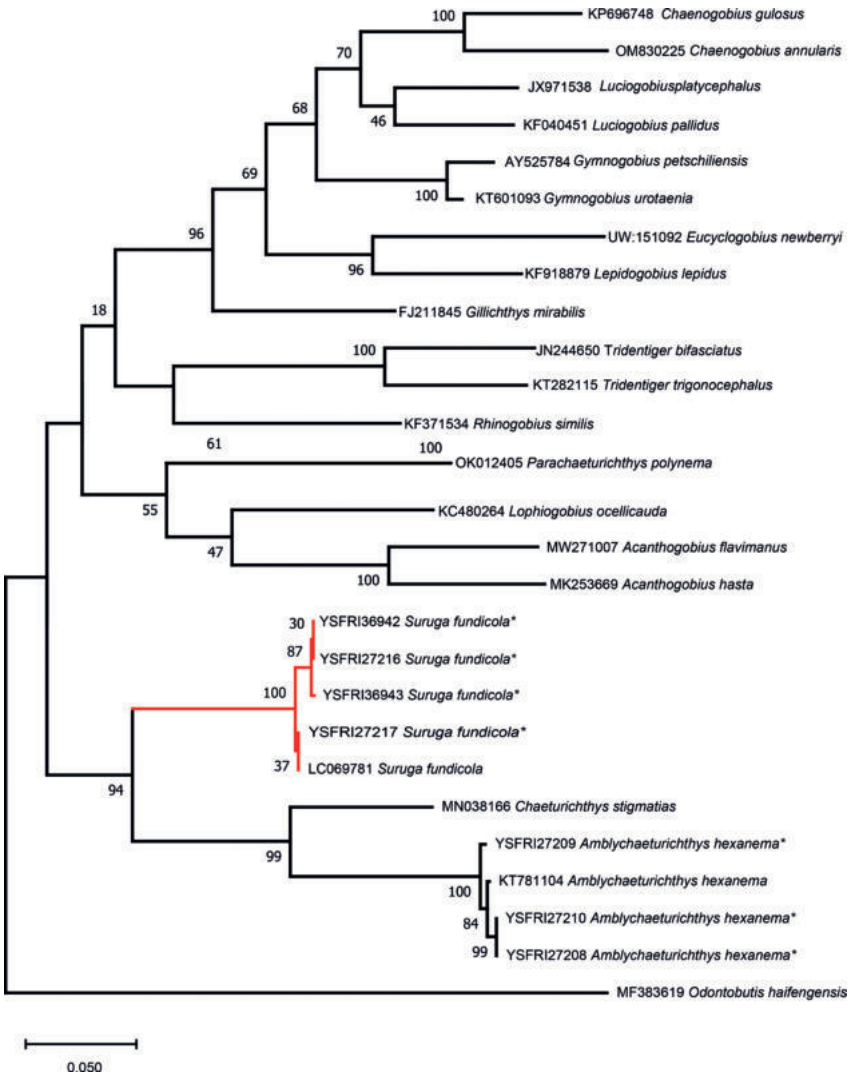

Figure 7. ML tree inferred from concatenated *COI* and *12S* sequences. Numbers at major internal nodes are bootstrap probability values. Sequences with * were sequenced in the present study.

had a sister group relationship with the lineage formed by *A. hexanema* and *C. stigmatias*.

Material examined. YSFRI27216–27217, 2 specimens, 51.2–63.5 mm SL, station H27, Yellow Sea, off Qingdao, Shandong Province, China (35°59.69'N, 123°07.63'E), collected by Changting An on 15 April, 2022; YSFRI36942, 1 specimen, 60.5 mm SL, station H12, Yellow Sea, off Lianyungang, Jiangsu Province, China (33°59.88'N, 123°24.14'E), collected by Hongyue Sun, on 16 July, 2022; YSFRI36943, 1 specimen, 59.1 mm SL, station H27, Yellow Sea, off Qingdao, Shandong Province, China (35°56.03'N 123°07.54'E), collected by Hongyue Sun, on 20 July, 2022.

Discussion

According to Jordan & Snyder's (1901) record, the type specimen (USNM 49744) was caught in a depth of 65 fathoms (119 meters), off Sagama, Japan. Unfortunately, the holotype of this species cannot be examined now, for it was lost in 1980 (Fricke et al. 2023). Our photographic

Table 4. Genetic distances (%) based on concatenated *COI* and *12S* sequences computed by MEGA X among 21 groups. *S. fundicola* * was sequenced for the present study.

	Group	Intragroup	Intergroup																			
			1	2	3	4	5	6	7	8	9	10	11	12	13	14	15	16	17	18	19	20
1.	*Suruga fundicola* *	0.5																				
2.	*S. fundicola*	n/c	0.2																			
3.	*Am. hexanema*	0.5	21.5	19.5																		
4	*Ac. flavimanus*	n/c	23.9	26.5	26.6																	
5	*Ac. hasta*	n/c	24.4	22.9	23.7	13.6																
6	*C. stigmatias*	n/c	19.2	17.9	15.1	25.6	22.8															
7	*Lo. ocellicauda*	n/c	21.6	20.1	27.3	21.2	20.9	25.5														
8	*Ch. gulosus*	n/c	23.5	14.8	26.6	24.6	25.2	23.4	20.2													
9	*Ch. annularis*	n/c	23.9	16.1	25.7	26.3	25.3	25.0	25.3	11.2												
10	*Gy. urotaenia*	n/c	21.4	18.7	25.0	24.3	22.6	23.7	23.6	15.2	15.4											
11	*Gy. petschiliensis*	n/c	23.5	22.2	25.9	26.0	23.8	25.3	24.0	16.9	16.2	2.8										
12	*P. polynema*	n/c	24.0	21.8	27.9	22.9	26.1	26.3	21.3	27.0	28.5	23.9	23.1									
13	*E. newberryi*	n/c	26.3	22.6	31.4	25.0	24.5	28.2	26.8	19.7	21.6	21.0	21.8	26.9								
14	*Gi. mirabilis*	n/c	20.9	12.6	23.9	24.7	21.4	23.3	20.6	17.4	21.4	17.1	18.7	23.4	20.1							
15	*Le. lepidus*	n/c	21.1	16.1	24.9	24.1	22.9	22.0	24.3	19.2	20.2	16.0	16.9	24.7	17.2	16.2						
16	*Lu. platycephalus*	n/c	21.4	15.5	24.5	23.2	23.8	23.6	22.2	13.7	14.0	14.1	14.8	23.3	19.3	15.6	17.5					
17	*Lu. pallidus*	n/c	22.8	20.2	22.8	23.5	22.3	21.2	24.2	15.4	15.4	13.1	14.0	24.6	19.3	15.9	16.5	10.9				
18	*T. bifasciatus*	n/c	25.0	29.0	26.2	26.3	25.4	24.7	24.5	24.4	25.1	23.2	23.5	25.0	24.4	24.7	25.3	25.1	24.6			
19	*T. trigonocephalus*	n/c	23.7	29.0	26.2	25.4	25.8	26.9	26.8	27.5	26.1	24.8	24.8	24.3	28.0	24.6	25.5	24.0	24.8	12.9		
20	*R. similis*	n/c	20.1	14.8	23.0	23.8	24.0	22.2	23.3	19.4	21.4	18.7	19.7	22.2	22.9	18.6	19.2	18.3	20.0	21.1	21.9	
21	*O. haifengensis*	n/c	22.5	23.5	27.1	24.1	26.2	26.3	24.5	25.7	26.4	22.4	21.8	24.1	24.8	24.4	22.8	22.7	20.9	29.7	27.3	22.3

examination based on two paratypes AMNH I-3549 (48.2–60.3 mm SL, Fig. 8) and their X-ray images, found that this species has notably large eyes, a very narrow interorbital space, jaws equal, eight dorsal spines and 17–18 dorsal-fin branched rays, dorsal-pterygiophore formula 3/I II II I I I 0 i /12, 17–18 anal-fin branched rays, and 35 (14 AV and 21 CV) vertebrae, as stated in its original description. All these characters are shared by the four specimens collected from the Yellow Sea of China, which are therefore conspecific with this species.

Clearly, the four specimens AMNH I-35829 (91.40–104.55 mm SL, Fig. 9), caught by Pope from Foochow (=Fuzhou), Fukien (=Fujian), China, were misidentified as they have relatively small eyes (less than the snout length), a broad interorbital space, a lower jaw projecting beyond the upper jaw, eight spines of the first dorsal fin and 16–17 branched rays of the second dorsal fin, the dorsal-fin pterygiophore formula 3/I II II I I I 0 i/11, 17–18 anal fin rays, and 34 (13 AV and 21 CV) vertebrae. Based on the number of rays in the second dorsal finI-16 (4), they can be distinguished from species of *Chaeturichthys* (I-20–22), *Siphonogobius* (I-12–13), *Pterogobius* (I-18–27), and *Acanthogobius* (I-18–20). Based on the number of anal fin rays (17–18), they are distinct from species of *Sagamia* (13–14), and *Amblychaeturichthys* (11–13). In comparison to *S. fundicola*, the eye diameter is clearly less than the snout length (vs. longer). To sum up, all the above-mentioned characters of the four specimens AMNH I-35829 are consistent with *Lophiogobius ocellicauda* Günther, 1873, as recorded by Wu and Zhong (2008).

Despite the recognition of four specimens from the Yellow Sea as *S. fundicola*, the following characteristics slightly differ from the data given in the original description. The head depth and width were less than those of the body (vs. head deeper and broader than those of the body). Based on Fig. 2, the dorsal fin has two or three light orange stripes (vs. fins dusky) and the head and dorsum of the body are dusky with several yellow markings (vs. dusky above). This body coloration is similar to that described by Shibukawa and Aonuma (2007). Nonetheless, the sampling location of the sequence (LC069781) is Kanagawa, Miura, off the west of Jogashima Island, very close to the type locality of *S. fundicola* given a 0.5% sequence divergence between this sequence and four sequences from the Yellow Sea samples, the voucher specimens of the four sequences can be recognized as the species *S. fundicola*. The aforementioned variations are probably intraspecific.

A total of 15 goby specimens from Tongyeong of South Korea were recognized as *S. fundicola* by Choi and Lee (2019). Most characteristics of the specimens are consistent with our examination of the specimens from the Yellow Sea. This study disagrees with Choi and Lee's (2019) report in two characters: head width and body depth at the anal-fin origin (Table 1). These variations can be caused by many factors, such as size-related, specimen condition, measuring method, and so on, which needs further examination. It is worth mentioning that our samples from the Yellow Sea of China (51.8–63.5 mm SL) are a bit larger than Choi and Lee's (2019) specimens of this species (44.3–51.8 mm SL).

The larval specimens, collected from two stations of the East China Sea by beam trawl in June 1956 [orange full circle 8 (32°04'N, 123°03'E) and 9 (31°53'N, 123°26'E); Fig. 1], were identified as *S. fundicola* (Okiyama 2014). We have no access to these juvenile specimens, so the possibility cannot be ruled out that they were misidentified. But, considering that the sampling locations are not far from station H12, we believe that this historical record is credible.

The species is regarded as the deepest dwelling Gobiidae in Japan, at depths from 40 to 400 meters with

Figure 8. Digital photos (**a**) and X-ray images (**b**) of the lateral body in paratypes of *S. fundicola* AMNH 3549, 48.2–60.3 mm SL, collected by D.S Honshu from Island, Japan.

Figure 9. Digital photos (**a**) and X-ray images (**b**) of the lateral body in four goby specimens AMNH 35829, 91.40–104.55 mm SL, collected by Pope from Fuzhou, Fujian Province.

a sandy silt bottom (Akihito et al. 2013; Choi and Lee 2019). The species was only discovered in two stations (H12 and H27, with a depth of about 70 m) of this survey, with a relatively low temperature of about 10 °C in summer. Moreover, many studies indicate that the Yellow Sea Cold Water Mass (YSCWM) can help the low-temperature species to escape the high temperature stress in the summer, by providing an appropriate over-summering habitat (Zhu et al. 2018; Li et al. 2021). However, up until now, there is no study indicating that *S. fundicola* is a true low-temperature species. Considering the water depth and temperature of its habitat, it is inferred that it must have some biological adaption to help it to live in this habitat. This goby species can possibly be used as an ideal experimental model for the study of adaptive evolution in a population of deep water gobies.

Suruga fundicola was assigned to the *Acanthogobius*-group based on morphological evidence (Birdsong et al. 1988; Shibukawa and Iwata 2013). But there was no molecular phylogenetic study which included a sequence of *S. fundicola*. This study also represents the first effort to address the issue about the relationship of *Suruga* within the *Acanthogobius*-lineage. The phylogenetic trees, based on concatenated *COI* and *12S* genes, indicate that *S. fundicola* has a close relationship with *A. hexanema*, and *C. stigmatias*. Based on genetic distances of the concatenated genes in our admittedly limited sampling, *S. fundicola* has the smallest genetic distances with *C. stigmatias* (19.2%). In the present study, 6 species from the *Acanthogobius*-group were clustered into two different lineages, opposite of the result of Shibukawa and Iwata (2013a). Maybe the nucleotide sequences used by us are too short and somewhat uninformative to provide a sufficient phylogenetic signal. Therefore, it is necessary to conduct more phylogenetic studies with the help of data sets based on combined nuclear and mitochondrial genes from more species to provide a more realistic insight into the phylogeny of the *Acanthogobius*-lineage (Gobiidae).

Comparative material

Suruga fundicola: AMNH I-3549, paratypes, 2 specimens, 48.2–60.3 mm SL; 1900; Suruga bay, Honshu Island, Japan (photograph examined).

Lophiogobius ocellicauda: AMNH I-35829, 4 specimens, 91.40–104.5 mm SL; Mar 1926; Foochow (=Fuzhou), Fukien (=Fujian Province), China (photograph examined).

Amblychaeturichthys hexanema: YSFRI27207–27210, 4 specimens, 60.9–85.5 mm SL; Sept 2022; Qiangdao, Shandong Province, China.

Chaeturichthys stigmatias: YSFRI 34428–34429; 12 specimens; 68.9–95.5 mm SL; Dandong, Liaoning Province, China. YSFRI 34407–34408; 2 specimens; 68.9–70.8 mm SL; Dandong, Liaoning Province, China.

Acanthogobius hasta: YSFRI 34422–34431; 10 specimens; 67.5–98.5 mm SL; Dandong, Liaoning Province, China.

Acknowledgments

Our sincere thanks should be given to Mingwei Zhang (Ocean University of China, Qingdao, China), who shared the specimens with us, and the whole staff of the Lanhai 101 for their help. Especially grateful to Prof. E Zhang of Institute of Hydrobiology, Chinese Academy of Sciences, Wuhan, China (IHB), who provided constructive suggestions for this manuscript, and Dongming Guo for taking X-radiographs and Micro-CT images. Thanks to Xiao-dong Bian (Yellow Sea Fisheries Research Institute, Chinese Academy of Fishery Sciences), for providing valuable advice and valuable materials. Thanks should be given to Junsheng Zhong, who provided kindhearted guidance for the observation of sensory canals and papillae. We thank Radford Arrindell (AMNH) for friendly help in providing photographs and X-radiographs. Special thanks go to Xiao Chen (Anhui Agricultural University), who provided friendly help with this manuscript. This research was funded by the National Key R&D Program (2018YFD0900803), National Marine Aquatic Germplasm Bank Project, Central Public-interest Scientific Institution Basal Research Fund, YSFRI, CAFS (NO.20603022022024). Data and samples were collected onboard of R/V "Lanhai 101" implementing the open research cruise NORC2022-01 supported by NSFC Shiptime Sharing Project (project number: 42149901).

Shufang Liu and Zhimeng Zhuang contributed to the design of the study. Shufang Liu supervised, reviewed, and edited the manuscript. Hongyue Sun, Changting An, and Kaiying Liu participated in the collection of specimens. Ang Li, Huang Wang and Busu Li provided constructive suggestions for this manuscript. Changting An analyzed the data and drafted the manuscript. Richard van der Laan provided many scientific suggestions and improved the English writing. All authors contributed to the writing of the paper.

All procedures described in this paper were in accordance with Chinese laws and were licensed by the Ministry of Ecology and Environment of the People's Republic of China.

Reference

Agorreta A, San Mauro D, Schliewen U, Van Tassell J L, Kovačić M, Zardoya R, Rüber L (2013) Molecular phylogenetics of Gobioidei and phylogenetic placement of European gobies. Molecular phylogenetics and evolution 69(3): 619–633. https://doi.org/10.1016/j.ympev.2013.07.017

Akihito PM, Hayashi T, Yoshino K, Shimada H, Senou, Yamamoto T (1984) Suborder Gobioidei. The Fishes of the Japanese Archipelago. Tokai University Press, Tokyo, 236–289. [English text]

Akihito SK, Ikeda Y, Aizawa M (2013) Suborder Gobioidei. Fishes of Japan with pictorial keys (3rd ed.). Tokai University Press, Tokyo, 1347–1608.

Birdsong RS, Murdy EO, Pezold FL (1988) A study of the vertebral column and median fin osteology in gobioid fishes with comments on gobioid relationships. Bulletin of Marine Science 42(2): 174–214.

Choi Y, Lee HH (2019) First record of the Goby, *Suruga fundicola* (Perciformes: Gobiidae) from Tongyeong, Korea. Korean Journal of Ichthyology 31(4): 255–258. https://doi.org/10.35399/ISK.31.4.10

Edgar RC (2004) MUSCLE: multiple sequence alignment with high accuracy and high throughput. Nucleic acids research 32(5): 1792–1797. https://doi.org/10.1093/nar/gkh340

Fricke R, Eschmeyer WN, Van der Laan R [Eds] (2023) Catalog of fishes: genera, species, references. California Academy of Sciences, San Francisco. http://researcharchive.calacademy.org/research/ichthyology/catalog/fishcatmain.asp

Fujiwara K, Shibukawa K (2022) Description of a new species of *Obliquogobius* (Gobiidae: Gobiinae) from the East China Sea off the Ryukyu Islands, southern Japan. Ichthyological Research. https://doi.org/10.1007/s10228-022-00901-1

Iwata A, Kobayashi T, Ikeo K, Imanishi T, Ono H, Umehara Y, Hamamatsu C, Sugiyama K, Ikeda Y, Sakamoto K (2000) Evolutionary aspects of gobioid fishes based upon a phylogenetic analysis of mitochondrial cytochrome *b* genes. Gene 259(1–2): 5–15. https://doi.org/10.1016/S0378-1119(00)00488-1

Iwatsuki Y, Nagino H, Tanaka F, Wada H, Tanahara K, Wada M, Tanaka H, Hidaka K, Kimura S (2017) Annotated checklist of marine and freshwater fishes in the Hyuga Nada area, southwestern Japan. Bulletin of the Graduate School of Bioresources. Mie University 43: 27–55.

Jordan DS, Snyder JO (1901) A review of the gobioid fishes of Japan, with descriptions of twenty-one new species. Proceedings of the United States National Museum 24(1244): 33–132. https://doi.org/10.5479/si.00963801.24-1244.33

Kimura M (1980) A simple method for estimating evolutionary rates of base substitutions through comparative studies of nucleotide sequences. Journal of Molecular Evolution 16: 111–120. https://doi.org/10.1007/BF01731581

Kumar S, Stecher G, Li M, Knyaz C, Tamura K (2018) MEGA X: Molecular evolutionary genetics analysis across computing platforms. Molecular Biology and Evolution 35(6): 1547–1549. https://doi.org/10.1093/molbev/msy096

Kuroda N (1957) Additions and corrections to the list of fishes of Suruga Bay. XVI. Zoological Magazine 66(12): 22–23.

Li J, Jiang F, Wu R, Zhang C, Tian Y, Sun P, Yu H, Liu Y, Ye Z, Ma S, Liu S, Dong X (2021) Tidally induced temporal variations in growth of young-of-the-year pacific cod in the Yellow Sea. Journal of Geophysical Research: Oceans 126(6): e2020JC016696. https://doi.org/10.1029/2020JC016696

Liu J, Chen Y, Ma L (2015) Fishes of the Bohai Sea and Yellow Sea. Science Press, Beijing, 376 pp. [in Chinese]

Miya M, Sato Y, Fukunaga T, Sado T, Poulsen J, Sato K, Minamoto T, Yamamoto S, Yamanaka H, Araki H, Kondoh M, Iwasaki W (2015) MiFish, a set of universal PCR primers for metabarcoding environmental DNA from fishes: Detection of more than 230 subtropical marine species. Royal Society Open Science 2(7): e150088. https://doi.org/10.1098/rsos.150088

Okiyama M (2014) An Atlas of Early Stage Fishes in Japan. Tokai University Press, 1294–2495. [in Japanese]

Parenti P (2021) A checklist of the gobioid fishes of the world (Percomorpha: Gobiiformes). Iranian Journal of Ichthyology 8: 1–480.

Sanzo L (1911) Distribuzione delle papille cutanee (organi ciatiformi) e suo valore sistematico nei Gobi. Mittheilungen aus der Zoologischen Station zu Neapal 20: 249–328.

Shibukawa K (1997) Systematic revision of the East Asian gobiid genus *Acanthogobius* and its relatives. PhD Thesis Tokyo University of Fisheries.

Shibukawa K, Aonuma Y (2007) Three new species of the deep-dwelling goby genus *Obliquogobius* (Perciformes: Gobiidae: Gobiinae) from Japan, with comments on the limits of the genus. Bulletin of the National Museum of Nature and Science, Series A, 137–152.

Shibukawa K, Aizawa M (2013) *Cabillus pexus*, a new marine goby (Teleostei, Gobiidae) from amami-oshima island, ryukyu islands, japan. Zoology. Bulletin of the National Museum of Nature and Science, Series A 39(3): 133–142.

Shibukawa K, Iwata A (2013) Review of the east Asian gobiid genus *Chaeturichthys* (Teleostei: Perciformes: Gobioidei), with description of a new species. Bulletin of the National Museum of Nature and Science, Series A (Suppl 7): 31–55.

Shinohara G, Endo H, Matsuura K, Machida Y, Honda H (2001) Annotated Checklist of the Deepwater Fishes from Tosa Bay, Japan. National Science Museum Monographs 20: 283–343.

Shinohara G, Sato T, Aonuma Y, Horikawa H, Matsuura K, Nakabo T, Sato K (2005) Annotated checklist of deep-sea fishes from the waters around the Ryukyu Islands, Japan. National Science Museum Monographs (29): 385–452.

Sonoyama T, Ogimoto K, Hori S, Uchida Y, Kawano M (2020) An Annotated checklist of marine fishes of the Sea of Japan off Yamaguchi Prefecture, Japan, with 74 new records. Bulletin of the Kagoshima University Museum 11: 1–152.

Sudhir K, Glen S, Michael L, Christina K, Koichiro T (2018) MEGA X: Molecular Evolutionary Genetics Analysis across computing platforms. Molecular Biology and Evolution 35(6): 1547–1549. https://doi.org/10.1093/molbev/msy096

Thacker CE, Roje DM (2011) Phylogeny of Gobiidae and identification of gobiid lineages. Systematics and Biodiversity 9(4): 329–347. https://doi.org/10.1080/14772000.2011.629011

Thacker CE (2013) Phylogenetic placement of the European sand gobies in Gobionellidae and characterization of gobionellid lineages (Gobiiformes: Gobioidei). Zootaxa 3619(3): 369–382. https://doi.org/10.11646/zootaxa.3619.3.6

Vaidya G, Lohman DJ, Meier R (2011) SequenceMatrix: Concatenation software for the fast assembly of multi-gene datasets with character set and codon information. Cladistics-the International Journal of the Willi Hennig Society 27(2): 171–180. https://doi.org/10.1111/j.1096-0031.2010.00329.x

Ward RD, Zemlak TS, Innes BH, Last PR, Hebert PD (2005) DNA barcoding Australia's fish species. Philosophical Transactions of the Royal Society of London, Series B, Biological Sciences 360(1462): 1847–1857. https://doi.org/10.1098/rstb.2005.1716

Wu HL, Zhong JS (2008) Gobioidei, Perciformes V, Osteichthyes, Fauna Sinica. Science Press Beijing, 922 pp. [in Chinese]

Wu HL, Zhong JS (2021) Gobioidei, Key to Marine and Estuarial Fishes of China. China Agriculture Press, Beijing, 1034–1132. [in Chinese]

Yamamuta O, Inada T, Shimazaki K (1993) Demersal fish assemblages and macro habitat niche overlaps among gadiform dominant species off Sendai Bay, north Japan. Scientific Reports of the Hokkaido Fisheries Experimental Station 42: 241–250.

Zhu J, Shi J, Guo X, Gao H, Yao X (2018) Air-sea heat flux control on the Yellow Sea Cold Water Mass intensity and implications for its prediction. Continental Shelf Research 152: 14–26. https://doi.org/10.1016/j.csr.2017.10.006

Zoosyst. Evol. 99 (2) 2023, 503–517 | DOI 10.3897/zse.99.110878

PENSOFT

für Natur MUSEUM FÜR NATURKUNDE BERLIN

Mammalian type material from Cameroon in the Museum für Naturkunde Berlin

Paul Taku Bisong[1], Jason Dunlop[1], Catarina Madruga[2]

1 *Museum für Naturkunde, Leibniz Institute for Evolution and Biodiversity Science, Invalidenstraße 43, 10115 Berlin, Germany*

2 *German Foundation for Lost Art (DZK), and Centre for Humanities of Nature, Museum für Naturkunde, Leibniz Institute for Evolution and Biodiversity Science, Invalidenstraße 43, 10115 Berlin, Germany*

https://zoobank.org/F6C6E092-BD56-49C2-A0D4-6F552B36C4B9

Corresponding author: Paul Taku Bisong (pbisong@hotmail.com)

Academic editor: M. TR Hawkins ♦ **Received** 9 August 2023 ♦ **Accepted** 22 September 2023 ♦ **Published** 19 October 2023

Abstract

Historical data, combined with current data on species distribution, are a valuable resource for tracking changes in biodiversity and can potentially be applied to developing models in conservation biology and designing and assessing conservation strategies. Historical data supporting current knowledge on the natural history of the African continent are primarily held in Western museums. The Zoologisches Museum Berlin (ZMB), which is today part of the Museum für Naturkunde Berlin (MfN), is the primary source of reference for zoological collections from former German colonial territories including Cameroon. Here, we document for the first time a catalogue of the type material in the mammal collection of the MfN from the point of view of a geographical region. The type collection includes 91 type specimens identified in the catalogues as originating from German 'Kamerun' and which correspond to 31 described species, of which 12 are currently accepted (valid) species names. Of the 31 described species, 21 are represented by holotypes, three para-holotype series, one para-lectotype series and six syntype series. We hope that this first analysis of zoological objects, based on geographical location, will lead to similar research on other geographical locations of collection. This could provide more information on the provenance of collections and on colonial collecting practices, as well as contribute to the accessibility of collections in Western museums.

Key Words

Africa, colonial collecting, historical collections, Mammalia, type material, specimen, Zoologisches Museum Berlin

Introduction

Zoological collections have been described as the main archive of animal biodiversity on Earth (Bogutskaya et al. 2022) and constitute a long-standing physical record of past species occurrences (Boakes et al. 2010; Johnson et al. 2011; Holmes et al. 2016). They represent a much more extensive record than ecological long-term surveys which only became established in the 1980s. Researchers have emphasised the role of natural history collections as a resource for detecting long-term changes in geographic range, phenology, abundance and species' evolution (Boakes et al. 2010). Furthermore, it is predicted that zoological collections could enable a better understanding of current condition of biomes and contribute to the development of better strategies for the management of biological resources (Ade et al 2001; Suarez and Tsutsui 2004). Type specimens are the original and unique representatives of a taxon and are the most important part of a zoological collection (Bogutskaya et al. 2022). Their descriptions have been published and would ideally contain information on the collector of the specimen, the locality of collection, the date of collection, the author of the description and the characteristics attributed to the specimen by the author. Hence, they represent physical vouchers that retain the diagnostic characters underlying the description of a new taxon. In addition to being the reference for a sci-

entific name, they also serve as a scientific memory for later research (Acharya and Subedi 2005).

Historical data supporting current knowledge of the natural history of the African continent are primarily held in Western museums and similar collections (Ashby and Machin 2021). Between 1891 and 1920, Berlin held a mandate as a clearing house for all zoological, paleontological, botanical and ethnographic collections obtained on German official expeditions in colonial territories (Kaiser 2021). The Museum für Naturkunde Berlin (MfN), part of which was formerly known as the Zoologisches Museum Berlin and whose zoological collections are abbreviated as 'ZMB', is thus the primary source of reference for all colonial zoological collections in Germany from former German colonial territories including German 'Kamerun'.

Cameroon continues to seek ways to improve conservation policies and the sustainable use of biological resources. Historical data, combined with current data on species distributions, are a valuable resource for tracking changes in biodiversity and can potentially be applied to developing models in conservation biology, designing and assessing conservation initiatives and tracking progress in conserving overall biodiversity (Boakes et al. 2010). Hence, information on collections and research on species' distribution and biodiversity loss in Cameroon could contribute to the establishment of better conservation policies, especially when applied to specific localities. In 2015, Cameroon's Ministry of Agriculture and Rural Development (MINADER) requested that research organisations on Cameroon's biome make their research findings available to policy-makers in the country for consideration of legislative procedures on its biodiversity (MINADER 2015). Therefore, there is a strong incentive to make the Berlin Museum's data on Cameroon collections available to both the country's government and to Cameroonian researchers or other interested parties who cannot access the Museum directly. This paper, therefore, offers an initial study exploring the potential of data repatriation to Cameroon.

Here, we focus on documenting type material in the MfN's mammal collection which are considered in the catalogues as originating from German 'Kamerun', which includes the contemporary territory of Cameroon and parts of today's Central African Republic and Nigeria. By accessing a range of source materials on specimens, including their original tags, skull inscriptions, scientific publications, historical catalogues and archival shipment lists, we present for the first time a complete inventory of the type specimens from 'Kamerun' in the mammal collection, including the implicated suppliers, collection dates and type localities (incompletely documented). Unfortunately, the available information in the catalogues and historical sources consulted do not allow for more precise details on habitat, elevation and actual geographical coordinates, which would have been desirable. However, the results of this study may be valuable to several stakeholders, including conservation biologists, taxonomists, ecologists and historians, as well as the Cameroonian Government and collection managers. The data presented here may be improved and expanded in the future, to include more detailed information and, therefore, contribute to extrapolating species distributions from the particular historical time period, in the specific localities in West Africa. This study also aims to provide a starting point for the discussion of digital and physical access to the collections, as well as considerations on data repatriation from German museums to former colonial regions where they could be of more relevance. This was the first step of a collaborative project on the identification of shipments of natural history specimens from the territories of 'Kamerun' during the period of German occupation.

Methods

Ninety-one specimens with potential type status from 'Kamerun' registered in the digital database ("Specify") of the mammal collections of the Museum für Naturkunde Berlin were assessed, including those whose type status required clarification. The specimens included dry preparations of skins, skulls and skeletal parts, as well as wet collections in 70% ethanol. Specimen reference numbers are in the format ZMB_Mam_XXXXX, where "ZMB" is the universally accepted abbreviation for the Zoologisches Museum Berlin and "Mam" is the shorthand for the mammal collection. The number refers to the five-digit general catalogue number of the specimen. For each specimen, we also assessed, when available, the shipment number and shipment entry in the accession catalogue (the "A-catalogue" number). Where necessary, we employed Article 73.2.3 of the International Code of Zoological Nomenclature (ICZN, 4th Edition 1999), which places the collection locality of the holotype or lectotype as the collection locality of the species or sub-species over those of the paratypes or paralectotypes. In other words, for a type series with specimens from different collection localities, the collection locality of the designated holotype or lectotype becomes the *locus typicus* of the species. We also included the conservation status of each species drawing on the Red List of threatened species from the International Union for Conservation of Nature (IUCN). The annotated list of type specimens collected from Cameroon in the Mammal Department of the Museum (see Results) is arranged in alphabetical order. Nomenclature follows the Integrated Taxonomic Information System (ITIS) with respect to valid names and synonyms. Photographs of the relevant type material are being made as part of the wider digitisation projects at the MfN and will subsequently be available online through the museum portal. These will also contribute to further planned detailed studies (Taku Bisong, in prep.) addressing specific aspects of the Cameroon holdings in this collection.

Results

The type collection in Berlin includes 31 described and named species, of which 12 are currently accepted (valid and available) species names described in the databank as "from Cameroon." Of the 31 described species, 21 are represented by holotypes, three para-holotype series, one para-lectotype series and six syntype series. Most of the type species (21) were described by Paul Matschie (1861–1926), curator of the Mammal Department in Berlin in the period from 1895–1926, i.e. during the main phase of colonial activity and collection expansion. The type specimens were collected by at least 21 collectors from one or more of 26 collecting localities in Cameroon. Approximately a quarter of the specimens were supplied by a single individual, Georg Zenker (1855–1922), who shipped collections from Bipindi and the military station in Yaoundé in the period 1889–1922. If any of the relevant information for a specimen is unavailable, the field for the information is not included.

Order Artiodactyla Owen, 1848
Family Bovidae Gray, 1821

***Adenota pousarguesi* Neumann, 1905**

MfN specimen. Skull. ZMB_Mam_86187.

Author of name and type description. Oscar Rudolph Neumann (1905).

Present name. *Kobus kob* (Erxleben, 1777).

Dedication of name (patronym). Eugène de Pousarges (1859–1901).

Specimen information in general catalogue. • "♂*, *Adenota pousarguesi*, Sch, A1[a].03, Semikore, Sanaga-Fluss, W-Kamerun, Sheunemann 8.X.1902, O. Neumann" Vol. 9, p. 256.

Shipment information (A-catalogue number). Listed in specify as A 19.03. but A-catalogue Information does not match this specimen. Most probably refers to shipment in A-catalogue under reference A 11.03: "Sammlung, Yaunde, Kamerun, Ober Lt. Scheunemann".

Collecting information in description • "Typus von *Adenota pousarguesi*. Schädel eines alten Bockes von Lt. Scheunemann am oberen Sanaga in Süd-Kamerun (Berl. Mus.) erlegt [Type for *Adenota pousarguesi*. Skull of an old male, shot by Lieutenant Scheunemann in the Upper Sanaga [river] in South Cameroon]" (Neumann 1905: 92).

Specifics of specimen in the description. Male specimen

Information on the specimen. Specimen not available for consultation as of 16.09.2022.

Collecting locality. • "Semikore, Sanaga-Fluss, W-Kamerun [At the time of German presence in 'Kamerun', 'Semikore' was the Chief of the Yesum people, a clan of the Ewondo (Yaounde) tribe close to the Sanaga River (Wirz 1972)]".

Collected by. Peter Scheunemann (1870–1937).

Type status based on description. Holotype (single specimen).

IUCN conservation status. Least Concern.

Remarks. Corresponding shipment is mentioned in MfN archive folder MfN, HBSB, ZM S III Scheunemann Hauptmann. According to Neumann, a female of this species, shipped from Cameroon, lived in the Berlin Zoological Garden for several years. Information on the collecting date was missing from all sources assessed.

Order Carnivora Bowdich, 1821
Family Canidae Fischer de Waldheim, 1817

***Canis (Cynalopex) pallidus oertzeni* Matschie, 1910**

MfN specimens. Round skins. ZMB_Mam_39927; ZMB_Mam_39929; ZMB_Mam_39930; ZMB_Mam_39931. Skulls. ZMB_Mam_65796; ZMB_Mam_65797.

Author of name and type description. Paul Matschie (1910).

Present name. *Vulpes pallida oertzeni* Matschie, 1910.

Dedication of name (patronym). Jasper Martin Otto von Oertzen (1880–1948).

Specimen information in the general catalogue. All round skins • "B, Dikoa, Hinterland von Kamerun, 26.III.10, Umlauff, A 165/10" Vol. 4, p. 411. All skulls • "Schädel, Dikoa, Hinterland von Kamerun, 26.III.1910 Umlauff, IX.09 Oertzen, A165/10" Vol. 7, p. 239.

Shipment information (A-catalogue number). A 165.10 • "[9 items], Dikoa, Hinterland von Kamerun, 26.III.10, von Oertzen und Umlauff [Dikoa, Cameroon hinterland, 26.III.10, from Oertzen and Umlauff]".

Collecting information in description. • "1 ♂, 3 ♀ Felle, von denen 1 ♂ und 1 ♀ mit Schädeln versehen sind. Dikoa, Nordost-Kamerun. September 1909. Von Herrn Oberleutnant von Oertzen gesammelt und dem Berliner Zoologischen Museum geschenkt [1 ♂, 3 ♀ skins, from which 1 ♂ and 1 ♀ came with skulls. Dikoa, Northeast Cameroon. September 1909. Collected by Mr. Oberleutnant von Oertzen and offered by the Berlin Zoological Garden]" (Matschie 1910: 370).

Specifics of specimen in the description. Single male specimen (skin and skull) preserved with indication "A. 165,10,1" and designated as the holotype.

Information on specimen. All specimens available

Collecting locality • "Dikoa [which was part of northern German 'Kamerun', today part of northern Nigeria with current English transcription as 'Dikwa']".

Collected by. Jasper Martin Otto von Oertzen (1880–1948), via the trading company Umlauff, based in Hamburg.

Collecting date. September 1909

Type status based on description. Para-holotype. Based on the sequence of this assessment, the male skull (Holotype) is probably ZMB_Mam_65796 as skull parameters measured were approximate with that in the description. Skull ZMB_Mam_65797 is a paratype. Male skin (Holotype) could not be identified as the skin parameters measured did not correspond to those in the description.

IUCN conservation status. Least Concern.

Remarks. Skin measurement differences are probably a consequence of fixing or long-term preservation. Collecting locality was part of "German Kamerun" and was registered in the databank as Cameroon, but is part of today's northern Nigeria.

Family Hyaenidae Gray, 1821

***Hyaena (Crocotta) noltei* Matschie, 1900**

MfN specimen. Skull. ZMB_Mam_82552.

Author of name and type description. Paul Matschie (1900b).

Present name. *Crocuta crocuta* Erxleben, 1777.

Dedication of name (patronym). Hermann Nolte (1869–1902).

Specimen information in general catalogue. • "**Hyaena (Crocotta) noltei* Schädel Yoko, oberer Sanaga, S-Kamerun/WA Nolte Sept.1899" Vol. 9, p. 109.

Shipment information (A-catalogue number). A 17.00 • "[1 item], Schädel von Hyaena, Yoko Kamerun, 28.VII.00, Nolte".

Collecting information in description. • "Herr Oberleutnant in der Kaiserlichen Schutztruppe für Kamerun, Nolte, hat im September 1899 auf der Station Yoko im Gebiete des oberen Sanaga, Süd Kamerun, eine gefleckte Hyaene erlegt, deren Schädel er dem Berliner Museum für Naturkunde freundlichst überlassen hat [Mr Nolte, Oberleutnant for the Imperial Schutztruppen [Protection Forces] in Cameroon, hunted a spotted Hyena in September 1899 in the Yoko Station in the district of the Upper Sanaga, South Cameroon, and kindly donated its skull to the Berlin Museum für Naturkunde]" (Matschie 1900b: 211).

Specifics of specimen in the description. The tail tassel of the specimen is incomplete therefore its full length could not be determined for comparison.

Information on the specimen. Specimen available.

Collecting locality. Yoko, by the Sanaga River, Cameroon.

Collected by. Hermann Nolte (1869–1902).

Collecting date. September 1899.

Type status based on description. Holotype (single specimen).

IUCN conservation status. Least Concern.

Remarks. A skin was also described by Matschie. He included an image of it in the description but did not mention whether the skin remained a property of the museum; the skin could not be traced at the time of publication.

Family Mustelidae G. Fischer, 1817

***Aonyx capensis microdon* Pohle, 1920**

MfN specimens. Skin. ZMB_Mam_30703. Skull. ZMB_Mam_30704.

Author of name and type description. Hermann Pohle (1919).

Present name. *Aonyx capensis* Schinz, 1821.

Specimen information in general catalogue. Skin • "*Aonyx microdon* Pohle* Fell, A.110.14, Nana Fluß bei Bomse Dr. Elbert 10.II.14, 388" Vol. 4, p. 31. Skull • "*Aonyx microdon* Pohle*, Schädel, A.110.14, Nana Fluß bei Bomse, Dr. Elbert, 10.II.14, 388" Vol. 4, p. 31.

Shipment information (A-catalogue number). A 110.14 • "[67 items], Kamerun Exped. des Reichs-Kolonialamt, 1.VII.14, Dr. Elbert [Cameroon Expedition of the Imperial Colonial Office, 1.VII.14, Dr. Elbert]".

Collecting information in description. • "Nana-Fluß, bei Dorf Bomse, Kamerun [River Nana, near the village Bomse, Cameroon]" (Pohle 1919: 145).

Information on specimen. All specimens available

Collecting Locality. Nana River, near Samba village in today's Central African Republic.

Collected by. Johannes Elbert (1878–1915).

Type status based on description. Holotype (Single specimen).

IUCN conservation status. Near Threatened.

Remarks. Mandible detached from the skull. A shipment label included with the skin. Collecting locality registered in the catalogue as "Cameroon", but is part of today's Central African Republic.

Order Chiroptera Blumenbach, 1779
Family Pteropodidae Gray, 1821

***Scotonycteris ophiodon* Pohle, 1943**

MfN specimens. Skull; Skin in Alcohol. ZMB_Mam_50001.

Author of name and type description. Hermann Pohle (1943).

Present name. *Casinycteris ophiodon* (Pohle, 1943).

Specimen information in general catalogue. • "♀ ad., *Scotonycteris ophiodon* Pohle *, 105/1/14/22., Alk? Sch(v), A. 00, Bipindi, Bez. Kribi, Kamerun, 05.1899, G. Zenker S.V, 327" Vol. 6, p. 1.

Collecting information in description. • "Typus. Nr. 50051 des Berl. Mus.; ♀ juv.-ad. von Bipindi, Bez. Kribi, Kamerun, Mai 1899, Georg A. Zenker S. V. Die Zähne (auch die Eckzähne) sind voll in Stellung, die Basalnaht ist noch offen. Das Tier liegt in Alkohol; der leider auf der rechten Seite unter Verlust der Hirnkapselwand verletzte Schädel ist gereinigt [Type. N. 50051 of the Berlin Museum; ♀ juv.-ad. from Bipindi, district of Kribi, Cameroon, May 1899, Georg A. Zenker, Supplier. The teeth (including canines) are all in place, the base suture is still open. The animal is in alcohol; the skull, unfortunately injured on the right side with loss of the brain capsule wall, is cleaned] (Pohle 1943:78).

Specifics of specimen in the description. This specimen is stated to have been in alcohol for 44 years prior to the description, so the original colour of the specimen could not be determined at the time of description.

Information on specimen. All specimens available.

Collecting locality. Bipindi, Cameroon.

Collected by. George A. Zenker (1855–1922).

Collecting date. May, 1899.

Type status based on description. Holotype (single specimen).

IUCN Conservation status. Near Threatened.

Remarks. In the description, Pohle pays tribute to Zenker who died 12.2.1922 at Bipindihof. He acknowledges other contributions to the museum's type specimens including *Scotonycteris zenkeri* Mtsch., *Idiurus zenkeri* Mtsch., *Zenkerella insignis* Mtsch., and *Cercocebus albigena zenkeri* (page 87). The description cites this specimen as having collection number Nr. 50051 instead of 50001. Information on A-catalogue missing from sources accessed.

Scotonycteris zenkeri Matschie, 1894

MfN specimens. Skull; Skin in Alcohol. ZMB_Mam_66533.

Author of name and type description. Paul Matschie (1894).

Present name. *Scotonycteris zenkeri* Matschie, 1894

Specimen information in general catalogue. • "*Scotonycteris zenkeri**, ♀ ad, Sch Alk, Yaunde, Süd-Kamerun, Zenker, Lectotype" Vol. 7, p. 268.

Collecting information in description • "♀ ad. Yaunde Station. Zenker coli" (Matschie 1894:202).

Specifics of specimen in the description. • "Das einzige Exemplar, welches mir vorliegt, ist ein Weibchen mit starken Brustwarzen. Der Schädel ist dem von *Epomophorus* ähnlich [The only specimen I have is a female with 'developed' nipples. The skull is similar to that of *Epomophorus*]" (Matschie 1894:203).

Information on the specimen. All specimens available

Collecting locality. Yaounde, Cameroon.

Collected by. George August Zenker (1855–1922).

Type status based on description. Holotype (single specimen) [although labelled as a Lectotype].

IUCN conservation status. Near threatened.

Remarks. Information on the A-catalogue and collection date missing from all sources accessed.

Order Hyracoidea Huxley, 1869
Family Procaviidae Thomas, 1892

Procavia (Dendrohyrax) adametzi Brauer, 1912

MfN specimen. Skull, Round skin. ZMB_Mam_21062.

Author of name and type description. August Brauer (1912).

Present name. *Dendrohyrax dorsalis nigricans* Peters, 1879.

Dedication of name (patronym). Karl Wilhelm Adametz (1877–?).

Specimen information in general catalogue. • "*Male, *Dendrohyrax adametzi*. A.Br. Fell, A 4614, Barombi Station, Zeuner" Vol. 3, p. 47.

Shipment information (A-catalogue number). A 46.14 • "**Hyrax Dorsalis* tras., Kamerun, 2.10.88, 21062".

Collecting information in description. • "Diese Art, die das Zoologische Museum vom Barombi-See bei Johann-Albrechts-Höhe in Kamerun erhalten hat und die ich zu Ehren des um die Kenntnis der Fauna West-Kameruns sehr verdienten Herrn Oberleutnant Adametz benenne [This species, which the Zoological Museum received from Lake Barombi near Johann-Albrechts-Höhe in Cameroon and which I name in honour of Lieutenant Adametz, who was very deserving of the knowledge of the fauna of West Cameroon]" (Brauer 1912:412–413).

Specifics of specimen in the description. Largest skull length (gnathion condylion) 11.85, greatest among the *Procaviidae.*

Information on specimen. All specimens available.

Collecting locality. Barombi, Cameroon.

Collected by. Karl Ludwig Zeuner (1852–1890).

Type status based on description. Holotype (Single specimen).

IUCN conservation status. Least concern.

Remarks. According to the description, there should be three specimens (2 skulls, 1 round skin). In the general catalogue, only 1 skull and 1 round skin from Barombi were mentioned. The whereabouts of the other skull is unknown.

Procavia (Dendrohyrax) adametzi zenkeri Brauer, 1914

MfN specimens. Skull; Skeleton; Skin. ZMB_Mam_21052; ZMB_Mam_21050; ZMB_Mam_21065; ZMB_Mam_21069. Skull. ZMB_Mam_21077.

Author of name and type description. August Brauer (1914).

Present name. *Dendrohyrax dorsalis nigricans* Peters, 1879.

Dedication of name (patronym). August Zenker (1855–1922).

Collecting information in description. Thirteen specimens mentioned in the description (6 skins and 7 skulls used) were collected from Bipindi, Edea, Namajong, Yaounde, Lolodorf, Alen -locality in E. Guinea and one skin of unknown locality. Collectors are Krücke, Conrad, Zenker and donations from 'Großh. Museum' in Karlsruhe - a Yaoundé skin specimen and from the 'Naturalienkabinett' in Stuttgart - the skin specimen of an unknown locality (Brauer 1914:38).

Specifics of specimen in the description. The dorsal patch is generally less conspicuous than in *D. adametzi.*

Information on specimen. All specimens available.

Type status based on description. Syntypes.

IUCN conservation status. Least Concern.

More specific collection and catalogue information for each specimen are summarised on Table 1.

Table 1. Specifics of individual *Pr. (Dendrohyrax) adametzi zenkeri* specimens.

MfN specimen (preparations)	Specimen information in General Catalogue	Shipment information (A-number)	Collecting locality	Collected by	Remarks
ZMB_Mam_21052 ZMB_Mam_21050 (Skull, Skeleton, Skin)	"*Dendrohyrax*, Fell, Shadel, A 54.13, Lolodorf, Kamerun, Conrad" Vol. 3, p. 47	(A 54.13) "[3 items] Lolodorf S. Kamerun, 22.V.13, Erich Conrad S"	Lolodorf, Cameroon	Leopold Conradt	Skin specimen for ZMB_Mam_21050 not available as of 08.09.2022.
ZMB_Mam_21065 (Skull, Skeleton, Skin)	"*Dendrohyrax adametzi zenkeri*. A.Br. Fell, Shadel, Skelett, A 384.11, 19km geradesüdl v. Edea, Kamerun, Wegemst. Behrens, Bez. Amtm. Krücke" Vol. 3, p. 48	(A 384.11) "[3 items] Edea, Kamerun, 30.03.1912, Bez. Amtm. Krücke."	Edea, Cameroon	Behrens	First skin label: *Dendrohyrax dorsalis* (Fraser, 1854). Second skin label: *Dendrohyrax d. nigricans*. However, skull label and skull inscription confirm specimen ZMB_Mam_21065 as *Dendrohyrax dorsalis nigricans*
ZMB_Mam_21069 (Skull, Skeleton, Skin)	"*Dendrohyrax*, Fell, Shadel, A 15.09, Bipindihof, Zenker" Vol. 3, p. 48	(A 15.09) "[3 items] Bipindi, 15.IV.08, Zenker"	Bipindi, Cameroon	George August Zenker	The skin specimen was not available as of 08.09.2022.
ZMB_Mam_21077 (Skull)	"*Dendrohyrax adametzi zenkeri*. A.Br. Shadel, A 63.12, Namanjong b/.Lolodorf, Conradt" Vol. 3, p. 48	(A 63.12) "[1 items] Namanjong b/ Lolodorf, 07.VI.12, Conradt S., Ulbrich V"	Lolodorf, Cameroon	Leopold Conradt	'Namanjong' locality could not be traced in today's Cameroon

***Dendrohyrax tessmanni* Brauer, 1912**

MfN specimen. Skull, Skin. ZMB_Mam_21080.

Author of name and type description. August Brauer (1912).

Present name. *Dendrohyrax dorsalis nigricans* Peters, 1879.

Dedication of name (Patronym). Günther Tessmann (1884–1969).

Specimen information in general catalogue. • "*Dendrohyrax adamtzi tessmanni* A. Br *, Fell, Shadel, A 102.09, Akonangi, Tessmann" Vol. 3, p. 48.

Shipment information (A-catalogue number). A 102.09 • "[21 items], 22.IX.09, Tessmann".

Collecting information in description. • "Von Herrn G. Tessmann erhielt das Zoologische Museum das Fell und den Schädel eines neuen großen Baumschliefers, den er in Akonangi (Spanisch-Guinea) erlegt hatte [The Zoological Museum received from Mr G. Tessmann the skin and skull of a large new tree hyrax, which he hunted in Akonangi (Spanish-Guinea)]" (Brauer 1912:411).

Specifics of specimen in the description. Specimen is a male.

Information on specimen. All specimens available.

Collecting locality. Akonangi, Cameroon. The collecting locality "Akonangi" is possibly part of what was considered Cameroon by German troops (Languy et al. 2005).

Collected by. Günther Tessmann (1884–1969).

Type status based on description. Holotype (Single specimen).

IUCN conservation status. Least Concern.

Remarks. Skull label refers to A 108.09 with collection date 22.09.09, but the collecting information for this entry in the A-catalogue is not consistent with its corresponding entry in the general catalogue.

***Procavia capensis bamendae* Brauer, 1913**

MfN specimen. Skull, Skin. ZMB_Mam_21490.

Author of name and type description. August Brauer (1913).

Present name. *Procavia capensis bamendae* Brauer, 1913.

Dedication of name (patronym). Karl Wilhelm Adametz (1877–?).

Specimen information in general catalogue. • "*Procavia kerstingi bamendae*, A. Br., Fell, Schädel, A. 278,12, Bamenda, Adametz" Vol. 3, p. 65.

Shipment information (A-catalogue number). (A. 278.12) • "[28 items], Nord Kamerun, 28. XII.12, Oblt. Adametz".

Collecting information in description. • "Diese neue Art verdankt das Zoologische Museum Herrn Oberleutnant Adametz; ihr Fundort ist Bamenda, Südwestkamerun [The Zoological Museum owes this new species to Lieutenant Adametz; it was found in Bamenda, Southwest Cameroon]" (Brauer 1913:127).

Specifics of specimen in the description. Skull is an adult male.

Information on specimen. All specimens available.

Collecting locality. Bamenda, Cameroon.

Collected by. Karl Wilhelm Adametz (1877–?).

Type status based on description. Holotype (Single specimen).

IUCN Conservation status. Least Concern.

Remarks. Inscription with "A 275.12" cancelled out and slightly wiped off on the skin label and skull inscription, respectively. Shipment information on A 275.12 does not correspond with that in the general catalogue and specimen labels or inscriptions. The correct A-catalogue number should read A 278.12, as written in the general catalogue and verified (14.04.2023).

Order Primates Linnaeus, 1758
Family Cercopithecidae Gray, 1821

***Stachycolobus zenkeri* Matschie, 1917**

MfN specimens. Skins. ZMB_Mam_24217; ZMB_Mam_24219; ZMB_Mam_24221; ZMB_Mam_24645; ZMB_Mam_11472**.** Skulls. ZMB_Mam_24218; ZMB_Mam_24209.

Author of name and type description. Paul Matschie (1917).

Present name. *Colobus satanas* Waterhouse, 1838.

Information on specimen. All specimens available.

Collecting locality. Bipindi, Cameroon.

Collected by. George August Zenker (1855–1922).

Type status based on description. Para-holotype.

IUCN conservation status. Threatened.

Remarks. The description mentions other specimens included. 11472*/24209**, 24217*/24218**, 24645*, 24219*/24220**, 24440**, 24441**, 24442**, 24443**, 24221*/24222**, 4323/10.

where: * Skin specimen; ** Skull specimen; / Skin and corresponding skull.

More specific collection and catalogue information for each specimen are summarised on Table 2.

Erythrocebus langheldi Matschie, 1905

MfN specimen. Skull, Skin. ZMB_Mam_13212.

Author of name and type description. Paul Matschie (1905a).

Present name. *Erythrocebus patas* Schreber, 1775.

Dedication of name (patronym). Wilhelm Langheld (1867–1917).

Specimen information in general catalogue. • "*Erythrocebus langheldi* Mtsch*, Balg, Schädel, I.06, Garua, Benue, Langheld" Vol. 2, p. 138.

Collecting information in description. • "Im hiesigen Zoologischen Garten leben augenblicklich zwei Husarenaffen, die Herr Hauptmann Langheld bei Garua am oberen Benue in Kamerun gesammelt hat. [Two hussar monkeys [common patas monkey], collected by Captain Langheld from Garua on the upper Benue in Cameroon, currently live in the zoological garden [Berlin]" (Matschie 1905a:275).

Specifics of specimen in the description. Young female specimen.

Information on specimen. All specimens available.

Collecting locality. Garoua, Cameroon.

Collected by. Wilhelm Langheld (1867–1917).

Type status based on description. Holotype (Single specimen).

IUCN conservation status. Near Threatened.

Remarks. Matschie identified this specimen as a young female, today (according to information on "Specify") the specimen has been identified as a young male.

Papio yokoensis Matschie, 1900

MfN specimen. Round skin. dummy_4484.

Author of name and type description. Paul Matschie (1900a).

Present name. *Papio hamadryas* Linnaeus, 1758.

Collecting information in description. • "Die Sammlung des Herrn Major von Kamptz enthält folgende Arten. *Papio yokoensis* Mtsch. spec. nov. 2 ♂♂ und 1 ♀ aus Yoko am Sanaga [The collection of Major von Kamptz contains the following species. *Papio yokoensis* Mtsch. spec. nov. 2 ♂♂ and 1 ♀ from Yoko at Sanaga]" (Matschie 1900a:89).

Specifics of specimen in the description. 2 male skins, 2 male skulls and 1 female skin were used for the description.

Table 2. Specifics of Individual *Stachycolobus zenkeri* specimens.

ZMB number (preparation)	Specimen information in the general catalogue	Shipment information (A-number)	Collecting information in the description	Specifics of Specimen in the description	Collecting Date	Type status based on the description
ZMB_Mam_24217 (Skin) And ZMB_ Mam_24218 (Skull)	"♂, *Colobus satanas* Mtsch, Fell, Bipindi, Kamerun, Zenker" Vol. 3, p 175	(A 15.09) "[3 items] Bipindi, 15.IV.1908, Zenker"	ZMB_Mam_24217. "♂ ad. Nr 24217/24217. Fell mit Schädel. Ebendaher und von demselben im Dezember 1907 oder Januar 1908 während der Trockenzeit erbeutet." p. 158. No information for ZMB_ Mam_24218.	Male specimen. The skin ZMB_Mam_24217 associated with the skull ZMB_Mam_24218	22.03.1905	Paratype
ZMB_Mam_24219 (Skin)	"♂ juv. *Colobus satanas* Mtsch, Fell, Bipindi, Kamerun, Zenker" Vol. 3, p. 175	N/A (A-number missing from all sources examined)	"♂ juv. 24219/24220. Fell mit Schädel. Aus der Trockenzeit des Frühjahres 1903. Der Affe war ungefähr 2 1\2 Jahr alt." p. 159	According to the general catalogue and the description, specimen is a Juvenile male, but is identified as a female in "Specify".	Spring 1903	Paratype
ZMB_Mam_24221 (Skin)	"♂ ad, *Colobus satanas* Mtsch, Fell, Bipindi, Kamerun, Zenker" Vol. 3, p. 175	(A 38.03) "[5 items], Bipindi, Kamerun, 6.X.03, G. Zenker"	"Nur ein Fell mit Schädel Nr. 24221/24222, ♂ ad. aus Zenker's Sammlungen" p. 159	Male specimen	06.10.1903	Paratype
ZMB_Mam_24645 (Skin)	"*Colobus satanas*, Fell, A 32.03, Bipindi, Zenker" Vol. 3, p. 192	(A 32.03) "[2 items] Bipindi, 10.II.03, Zenker"	"♀ ad. Nr. 24645. Fell ohne Schädel. Ebendaher und von demselben. Im Dezember 1902 erlegt. Das Fell hat kürzeren Schulterbehang als das vorige." p. 158	Female specimen	10.02.1903	Paratype
ZMB_Mam_11472 (Skin) And ZMB_ Mam_24209 (Skull)	ZMB_Mam_24209. "♂ *Stachycolobus zenkeri* Mtsch*, Waterh., Schädel, A 62.04, Bipindi, Zenker,Fell 11472" Vol. 3, p. 174. ZMB_Mam_11472. "♂*, *Colobus satanas* Waterh. Balg, 5.1.98, Bipindi, Kamerun, Zenker. Typus von *Stachycolobus zenkeri* Mtsch., Zur Schädel 24209" Vol. 2, p. 62	(A 62.04) "[34 items] 7 skins, 10 skulls, 2 skeleton, 6 animals in alcohol, 9 embryos], Bipindi, Zenker, 26.IV.04"	"Typus: ♂ ad. Nr. 11472/24209. Fell mit Schädel. Von G. Zenker im September oder Oktober 1897 bei Bipindi am Lokundje in Kamerun während der Regenzeit erbeutet." p. 158	Male specimen. Designated Holotype	05.01.1898	Holotype

Information on specimen. Specimen available.

Collecting locality. Yoko, Cameroon.

Collected by. Oltwig von Kamptz (1857–1921).

Type status based on description. Syntypes.

IUCN conservation status. Least concern.

Remarks. 'dummy' specimen has no ZMB number and no A-catalogue number. According to "Specify", the valid name for *Papio yokoensis* is *Papio hamadryas*.

***Piliocolobus preussi* Matschie, 1900**

MfN specimen. Skin. ZMB_Mam_6588.

Author of name and type description. Paul Matschie (1900c).

Present name. *Piliocolobus preussi* Matschie, 1900.

Specimen information in general catalogue. • "*Colobus temminckii*, Kühl Fell ohne Schadel, Barombi, Kamerun, Preuss; Typus von *Piliocolobus preussi* Mtsch." Vol. 1. p. 236.

Collecting information in description. • "von Dr. Preuss bei Barombi am Elefanten-See in Nord-Kamerun [by Dr. Preuss on the Elephant Lake at Barombi in north Cameroon]" (Matschie 1900c:183).

Specifics of specimen in the description. Male specimen.

Information on specimen. Specimen available.

Collecting locality. Barombi Mbo, Cameroon.

Collected by. Paul Rudolph Preuss (1861–1926).

Type status based on description. Holotype (Single specimen).

IUCN conservation status. Critically Endangered.

Remarks. The general catalogue entry for 6588 states "*Colobus temminckii*, Kühl…Typus von *Piliocolobus preussi* Mtsch". Both species are mentioned in the same description as different species, but the reason for this name change in the general catalogue is not clear.

Order Primates Linnaeus, 1758
Family Hominidae Gray, 1825

***Gorilla diehli* Matschie, 1904**

MfN specimens. Skulls. ZMB_Mam_12789; ZMB_Mam_12790; ZMB_Mam_12792; ZMB_Mam_12793; ZMB_Mam_12794; ZMB_Mam_12795; ZMB_Mam_12796.

Skull and skeleton parts. ZMB_Mam_12791.

Author of name and type description. Paul Matschie (1904).

Present name. *Gorilla gorilla diehli* Matschie, 1904.

Dedication of name (Patronym). Adolf Diehl (1870–1943).

Collecting information in description. • "Herr Diehl sammelte in dem Gebiete des Mun-Aya oder Wadye, der in den Cross-Fluss strömt, 4 Schädel von ausgewachsenen männlichen, 5 Schädel von ausgewachsenen weiblichen Gorillas [Mr. Diehl collected in the area of the Mun-Aya or Wadye, which flows into the Cross River, 4 skulls of adult male, 5 skulls of adult female gorillas]" (Matschie 1904:52).

Information on specimen. All specimens are available.

Collected by. Adolf Diehl (1870–1943).

Type status based on description. Para-holotype.

IUCN conservation status. Critically Endangered.

General remark. A-catalogue number, collection and accession dates missing from all historical sources examined. Although the original description mentions nine specimens, only eight specimens are indicated for this species on "Specify".

More specific collection and catalogue information for each specimen are summarised on Table 3.

***Gorilla hansmeyeri* Matschie, 1914**

MfN specimens. Skull, Skeleton. ZMB_Mam_17960. Skin. ZMB_Mam_17961.

Author of name and type description. Paul Matschie (1914).

Present name. *Gorilla gorilla gorilla* Savage, 1847.

Dedication of name (patronym). No specific mention of a dedication, nevertheless, refers to the supplier Hans Meyer (1877–1964).

Specimen information in general catalogue. • "♂ *Gorilla hansmeyeri*, Mtsch. * Typ, Fell, Bunda und Dume, Kamerun, Peters. Geh, Prof. Hans Meyers. S." Vol. 2, p. 339.

Collecting information in description. • "Typus. ♂ ad. 17 961 in der Schausammlung des Berliner Zoologischen Museums aufgestellt, hierzu Skelet 17 960. Von Feldwebel Peter am 27. Januar 1907 auf der Straße von Assobam zwischen Mensima und Bimba südlich Dumeflusse westlich von Mokbe erlegt und von Geheimrat Professor Dr. Hans Meyer in Leipzig geschenkt [Type. ♂ ad. 17961 placed in the display collection of the Berlin Zoological Museum, associated with skeleton 17960. Shot by Sergeant Peter on 27 January 1907 on the Assobam Road between Mensima and Bimba south of Dumé River west of Mokbe and donated by Professor Dr. Hans Meyer in Leipzig]" (Matschie 1914:325).

Specifics of specimen in the description. • "Typus. ♂ ad. 17961 in der Schausammlung des Berliner Zoologischen Museums aufgestellt, hierzu Skelet 17960 [translation: Type. ♂ ad. 17961 displayed in the exhibition of the Berlin Zoological Museum, refers to skeleton 17960]" (Matschie 1914:325).

Information on specimen. Skin, available; Skull, Skeleton not available.

Collecting locality. • "zwischen Bumba und Dume, Kamerun [between Bumba and Dumé, Cameroon]".

Collected by. Peter Scheunemann (1870–1937).

Collecting date. 27.01.1907.

Type status based on description. Holotype (Single specimen).

IUCN conservation status. Critically Endangered.

Remarks. Skull and skeleton not accessed as of 09.12.2022. The skull and skeleton 17960 are described to be associated with the skin 17961. Based on the de-

Table 3. Specifics of Individual *Gorilla diehli* specimens.

MfN specimen	Specimen Information in the general catalogue	Specifics of specimen in the description	Collecting locality	Type status	Specific remarks
ZMB_Mam_12789 (skull)	"♂ *Gorilla diehli* Mtsch*, Schädel mit Unterkiefer, Dakbe, Cross-Flussgebiet Diehl S.G" Vol. 2, p. 121	Adult Male	Takpe, Cameroon	Holotype	Skull with mandible. Verbatim locality 'Dakbe', in Cameroon could not be traced. Sarmiento and Oates (2000) confirmed *Gorilla gorilla diehli* as a distinct subspecies and identified the collection locality as Takpe. p 12
ZMB_Mam_12792 (skull)	"♂ *Gorilla diehli* Mtsch*, Schädel mit Unterkiefer, Dakbe, Cross-Flussgebiet Diehl S.G" Vol. 2, p. 121	Adult Male. "Diese Schädel sind zum Theil durch Brand verletzt" (page 52)	Takpe, Cameroon	Paratype	The specimen appears burnt. Matschie wrote that it probably served as a fetish object before collection, hence supposedly possessed mystical powers. The general catalogue states that the mandible for this skull is available, but it is absent. The specimen box includes a tube containing a loose tooth from the skull.
ZMB_Mam_12790 (skull)	"♂, *Gorilla diehli* Mtsch*, Schädel mit Unterkiefer, von Gadyifu bei Oboni erlegt., Diehl S.G" Vol. 2, p. 121	Adult Male	Obonyi, Cameroon	Paratype	Skull with mandible
ZMB_Mam_12791 (skull and skeleton parts)	"♂ *Gorilla diehli* Mtsch*, Schädel mit Unterkiefer, Oboni, Diehl S.G" Vol. 2, p. 121	Adult Male. "Diese Schädel sind zum Theil durch Brand verletzt" (page 52)	Obonyi, Cameroon	Paratype	The specimen appears burnt. Matschie wrote that it probably served as a fetish object before collection, hence supposedly possessed mystical powers. The general catalogue states that the mandible for this skull is available, but it is absent.
ZMB_Mam_12796 (ZMB_Mam_85826) (skull)	"♀ *Gorilla gorilla diehli*, Sch Ukf, Oboni, Diehl, Paratypus" Vol. 9, p. 241	Adult Female	Obonyi, Cameroon	Paratype	Skull without mandible. Specimen in General catalogue as ZMB_Mam_85826
ZMB_Mam_12793 (skull)	"♀ *Gorilla diehli* Mtsch*, Schädel ohne Unterkiefer, Basho, Diehl S.G" Vol. 2, p. 121	Adult Female	Basho, Cameroon	Paratype	Skull without mandible.
ZMB_Mam_12794 (skull)	"♀ *Gorilla diehli* Mtsch*, Schädel ohne Unterkiefer, Basho, Diehl S.G" Vol. 2, p. 121	Adult Female. "Diese Schädel sind zum Theil durch Brand verletzt" (page 52)	Basho, Cameroon	Paratype	Skull without mandible. The specimen appears burnt. Matschie wrote that it probably served as a fetish object before collection, hence supposedly possessed mystical powers. The general catalogue states that the mandible for this skull is available, but it is absent.
ZMB_Mam_12795 (ZMB_Mam_85825) (skull)	"*Gorilla gorilla diehli*, Sch Ukf, Basho/ Kamerun, Diehl, Paratypus" Vol. 9, p. 241	Adult Female	Basho, Cameroon	Paratype	Skull without mandible. Matschie identified this specimen as a female, but is identified as a male on "Specify". The specimen box includes a tube containing a loose tooth from the skull. Specimen available in General catalogue as ZMB_Mam_85825

scription, this skin should be labelled 17961, but the label on the skin specimen reads 17960.

Gorilla zenkeri Matschie, 1914

MfN specimens. Skull. ZMB_Mam_30261(2); Skin, Skeleton. ZMB_Mam_30260.

Author of name and type description. Paul Matschie (1914).

Present name. *Gorilla gorilla gorilla* Savage, 1847.

Dedication of name (patronym). No particular mention of a dedication, nevertheless name refers to supplier George Zenker (1855–1922).

Specimen information in general catalogue. • "♂*Gorilla zenkeri* Mtsch *, Fell, Schädel, Skelett, 15.09 [this is the A number], Mbiawe, Lokundje, Zenker "Vol. 4, p. 11.

Shipment information (A-catalogue number). A 15.09 • "[3 items], Bipindi, 14. IV.08, Zenker".

Collecting information in description. • "Typus. ♂ juv. ad. A. 15, 09, 1. Fell aufgestellt. Skelet vorhanden. Von G. Zenker bei Mbiawe am Lokundje, 6 Stunden flußabwärts von Bipindi am weißen Berge im Januar 1908 gesammelt [Type. ♂ juv. ad. A. 15, 09, 1. Skin mounted. Skeleton present. Collected by G. Zenker at Mbiawe in Lokundje, 6 hours downstream from Bipindi on White Mountain in January 1908]" (Matschie 1914:325–326).

Specifics of specimen in the description. Male specimen • "Die Gesichtshaut war an vielen Stellen krankhaft verändert, ähnlich wie bei Lues…Die Sutura basilaris ist noch geöffnet. Das linke Auge war zerstört. Im Schädel sitzt dicht am unteren Rande der Augenhöhle im Jugale ein Stück Eisen. Am rechten Rande des Planum nuchale auf der Sutura occipito-mastoidea ist eine verheilte Verletzung des Knochens sichtbar [The face skin was abnormally damaged in many places, similar to lues [syphillis]...The sutura basilaris is still open. The left eye was damaged. In

the skull, close to the lower edge of the orbit in the jugal bone, lies a piece of iron. On the right edge of the planum nuchale on the sutura occipito-mastoidea a healed injury of the bone is visible]" (Matschie 1914:327).

Information on the specimen. Skull, available; Skin, Skeleton, not available.

Collecting locality. Mbiawe [Mbiame?], Cameroon.

Collected by. Georg Zenker (1855–1922).

Collecting date. 01.1908.

Type status based on description. Holotype (Single specimen).

IUCN conservation status. Critically Endangered.

Remarks. Skin and skeleton specimens are not accessible as of 21.12.2022. The skull ZMB_Mam_30261(2) is now changed to ZMB_Mam_30260 i.e. associated with the same inventory number as its skin and skeleton.

Gorilla jacobi Matschie, 1905

MfN specimens. Skulls. ZMB_Mam_83558; ZMB_Mam_83862.

Author of name and type description. Paul Matschie (1905b).

Present name. *Gorilla gorilla gorilla* Savage, 1847.

Dedication of name (patronym). No mention of a dedication, nevertheless, refers to the name of supplier Gerhard Jacob (1878–1914).

Specimen information in general catalogue. ZMB_Mam_83558 • "♂, *Gorilla gorilla*, Sch, Lobo-mündung, Kam., Jacob, A 28,05 / 10.VII.05, 2" Vol. 9, p. 149.

ZMB_Mam_83862 • "**Gorilla jacobi* , Matschie 1905, Sch, Lobo-mündung, Kamerun, Jacob, Holotypus unter Vorbehalt; ♀ A 28,05 1, ♀ von Matschie unter 28051" Vol. 9, p. 161.

Shipment information (A-catalogue number). A 28.05 • "[35 items], Lobo-Mündung, Süd-Kamerun, 10.VII.05, Lt. Jacob".

Collecting information in description. • "Einen Schädel den Herr Leutnant Jacob auf der Station Lobo-Mündung (…) [A skull found by Lieutenant Jacob at the River Lobo Estuary Station]" (Matschie 1905b:282).

Specifics of specimen in the description. Male specimen ZMB_Mam_83558. Female specimen ZMB_Mam_83862. Both with forward protruding eyebrows, broad faces and occiputs.

Information on specimens. All specimens available.

Collecting locality. Lobo River Estuary, Cameroon.

Collected by. Gerhard Jacob (1878–1914).

Type status based on description. Syntypes.

IUCN conservation status. Critically Endangered.

Remarks • The skull ZMB_Mam_28051 (Matschie 1905b:282), is confirmed today as ZMB_Mam_83862. The skull ZMB_Mam_83558 is a skull without a mandible.

Anthropopithecus reuteri Matschie, 1914

MfN specimens. Skull and Skin. ZMB_Mam_83869. Skeleton. ZMB_Mam_83700.

Author of name and type description. Paul Matschie (1914).

Present name. *Pan troglodytes* Blumenbach, 1775.

Dedication of name (patronym). Franz Reuter (?–?).

Specimen information in general catalogue. ZMB_Mam_83869 • "*♂ ad, *Anthropopithecus reuteri* Matschie 1914, Sch, Dumemündung, Kamerun, F. Reuter 1908, A 39.09.1? Holotypus Sk. of 83700" Vol. 9, p. 161

ZMB_Mam_83700 • "**Pan troglodytes*, Sk, Dumemündung, Kam., Reuters 29. VI.1909, A 39.09, Siehe Sch 83869" Vol. 9, p. 154.

Shipment information (A-catalogue number). A 39.09 • "Düme, 29. VI.09, Reuter".

Collecting information in description. • "*Pan* —? Specimen from Dünne, the interior of Southern Cameron, Elliot, 1. c. III, 252, Typus. ♂ ad. A. 39, 09, 1. Fell mit Skelet. In der Nähe der Einmündung des Dume-Flusses in den Kadei in Kamerun von, Oberleutnant Franz Reuter † im Herbst 1908 erlegt [Type. ♂ adult A 39.09,1. Skin with skeleton. Hunted by Oberleutnant Franz Reuter † in Autumn 1908, in the vicinity of the confluence of River Dumé and River Kadeï in Cameroon]" (Matschie 1914:328).

Specifics of specimen in the description. Male fur with skeleton and skull.

Information on the specimen. Skull and Skeleton are available, but Skin is not available.

Collecting locality. Doumé River Estuary, Cameroon.

Collected by. Franz Reuter (1881–1908).

Collecting date. Autumn 1908.

Type status based on description. Holotype (single specimen).

IUCN conservation status. Endangered.

Remarks. Skin not found as of 05.01.2023.

Anthropopithecus oertzeni Matschie, 1914

MfN specimens. Skin. ZMB_Mam_83867. Skeleton. ZMB_Mam_83716.

Author of name and type description. Paul Matschie (1914).

Present name. *Pan troglodytes* Blumenbach, 1775.

Dedication of name (Patronym). Jasper Martin Otto von Oertzen (1880–1948).

Specimen information in general catalogue. • "*♂ Juv. *Pan Troglodytes*, F + Sk, Bascho, Kamerun, Oertzen 29. VI.1909, A60.05 I".

Skin ZMB_Mam_83867, Vol. 9, p. 161; Skeleton ZMB_Mam_83716, Vol. 9, p. 155.

Shipment information (A-catalogue number). A 60.05 • "[89 items], Säugetier von Bascho, Nord.Kamerun, 20. XI.05, Leutenant von Oertzen".

Collecting information in description. • "*Pan* —? Specimen from Basho. Elliot, 1. c. III, 252 partim. Typus. ♂ ad. A. 60, 05, 1. Fell mit Skelet ohne Schädel. (Der Schädel ist im Besitz des Herrn Hauptmann v. Oertzen). Von diesem im Jahre 1905 in der Nähe von Bascho in Nordkamerun gesammelt.[Type. ♂ ad. A 60.05,1. Skin with skeleton without skull. (The skull is property of Mr

Hauptmann v. Oertzen). Collected in 1905 in the vicinity of Baschéo in north Cameroon" (Matschie 1914:327).

Specifics of specimen in the description. The specimen is a male skin with a skeleton and no skull.

Information on specimen. All specimens available.

Collecting locality. Bashéo, Cameroon.

Collected by. Jasper Martin Otto von Oertzen (1880–1948).

Collecting date. 20.11.1905.

Type status based on description. Holotype (Single specimen).

IUCN conservation status. Endangered.

Remarks. The label for skeleton ZMB_Mam_83716 is also attached to the skin specimen.

Anthropopithecus papio Matschie, 1919

MfN specimens. Skull, Round skin. ZMB_Mam_83865.

Author of name and type description. Paul Matschie (1919).

Present name. *Pan troglodytes* Blumenbach, 1775.

Specimen information in general catalogue. • "*♂, *Anthropopithecus papio* Matschie 1919, Sch B, J.-Albrechtshohe, Kamerun, Puttkammer G.S 1903, A 48.03 Syntypus, beschr. Zeitsch. f. Ethnologie 1919, H 1. p 79/80" Vol. 9, p. 161.

Shipment information (A-catalogue number). A 48.03 • "[2 items], Fell mit Schädel von *Anthropopithecus*, Albrechtshohe, Kamerun, 30.VI.03, von Puttkammer".

Collecting information in description. • "Bei Barombi am Elefanten-See in der nächsten Nähe der Station Johann Albrechtshöhe nordwestlich von Mundame zwischen dem oberen Mungo und dem zum Oberen Meme abwässernden Uwe hat Herr Gouverneuer J. v. Puttkamer im Februar 1903 einen männlichen Schimpansen erlegt [Governor J. v. Puttkamer hunted a male chimpanzee in February 1903, near Barombi at the Elephant lake, close to the Station Johann Albrechtshöhe, northwest from Mundame, between the Upper Mungo and the drainage basin of the Uwe River]" (Matschie 1919:79).

Specifics of specimen in the description. Male specimen • "Dieser Schimpanse, den man wegen seiner dem Pavian ähnlich vorspringendee Schnauze *Anthropopithecus papio* nennen könnte [This chimpanzee could be called *Anthropopithecus papio* because of its protruding snout similar to that of the baboon]" (Matschie 1919:80).

Information on specimen. All specimens available.

Collecting locality. Barombi (Lake Barombi Mbo) Mountains, near Kumba, Cameroon.

Collected by. Jesco von Puttkamer (1855–1917).

Collecting date. 02.1903.

Type status based on description. Holotype (Single specimen).

IUCN conservation status. Endangered.

Anthropopithecus ellioti Matschie, 1914

MfN specimens. Skin. ZMB_Mam_83868. Skeleton. ZMB_Mam_83709.

Author of name and type description. Paul Matschie (1914).

Present name. *Pan troglodytes ellioti* Matschie, 1914

Dedication of name (patronym). Daniel Giraud Elliot (1835–1915).

Specimen information in general catalogue. • "**Pan troglodytes*, F + Sk, Basho, Kam., v. Oertzen, A 60.05 II." ZMB_Mam_83868, Vol. 9, p. 161; ZMB_Mam_83709, Vol. 9, p. 155.

Shipment information (A-catalogue number). A 60.05 • "[89 items], Säugetier von Bascho, Nord.Kamerun, 20. XI.05, Leutenant von Oertzen".

Collecting information in description. • "Als Typus von *A. ellioti* möge das ♂ ad. A. 60, 05, 2 Fell ohne Schädel gelten, das in der Nähe von Bascho durch Herrn v. Oertzen gesammelt worden ist; den Schädel hat der Sammler behalten [Type for *A. ellioti* is possibly the ♂ adult A 60.05, 2 skins without skulls, which were captured in the vicinity of Bascho by Mr. v. Oertzen; the collector kept the skull]" (Matschie 1914:327).

Specifics of specimen in the description. The specimen is a male skin with a skeleton - no skull.

Information on specimen. All specimens available.

Collecting locality. Bashéo, Cameroon.

Collected by. Jasper Martin Otto von Oertzen (1880–1948).

Collecting date. 20.11.1905.

Type status based on description. Holotype (Single specimen).

IUCN conservation status. Endangered.

Remarks. The label for skeleton ZMB_Mam_83709 is also attached to the skin specimen.

Order Proboscidea Illiger, 1811
Family Elephantidae Gray, 1821

Elephas (Loxodonta) cyclotis Matschie, 1900

MfN specimen. Skull. ZMB_Mam_13501.

Author of name and type description. Paul Matschie (1900d).

Present name. *Loxodonta cyclotis* Matschie, 1900.

Specimen information in general catalogue. • "♂ *Loxodonta cyclotis* Mtsch *, Schädel, 21.VIII.07" Vol. 2, p. 151

Collecting information in description • "Als Original-Exemplar diene das von Herrn Oberleutnant Dominick dem hiesigen Zoologischen Garten überwiesene Männchen [Original specimen is the male shipped to the Zoological Garden by Oberleutnant Dominik" (Matschie 1900d:194).

Specifics of specimen in the description. • "Männchen [male]" (Matschie 1900d:194).

Information on specimen. Specimen available.

Collecting locality. Yaounde, Cameroon.

Collected by. Hans Dominik (1870–1910).

Type status based on description. Holotype (Single specimen).

IUCN conservation status. Critically Endangered.

Remarks. This individual was described as a new species while still alive in the Berlin Zoological Garden, its oval ear lobes being the main defining morphological character considered by Matschie. It was called by the colonial press as "the first German elephant" and died in the Zoo in 20.05.1907, after which its skull was accessioned to the MfN. The skull possibly underwent autopsy and a calotte was cut from the main skull, the lower mandible was also present.

Order Rodentia Bowdich, 1821
Family Anomaluridae Gervais, 1849

***Idiurus zenkeri* Matschie, 1894**

MfN specimen. Skull, Skin and Body in alcohol. ZMB_Mam_7993.

Author of name and type description. Paul Matschie (1894).

Present name. *Idiurus zenkeri* Matschie, 1894.

Specimen information in general catalogue. • "*7993♀, *Idiurus zenkeri* Mtsch, F Sch. K, A. 3.93, Yaunde, Kamerun, G. Zenker" Vol. 1, p. 286.

Shipment information (A-catalogue number). A 3.93 is an older A-catalogue number that could not yet be traced in the archival materials.

Specifics of specimen in the description. • "Das vorliegende Exemplar ist ein sehr altes Weibchen [The present specimen is a very old female]" (Matschie 1894:200).

Information on specimen. All specimens available.

Collecting locality. Yaoundé, Cameroon.

Collected by. George Zenker (1855–1922).

Type status based on description. Holotype (Single specimen).

IUCN conservation status. Least Concern.

Remarks. Only the body is in alcohol; the skin is a dry specimen.

***Zenkerella insignis* Matschie, 1898**

MfN specimens. Skull, Skeleton parts, Round Skin. ZMB_Mam_10085.

Author of name and type description. Paul Matschie (1898).

Present name. *Zenkerella insignis* Matschie, 1898.

Specimen information in general catalogue. • "♂ *Zenkerella insignis* Mtsch *, Fell Sch, A 3 98, Yaunde, Zenker, 13.5.98" Vol. 2, p. 5.

Shipment information (A-catalogue number). A 3.98 is an older A-catalogue number that could not yet be traced in the archival materials.

Collecting information in description. • "Hab. Kamerun, Afr. occ, Yaunde. Zenker coli [Provenance Cameroon, West Africa, Yaoundé, Zenker's shipment]" (Matschie 1898:24).

Specifics of specimen in the description. According to Matschie, the specimen was in poor condition and the hair fell off the skin easily, measurements of the ear and feet are only approximate. The specimen was likely a male juvenile. (Matschie 1898:24).

Information on specimen. All specimens available.

Collecting locality. Yaoundé, Cameroon.

Collected by. George Zenker (1855–1922).

Type status based on description. Holotype (Single specimen).

IUCN conservation status. Least Concern.

Family Muridae Illiger, 1811

***Mus (nannomys) setulosus* Peters, 1876**

MfN specimen. Specimen in alcohol. ZMB_Mam_5047

Author of name and type description. Wilhelm Peters (1876).

Present name. *Mus setulosus* Peters, 1876.

Specimen information in general catalogue • "**Mus (Nannomys) setulosus* Pter* Victoria Aug. 74 Buchholz" Vol. 1, p. 183.

Collecting information in description. • "Ein Männchen wurde im August 1874 in Victoria gefangen, ein jüngeres Weibchen brachte Hr. Dr. Reichenow von Cameruns [A male was captured in Victoria in August 1874, a younger female was brought by Dr. Reichenow from Cameruns[sic]]" (Peters 1876:481).

Specifics of specimen in the description. Male specimen • "was ich zur Begründung einer neuen Untergattung, *Nannomys*, anführe, den ersten Backzahn viel länger, als die beiden andern zusammengenommen [what I use to justify a new subgenus, *Nannomys*, the first molar is much longer than the other two taken together]" (Peters 1876:481).

Information on specimen. Specimen available.

Collecting locality. Limbe, Cameroon.

Collected by. Reinhold Buchholz (1837–1876).

Collecting date. 08.1874.

Type status based on description. Syntypes.

IUCN conservation status. Least concern.

Remarks. The description is 'Peters 1876', but the jar label reads 'Peters 1852', no description for 'Peters 1852' for this species could be traced. The description 'Peters 1876' also mentions a female of the species collected by Reichenow and delivered to Peters, but this specimen which constitutes the other syntype of this species could not be traced at time of publication.

Family Sciuridae Fischer de Waldheim, 1817

***Sciurus auriculatus* Matschie, 1891**

MfN specimens. Skin. ZMB_Mam_46674. Round Skin. ZMB_Mam_46675.

Author of name and type description. Paul Matschie (1891).

Present name. *Funisciurus leucogenys auriculatus* Matschie, 1891.

Specimen information in general catalogue. ZMB_Mam_46674 • "[1 specimen] **Funisciurus leucogenys*, Fell, Barombe, Preuß, 1891" Vol. 5, p.270.

ZMB_Mam_46675 • "[1 specimen] **Funisciurus leucogenys* Mtsch, Balg, Kamerun, Dr. Preuß" Vol. 5, p. 270.

Specifics of specimen in the description. Male specimen. "3 Felle ohne Schädel. [3 skins without skull]" (Matschie 1891:353).

Information on specimen. All specimens available.

Collecting locality. Barombi Mbo, Cameroon.

Collected by. Paul Rudolph Preuss (1861–1926).

Type status based on description. Syntypes.

IUCN conservation status. Least Concern.

Remarks. The description mentions three skins. Only two skins are mentioned in "Specify", one skin is still unaccounted for.

Sciurus calliurus Peters, 1874

MfN specimen. Skull, Skin**.** ZMB_Mam_4696.

Author of name and type description. Wilhelm Peters (1874).

Present name. *Protoxerus stangeri* Waterhouse, 1842.

Specimen information in general catalogue. • "*Sciurus calliurus* Buchholtz*, Mai, Mungo Cameroon, Buchholz 4696" Vol. 1, p. 171.

Collecting information in description. • "Ein männliches Exemplar in Mungo, am 11. Mai 1874 erlegt. Ausser dieser Art wurde auch *Sc. pyrrhopus* Fr. Cuv. in derselben Gegend gefunden [One male specimen hunted in Mungo, in 11 May 1874. Besides this species, *Sc. pyrrhopus* Fr. Cuv. was also found in the same location]" (Peters, 1874:708).

Specifics of specimen in the description. Male specimen.

Information on specimen. Only skin specimen was available for consultation.

Collecting locality. Mungo, Cameroon.

Collected by. Reinhold Buchholz (1837–1876).

Collecting date. 11.05.1874.

Type status based on description. Holotype (single specimen).

IUCN conservation status. Least Concern.

Remarks. Skull specimen could not be assessed as of 24.11.2022.

Order Eulipotyphla Waddell et al., 1999
Family Soricidae Fischer, 1814

Crocidura vulcani Heim de Balsac, 1956

MfN specimen. Skull, Skin. ZMB_Mam_91354.

Author of name and type description. Heim de Balsac (1956).

Present name. *Crocidura virgata* Sanderson, 1940.

Specimen information in general catalogue. • "**Crocidura vülcani* von Prof. Heim de Balsac, F Sch, 58/45/11/7, A _39, Kamerunberg, Kamerun 1600 m, 4.5.1938, Dr. Martin Eisentraut, Buhr S." Vol. 10, p. 56.

Shipment information (A-catalogue number). A _39 [Incomplete shipment information in general catalogue; shipment number not given].

Collecting information in description. • "Peau (sans sexe indiqué) et crane d'un specimen provenant du cratère Bibundi (1.600 m), Mt. Cameroun, 4–5-1938, Musée de Humboldt, Berlin, n° 91354. Procurée par M. Eisentraut [Skin (no sex indicated) and skull of a specimen from the Bibundi crater (1,600 m), Mount Cameroon, 4–5-1938, Humboldt Museum, Berlin, n° 91354. Procured by Mr. Eisentraut]" p. 134.

Specifics of specimen in the description. Mounted skin. No sex indicated on either specimen.

Information on specimen. All specimens available.

Collecting locality. Bibundi Crater, Mount Cameroon.

Collected by. Martin Bruno Eisentraut (1902–1994).

Collecting date. 04.05.1938.

Type status based on description. Holotype (Single specimen).

IUCN conservation status. Least Concern.

Remarks. According to Turni et al. (2007), for *Crocidura vulcani*, the valid name today is *Crocidura virgata*.

Crocidura dolichura Peters, 1876

MfN specimen. Skull, Skin. ZMB_Mam_5037.

Author of name and type description. Wilhelm Peters (1876).

Present name. *Crocidura dolichura* Peters, 1876.

Specimen information in general catalogue. • "*Crocidura (Crocidura) dolichura*, Pter*, Fem., Bonjongo, Buchholtz" Vol. 1, p. 183.

Collecting information in description. • "Ein weibliches Exemplar dieser ausgezeichneten Art aus Bonjongo [A female specimen of this magnificent species from Bonjongo]" (Peters 1876:476).

Specifics of specimen in the description. Female specimen.

Information on specimen. All specimens available.

Collecting locality. Bonjongo, Cameroon.

Collected by. Reinhold Buchholz (1837–1876).

Type status based on description. Holotype (single specimen).

IUCN Conservation status. Least concern.

Remarks. Both skin and skull specimens are available and observed on 06.01.2023, but only the skull specimen is mentioned in "Specify" at the time of publication.

Myosorex preussi Matschie, 1893

MfN specimen. Skull, skin. ZMB_Mam_6990. Skull, skin. ZMB_Mam_6991. Skull, skin. ZMB_Mam_6992.

Author of name and type description. Paul Matschie (1893).

Present name. *Sylvisorex morio* Gray, 1862.

Specimen information in general catalogue. • "*Myosorex preussi* Mtsch*, Fell m. Schädel, Buea, Preuss" Vol. 1, p. 249.

Collecting information in description. • "Die drei vorliegenden Stücke wurden in der Umgebung von Buea auf dem Kamerun-Gebirge von Dr. Preuss gefangen [The three present pieces were caught in the vicinity of Buea on the Cameroon Mountains by Dr. Preuss]" (Matschie 1893:178).

Specifics of specimen in the description. Three female specimens.

Information on specimen. All specimens available.

Collecting locality. Buea, Cameroon.

Collected by. Paul Rudolph Preuss (1861–1926).

Type status based on description. Syntypes.

IUCN conservation status. Endangered.

Remarks. According to Turni et al (2007), for *Myosorex preussi* the valid name, today is *Sylvisorex morio*.

Conclusion

The analysis of type specimens from the MfN mammal collections presented here illustrates the complexity of dealing with historical natural history collection records. This assessment attempted, for the first time, to identify all type material identified in the catalogue as originating from a particular geographical location, that was also a political unit defined at that time as German 'Kamerun.' The type status, collecting localities, collectors and dates mentioned herein are based on an assessment of the available information from catalogues, specimen tags and descriptions. Most of the specimens examined have incomplete collection records due to diverse circumstances, including insufficient labelling at the time of collection, shipping, accession, description and storage. We assume that further information on these collecting events can be determined with further provenance research. We hope this work contributes to an understanding of how natural history specimens are catalogued and stored in the MfN collections and encourage further studies on all West African collections in the MfN and other Western museums. Hence, further funding for projects, such as the one presented here, is crucial for an assessment of museum storage processes and past collecting practices. Our study also attempts to disambiguate the documented type specimen localities of collection in the hope to facilitate a future determination of these localities and, as such, an increasingly detailed understanding of the faunal situation from the perspective of geographical region, which may include flagging endemic species, their abundance and distribution over time, potentially contributing to a better and shared knowledge of global and local biodiversity.

Acknowledgements

This research was supported by the Museum für Naturkunde Berlin and the German Lost Art Foundation. Paul Taku Bisong and Catarina Madruga cooperated in the context of the project "Koloniale Provenienzen der Natur. Der Ausbau der Säugetiersammlung des Museums für Naturkunde Berlin, um 1900" (2020–2023), funded by the German Lost Art Foundation (Deutsches Zentrum Kulturgutversluste) and hosted at the Centre for the Humanities of Nature, MfN. The authors would like to thank the MfN Mammal Department especially Frieder Mayer for useful comments and suggestions and Christiane Funk for providing access to the specimens and historical catalogues; and to the MfN digitisation team, in particular Eileen Westwig, Bernhard Schurian, Eran Wolff and Oskar Werb, for their support in the photographic records of the valid types. We acknowledge the team of the Centre for the Humanities of Nature, MfN, for the bureaucratic and scientific support that made this work possible, particularly Polichronia Kiourtidis, Katja Kaiser and Ina Heumann. The authors would also like to thank the editor and peer-reviewers for the improvements suggested to the manuscript.

References

Acharya N, Subedi MN (2005) Type specimens. Bulletin of Department of Plant Resources, Kathmandu, Nepal., 1–2. http://kath.gov.np/image/data/TYPE%20SPECIMEN.pdf

Ade M, Frahnert S, Starck C (2001) Analysing databases of Southern African material at the Museum für Naturkunde in Berlin. Mitteilungen aus dem Museum für Naturkunde in Berlin, Zoologische Reihe 77: 325–331 https://doi.org/10.1002/mmnz.4850770215

Ashby J, Machin R (2021) Legacies of colonial violence in natural history collections. Journal of Natural Science Collections 8: 45. http://www.natsca.org/sites/default/files/publications/JoNSC-Vol8-Ashby_and_Machin_2021_0.pdf [May 21, 2023]

Boakes EH, McGowan PJK, Fuller RA, Chang-qing D, Clark NE, O'Connor K, Mace GM (2010) Distorted views of biodiversity: Spatial and temporal bias in species occurrence data. PLoS Biology 8: e1000385. https://doi.org/10.1371/journal.pbio.1000385

Bogutskaya NG, Mikschi E, Riedl MD, Szeiler S, Frade PR, Palandačić A (2022) An annotated catalogue of the type specimens described by Maximilian Holly housed in the Natural History Museum of Vienna. Part. 1. Chordata: Actinopterygii and Echinodermata: Asteroidea. Annalen des Naturhistorischen Museums in Wien. Serie B für Botanik und Zoologie 124: 20–21.

Brauer A (1912) Zwei neue Baumschlieferarten aus Westafrika. Sitzungsberichte der Gesellschaft Naturforschender Freunde zu Berlin 1912: 411–414. https://www.biodiversitylibrary.org/page/43604471

Brauer A (1913) Weitere neue *Procavia*- Arten aus dem Kgl. Zoologischen Museum in Berlin. Sitzungsberichte der Gesellschaft Naturforschender Freunde zu Berlin 1913: 125–127. https://www.biodiversitylibrary.org/page/43606987

Brauer A (1914) Neue Klipp- und Baumschliefer aus Südwest- und Westafrika. Sitzungsberichte der Gesellschaft Naturforschender Freunde zu Berlin 1914: 38–39. https://www.biodiversitylibrary.org/page/43608067

Heim De Balsac H (1956) Diagnoses De *Crocidura* Inédites D'afrique Occidentale. Mammalia 20(2): 131–139. https://doi.org/10.1515/mamm.1956.20.2.131

Holmes MW, Hammond TT, Wogan GOU, Walsh RE, LaBarbera K, Wommack EA, Martins FM, Crawford JC, Mack KL, Bloch LM, Nachman MW (2016) Natural history collections as windows on evolutionary processes. Molecular Ecology 25: 864–881. https://doi.org/10.1111/mec.13529

International Commission on Zoological Nomenclature, Ride WDL, International Trust for Zoological Nomenclature, Natural History Museum (London, England), International Union of Biological Sciences [Eds] (1999) International code of zoological nomenclature: Code international de nomenclature zoologique. 4th edn. International Trust for Zoological Nomenclature, Natural History Museum, London.

Johnson KG, Brooks SJ, Fenberg PB, Glover AG, James KE, Lister AM, Michel E, Spencer M, Todd JA, Valsami-Jones E, Young JR, Stewart JR (2011) Climate Change and Biosphere Response: Unlocking the Collections Vault. BioScience 61: 147–153. https://doi.org/10.1525/bio.2011.61.2.10

Kaiser K (2021) Wirtschaft, Wissenschaft: Die Botanische Zentralstelle für die deutschen Kolonien am Botanischen Garten und Museum Berlin (1891–1920). Peter Lang, Berlin.

Languy M, Bobo KS, Njie FM, Njabo KY, Lapios JM, Demey R (2005) New bird records from Cameroon. Malimbus 27: 1–12. https://free.fr/articles/V27/27001012.pdf

Matschie P (1891) Über einige Säugetiere aus Kamerun und dessen Hinterlande. Archiv für Naturgeschichte 57: 351–356. https://www.biodiversitylibrary.org/page/6400758

Matschie P (1893) Einige afrikanische Säugethiere. Sitzungsberichte der Gesellschaft Naturforschender Freunde zu Berlin: 175–178. https://doi.org/10.5962/bhl.part.9925

Matschie P (1894) Neue Saugetiere aus den Sammlungen der Herren Zenker, Neumann, Stuhlmann und Emin. Sitzungsberichte der Gesellschaft Naturforschender Freunde zu Berlin 1894: 197–203. https://www.biodiversitylibrary.org/page/43581304

Matschie P (1898) Eine neue mit *Idiurus* Mtsch. verwandte Gattung der Nagetiere. Sitzungsberichte der Gesellschaft Naturforschender Freunde zu Berlin 1898: 23–30. https://www.biodiversitylibrary.org/page/8790743

Matschie P (1900a) Einige Säugetiere aus dem Hinterlande von Kamerun. Sitzungsberichte der Gesellschaft Naturforschender Freunde zu Berlin, 87–100. https://www.biodiversitylibrary.org/item/35603#page/9/mode/1up

Matschie P (1900b) Über die Fleckenhyäne des Hinterlandes von Kamerun. Sitzungsberichte der Gesellschaft Naturforschender Freunde zu Berlin, 211–215. https://www.biodiversitylibrary.org/page/8797217

Matschie P (1900c) Über einige Formen der Gattung *Colobus*. Sitzungsberichte der Gesellschaft Naturforschender Freunde zu Berlin 1900: 181–189. https://www.biodiversitylibrary.org/page/8797190

Matschie P (1900d) Über geographische Abarten des afrikanischen Elefanten. Sitzungsberichte der Gesellschaft Naturforschender Freunde zu Berlin 1900: 189–197. https://www.biodiversitylibrary.org/page/8797195

Matschie P (1904) Bemerkungen über die Gattung *Gorilla*. Sitzungsberichte der Gesellschaft Naturforschender Freunde zu Berlin 1904: 45–53. https://www.biodiversitylibrary.org/page/7673816

Matschie P (1905a) Einige Anscheinend neue Meerkatzen. Sitzungsberichte der Gesellschaft Naturforschender Freunde zu Berlin 1905: 262–276. https://www.biodiversitylibrary.org/page/7897367

Matschie P (1905b) Merkwürdige Gorilla-Schädel aus Kamerun. Sitzungsberichte der Gesellschaft Naturforschender Freunde zu Berlin, 279–283. https://www.biodiversitylibrary.org/page/7897374

Matschie P (1910) Ein Steppenfuchs aus Kamerun. Sitzungsberichte der Gesellschaft Naturforschender Freunde zu Berlin, 370–371. https://www.biodiversitylibrary.org/page/43615821

Matschie P (1914) Neue Affen aus Mittelafrika. Sitzungsberichte der Gesellschaft Naturforschender Freunde zu Berlin 1914: 325–332. https://www.biodiversitylibrary.org/page/43608393

Matschie P (1917) Die Untergattung *Stachycolobus* ROCHEBR. Sitzungsberichte der Gesellschaft Naturforschender Freunde zu Berlin 1917: 152–163. https://www.biodiversitylibrary.org/page/43576253

Matschie P (1919) Neue Ergebnisse der Schimpansenforschung. Zeitschrift für Ethnologie 1919: 62–82. https://digi.evifa.de/viewer/image/1569514108988/125/#topDocAnchor

Ministry of Agriculture and Rural Development (MINADER) (2015) The State of Biodiversity for Food and Agriculture in the Republic of Cameroon. Food and Agricultural Organisation 2015: 1–2.

Neumann O (1905) Über neue Antilopen -Arten. Sitzungsberichte der Gesellschaft Naturforschender Freunde zu Berlin 1905: 91–92. https://www.biodiversitylibrary.org/page/7897168

Peters W (1874) Über eine neue Art der Säugethiergattung *Bassaris* aus Centralamerica und eine neue Eichhornart aus Westafrica. Monatsberichte der Königlichen Preussische Akademie des Wissenschaften zu Berlin 1874: 707–708. https://www.biodiversitylibrary.org/page/36627077

Peters W (1876) Hr. W. Peters las über die von dem verstorbenen Professor Dr. Reinhold Buchholz in Westafrika gesammelten Säugethiere. Monatsberichte der Königlichen Preussische Akademie des Wissenschaften zu Berlin 1876: 475–481. https://www.biodiversitylibrary.org/page/35329852

Pohle H (1919) Die Unterfamilie der Lutrinae. (Eine systematisch-tiergeographische Studie an dem Material der Berliner Museen). Archiv für Naturgeschichte 1919: 145–147. https://www.biodiversitylibrary.org/page/45490215

Pohle H (1943) *Scotonycteris ophiodon* sp. n., eine neue Art epomophoroider Flughunde. Sitzungsberichte der Gesellschaft Naturforschender Freunde zu Berlin 1942: 78–87.

Sarmiento EE, Oates JF (2000) The Cross River Gorillas: A Distinct Subspecies, *Gorilla gorilla* Diehli Matschie 1904. American Museum of Natural History, 55 pp. https://doi.org/10.1206/0003-0082(2000)3304%3C0001:TCRGAD%3E2.0.CO;2

Suarez AV, Tsutsui ND (2004) The value of museum collections for research and society. BioScience 54(1): 66–74. https://doi.org/10.1641/0006-3568(2004)054[0066:TVOMCF]2.0.CO;2

Taku Bisong P (in prep.) Cameroon in Berlin 1. Collections. Report on mammal collections of the Museum für Naturkunde Berlin.

Turni H, Hutterer R, Asher R (2007) Type specimens of “insectivoran” mammals at the Museum für Naturkunde, Berlin. Zootaxa 1470: 1–33. https://doi.org/10.11646/zootaxa.1470.1.1

Wirz A (1972) Vom Sklavenhandel zum kolonialen Handel: Wirtschaftsräume und Wirtschaftsformen in Kamerun vor 1914. Atlantis, Zürich, Freiburg, 125–126. https://docs.google.com/file/d/0B-6Bw-KX3F6HXMERBVldpWUtkZjQ/edit?resourcekey=0-WoR-WVE9DZEIqCjEvAKjefQ [September 22, 2023]

Zoosyst. Evol. 99 (2) 2023, 519–533 | DOI 10.3897/zse.99.109097

PENSOFT

für Natur MUSEUM FÜR NATURKUNDE BERLIN

A new species of free-living marine nematode, *Fotolaimus cavus* sp. nov. (Nematoda, Oncholaimida, Oncholaimidae), isolated from a submarine anchialine cave in the Ryukyu Islands, southwestern Japan

Daisuke Shimada[1,2], Keiichi Kakui[1], Yoshihisa Fujita[3]

1 *Department of Biological Sciences, Faculty of Science, Hokkaido University, Sapporo 060-0810, Japan*
2 *Center for Molecular Biodiversity Research, National Museum of Nature and Science, Tsukuba 305-0005, Japan*
3 *Okinawa Prefectural University of Arts, 1-4 Shuri-Tounokura, Naha, Okinawa 903-8602, Japan*

https://zoobank.org/75589A9A-94C3-4F20-BBEC-A4C7D3799836

Corresponding author: Daisuke Shimada (oncholaimus@gmail.com)

Academic editor: Pavel Stoev ♦ **Received** 6 July 2023 ♦ **Accepted** 6 October 2023 ♦ **Published** 6 November 2023

Abstract

Fotolaimus cavus **sp. nov.** was described from a submarine anchialine cave called Akuma-no-yakata on the Shimoji Island, Miyako Island Group, Ryukyu Islands, southwestern Japan. This is the first free-living marine nematode isolated from a submarine cave in Japan, and the third species of the genus *Fotolaimus*. This new species differs from its congeners by its small body size, wide amphids, long buccal cavity, long conico-cylindrical tail, and proximally curved gubernaculum. We provide amended dichotomous keys to genera in the subfamily Oncholaiminae and species in *Fotolaimus*. We also analyzed partial DNA sequences encoding ribosomal small subunit RNA and cytochrome *c* oxidase subunit I from *Fotolaimus cavus* **sp. nov.** and six other species of Oncholaimidae collected from Japanese waters. The phylogenetic tree based on the ribosomal small subunit RNA sequences using maximum likelihood analysis suggested a close relationship between *Fotolaimus* and *Wiesoncholaimus* as well as *Oncholaimus*. The topology of the tree was similar to those from previous studies; however, it suggested a new phylogenetic position of *Adoncholaimus* as a sister clade for *Viscosia* and *Oncholaimus*.

Key Words

cave scuba diving, Enoplea, meiofauna, Miyako Island Group, molecular phylogeny, Oncholaiminae

Introduction

Free-living nematodes are the most abundant taxon in the marine environment and the dominant organisms in the meiobenthos of submarine caves, including anchialine caves (D'Addabbo et al. 2008; Arunimaand and Mohan 2021). However, surveys of meiofauna, including nematodes, in submarine caves have only been conducted in the Canary Islands (García-Valdecasas Huelín 1985; Riera et al. 2018), Hong Kong (Zhou and Zhang 2003, 2008), Italy (Wieser 1954; Ape et al. 2015; Onorato and Belmonte 2017), and Cuba (Pérez-García et al. 2018). Thus, our taxonomic and ecological knowledge of nematodes from submarine caves is insufficient.

In the present study, we describe a new species of the free-living marine nematode genus *Fotolaimus* Belogurova & Belogurov, 1974 collected from an anchialine cave called Akuma-no-yakata (= Devil's Palace) and located on the Shimoji Island (or Shimojijima Island), Miyako Island Group, Ryukyu Islands, southwestern Japan. Osawa and Fujita (2019) have provided a detailed description of this cave, and faunal surveys conducted in Akuma-no-yakata in recent years identified the following organisms in the cave: crustaceans (Fujita et al. 2013, 2017; Anker and Fujita 2014; Osawa and Fujita 2016, 2019; Kakui and Fujita 2018, 2020; Saito and Fujita 2022), ophiuroids (Okanishi and Fujita 2018, 2019), annelids (Worsaae et al. 2021), molluscs (Mizuyama et

al. 2022), sponges (Ise et al. 2023), and pycnogonids (Kakui and Fujita 2023).

Belogurova and Belogurov (1974) established the genus *Fotolaimus* in Oncholaimidae Filipjev, 1916. Currently, this genus contains two species, i.e., *F. marinus* Belogurova & Belogurov, 1974 (type species) and *F. apostematus* (Wieser, 1959) Belogurova & Belogurov, 1974. *Fotolaimus* belongs to the subfamily Oncholaiminae Filipjev, 1916, based on its left ventrosublateral tooth being larger than the other two teeth and the presence of a prodelphic ovary. Members of *Fotolaimus* resemble those of *Metoncholaimus* Filipjev, 1918 as males have a gubernaculum and females have a Demanian system, but differ from the *Metoncholaimus* species by the presence of ten or more terminal ducts and pores (whereas *Metoncholaimus* members have two ducts and two pores) (Belogurova and Belogurov 1974; Belogurov and Belogurova 1988; Smol et al. 2014). However, there are currently no molecular data supporting the phylogenetic position of *Fotolaimus*.

In a recent classification system by Hodda (2022), the family Oncholaimidae belongs to the order Oncholaimida Siddiqi, 1983 = suborder Oncholaimina De Coninck, 1965 = superfamily Oncholaimoidea Filipjev, 1916 with two other families, i.e., Enchelidiidae Filipjev, 1918 and Thalassogeneridae Orton Williams & Jairajpuri, 1984. Thalassogeneridae is a terrestrial family that includes only the type genus *Thalassogenus* Andrássy, 1973, and several authors do not include Thalassogeneridae in Oncholaimoidea based on morphological data (Jensen 1976; Lorenzen 1981). Since molecular data do not allow any conclusion, only Oncholaimidae and Enchelidiidae are considered members of Oncholaimoidea sensu stricto. Several molecular phylogenetic analyses strongly support the monophyly of the clade composed of Oncholaimoidea sensu stricto (Meldal et al. 2007; van Megen et al. 2009; Bik et al. 2010a, b; Pereira et al. 2010; Smythe 2015; Smythe et al. 2019; Ahmed et al. 2022). However, analyses of ribosomal small subunit RNA sequences (Meldal et al. 2007; Bik et al. 2010a, b; Smythe 2015) and whole-genome/transcriptome (Smythe et al. 2019; Ahmed et al. 2022) do not support monophyly of Oncholaimidae. The monophyly of the seven subfamilies comprising Oncholaimidae (for three of which there are no molecular data) is also not supported by molecular analyses (Bik et al. 2010a, b; Smythe 2015), and phylogenetic relationships within Oncholaimoidea that have been supported by morphological analyses (e.g., Smol et al. 2014; Hodda 2022) are considered to require significant revision.

Materials and methods

Sampling and morphological observation

Sediment samples were collected by scuba diving from a completely dark, anchialine zone at 7–20 m depth ("second slope zone," Osawa and Fujita 2019) in the submarine cave Akuma-no-yakata, Shimoji Island, Miyako Island Group, Ryukyu Islands, southwestern Japan (24°49'22.5"N, 125°08'07.8"E) on 26 Oct. 2018. Thirteen nematode individuals were isolated from the sediments and preserved in DESS solution (Yoder et al. 2006). We considered that these individuals belonged to the same species in the family Oncholaimidae. Three males and four females were permanently mounted in anhydrous glycerin (Shimada et al. 2021), observed using a BX51 light microscope (Olympus, Japan) with differential interference contrast, and photographed with an PCM500 digital camera (AS ONE, Japan). One male and one female were dried using the hexamethyldisilazane method (Nation 1983), sputter-coated with gold to a thickness of 20 nm, and observed using an S-3000N scanning electron microscope (SEM; Hitachi, Japan). We edited digital photographs using GIMP ver. 2.10 (https://www.gimp.org) and generated measurements and drawings from digital photographs using Inkscape ver. 1.0 (https://inkscape.org). We deposited all specimens examined in the Invertebrate Collection of Hokkaido University Museum (ICHUM). The terminology used to describe the arrangement of morphological features such as setae follows that of Decraemer et al. (2014). The following de Man's ratios (Hooper 1986) were used: a, ratio of body length to maximum body diameter; b, ratio of body length to pharyngeal length; c, ratio of body length to tail length; c', ratio of tail length to body diameter at cloacal opening or anus; and V, position of vulva from anterior body end expressed as percentage of body length.

Molecular experiments

Two males and two females isolated from the Akuma-no-yakata cave were used. Additionally, we included 18 individuals of six oncholaimid species from Japanese waters, i.e., *Oncholaimus secundicollis* Shimada, Kajihara, & Mawatari, 2009, *Oncholaimus* cf. *oxyuris* Ditlevsen, 1911, *Oncholaimus* cf. *vesicarius* (Wieser, 1959), *Wiesoncholaimus jambio* Shimada & Kakui, 2021, *Adoncholaimus daikokuensis* Shimada & Kajihara, 2014, and *Adoncholaimus pseudofervidus* Shimada & Kajihara, 2014, for phylogenetic analysis (Table 1). Total DNA was extracted using an ISOHAIR extraction kit (NIPPON GENE, Japan) following the protocols described by Tanaka et al. (2012) and Iwahori (2014) with minor modifications. Each nematode was placed in 20 µL dissolving solution containing 18.5 µL 1% extraction buffer in TE buffer pH 8.0, 0.5 µL lysis solution, and 1.0 µL enzyme solution and incubated at 55 °C for 60 min (extraction buffer, lysis solution, and enzyme solution are included in the kit). Nearly full-length sequences encoding ribosomal small subunit RNA (18S) and mitochondrial cytochrome *c* oxidase subunit I (COI) were amplified by PCR using KOD One PCR Master Mix (TOYOBO, Japan). PCR primers for 18S amplification were as follows: forward EukA (AACCTGGTTGATCCTGCCAGT) (Díez et al. 2001)

Table 1. List of nematodes sequenced from Japanese waters with INSD accession numbers. *Type locality.

Species	N	Date	Locality	Accession numbers	
				18S	COI
Fotolaimus cavus sp. nov.	4	26 Oct. 2018	Akuma-no-yakata	LC746839–LC746842	LC746861–LC746864
Wiesoncholaimus jambio	4	25 Jun. 2015	*off Misaki, Sagami Bay	LC746843–LC746846	LC759639–LC759641
Oncholaimus secundicollis	2	13 Jul. 2014	*Akkeshi, Hokkaido	LC746847, LC746848	–
Oncholaimus cf. *oxyuris*	5	23 Jun. 2013	Hamanaka, Hokkaido	LC746849, LC746850	LC746865–LC746869
Oncholaimus cf. *vesicarius*	18	17 Mar. 2015	Akkeshi, Hokkaido	LC746851, LC746852	LC746870–LC746887
Adoncholaimus daikokuensis	4	19 Jun. 2012	*Daikoku Island, Hokkaido	LC746853–LC746856	LC746888–LC746891
Adoncholaimus pseudofervidus	4	20 May 2012	*Mukawa, Hokkaido	LC746857–LC746860	LC746892–LC746895

and reverse 26R (CATTCTTGGCAAATGCTTTCG), forward 9FX (AAGTCTGGTGCCAGCAGCCGC) and reverse 13R (GGGCATCACAGACCTGTTA), and forward 2FX (GGAAGGGCACCACCAGGAGTGG) and reverse 18P (TGATCCWKCYGCAGGTTCAC) (De Ley et al. 2002). PCR primers for COI amplification were forward F1 (CCTACTATGATTGGTGGTTTTGGTAATTG) and reverse R2 (GTAGCAGCAGTAAAATAAGCACG) (Kanzaki and Futai 2002) and forward JB3 (TTTTTTGGGCATCCTGAGGTTTAT) and reverse JB5 (AGCACCTAAACTTAAAACATAATGAAAATG) (Derycke et al. 2005). The thermal cycling program consisted of 35 cycles at 98 °C for 10 s, 50 °C for 5 s, and 68 °C for 10 s. We determined the nucleotide sequences by direct sequencing using a BigDye Terminator Kit ver.3.1 (Applied Biosystems, USA) with a 3730 Genetic Analyzer (Applied Biosystems). Fragments were joined into a single sequence using MEGA X (Kumar et al. 2018). We deposited the obtained sequences (Table 1) in the International Nucleotide Sequence Database (INSD) through the DNA Data Bank of Japan.

Phylogenetic analysis

The 18S dataset (1442 bp long after alignment) used for phylogenetic analysis included 21 oncholaimid sequences obtained in the present study, and 38 oncholaimid sequences, 12 enchelidiid sequences, and three outgroup sequences (*Enoplus* Dujardin, 1845 and *Enoploides* Ssaweljev, 1912) obtained from the INSD (Table 2). All sequences were aligned according to the secondary structure predicted using RNAfold WebServer (Gruber et al. 2008; Lorenz et al. 2011). Sequences were trimmed in MEGA X and alignment-ambiguous sites were then removed using Gblocks ver. 0.91b (Castresana 2000) in NGPhylogeny.fr (Lemoine et al. 2019) and the "relaxed" parameters described in Talavera and Castresana (2007). The optimal substitution model was GTR+F+R3, determined under the corrected Akaike information criterion option in ModelFinder (Kalyaanamoorthy et al. 2017). A maximum likelihood (ML) analysis was constructed based on the 18S dataset using IQ-TREE ver. 2.1.2 (Minh et al. 2020) under the 'bnni' option (Hoang et al. 2018). Clade support was estimated using 1,000 replicates for both SH-like approximate likelihood ratio tests (SH-aLRT; Guindon et al. 2010) and ultrafast bootstraps (UFBoot; Hoang et al. 2018) as a function of IQ-TREE. The ML tree was drawn using FigTree ver. 1.4.4 (http://tree.bio.ed.ac.uk) and processed using Illustrator CS6 (Adobe, USA).

Results

Taxonomy

Subfamily Oncholaiminae Filipjev, 1916

Type genus. *Oncholaimus* Dujardin, 1945.

Diagnosis (modified from Belogurova and Belogurov 1974; Smol et al. 2014). Oncholaimidae. Cuticle smooth. Buccal cavity barrel-shaped, with three teeth. Left ventrosublateral tooth larger than other teeth (usual) or left and right ventrosublateral teeth of same size. Spicules short or long, gubernaculum present or absent. Copulatory bursa absent. Female reproductive system monodelphic-prodelphic with an antidromously reflexed ovary. Demanian system present or absent.

Remarks. Cobb (1930) established the new genus *Oncholaimium* Cobb, 1930, which differs from *Oncholaimus* mainly by the presence of a distinct precloacal appendicule (papilla) in males. Subsequently, Kreis (1932) established *Pseudoncholaimus* Kreis, 1932 based on the lack of Demanian system. Kreis (1934) also distinguished *Oncholaimium* from *Oncholaimus* based on the Demanian system, which is without terminal pore in *Oncholaimium* and with terminal pores in *Oncholaimus*. However, Rachor (1969) synonymized *Oncholaimium* and *Pseudoncholaimus* to *Oncholaimus*, because the presence of a Demanian system is unknown for many species of *Oncholaimus*. Belogurov and Belogurova (1988), who proposed the currently accepted taxonomic system of Oncholaimidae, treated *Oncholaimium* and *Pseudoncholaimus* as valid genera. *Pseudoncholaimus* is still considered valid by several researchers (e.g., Smol et al. 2014; Tsalolikhin 2015; Milovankina and Fadeeva 2019). However, because it is unclear for numerous species whether they rather belong to *Oncholaimus*, *Oncholaimium*, or *Pseudoncholaimus*, we included the latter two in *Oncholaimus* sensu lato as described by Rachor (1969). Thus, the subfamily Oncholaiminae comprises six genera, i.e., *Oncholaimus*, *Metoncholaimus*, *Prooncholaimus* Micoletzky, 1924, *Metaparoncholaimus* De Coninck &

Table 2. List of nematode sequences from the INSD including the phylogenetic analysis. Abbreviations: A = Atlantic Ocean side; FS = French Southern and Antarctic Lands; nd = no data; P = Pacific Ocean side. *Outgroup.

Family	Subfamily	Species		Accession number	Reference
Oncholaimidae	Oncholaiminae	*Oncholaimus* sp. AUK23	UK	HM564402	Bik et al. (2010b)
		Oncholaimus sp. AUK35	UK	HM564474	Bik et al. (2010b)
		Oncholaimus sp. AUK36	UK	HM564475	Bik et al. (2010b)
		Oncholaimus sp. BUS1	USA (A)	HM564404	Bik et al. (2010b)
		Oncholaimus sp. BUS4	USA (A)	HM564409	Bik et al. (2010b)
		Oncholaimus sp. BUS5	USA (A)	HM564410	Bik et al. (2010b)
		Oncholaimus sp. BUS7	USA (A)	HM564411	Bik et al. (2010b)
		Oncholaimus sp. NAR4	USA (A)	HM564429	Bik et al. (2010b)
		Oncholaimus sp. NAR7	USA (A)	HM564432	Bik et al. (2010b)
		Oncholaimus sp. NAR16	USA (A)	HM564426	Bik et al. (2010b)
		Oncholaimus sp. NUS2	USA (A)	HM564438	Bik et al. (2010b)
		Oncholaimus sp. NUS5	USA (A)	HM564444	Bik et al. (2010b)
		Oncholaimus sp. NUS6	USA (A)	HM564445	Bik et al. (2010b)
		Oncholaimus sp. NUS7	USA (A)	HM564446	Bik et al. (2010b)
		Oncholaimus sp. OUS2	USA (A)	HM564450	Bik et al. (2010b)
		Oncholaimus sp. SBA2	South Africa	HM564592	Bik et al. (2010b)
		Oncholaimus sp. SBA3	South Africa	HM564593	Bik et al. (2010b)
		Oncholaimus sp. SBA5	South Africa	HM564594	Bik et al. (2010b)
		Oncholaimus sp. AS479	Japan	KR265044	Smythe (2015)
		Oncholaimus sp. DS-2015	Japan	LC093124	Shimada (unpubl.)
		Pseudoncholaimus sp. AS89	USA (A)	KR265048	Smythe (2015)
	Adoncholaiminae	*Adoncholaimus* sp.	nd	AF036642	Mullin et al. (2005)
	Oncholaimellinae	*Viscosia* sp. AUK10	UK	HM564399	Bik et al. (2010b)
		Viscosia sp. HCL9	UK	HM564570	Bik et al. (2010b)
		Viscosia sp. HCL10	UK	HM564557	Bik et al. (2010b)
		Viscosia sp. HCL11	UK	HM564558	Bik et al. (2010b)
		Viscosia sp. HCL15	UK	HM564560	Bik et al. (2010b)
		Viscosia sp. HCL24	UK	HM564565	Bik et al. (2010b)
		Viscosia sp. HCL27	UK	HM564566	Bik et al. (2010b)
		Viscosia sp. LUK1	UK	HM564417	Bik et al. (2010b)
		Viscosia sp. LUK3	UK	HM564419	Bik et al. (2010b)
		Viscosia sp. SBN2	UK	HM564595	Bik et al. (2010b)
		Viscosia sp. SBN4	UK	HM564597	Bik et al. (2010b)
		Viscosia dossena Leduc & Zhao, 2023	New Zealand	OK317193	Leduc and Zhao (2023)
		Oncholaimellinae sp. AS71	USA (A)	KR265043	Smythe (2015)
	Pontonematinae	*Pontonema* sp. Nem.209	USA (P)	MN250102	Pereira et al. (2020)
		Pontonema sp. Nem.213	USA (P)	MN250105	Pereira et al. (2020)
Enchelidiidae		*Bathyeurystomina* sp. Cr78a	FS	HM564537	Bik et al. (2010b)
		Bathyeurystomina sp. Cr80b	FS	HM564539	Bik et al. (2010b)
		Bathyeurystomina sp. TCR81	USA (P)	HM564646	Bik et al. (2010b)
		Bathyeurystomina sp. TCR109	USA (P)	HM564602	Bik et al. (2010b)
		Calyptronema sp. 1068	the Netherlands	FJ040503	van Megen et al. (2009)
		Calyptronema sp. AUK13	UK	HM564400	Bik et al. (2010b)
		Calyptronema sp. LUK7	UK	HM564421	Bik et al. (2010b)
		Calyptronema sp. LUK12	UK	HM564418	Bik et al. (2010b)
		Eurystomina sp. AS485	Japan	KR265038	Smythe (2015)
		Pareurystomina sp. BCA3	Antarctica	HM564491	Bik et al. (2010b)
		Pareurystomina sp. NUS1	USA (A)	HM564435	Bik et al. (2010b)
		Symplocostoma sp. AS520	Panama (A)	KR265050	Smythe (2015)
Enoplidae		**Enoplus brevis* Bastian, 1865	nd	U88336	Aleshin et al. (1998)
		**Enoplus meridionalis* Steiner, 1921	Croatia	Y16914	Kampfer et al. (1998)
Thoracostomopsidae		**Enoploides* sp. 1252	the Netherlands	FJ040490	van Megen et al. (2009)

Schuurmans Stekhoven, 1933, *Wiesoncholaimus* Inglis, 1966, and *Fotolaimus*. Members of the Oncholaiminae can be distinguished from these of the other six subfamilies as follows. They are distinct from Krampiinae De Coninck, 1965, Adoncholaiminae Gerlach & Riemann, 1974, and Pontonematinae Gerlach & Riemann, 1974 as they have only one ovary (whereas the three other genera have two); from Pelagonematinae De Coninck, 1965

and Octonchinae De Coninck, 1965 as they have three distinct teeth (whereas Pelagonematinae member have minute or no tooth and Octonchinae have eight or more); and from Oncholaimellinae De Coninck, 1965 because their left ventrosublateral tooth is larger than the other two teeth (right ventrosublateral tooth is larger in Oncholaimellinae). Recent revisional works were provided by Mawson (1958) for *Metaparoncholaimus*, Yoshimura (1982) for *Metoncholaimus*, and Chen et al. (2015) for *Prooncholaimus*.

Genus *Fotolaimus* Belogurova & Belogurov, 1974

Type species. *Fotolaimus marinus* Belogurova & Belogurov, 1974.

Diagnosis (modified from Belogurova and Belogurov 1974). Oncholaiminae. Left ventrosublateral tooth larger than the two other teeth. Spicules shorter than 2.0 cloacal body diameters. Gubernaculum present. Demanian system present, posterior end of main duct forming two symmetrical sacs each with five or more terminal ducts.

Remarks. The genus *Fotolaimus* can be distinguished from *Metaparoncholaimus* and *Wiesoncholaimus* by the left ventrosublateral tooth being larger than the right ventrosublateral tooth (left and right ventrosublateral teeth are equal in size in *Metaparoncholaimus* and *Wiesoncholaimus*). It also differs from *Prooncholaimus* by the absence of the large bubble-like cells in pseudocoelom (presence in *Prooncholaimus*). *Fotolaimus*, *Oncholaimus*, and *Metoncholaimus* are similar to each other and are distinguished by the morphological characters of the terminal ducts of the Demanian system. Belogurova and Belogurov (1974) characterized the Demanian system of *Fotolaimus* as follows: the posterior end of the main duct forms two symmetrical sacs, each of which is pierced by five terminal ducts ending in terminal pores. On the other hand, the main ducts of *Oncholaimus* and *Metoncholaimus* do not form a sac at the posterior end, but branch separately into two or more terminal ducts (Belogurov and Belogurova 1988). Belogurov and Belogurova (1977) distinguished *Metoncholaimus* from *Oncholaimus* in that the terminal ducts are covered with moniliform glands. However, some *Metoncholaimus* species do not mention the shape of the terminal duct in their description (e.g., Mawson 1958; Salma et al. 2017). For convenience, a species may be considered belonging to *Oncholaimus* if it has short (equal to cloacal body diameter) spicules and without gubernaculum, and belonging to *Metoncholaimus* if it has longer spicules (with or without gubernaculum) or short spicules with gubernaculum (cf. Platt and Warwick 1983). The distinction between *Oncholaimus* and *Metoncholaimus* will need to be reexamined in the future.

Key to genera in Oncholaiminae (cf. Belogurov and Belogurova 1988; Smol et al. 2014).

1	Right and left ventrosublateral teeth of same size	2
–	Left ventrosublateral tooth larger than the other teeth	3
2	Spicule length almost equal to cloacal body diameter	*Metaparoncholaimus*
–	Spicules longer than 3.0 cloacal body diameters	*Wiesoncholaimus*
3	Large bubble-like cells present in pseudocoelom	*Prooncholaimus*
–	Large bubble-like cells absent	4
4	Demanian system including two posterior sacs	*Fotolaimus*
–	Demanian system absent, or present but without posterior sacs	5
5	Terminal ducts covered with moniliform glands	*Metoncholaimus*
–	Terminal ducts not covered with moniliform glands	*Oncholaimus*

Fotolaimus cavus sp. nov.

https://zoobank.org/A0509360-77DD-4387-9FAD-92B14758952F

Figs 1–4, Table 3

Material examined. ***Holotype*.** Japan • male (permanent whole mount in glycerin); Ryukyu Islands, Miyako Island Group, Shimoji Island, a submarine cave called Akuma-no-yakata; 24°49'22.5"N, 125°08'07.8"E; 26 Oct. 2018; anchialine zone, depth 7 m, collected by Yoshihisa Fujita; ICHUM 8474.

***Paratypes*.** Japan • two males (permanent whole mounts in glycerin); same collection data as for holotype; 26 Oct. 2018; anchialine zone, depth 20 m, collected by Yoshihisa Fujita; ICHUM 8475 and 8476 • four females (permanent whole mounts in glycerin); same collection data as for preceding; ICHUM 8477–8480.

Other material. Japan • one male (SEM specimen); same collection data as for paratypes; • one female (SEM specimen); same collection data as for preceding.

Etymology. The specific name *cavus* (cave) is a Latin noun in apposition derived from the type locality.

Description. Body (Fig. 1A, B) elongated, almost cylindrical but gradually tapering toward both extremities. Cuticle smooth throughout body besides oblique striations (Fig. 2A; cf. Leduc 2013) crossing at angle of ca. 120° between amphids and anteriormost cervical setae visualized using SEM. Somatic sensilla arranged in eight longitudinal rows: setiform in anterior half of cervical (Figs 1C, 2B) and caudal (Fig. 2C) regions; papilliform or very short setiform in rest of body (Fig. 2D), difficult to observe without SEM. Cephalic region (Figs 1D–F, 2E–G, 3A–D) rounded at anterior end, with six lips, slightly

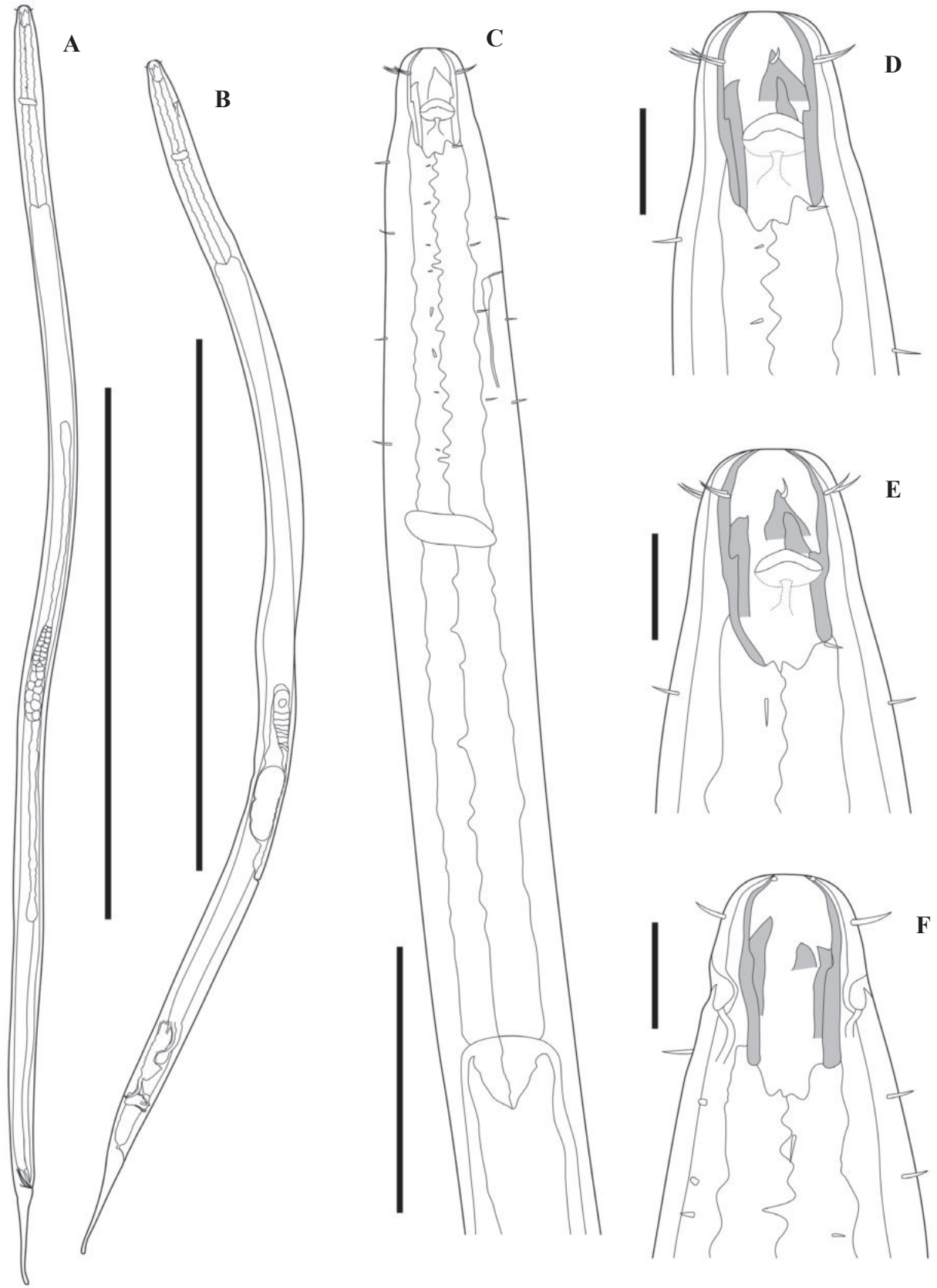

Figure 1. Line drawings of *Fotolaimus cavus* sp. nov. **A, C, D.** Holotype (ICHUM 8474); **B, E.** Paratype (ICHUM 8477); **F.** Paratype (ICHUM 8479). **A.** Male body, right lateral view; **B.** Female body, right lateral view; **C.** Male cervical region, right lateral view; **D.** Male cephalic region, right lateral view; **E.** Female cephalic region, right lateral view; **F.** Female cephalic region, dorsal view. Scale bars: 1 mm (**A, B**); 100 µm (**C**); 20 µm (**D–F**).

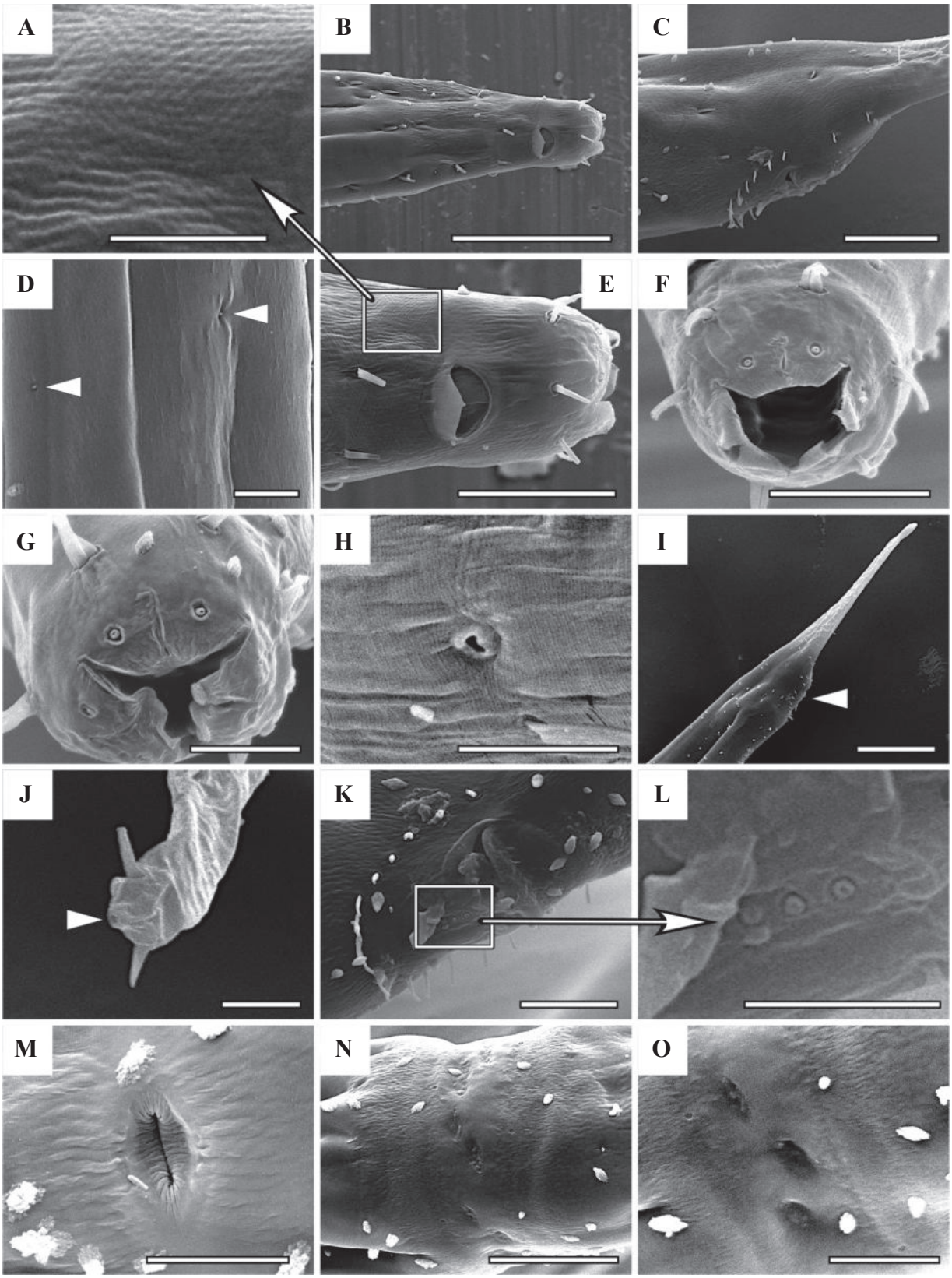

Figure 2. SEM photographs of *Fotolaimus cavus* sp. nov. **A, B, D–F, M–O.** Non-type female; **C, G–L.** Non-type male. **A.** Oblique striations on cuticle; **B.** Anterior region; **C.** Male cloacal region; **D.** Papilliform somatic sensilla (arrowheads); **E.** Female cephalic region, lateral view; **F.** Female cephalic region, anterior view; **G.** Male cephalic region, anterior view; **H.** SE-pore; **I.** Male posterior region with cloacal opening (arrowhead); **J.** Tail tip with spinneret (arrowhead); **K.** Cloacal region, subventral view; **L.** Ventral papillae; **M.** Vulva; **N.** Circle of terminal pores; **O.** Terminal pores. Scale bars: 5 μm (**A, H, J, L**); 50 μm (**B, I**); 20 μm (**C, E, N**); 10 μm (**D, F, G, K, M, O**).

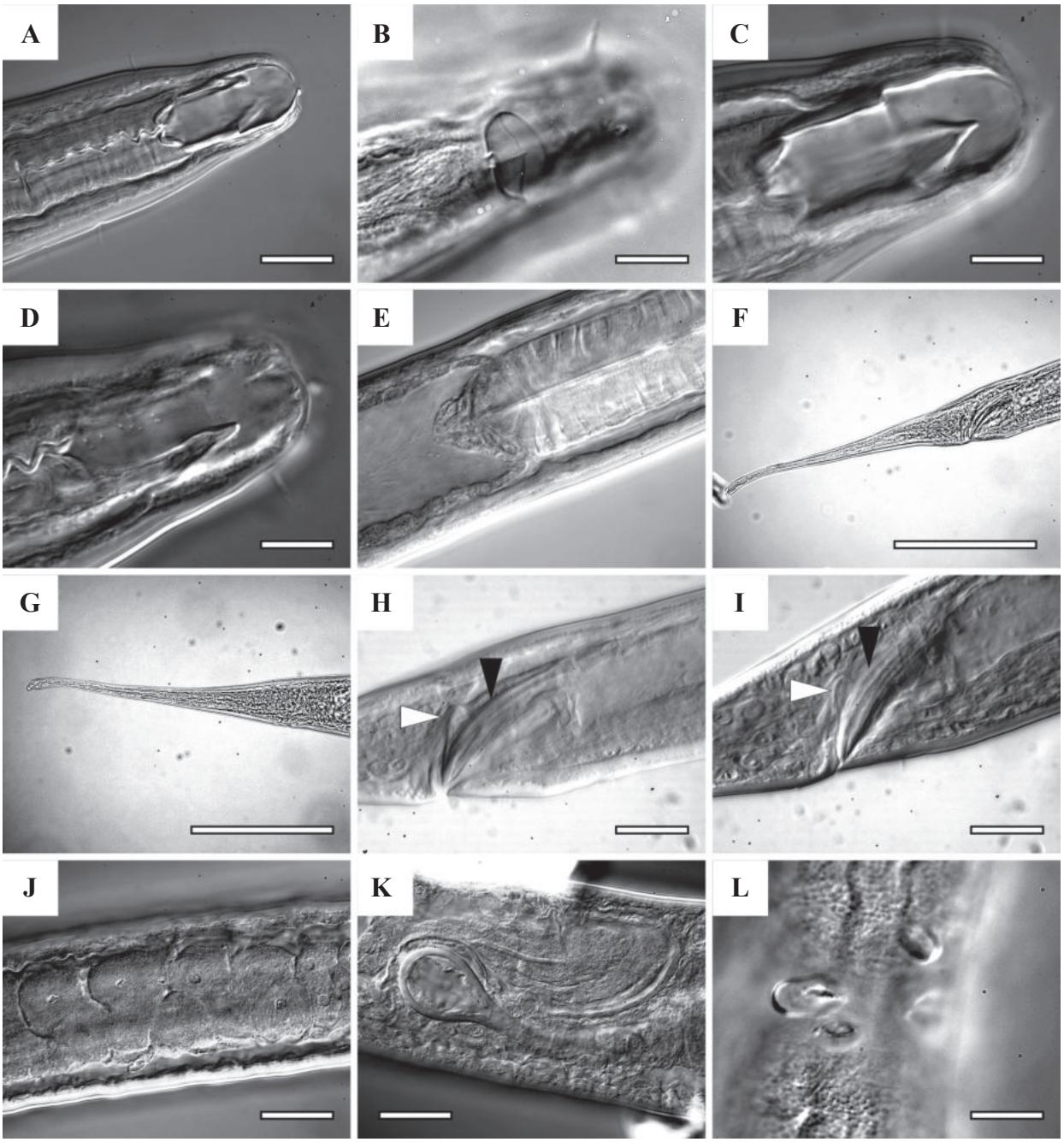

Figure 3. Light micrographs of *Fotolaimus cavus* sp. nov. **A–F, H, J.** Holotype (ICHUM 8474); **G, K.** Paratype (ICHUM 8477); **I.** Paratype (ICHUM 8475); **L.** Paratype (ICHUM 8479). **A.** Anterior region; **B.** Amphid; **C.** Buccal cavity with left ventrosublateral tooth; **D.** Buccal cavity with right ventrosublateral tooth; **E.** Posterior end of pharynx with cardia; **F.** Male tail; **G.** Female tail; **H, I.** Spicule (black arrowhead) and gubernaculum (white arrowhead); **J.** Sperms in seminal vesicle; **K.** Uvette and ductus entericus; **L.** Terminal pores. Scale bars: 20 μm (**A, E, H–K**); 10 μm (**B–D, L**); 100 μm (**F, G**).

constricted posterior to amphids, as wide as 0.3–0.4 maximum body diameters at cephalic sensilla level. Six inner labial sensilla papilliform. Six outer labial and four cephalic sensilla setiform, arranged in single circle, 5–8 μm or 0.20–0.30 corresponding body diameters long in males and 6–9 μm or 0.25–0.35 corresponding body diameters long in females. Amphids (Figs 1D, E, 2E, 3B) pocket-like, with elliptical aperture and cup-shaped fovea, 0.40–0.45 corresponding body diameters wide in males and 0.35–0.40 corresponding body diameters wide in females, anterior margin located at 0.4–0.5 buccal cavity lengths from anterior body end. Buccal cavity (Figs 1D–F, 3C, D) barrel-shaped, length/width = 2.5–3.0, surrounded by pharyngeal tissue in posterior 15%–25%. Three well-developed teeth: left ventrosublateral tooth largest, 4–6 μm longer than right and dorsal teeth. Tip of left ventrosublateral tooth at 0.2 buccal cavity lengths from anterior body end (i.e., level of cephalic sensilla). Pharynx (Figs 1C, 3E) cylindrical, evenly muscular, gradually widened toward posterior end. Cardia surrounded by intestine. Rectum

Figure 4. Line drawings of *Fotolaimus cavus* sp. nov. **A, C, D.** Holotype (ICHUM 8474); **B, E, F.** Paratype (ICHUM 8477); **G.** Paratype (ICHUM 8479). **A.** Male posterior region, right lateral view; **B.** Female posterior region, right lateral view; **C.** Spicule and gubernaculum, right lateral view; **D.** Male reproductive system, right lateral view; **E.** Female reproductive system, right lateral view; **F.** Demanian system, right lateral view; **G.** Demanian system, dorsal view. Scale bars: 50 µm (**A, B**); 10 µm (**C**); 100 µm (**D–G**).

(Fig. 4A, B) slightly longer than cloacal body diameter. Pore of secretory-excretory system (Figs 1C, 2H; SE-pore) with ampulla, at 2.0–2.2 buccal cavity lengths or 0.2 pharyngeal lengths from anterior body end. Renette cell not observed. Nerve ring (Fig. 1C) located at 0.45–0.50 pharyngeal lengths from anterior body end. Tail sexually dimorphic: male tail (Figs 2I, J, 3F, 4A) strongly tapering in anterior 1/5, gradually tapering in next 2/5, and almost cylindrical in posterior 2/5, as long as 3.9–5.7 cloacal body diameters; female tail (Figs 3G, 4B) more gradually tapering throughout its length, as long as 5.5–6.1 anal body diameters. Tail tip slightly expanded, with spinneret and one pair of subterminal setae in both sexes. Body diameter at level of cloacal opening or anus equal to 0.5 maximum body diameters, at cylindrical portion of tail equal to 0.20–0.25 cloacal body diameters. Caudal glands inconspicuous. Caudal setae arranged in longitudinal rows, number and location varying from individuals.

Table 3. Morphometrics of *Fotolaimus cavus* sp. nov. All measurements are in μm and in the form: mean ± s.d. (range). *Distance from the anterior body end.

	Male		Female
	Holotype	**Paratype**	**Paratype**
n	–	2	4
Body length	2417	2169 ± 109 (2060–2277)	2481 ± 284 (2266–2970)
a	39.6	31 ± 1.2 (29.9–32.1)	34.2 ± 4.0 (30.7–40.7)
b	6.2	6.1 ± 0.1 (6.1–6.2)	6.2 ± 0.6 (5.8–7.2)
c	13.3	13.5 ± 1.7 (11.8–15.1)	12.7 ± 0.8 (11.9–13.7)
V	–	–	66.0 ± 1.1 (64.9–67.5)
Body diameter at cephalic sensilla	25	24.5 ± 0.5 (24–25)	25.8 ± 0.5 (25–26)
Body diameter at amphids	29	30	31 ± 1.6 (29–33)
Maximum body diameter	61	70.0 ± 1.0 (69–71)	72.8 ± 2.3 (69–75)
Body diameter at vulva	–	–	68.3 ± 2.8 (65–71)
Body diameter at cloacal opening or anus	32	35	35 ± 0.9 (34–36)
Outer labial and cephalic setae length	5.0–7.5	6.4 ± 0.8 (5.0–7.4)	6.9 ± 1.0 (5.5–9.1)
Amphid position*	20	18 ± 1.0 (17–19)	20 ± 1.9 (18–23)
Amphid width	13	12.5 ± 0.5 (12–13)	12
Buccal cavity length	40	41 ± 1.0 (40–42)	42 ± 0.8 (41–43)
Buccal cavity width	16	15.5 ± 0.5 (15–16)	15.5 ± 0.5 (15–16)
Pharyngeal length	389	356 ± 13 (343–369)	403 ± 11 (386–416)
SE-pore*	85	81	88
Nerve ring*	175	165 ± 8 (157–173)	180 ± 5 (172–185)
Tail length on arc	182	165 ± 28 (137–193)	199 ± 13 (189–218)
Spicule length on arc	47	48 ± 2.5 (45–50)	–
Gubernaculum length on arc	17	20 ± 3.0 (17–23)	–
Anterior gonad*	785	760 ± 55 (705–814)	1302 ± 94 (1214–1460)
End of posterior gonad*	1732	1546 ± 60 (1486–1606)	–
Vulva*	–	–	1638 ± 200 (1473–1975)
Uvette*	–	–	2067 ± 278 (1839–2541)
Terminal pores*	–	–	2163 ± 268 (1961–2622)

Spicules (Figs 3H, I, 4A, C) paired, arcuate, distally acute with subterminal opening, proximally with capitulum, as long as 1.3–1.5 cloacal body diameters or 0.25–0.35 tail lengths. Gubernaculum (Figs 3H, I, 4A, C) plate-like, distally associated with spicules, proximally curved, shape similar to that of gubernaculum from *Admirandus belogurovi* Tchesunov, Mokievsky & Nguyen, 2010 (Tchesunov et al. 2010), as long as 0.5–0.7 cloacal body diameters or 0.3–0.5 spicule lengths. No precloacal supplement. Circumcloacal setae (Fig. 2C, K) arranged in single circle, 9–12 setae in each body side. Three ventral papillae (Fig. 2L) present just anterior to cloacal opening, arranged in single longitudinal row, observed only with SEM. Male reproductive system (Fig. 4D) diorchic. Two opposed and outstretched telogonic testes, both situated on right side of intestine: germinal zone filled with small cells not arranged in rows; growth zone with larger cells arranged in single row. Blind end of anterior testis at 30%–40% of body length from anterior end; blind end of posterior testis at 70% of body length from anterior end. Seminal vesicle including two (dorsal and ventral) rows of sperms (Fig. 3J). Vas deference located on ventral side of intestine, anteriorly filled by single row of sperms.

Female reproductive system (Fig. 4E) monodelphic-prodelphic. Telogonic ovary antidromously reflexed, situated on right side of intestine, as long as 6%–10% of body length; anterior end connecting with oviduct at 50%–55% of body length from anterior end; blind end located at 60%–65% of body length from anterior end; germinal zone with small cells not arranged in rows; growth zone with gradually growing cells arranged in two (right and left) rows; ripening zone with grown oocytes arranged in single row. Oviduct situated on left side of ovary (between intestine and ovary). Uterus well developed in two specimens (ICHUM 8477 and 8478), ca. 200 μm in length, each containing one egg (131–141 μm long and 48–62 μm wide). In other two individuals, uterus very short without egg and blind end of ovary located just anterior to vulva. However, the size and degree of maturity of the ovaries similar to those of egg-bearing specimens. Vulva (Figs 2M, 4E) transverse slit with thick cuticular walls, located at 2/3 from anterior body end. Vagina weakly sclerotized. Demanian system (Figs 3K, 4F, G) oncholaimoid type variant D (cf. Belogurov and Belogurova 1988). Ductus uterinus anteriorly inconspicuous. Uvette well-developed, spherical with thick sclerotized wall, situated on right side of intestine at 80%–85% of body lengths, connected to main duct with posterior tip. Main duct on dorsal side of intestine, anteriorly forming one short sac with thick sclerotized wall and filled with sperms, posteriorly forming two sacs on both sides. Ductus entericus very short, situated subterminally on the left side of anterior sac of main duct. Osmosium inconspicuous, may be simple pore. Terminal ducts branching off from posterior sacs of main duct, five or more in number on both sides. Terminal pores (Figs 2N, O, 3L, 4F, G) arranged in single circle surrounding body, 3–4 anal body diameters anterior to anus.

Diagnosis. *Fotolaimus cavus* sp. nov. is characterized by small body size (2.1–3.0 mm), wide amphids (0.35–0.45 corresponding body diameters), a long buccal cavity (length/width = 2.5–3.0), a long (c = 12–15, c' = 3.9–6.1) conico-cylindrical tail, and a proximally curved gubernaculum.

Remarks. *Fotolaimus cavus* sp. nov. differs from the other two species of the genus, i.e., *F. marinus* and *F. apostematus*, by the curved shape of the gubernaculum (not curved and smaller in *F. marinus* and *F. apostematus*). *Fotolaimus cavus* sp. nov. is also different from *F. marinus* by its shorter body (2.1–3.0 mm in *F. cavus* sp. nov. vs 5.8–6.2 mm in *F. marinus*) and longer tail (c = 12–15, c' = 3.9–6.1 in *F. cavus* sp. nov. vs c = 39–51, c' = 2.3–3.8 in *F. marinus*) with conico-cylindrical shape (vs clavate in *F. marinus*) (cf. Wieser 1959; Belogurova and Belogurov 1974).

Key to Fotolaimus species (cf. Wieser 1959; Belogurova and Belogurov 1974)

1 Tail clavate, as long as 2.0–2.5 cloacal body diameters ..... *F. marinus*
– Tail conico-cylindrical, longer than 3.0 cloacal body diameters 2
2 Gubernaculum almost straight ..... *F. apostematus*
– Gubernaculum proximally curved ..... *F. cavus* sp. nov.

Phylogenetic analysis

We obtained 38 partial COI sequences (315–801 bp) and 22 partial 18S sequences (1221–1692 bp) for seven oncholaimid species including *F. cavus* sp. nov. (Table 1). The DNA sequences isolated from *Fotolaimus* species were deposited in the INSD for the first time.

The ML tree based on 18S sequences (Fig. 5) suggested, albeit with low support values, the presence of two major clades within the Oncholaimoidea. The first major clade was composed of two highly supported subclades: all sequences from *Adoncholaimus* Filipjev, 1918 (SH-aLRT = 100% and UFBoot = 100%), and all sequences from *Viscosia* de Man, 1890 and several sequences from *Oncholaimus*, including *Pseudoncholaimus* (SH-aLRT = 97.3% and UFBoot = 99%). *Oncholaimus* from South Africa (SBA) and the Atlantic side of the USA (BUS, NAR, NUS, and OUS) did not form clades. *Oncholaimus* from the UK (AUK) and Japan placed in another major clade. Within the genus *Viscosia*, 11 sequences from the UK (AUK, HCL, LUK, and SBN) formed one clade, which did not include *V. dossena* Leduc & Zhao, 2023 from New Zealand. The second major clade contained *Pontonema* sp. and four well- or moderately-supported subclades: (1) *Eurystomina* Filipjev, 1921 and *Pareurystomina* Micoletzky, 1930 (SH-aLRT = 95% and UFBoot = 85%); (2) *Bathyeurystomina* Lambshead & Platt, 1979 (SH-aLRT ≥ 90% and UFBoot = 100%); (3) *Calyptronema* Marion, 1870 and *Symplocostoma* Bastian, 1865 (SH-aLRT = 94.8% and UFBoot = 97%); and (4) parts of *Oncholaimus* with all *Wieseoncholaimus*, *Fotolaimus*, *Meyersia* Hopper, 1967 and Oncholaimellinae sp. (SH-aLRT = 90.7% and UFBoot = 90%). The support values for a second major clade were not well-supported (SH-aLRT < 70% and UFBoot < 80%).

Discussion

The 18S phylogenetic tree (Fig. 5) suggested that *Fotolaimus cavus* sp. nov. was assembled in one major clade with some members of *Oncholaimus* and all members of *Wieseoncholaimus* and Oncholaimellinae sp. with a high level of support (SH-aLRT = 96.3% and UFBoot = 97%). *Fotolaimus* and *Wieseoncholaimus* are included, with *Oncholaimus*, in the subfamily Oncholaiminae (Hodda 2022), and they all present an oncholaimid-type Demanian system (Belogurov and Belogurova 1988). Therefore, the position of *Fotolaimus* in the Oncholaiminae based on the morphology was supported by molecular phylogeny.

Oncholaimus sp. (KR265044) from Wakayama (Pacific side of central Japan) is considered to be *O. secundicollis* because DNA sequences obtained from the former was identical to those from the topotypes of *O. secundicollis*. *Oncholaimus secundicollis* is distributed on the Pacific and Sea of Japan sides of northeastern Japan (Shimada unpubl.) and on the Sea of Japan side of South Korea (Lee et al. 2015). Wieser (1955) also reported on *O. dujardinii* de Man, 1876 from Wakayama but provided limited morphological information and no illustration. A redescription of *O. dujardinii* by the same author (Wieser 1953) mentions a gubernaculum (Zhang and Platt 1983), which should be absent in *Oncholaimus*. Therefore, *O. dujardinii* sensu Wieser (1955) may not be a true *Oncholaimus*.

Meyersia branch has been assembled (SH-aLRT = 90.7% and UFBoot = 90%) with the *Oncholaimus–Wieseoncholaimus–Fotolaimus* clade. *Meyersia* did not form the clade with *Adoncholaimus*, indicating that monophyly of Adoncholaiminae is unlikely. Members of Adoncholaiminae possess two ovaries and a well-developed Demanian system, but other morphological features distinguish *Meyersia* from the other three genera. *Adoncholaimus* (including *Metoncholaimoides* Wieser, 1954), *Admirandus* Belogurov & Belogurova, 1979, and *Kreisoncholaimus* Rachor, 1969 have larger teeth on the right side, and the terminal pores of the Demanian system are located near the anus (i.e., much posterior to both ovaries). In contrast, in *Meyersia*, right and left teeth are large, and the terminal pores of the Demanian system are located at the level of the vulva (i.e., between both ovaries).

Monophyly of Enchelidiidae was not supported by our phylogenetic tree, although previous studies by Bik et al. (2010a, b) evidenced monophyly with 95% of bootstrap

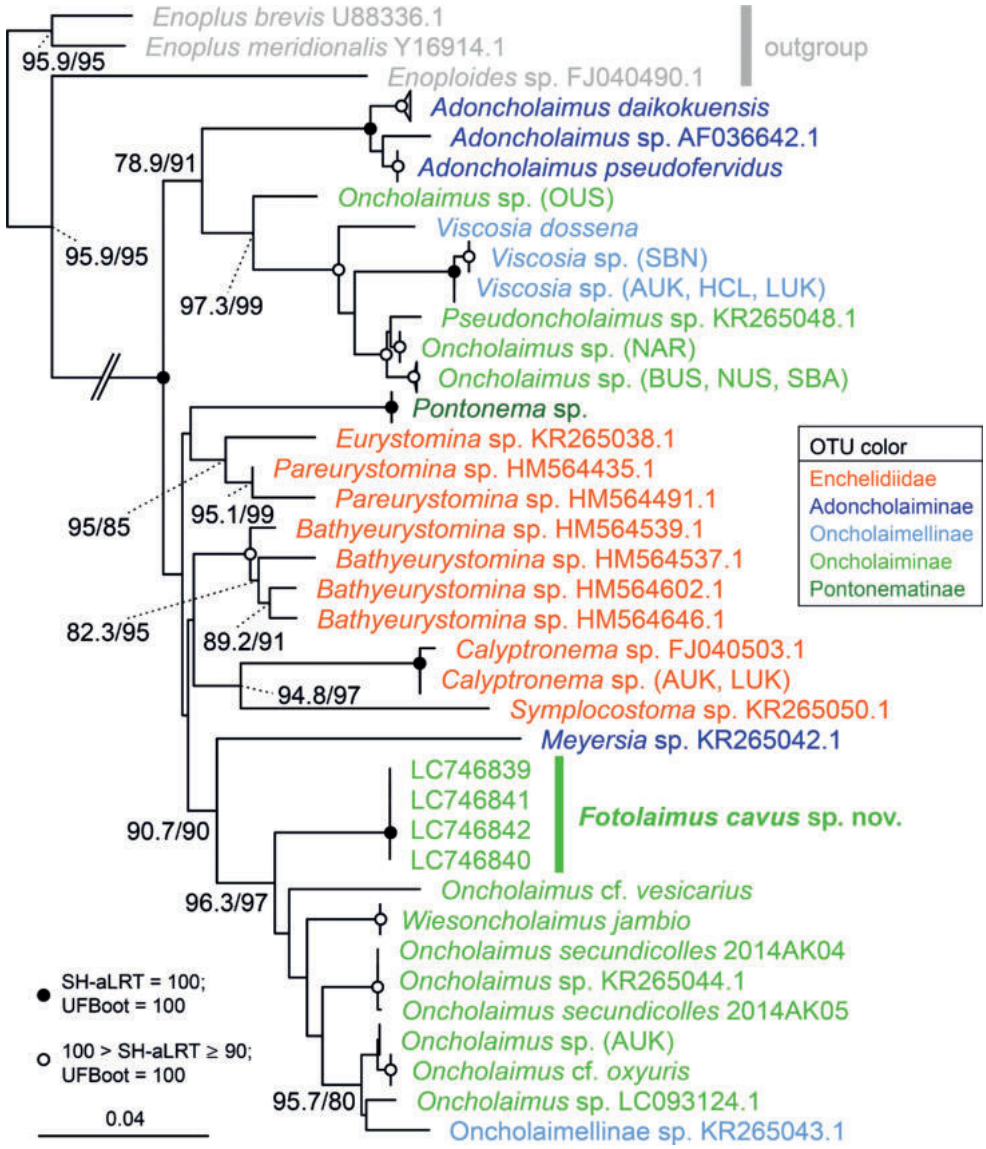

Figure 5. ML tree of Oncholaimoidea based on 18S DNA sequences. Numbers at the nodes are SH-aLRT (left) greater than 70% and UFBoot (right) greater than 80%.

values. Monophyly of the clade comprising *Calyptronema* and *Symplocostoma* was well supported (SH-aLRT = 94.8% and UFBoot = 97%). Both genera present a sexually dimorphic cephalic region, elongated spicules, and papilliform (not winged) precloacal supplements, and have been considered, together with *Symplocostomella* Micoletzky, 1930, which has the same three characteristics, closely related groups within Enchelidiidae. *Pontonema* appeared to be a sister group of the clade consisting of *Eurystomina* and *Pareurystomina* Micoletzky, 1930; however, the support values are quite low (SH-aLRT < 70% and UFBoot < 80%), consequently, the position of *Pontonema* remains uncertain.

Some members of *Oncholaimus* and all members of *Pseudoncholaimus* and *Viscosia* appear to be monophyletic (SH-aLRT = 97.3% and UFBoot = 99%). As aforementioned, *Pseudoncholaimus* is considered a junior synonym of *Oncholaimus*, but both taxa can be distinguished by the presence or absence of Demanian system. Our tree strongly suggested that unidentified *Oncholaimus* spp. was not clustered in a single clade. The species of *Oncholaimus* clustered with *Pseudoncholaimus* might not have a Demanian system. In fact, the species that doubtlessly had a Demanian system (*O. secundicollis*) belonged to a separate clade from *Pseudoncholaimus*. *Fotolaimus* and *Wiesoncholaimus*, suggested to be closely related to *O. secundicollis*, also have a Demanian system. Therefore, there was no evidence supporting the synonymization of *Pseudoncholaimus* with *Oncholaimus*. Because members of *Oncholaimus* (in which the left tooth is the largest) are included in two well-supported clades, which both contain Oncholaimellinae spp. (in which the right tooth is the largest), it is likely that the size of the left and right teeth does not reflect phylogenetic relationships. Additionally, *Wiesoncholaimus*, in which left and right teeth are large, was in the same clade as *Oncholaimus* and *Fotolaimus*, suggesting that the teeth size has evolved independently many times.

In Bik et al. (2010a, b) and Smythe (2015), the phylogenetic position of *Adoncholaimus* within Oncholaimoidea was not clear. Our phylogenetic analysis suggested that

Adoncholaimus is a sister clade of *Oncholaimus–Pseudoncholaimus–Viscosia* clade with a certain degree of support (SH-aLRT = 78.9% and UFBoot = 91%).

Acknowledgements

We wish to thank Hiroki Ichi (Irabu-jima Fishery Cooperative), Masaru Mizuyama (Meio University), Katrine Worsaae (University of Copenhagen), Peter Rask Møller (Natural History Museum Denmark, University of Copenhagen), and Go Tomitani (Diving Service "Marines Pro Miyako") for helping with scuba diving and sampling in the submarine cave. Thanks are also extended to Hiroaki Nakano (Shimoda Marine Research Center, University of Tsukuba), Hisanori Kohtsuka (Misaki Marine Biological Station, the University of Tokyo), and all the other participants to the 7th Japanese Association for Marine Biology (JAMBIO) Coastal Organism Joint Survey for their help in collecting *Wiesoncholaimus jambio*. We would like to thank Enago (https://www.enago.jp/) for the English language review. This study was partly supported by JSPS KAKENHI Grant Numbers JP21K06299 to DS and JP20H03313 to YF and KK.

References

Ahmed M, Roberts NG, Adediran F, Smythe AB, Kocot KM, Holovachov O (2022) Phylogenomic analysis of the phylum Nematoda: Conflicts and congruences with morphology, 18S rRNA, and mitogenomes. Frontiers in Ecology and Evolution 9: e769565. https://doi.org/10.3389/fevo.2021.769565

Aleshin VV, Milyutina IA, Kedrova OS, Vladychenskaya NS, Petrov NB (1998) Phylogeny of Nematoda and Cephalorhyncha derived from 18S rDNA. Journal of Molecular Evolution 47(5): 597–605. https://doi.org/10.1007/PL00006416

Anker A, Fujita Y (2014) On the presence of the anchialine shrimp *Calliasmata pholidota* Holthuis, 1973 (Crustacea: Decapoda: Caridea: Barbouriidae) in Shimoji Island, Ryukyu Islands, Japan. Fauna Ryukyuana 17: 7–11.

Ape F, Arigò C, Gristine M, Genovese L, di Franco A, di Lorenzo M, Baiata P, Aglieri G, Milisenda G, Mirto S (2015) Meiofaunal diversity and nematode assemblages in two submarine caves of a Mediterranean marine protected area. Mediterranean Marine Science 17(1): 202–215. https://doi.org/10.12681/mms.1375

Arunimaand TKA, Mohan PM (2021) Meiofauna from marine and anchialine caves. Journal of the Andaman Science Association 26(2): 131–140.

Belogurov OI, Belogurova LS (1977) Systematics and evolution of Oncholaiminae (Nematoda). I. Significance of the de Manian system. Biologiya Morya [Биология моря] 1977(3): 36–47. [In Russian with English abstract]

Belogurov OI, Belogurova LS (1988) Morphology and systematics of free-living Oncholaimidae (Nematoda: Enoplida: Oncholaimina). Far Eastern Branch of the USSR Academy of Sciences, Vladivostok, 99 pp. [In Russian]

Belogurova LS, Belogurov OI (1974) *Fotolaimus marinus* gen. et sp. n. (Nematoda, Oncholaimidae) from the Schikotan Island (Kuril Islands). Zoologicheskiy jurnal [Зоологический журнал] 53(10): 1566–1568. [In Russian with English abstract]

Bik HM, Lambshead PJD, Thomas WK, Lunt DH (2010a) Moving towards a complete molecular framework of the Nematoda: A focus on the Enoplida and early-branching clades. BMC Evolutionary Biology 10(1): e353. https://doi.org/10.1186/1471-2148-10-353

Bik HM, Thomas WK, Lunt DH, Lambshead PJD (2010b) Low endemism, continued deep-shallow interchanges, and evidence for cosmopolitan distributions in free-living marine nematodes (order Enoplida). BMC Evolutionary Biology 10(1): e389. https://doi.org/10.1186/1471-2148-10-389

Castresana J (2000) Selection of conserved blocks from multiple alignments for their use in phylogenetic analysis. Molecular Biology and Evolution 17(4): 540–552. https://doi.org/10.1093/oxfordjournals.molbev.a026334

Chen CA, Nguyen DT, Smol N (2015) Two new free-living marine nematode species from an intertidal sandy-rocky shore on Pulau Ubin, Singapore with a key to the valid species of the genera *Prooncholaimus* and *Acanthonchus*. The Raffles Bulletin of Zoology (Supplement 31): 68–74.

Cobb NA (1930) The demanian vessels in nemas of the genus *Oncholaimus*; with notes on four new oncholaims. Journal of the Washington Academy of Sciences 20(12): 225–241.

D'Addabbo R, De Leonardis C, Sandulli R, Gallo M (2008) Further studies of meiofauna and tardigrade fauna in two Italian marine protected areas. Biologia Marina Mediterranea 15(1): 262–263.

De Ley IT, De Ley P, Vierstraete A, Karssen G, Moens M, Vanfleteren J (2002) Phylogenetic analyses of *Meloidogyne* small subunit rDNA. Journal of Nematology 34(4): 319–327.

Decraemer W, Coomans A, Baldwin J (2014) Morphology of Nematoda. In: Schmidt-Rhaesa A (Ed.) Handbook of Zoology. Gastrotricha, Cycloneuralia and Gnathifera (Vol. 2). Nematoda. De Gruyter, Berlin and Boston, 1–59. https://doi.org/10.1515/9783110274257.1

Derycke S, Remerie T, Vierstraete A, Backeljau T, Vanfleteren J, Vincx M, Moens T (2005) Mitochondrial DNA variation and cryptic speciation within the free-living marine nematode *Pellioditis marina*. Marine Ecology Progress Series 300: 91–103. https://doi.org/10.3354/meps300091

Díez B, Pedrós-Alió C, Massana R (2001) Study of genetic diversity of eukaryotic picoplankton in different oceanic regions by small-subunit rRNA gene cloning and sequencing. Applied and Environmental Microbiology 67(7): 2932–2941. https://doi.org/10.1128/AEM.67.7.2932-2941.2001

Fujita Y, Naruse T, Yamada Y (2013) Two submarine cavernicolous crabs, *Atoportunus gustavi* Ng & Takeda, 2003, and *Neoliomera cerasinus* Ng, 2002 (Crustacea: Decapoda: Brachyura: Portunidae and Xanthidae), from Shimojijima Island, Miyako Group, Ryukyu Islands, Japan. Fauna Ryukyuana 1: 1–9. [In Japanese with English abstract]

Fujita Y, Mizuyama M, Yamada Y (2017) *Bresilia rufioculus* Komai & Yamada, 2011 (Decapoda: Caridea: Bresiliidae) from a submarine cave in Shimoji-jima Island, Miyako Island Group, southern Ryukyus, Japan. Fauna Ryukyuana 37: 31–33.

García-Valdecasas Huelín A (1985) Estudio faunístico de la cueva submarina ‹‹Túnel de la Atlántida››, Jameos del Agua, Lanzarote. Naturalia Hispanica 27: 1–56.

Gruber AR, Lorenz R, Bernhart SH, Neuböck R, Hofacker IL (2008) The Vienna RNA Websuite. Nucleic Acids Research 36: W70–W74. https://doi.org/10.1093/nar/gkn188

Guindon S, Dufayard JF, Lefort V, Anisimova M, Hordijk W, Gascuel O (2010) New algorithms and methods to estimate maximum-likelihood phylogenies: Assessing the performance of PhyML 3.0. Systematic Biology 59(3): 307–321. https://doi.org/10.1093/sysbio/syq010

Hoang DT, Chernomor O, von Haeseler A, Minh BQ, Vinh LS (2018) UFBoot2: Improving the ultrafast bootstrap approximation. Molecular Biology and Evolution 35(2): 518–522. https://doi.org/10.1093/molbev/msx281

Hodda M (2022) Phylum Nematoda: A classification, catalogue and index of valid genera, with a census of valid species. Zootaxa 5114(1): 1–289. https://doi.org/10.11646/zootaxa.5114.1.1

Hooper DJ (1986) Drawing and measuring nematodes. In: Southey JF (Ed.) Laboratory Methods for Work with Plant and Soil Nematodes (6th Edn.). Her Majesty's Stationery Office, London, 87–94.

Ise Y, Vacelet J, Mizuyama M, Fujita Y (2023) New lithistid sponge of the genus *Sollasipelta* (Porifera, Demospongiae, Tetractinellida, Neopeltidae) from submarine caves of the Ryukyu Islands, southwestern Japan, with redescription of *S. sollasi*. Zootaxa 5285(2): 293–310. https://doi.org/10.11646/zootaxa.5285.2.4

Iwahori H (2014) Senchū kara no DNA chūshutsuhō [DNA extraction methods for nematodes]. In: Mizukubo T, Futai K (Eds) Senchūgaku Jikkenhō [Nematological Experimentation]. Kyoto University Press, Kyoto, 50–55. [In Japanese]

Jensen P (1976) Redescription of the marine nematode *Pandolaimus latilaimus* (Allgen, 1929), its synonyms and relationships to the Oncholaimidae. Zoologica Scripta 5(1–4): 257–263. https://doi.org/10.1111/j.1463-6409.1976.tb00707.x

Kakui K, Fujita Y (2018) *Haimormus shimojiensis*, a new genus and species of Pseudozeuxidae (Crustacea: Tanaidacea) from a submarine limestone cave in Northwestern Pacific. PeerJ 6: e4720. https://doi.org/10.7717/peerj.4720

Kakui K, Fujita Y (2020) *Paradoxapseudes shimojiensis* sp. nov. (Crustacea: Tanaidacea: Apseudidae) from a submarine limestone cave in Japan, with notes on its chelipedal morphology and sexual system. Marine Biology Research 16(3): 195–207. https://doi.org/10.1080/17451000.2020.1720249

Kakui K, Fujita Y (2023) New sea spider species (Pycnogonida: Austrodecidae) from a submarine cave in Japan. Journal of the Marine Biological Association of the United Kingdom 103: E44. https://doi.org/10.1017/S0025315423000322

Kalyaanamoorthy S, Minh BQ, Wong TKF, von Haeseler A, Jermiin LS (2017) ModelFinder: Fast model selection for accurate phylogenetic estimates. Nature Methods 14(6): 587–589. https://doi.org/10.1038/nmeth.4285

Kampfer S, Sturmbauer C, Ott J (1998) Phylogenetic analysis of rDNA sequences from adenophorean nematodes and implications for the Adenophorea-Secernentea controversy. Invertebrate Biology 117(1): 29–36. https://doi.org/10.2307/3226849

Kanzaki N, Futai K (2002) A PCR primer set for determination of phylogenetic relationships of *Bursaphelenchus* species within the *xylophilus* group. Nematology 4(1): 35–41. https://doi.org/10.1163/156854102760082186

Kreis HA (1932) Papers from Dr. Th. Mortensen's Pacific Expedition 1914–16. LXI. Freilebende marine Nematoden von den Sunda-Inseln. II. Oncholaiminae. Videnskabelige Meddelelser fra Dansk naturhistorisk Forening i København 93: 23–69.

Kreis HA (1934) Oncholaiminae Filipjev, 1916. Eine monographische Studie. Capita Zoologica 4(5): 1–271.

Kumar S, Stecher G, Li M, Knyaz C, Tamura K (2018) MEGA X: Molecular evolutionary genetics analysis across computing platforms. Molecular Biology and Evolution 35(6): 1547–1549. https://doi.org/10.1093/molbev/msy096

Leduc D (2013) *Deontostoma tridentum* n. sp. (Nematoda, Leptosomatidae) from the continental slope of New Zealand. Zootaxa 3722(4): 483–492. https://doi.org/10.11646/zootaxa.3722.4.3

Leduc D, Zhao ZQ (2023) The marine biota of Aotearoa New Zealand. Ngā toke o Parumoana: Common free-living Nematoda of Pāuatahanui Inlet, Te Awarua-o-Porirua Harbour, Wellington. NIWA Biodiversity Memoir 135: 1–212.

Lee HJ, Rho HS, Jung J (2015) New record of the genus *Oncholaimus* nematode species (Nematoda: Oncholaimidae) from the East Sea of Korea. Hangug Hwangyeong Saengmul Haghoeji 33(2): 170–176. https://doi.org/10.11626/KJEB.2015.33.2.170

Lemoine F, Correia D, Lefort V, Doppelt-Azeroual O, Mareuil F, Cohen-Boulakia S, Gascuel O (2019) NGPhylogeny.fr: New generation phylogenetic services for non-specialists. Nucleic Acids Research 47(W1): W260–W265. https://doi.org/10.1093/nar/gkz303

Lorenz R, Bernhart SH, Höner zu Siederdissen C, Tafer H, Flamm C, Stadler PF, Hofacker IL (2011) ViennaRNA Package 2.0. Algorithms for Molecular Biology 6: e26. https://doi.org/10.1186/1748-7188-6-26

Lorenzen S (1981) Entwurf eines phylogenetischen Systems der freilebenden Nematoden. Veröffentlichungen des Instituts für Meeresforschung in Bremerhaven (Supplement 7): 1–472.

Mawson PM (1958) Free-living nematodes. Section 3: Enoploidea from Subantarctic stations. British, Australian, and New Zealand Antarctic Research Expedition 1929–1931. Reports Series B. Zoology and Botany 6(14): 309–358.

Meldal BHM, Debenham NJ, De Ley P, De Ley IT, Vanfleteren JR, Vierstraete AR, Bert W, Borgonie G, Moens T, Tyler PA, Austen MC, Blaxter ML, Rogers AD, Lambshead PJD (2007) An improved molecular phylogeny of the Nematoda with special emphasis on marine taxa. Molecular Phylogenetics and Evolution 42(3): 622–636. https://doi.org/10.1016/j.ympev.2006.08.025

Milovankina AA, Fadeeva NP (2019) Spatial distribution of nematode communities along the salinity gradient in the two estuaries of the Sea of Japan. Russian Journal of Nematology 27(1): 1–12.

Minh BQ, Schmidt HA, Chernomor O, Schrempf D, Woodhams MD, von Haeseler A, Lanfear R (2020) IQ-TREE 2: new models and efficient methods for phylogenetic inference in the genomic era. Molecular Biology and Evolution 37: 1530–1534. https://doi.org/10.1093/molbev/msaa015

Mizuyama M, Kudo H, Fujita Y (2022) Discovery of living *Chama cerion* Matsukuma, Paulay & Hamada, 2003 (Mollusca: Bivalvia: Chamidae) from submarine caves in the Ryukyu Islands, southwestern Japan. Fauna Ryukyuana 64: 65–73.

Mullin PG, Harris TS, Powers TO (2005) Phylogenetic relationships of Nygolaimina and Dorylaimina (Nematoda: Dorylaimida) inferred from small subunit ribosomal DNA sequences. Nematology 7(1): 59–79. https://doi.org/10.1163/1568541054192199

Nation JL (1983) A new method using hexamethyldisilazane for preparation of soft insect tissues for scanning electron microscopy. Stain Technology 58(6): 347–351. https://doi.org/10.3109/10520298309066811

Okanishi M, Fujita Y (2018) A new species of *Ophioconis* (Echinodermata: Ophiuroidea) from Ryukyu Islands, southwestern Japan. Proceedings of the Biological Society of Washington 131(1): 163–174. https://doi.org/10.2988/18-00001

Okanishi M, Fujita Y (2019) A comprehensive taxonomic list of brittle stars (Echinodermata: Ophiuroidea) from submarine caves of the Ryukyu Islands, southwestern Japan, with a description of a rare

species, *Dougaloplus echinatus* (Amphiuridae). Zootaxa 4571(1): 73–98. https://doi.org/10.11646/zootaxa.4571.1.5

Onorato M, Belmonte G (2017) Submarine caves of the Salento pensinsula: faunal aspects. Thalassia Salentin 39: 47–72. https://doi.org/10.1285/i15910725v39p47

Osawa M, Fujita Y (2016) Stomatopods and decapods of Axiidea, Gebiidea and Anomura (Crustacea: Malacostraca) from Irabu-jima and Shimojijima Islands, Miyako Group, southern Ryukyus, Japan. Fauna Ryukyuana 28: 37–56. [In Japanese with English abstract]

Osawa M, Fujita Y (2019) Submarine cave hermit crabs (Crustacea: Decapoda: Anomura: Paguroidea) from three islands of the Ryukyu Islands, southwestern Japan. Zootaxa 4560(3): 463–482. https://doi.org/10.11646/zootaxa.4560.3.3

Pereira TJ, Fonseca G, Mundo-Ocampo M, Guilherme BC, Rocha-Olivares A (2010) Diversity of free-living marine nematodes (Enoplida) from Baja California assessed by integrative taxonomy. Marine Biology 157(8): 1665–1678. https://doi.org/10.1007/s00227-010-1439-z

Pereira TJ, De Santiago A, Schuelke T, Hardy SM, Bik HM (2020) The impact of intragenomic rRNA variation on metabarcoding-derived diversity estimates: A case study from marine nematodes. Environmental DNA 2(4): 519–534. https://doi.org/10.1002/edn3.77

Platt HM, Warwick RM (1983) Free-living Marine Nematodes. Part I. British Enoplids. Cambridge University Press, Cambridge, 307 pp.

Pérez-García JA, Díaz-Delgado Y, García-Machado E, Martínez-García A, Gonzalez BC, Worsaae K, Armenteros M (2018) Nematode diversity of freshwater and anchialine caves of western Cuba. Proceedings of the Biological Society of Washington 131(1): 144–155. https://doi.org/10.2988/17-00024

Rachor E (1969) Das de Mansche Organ der Oncholaimidae, eine genito-intestinale Verbindung bei Nematoden. Zoomorphology 66(2): 87–166. https://doi.org/10.1007/BF00277650

Riera R, Monterroso Ó, Núñez J, Martínez A (2018) Distribution of meiofaunal abundances in a marine cave complex with secondary openings and freshwater filtrations. Marine Biodiversity 48(1): 203–215. https://doi.org/10.1007/s12526-016-0586-y

Saito T, Fujita Y (2022) A new shrimp of the genus *Odontozona* Holthuis, 1946 (Decapoda: Stenopodidea: Stenopodidae) from a submarine cave of the Ryukyu Islands, Indo-West Pacific. Zootaxa 5175(4): 439–452. https://doi.org/10.11646/zootaxa.5175.4.2

Salma J, Nasira K, Saima M, Shahina F (2017) Morphological and molecular identification of four new species of marine nematodes. Pakistan Journal of Nematology 35(2): 113–150. https://doi.org/10.18681/pjn.v35.i02.p113-150

Shimada D, Suzuki AC, Tsujimoto M, Imura S, Kakui K (2021) Two new species of free-living marine nematodes (Nematoda: Axonolaimidae and Tripyloididae) from the coast of Antarctica. Species Diversity 26(1): 49–63. https://doi.org/10.12782/specdiv.26.49

Smol N, Muthumbi A, Sharma J (2014) Order Enoplida. In: Schmidt-Rhaesa A (Ed.) Handbook of Zoology. Gastrotricha, Cycloneuralia and Gnathifera (Vol. 2). Nematoda. De Gruyter, Berlin and Boston, 193–249. https://doi.org/10.1515/9783110274257.193

Smythe AB (2015) Evolution of feeding structures in the marine nematode order Enoplida. Integrative and Comparative Biology 55(2): 228–240. https://doi.org/10.1093/icb/icv043

Smythe AB, Holovachov O, Kocot KM (2019) Improved phylogenomic sampling of free-living nematodes enhances resolution of higher-level nematode phylogeny. BMC Evolutionary Biology 19(1): e121. https://doi.org/10.1186/s12862-019-1444-x

Talavera G, Castresana J (2007) Improvement of phylogenies after removing divergent and ambiguously aligned blocks from protein sequence alignments. Systematic Biology 56(4): 564–577. https://doi.org/10.1080/10635150701472164

Tanaka R, Kikchi T, Aikawa T, Kanzaki N (2012) Simple and quick methods for nematode DNA preparation. Applied Entomology and Zoology 47(3): 291–294. https://doi.org/10.1007/s13355-012-0115-9

Tchesunov AV, Mokievsky VO, Nguyen VT (2010) Three new free-living nematode species (Nematoda, Enoplida) from mangrove habitats of Nha Trang, Central Vietnam. Russian Journal of Nematology 18(2): 155–172.

Tsalolikhin SY (2015) *Pseudoncholaimus spartacus* sp. n. (Nematoda, Enoplida, Oncholaimidae) from western India. Zoologicheskiy jurnal [Зоологический журнал] 94(8): 985–988. https://doi.org/10.7868/S0044513415080164 [In Russian with English abstract]

van Megen H, van den Elsen S, Holterman M, Karssen G, Mooyman P, Bongers T, Holovachov O, Bakker J, Helder J (2009) A phylogenetic tree of nematodes based on about 1200 full-length small subunit ribosomal DNA sequences. Nematology 11(6): 927–950. https://doi.org/10.1163/156854109X456862

Wieser W (1953) Reports of the Lund University Chile Expedition 1948–1949. 10. Free-living marine nematodes. I. Enoploidea. Acta Universitatis Lundensis. Nova Series. Andra Afdelningen 49(6): 1–155.

Wieser W (1954) Beiträge zur Kenntnis der Nematoden submariner Höhlen. Ergebnisse der österreichischen Tyrrhenia-Expedition 1952, Teil II. Österreichische Zoologische Zeitschrift 5: 172–230.

Wieser W (1955) A collection of marine nematodes from Japan. Publications of the Seto Marine Biological Laboratory 4(2–3): 159–181. https://doi.org/10.5134/174529

Wieser W (1959) Free-living Nematodes and Other Small Invertebrates of Puget Sound Beaches. University of Washington Press, Seattle, 179 pp.

Worsaae K, Hansen MJ, Axelsen O, Kakui K, Møller PR, Osborn KJ, Martínez A, Gonzalez BC, Miyamoto N, Fujita Y (2021) A new cave-dwelling genus and species of Nerillidae (Annelida) from the Ryukyu Islands, Japan. Marine Biodiversity 51(4): e67. https://doi.org/10.1007/s12526-021-01199-4

Yoder M, Tandingan De Ley I, King IW, Mundo-Ocampo M, Mann J, Blaxter M, Poiras L, De Ley P (2006) DESS: A versatile solution for preserving morphology and extractable DNA of nematodes. Nematology 8(3): 367–376. https://doi.org/10.1163/156854106778493448

Yoshimura K (1982) Free-living marine nematodes from Kii Peninsula. II. Publications of the Seto Marine Biological Laboratory 27(1–3): 133–142. https://doi.org/10.5134/176043

Zhang ZN, Platt HM (1983) New species of marine nematodes from Qingdao, China. Bulletin of the British Museum (Natural History). Bulletin of the British Museum, Natural History. Zoology 45(5): 253–261. https://doi.org/10.5962/p.28001

Zhou H, Zhang Z (2003) New records of freeliving marine nematodes from Hong Kong, China. Journal of the Ocean University of Qingdao 2(2): 177–184. https://doi.org/10.1007/s11802-003-0048-6

Zhou H, Zhang ZN (2008) Nematode assemblages from submarine caves in Hong Kong. Journal of Natural History 42(9–12): 781–795. https://doi.org/10.1080/00222930701850448

Zoosyst. Evol. 99 (2) 2023, 535–543 | DOI 10.3897/zse.99.110610

PENSOFT

für Natur MUSEUM FÜR NATURKUNDE BERLIN

The Caucasus is neither a cradle nor a museum of diversity of the land snail genus *Helix* (Gastropoda, Stylommatophora, Helicidae), while Crimea is home to an ancient lineage

Ondřej Korábek[1,2], Igor Balashov[3], Marco T. Neiber[4], Frank Walther[4], Bernhard Hausdorf[1,4]

1 *Leibniz Institute for the Analysis of Biodiversity Change, Zoological Museum, Martin-Luther-King-Platz 3, 20146 Hamburg, Germany*
2 *Department of Zoology, Faculty of Science, Charles University, Viničná 7, 12844 Praha 2, Czech Republic*
3 *Schmalhausen Institute of Zoology, National Academy of Sciences of Ukraine, B. Khmelnitsky str. 15, Kyiv 01030, Ukraine*
4 *Universität Hamburg, Martin-Luther-King-Platz 3, 20146 Hamburg, Germany*

https://zoobank.org/7F4E305A-A732-470C-AEB5-58F5E58605BF

Corresponding author: Ondřej Korábek (ondrej.korabek@gmail.com)

Academic editor: Frank Köhler ♦ **Received** 6 August 2023 ♦ **Accepted** 10 October 2023 ♦ **Published** 15 November 2023

Abstract

The Caucasus and the adjacent Pontic Mountains in north-eastern Anatolia are home to numerous endemic land snail genera and species. The diversity of the region is the result of both intra-regional speciation and the persistence of relict lineages. The same seemed to be true for the genus *Helix*, which has been present in the Greater Caucasus since the Miocene. In the Caucasus region, there are three *Helix* species. *Helix buchii* (Pontic Mountains and Georgia) and *Helix albescens* (southern Ukraine to northern Lesser Caucasus) are both separated by deep splits from the major *Helix* clades in the mitochondrial phylogeny. In contrast, *Helix lucorum* belongs to the Anatolian radiation of *Helix*. At least part of its intraspecific diversification may have occurred in north-eastern Anatolia and the adjacent parts of the Caucasus. Here, we report new evidence suggesting that the Caucasus and the Pontus regions were less important as a refugium of ancient *Helix* lineages or as a diversification centre than previously hypothesised. *Helix lucorum* probably diversified more westwards, while *H. buchii* is a less ancient lineage than previously thought. *Helix albescens* had its long-term refugium on the Crimean Peninsula in southern Ukraine, not in the Caucasus. The Caucasus is close to the eastern limit of the distribution range of the genus and, although the fossil record shows that *Helix* was present there as early as the Miocene, the current diversity of the genus there is the result of much later colonisation.

Key Words

Anatolia, fossil, land snail, phylogeography, refugia, Ukraine

Introduction

The Caucasus ecoregion (Zazanashvili et al. 2020) is one of the global biodiversity hotspots, areas of high endemic diversity threatened by ongoing habitat loss (Myers et al. 2000; Marchese 2015). Mountainous topography and climatic stability can explain accumulation of diversity (Harrison and Noss 2017; Rahbek et al. 2019) and these two factors combine in the region. There are high mountains and there are climatic refugia as well. For example, some representatives of the late Neogene woody flora (Browicz 1989; Denk et al. 2001; Nakhutsrishvili et al. 2015; Magri et al. 2017; Maharramova et al. 2018), as well as some endemic land snails (Pokryszko et al. 2011; Walther et al. 2014; Neiber and Hausdorf 2017; Neiber et al. 2017; Mumladze et al. 2023) and other taxa (Tarkhnishvili et al. 2000), survived in the Colchis refugium in the eastern part of the Euxine floristic province of humid temperate forests, which extends along the southern Black Sea coast to the western Greater Caucasus (Browicz 1989). Quaternary glacial forest refugia extended from the western Caucasus along northern Anatolia approximately to Ordu in northern Turkey (Tarkhnishvili et al. 2012).

Phylogenetic relationships between some Pontic land snail taxa on the one hand and those from southern Anatolia on the other hand suggest that the Pontic region contains relicts of lineages that were eliminated in central Anatolia by the uplift and aridification of the Anatolian Plateau and its surrounding mountain ranges (Neiber and Hausdorf 2017; Neiber et al. 2021). The uniqueness of the land snail fauna of the Caucasus and the adjacent Pontus Mountains (north-eastern Turkey) is demonstrated by the many species and genera that occur only in the easternmost part of the Pontic Mountains, especially on the northern seaward side around Artvin (Cook 1997; Schütt 2005). Other unique lineages live in the Greater Caucasus (e.g. Walther et al. (2018)). In light of this, the presence of two species of the genus *Helix* without close relatives in the Caucasus and Pontus regions seemed to add to the list of ancient lineages preserved in this long-term refugium (Korábek et al. 2015), the more that there are Micoene and Pliocene *Helix* fossils in the Greater Caucasus (Steklov 1966). The first, *Helix buchii* Dubois de Montpéreux, 1840, is mainly distributed in the Pontus Mountains and in Georgia. The available data suggest that the diversity of mitochondrial lineages is greatest in the western part of its range (Korábek et al. 2022). The other species, *Helix albescens* Rossmässler, 1839 is widely distributed in the Greater Caucasus and southern Ukraine, as far west as Odesa Oblast. Until recently, the species was thought to live as far west as Bulgaria (e.g. Irikov and Erőss (2008)), but this was based on misidentifications (Korábek et al. 2022) and the confusion with *Helix philibinensis* Rossmässler, 1839 (as in Schileyko 1978). The distribution of its intraspecific genetic diversity is unknown.

In addition to the two possibly relictual species, there is a third *Helix* species in the Caucasus, *Helix lucorum* Linnaeus, 1758. It is distributed all over the Caucasus region, Anatolia and the southern Balkan Peninsula. The occurrence of most of the main intraspecific mitochondrial clades in the Caucasus region or adjacent north-eastern Anatolia, with endemic clades in the south-eastern Caucasus (Korábek et al. 2022) may indicate an origin of the species in north-eastern Anatolia or the Caucasus. It was hypothesised that the Pontus region could be a source region of its Holocene expansion to the western Caucasus as well as to the Balkans (Korábek et al. 2018).

Based on our expanded sampling, we tested the hypothesis that the Caucasus region and the Pontic Mountains were the area where the intraspecific diversity of *H. lucorum* originated and that the other two species are old, phylogenetically isolated lineages that persisted in the Caucasus (*H. albescens*) or the Pontic Mountains (*H. buchii*).

Methods

Partial sequences of the mitochondrial genes for cytochrome c oxidase subunit I (*cox1*), 16S rRNA (*rrnL*) and 12S rRNA (*rrnS*) were analysed. Laboratory methods were as described in Korábek et al. (2022) with some modifications. DNA was extracted as described by Scheel and Hausdorf (2012). The primers 16Sar, 16Sbr (Palumbi et al. 1991), 16S_MN3R (Neiber et al. 2017), 16Scs1 and 16Scs2 (Chiba 1999) were used for amplification and sequencing of the *rrnL* gene, a modified pair LCO1490 and HCO2198 (Hausdorf et al. 2003) for *cox1* and 12SGast_fwd2 and 12SGast_rev3 (Cadahía et al. 2014) for the *rrnS*. Internal primers were designed for PCR and sequencing of *cox1* in a number of *H. buchii* samples: COI_buchii_F: TATTTGGCGTGTGATGTGGC, COI_buchii_R: TAATAGCTCCGGCCAAAACA.

The new data were combined with previously published sequences (Korábek et al. 2022 and references therein). Only seven samples of *H. albescens*, one of them from outside its autochthonous distribution range (Bulgaria), have been analysed previously (Korábek et al. 2022); we added 40 more from 15 additional localities within the presumed native range and two from introduced populations in Ukraine (Kyiv, Poltava). For *H. buchii*, we analysed 57 (27 new) individuals from 32 (13 new) localities (Fig. 1B). Finally, 91 newly-added individuals from 88 sites were analysed for *H. lucorum*, mainly from south-eastern Balkans and the Caucasus region. All the sequences used are listed, along with locality information, in Suppl. material 1: table S1.

Alignments were done with MAFFT 7.487 (E-INS-i algorithm; Katoh and Standley (2013)). Substitution model selection was performed with IQ-TREE 1.6.12 (Nguyen et al. 2015; Kalyaanamoorthy et al. 2017; partitioning into 3 *cox1* codon positions and the two rRNA genes). Concatenated alignments of *cox1*, *rrnL* and, in *H. buchii*, *rrnS* sequences were analysed with BEAST 1.10.4 (Suchard et al. 2018) for each species separately. *Helix nicaeensis* Férussac, 1821, the sister species of *H. lucorum*, was used as an outgroup for *H. lucorum*; the other two species lack close relatives. BEAST was used to produce ultrametric trees where comparably old clades may be defined. Tree prior was set to Bayesian Skyline (a flexible prior not imposing strong constraints on the distribution of branch lengths), using a lognormal relaxed clock and no calibration. However, we specified the same mean rate for all species for approximate comparability. We ran the analyses in two replicates and collected a total of 10,000 post-burn-in trees for each of the three analysed species, making sure that effective sample sizes were > 800 for all parameters, except the skyline model.

PCR and sequencing with the primer pair LCO1490 and HCO219 targeting the "barcoding" fragment of *cox1* produced for two *H. buchii* individuals an incomplete pseudogene sequence containing an in-frame stop codon and frame-shift indels. Two phylogenetically distant mitochondrial lineages are known from *H. buchii*, one of which was probably acquired from an unknown, possibly extinct species (Korábek et al. 2015). A phylogenetic analysis of the pseudogene could reveal which of the mitochondrial lineages is more likely to be the original one for *H. buchii*. We used a representative set of *Helix* and *Maltzanella* Hesse, 1917 *cox1* and *rrnL* sequences

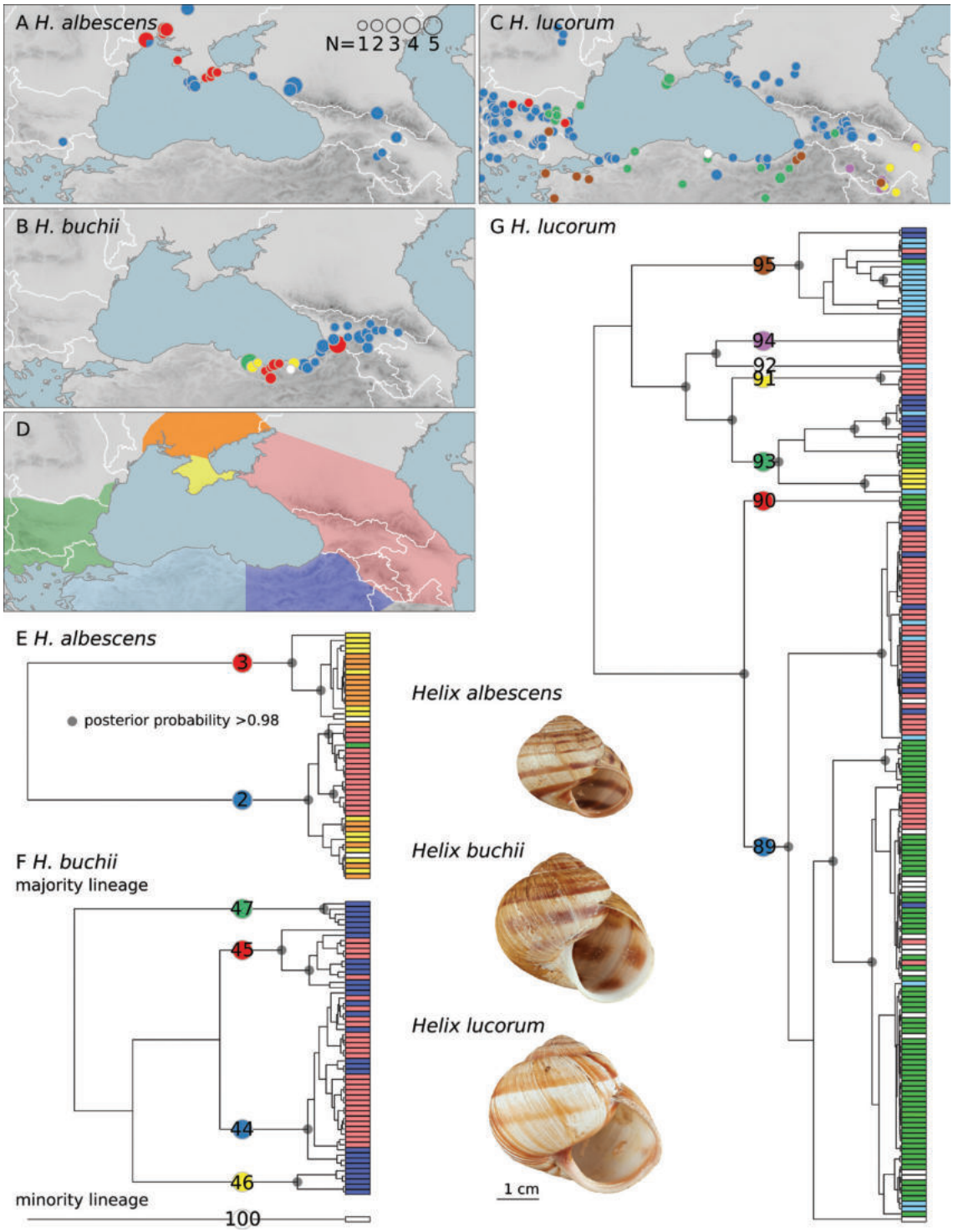

Figure 1. Intraspecific mitochondrial lineages of the Caucasian *Helix* species and their distribution. **A–C.** Distribution of major clades (i.e. the branches labelled with correspondingly coloured circles in the trees). Non-native or potentially non-native occurrences are not distinguished. **A.** *H. albescens*; **B.** *H. buchii*; **C.** *H. lucorum*; **D.** Classification of the discussed regions: southern Ukraine (mainland, orange), Crimea (yellow), the Caucasus region (red), eastern and western part of Anatolia (dark and light blue) and the Balkans (green). The east-west division of Anatolia is for plotting purposes only and coincides with the western distribution limit of *H. buchii*, which also marks the limit of the wettest area of the Pontic Mountains; **E–G.** Bayesian mitochondrial trees based on concatenated alignments of partial *rrnL*, *rrnS* (only in *H. buchii*) and *cox1* sequences. Supported nodes are indicated by small circles at nodes (omitted from the shallowest nodes), large circles on branches denote the clades used for plotting the maps along with the corresponding numbers of the clades as given in Korábek et al. (2022). Tips are labelled with colour indicating the area of origin as in D (samples from outside the covered area are coloured white). The species are illustrated by shells from Georgia: Patara Dmanisi (*H. buchii*, ZMH 100320), Armenia: Gegha Valley by Kavchut (*H. lucorum*, ZMH 101308) and Russia: Kamennomostkiy in Adygea (*H. albescens*, ZMH 86704).

(from a dataset used by Korábek et al. (2022): fig 3) to analyse the phylogenetic position of the *cox1* nuclear pseudogene sequences obtained from *H. buchii* (merged for the analysis into a single sequence at their 404 bp overlap). The sequences used are listed in Suppl. material 1: table S2. The merged pseudogene sequence was added manually to the alignment from Korábek et al. (2022) and the data were analysed with Maximum Likelihood phylogenetic analysis in IQ-TREE following partitioning and automated model selection as above. The support was assessed with 500 bootstraps.

The sequence data underlying this article are available from the NCBI Nucleotide database (available at: www.ncbi.nlm.nih.gov/Genbank). Accession numbers are provided in the online supplementary material along with sampling localities and voucher information.

Results

Helix albescens Rossmässler, 1839

We found two major clades, each of them with only shallow internal divergences (Fig. 1E). Only one was found in the Caucasus, but both are present in southern Ukraine. In the Crimean Mountains, the two clades are parapatric, one occurring in the west and the other in the east. The eastern clade has its basal-most haplotype there. The western clade is surprisingly the one found also in the Caucasus. We observed three groups of haplotypes in this clade, one (without strong support) in southern Ukraine inclusive of Crimea and the other two on the southern (Georgia, Armenia) and northern (Russia) side of the Greater Caucasus, respectively.

Helix buchii Dubois de Montpéreux, 1840

Two divergent lineages have been found in *H. buchii*. All but one of the analysed individuals yielded haplotypes belonging to the 'majority lineage', which is deeply separated from the major *Helix* radiations (Figs 1F, 2). The data show generally low intraspecific diversity in Georgia, whereas multiple lineages including the 'minority lineage', which is likely the sister lineage of *Helix pathetica* Mousson, 1854 within the Anatolian radiation of *Helix* (Fig. 2), were found in north-eastern Turkey. The oldest split of the majority lineage separated a clade (47 as numbered by Korábek et al. (2022); Fig. 1F) from the westernmost sampling site from all other haplotypes. Almost all Georgian samples are closely related to each other and the adjacent eastern Turkish samples. An exception to these are samples from the Goderdzi Pass in south-western Georgia (Mumladze et al. 2013), which were described as *Helix goderdziana* Mumladze, Tarkhnishvili & Pokryszko, 2008, sharing a mitochondrial lineage (45) with some individuals from the west of the species range.

Partial, but overlapping *cox1* pseudogene sequences, were obtained from two individuals (GenBank accessions: isolate SP2 OQ148366, isolate 6916 OQ148367). These samples otherwise yielded haplotypes of the clades 44 and 45 of the majority lineage. Phylogenetic analysis placed the pseudogene sequences into the Anatolian clade of *Helix* (Korábek et al. 2015), along with the sole sample of the minority mitochondrial lineage collected near Sümela Monastery in Turkey (Fig. 2).

Helix lucorum Linnaeus, 1758

In Armenia and Azerbaijan, all but one sample (from Tatev Monastery, Armenia) yielded haplotypes from two co-occurring clades (Fig. 1G), which as yet have not been found elsewhere, while almost all samples from Georgia and Russia belong to an unrelated clade that is otherwise distributed in northern Anatolia and accounts also for the majority of the occurrences in the Balkans, as well as introduced populations in various parts of Europe. This widespread intraspecific clade (number 89 in Korábek et al. (2022), blue in the map in Fig. 1C), is associated with conical to flattened conical shells in contrast to more globular ones typical for more southerly populations in Anatolia and the Lesser Caucasus (Korábek et al. 2018).

The haplotypes of the clade 89 form four well-supported groups. One of them was found only in a non-native sample from Spain, but one was recorded so far only in the eastern Balkans and none of the remaining two is unique to the Caucasus and Pontus. Furthermore, there are nearly identical haplotypes (1 bp difference over 1469 bp of the *rrnL+cox1* alignment) in the Caucasus on the one hand and the eastern Balkans on the other hand. The sister lineage of the whole clade (red in Fig. 1C) was found exclusively in the eastern Balkans.

Populations with globular shells, which share mitochondrial clade 93 (green in Fig. 1C), are widespread in northern Anatolia, but are also found in Crimea and north-eastern Bulgaria. The geographically isolated populations of this lineage in Bulgaria differ in shell shape and colouration from the majority of Bulgarian *H. lucorum*.

Discussion

Helix albescens Rossmässler, 1839

Both major mitochondrial clades within *H. albescens* occur in the Crimean Mountains and the lowlands of southern Ukraine, while only one of them occurs in the Caucasus (Fig. 1A). It is possible that *H. albescens* was present in the Caucasus already before the Last Glacial, as we found some differentiation of Caucasian populations on both sides of the Greater Caucasus ridge. However, it is unlikely that *H. albescens* has persisted in the Caucasus for an extended period of time. Instead, the Crimean Mountains, where its two main clades appear

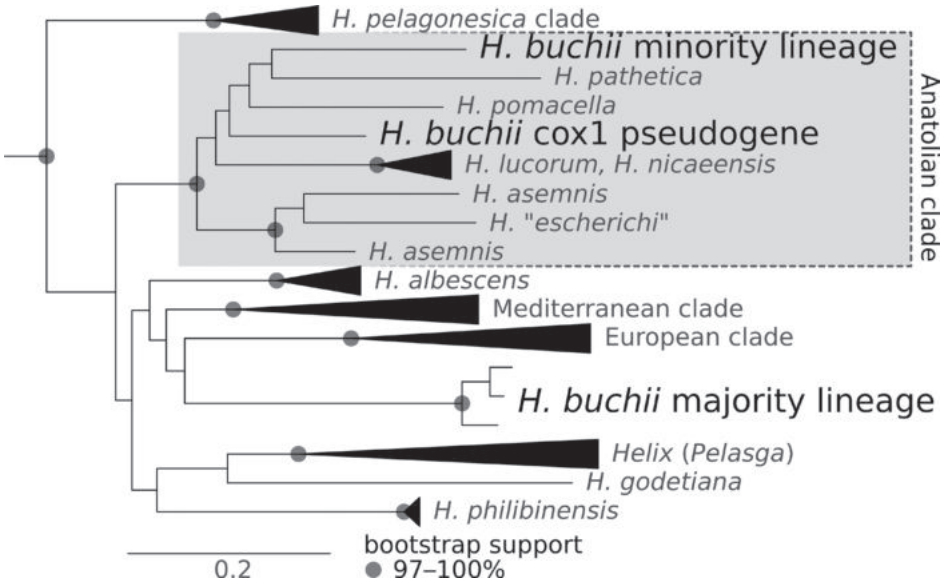

Figure 2. Maximum Likelihood tree based on *rrnL* and *cox1* sequences showing the relationships of *H. buchii*. Both mitochondrial lineages and the *cox1* pseudogene (presumed NUMT) sequence obtained from two of its individuals with the majority lineage mitochondrion are included. The samples listed in Suppl. material 1: table S2 were used; the tree is rooted with *Maltzanella* (not shown). Support values were obtained by standard bootstrapping.

to be parapatric (in contrast to the rest of Ukraine) are the most probable long-term refugium. The Crimean Mountains show some biogeographic affinities with the western Caucasus (Cameron et al. 2013; Turbanov and Balashov 2015; Neiber and Hausdorf 2017), but were a glacial refugium in their own right (e.g. Kukushkin et al. (2020)) and host a number of endemic land snail species and genera (Hausdorf 1994; Balashov and Baidashnikov 2013; Cameron et al. 2013; Balashov 2014, 2016; Neiber et al. 2019). The long-term stronghold of *H. albescens* in southern Crimea supported by our data, therefore, corresponds to known patterns. Furthermore, within Ukraine, the variability in shell shape was found to be the greatest in Crimea (Kramarenko 2016) and the diversity of banding patterns is greater in the Crimean Mountains than in the Crimean lowlands (Kramarenko and Leonov 2011).

The extent of the native distribution of *H. albescens* on the East European Plain is unclear. It is relatively continuously distributed across the steppe ecoregion of southern Ukraine and in adjacent regions of Russia south to the Caucasus, both in natural and transformed habitats. In Ukraine, there are no Quaternary fossil records of this species outside Crimea (Balashov 2016: 85). Since at least 2006, *H. albescens* has been present in Kyiv, central Ukraine, marking the first case of an evident invasion outside its native range far from its continuous distribution. Since then, it has also reached several other settlements in central and eastern Ukraine. Thus, *H. albescens* is now spreading northwards and it is possible that much of its distribution in the East European Plain is the result of recent expansion, possibly largely human-assisted. Similarly, several other stylommatophoran gastropods that originated or were isolated for a long time in the Crimean Mountains have relatively recently spread to the southern part of the East European Plain. To what extent this range extension is anthropogenic remains unclear. In particular, this applies to *Brephulopsis cylindrica* (Menke, 1828) (Enidae), *Helicopsis filimargo* (Krynicki, 1833) (Geomitridae) and *Monacha fruticola* (Krynicki, 1833) (Hygromiidae) (Balashov 2016; Neiber and Hausdorf 2017; Balashov et al. 2021). All these species, along with *H. albescens*, form a group of inhabitants of dry open and semi-open habitats that spread to the south of the East European Plain postglacially from Crimea and anthropogenic factors allow for continuation of this expansion.

Helix buchii Dubois de Montpéreux, 1840

Korábek et al. (2015) found two divergent mitochondrial lineages within *H. buchii*. One sample from Sümela (Trabzon Province of Turkey) yielded a lineage belonging to a group of largely Anatolian species ("Anatolian clade" sensu Korábek et al. (2015)). However, all other samples yielded a different, highly divergent lineage with no relatives and unaffiliated with any major clade within the genus. The majority lineage indicates that *H. buchii* could be an old species persisting in a long term refugium from the Neogene. One or the other lineage might be the result of an introgression from another species, but the source of the introgression remained unclear because neither lineage is closely related to other known extant species. It is unlikely that one of them is a nuclear pseudogene (NUMT), because the results for the *rrnL* and *cox1* genes were replicated here also with the *rrnS* gene, which is in Helicidae located in a different part of the mitogenome and coded on the other strand (Terrett et al. 1996; Groenenberg et al. 2012; Gaitán-Espitia et al. 2013; Korábek et al. 2019).

Based on the distribution of individual clades from the majority lineage, *Helix buchii* did not originate in the Caucasus hotspot or the centre of land snail diversity in the mountains around Artvin in Turkey. The data show generally low intraspecific diversity in Georgia, whereas multiple lineages (including the minority lineage) were found in north-eastern Turkey. Our results obtained with improved sampling thus confirm earlier observations (Mumladze et al. 2013; Korábek et al. 2022). The origins of *H. buchii* can be traced to the western part of the Eastern Pontic Mountains and the additional data confirm that its current presence in the Caucasus is the result of a recent range expansion from the west.

The phylogenetic placement of the *cox1* pseudogene (presumed NUMT) sequenced here in the Anatolian clade indicates that the minority mitochondrial lineage is the original mitochondrial lineage of *H. buchii*. This means that *H. buchii* is younger and less isolated than suggested by the sequence data representing the majority mitochondrial lineage. The origin of the majority lineage remains unclear. Perhaps the inferred early branching is an artefact caused by its long branch. In any case, the closest relatives of *H. buchii* appear to be species from the northwest of Anatolia.

Helix lucorum Linnaeus, 1758

With two sympatric lineages restricted to the south-eastern Caucasus region (Azerbaijan, Armenia, adjacent Iran), the species is not a complete newcomer to the area, although it is still only a very young group in the context of the *Helix* phylogeny (Korábek et al. 2022). However, the phylogenetic relationships of these two lineages suggest that they originated in Anatolia. The sister lineages of both are found there, one of them being distributed all over the north of Anatolia. As the sister group of *H. lucorum*, *Helix nicaeensis*, lives in north-western Anatolia, the likelihood that the species diversified near the Caucasus region seems low and the two endemic lineages are likely the result of an earlier, pre-Holocene colonisation.

The geographic origin of the widespread clade 89 (see Fig. 1C, G), which with one exception accounts for the distribution of *H. lucorum* in Russia and Georgia, is unclear, as sampling of Anatolia remains inadequate and the distribution ranges of the *H. lucorum* lineages are likely to have been affected by anthropogenic translocations. Mumladze (2015) raised reasonable doubts as to whether *H. lucorum* is native to Georgia and the new data add to these. The fact that the sister clade of clade 89 has, so far, been found only in Bulgaria suggests that the origin of this clade is located more westerly than the Pontus region, which was previously suggested as its area of origin (Korábek et al. 2018). Korábek et al. (2018) found one haplotype group in this clade to be unique to the Pontus Mountains and Georgia (apart from an introduced population in Moscow), but it is now also known from localities in the Provinces of Tokat and Sakarya, i.e. westwards up to the westernmost Anatolia. Very similar haplotypes at the western and eastern extremes of the range of clade 89 (i.e. eastern Balkans versus the western Caucasus), given the distance, suggest human-mediated dispersal in at least one direction, although natural dispersal cannot be excluded at present.

The current distribution of different *H. lucorum* lineages within the species' range is influenced by anthropogenic translocations (Korábek et al. 2018). The occurrence near the Tatev Monastery in Armenia could be such a case, as the lineage present there differs from the regional background. Similarly, globular-shelled populations of clade 93 (green in Fig. 1C, G) were found in north-eastern Bulgaria in an area disconnected from the main range of the clade in Anatolia. The presence of clade 93 in Crimea (a globular form previously separated as *H. lucorum taurica* Krynicki, 1833; see Korábek et al. (2018)) is also most easily explained by introduction (Korábek et al. 2018). The most conchologically similar individuals have so far been found in north-western Anatolia in the provinces of Bolu and Kastamonu. It is likely that translocations have also occurred within Anatolia. The co-occurrence of several lineages in a region must, therefore, be interpreted with caution, as they may have been brought together by humans, especially if samples come from synanthropic habitats.

Conclusion

It is likely that *Helix buchii* is not an ancient and isolated lineage of *Helix* in the Caucasus region, but part of a group of species that diversified in Anatolia (the 'Anatolian clade' of Korábek et al. (2015)). Our new data suggest that the species originated in the Pontus region in northern Anatolia and colonised the Caucasus region relatively recently. *Helix albescens* has also not been present in the Caucasus region for a long time, as its crown group probably originated in Crimea. The third Caucasian species, *H. lucorum*, is another member of the Anatolian clade of *Helix*. Populations of *H. lucorum* from Armenia and Azerbaijan have mitochondrial lineages that may be endemic to the region, suggesting that this species may have been present there for a longer period of time than the other two species. However, the more northerly populations in Georgia and Russia belong to a recently-spread clade, for which the new data suggest an origin elsewhere, possibly as far west as the Balkans, and which probably colonised the region only with human help.

The hypothesis of the Caucasus and the adjacent Pontus region of Turkey as a place where ancient lineages of *Helix* (not belonging to the European, Mediterranean or Anatolian clades of *Helix*) persisted for a long period of time (Korábek et al. 2015) can thus be rejected. Within the wider region, deeper intraspecific diversity was preserved or endemic species exist in the western Pontus, in the Lesser Caucasus and in Crimea, but the Greater Caucasus and the territory of Georgia were colonised relatively recently

(comparison with the central-European species *Helix pomatia* suggests as late as Late Pleistocene or Holocene; Korábek et al. (2023)). There appears to be no direct link between the *Helix* species that lived in the northern foothills of the Greater Caucasus (Chechnya, Dagestan) from the Middle Miocene and Late Pliocene to the Early Pleistocene (Steklov 1966; Beluzhenko 2014, 2015) and the *Helix* species currently living in the region. This is bad news for the potential use of the remarkable fossil record of this region for evolutionary analyses of *Helix*. Whether there is a link between Miocene *Helix* fossils from Crimea (Mayer 1856; Andrusov 1896; Wenz 1923) and *H. albescens* remains to be established, but it would be consistent with a previous estimate of the divergence time of *H. albescens* and the European clade of *Helix* at around 10 million years (Neiber and Hausdorf 2015).

Acknowledgements

We thank colleagues who provided us samples for analysis or helped with collecting, especially S. Kramarenko (Mykolayiv National Agrarian University, Ukraine), M. Son (Institute of Marine Biology NAS Ukraine, Odesa, Ukraine), E. Rybalchenko (Poltava, Ukraine) and P. Romanov (Kryvyi Rih, Ukraine). The work was funded by the Alexander von Humboldt Foundation. The publication of this article was funded by the Open Access Fund of the Leibniz Association.

References

Andrusov N (1896) Die südrussischen Neogenablagerungen (Eine kurze Uebersicht). 1-ter Theil. Alteres Miocän. Verhandlungen der Russisch-Kaiserlichen mineralogischen Gesellschaft zu St. Petersburg. Zweite Serie 34: 195–242. https://books.google.cz/books?id=J2tjAAAAIAAJ&redir_esc=y

Balashov IA (2014) *Taurinellushka babugana* gen. nov., sp. nov. (Stylommatophora: Pristilomatinae) from the Crimean Mountains (Ukraine) and revision of Crimean Mediterranea (Oxychilinae). Journal of Conchology 41: 575–584.

Balashov IA (2016) Fauna Ukrainȳ. Tom 29, Mollyuski. Vȳpusk 5, Stebel'chatoglazȳe (Stylommatophora). Naukova Dumka, Kyiv.

Balashov IA, Baidashnikov AA (2013) Nazemnȳe mollyuski redkolesiĭ mozhzhevel'nika vȳsokogo v Krȳmskykh gorakh. Zoologicheskiy jurnal [Зоологический журнал] 92: 257–263. https://doi.org/10.7868/S0044513413030033

Balashov IA, Neiber MT, Hausdorf B (2021) Phylogeny, species delimitation and population structure of the steppe-inhabiting land snail genus *Helicopsis* in Eastern Europe. Zoological Journal of the Linnean Society 193(3): 1108–1125. https://doi.org/10.1093/zoolinnean/zlaa156

Beluzhenko EV (2014) Neogene-Eopleistocene shelly limestones in the North Caucasus and Ciscaucasia regions. Stratigraphy and Geological Correlation 22(4): 406–425. https://doi.org/10.1134/S0869593814040029

Beluzhenko EV (2015) Stratigraficheskoe polozhenie i lateral'noe raspredelenie mshakovo-vodoroslevȳkh izvestnyakov miotsena severnogo Kavkaza. Byulleten' Moskovskogo obschestva ispȳtateleĭ prirodȳ. Otdel geologicheskiĭ 90: 50–61.

Browicz K (1989) Chorology of the Euxinian and Hyrcanian element in the woody flora of Asia. Plant Systematics and Evolution 162(1–4): 305–314. https://doi.org/10.1007/BF00936923

Cadahía L, Harl J, Duda M, Sattmann H, Kruckenhauser L, Fehér Z, Zopp L, Haring E (2014) New data on the phylogeny of Ariantinae (Pulmonata, Helicidae) and the systematic position of *Cylindrus obtusus* based on nuclear and mitochondrial DNA marker sequences. Journal of Zoological Systematics and Evolutionary Research 52(2): 163–169. https://doi.org/10.1111/jzs.12044

Cameron RAD, Pokryszko BM, Horsák M (2013) Forest snail faunas from Crimea (Ukraine), an isolated and incomplete Pleistocene refugium. Biological Journal of the Linnean Society, Linnean Society of London 109(2): 424–433. https://doi.org/10.1111/bij.12040

Chiba S (1999) Accelerated evolution of land snails *Mandarina* in the oceanic Bonin Islands: Evidence from mitochondrial DNA sequences. Evolution; International Journal of Organic Evolution 53(2): 460–471. https://doi.org/10.2307/2640782

Cook LM (1997) Geographic and ecological patterns in Turkish land snails. Journal of Biogeography 24(4): 409–418. https://doi.org/10.1111/j.1365-2699.1997.00139.x

Denk T, Frotzler N, Davitashvili N (2001) Vegetational patterns and distribution of relict taxa in humid temperate forests and wetlands of Georgia (Transcaucasia). Biological Journal of the Linnean Society. Linnean Society of London 72(2): 287–332. https://doi.org/10.1111/j.1095-8312.2001.tb01318.x

Gaitán-Espitia JD, Nespolo RF, Opazo JC (2013) The complete mitochondrial genome of the land snail *Cornu aspersum* (Helicidae: Mollusca): intra-specific divergence of protein-coding genes and phylogenetic considerations within Euthyneura. PLoS ONE 8(6): e67299. https://doi.org/10.1371/journal.pone.0067299

Groenenberg DS, Pirovano W, Gittenberger E, Schilthuizen M (2012) The complete mitogenome of *Cylindrus obtusus* (Helicidae, Ariantinae) using Illumina next generation sequencing. BMC Genomics 13(1): 114. https://doi.org/10.1186/1471-2164-13-114

Harrison S, Noss R (2017) Endemism hotspots are linked to stable climatic refugia. Annals of Botany 119(2): 207–214. https://doi.org/10.1093/aob/mcw248

Hausdorf B (1994) Additive typogenesis in *Thoanteus* (Gastropoda: Bulminidae). Zoological Journal of the Linnean Society 112(3): 353–361. https://doi.org/10.1111/j.1096-3642.1994.tb00325.x

Hausdorf B, Röpstorf P, Riedel F (2003) Relationships and origin of endemic Lake Baikal gastropods (Caenogastropoda: Rissooidea) based on mitochondrial DNA sequences. Molecular Phylogenetics and Evolution 26(3): 435–443. https://doi.org/10.1016/S1055-7903(02)00365-2

Irikov A, Erőss Z (2008) An updated and annotated checklist of Bulgarian terrestrial gastropods (Mollusca: Gastropoda). Folia Malacologica 16(4): 197–205. https://doi.org/10.12657/folmal.016.015

Kalyaanamoorthy S, Minh BQ, Wong TKF, von Haeseler A, Jermiin LS (2017) ModelFinder: Fast model selection for accurate phylogenetic estimates. Nature Methods 14(6): 587–589. https://doi.org/10.1038/nmeth.4285

Katoh K, Standley DM (2013) MAFFT multiple sequence alignment software version 7: Improvements in performance and usability.

Molecular Biology and Evolution 30(4): 772–780. https://doi.org/10.1093/molbev/mst010

Korábek O, Petrusek A, Neubert E, Juřičková L (2015) Molecular phylogeny of the genus *Helix* (Pulmonata: Helicidae). Zoologica Scripta 44(3): 263–280. https://doi.org/10.1111/zsc.12101

Korábek O, Juřičková L, Balashov I, Petrusek A (2018) The contribution of ancient and modern anthropogenic introductions to the colonization of Europe by the land snail *Helix lucorum* Linnaeus, 1758 (Helicidae). Contributions to Zoology (Amsterdam, Netherlands) 87(2): 61–74. https://doi.org/10.1163/18759866-08702001

Korábek O, Petrusek A, Rovatsos M (2019) Mitogenome of *Helix pomatia* and the basal phylogeny of Helicinae (Gastropoda, Stylommatophora, Helicidae). ZooKeys 827: 19–30. https://doi.org/10.3897/zookeys.827.33057

Korábek O, Juřičková L, Petrusek A (2022) Diversity of land snail tribe Helicini (Gastropoda: Stylommatophora: Helicidae): where do we stand after 20 years of sequencing mitochondrial markers? Diversity (Basel) 14(1): 24. https://doi.org/10.3390/d14010024

Korábek O, Adamcová T, Proćków M, Petrusek A, Hausdorf B, Juřičková L (2023) In both directions: Expansions of European land snails to the north and south from glacial refugia. Journal of Biogeography 40(4): 654–668. https://doi.org/10.1111/jbi.14531

Kramarenko SS (2016) Patterns of spatio-temporal variation in land snails: A multi-scale approach. Folia Malacologica 24(3): 111–177. https://doi.org/10.12657/folmal.024.008

Kramarenko SS, Leonov SV (2011) Phenetic population structure of the land snail *Helix albescens* (Gastropoda, Pulmonata, Helicidae) in the Crimea. Russian Journal of Ecology 42(2): 170–177. https://doi.org/10.1134/S1067413611020068

Kukushkin OV, Ermakov OA, Ivanov AY, Doronin IV, Sviridenko EY Sviridenko, Simonov EP, Gorelov RA, Khramova MA, Blokhin IG (2020) Cytochrome b mitochondrial gene analysis-based phylogeography of a Sand lizard in the Crimea: ancient refugium at the peninsula, late expansion from the North, and first evidence of *Lacerta agilis tauridica* and *L. a. exigua* (Lacertidae: Sauria) hybridization. Proceedings of the Zoological Institute RAS 324: 56–99. https://doi.org/10.31610/trudyzin/2020.324.1.56

Magri D, di Rita F, Aranbarri J, Fletcher W, González-Sampériz P (2017) Quaternary disappearance of tree taxa from Southern Europe: Timing and trends. Quaternary Science Reviews 163: 23–55. https://doi.org/10.1016/j.quascirev.2017.02.014

Maharramova E, Huseynova I, Kolabaia S, Gruenstaeudl M, Borsch T, Muller LAH (2018) Phylogeography and population genetics of the riparian relict tree *Pterocarya fraxinifolia* (Juglandaceae) in the South Caucasus. Systematics and Biodiversity 16(1): 14–27. https://doi.org/10.1080/14772000.2017.1333540

Marchese C (2015) Biodiversity hotspots: A shortcut for a more complicated concept. Global Ecology and Conservation 3: 297–309. https://doi.org/10.1016/j.gecco.2014.12.008

Mayer MC (1856) Description de coquilles fossiles des terrains tertiaires du midi de la Russie. Journal de Conchyliologie 5: 96–113. [pl. 4] https://www.biodiversitylibrary.org/item/53871#page/102/mode/1up

Mumladze L (2015) Species of the genus *Helix* (Mollusca, Gastropoda) in Georgia. Proceedings of the Institute of Zoology (Ilia State University, Tbilisi) 24: 148–157. http://eprints.iliauni.edu.ge/4295/

Mumladze L, Tarkhnishvili D, Pokryszko BM (2008) A new species of the genus *Helix* from the Lesser Caucasus (SW Georgia). Journal of Conchology 39: 483–485.

Mumladze L, Tarkhnishvili D, Murtskhvaladze M (2013) Systematics and evolutionary history of large endemic snails from the Caucasus (*Helix buchii* and *H. goderdziana*) (Helicidae). American Malacological Bulletin 31(2): 225–234. https://doi.org/10.4003/006.031.0202

Mumladze L, Grego J, Szekeres M (2023) The land snail family Clausiliidae (Gastropoda, Pulmonata, Stylommatophora) in Georgia: Overview, novel records and a new species. Caucasiana 2: 29–61. https://doi.org/10.3897/caucasiana.2.e101013

Myers N, Mittermeier RA, Mittermeier CG, da Fonseca GAB, Kent J (2000) Biodiversity hotspots for conservation priorities. Nature 403(6772): 853–858. https://doi.org/10.1038/35002501

Nakhutsrishvili G, Zazanashvili N, Batsatsashvili K, Montalvo Mancheno CS (2015) Colchic and Hyrcanian forests of the Caucasus: Similarities, differences and conservation status. Flora Mediterranea 25: 185–192. https://doi.org/10.7320/FlMedit25SI.185

Neiber MT, Hausdorf B (2015) Molecular phylogeny reveals the polyphyly of the snail genus *Cepaea* (Gastropoda: Helicidae). Molecular Phylogenetics and Evolution 93: 143–149. https://doi.org/10.1016/j.ympev.2015.07.022

Neiber MT, Hausdorf B (2017) Molecular phylogeny and biogeography of the land snail genus *Monacha* (Gastropoda, Hygromiidae). Zoologica Scripta 46(3): 308–321. https://doi.org/10.1111/zsc.12218

Neiber MT, Razkin O, Hausdorf B (2017) Molecular phylogeny and biogeography of the land snail family Hygromiidae (Gastropoda: Helicoidea). Molecular Phylogenetics and Evolution 111: 169–184. https://doi.org/10.1016/j.ympev.2017.04.002

Neiber MT, Helfenrath K, Walther F, Hausdorf B (2019) Ecological specialization resulting in restricted gene flow promotes differentiation in door snails. Molecular Phylogenetics and Evolution 141: 106608. https://doi.org/10.1016/j.ympev.2019.106608

Neiber MT, Walther F, Kijashko PV, Mumladze L, Hausdorf B (2021) The role of Anatolia in the origin of the Caucasus biodiversity hotspot illustrated by land snails in the genus *Oxychilus*. Cladistics 38(1): 83–102. https://doi.org/10.1111/cla.12479

Nguyen L-T, Schmidt HA, von Haeseler A, Minh BQ (2015) IQ-TREE: A fast and effective stochastic algorithm for estimating maximum-likelihood phylogenies. Molecular Biology and Evolution 32(1): 268–274. https://doi.org/10.1093/molbev/msu300

Palumbi S, Martin A, Romanco S, McMillan WO, Stice L, Grabowski G (1991) The simple fool's guide to PCR. Department of Zoology, University of Hawaii, Honolulu.

Pokryszko BM, Cameron RAD, Mumladze L, Tarkhnishvili D (2011) Forest snail faunas from Georgian Transcaucasia: Patterns of diversity in a Pleistocene refugium. Biological Journal of the Linnean Society, Linnean Society of London 102(2): 239–250. https://doi.org/10.1111/j.1095-8312.2010.01575.x

Rahbek C, Borregaard MK, Colwell RK, Dalsgaard B, Holt BG, Morueta-Holme N, Nogues-Bravo D, Whittaker RJ, Fjeldså J (2019) Humboldt's enigma: What causes global patterns of mountain biodiversity? Science 365(6458): 1108–1113. https://doi.org/10.1126/science.aax0149

Scheel BM, Hausdorf B (2012) Survival and differentiation of subspecies of the land snail *Charpentieria itala* in mountain refuges in the Southern Alps. Molecular Ecology 21(15): 3794–3808. https://doi.org/10.1111/j.1365-294X.2012.05649.x

Schileyko AA (1978) Nazemnȳe mollyuski nadsemeĭstva Helicoidea. In: Skarlato OA (Ed.) Fauna SSSR, Tom 3 vyp. 6. Nauka, Leningrad.

Schütt H (2005) Turkish land snails. 4th, revised and enlarged edition. Verlag Natur & Wissenschaft, Solingen.

Steklov AA (1966) Nazemnȳe mollyuski neogena Predkavkaz'ya i ikh stratigraficheskoe znachenie. Nauka, Moskva.

Suchard MA, Lemey P, Baele G, Ayres DL, Drummond AJ, Rambaut A (2018) Bayesian phylogenetic and phylodynamic data integration using BEAST 1.10. Virus Evolution 4(1): vey016. https://doi.org/10.1093/ve/vey016

Tarkhnishvili DN, Thorpe RS, Arntzen JW (2000) Pre-Pleistocene refugia and differentiation between populations of the Caucasian salamander (*Mertensiella caucasica*). Molecular Phylogenetics and Evolution 14(3): 414–422. https://doi.org/10.1006/mpev.1999.0718

Tarkhnishvili DN, Gavashelishvili A, Mumladze L (2012) Palaeoclimatic models help to understand current distribution of Caucasian forest species. Biological Journal of the Linnean Society, Linnean Society of London 105(1): 231–248. https://doi.org/10.1111/j.1095-8312.2011.01788.x

Terrett JA, Miles S, Thomas RH (1996) Complete DNA sequence of the mitochondrial genome of *Cepaea nemoralis* (Gastropoda: Pulmonata). Journal of Molecular Evolution 42(2): 160–168. https://doi.org/10.1007/BF02198842

Turbanov I, Balashov IA (2015) A second record of *Selenochlamys* (Stylommatophora: Trigonochlamydidae) from Crimea. Malacologica Bohemoslovaca 14: 1–4. https://doi.org/10.5817/MaB2015-14-1

Walther F, Kijashko P, Harutyunova L, Mumladze L, Neiber MT, Hausdorf B (2014) Biogeography of the land snails of the Caucasus region. Tentacle 22: 3–5. http://www.hawaii.edu/cowielab/Tentacle/Tentacle_22.pdf

Walther F, Neiber MT, Hausdorf B (2018) Systematic revision of the Caucasigenini (Gastropoda: Hygromiidae) from the Caucasus region. Archiv für Molluskenkunde 147(1): 129–169. https://doi.org/10.1127/arch.moll/147/129-169

Wenz W (1923) Fossilium Catalogus I: Animalia. Pars 18: Gastropoda extramarina tertiaria. II. W. Junk, Berlin. https://www.biodiversitylibrary.org/item/125702#page/1/mode/1up

Zazanashvili N, Manvelyan K, Askerov E, Mousavi M, Krever V, Kalem S, Garforth M (2020) The boundaries and bio-physical features of the Caucasus Ecoregion. In: Zazanashvili N, Garforth M, Bitsadze M (Eds) Ecoregional Conservation Plan for the Caucasus, 2020 Edition: Supplementary Reports. WWF, KfW, Tbilisi, 9–20. https://wwfint.awsassets.panda.org/downloads/ecp_2020_part_2.pdf

Supplementary material 1

List of sequences

Authors: Ondřej Korábek, Igor Balashov, Marco T. Neiber, Frank Walther, Bernhard Hausdorf

Data type: xlsx

Explanation note: **table S1.** List of sequences used for intraspecific phylogenetic analyses presented in Fig. 1. **table S2.** List of sequences used for inferring the phylogenetic position of a *cox1* pseudogene in Fig. 2.

Link: https://doi.org/10.3897/zse.99.110610.suppl1

Zoosyst. Evol. 99 (2) 2023, 545–556 | DOI 10.3897/zse.99.108032

PENSOFT

MUSEUM FÜR NATURKUNDE BERLIN

A new freshwater species of *Gnorimosphaeroma* (Crustacea, Isopoda, Sphaeromatidae) from Chichi-jima Island, Ogasawara Islands, Japan

Ko Tomikawa[1], Junpei Yoshii[1], Akari Noda[1], Chi-Woo Lee[2], Tetsuro Sasaki[3], Naoya Kimura[4], Noboru Nunomura[5]

1 *Graduate School of Humanities and Social Sciences, Hiroshima University, Higashihiroshima, Hiroshima 739-8524, Japan*
2 *Nakdonggang National Institute of Biological Resources, 137, Donam 2-gil, Sangju-si, Gyeongsangbuk-do 37242, Republic of Korea*
3 *Institute of Boninology, Nishi-machi, Chichi-jima, Ogasawara, Tokyo 100-2101, Japan*
4 *Tokiwazaka 1-7-18, Hirosaki, Aomori 036-8263, Japan*
5 *Noto Marine Laboratory, Institute of Nature and Environmental Technology, Kanazawa University, Ogi, Noto-chô, Kanazawa, Ishikawa 927-0553, Japan*

https://zoobank.org/55EB7C8D-3FA4-4DDF-9340-A54B33999627

Corresponding author: Ko Tomikawa (tomikawa@hiroshima-u.ac.jp)

Academic editor: Luiz F. Andrade ♦ **Received** 15 June 2023 ♦ **Accepted** 16 October 2023 ♦ **Published** 21 November 2023

Abstract

This study describes *Gnorimosphaeroma rivulare* **sp. nov.** from a stream on Chichi-jima Island, Ogasawara Islands, Japan. This is the second freshwater species of *Gnorimosphaeroma* and the third Sphaeromatidae from oceanic islands. *Gnorimosphaeroma rivulare* **sp. nov.** is morphologically similar to *G. boninense* Nunomura, 2006, *G. naktongense* Kwon & Kim, 1987 and *G. saijoense* Nunomura, 2013. However, *G. rivulare* **sp. nov.** differs from these species in various morphological features, such as the shape of pleotelson and pereopod 2, relative length of antennule peduncular articles and pleopod 3 rami, number of setae on maxillula and maxilliped, and setation on pereopod 3. Phylogenetic analyses revealed that *G. akanense* is sister to *G. saijoense*, and together they are sister to *G. hokurikuense*. This three taxa clade is sister to *G. rivulare* **sp. nov.** with *G. iriei* basal to them all. Our analysis concludes that *G. boninense* from Haha-jima Island, Ogasawara Islands is only distantly related to *G. rivulare* and may represent an independent colonization event.

Key Words

freshwater, inland water, isopod, molecular phylogeny, oceanic island, stream, taxonomy

Introduction

Generally, oceanic islands do not occur on continental shelves. These are islands that have never been connected to a continental landmass. Inland water-dwelling organisms cannot reach oceanic islands without crossing the ocean or speciating from organisms that find themselves in a new habitat to which they have adapted, e.g., marine and then isolated in freshwater. Therefore, the occurrence of freshwater fish and invertebrates on oceanic islands is generally limited (Lévêque et al. 2008; Strong et al. 2008; Väinölä et al. 2008; Wilson 2008).

The Ogasawara Islands, oceanic islands, are a group of approximately 30 islands located in the Pacific Ocean approximately 1000 km southeast of the Japanese archipelago. The Ogasawara Islands have small and well-developed rivers inhabited by freshwater crustaceans, molluscs, and caddisflies. These taxa have limited diversity on oceanic islands (Satake and Cai 2005; Nunomura and Satake 2006; Miura et al. 2008; Tomikawa et al. 2022; Ito et al. 2023).

More than 10,600 species of Isopoda have been described worldwide, occurring in diverse aquatic and terrestrial environments (Boyko et al. 2023). Approximately 950

species of isopods have been recorded from inland waters; however, the number of species occurring in inland waters of oceanic islands is far fewer, with only a few species recorded from Pacific Ocean islands (Jaume and Queinnec 2007; Wilson 2008). The aquatic sphaeromatid genus *Gnorimosphaeroma* Menzies, 1954 has 26 described species (Boyko et al. 2023). They are restricted to the Japanese Islands, Korean Peninsula, Mainland China, Alaska, and the eastern Pacific coast of North America (Tattersall 1921; Jang and Kwon 1993; Nunomura 2013; Wetzer et al. 2021). Most Sphaeromatidae are marine (Sket and Bruce 2004; Bruce 2005; Jaume and Queinnec 2007). The genus *Gnorimosphaeroma* is unusual because it includes not only marine species, but also has seven brackish and eight freshwater described species (Fig. 1, Table 1).

Satake and Ueno (2013) reported an unidentified species of *Gnorimosphaeroma* from a stream on Chichi-jima Island, Ogasawara Islands. A recent collection of *Gnorimosphaeroma* was made on Chichi-jima Island during the author's KT and NN research expedition to the Ogasawara Islands. A colleague provided an additional collection of seven specimens. In this study, we describe this previously undescribed species of *Gnorimosphaeroma*. To clarify the phylogenetic position of this *Gnorimosphaeroma* species, we performed a molecular phylogenetic analyses based on nuclear 18S rRNA and mitochondrial 16S rRNA genes.

Materials and methods

Samples

Specimens of an unidentified species were collected from under the boulders in the upper stream of Nagatani River, Chichi-jima Island, Ogasawara Islands, Japan (Fig. 2). Our molecular phylogenetic analysis includes nine described species of *Gnorimosphaeroma*, one unidentified species from Chiba, Japan, one unidentified species from San Francisco Bay, and the new undescribed freshwater species described in this paper (Table 2). The specimens were collected using a fine-mesh hand-net and samples were subsequently fixed in 70% or 99% ethanol in-situ. Specimens fixed in 70% ethanol were transferred to 99% ethanol in the laboratory.

Morphological observation

All appendages of *G. rivulare* sp. nov. were dissected in 80% ethanol and mounted in gum-chloral medium. The slides were examined using a stereomicroscope (Olympus SZX7, Japan) and a light microscope (Nikon Eclipse Ni, Japan), and the body and appendages were illustrated using a camera lucida. One male (paratype, NSMT-Cr 31507) was dehydrated through a graded ethanol series, and dried using hexamethyldisilazane (HMDS) (Nation 1983). They were then sputter-coated with gold and observed using scanning electron microscopy (SEM, JSM-6510LV). Body length was measured as a straight-line distance from the rostral point to the posterior margin of pleotelson within the nearest 0.1 mm. Type specimens were deposited at the National Museum of Nature and Science, Tsukuba, Japan (NSMT).

Molecular phylogenetic analyses

Genomic DNA was extracted from the appendage muscles of the specimen following procedures detailed by Tomikawa et al. (2014). The primer set 16Sar and 16Sbr (Palumbi et al. 1991) was used to target the mitochondrial 16S rRNA (16S), whereas the 18SF [5′-AAGATTAAGCCATGCATGTC-3′] and 18SR [5′- GCTGGAATTACCGCGGCTGC-3′] primer pair were designed to target the nuclear 18S rRNA (18S). PCR and DNA sequencing were performed using the method detailed by Tomikawa (2015). The newly obtained DNA sequences were deposited in the International Nucleotide Sequence Databases (INSD) through the DNA Data Bank of Japan (DDBJ) (Table 2).

The phylogenetic analyses were conducted based on 16S and 18S sequence data generated for this project and also includes previously published sequences. *Ancinus* sp. (Ancinidae) and two *Chitonosphaera* species (Sphaeromatidae), *C. lata* (Nishimura, 1968) and *C. salebrosa* (Nishimura, 1969) were used as the outgroup (Wetzer et al. 2013, 2018). The sequences were aligned using the Muscle algorithm implemented in MEGA XI (Tamura et al. 2021). The aligned lengths of the 16S and 18S were found to be 518 and 559 bp, respectively. Moreover, the concatenated sequences yielded 1077 bp of alignment positions.

Phylogenetic relationships were reconstructed via maximum likelihood (ML) and Bayesian inference (BI) and partitioned by 16S and 18S datasets. ML analyses were conducted using IQ-TREE web server (ver. 1.6.12, see http://www.iqtree.org/; Trifinopoulos et al. 2016) with 1000 ultrafast bootstrap replicates (Hoang et al. 2018). The best evolutionary models were selected based on the corrected Bayesian information criterion (BIC) using ModelFinder (Kalyaanamoorthy et al. 2017): for 16S, TIM2+F+G4; for 18S, TNe+G4. BI and Bayesian posterior probabilities (PPs) were estimated using MrBayes v. 3.2.5 (Ronquist et al. 2012). The best-fit partition scheme and models for each partition were selected with the BIC using PartitionFinder with the 'greedy' algorithm, and for 16S, GTR+G; for 28S, JC+I. Two independent runs of four Markov chains were conducted for 10 million generations, and the tree was sampled every 100 generations. The parameter estimates and convergence were checked using Tracer v. 1.7.1 (Rambaut et al. 2018), and the first 50,001 trees were considered burn-in and discarded.

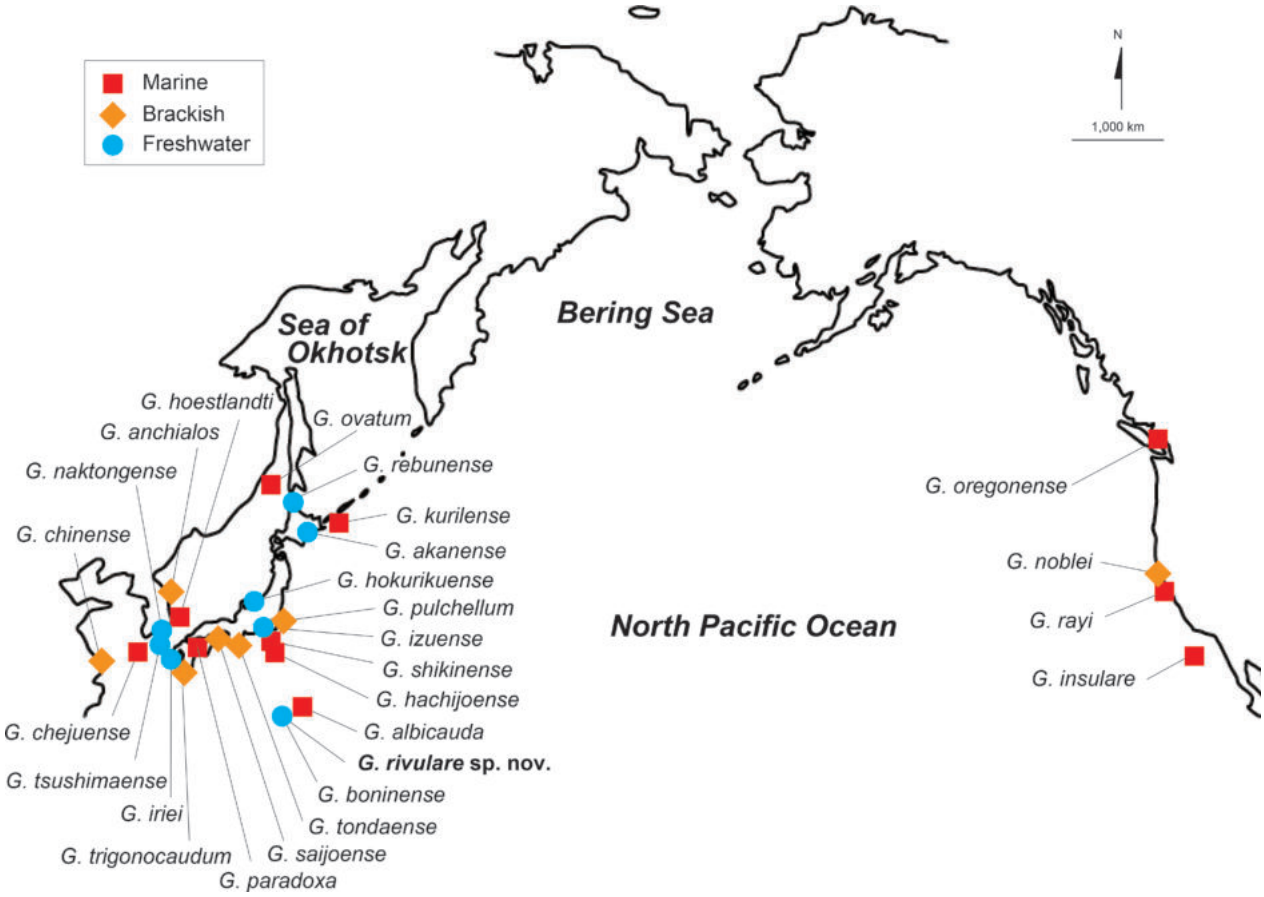

Figure 1. Map showing the type localities of *Gnorimosphaeroma* species.

Table 1. The type localities and habitats of *Gnorimosphaeroma* species.

Species	Type locality	Habitat
G. akanense Nunomura, 1998	Akan River, Hokkaido	freshwater
G. albicauda Nunomura, 2005	Hatsuneura, Chichi-jima Island, Ogasawara Islands	marine
G. anchialos Jang & Kwon, 1993	Lake Songjiho	brackish
G. boninense Nunomura & Satake, 2006	Haha-jima Island, Ogasawara Islands	freshwater
G. chejuense Kim & Kwon, 1988	Cheju Island	marine
G. chinense (Tattersall, 1921)	Whangpoo River, Shanghai	brackish
G. hachijoense Nunomura, 1999	Hachijo Island, Tokyo	marine
G. hoestlandti Kim & Kwon, 1985	Mukho	marine
G. hokurikuense Nunomura, 1998	Yomokuro-ike Pond, Toyama	freshwater
G. insulare (Van Name, 1940)	San Nicolas Island, California	marine
G. iriei Nunomura, 1998	Lake Ezu, Kumamoto	freshwater
G. izuense Nunomura, 2007	Izu, Shizuoka	freshwater
G. kurilense Kussakin, 1974	off Shikotan Island, Kuril Islands	marine
G. naktongense Kwon & Kim, 1987	Nakdong River, Busan	freshwater
G. noblei Menzies, 1954	Tomales Bay, California	brackish
G. oregonense (Dana, 1853)	Vancouver, British Columbia	marine
G. ovatum (Gurjanova, 1933)	Sea of Japan (details unknown)	marine
G. paradoxa (Nunomura, 1988)	Uwajima, Ehime	marine
G. pulchellum Nunomura, 1998	Obitsu River, Chiba	brackish
G. rayi Hoestlandt, 1969	Tomales Bay, California	marine
G. rebunense Nunomura, 1998	Rebun Island, Hokkaido	freshwater
***G. rivulare* sp. nov.**	Nagatani River, Chichi-jima Island, Ogasawara Islands	freshwater
G. saijoense Nunomura, 2013	Shiotori River, Ehime	brackish
G. shikinense Nunomura, 1999	Shikine Island, Tokyo	marine
G. tondaense Nunomura, 1999	Tonda River, Wakayama	brackish
G. trigonocaudum Nunomura, 2011	Hijikuro River, Nagasaki	brackish
G. tsutshimaense Nunomura, 1998	Tsushima Island	freshwater

Table 2. Samples used for the phylogenetic analyses. Sequences marked with an asterisk (*) were newly obtained in the present study. ND, no sequence available.

Species	Voucher or isolate #	Locality	INSD #		Note
			16S	18S	
Sphaeromatidae					
Gnorimosphaeroma akanense	G1913	Lake Akan, Hokkaido, Japan	LC765314*	LC765326*	Topotype
Gnorimosphaeroma boninense	G1814	Chibusa Dam, Haha-jima I., Ogasawara Is., Japan	LC765315*	LC765327*	Topotype
Gnorimosphaeroma hokurikuense	G1943	Ota, Toyama, Japan	LC765316*	LC765328*	Topotype
Gnorimosphaeroma iriei	G1894	Lake Ezu, Kumamoto, Japan	LC765317*	LC765329*	Topotype
Gnorimosphaeroma noblei	RW02.021.1541	Tomales Bay, California, USA	KU248168	JF699554	Topotype
Gnorimosphaeroma oregonense	RW10.003.3131	Vancouver, British Columbia, Canada	MH427781	ND	Topotype
Gnorimosphaeroma rayi	RW09.002.2567	Tomales Bay, California, USA	MH427784	ND	Topotype
Gnorimosphaeroma saijoense	G1902	Kamo R., Ehime, Japan	LC765319*	LC765331*	Topotype
***Gnorimosphaeroma rivulare* sp. nov.**	G1820	Nagatani River, Chichi-jima I., Ogasawara Is., Japan	LC765320*	LC765332*	Paratype
***Gnorimosphaeroma rivulare* sp. nov.**	NSMT-Cr 31490; G1826	Nagatani River, Chichi-jima I., Ogasawara Is., Japan	LC765321*	LC765333*	Paratype
***Gnorimosphaeroma rivulare* sp. nov.**	NSMT-Cr 31486; G1892	Nagatani River, Chichi-jima I., Ogasawara Is., Japan	LC765322*	LC765334*	Paratype
Gnorimosphaeroma sp.	G1954	Obitsu R., Chiba, Japan	LC765318*	LC765330*	
Gnorimosphaeroma sp.	RW02.060.2550	San Francisco Bay, California, USA	MH427743	ND	
Gnorimosphaeroma tondaense	G1972	Takase River, Wakayama, Japan	LC765323*	LC765335*	Topotype
Outgroup					
Ancinidae					
Ancinus sp.	RW05.010.1475	Naos Island, Republic of Panama	KU248307	JF699514	
Sphaeromatidae					
Chitonosphaera lata	G1935	Takase R., Wakayama, Japan	LC765324*	LC765336*	
Chitonosphaera salebrosa	G1937	Edura,Wakayama, Japan	LC765325*	LC765337*	

Results

Taxonomy

Family Sphaeromatidae Latreille, 1825
Genus *Gnorimosphaeroma* Menzies, 1954

Gnorimosphaeroma rivulare Tomikawa, Yoshii & Nunomura, sp. nov.

https://zoobank.org/E97CCBDD-F5FE-473F-BD78-B98DB4230BEB

Figs 2–7

New Japanese name: Chichijima-kotsubumushi

Type materials. ***Holotype*:** male 4.9 mm (NSMT-Cr 31485), upper stream of Nagatani River (27°04.051'N, 142°12.938'E), alt. 160 m, Chichi-jima Island, Ogasawara Islands, Tokyo, Japan, collected by Tetsuro Sasaki on 2 February 2021. ***Paratypes*:** 3 males, 5.3 mm (NSMT-Cr 31486; G1892), 4.7 mm (NSMT-Cr 31487; G1893), 5.2 mm (NSMT-Cr 31507) 1 female 3.2 mm (NSMT-Cr 31488), data same as for holotype; 2 males, 4.1 mm (NSMT-Cr 31489), 4.0 mm (NSMT-Cr 31490; G1826), locality same as for holotype, collected by Noboru Nunomura on 16 December 2019.

Type locality. Japan, Tokyo: Ogasawara Islands, Chichi-jima Island, upper stream of Nagatani River (Figs 1, 2A).

Diagnosis. Pleonites incompletely fused; anterior suture line longer than posterior one. Pleotelson posterior margin rounded. Maxillula medial lobe with 4 plumose setae and a short single seta; lateral lobe with 10 robust setae. Maxilla medial lobe with 17 setae; middle lobe with 12 setae; lateral lobe with 13 setae. Pereopod 1 basis with a single seta on posterodistal corner; merus with

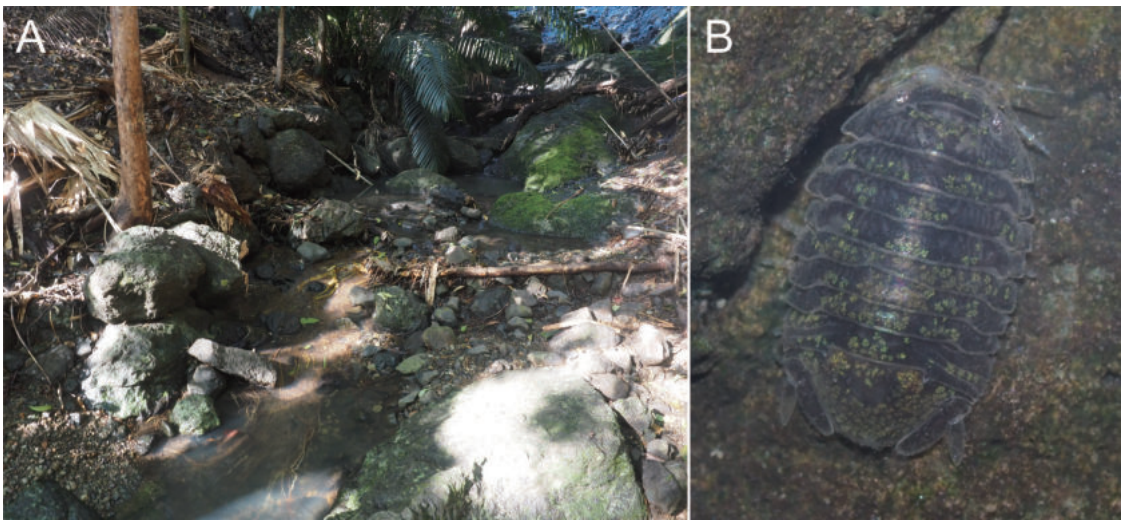

Figure 2. Habitat and live specimen of *Gnorimosphaeroma rivulare* sp. nov. **A.** Habitat; **B.** Living state of the holotype, male 4.9 mm (NSMT-Cr 31485).

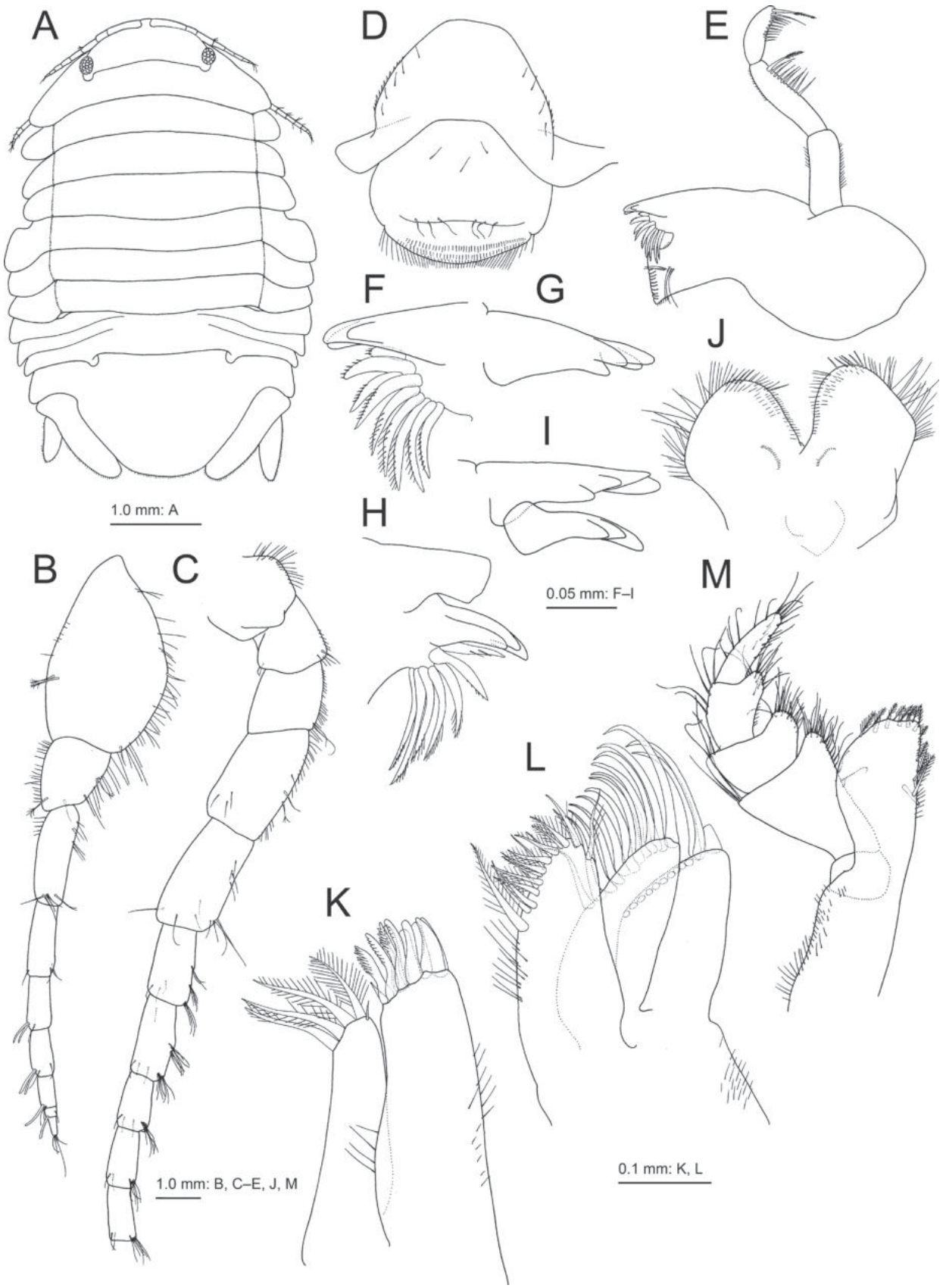

Figure 3. *Gnorimosphaeroma rivulare* sp. nov. **A–F, H, J–M.** Holotype, male 4.9 mm (NSMT-Cr 31485); **G, I.** Paratype, male 5.3 mm (NSMT-Cr 31486). **A.** Habitus, dorsal view; **B.** Antennula, medial view; **C.** Antenna, medial view; **D.** Labrum, dorsal view; **E.** Right mandible, medial view; **F.** Incisor and setal row of right mandible, medial view; **G.** Incisor of right mandible, lateral view; **H.** Incisor, lacinia mobilis and setal row of left mandible, medial view; **I.** Incisor and lacinia mobilis of left mandible, medial view; **J.** Paragnaths, posterior view; **K.** Maxillula, anterior view; **L.** Maxilla, anterior view; **M.** Maxilliped, anterior view.

4 setae on anterodistal corner. Pereopod 2 propodus subrectangular, not swollen. Pereopod 3 merus, carpus, and propodus sparsely setulose. Uropod exopod length 0.7 times as long as endopod.

Description. Male [NSMT-Cr 31485, holotype, 4.9 mm]. Body (Figs 2B, 3A) ovate, vaulted, ca. 1.5 times longer than wide, dorsal surface unornamented, without marginal setae; eyes ovate, simple. Coxal plates (Figs 3A, 7A) without visible distinct articulation to pereonites, partly overlapped, distal coxal margins rounded without setae; coxa 3 tapered anteriorly and posteriorly such that the animal can conglobulate. Pleon (Figs 3A, 7B) incompletely fused; pleonite 1 almost invisible, hidden by pereonite 7; anterior suture line between pleonites 2 and 3 longer than posterior one between pleonites 3 and 4; pleonite 5 fused with pleonite 4, barely recognizable. Pleotelson (Figs 3A, 7B) slightly narrower than pleon, length 0.5 times longer than wide, posterior margin entire, rounded, with minute setae.

Antennule (Fig. 3B) exceeding posterior margin of head; length ratio of peduncular articles 1–3 as 1.0: 0.4: 0.5; peduncular article 1 ovate, length 1.6 times as long as wide, anterior margin with a few setae, posterior margin lined with setae; peduncular article 2 subquadrate, length 1.2 times as long as wide, anterior and posterior margins lined with setae; peduncular article 3 rectangular, slender, length 3.0 times as long as wide, with setae on anterior and posterior margins; flagellum 6-articulate, articles 2 and 3 each with 2 aesthetaescs and articles 4 and 5 each with an aesthetasc. Antenna (Fig. 3C) reaching distal margin of pereonite 2; length ratio of peduncular articles 1–5 as 1.0: 0.9: 0.9: 1.5: 1.5; peduncular articles 1–3 subquadrate with fine setae on anterior margin; peduncular articles 4 and 5 subrectangular, each length 1.9 times longer than wide, anterior margin of article 4 with fine setae, article 5 with a few setae; flagellum 12-articulate (only the first five articles drawn in Fig. 3C).

Labrum (Fig. 3D) anterior margin rounded with fine setae. Mandibles (Fig. 3E–I) left and right incisors with 4 and 3 cusps, respectively; lacinia mobilis of left mandible with 3 cusps; setal row of left and right mandibles comprised 7 and 9 serrate setae; palp 3-articulate, length ratio of articles 1–3 as 1.0: 1.2: 0.8, article 1 with fine setae, article 2 with 10 setae on lateral margin and fine setae on medial margin, article 3 with 11 setae on lateral margin. Paragnaths (Fig. 3J) with rounded shoulders, bearing setae. Maxillula (Fig. 3K) medial lobe narrow, slightly shorter than lateral lobe, with 4 plumose setae and a short simple seta; lateral lobe with 10 robust setae, 4 of which serrate. Maxilla (Fig. 3L) medial lobe with 17 setae, some of which plumose; middle lobe with 12 setae; lateral lobe with 13 setae. Maxilliped (Fig. 3M) endite reaching distal margin of palp article 2, distal margin with 8 plumose setae and 5 simple setae, medial margin with a coupling hook and 4 plumose setae; palp 5-articulate, articles 2–4 with 3, 3 and 6 setae on lateral margin, respectively, produced mediodistally with setae, article 5 narrow with marginal setae.

Pereopod 1 (Fig. 4A, B) basis with a ventrodistal simple seta, ventral margin with fine setae; merus lobate dorsodistally, dorsodistal corner with 4 setae, ventral margin with robust setae and fine setae; carpus short with 2 robust setae and fine setae on ventral margin; propodus oval, swollen, length 2.5 times as long as wide, with 2 robust setae on ventral margin and 5 setulate setae close to ventral margin; dactylus length 0.6 times as long as propodus. Pereopod 2 (Fig. 4C, D) basis with a ventrodistal simple seta; merus weakly lobate dorsodistally, with 5 setae on dorsodistal corner, ventral margin with fine setae; carpus with 6 robust and 3 slender setae on distal surface, ventral margin with fine setae; propodus subrectangular, not swollen, length 2.8 times as long as wide, with 3 robust setae on ventral margin; dactylus length 0.5 times as long as propodus. Pereopod 3 (Fig. 4E, F) basis with a ventrodistal simple seta; merus lobate dorsodistally, dorsodistal corner with 6 setae, ventral margin with sparse fine setae; carpus with 5 robust and some slender setae on distal margin, ventral margin with sparse fine setae; propodus length 2.8 times as long as wide, with 2 robust setae and a slender single seta on ventral margin; dactylus length 0.5 times as long as propodus. Pereopod 4 (Fig. 4G) basis with a simple seta on ventrodistal corner and some broom setae on dorsal margin; ischium with fine setae on ventral margin; merus lobate dorsodistally with robust setae, dorsal and ventral margins with fine setae; carpus with sparse fine setae on ventral margin; propodus with 3 robust setae on ventral margin, dorsal and ventral margins with sparse fine setae. Pereopod 5 (Fig. 4H) basis with a simple seta on dorsodistal corner; merus and carpus with robust setae on distal margins; propodus with 3 robust setae on dorsal margin. Pereopods 6 and 7 (Fig. 5A, B) basis with a simple seta on dorsodistal corner; merus and carpus with robust setae on distal margins; propodus with 2 robust setae on dorsal margin.

Penial process (Fig. 5C) simple, length 3.5–4.2 times as long as basal width, close set.

Pleopod 1 (Fig. 5D) peduncle length 0.5 times width with 4 setae on mediodistal corner; exopod oval, length 1.9 times width, 1.2 times length of endopod, with plumose setae marginally; endopod subtriangular, length 1.4 times width, with distal plumose setae. Pleopod 2 (Fig. 5E) peduncle length 0.4 times width, mediodistal and laterodistal corners with 2 and 1 setae, respectively; exopod oval, length 1.8 times width, with marginal plumose setae; endopod subtriangular, length 1.6 times width, with plumose setae on distal margin; appendix masculina slender, length 6.0 times width, 1.2 times as long as endopod. Pleopod 3 (Fig. 5F) peduncle length 0.4 times width, mediodistal and laterodistal corners with 2 and 1 setae, respectively; exopod oval, length 1.9 times width, with transverse suture, bearing plumose setae marginally; endopod slightly shorter than exopod with plumose setae on distal margin. Pleopod 4 (Fig. 5G) peduncle small, length 0.5 times width, laterodistal corner with a single seta; exopod length 1.8 times width with transverse suture, bearing 4 plumose setae and simple setae marginally; endopod oval, length 1.4 times width,

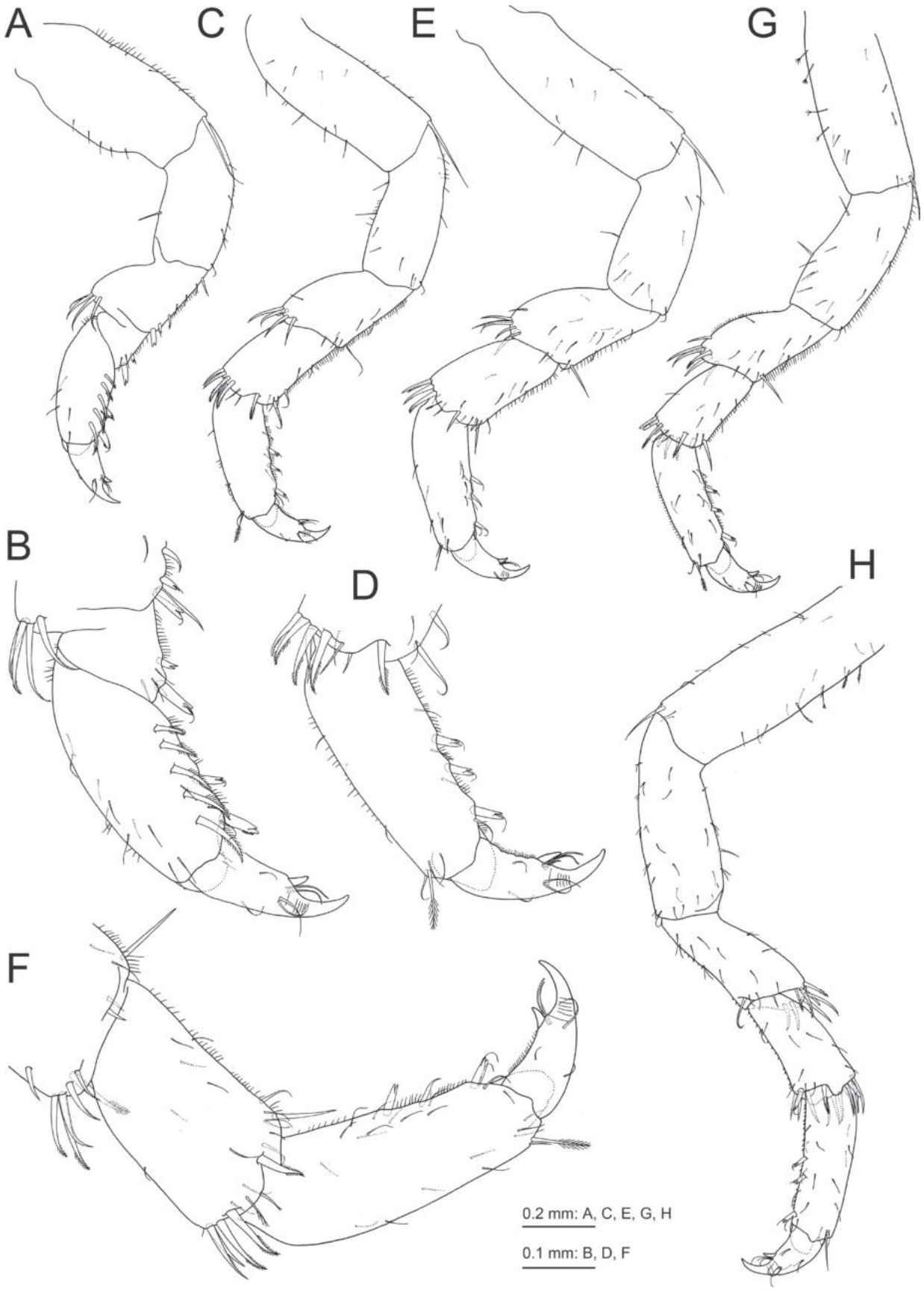

Figure 4. *Gnorimosphaeroma rivulare* sp. nov., holotype, male 4.9 mm (NSMT-Cr 31485). **A.** Right pereopod 1, medial view; **B.** Merus, carpus, propodus and dactylus of right pereopod 1, medial view; **C.** Right pereopod 2, medial view; **D.** Carpus, propodus and dactylus of right pereopod 2, medial view; **E.** Right pereopod 3, medial view; **F.** Merus, carpus, propodus and dactylus of right pereopod 3, medial view; **G.** Right pereopod 4, medial view; **H.** Right pereopod 5, medial view.

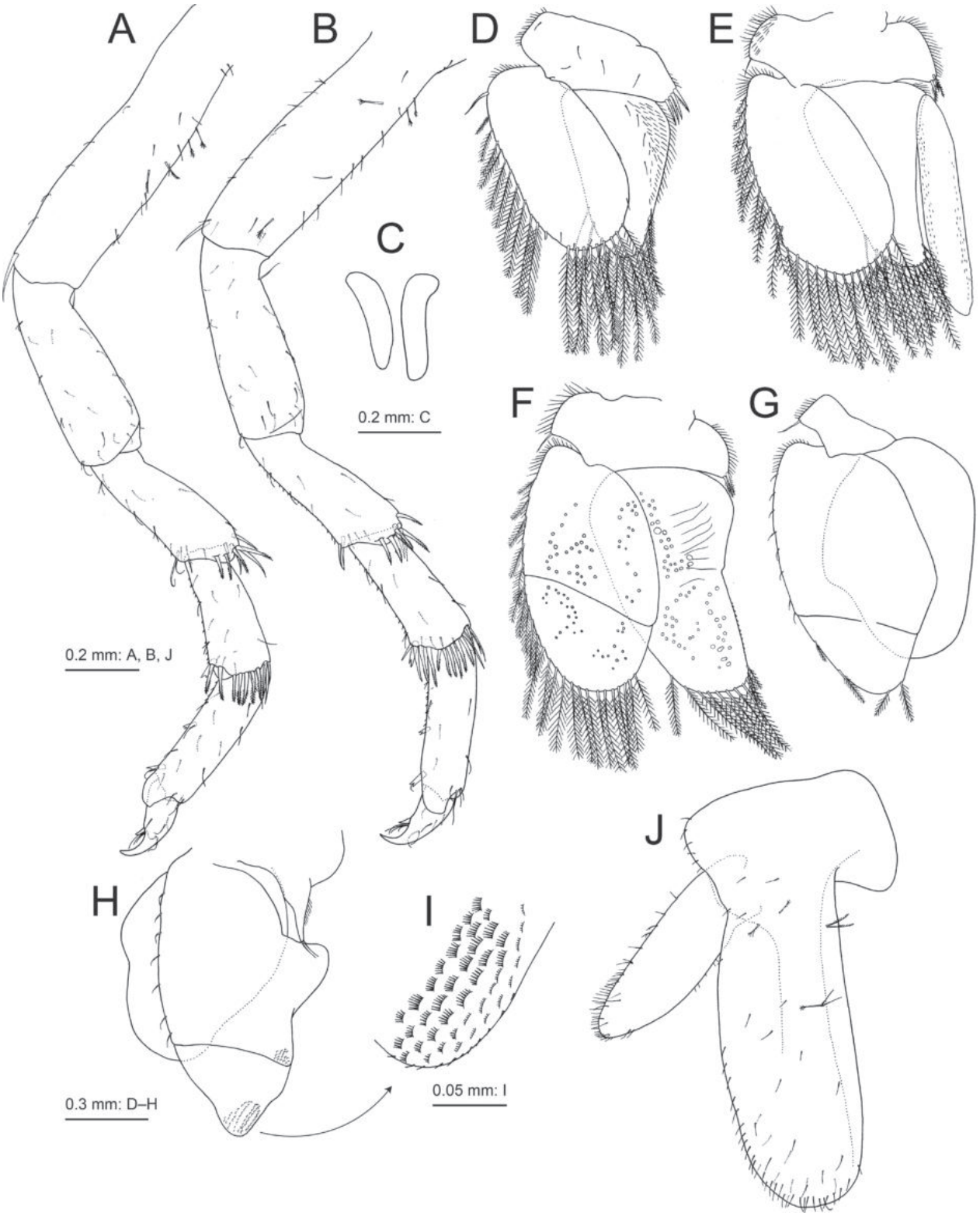

Figure 5. *Gnorimosphaeroma rivulare* sp. nov., holotype, male 4.9 mm (NSMT-Cr 31485). **A.** Right pereopod 6, medial view; **B.** Right pereopod 7, medial view; **C.** Penes, anterior view; **D.** Right pleopod 1, anterior view; **E.** Right pleopod 2, anterior view; **F.** Right pleopod 3, anterior view; **G.** Right pleopod 4, anterior view; **H.** Left pleopod 5, posterior view; **I.** Detail of distal endopod of pleopod 5, posterior view; **J.** Left uropod, dorsal view.

marginally bare. Pleopod 5 (Fig. 5H, I) peduncle with 2 setae on mediodistal corner; exopod length 1.6 times width transverse suture, bearing lateral and distal scale patches, lateral margin with simple setae; endopod oval, length 0.7 times as long as exopod, marginally bare.

Uropod (Figs 3A, 5J, 7B) not quite extending to posterior margin of pleotelson; peduncle rectangular, length 0.6 times width; exopod length 3.5 times width, 0.7 times as long as endopod, with fine sparse setae; endopod length 2.5 times width with fine setae.

Female [NSMT-Cr 31488, paratype, 3.2 mm]. Body shape similar to that of male. Body length 1.7 times width.

Pereopod 1 (Fig. 6A) propodus subrectangular, length 2.6 times as long as wide. Pereopod 2 (Fig. 6B) propodus subrectangular, length 3.1 times as long as wide, with 2 robust setae on posterior margin.

Pleopod 1 (Fig. 6C) peduncle length 0.5 times width with 3 setae on mediodistal corner; exopod oval, length 1.6 times width, 1.2 times length of endopod; endopod subtriangular, length 1.5 times width. Pleopod 2 (Fig. 6D) peduncle length 0.4 times width, mediodistal and laterodistal corners with 2 and 1 setae, respectively; exopod oval, length 1.8 times width; endopod subtriangular, length 1.6 times width.

Uropod (Fig. 6E) peduncle rectangular, length 0.6 times width; exopod length 3.0 times width, 0.7 times as long as endopod; endopod length 2.6 times width.

Variation. Mandible left incisor of paratype male (NSMT-Cr 31486) with 4 cusps.

Etymology. The specific name *rivulare* is derived from a Latin adjective *rivularis*, which means brook living, referring to the habitat of the new species.

Distribution and habitat. This species is known only from the type locality. The specimens were collected from beneath the cobbles in an upper stream of Nagatani River.

Remarks. *Gnorimosphaeroma rivulare* sp. nov. is morphologically similar to *G. boninense* Nunomura, 2006, *G. naktongense* Kwon & Kim, 1987, and *G. saijoense* Nunomura, 2013 in having anterior suture line longer than posterior one, maxilla middle and lateral lobes each with more than 10 setae, pereopod 1 basis with a simple seta on ventrodistal corner, pereopod 1 merus with 4 setae on dorsodistal corner, and uropodal exopod twice as long as endopod. However, *G. rivulare* sp. nov. differs from these three species by the following features (features of the species that are being compared are in parentheses): from *G. boninense*, pleotelson posterior margin rounded (almost straight), pereopod 3 carpus and propodus sparsely setulose (densely setulose), pereopod 2 propodus subrectangular (subtriangular), and pleopod 3 exopod almost same size as endopod (smaller than endopod); from *G. naktongense*, antennule peduncular article 3 not elongate, length 1.3 times as long as article 2 (elongate, 1.7 times as long as article 2), pereopod 2 propodus ventral margin straight (weakly expanded), and pleopod 5 endopod length 0.7 (0.9) times as long as exopod; from *G. saijoense*, maxillula medial lobe with 4 (5) plumose setae, maxilliped palp articles 2 and 3 each with 3 (1) setae on laterodistal corner, pereopod

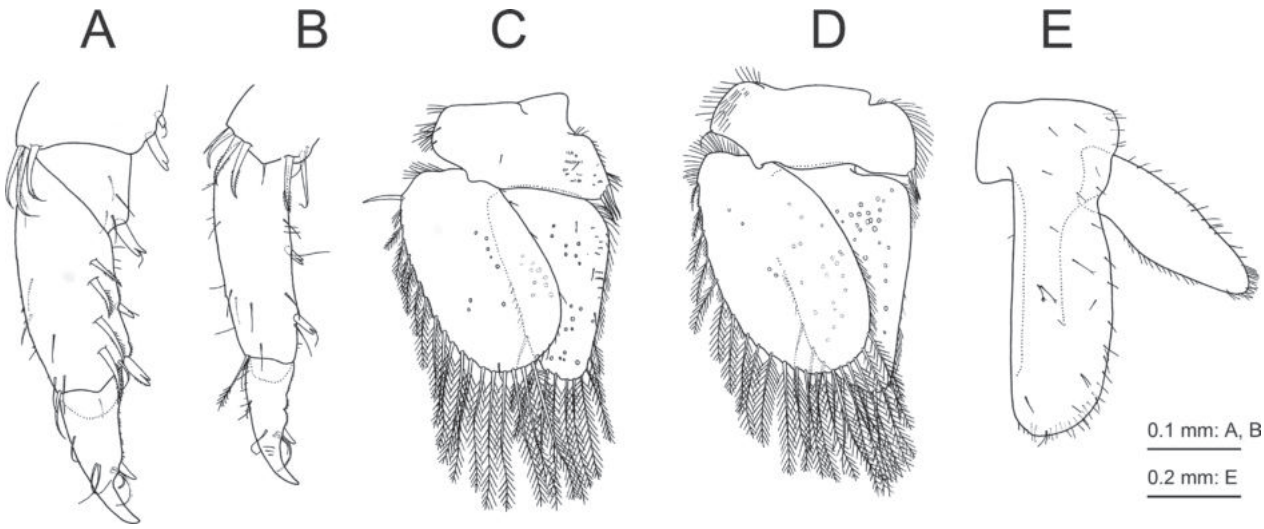

Figure 6. *Gnorimosphaeroma rivulare* sp. nov., paratype, female 3.2 mm (NSMT-Cr 31488). **A, B.** Merus, carpus, propodus and dactylus of right pereopods 1 and 2, medial views; **C, D.** Right pleopods 1 and 2, anterior views; **E.** Right uropod, dorsal view.

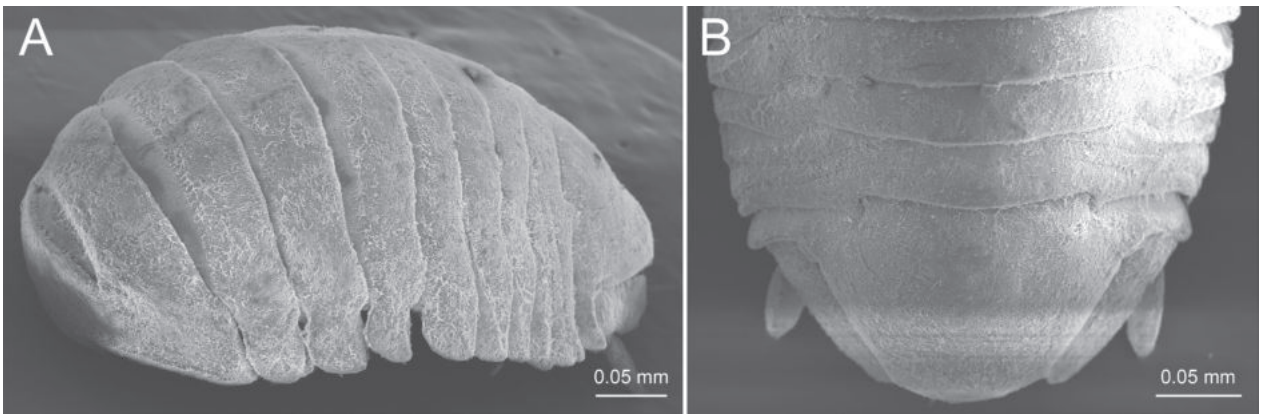

Figure 7. SEM photographs of *G. rivulare* sp. nov., paratype, male 5.2 mm (NSMT-Cr 31507). **A.** Habitus, lateral view; **B.** Pleon and pleotelson, dorsal view.

2 propodus ventral margin straight (weakly expanded), pereopod 3 merus, carpus, and propodus sparsely setulose (densely setulose).

Molecular phylogeny

Bayesian and ML phylogenies were similar. Only the ML is shown (Fig. 8). *Gnorimosphaeroma rivulare* sp. nov. forms a monophyletic clade with *G. akanense* Nunomura, 1998, *G. hokurikuense* Nunomura, 1998, *G. iriei* Nunomura, 1998, and *G. saijoense* (Fig. 8). Genetic differentiation of *G. akanense*, *G. hokurikuense*, and *G. saijoense* was small, with a *p*-distance of 0.4–1.7% for 16S rRNA sequences. Marine *G. rayi* Hoestlandt, 1969 and brackish water *G. tondaense* Nunomura, 1999 are sister group. The 16S rRNA sequences of unidentified species from Chiba, Japan and California were identical.

Discussion

Our molecular phylogenetic analyses revealed that marine, brackish, and freshwater taxa appear mixed throughout the tree. *Gnorimosphaeroma boninense* from a small stream on Haha-jima Island, Ogasawara Islands and *G. rivulare* sp. nov. are not sister taxa; however, the latter forms a monophyletic clade with *G. akanense* from Akan River, *G. hokurikuense* from freshwater streams in Honshu, *G. iriei* from springs in Kyushu, and *G. saijoense* from brackish waters at the mouths of rivers in Shikoku. This suggests that *G. boninense* and *G. rivulare* sp. nov. may have colonised the Ogasawara Islands independently. However, without including all *Gnorimosphaeroma* species in the analyses and also carefully reviewing the ecologies of each species it is not possible to definitively determine invasion and evolutionary history. Multiple invasions of freshwater invertebrates into the Ogasawara Islands have been reported for the amphipod Crustacea (Tomikawa et al. 2022). Tomikawa et al. (2022) showed that two species of melitid amphipods, *Melita nunomurai* Tomikawa & Sasaki, 2022 and *M. ogasawaraensis* Tomikawa & Sasaki, 2022, which occur in freshwater of Ogasawara Islands, are closely related to the species occurring on Honshu Island and the Nansei Islands, respectively. Possibly, they may originate from different regions. Although the origin of freshwater *Gnorimosphaeroma* on the Ogasawara Islands cannot been clarified in this study, we suggest that further elucidation of the evolutional history of freshwater isopods on oceanic islands will be possible with enhanced taxon sampling and broad genetic sampling in the future.

The freshwater invertebrate fauna of Chichi-jima Island, Ogasawara Islands, has been relatively well investigated (Satake and Ueno 2013; Satake et al. 2019). However, *G. rivulare* sp. nov. has only been found at one site in the upper reaches of Nagatani River on Chichi-jima Island (Satake and Ueno 2013). In addition to the low water volume in this species' habitat, the water flow is being dammed up by the roots of the non-native plant Bishop wood, *Bischofia javanica*. Freshwater *Gnorimosphaeroma* have been found in springs and mountain streams (e.g. Nunomura 1998) and is considered to prefer oxygenated

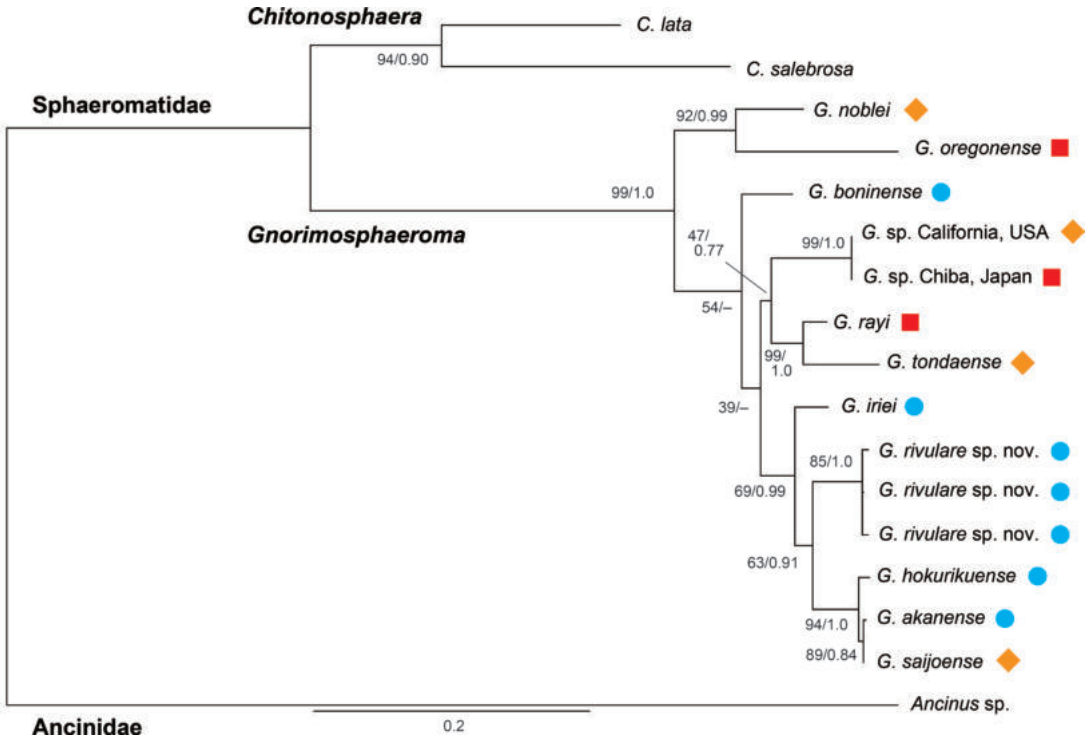

Figure 8. Maximum likelihood tree for 1077 bp of 16S rRNA and 18S rRNA markers. Numbers on nodes represent ultra-bootstrap values for maximum likelihood and Bayesian posterior probabilities. Symbols beside the species name indicate the habitats shown in Fig. 1.

lotic waters. A stagnant bottom environment may not be favourable for *G. rivulare* sp. nov., and could severely limit its future persistence. For this newly described species survive, conservation of this restricted habitat is an urgent issue that needs to be addressed.

Author contributions

KT, JY, AN, TS, NK, and NN collected the samples used in this study. KT, JY, AN, and CL performed molecular phylogenetic analyses. KT, JY, and NN were responsible for describing and naming the new species. This manuscript was compiled by KT and carefully reviewed and finalized by all authors.

Acknowledgements

We thank Drs Regina Wetzer of Natural History Museum of Los Angeles County and Brenda L. Doti of Universidad de Buenos Aires for their critical reading and valuable comments on our manuscript. This work was partly supported by the Japan Society for the Promotion of Science KAKENHI grants JP21H00910, JP22H01011, JP22K06373, and JP22K06371 to KT. This work was also supported by grants from the Nakdonggang National Institute of Biological Resources (NNIBR) funded by the Ministry of Environment (MOE) of the Republic of Korea (NNIBR202302102) to CL. We would like to thank Editage (www.editage.com) for English language editing.

References

Boyko CB, Bruce NL, Hadfield KA, Merrin KL, Ota Y, Poore GCB, Taiti S (2023) World Marine, Freshwater and Terrestrial Isopod Crustaceans database. https://doi.org/10.14284/365

Bruce NL (2005) New sphaeromatids (Crustacea: Isopoda: Sphaeromatidea) from coastal and freshwater habitats in New Zealand. Zootaxa 1002(1): 1–20. https://doi.org/10.11646/zootaxa.1002.1.1

Hoang DT, Chernomor O, von Haeseler A, Minh BQ, Vinh LS (2018) UFBoot2: Improving the Ultrafast Bootstrap Approximation. Molecular Biology and Evolution 35(2): 518–522. https://doi.org/10.1093/molbev/msx281

Hoestlandt H (1969) Sur un sphérome nouveau de la côte pacifique américaine, *Gnorimosphaeroma rayi* n. sp. (isopode flabellifère). Comptes rendus hebdomadaires des séances de l'Académie des sciences, série D 268: 325–327.

Ito T, Sasaki T, Takahashi C, Sugawara H, Hayashi F (2023) The family Hydroptilidae Curtis (Trichoptera) in the Ogasawara Islands, northwestern Pacific, with particular reference to adaptive radiation in the oceanic islands. Zootaxa 5231(2): 141–164. https://doi.org/10.11646/zootaxa.5231.2.2

Jang IK, Kwon DH (1993) A new species of the genus *Gnorimosphaeroma* (Crustacea, Isopoda, Sphaeromatidae) from a brackish-water lake in Korea. Tongmul Hakhoe Chi 36: 402–407.

Jaume D, Queinnec E (2007) A new species of freshwater isopod (Sphaeromatidea: Sphaeromatidae) from an inland karstic stream on Espíritu Santo Island, Vanuatu, southwestern Pacific. Zootaxa 1653(1): 41–55. https://doi.org/10.11646/zootaxa.1653.1.3

Kalyaanamoorthy S, Minh BQ, Wong TKF, von Haeseler A, Jermiin LS (2017) ModelFinder: Fast model selection for accurate phylogenetic estimates. Nature Methods 14(6): 587–589. https://doi.org/10.1038/nmeth.4285

Kwon DH, Kim HS (1987) A new species of the genus *Gnorimosphaeroma* (Crustacea, Isopoda, Sphaeromatidae) from the Naktong River, with a key to the Korean species of the genus. Korean Journal of Systematic Zoology 3: 51–56.

Latreille PA (1825) Familles naturelles du règne animal, exposées succinctement et dans un ordre analytique, avec l'indication de leurs genres. Jean-Baptiste Baillière, Paris, 570 pp. https://doi.org/10.5962/bhl.title.16094

Lévêque C, Oberdorff T, Paugy D, Stiassny MLJ, Tedesco PA (2008) Global diversity of fish (Pisces) in freshwater. Hydrobiologia 595(1): 545–567. https://doi.org/10.1007/s10750-007-9034-0

Menzies RJ (1954) A review of the systematics and ecology of the genus "*Exosphaeroma*" with the description of a new genus, a new species, and a new sub-species (Crustacea, Isopoda, Sphaeromidae). American Museum Novitates 1683: 1–24.

Miura M, Mori H, Nakai S, Satake K, Sasaki T, Chiba S (2008) Molecular evidence of the evolutionary origin of a Bonin Islands endemic Stenomelania boninensis. The Journal of Molluscan Studies 74(2): 199–202. https://doi.org/10.1093/mollus/eyn003

Nation JL (1983) A new method using hexamethyldisilazane for preparation of soft insect tissues for scanning electron microscopy. Stain Technology 58(6): 347–351. https://doi.org/10.3109/10520298309066811

Nishimura S (1968) *Gnorimosphaeroma lata* n. sp., a new marine isopod from Kii, Japan. Publications of the Seto Marine Biological Laboratory 16(4): 273–280. https://doi.org/10.5134/175549

Nishimura S (1969) *Gnorimosphaeroma salebrosa* sp. nov. from the coast of Kii, Japan (Isopoda: Sphaeromatidae). Publications of the Seto Marine Biological Laboratory 16(6): 385–393. https://doi.org/10.5134/175563

Nunomura N (1998) On the genus *Gnorimosphaeroma* (Crustacea, Isopoda, Sphaeromatidae) in Japan with descriptions of six new species. Bulletin of the Toyama Science Museum 21: 23–54.

Nunomura N (1999) A new Species of the Genus *Gnorimosphaeroma* (Isopoda, Sphaeromatidae) from the Mouth of Tonda River Kii Pemnsula, Southern Japan. Bulletin of the Toyama Science Museum 22: 1–5.

Nunomura N (2013) Isopod crustaceans from Shikoku, western Japan-1, specimens from Ehime Prefecture. Bulletin of the Toyama Science Museum 446: 19–78.

Nunomura N, Satake K (2006) A new species of the genus *Gnorimosphaeroma* (Crustacea: Isopoda) from Hahajima, Bonin islands, southern Japan. Bulletin of the Toyama Science Museum 29: 1–6.

Palumbi S, Martin A, Romano S, McMillan WO, Stice L, Grabowski G (1991) The simple fool's guide to PCR. Version2.0. Honolulu, HL: Department of Zoology and Kewalo Marine Laboratory, University of Hawaii.

Rambaut A, Drummond AJ, Xie D, Baele G, Suchard MA (2018) Posterior summarization in bayesian phylogenetics using Tracer 1.7. Systematic Biology 67(5): 901–904. https://doi.org/10.1093/sysbio/syy032

Ronquist F, Teslenko M, van der Mark P, Ayres DL, Darling A, Höhna S, Larget B, Liu L, Suchard MA, Huelsenbeck JP (2012) MRBAYES 3.2: Efficient Bayesian phylogenetic inference and model selection across a large model space. Systematic Biology 61(3): 539–542. https://doi.org/10.1093/sysbio/sys029

Satake K, Cai Y (2005) *Paratya boninensis*, a new species of freshwater shrimp (Crustacea: Decapoda: Atyidae) from Ogasawara, Japan. Proceedings of the Biological Society of Washington 118(2): 306–311. https://doi.org/10.2988/0006-324X(2005)118[306:PBANSO]2.0.CO;2

Satake K, Ueno R (2013) Distribution of freshwater macroinvertebrates in streams with dams and associated reservoirs on a subtropical oceanic island off southern Japan. Limnology 14(2): 211–221. https://doi.org/10.1007/s10201-012-0393-5

Satake K, Ueno R, Sasaki T (2019) Freshwater and brackish-water macroinvertebrates in the Ogasawara Islands. Global Environmental Research 23: 73–75.

Sket B, Bruce NL (2004) Sphaeromatids (Isopoda, Sphaeromatidae) from New Zealand fresh and hypogean waters, with description of *Bilistra* n. gen. and three new species. Crustaceana 76: 1347–1370. https://doi.org/10.1163/156854003323009858

Strong EE, Gargominy O, Ponder WF, Bouchet P (2008) Global diversity of gastropods (Gastropoda; Mollusca) in freshwater. Hydrobiologia 595(1): 149–166. https://doi.org/10.1007/s10750-007-9012-6

Tamura K, Stecher G, Kumar S (2021) MEGA11: Molecular Evolutionary Genetics Analysis version 11. Molecular Biology and Evolution 38(7): 3022–3027. https://doi.org/10.1093/molbev/msab120

Tattersall WM (1921) Mysidacea, Tanaidacea, and Isopoda. Pt. 7. In: Zoological results of a tour in the Far East. Memoires of the Asiatic Society of Bengal 6: 403–443.

Tomikawa K (2015) A new species of *Jesogammarus* from the Iki Island, Japan (Crustacea, Amphipoda, Anisogammaridae). ZooKeys 530: 15–36. https://doi.org/10.3897/zookeys.530.6063

Tomikawa K, Kobayashi N, Kyono M, Ishimaru S-i, Grygier MJ (2014) Description of a new species of *Sternomoera* (Crustacea: Amphipoda: Pontogeneiidae) from Japan, with an analysis of the phylogenetic relationships among the Japanese species based on the 28S rRNA gene. Zoological Science 31(7): 475–490. https://doi.org/10.2108/zs140026

Tomikawa K, Sasaki T, Aoyagi M, Nakano T (2022) Taxonomy and phylogeny of the genus *Melita* (Crustacea: Amphipoda: Melitidae) from the West Pacific Islands, with descriptions of four new species. Zoologischer Anzeiger 296: 141–160. https://doi.org/10.1016/j.jcz.2021.12.005

Trifinopoulos J, Nguyen LT, von Haeseler A, Minh BQ (2016) W-IQ-TREE: A fast online phylogenetic tool for maximum likelihood analysis. Nucleic Acids Research 44(W1): W232–W235. https://doi.org/10.1093/nar/gkw256

Väinölä R, Witt JDS, Grabowski M, Bradbury JH, Jazdzewski K, Sket B (2008) Global diversity of amphipods (Amphipoda; Crustacea) in freshwater. Hydrobiologia 595(1): 241–255. https://doi.org/10.1007/s10750-007-9020-6

Wetzer R, Pérez-Losada M, Bruce NL (2013) Phylogenetic relationships of the family Sphaeromatidae Latreille, 1825 (Crustacea: Peracarida: Isopoda) within Sphaeromatidea based on 18S-rDNA molecular data. Zootaxa 3599(2): 161–177. https://doi.org/10.11646/zootaxa.3599.2.3

Wetzer R, Bruce NL, Pérez-Losada M (2018) Relationships of the Sphaeromatidae genera (Peracarida: Isopoda) inferred from 18S rDNA and 16S rDNA genes. Arthropod Systematics & Phylogeny 76(1): 1–30. https://doi.org/10.3897/asp.76.e31934

Wetzer R, Wall A, Bruce NL (2021) Redescription of *Gnorimosphaeroma oregonense* (Dana, 1853) (Crustacea, Isopoda, Sphaeromatidae), designation of neotype, and 16S-rDNA molecular phylogeny of the north-eastern Pacific species. ZooKeys 1037: 23–56. https://doi.org/10.3897/zookeys.1037.63017

Wilson GDF (2008) Global diversity of Isopod crustaceans (Crustacea; Isopoda) in freshwater. Hydrobiologia 595(1): 231–240. https://doi.org/10.1007/s10750-007-9019-z

Zoosyst. Evol. 99 (2) 2023, 557–574 | DOI 10.3897/zse.99.107974

PENSOFT

für Natur MUSEUM FÜR NATURKUNDE BERLIN

A new species of *Cerapus* (Amphipoda, Senticaudata, Ischyroceridae) from Mae Klong Estuary, with a discussion on their nesting and types of mating behaviour

Chanikan Katnoum[1,2], Tosaphol Saetung Keetapithchayakul[1], Azman Abdul Rahim[3], Koraon Wongkamhaeng[1,2]

1 *Department of Zoology, Faculty of Science, Kasetsart University, Bangkok 10900, Thailand*

2 *Biodiversity Center Kasetsart University, Bangkok 10900, Thailand*

3 *Marine Ecosystem Research Centre, Faculty of Science and Technology, Universiti Kebangsaan Malaysia, 43600 UKM Bangi, Selangor, Malaysia*

https://zoobank.org/1549ABF3-4A14-448B-89AF-549F2088D947

Corresponding author: Koraon Wongkamhaeng (koraon@gmail.com)

Academic editor: Luiz F. Andrade ♦ **Received** 14 June 2023 ♦ **Accepted** 9 November 2023 ♦ **Published** 4 December 2023

Abstract

The first representative of the genus *Cerapus* in the Gulf of Thailand, *Cerapus rivulus* sp. nov., is described from specimens sampled from Mae Klong Estuary, the inner Gulf of Thailand. The main identifying characteristics of this new amphipod species are pereonites 1 and 2 without constriction; male gnathopod propodus palm transverse with long posterior defining tooth and well-developed anterodistal recurved tooth adjacent to propodus articulation; pereopod 6 coxa without fine fringe setae ventrally, basis with setae on posterior margin; and telson with deep cleft. An updated identification key for the 25 known species in the genus is also presented. A discussion on their nesting and types of mating behaviour is provided.

Key Words

Amphawa, *Cerapus*, mating behaviour, nesting behaviour

Introduction

Lowry and Berents (1996) recognised five genera of tube building amphipods in the Cerapodini (*Cerapus* Say, 1817, *Runanga* Barnard, 1961, *Paracerapus* Budnikova, 1989, *Bathypoma* Lowry & Berents, 1996 and *Notopoma* Lowry & Berents, 1996). In 2018, Berents and Lowry (2018) proposed a new genus from Australia (*Kapalana* Berents and Lowry 2018). The tubicolous genus *Cerapus* can be recognised by: 1) antenna 1 without vestigial accessory flagellum, 2) antenna 1 peduncular article 1 posterior margin with strong posterior projection, 3) gnathopod 2 of adult male, carpochelate, subchelate in female, 4) pereopod 5 with the distal part directed posteriorly, 5) dactyli of pereopods 6 and 7 with 1–2 small accessory spines, 6) pleopods 2 and 3 with inner rami reduced, 1-articulate, 7) uropod 1 with the outer margin of the ramus dentate, 8) uropod 2 uniramus, outer margin of the ramus dentate, without robust setae and 9) uropod 3 uniramous, ramus vestigial bearing recurved spines (Lowry and Berents 1996; Souza-Filho and Serejo 2014; Berents and Lowry 2018; Nurshazwan et al. 2020).

Most species of Cerapodini are found on the soft bottom of estuaries and various coastal habitats, i.e. seagrass beds, algal beds, mangrove forests and coral reefs (Shen 1936; Lowry and Berents 2002; Lowry and Berents 2005; Nurshazwan et al. 2020). There are various types of tubes, with Lowry and Berents (2005) classifying *Cerapus* tubes into three types: the detrital tube, algal tube and sandy tube. Most tubes are constructed in a turf of the interwoven tube with various substrates attached, including hydroids, algae, fleshy and calcareous gorgonians and sponges (Lowry and Thomas 1991). The study of Nurshazwan et al. (2020) reported 23 species, but did not include *C. longicervicum*

Lim, Park & Min, 2008 from South Korea (Lim et al. 2008). Adding the newly-discovered *C. rivulus* sp. nov., there are now a total of 25 *Cerapus* species worldwide. From that, only six species of *Cerapus* have been described in the waters of Southeast Asia, including Singapore: *C. tubularis* Say, 1817; Thailand: *C. chaomai* Lowry & Berents, 2002 and *C. yuyatalay* Lowry & Berents, 2002; Korea: *C. longirostris* Shen, 1936 and *C. longicervicum* Lim, Park & Min, 2008; Malaysia: *C. bumbumiensis* Nurshazwan, Ahmad-Zaki & Azman, 2020. However, there have been no recorded species from the South China Sea, including the Gulf of Thailand (Lowry and Berents 2002; Lim et al. 2008; White 2015; Nurshazwan et al. 2020; Azman 2022).

The present study describes *Cerapus rivulus* sp. nov. as a new species from the Gulf of Thailand. A distribution map with brief biological notes and a key to the world species of the genus are also provided.

Materials and methods

The *Cerapus* sampling was carried out using the experimental model set, based on Aikins and Kikuchi (2001). The experimental models were set up around Mae Klong estuarine for two and four months (Fig. 1).

The Mae Klong River is located in west-central Thailand and passes through Kanchanaburi, Ratchaburi and Samut Songkhram before reaching the upper Gulf of Thailand. Along the river, there are urban and aquaculture zones which make this area important for fishing activities and aquaculture. The Mae Klong Estuary is situated in the Amphawa District of Samut Songkhram Province with salinity ranges from 0.05–2.00 ppt due to tide and water runoff.

The specimens were selected from experimental material and preserved in 95% ethanol. The male holotype and female paratype specimens were transferred from ethanol on to a glycerol slide for morphological study in the laboratory. Drawings were made using a camera lucida attached to an Olympus CH30 light microscope. The pencil drawings were scanned and digitally inked using a WACOM bamboo CTH-970 graphics board in Adobe Illustrator CC 2017, following the method described in Coleman (2003). Terminology for setae and mouthparts described by Zimmer et al. (2009).

The representative specimens were dehydrated with absolute ethanol, critical-point-dried using carbon dioxide, placed on holders and coated with gold for examination with an FEI Quanta 450 scanning electron microscope. Institutional abbreviation: THNHM, Thailand Natural History Museum, Bangkok, Thailand.

Figure 1. Map showing the three river mouths along the Gulf of Thailand. Red circle represents the type locality of *Cerapus rivulus* sp. nov.

Systematics

Suborder Senticaudata Lowry & Myers, 2013
Infraorder Corophiida Leach, 1814 (*sensu* Lowry & Myers, 2013)
Parvorder Caprellidira Leach, 1814 (*sensu* Lowry & Myers, 2013)
Superfamily Photoidea Boeck, 1871
Family Ischyroceridae Stebbing, 1899
Subfamily Ischyrocerinae Stebbing, 1899
Tribe Cerapodini Smith, 1880

Genus *Cerapus* Say, 1817

Type species. *Cerapus tubularis* Say, 1817

Current species composition. *Cerapus* contains 24 species + 1 new species: *C. tubularis* Say, 1817, *C. calamicola* (Giles, 1885), *C. longirostris* Shen, 1936, *C. erae* Bulyčeva, 1952, *C. benthophilus* Thomas & Heard, 1979, *C. alquirta* (Barnard & Drummond, 1981), *C. oceanicus* Lowry, 1985, *C. pacificus* Lowry, 1985, *C. cudjoe* Lowry & Thomas, 1991, *C. micronesicus* Myers, 1995, *C. thomasi* Ortiz & Lemaitre, 1997, *C. chaomai* Lowry & Berents, 2002, *C. yuyatalay* Lowry & Berents, 2002, *C. bundegi* Lowry & Berents, 2005, *C. murrayae* Lowry & Berents, 2005, *C. volucola* Lowry & Berents, 2005, *C. orteai* Ortiz & Thomas, 2007, *C. jonsoni* Valério-Berardo, Thiago de Souza & Waiteman Rodrigues, 2008, *C. longicervicum* Lim, Park & Min, 2008, *C. nudus* Just, 2009, *C. maculanigra* Zeina & Asakura, 2017, *C. ryanadamsi* Drumm, 2018, *C. slayeri* Drumm, 2018, *C. bumbumiensis* Nurshazwan, Ahmad-Zaki & Azman, 2020; *C. rivulus* sp. nov.

Cerapus rivulus sp. nov.

https://zoobank.org/3074048C-ECA2-499C-A3D4-C54C6DAECB7C
Figs 2–10

Material examined. *Holotype*. THAILAND • ♂, 10 mm; Samut Songkhram Province, Mae Klong River, Darunanukroh School; 13°29'41.0"N, 99°55'25.3"E; 5 m depth; 10 Apr 2021; C. Katnoum leg.; THNHM-lv-19376.

***Paratype*.** THAILAND • 5 ♂, 5 ♀; same data as for holotype • THNHM-lv-19379.

Type locality. Darunanukroh School (13°29'41.0"N, 99°55'25.3"E) Mae Klong River, Amphawa District, Samut Songkhram Province, Thailand.

Habitat. Freshwater and brackish water (0.05–2.03 ppt) in Mae Klong River of Amphawa District, Samut Songkhram Province, Thailand.

Figure 2. *Cerapus rivulus* sp. nov. **A.** Holotype male lateral (THNHM -19377); **B.** A specimen in its tube with protruding head and antennae; **C.** Paratype female front (THNHM-19379).

Etymology. The species is named after their habitat which is located in the river (*Rivulus*: Latin for river/stream).

Description. Based on holotype, male, size 10 mm, body elongated, cylindrical THNHM-lv-19376.

Head. (Fig. 3A) ***Eye*** medium, 0.1 mm (0.14× head length); rostrum short (0.16× length of head), acute; Head lateral cephalic lobe well-developed and distally round. ***Antenna 1*** (Fig. 3B) anterior margin with short setae, posterior margin with long setae, about 0.4× the body length, peduncle 3.1× the length of flagellum peduncle article 1 with proximoventral swelling, peduncle article 3 subequal to peduncle article 2, both are slender, several aesthetascs, flagellum with 5 articles, article 1 being the longest, flagellum article 5 the shortest with 1 aesthetasc. ***Antenna 2*** (Fig. 3C) anterior margin with short setae, posterior margin with long setae, slightly shorter than antenna 1, setation similar to antenna 1; peduncle article 5 subequal to article 4.

Upper lip (Fig. 6F) symmetrical, notched, with small setulae apically. ***Lower lip*** (Fig. 6G) with inner lobe, smooth, setulose on inner and outer lobes. ***Mandibles*** (Fig. 6A, B) left incisor with 4 teeth; right lacinia mobilis 4-cuspidate (4 teeth); right mandible with 3 broad accessory spines; molar triturative; molar flake absent; palp elongated, robust; article 2 1.3× as long as article 3, with 17 marginal setae; article 3 with 10 long setae. ***Maxilla 1*** (Fig. 6E) inner plate small without seta; outer plate with 7 apical robust setae; palp biarticulate, with 6 serrated apical robust setae and 4 subapical setae. ***Maxilla 2*** (Fig. 6D) outer plate broader than inner plate, with 12 simple setae; inner plate with 12 setae.

Pereon. ***Gnathopod 1*** (Fig. 3D, E) length ratio from basis to dactylus 2.6:1:1:1.7:1.8; coxa 2× as broad as deep, carpus subequal length to propodus, lobate posterior margin with setae and plumose setae, anterior margin less setae; propodus oval, length 1.7× the width, posterior margin with setae and plumose setae, palm oblique, serrated and with setae; dactylus well developed, palmar margin serrated, crenulated posterior margin withone robust seta. ***Gnathopod 2*** (Fig. 3F, G) carpochelate, length ratio from basis to dactylus 3:1:2:3.5:3:2.5; coxa broader than deep, subequal to coxa 1; basis longer than wide, with 2 marginal setae on anterior margin; carpus massive, length 1.6× the width, palm margin transverse with long posterior defining tooth and well-developed anterodistal recurved spine adjacent to propodus articulation; propodus length 2× the width, with two acute spines and 1 rounded projection on posterior margin, with long setae on anterior and posterior margins; dactylus length 3× the width, with long setae on posterior margin and one seta on anterior margin.

Pereopod 3 (Fig. 4A) length ratio from basis to dactylus 14:6:4.5:4:5.5:3.5; coxa 2.2× as broad as deep, with 2 anterodistal setae; basis length 2.2× the width, anterior margin with 10 setae; merus with 3 anterodistal setae and 3 posterodistal plumose setae; carpus with 2 anterodistal setae and 2 posterodistal setae; propodus with 3 anterodistal setae.

Pereopod 4 (Fig. 4B) length ratio from basis to dactylus 12.5:6.5:6:4:5:3; coxa 1.8× as broad as deep, with a anterodistal seta; basis, length 1.9× the width, anterior margin with 8 setae; ischium subequal to merus, with 4 posterodistal setae; merus without ridges, with a posterodistal plumose seta; carpus with an anterodistal seta and 2 posterodistal setae; propodus with 4 posteromarginal setae; dactylus with unguis.

Pereopod 5 (Fig. 4C) length ratio from basis to dactylus 8:3:4.5:3:5.5: 3; coxa 1.2× as broad as deep; basis globular, length equals to width; ischium subrectangular; merus posterior lobe with 1 plumose seta, smaller anterior lobe with 1 seta; carpus smaller than merus, posterior lobe with fine hair, bearing a seta; propodus subovate; dactylus unguis with 2 accessory hooks.

Pereopod 6 (Fig. 4D) length ratio from basis to dactylus 8.5:2:4:3:5:3; coxa lobate, about 1.3× as broad as deep; basis length 1.6× the width, with setae on posterior margin; ischium subrectangular, length 1.25× width; merus 2.1× as long as broad with distal setae on both sides; carpus as long as broad, with 3 long setae on anterodistal corner and 2 long setae on posterodistal corner; propodus with 2 anterodistal long setae and 1 short marginal seta; dactylus unguis with 2 accessory hooks, with 1 seta on anterior side.

Pereopod 7 (Fig. 4E) length ratio from basis to dactylus 9:3:5:3:5:3; coxa lobate, about 1.6× as broad as deep; basis length 2.25× the width, with setae on anterior margin; ischium subrectangular, length 1.5× the width; merus 2× as long as broad with distal long setae on both sides; carpus as long as broad broad, with 1 marginal seta and 3 long setae on anterodistal corner and 3 long setae on posterodistal corner; propodus with 3 marginal setae on both sides and 8 long posterodistal setae ; dactylus unguis with 2 accessory hooks.

Pleon. Pleopods 1 to 3 decreasing in size. ***Pleopod 1*** (Fig. 5A) peduncle bearing 2 retinacula, without setae; outer ramus slightly shorter than inner ramus, with 6 articles; outer ramus broader than inner ramus, with 2 articles, first article is the largest. ***Pleopod 2*** (Fig. 5B) peduncle with 2 retinacula, without setae; outer ramus 3.1× as long as inner ramus, with a single article; inner ramus reduced, 1.6× as long as broad, 1 plumose seta and single article. ***Pleopod 3*** (Fig. 5C) peduncle with 2 retinacula, without plumose setae distomarginally; outer ramus 3× as long as inner ramus; single article; inner ramus reduced, about 1.75× as long as broad, single article with 1 plumose seta.

Urosome. (Fig. 5D**)** ***Uropod 1*** (Fig. 5E) biramous; peduncle 2.1× as long as wide, with 3 dorsodistal setae; outer ramus shorter than peduncle, 1.5× longer than inner ramus, with outer row of spinules and 1 large apical robust seta, inner ramus with a large apical robust seta, corona of short robust setae surrounding large terminal robust seta.

Uropod 2 (Fig. 5D) uniramous; peduncle 3.75× as long as broad, 6.3× as long as vestigial ramus; ramus with 1 row of short setae and a terminal seta. ***Uropod 3*** (Fig. 5D) uniramous; peduncle 2.7× as long as wide, with

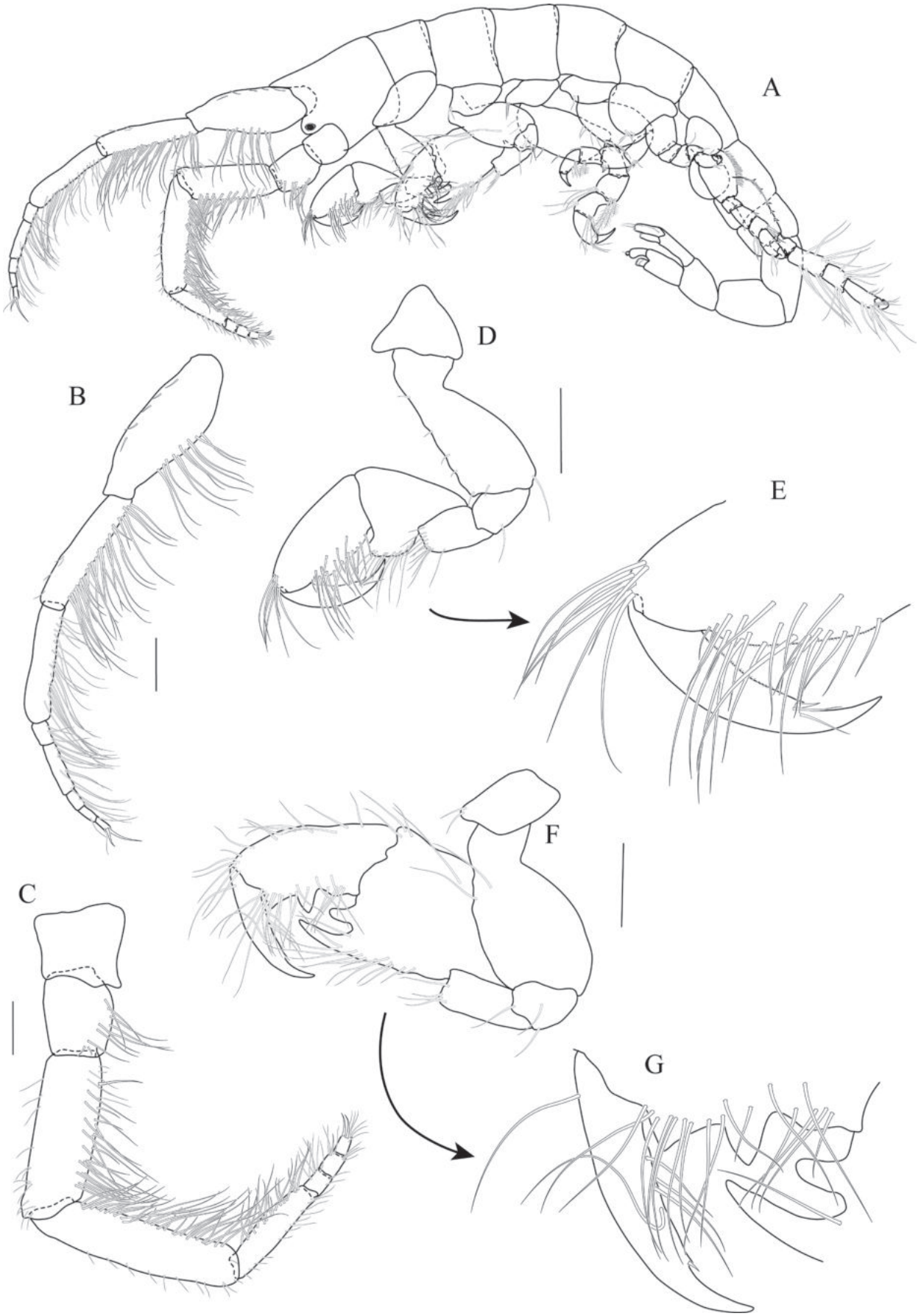

Figure 3. *Cerapus rivulus* sp. nov., holotype, male (THNHM -19377). **A.** Habitus of the male holotype; **B.** Antenna 1; **C.** Antenna 2; **D.** Gnathopod 1; **E.** Palm of gnathopod 1; **F.** Gnathopod 2; **G.** Palm of gnathopod 2. Scale bars: 0.2 mm.

Figure 4. *Cerapus rivulus* sp. nov., holotype, male (THNHM -19377). **A.** Pereopod 3; **B.** Pereopod 4; **C.** Pereopod 5; **D.** Pereopod 6; **E.** Pereopod 7. Scale bars: 0.2 mm.

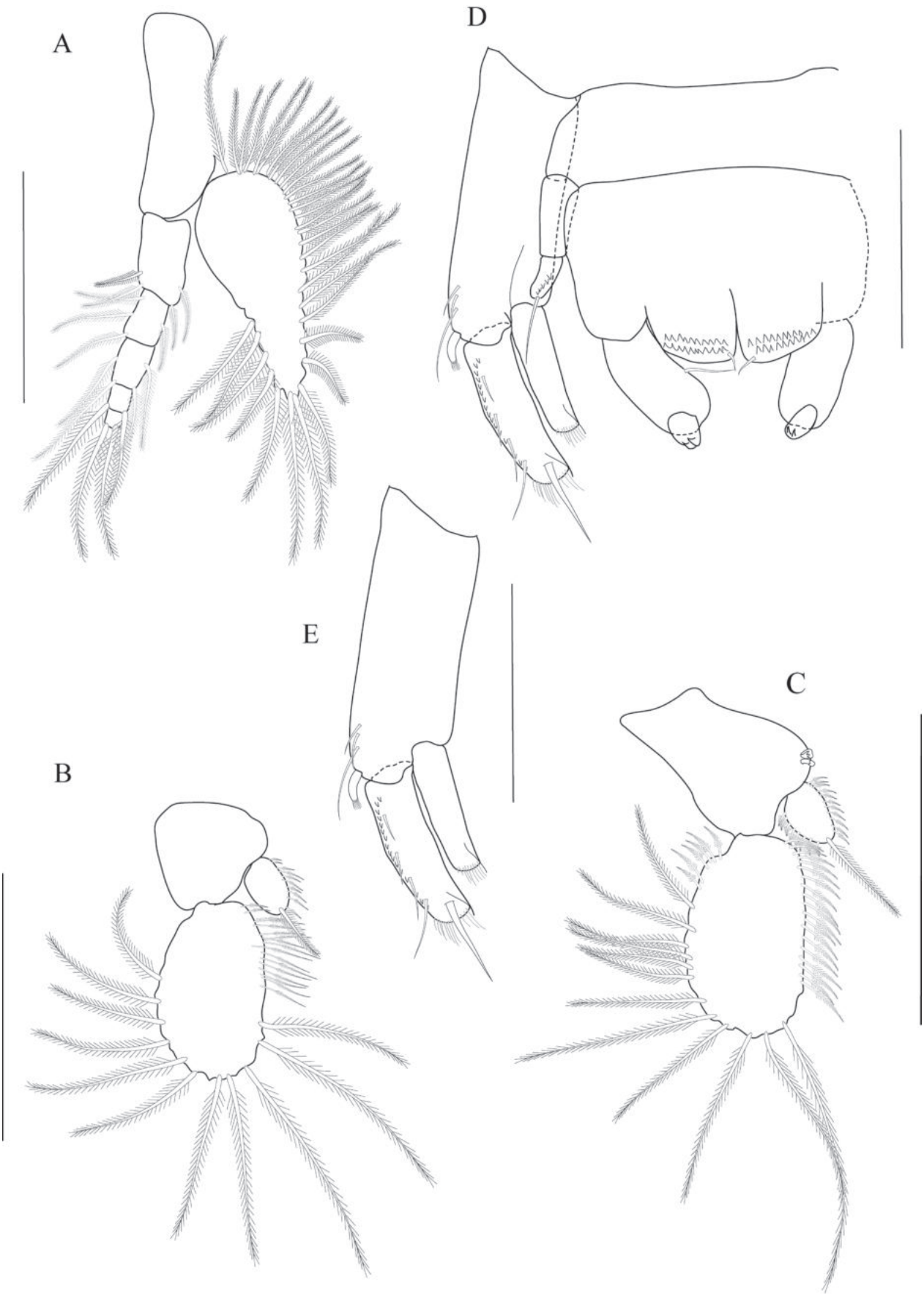

Figure 5. *Cerapus rivulus* sp. nov., holotype, male (THNHM -19377). **A.** Pleopod 1; **B.** Pleopod 2; **C.** Pleopod 3; **D.** Uropods 1–3 and Telson; **E.** Uropod 1. Scale bars: 0.1 mm.

Figure 6. *Cerapus rivulus* sp. nov., holotype, male (THNHM -19377). **A.** Left mandible; **B.** Right mandible; **C.** Maxilliped; **D.** Maxilla 2; **E.** Maxilla 1; **F.** Upper lip; **G**. Lower lip. Scale bars: 0.1 mm.

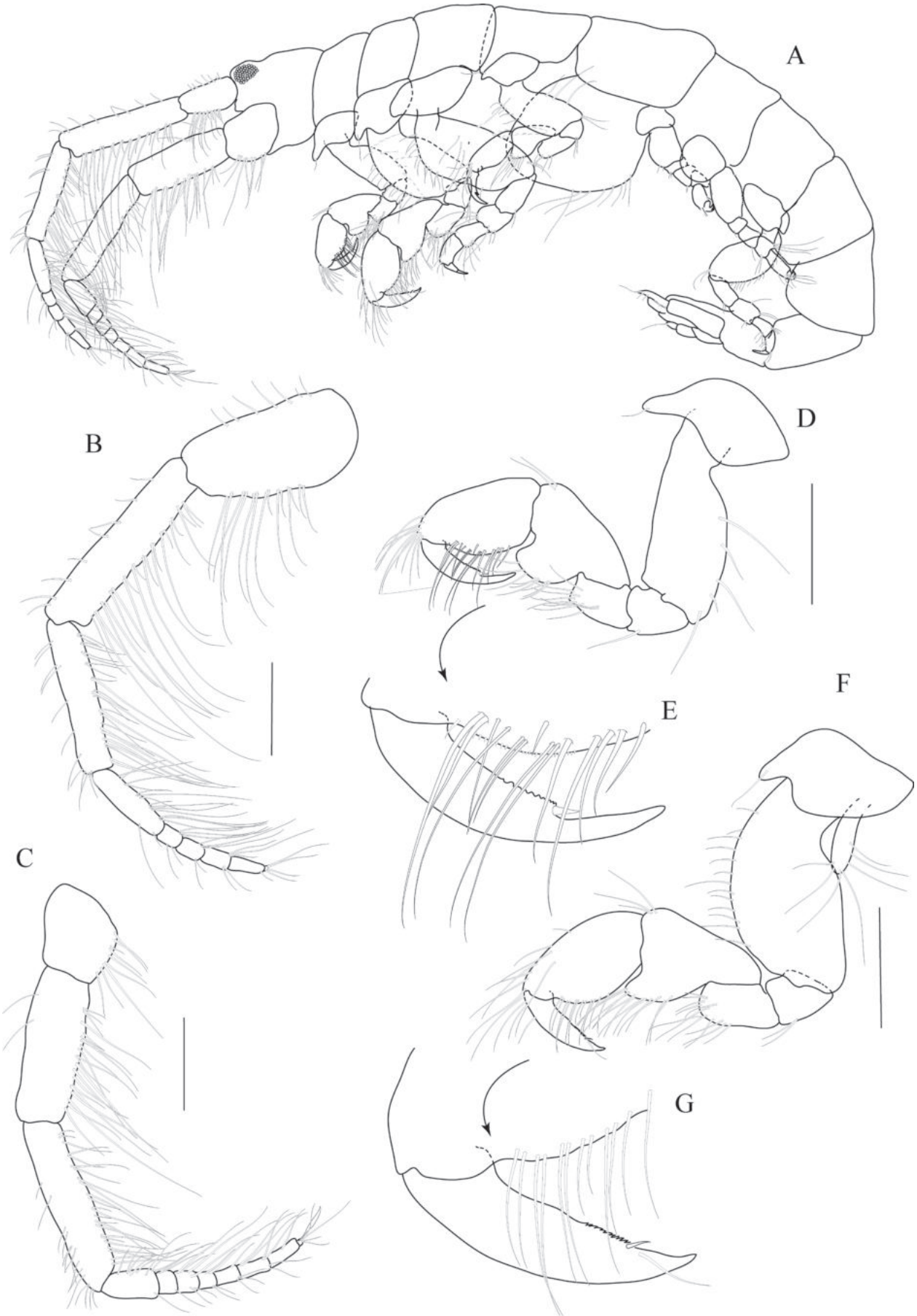

Figure 7. *Cerapus rivulus* sp. nov., paratype, female (THNHM -19379). **A.** Habitus of the female paratype; **B.** Antenna 1; **C.** Antenna 2; **D.** Gnathopod 1; **E.** Palm of gnathopod 1; **F.** Gnathopod 2; **G.** Palm of gnathopod 2. Scale bars: 0.2 mm.

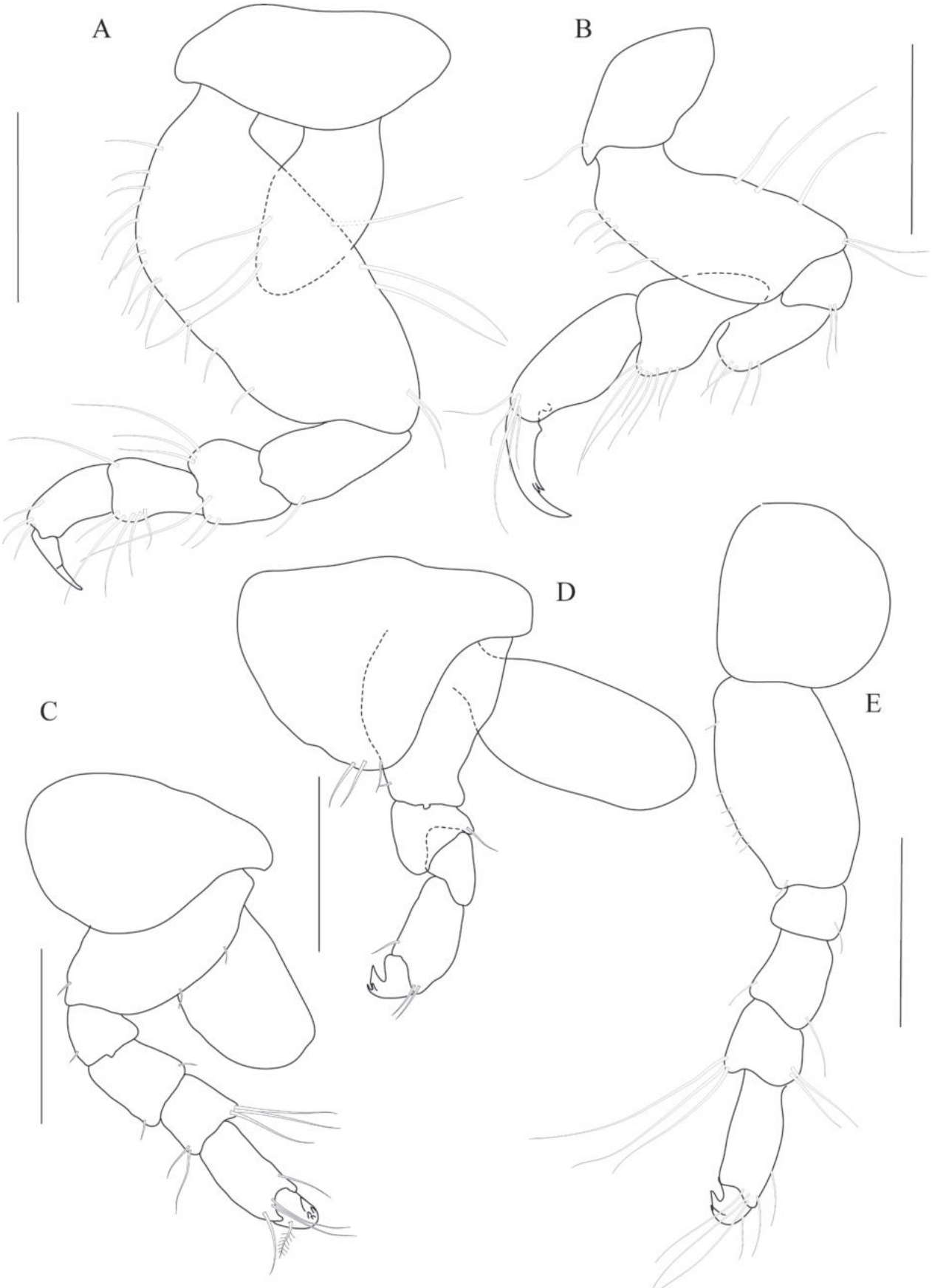

Figure 8. *Cerapus rivulus* sp. nov., paratype, female (THNHM -19379). **A**. Pereopod 3; **B.** Pereopod 4; **C.** Pereopod 5; **D.** Pereopod 6; **E.** Pereopod 7. Scale bars: 0.2 mm.

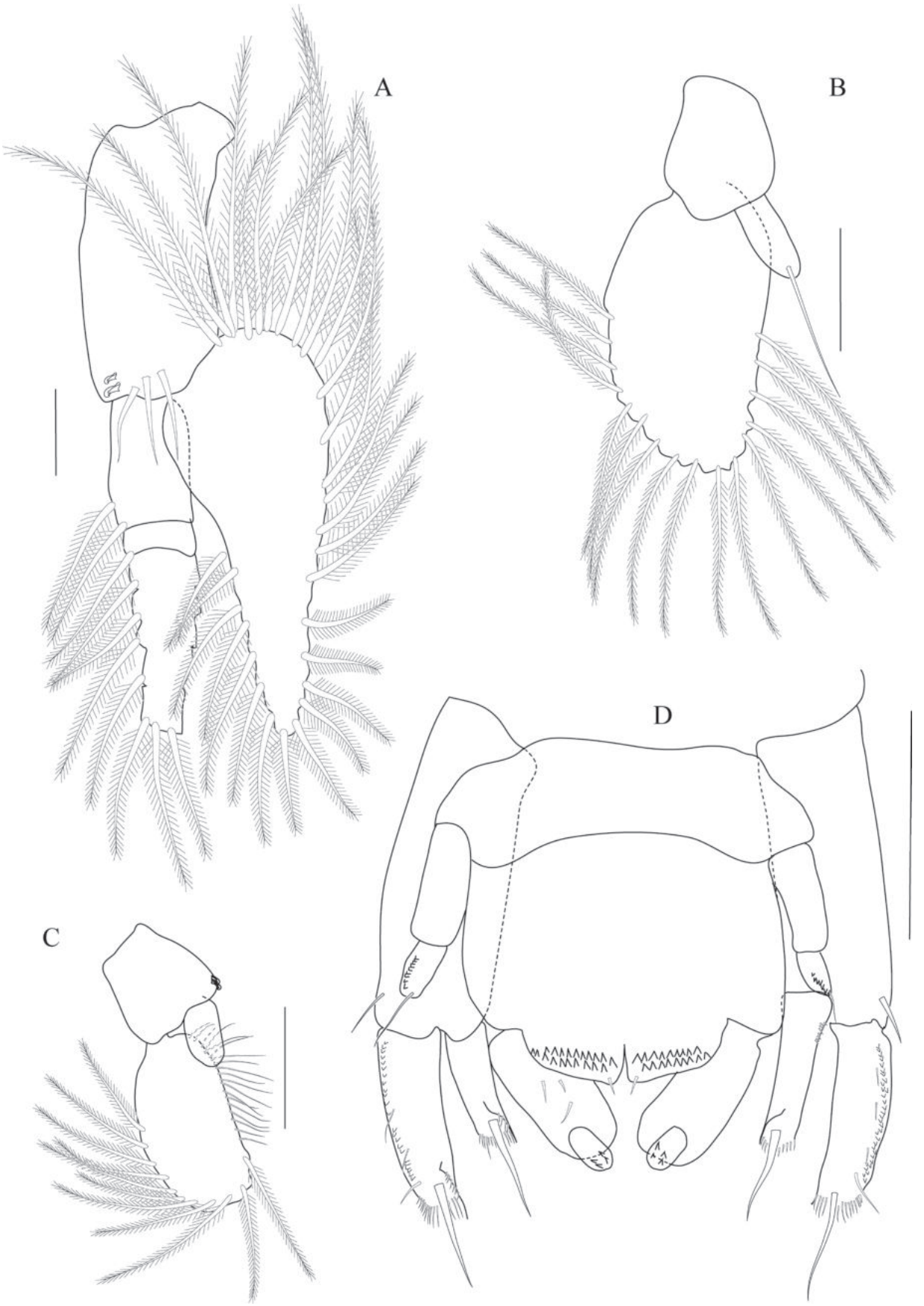

Figure 9. *Cerapus rivulus* sp. nov., paratype, female (THNHM -19379). **A.** Pleopod 1; **B.** Pleopod 2; **C.** Pleopod 3; **D.** Uropods 1–3 and Telson. Scale bars: 0.1 mm (**A–C**); 0.2 mm (**D**).

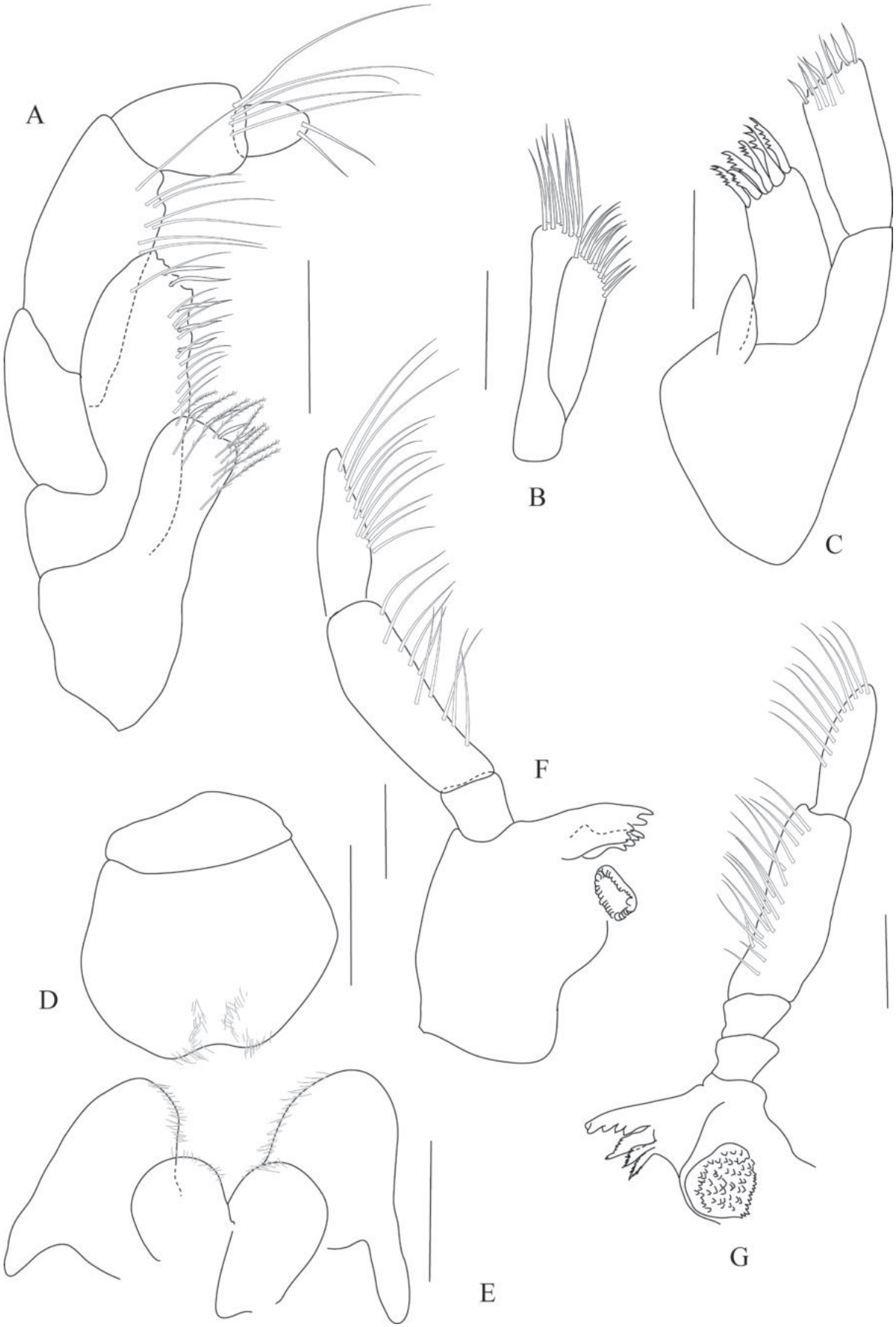

Figure 10. *Cerapus rivulus* sp. nov., paratype, female (THNHM -19379). **A.** Maxilliped; **B.** Maxilla 2; **C.** Maxilla 1; **D.** Upper lip; **E.** Lower lip; **F.** Left mandible; **G.** Right mandible. Scale bars: 0.2 mm.

one seta on inner margin; ramus vestigial, inconspicuously small with 2 hooks. ***Telson*** (Fig. 5D) deeply cleft, 0.5× the length of uropod 3, each lobe with 19 or 20 recurved hooks in two rows and an apical seta.

Female (Figs 7–10) (Sexually dimorphic characters). Based on allotype (THNHM-iv-19379), length 3.5 mm (Fig. 7A). Similar to male, except for the following: ***Antenna 1*** (Fig. 7B) with fewer setae and fewer aesthetascs. ***Antenna 2*** (Fig. 7C) more slender than in male. ***Gnathopod 1*** (Fig. 7D, E) dactylus posterior margin serrated, with one spine. ***Gnathopod 2*** (Fig. 7F, G) slightly larger than gnathopod 1; carpus triangular, posterodistal corner with plumose setae and normal setae; propodus palm not serrated, with plumose setae and simple setae; dactylus posterior margin crenulated. ***Pereopod 5*** (Fig. 8C) coxa larger, about 2.7× as broad as deep, about 6.3× longer than the basis width; basis slightly globular; dactylus with 2 accessory hooks; with a pair of oostegites on each segment from 4 to 6.

Remarks. *Cerapus rivulus* sp. nov. is similar to *C. nudus* and *C. longirostris* which has synapomorphic character states, such as: (1) pereonites 1–2 without constriction; (2) pereopod 5 merus without plumose seta on posterior lobe; (3) pereopod 6 coxa without setae on ventral margin; (4) uropod 1 without hook on ventrodistal margin. They are distinguished by the following: (1) head subequal in length to pereonites 1 + 2 [*C. nudus* longer than pereonites 1 + 2, *C. longirostris* subequal to pereonites 1 + 2]; (2) gnathopod 2 propodus twice as long as wide [*C. nudus* and *C. longirostris* less than twice as long as wide]; (3) telson deeply cleft (> 50%) [*C. nudus* and *C. longirostris* semi-cleft]; (4) telsonic lobe with 19–20 hooks in two transverse rows [*C. nudus* with ten recurved hooks on three transverse rows and *C. longirostris* with eight recurved hooks on two transverse rows.

This study brings the number of identified *Cerapus* species from Southeast Asia to seven. *Cerapus rivulus* sp. nov. can be separated from Southeast Asian congeners by a combination of characteristics as follows (other species in paratheses): absence of constriction between pereonite 1 and 2 (present in *C. yuyatalay*, *C. bumbumiensis* and *C. longicervicum*); antenna 1 peduncular article 1 shorter than article 3 (longer in *C. chaomai*, *C. bumbumiensis* and *C. longicervicum*); gnathopod 2 propodus with tooth in male (without tooth in *C. chaomai*, *C. yuyatalay*, *C. bumbumiensis* and *C. longicervicum*); telson fused with pleonite 3 (not fused in *C. yuyatalay*, *C. bumbumiensis*, and *C. longicervicum*); telson with more than ten hooks (fewer than ten in *C. bumbumiensis*).

C. tubularis was described from Long Island Sound, New York, U.S.A. and after that reported in Japan by Morino (1976). However, Lowry and Berents (1989) re-described *C. tubularis* and excluded the record of Morino (1976). Lastly, White (2015) reported *Cerapus* sp. in Singapore and noted that the amphipod resembles *C. tubularis* and possibly was introduced to Singapore. The presence of *C. tubularis* in the eastern Pacific and South China Sea is still unclear and needs clarification.

Geographic distribution. The *Cerapus* are distributed worldwide and mainly inhabit marine and brackish water (Fig. 11) (Lowry and Thomas 1991; Lowry and Berents 2002; Drumm 2018; Nurshazwan et al. 2020). Interestingly, *C. rivulus* sp. nov. was found in freshwater and brackish water (salinity less than 3 ppt), so this is the first report for freshwater habitats. They were dominant in the coarse filter substrate used for benthos sampling because the tubes are retained on the coarse filter.

Biological notes. Generally, tube-building amphipods build tubes using amphipod silk which is observed as silk strands adhering to the tip of the dactylar surface close to the pore on P3 and P4 (Kronenberger et al. 2012).

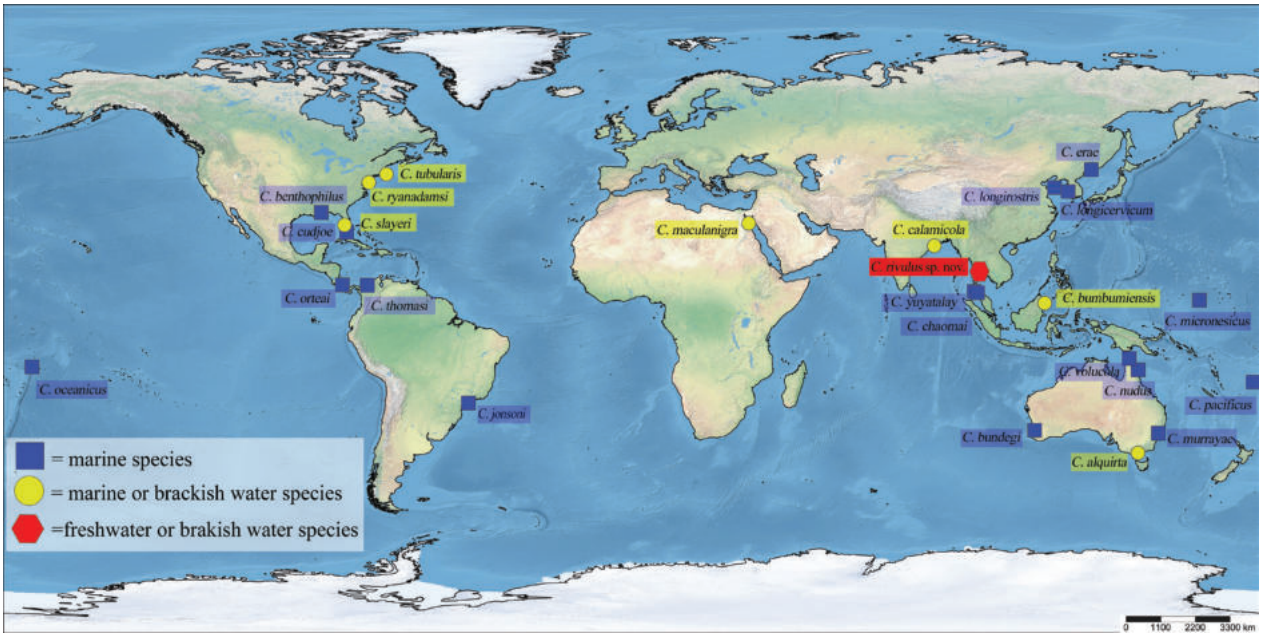

Figure 11. Distribution of *Cerapus* spp.

Cerapus rivulus sp. nov. also presents this characteristic (Fig. 12). The outer surface of the tube consists of uniformly coarse sediment and detritus with a mix of fragmented fibres and algae (Fig. 2) (small tubes of juvenile attached to the larger tube) (Fig. 13A–D); the inner surface, on the other hand, exhibits a fine network of amphipod silk. Laboratory observations on *C. rivulus* sp. nov.: feeding behaviour, both antennae 1 and 2 were used to gather food and move chunks of organic material back inside their tube. From the gut content analysis, the major food items consist of fungus, algae, diatoms, organic substances and protozoa. Moreover, mating behaviour showed that males wander about the habitat investigating the tube of female individuals. During these encounters, males try to contact females with their antennae. After that, females withdraw the posterior part of the body into their tubes, while males use their urosome to stimulate the ventral surface of the female pleosome. These situations are assumed to be a possible prelude to mating (Fig. 14).

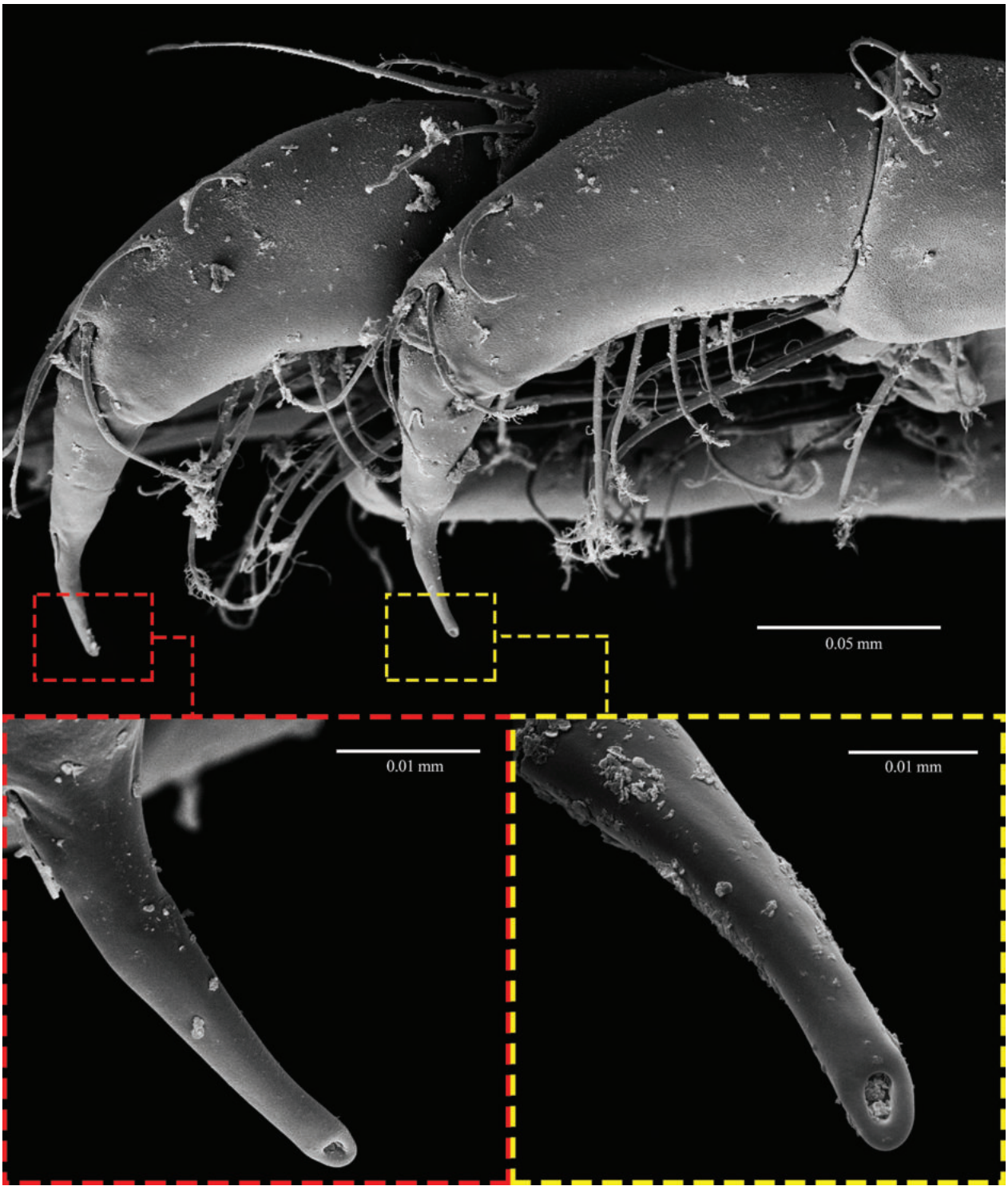

Figure 12. Distal end of P3 and P4 of *Cerapus rivulus* sp. nov. Red dash line represents distal end of P3 dactylus with amphipod silk opening and yellow dash line represents distal end of P4 dactylus with amphipod silk opening.

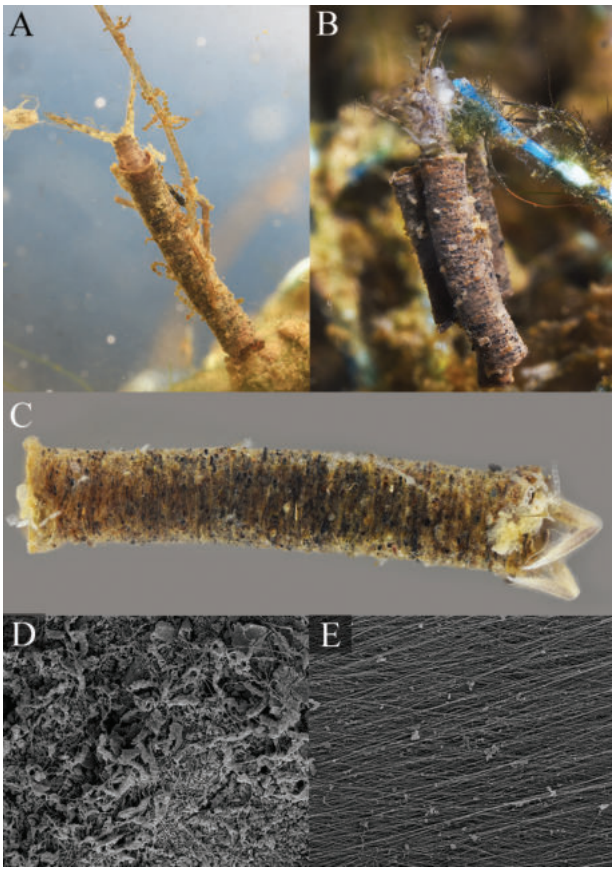

Figure 13. *Cerapus rivulus* sp. nov. **A.** Showing a mix of fragmented fibres and algae on its tube; **B.** Showing small tubes of juvenile attached on the larger tube; **C**. Uniformly coarse sediment on the outer surface of the tube; **D.** Ultrastructure of uniformly coarse sediment on the outer surface of the tube (scanning electron microscope); **E.** Ultrastructure of fine network of amphipod silks on the inner surface of the tube (scanning electron microscope).

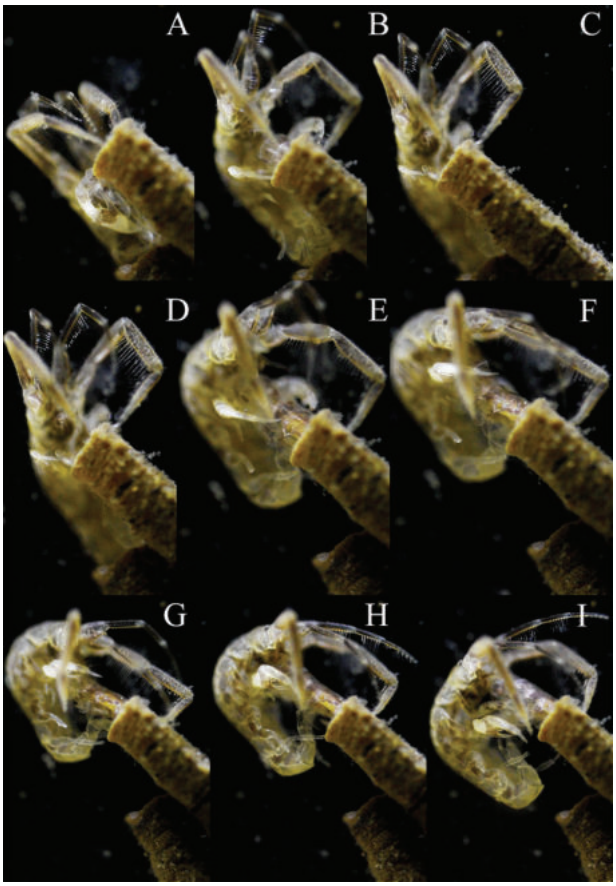

Figure 14. Series of mating of *Cerapus rivulus* sp. nov. (created from video of Suppl. material 1).

Key to world species of *Cerapus*

1	Uropod 1 with conspicuously large lateral peduncular hook on ventrodistal margin 2
–	Uropod 1 without hook on ventrodistal margin 5
2(1)	Pereonites 1–2 with constriction ..... *C. cudjoe* Lowry & Thomas, 1991
–	Pereonites 1–2 without constriction 3
3(2)	Head longer than pereonite 1+2 ..... *C. slayeri* Drumm, 2018
–	Head subequal in length to pereonites 1+2 4
4(3)	Rostrum well developed, more than 20% of head length; antennal flagella 1 and 2 conspicuously short, composed of two or three articles; telson with 11 or 12 recurved spines ..... *C. ryanadamsi* Drumm, 2018
–	Rostrum conspicuously short, less than 20% of head length; antennal flagella 1 and 2 long, composed of more than three articles; telson with 9 or 10 recurved spines ..... *C. thomasi* Ortiz & Lemaitre, 1997
5(1)	Pereonites 1–2 with constriction 6
–	Pereonites 1–2 without constriction 12
6(5)	Telson entirely cleft 7
–	Telson semi-cleft 8
7(6)	Antenna 2 shorter than antenna 1, peduncle article 4 shorter than 5 ..... *C. micronesicus* Myers, 1995
–	Antenna 2 longer than antenna 1, peduncle article 4 longer than 5 ..... *C. longicervicum* Lim, Park & Min, 2008
8(7)	Telson with deep cleft (> 50%) 9
–	Telson with shallow cleft (< 45%) 10
9(8)	Telsonic lobe with 3–5 recurved spines on two transverse rows ..... *C. bumbumiensis* Nurshazwan, Ahmad-Zaki & Azman, 2020
–	Telsonnic lobe with 9–11 recurved spines on two transverse rows ..... *C. yuyatalay* Lowry & Berents, 2002

10(8) Rostrum well developed, more than 20% of head length; antenna 2 longer than antenna 1; pereopod 5 merus without plumose seta on posterior lobe ..... *C. benthophilus* Thomas & Heard, 1979
– Rostrum short, less than 20% of head length; antenna 2 shorter than antenna 1; pereopod 5 merus with more than one plumose seta on posterior lobe 11
11(10) Pereopod 5 merus with three to six plumose setae at posterior lobe ..... *C. jonsoni* Valério-Berardo, Thiago de Souza & Waiteman Rodrigues, 2008
– Pereopod 5 merus with seven to ten plumose setae at posterior lobe ..... *C. murrayae* Lowry & Berents, 2005
12(5) Pereopod 6 coxa with long or short setae on ventral margin 13
– Pereopod 6 coxa without setae on ventral margin 17
13(12) Pereopod 5 merus without plumose seta on posterior lobe ..... *C. longirostris* Shen, 1936
– Pereopod 5 merus with one or more than one plumose setae on posterior lobe 14
14(13) Pereopod 5 with one plumose seta on posterior lobe ..... *C. chaomai* Lowry & Berents, 2002
– Pereopod 5 merus with more than one plumose seta on posterior lobe 15
15(14) Male gnathopod 2 palm without inner tooth ..... *C. pacificus* Lowry, 1985
– Male gnathopod 2 palm with inner tooth 16
16(15) Pereopod 5 merus with two plumose setae at posterior lobe ..... *C. calamicola* (Giles, 1885)
– Pereopod 5 merus with three to six setae at posterior lobe ..... *C. erae* Bulyčeva, 1952
17(12) Pereopod 5 merus without plumose seta on posterior lobe 18
– Pereopod 5 merus with one or more than one plumose setae on posterior lobe 20
18(17) Rostrum conspicuously short; pereopod 5 merus with one seta at posterior lobe ..... *C. rivulus* sp.nov.
– Rostrum well developed; pereopod 5 merus without setae at posterior lobe 19
19(18) Telsonic lobe with ten recurved hooks on three transverse rows ..... *C. nudus* Just, 2009
– Telsonic lobe with eight recurved hooks on two transverse rows ..... *C. longirostris* Shen, 1936
20(17) Pereopod 5 merus with one plumose seta on posterior lobe ..... *C. alquirta* (Barnard & Drummond, 1981)
– Pereopod 5 merus with more than one plumose setae on posterior lobe 21
21(20) Pereopod 7 basis with spines along posteroproximal margin ..... *C. tubularis* Say, 1817
– Pereopod 7 basis without spines along posteroproximal margin 22
22(21) Telson entirely cleft 23
– Telson semi-cleft 24
23(22) Rostrum well developed; antenna 2 longer than antenna 1 ..... *C. oceanicus* Lowry, 1985
– Rostrum conspicuously short; antenna 1 longer than antenna 2 ..... *C. erae* Bulyčeva, 1952
24(22) Telson with 6–7 longitudinal rows of spines ..... *C. orteai* Ortiz & Thomas, 2007
– Telson with two transverse rows of spines 25
25(24) Antenna 2 longer than antenna 1 ..... *C. maculanigra* Zeina & Asakura, 2017
– Antenna 1 longer than antenna 2 26
26(25) Pereopod 5 merus with two plumose setae at posterior lobe ..... *C. volucola* Lowry & Berents, 2005
– Pereopod 5 merus with four plumose setae at posterior lobe ..... *C. bundegi* Lowry & Berents, 2005

Acknowledgements

The authors thank Kasetsart University for providing a Master's degree student scholarship through the Biodiversity Center Kasetsart University. This project is funded by the National Research Council of Thailand (NRCT) (Grant no. N25A660322). In remembrance and thanks also to Assistant Professor Pongrat Dumrongrojwattana for his invaluable advice on the nomenclature of the new taxa. We are grateful to Ms. Nattavadee Tipsut for provided information of gut contents in this study. We express our gratitude to Dr. Alan Myers, Dr. Jesser Fidelis de Souza Filho and Dr. Penny Berents for their valuable evaluations of a previous draft of the manuscript. Furthermore, we extend our appreciation to Dr. Luiz F. Andrade, the subject editor, for promptly facilitating and overseeing the publication process in a gracious manner. We thank the Department of Zoology, Faculty of Science, Kasetsart University, for the laboratory facilities.

References

Aikins S, Kikuchi E (2001) Studies on habitat selection by amphipods using artificial substrates within an estuarine environment. Hydrobiologia 457(1/3): 77–86. https://doi.org/10.1023/A:1012261116232

Azman AR, Sivajothy K, Shafie BB, Ja'afar N, Wongkamhaeng K, Bussarawit S, Alip AE, Lee YL, Metillo EB, Won MEQ (2022) The amphipod (Crustacea: Peracarida) of the Southeast Asia and the neighbouring waters: an updated checklist with new records of endemic species. Research Bulletin - Phuket Marine Biological Center 79(1): 42–84.

Barnard JL, Drummond MM (1981) Three corophioids (Crustacea, Amphipoda) from Western Port, Victoria. Proceedings of the Royal Society of Victoria 93(1–2): 31–41.

Berents PB, Lowry JK (2018) The new crustacean amphipod genus *Kapalana* from Australian waters (Senticaudata, Ischyroceridae, Ischyrocerinae, Cerapodini). Records of the Australian Museum 70(4): 391–421. https://doi.org/10.3853/j.2201-4349.70.2018.1711

Boeck A (1871) Crustacea Amphipoda borealia et arctica. Forhandlinger Videnskabs-Selskabet i Christiania 1870: 81–280. https://doi.org/10.5962/bhl.title.2056

Bulyčeva AI (1952) Novye vidy bokoplavov (Amphipoda, Gammaridea) iz Japonskogo Morja. Trudy Zoologicheskogo Instituta Akademii Nauk S.S.S.R. 12: 195–250. [Nouvelles espèces 'amphipodes (Amphipoda, Gammaridea) de la Mer du Japon]

Coleman C (2003) "Digital inking": How to make perfect line drawings on computers. Organisms, Diversity & Evolution 3(4): 1–14. https://doi.org/10.1078/1439-6092-00081

Drumm DT (2018) Two new species of *Cerapus* (Crustacea: Amphipoda: Ischyroceridae) from the Northwest Atlantic and Gulf of Mexico. Zootaxa 4441(3): 495–510. https://doi.org/10.11646/zootaxa.4441.3.4

Giles GM (1885) Natural history notes from H.M.'s Indian marine survey steamer "Investigator", commander Alfred Carpenter, R.N. commanding. N° 1. On the structure and habits of *Cyrtophium calamicola*, a new tubicolous amphipod from the Bay of Bengal. Journal of the Asiatic Society of Bengal 54: 54–59.

Just J (2009) Ischyroceridae. In: Lowry JK, Myers AA (Eds) Benthic Amphipoda (Crustacea: Peracarida) of the Great Barrier Reef, Australia. Zootaxa 2260: 1–930. https://doi.org/10.11646/zootaxa.1980.1.1

Kronenberger K, Moore PG, Halcrow K, Vollrath F (2012) Spinning a Marine Silk for the Purpose of Tube-Building. Journal of Crustacean Biology 32(2): 191–202. https://doi.org/10.1163/193724011X615532

Lim B, Park J, Min G (2008) A New Species of *Cerapus* from Korea (Crustacea: Amphipoda: Ischyroceridae). Animal Systematics, Evolution and Diversity 24(1): 9–16. https://doi.org/10.5635/KJSZ.2008.24.1.009

Lowry JK (1985) Two new species of *Cerapus* from Samoa and Fiji (Crustacea: Amphipoda: Ischyroceridae). Records of the Australian Museum 36(4): 157–168. https://doi.org/10.3853/j.0067-1975.36.1985.344

Lowry JK, Berents PB (1989) A redescription of *Cerapus tubularis* Say, 1818, based on material of the first reviewer, S.I. Smith, 1880, (Crustacea: Amphipoda: Corophioidea). Journal of Natural History 23: 1341–135. https://doi.org/10.1080/00222938900770711

Lowry JK, Berents PB (1996) The *Ericthonius* group, a new perspective on an old problem (Crustacea: Amphipoda: Corophioidea). Records of the Australian Museum 48(1): 75–109. https://doi.org/10.3853/j.0067-1975.48.1996.281

Lowry JK, Berents PB (2002) The genus *Cerapus* in the Andaman Sea (Crustacea, Amphipoda, Ischyroceridae). Phuket Marine Biological Center Special Publication 23: 189–196.

Lowry JK, Berents PB (2005) Algal-tube Dwelling Amphipods in the Genus *Cerapus* from Australia and Papua New Guinea (Crustacea: Amphipoda: Ischyroceridae). Records of the Australian Museum 57(2): 153–164. https://doi.org/10.3853/j.0067-1975.57.2005.1439

Lowry JK, Myers AA (2013) A phylogeny and classification of the Senticaudata subord. nov. (Crustacea: Amphipoda). Zootaxa 3610(1): 1–80. https://doi.org/10.11646/zootaxa.3610.1.1

Lowry JK, Thomas JD (1991) A new species of *Cerapus* from Cudjoe Channel, Lower Florida Keys, USA, with notes on male behaviour (Crustacea: Amphipoda: Corophioidea). Journal of Natural History 25(6): 1461–1467. https://doi.org/10.1080/00222939100770931

Morino H (1976) On two new forms of *Cerapus tubularis*, a tube dwelling Amphipoda, from shallow waters of Japan. Publications of the Seto Marine Biological Laboratory 23(1/2): 179–189. https://doi.org/10.5134/175915

Myers AA (1995). Marine Amphipoda of Micronesia: Kosrae. Records of the Australian Museum 47: 27–38. https://doi.org/10.3853/j.0067-1975.47.1995.4

Nurshazwan J, Ahmad-Zaki AB, Azman BAR (2020) A new species of *Cerapus* (Amphipoda: Senticaudata: Ischyroceridae) from Pulau Bum Bum, Sabah, Malaysia, with an identification key to *Cerapus* species. Zootaxa 4802(3): 519–533. https://doi.org/10.11646/zootaxa.4802.3.7

Ortiz M, Lemaitre R (1997) Seven new amphipods (Crustacea: Peracarida: Gammaridea) from the Caribbean coast of South America. Boletin de Investigaciones Marinas y Costeras 26: 71–104. https://doi.org/10.25268/bimc.invemar.1997.26.0.365

Ortiz M, Thomas JD (2007) *Cerapus orteai* (Corophioidea: Corophiidae) a new amphipod crustacean from the Caribbean coast of Costa Rica. Avicennia 19: 17–24.

Say T (1817) On a new genus of Crustacea, and the species on which it is established. Journal of the Academy of Natural Sciences of Philadelphia 1(4): 49–52.

Shen CJ (1936) Description of a new tube-dwelling amphipod collected on the coast of Shantung peninsula. Bulletin of the Fan Memorial Institute of Biology (Zoology) 6: 265–273.

Smith SI (1880) On the amphipodous genera, *Cerapus*, *Unciola*, and *Lepidactylis*, described by Thomas Say. Transactions of the Connecticut Academy of Arts and Sciences 4: 268–285.

Souza-Filho JF, Serejo CS (2014) On the phylogeny of Ischyroceridae (Amphipoda, Senticaudata, Corophiida), with the description of a new genus and eight new species from deep-sea Brazilian waters. Zoological Journal of the Linnean Society 170(1): 34–85. https://doi.org/10.1111/zoj12099

Thomas JD, Heard RW (1979) A new species of *Cerapus* Say, 1817 (Crustacea: Amphipoda) from the northern Gulf of Mexico with notes on its ecology. Proceedings of the Biological Society of Washington 92(1): 98–105.

Valério-Berardo MT, De Souza AMT, Rodrigues CW (2008) Description of two new species of Ischyroceridae (Crustacea: Amphipoda) from the coast of Southeastern Brazil. Zootaxa 1857(1): 55–65. https://doi.org/10.11646/zootaxa.1857.1.5

White K (2015) A checklist of Amphipoda (Crustacea) collected from the mudflats of Pulau Ubin, Singapore. The Raffles Bulletin of Zoology 31: 139–142.

Zeina A, Asakura A (2017) A new species of *Cerapus* Say, 1817 (Amphipoda: Ischyroceridae) from the Red Sea, with a key to the worldwide species of the genus. Journal of Crustacean Biology 37(3): 296–302. https://doi.org/10.1093/jcbiol/rux024

Zimmer A, Arriagada A, Bond Buckup G (2009) Diversity and arrangement of the cuticular structures of *Hyalella* (Crustacea: Amphipoda: Dogielinotidae) and their use in taxonomy. Zoologia 26(1): 127–142. https://doi.org/10.1590/S1984-46702009000100019

Supplementary material 1

Video of mating of *Cerapus rivulus* sp. nov.

Authors: Chanikan Katnoum, Tosaphol Saetung Keetapithchayakul, Azman Abdul Rahim, Koraon Wongkamhaeng

Data type: mp4

Link: https://doi.org/10.3897/zse.99.107974.suppl1